



SIGGRAPH THINK
BEYOND
2020 S2020.SIGGRAPH.ORG

PHYSICS-BASED DIFFERENTIABLE RENDERING
A COMPREHENSIVE INTRODUCTION

Shuang Zhao
Wenzel Jakob
Tzu-Mao Li

University of California, Irvine
EPFL, Lausanne, Switzerland
MIT CSAIL, Cambridge



SHUANG ZHAO
ASSISTANT PROFESSOR
University of California, Irvine



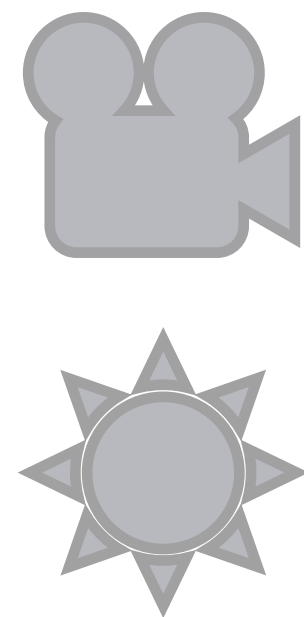
WENZEL JAKOB
ASSISTANT PROFESSOR
EPFL, Lausanne, Switzerland



TZU-MAO LI
POSTDOCTORAL RESEARCHER
MIT CSAIL, Cambridge
(joining UCSD as an assistant professor in 2021)



FORWARD VS. INVERSE RENDERING



Rendering



$$\mathbf{y} = f(\mathbf{x})$$

Inverse rendering



$$\mathbf{x} = f^{-1}(\mathbf{y})?$$

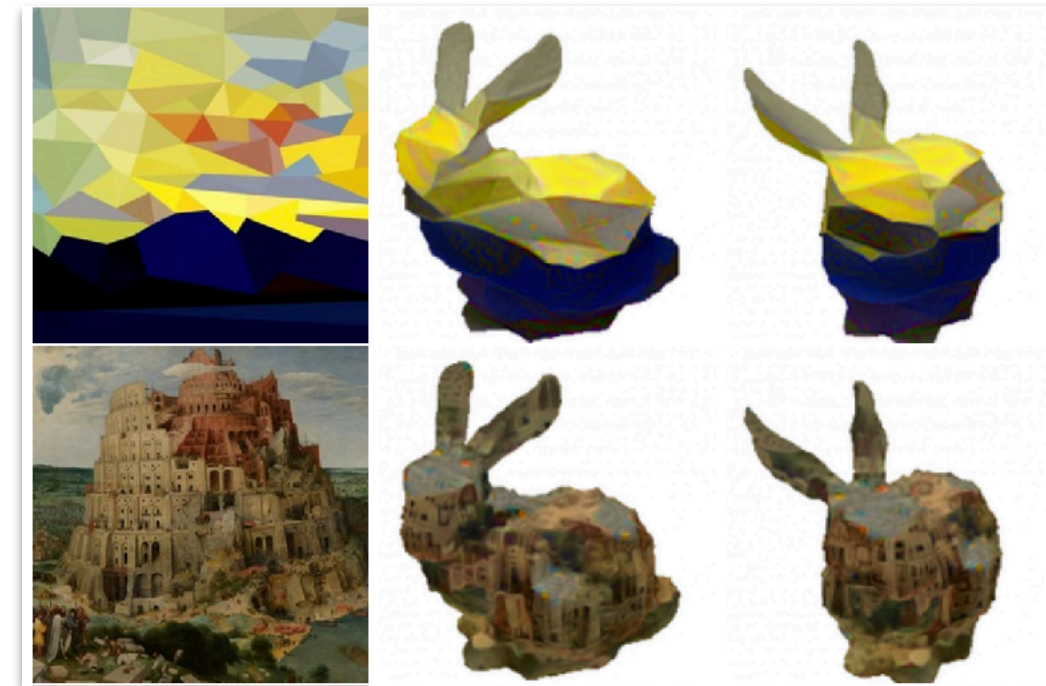
Geometry, materials, emitters, ...



Scene: "bed classic" from jiraniano



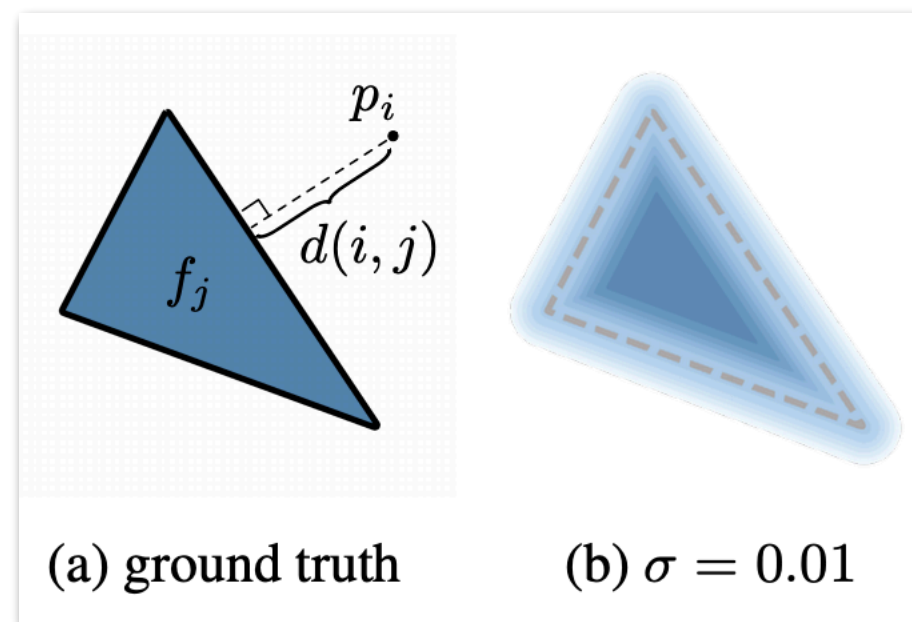
OpenDR: an Approximate Differentiable Renderer
[Loper et al. 2014]



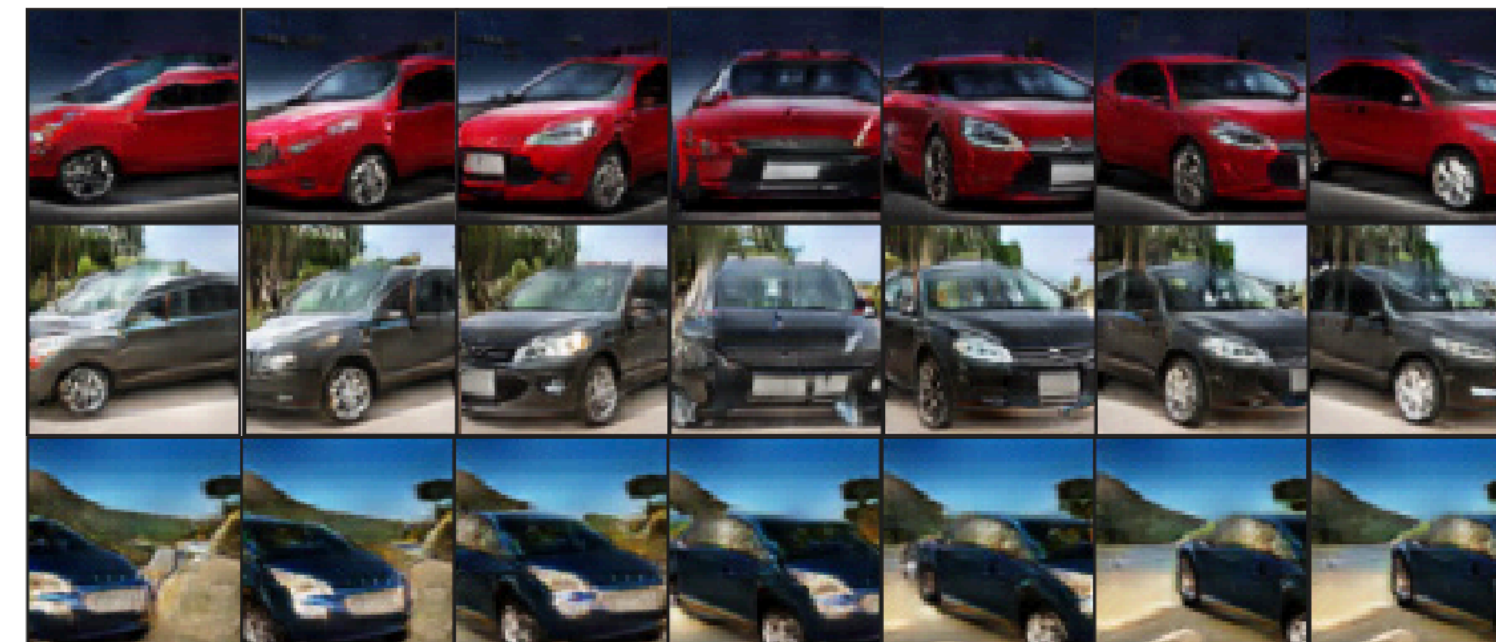
Neural 3D Mesh Renderer
[Kato et al. 2017]



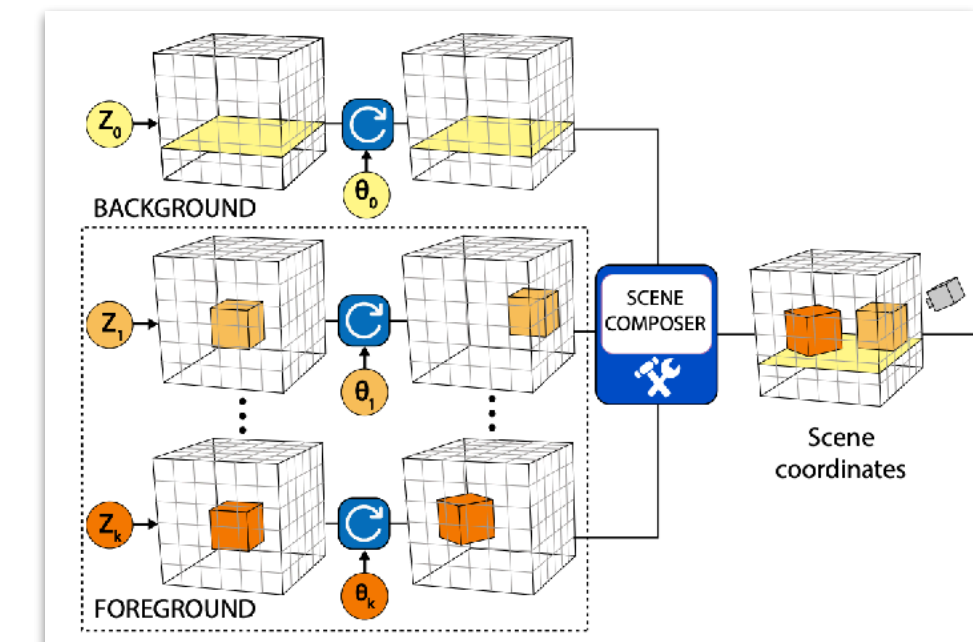
Unsupervised Geometry-Aware Representation for 3D Human Pose Estimation
[Rhodin et al., 2016]



Soft Rasterizer: Differentiable Rendering for Unsupervised Single-View Mesh Reconstruction
[Liu et al. 2019]



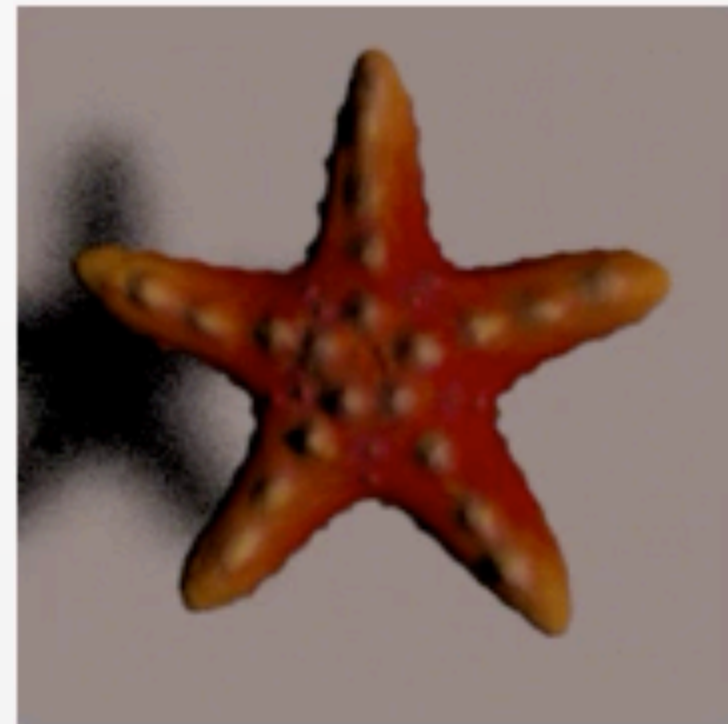
HoloGAN: Unsupervised Learning of 3D Representations From Natural Images.
[Nguyen-Phuoc et al. 2019]



BlockGAN: Learning 3D Object-aware Scene Representations from Unlabelled Images
[Nguyen-Phuoc et al. 2020]

- Focus on inverse rendering for realistic functions $f(\mathbf{x})$

Global illumination, complex materials, participating media, polarization, color spectra, etc.



Target



Target



Target

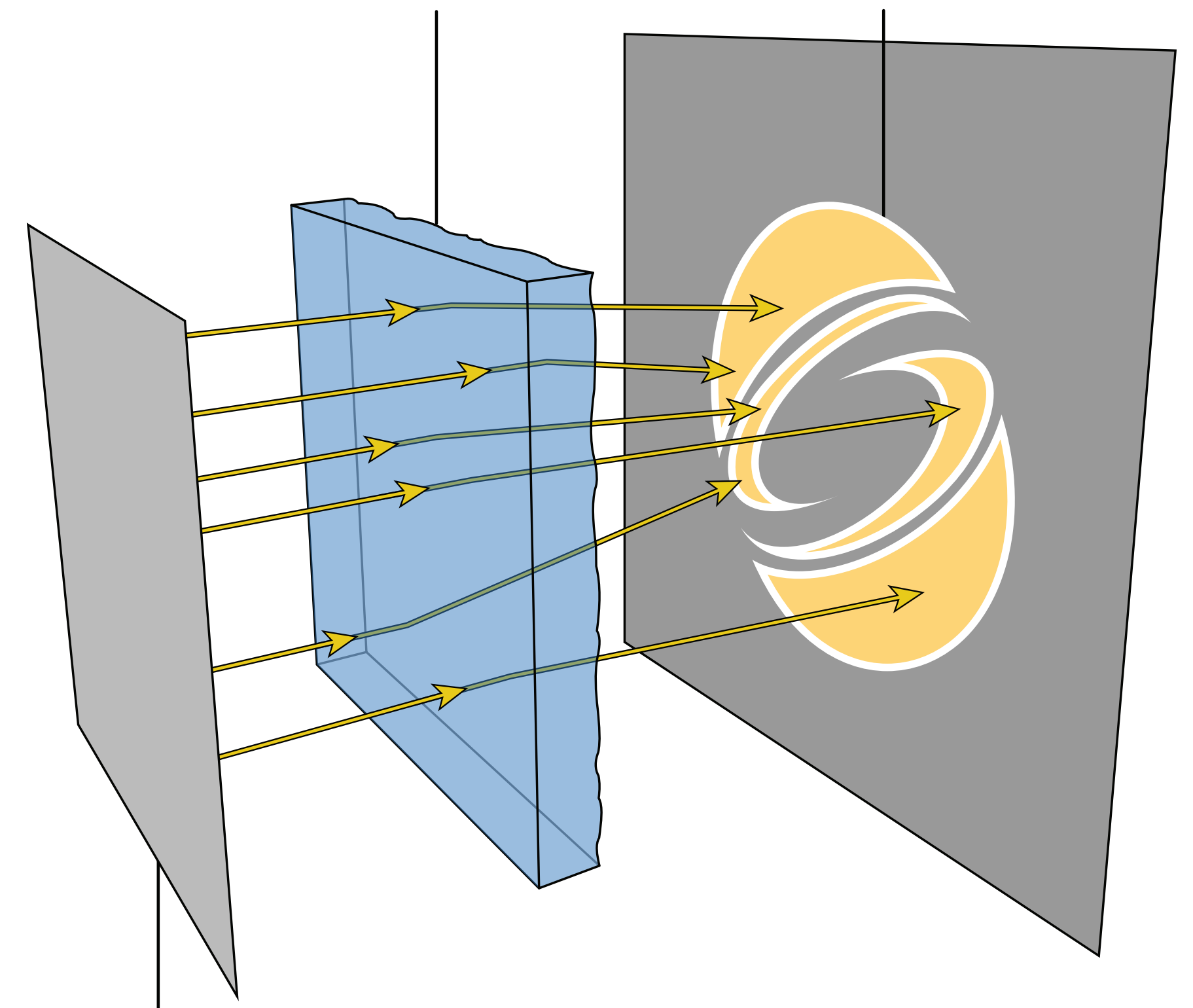


Target



Schwartzburg et al. 2014

Optimized geometry Projected caustic

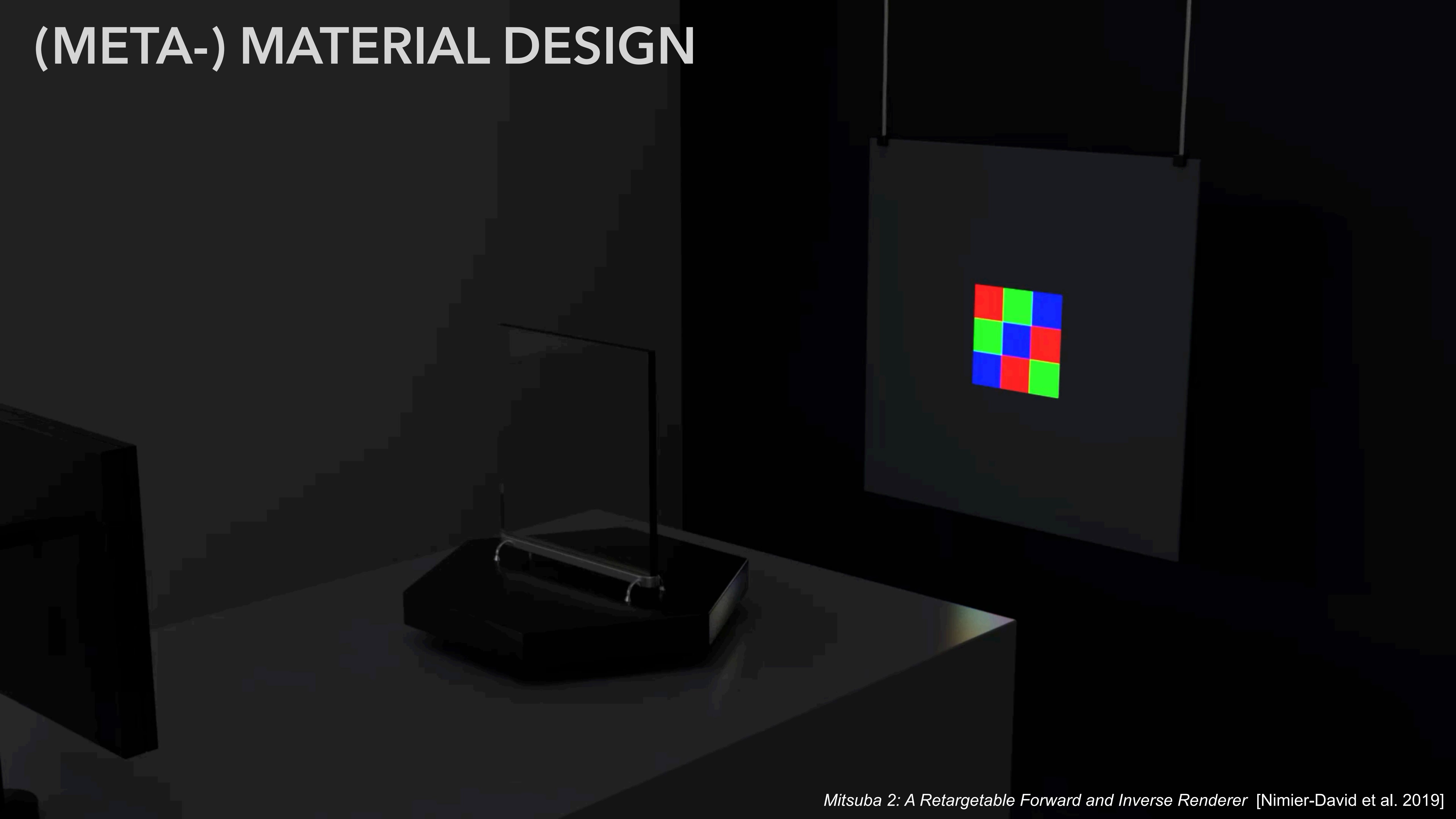


Directional area light

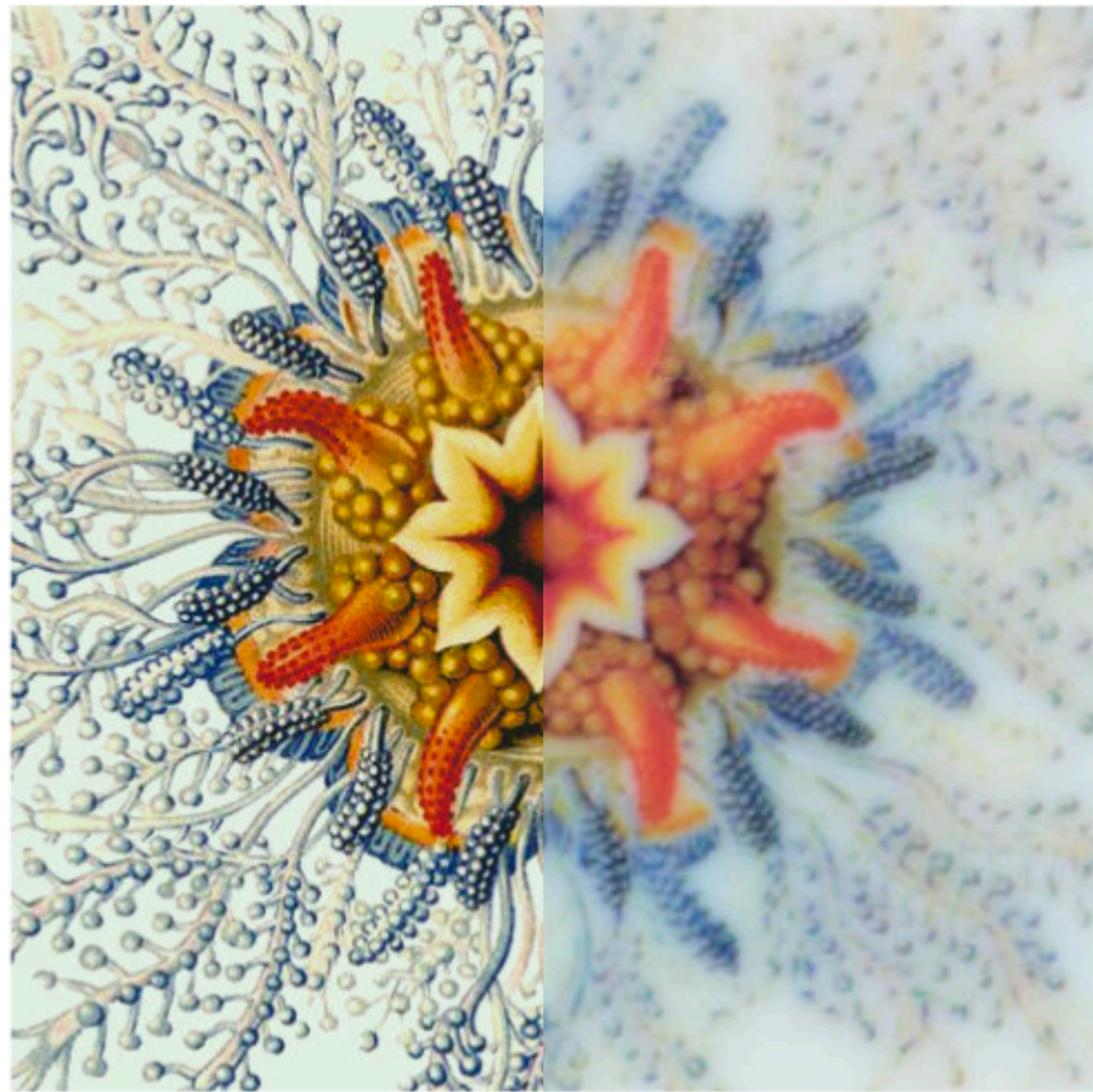
(META-) MATERIAL DESIGN



(META-) MATERIAL DESIGN

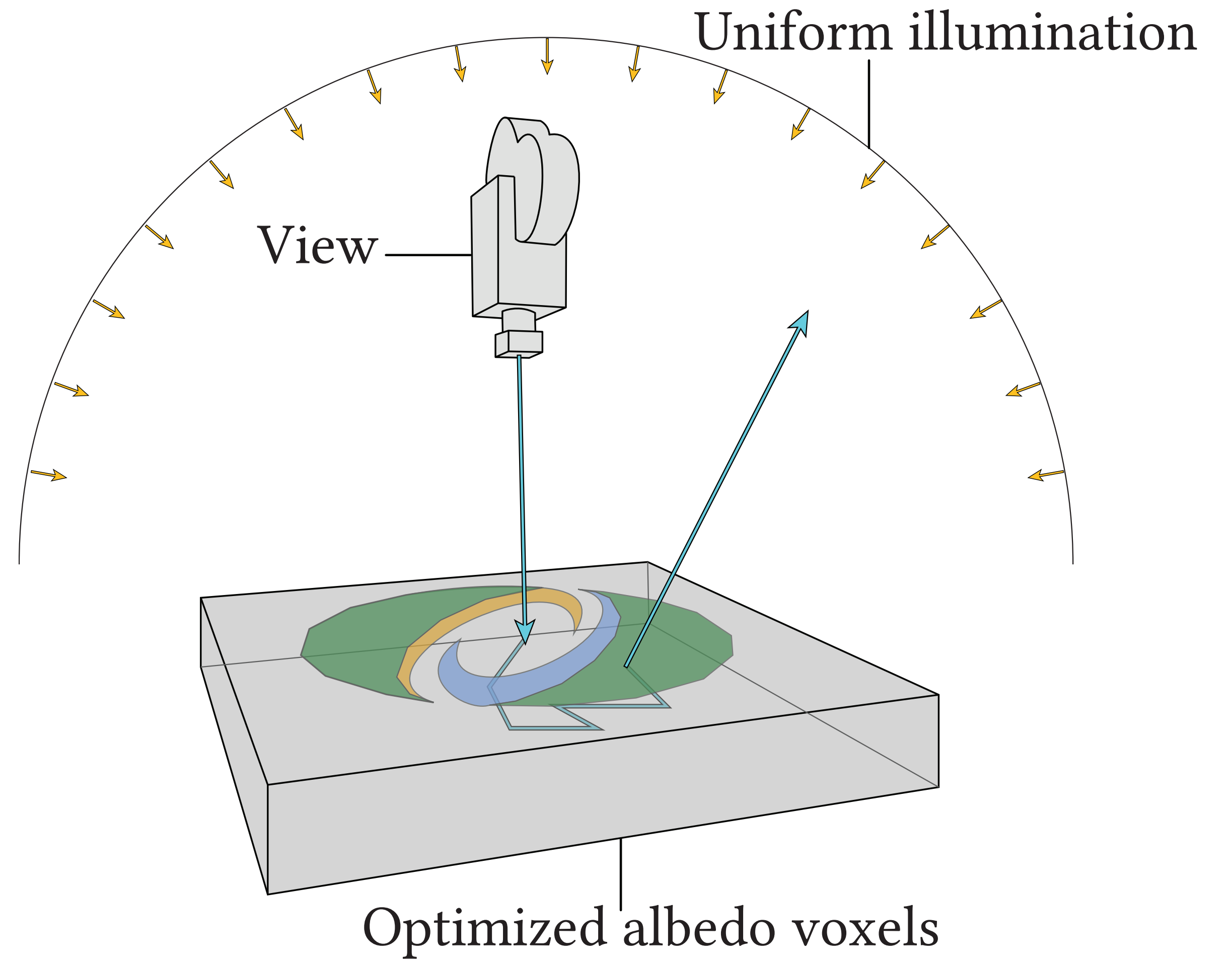


Elek et al. 2017



Target

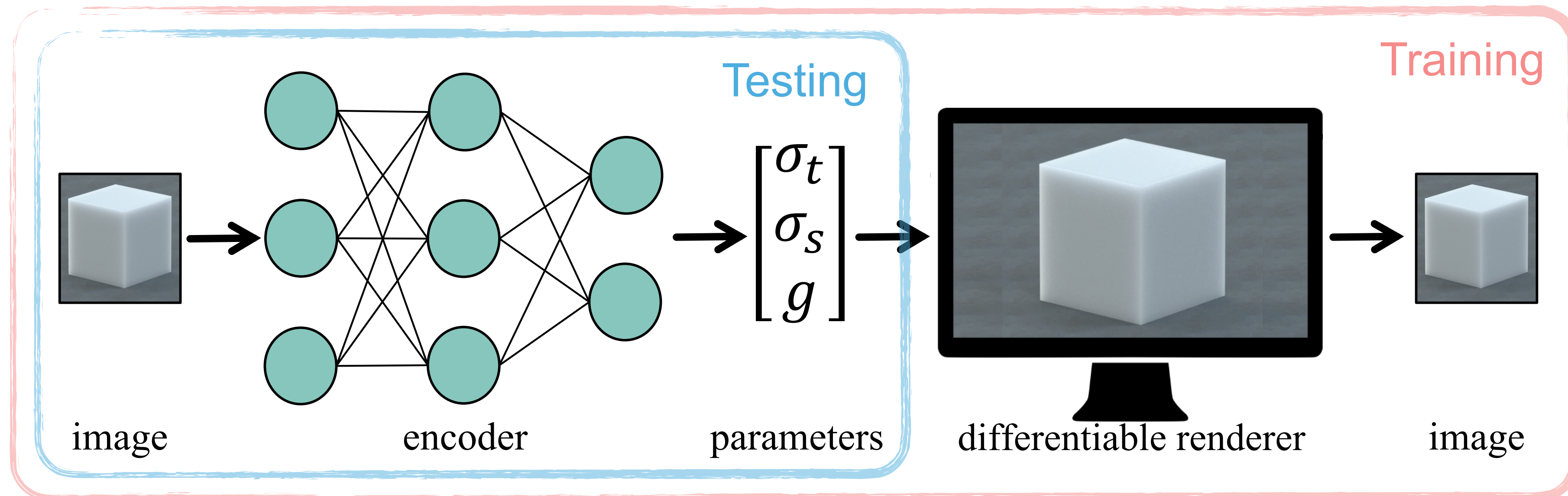
Naive print





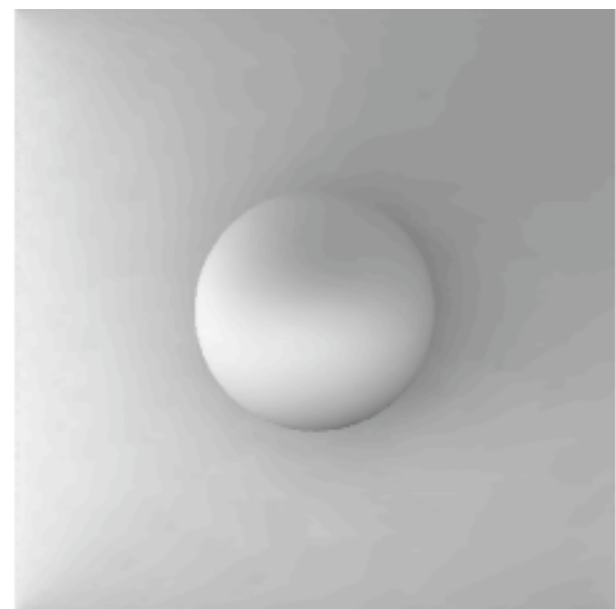
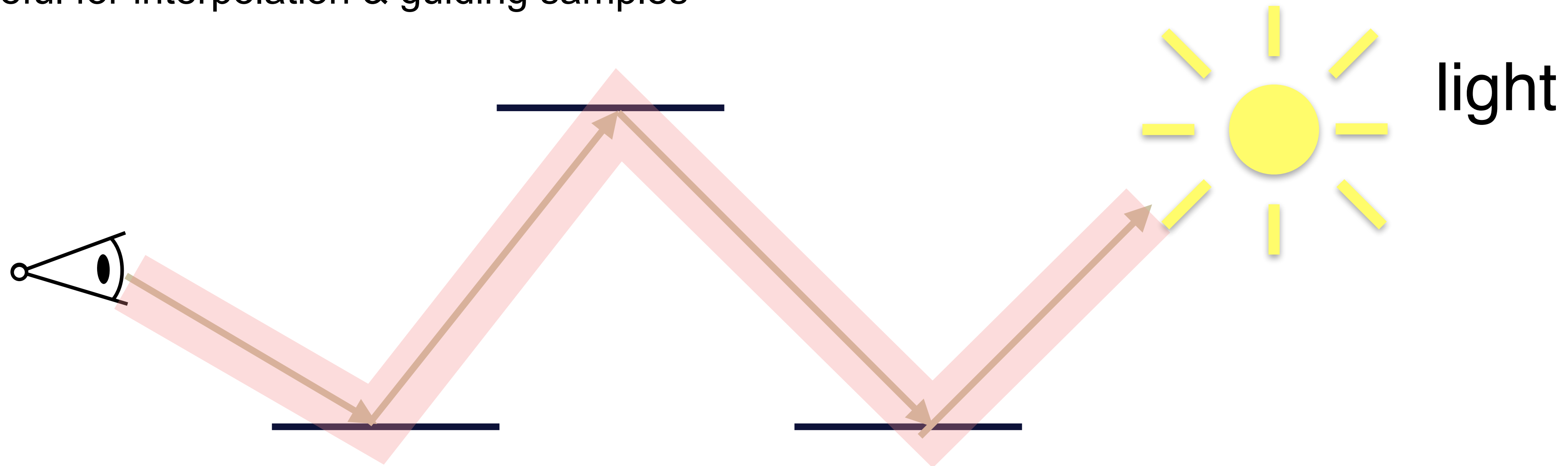
Reference: diffuse surface texture

- Integrating physics-based rendering into **machine learning & probabilistic inference** pipelines
- Inverse subsurface scattering [Che et al. 2020]

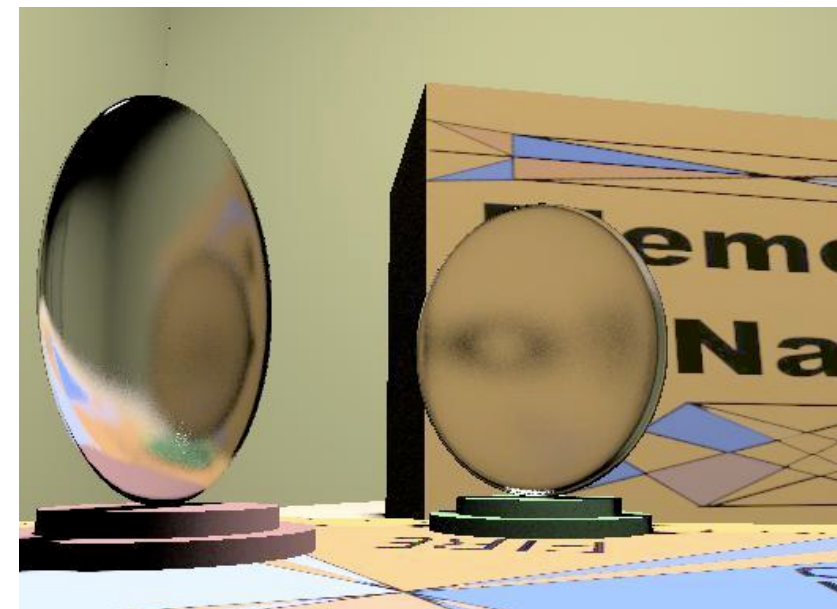


- Utilizing *image loss* (provided by a volume path tracer) to regularize training
- Use the trained encoder to solve inverse problems during testing

- Derivatives reveal neighborhood information of light paths
 - useful for interpolation & guiding samples



irradiance gradient
[Ward 1992]



path differentials
[Suykens and Williams 2001]

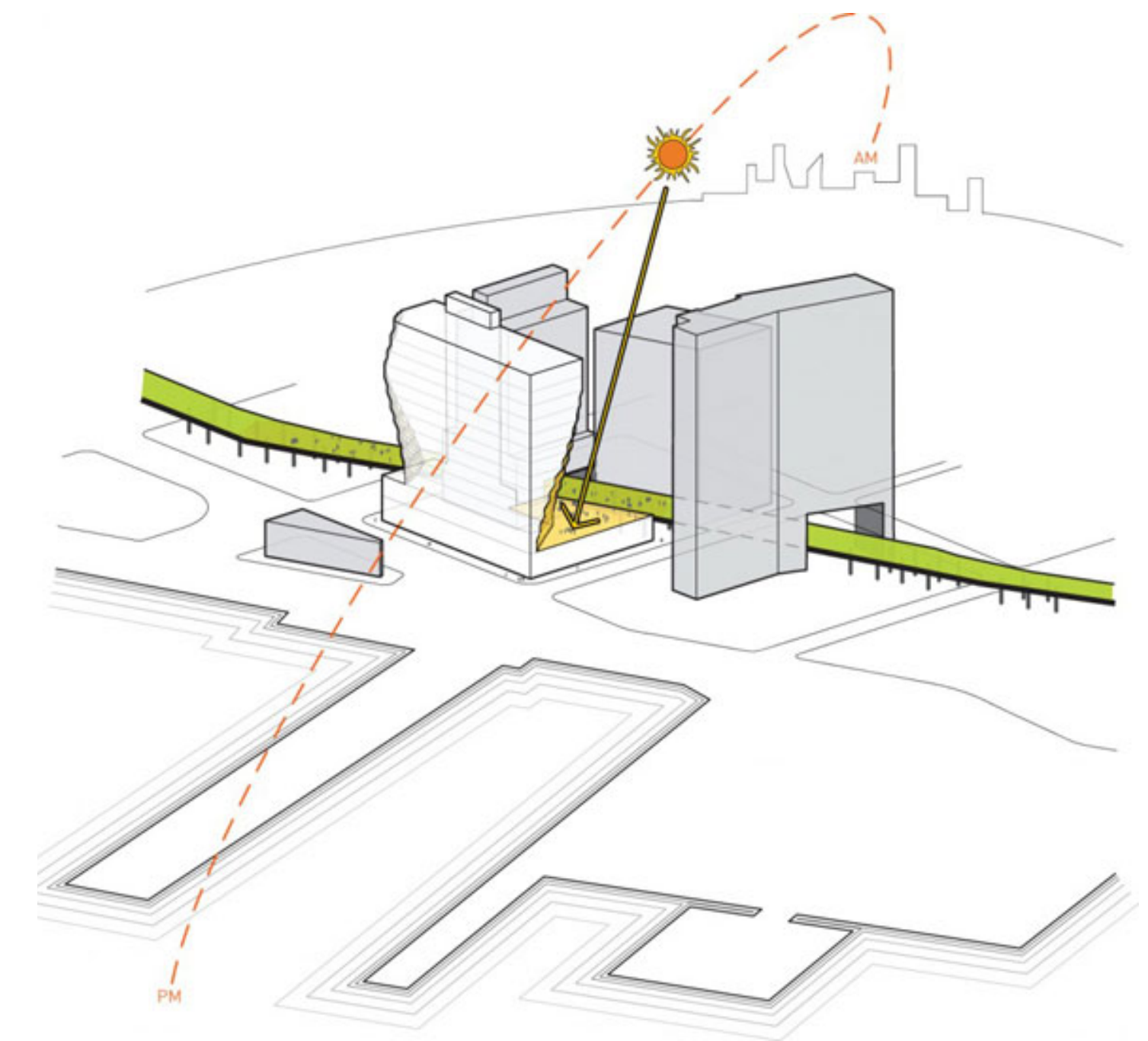
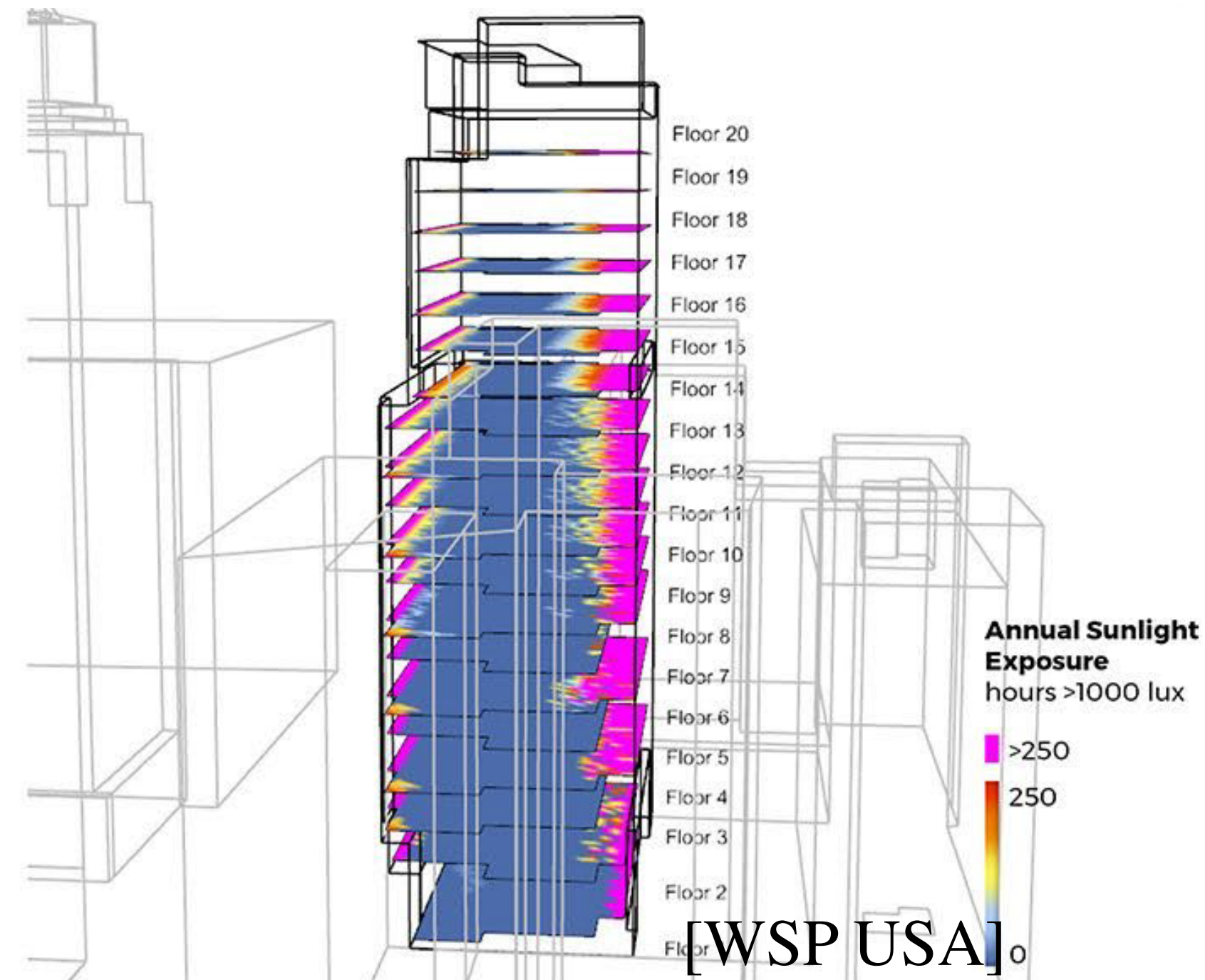
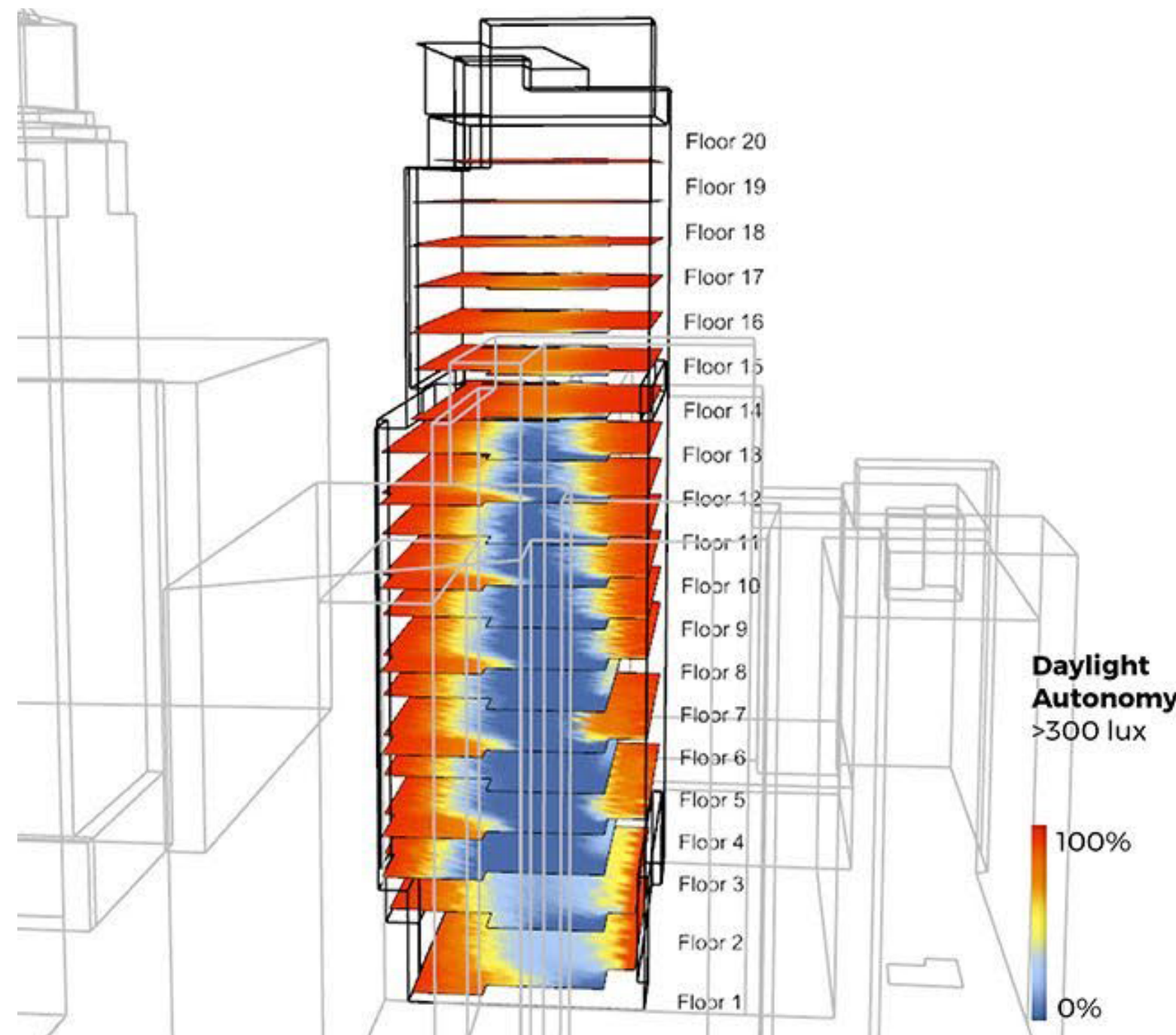


H2MC
[Li et al. 2015]



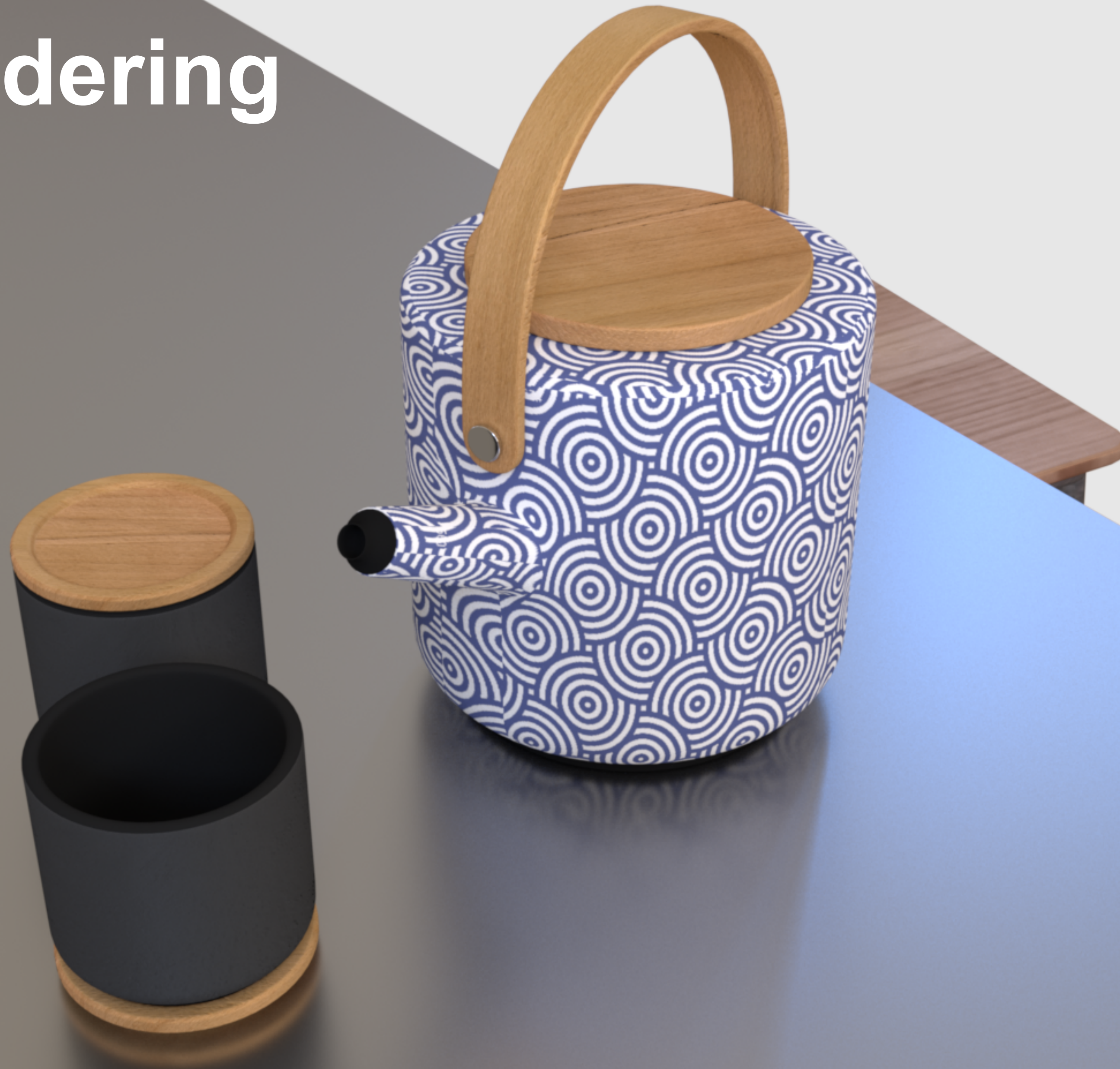
Langevin MC
[Luan et al. 2020]

- Many disciplines rely on understanding or controlling the behavior of light in images or other kinds of measurements.



[Solar Carve Tower - Studio Gang]

Target rendering



OBJECTIVE FUNCTION (A.K.A. "LOSS")

$$g\left(\text{img}\right) = \left\| \left[\text{img}_{\text{Rendering}} - \text{img}_{\text{Target}} \right] \right\|_2^2$$

The equation shows the objective function g applied to an image. The image is the difference between a rendered image and a target image. The rendered image shows a teapot and a cup on a table, both in a dark grey color. The target image shows the same scene, but the teapot and cup are light blue with a white pattern. The difference image is the result of subtracting the target from the rendering, showing the dark grey areas where the rendering differs from the target.

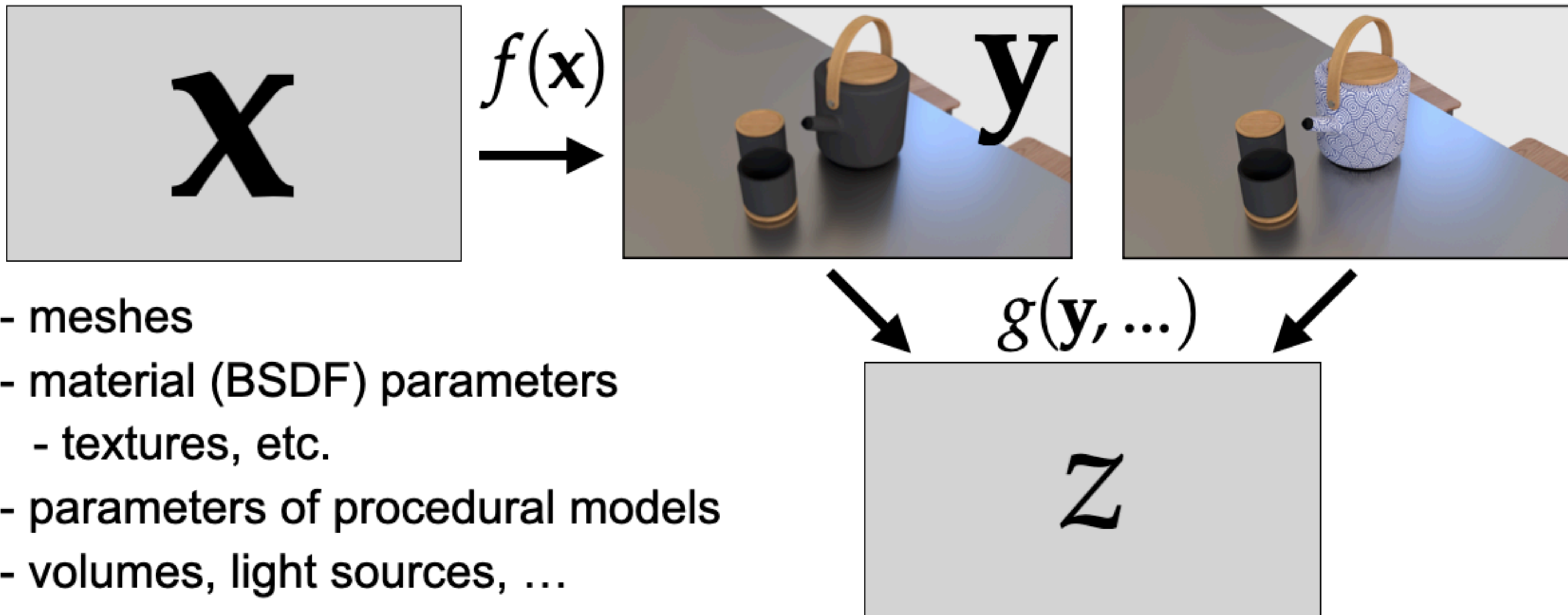
The problem: minimize $g(f(\mathbf{x}))$

$\mathbf{x} \in \mathcal{X}$

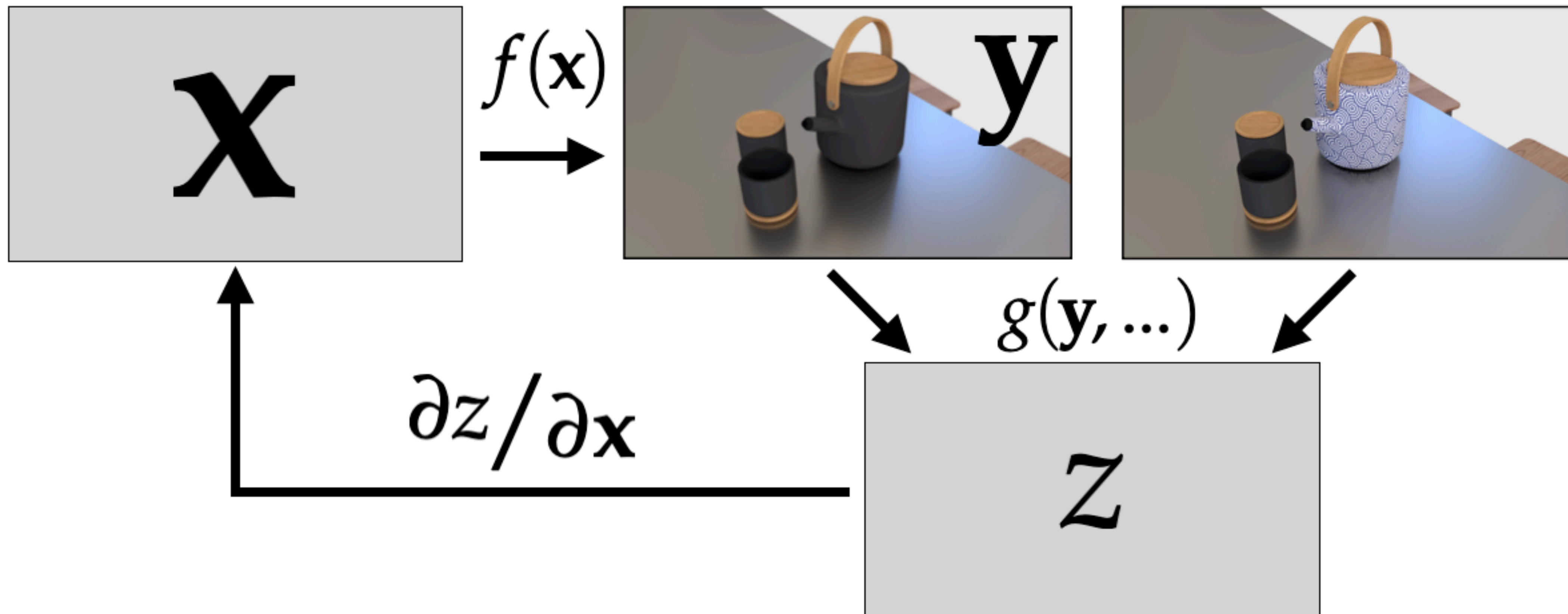
Objective \nearrow g \nwarrow Rendering algorithm

Scene parameters \nearrow f

The problem: minimize $g(f(\mathbf{x}))$
 $\mathbf{x} \in \mathcal{X}$



The problem: minimize $g(f(\mathbf{x}))$
 $\mathbf{x} \in \mathcal{X}$



DIFFERENTIABLE RENDERING

Vector

$$\frac{\partial z}{\partial x} = \frac{\partial z}{\partial y} \cdot \frac{\partial y}{\partial x}$$

Matrix

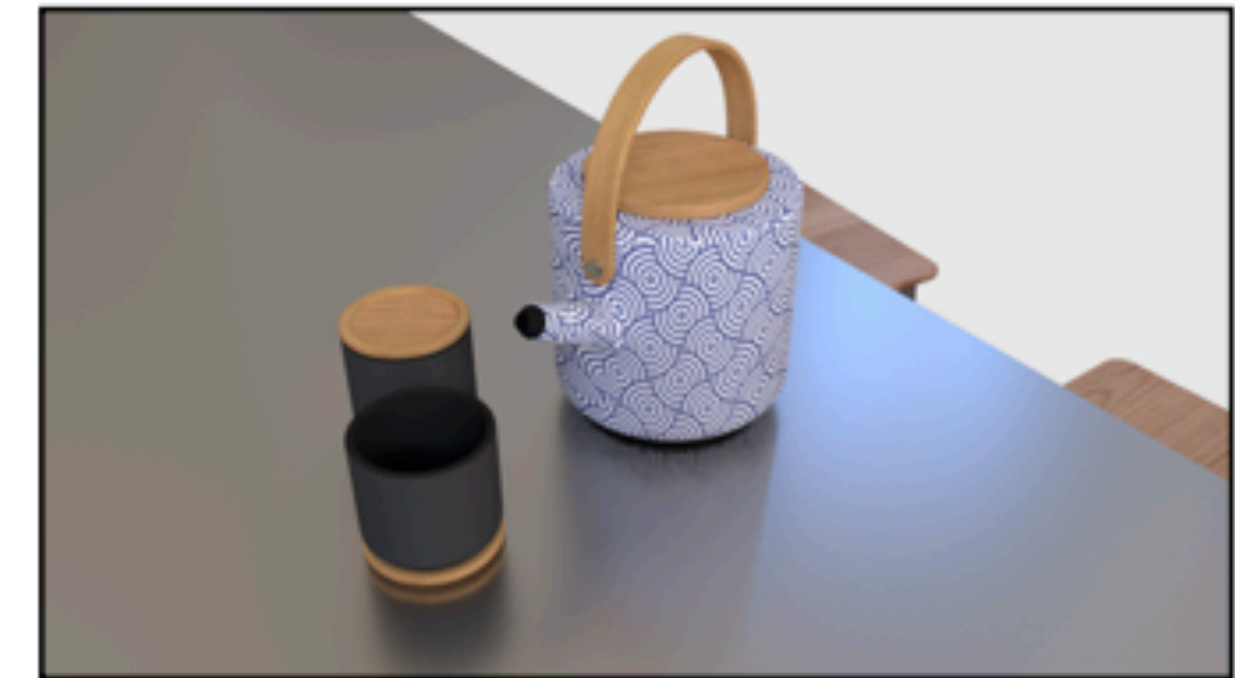
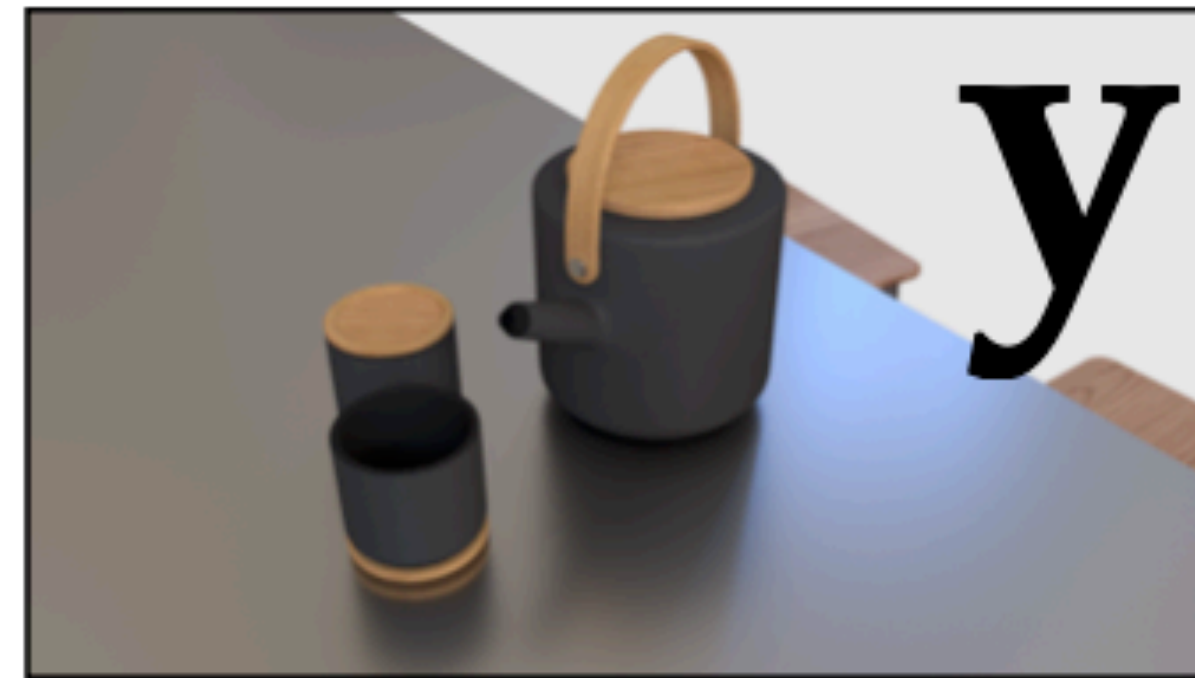
CHAIN RULE

x

$f(\mathbf{x})$



y



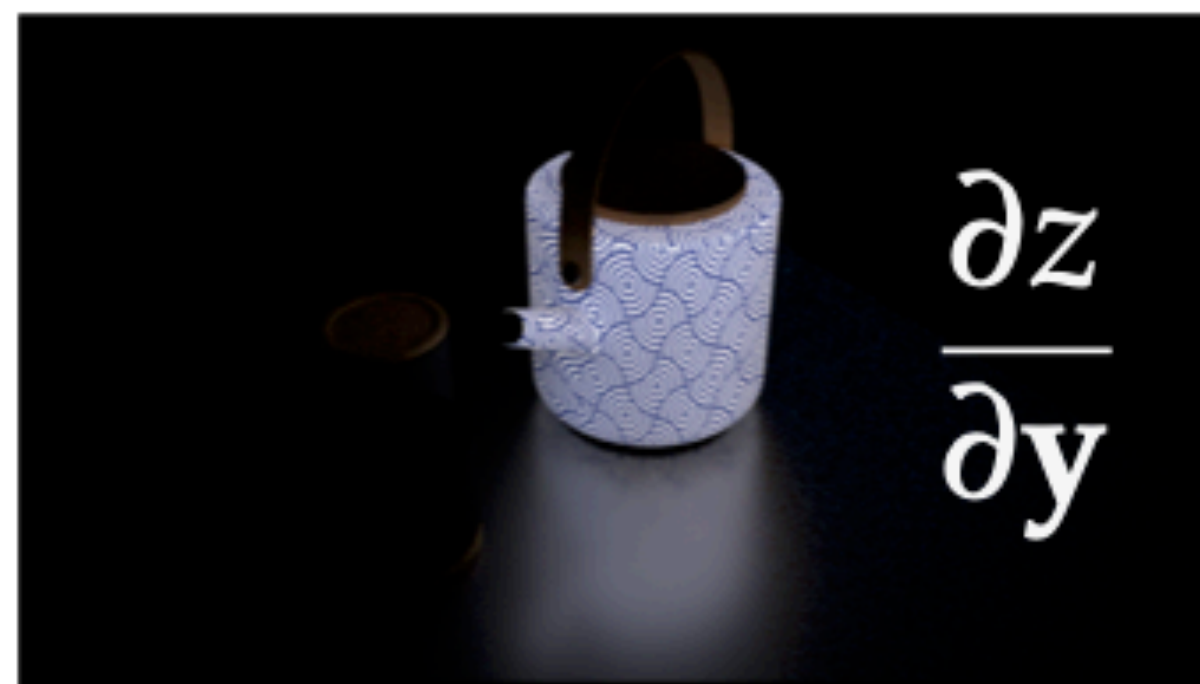
$g(\mathbf{y}, \dots)$



z

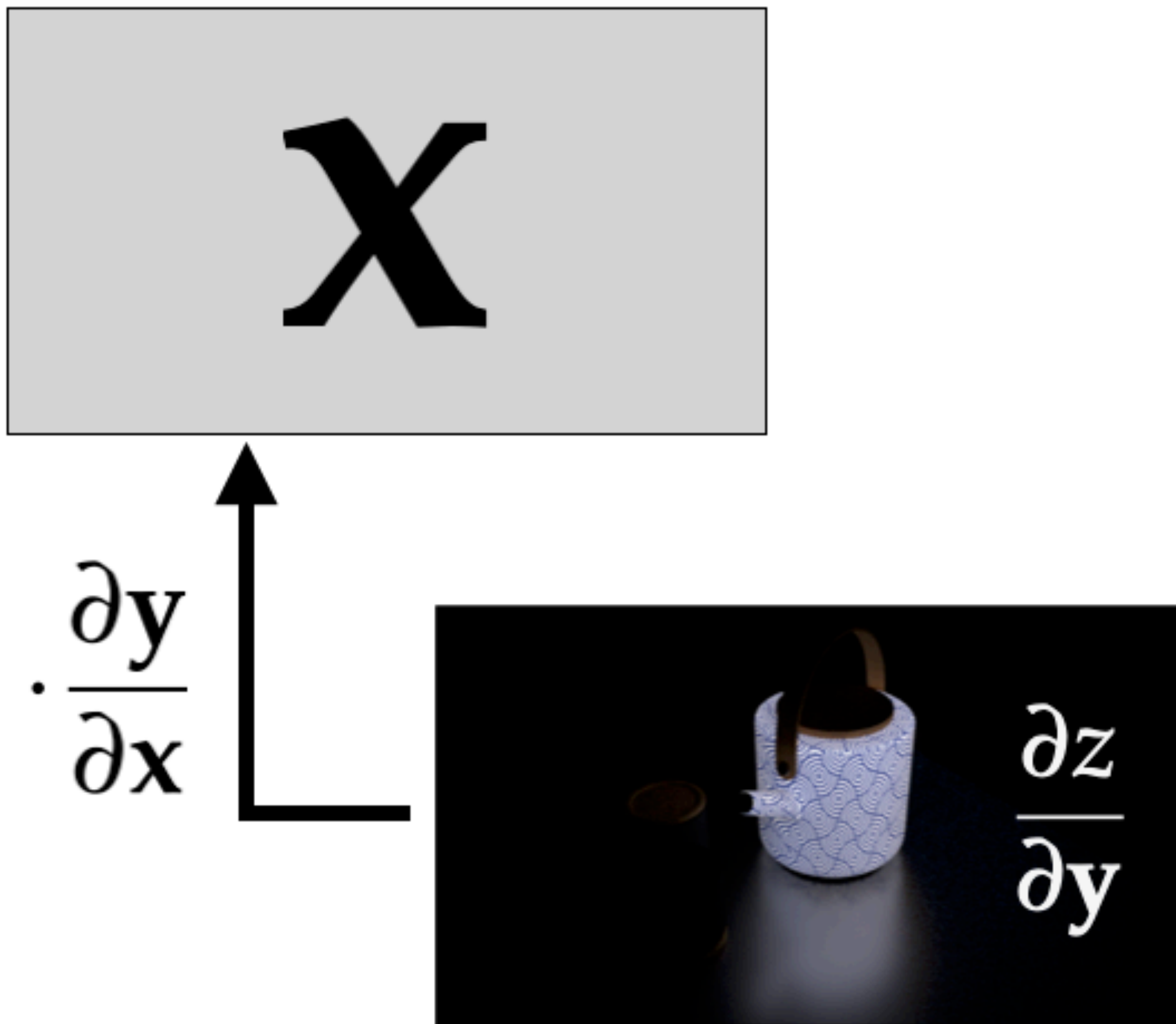


$\frac{\partial y}{\partial x}$



$\frac{\partial z}{\partial y}$

$$\frac{\partial z}{\partial x} = \frac{\partial z}{\partial y} \cdot \frac{\partial y}{\partial x}$$



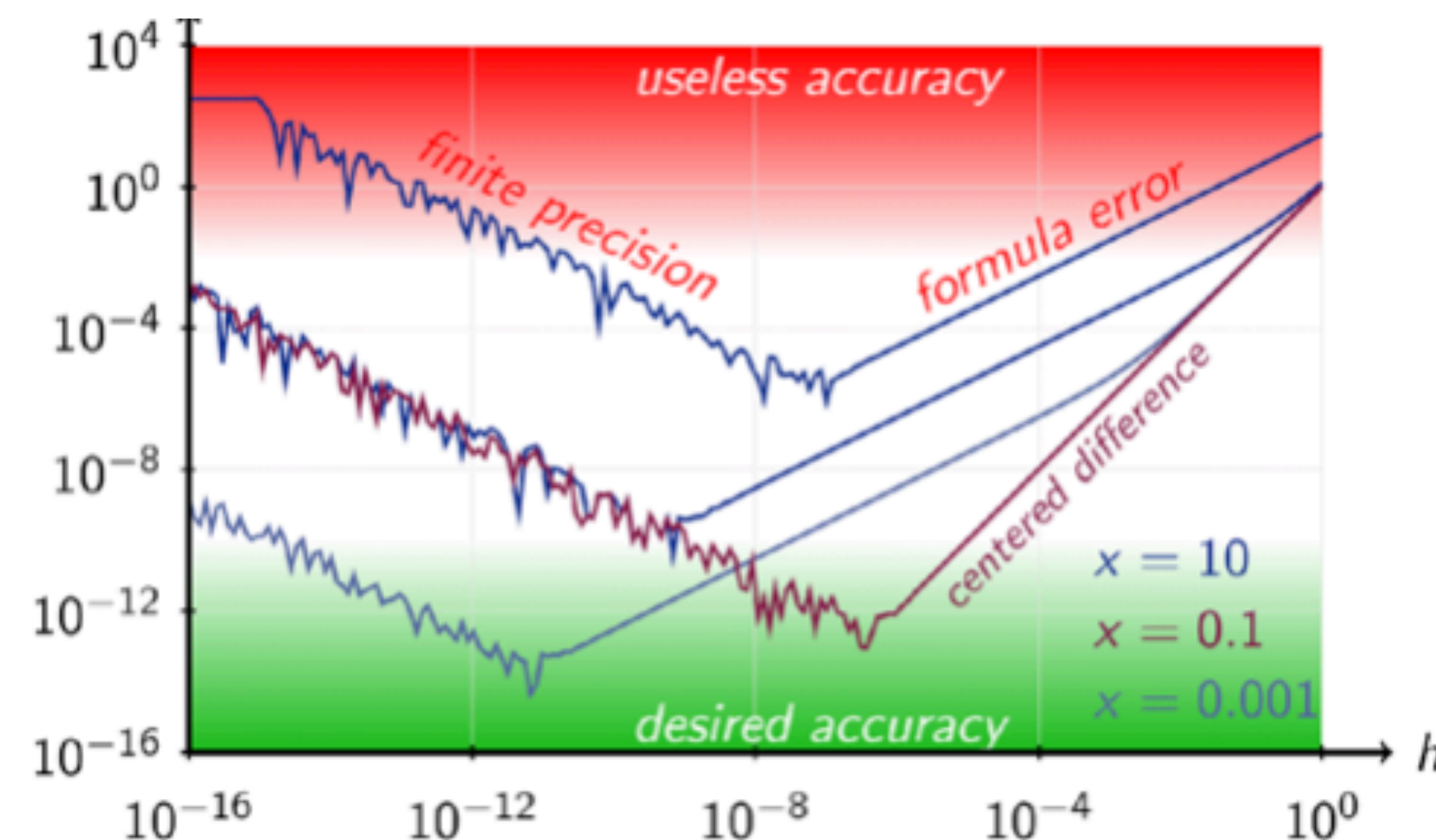
Challenges

1. Differentiating f
2. Matrix multiplication
3. Efficiency?
4. How to deal with edges?

HOW TO DO THIS (AT ALL?)

Use finite differences!

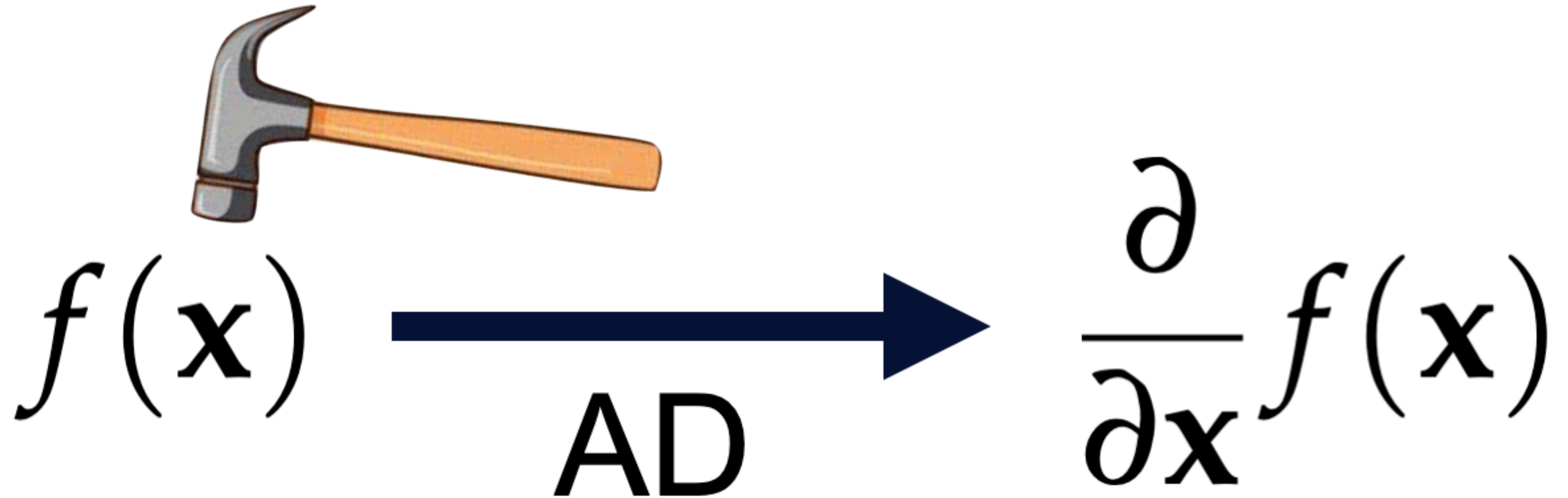
$$\frac{\partial \mathbf{y}}{\partial x_i} = \frac{f(\mathbf{x} + \varepsilon \mathbf{e}_i) - f(\mathbf{x} - \varepsilon \mathbf{e}_i)}{2\varepsilon}$$



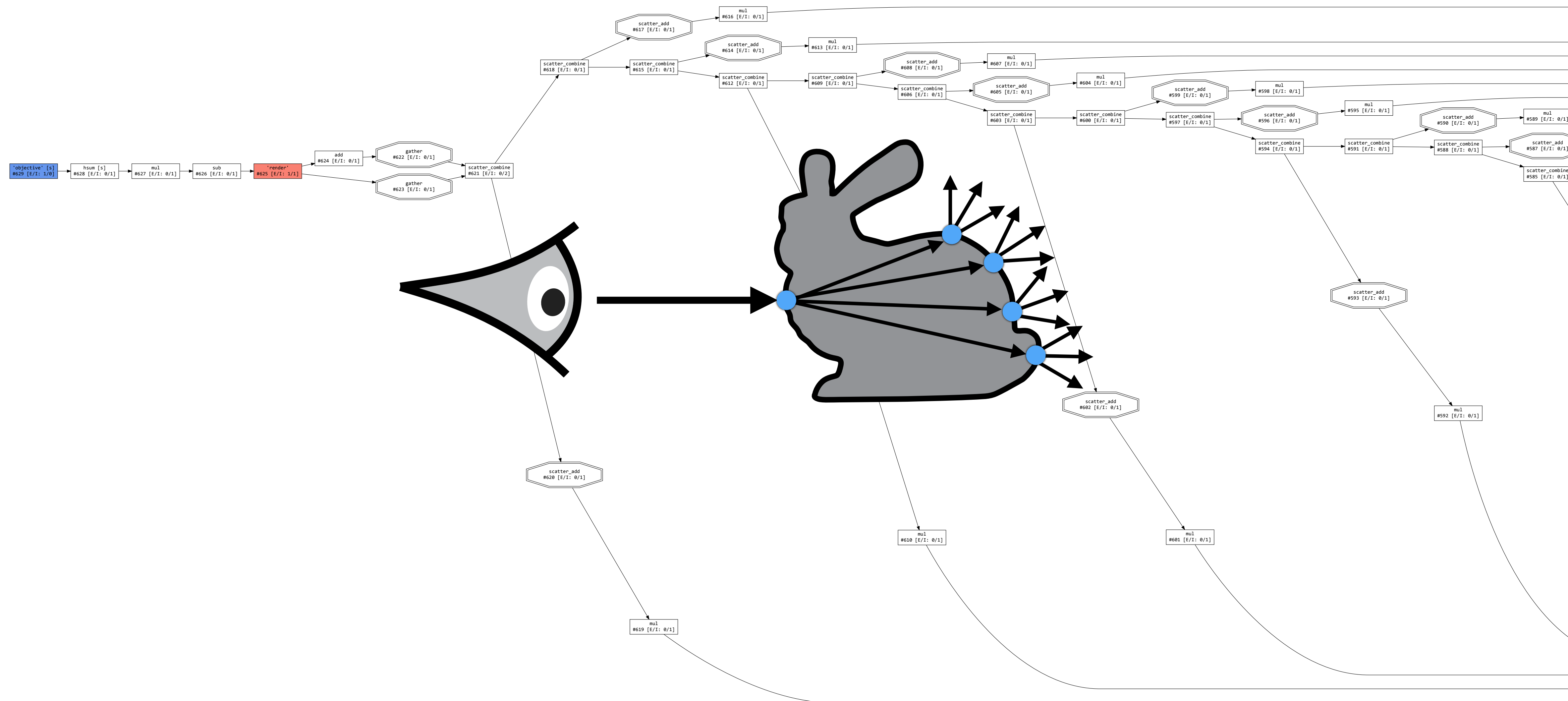
[Wikipedia]

Potential problems:

- Bad approximation (big ε), rounding error (small ε)
- Need to correlate Monte Carlo samples
- Extremely slow when many there are many parameters.



ISSUES WITH AUTOMATIC DIFFERENTIATION (AD)



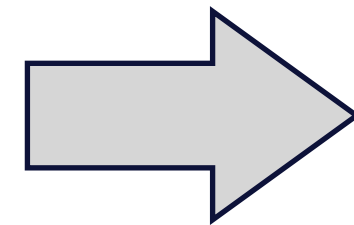
- Precautions must be taken to ensure **correctness**
 - Symbolically differentiating a Monte Carlo estimator path tracer does not always work!

- **Example 1:** Distributional parameters

Estimate $\int_0^\infty f(\lambda, x) dx$ (with λ given)

(Single-sample) Monte Carlo estimator:

- Draw $x \sim \text{Exp}[\lambda]$
- $f \leftarrow f(\lambda, x)$
- $p \leftarrow \lambda e^{-\lambda x}$ # This is the pdf of $\text{Exp}[\lambda]$
- Return f/p



Estimate $\frac{d}{d\lambda} \int_0^\infty f(\lambda, x) dx = \int_0^\infty \frac{\partial f}{\partial \lambda}(\lambda, x) dx$

(Single-sample) Monte Carlo estimator:

- Draw $x \sim \text{Exp}[\lambda]$ x has zero gradient
- $f' \leftarrow \frac{\partial f}{\partial \lambda}(\lambda, x)$
- $p \leftarrow \lambda e^{-\lambda x}$ p is NOT differentiated
- Return f'/p

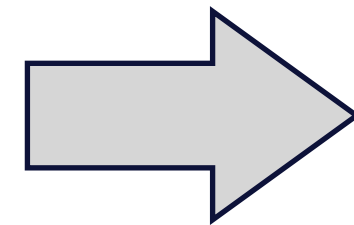
- Precautions must be taken to ensure **correctness**
 - Symbolically differentiating a Monte Carlo estimator path tracer does not always work!

- **Example 1:** Distributional parameters, with $\xi = e^{-\lambda x}$

$$\text{Estimate } \int_0^{\infty} f(\lambda, x) dx = \int_0^1 \frac{f(\lambda, x)}{\lambda \xi} d\xi$$

(Single-sample) Monte Carlo estimator:

- Draw $\xi \sim U[0,1)$
- $x \leftarrow -\log(\xi)/\lambda$ # $x \sim \text{Exp}(\lambda)$
- $f \leftarrow f(\lambda, x)$
- $p \leftarrow \lambda e^{-\lambda x}$ # $p = \lambda \xi$
- Return f/p



$$\text{Estimate } \frac{d}{d\lambda} \int_0^{\infty} f(\lambda, x) dx = \int_0^1 \frac{\partial}{\partial \lambda} \frac{f(\lambda, x)}{\lambda \xi} d\xi$$

(Single-sample) Monte Carlo estimator:

- Draw $\xi \sim U[0,1)$
- $x \leftarrow -\log(\xi)/\lambda$ x has nonzero gradient
- $f \leftarrow f(\lambda, x)$
- $p \leftarrow \lambda e^{-\lambda x}$ # $p = \lambda \xi$
- Return $\partial(f/p)/\partial \lambda$ f and p are both differentiated

- Precautions must be taken to ensure **correctness**
 - Symbolically differentiating a Monte Carlo estimator path tracer does not always work!

- **Example 1:** Distributional parameters

$$\text{Estimate } \frac{d}{d\lambda} \int_0^\infty f(\lambda, x) dx = \int_0^\infty \frac{\partial f}{\partial \lambda}(\lambda, x) dx$$

(Single-sample) Monte Carlo estimator:

- Draw $x \sim \text{Exp}[\lambda]$ x has zero gradient
- $f' \leftarrow \frac{\partial f}{\partial \lambda}(\lambda, x)$
- $p \leftarrow \lambda e^{-\lambda x}$ p is NOT differentiated
- Return f'/p

Whether to differentiate the *sampling* and the *pdf* should be **consistent!**

$$\text{Estimate } \frac{d}{d\lambda} \int_0^\infty f(\lambda, x) dx = \int_0^1 \frac{\partial}{\partial \lambda} \frac{f(\lambda, x)}{\lambda \xi} d\xi$$

(Single-sample) Monte Carlo estimator:

- Draw $\xi \sim U[0,1)$
- $x \leftarrow -\log(\xi)/\lambda$ x has nonzero gradient
- $f \leftarrow f(\lambda, x)$
- $p \leftarrow \lambda e^{-\lambda x}$ # $p = \lambda \xi$
- Return $\frac{\partial(f/p)}{\partial \lambda}$ f and p are both differentiated

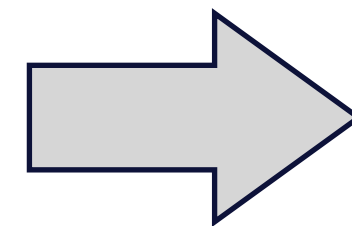
- Precautions must be taken to ensure **correctness**
 - Symbolically differentiating a Monte Carlo estimator path tracer does not always work!

- **Example 2: Discontinuities**

Estimate $\int_0^1 (x < p ? 1 : 0.5) dx$ with $0 < p < 1$

(Single-sample) Monte Carlo estimator:

- Draw $X \sim U[0, 1)$
- Return $X < p ? 1 : 0.5$



Estimate $\frac{d}{dp} \int_0^1 (x < p ? 1 : 0.5) dx$ with $0 < p < 1$

(Single-sample) Monte Carlo estimator:

- Draw $X \sim U[0, 1)$
- Return $d(X < p ? 1 : 0.5)/dp$ **Zero! (constant)**

Ground-truth:

$$\int_0^1 (x < p ? 1 : 0.5) dx = \int_0^p dx + \int_p^1 0.5 dx = \frac{1+p}{2}$$

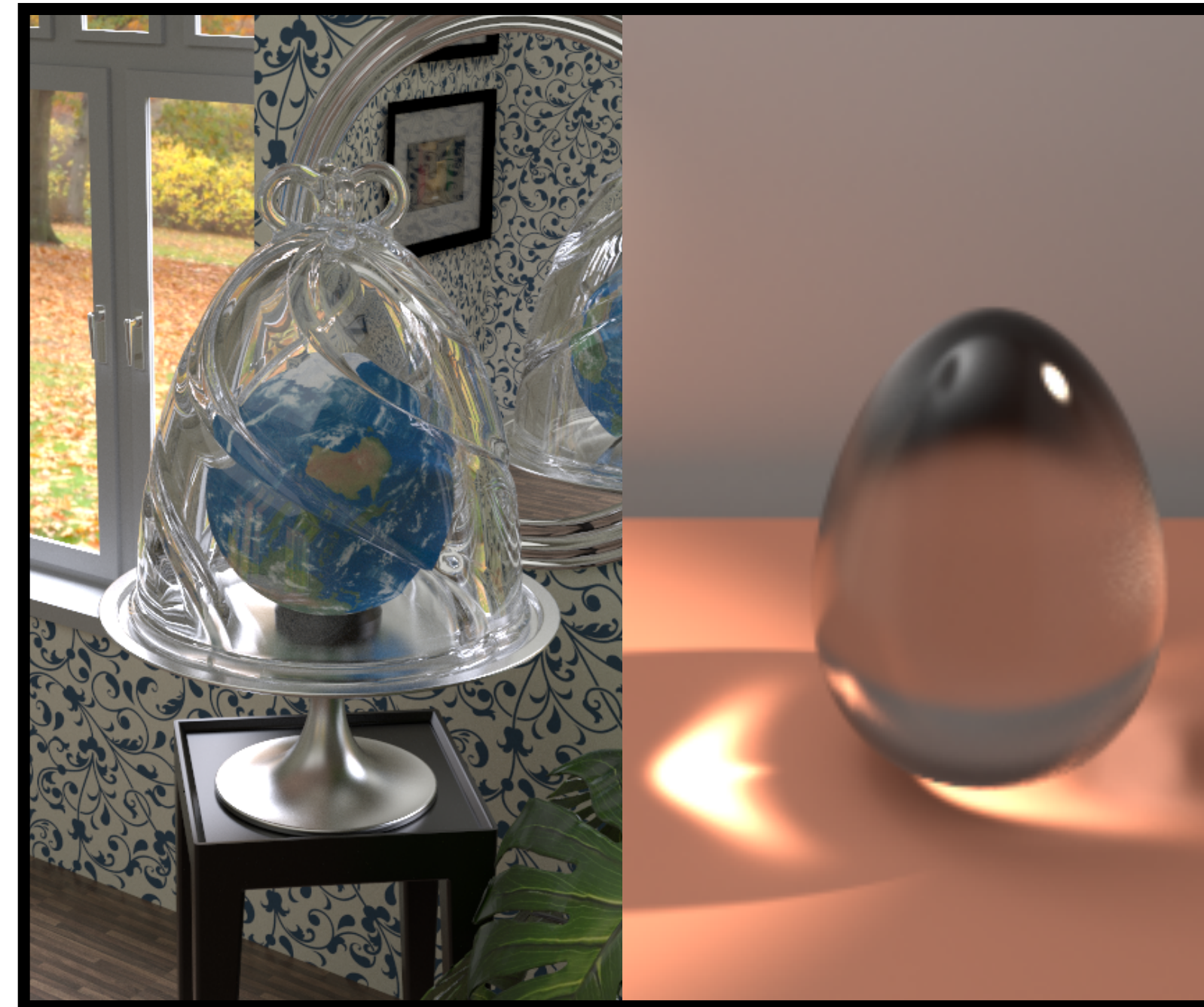
Ground-truth:

$$\frac{d}{dp} \int_0^1 (x < p ? 1 : 0.5) dx = \frac{d}{dp} \frac{1+p}{2} = \frac{1}{2}$$

More on this example later



Basics



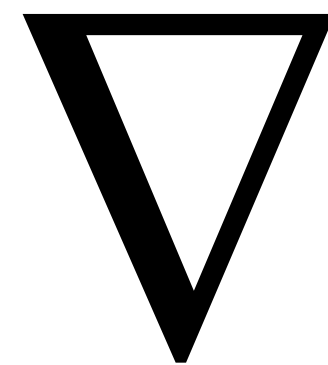
State-of-the-art theories
and algorithms



Implementation
details

BASICS

- a crash course on automatic differentiation
- differentiating discontinuities in rendering
- discussions & limitations



```
auto scatter_contrib = Vector3{0, 0, 0};
auto scatter_bsdf = Vector3{0, 0, 0};
if (bsdf_isect.valid()) {
    const auto &bsdf_shape = scene.shapes[bsdf_isect.shape_id];
    auto dir = bsdf_point.position - p;
    auto dist_sq = length_squared(dir);
    auto wo = dir / sqrt(dist_sq);
    auto pdf_bsdf = bsdf_pdf(material, shading_point, wi, wo, min_rough);
    if (dist_sq > 1e-20f && pdf_bsdf > 1e-20f) {
        auto bsdf_val = bsdf(material, shading_point, wi, wo, min_rough);
        if (bsdf_shape.light_id >= 0) {
            const auto &light = scene.area_lights[bsdf_shape.light_id];
            if (light.two_sided || dot(-wo, bsdf_point.shading_frame.n) > 0) {
                auto light_contrib = light.intensity;
                auto light_pmf = scene.light_pmf[bsdf_shape.light_id];
                auto light_area = scene.light_areas[bsdf_shape.light_id];
                auto inv_area = 1 / light_area;
                auto geometry_term = fabs(dot(wo, bsdf_point.geom_normal));
                auto pdf_nee = (light_pmf * inv_area) / geometry_term;
                auto mis_weight = Real(1 / (1 + square((double)pdf_nee / pdf_bsdf)));
                scatter_contrib = (mis_weight / pdf_bsdf) * bsdf_val * light_contrib;
            }
        }
    }
    scatter_bsdf = bsdf_val / pdf_bsdf;
    next_throughput = throughput * scatter_bsdf;
}
```



- automatic differentiation v.s. symbolic differentiation

```
function f(x):  
    result = x  
    for i = 1 to 8:  
        result = exp(result)  
    return result
```


- automatic differentiation v.s. symbolic differentiation

symbolic differentiation (37 exponents):

$$\frac{df(x)}{dx} = e^{x+e^{e^{e^{e^{e^{e^{e^x}}}}}}}} + e^{e^{e^{e^{e^{e^{e^x}}}}} + e^{e^{e^{e^{e^{e^x}}}}} + e^{e^{e^{e^{e^x}}} + e^{e^{e^{e^x}}} + e^{e^{e^x}} + e^{e^x} + e^x$$

```
function f(x):
    result = x
    for i = 1 to 8:
        result = exp(result)
    return result
```


- automatic differentiation v.s. symbolic differentiation

symbolic differentiation (37 exponents):

$$\frac{df(x)}{dx} = e^{x+e^{e^{e^{e^{e^{e^{e^x}}}}}}}} + e^{e^{e^{e^{e^{e^x}}}}} + e^{e^{e^{e^{e^x}}} + e^{e^{e^{e^x}}} + e^{e^{e^x}} + e^{e^x} + e^x$$

```
function f(x):
    result = x
    for i = 1 to 8:
        result = exp(result)
    return result
```

forward-mode automatic differentiation (8 exponents):

```
function d_f(x):
    result = x
    d_result = 1
    for i = 1 to 8:
        result = exp(result)
        d_result = d_result * result
    return d_result
```


- key idea: chain rules, but applied in a smart way

$$y = f(x)$$

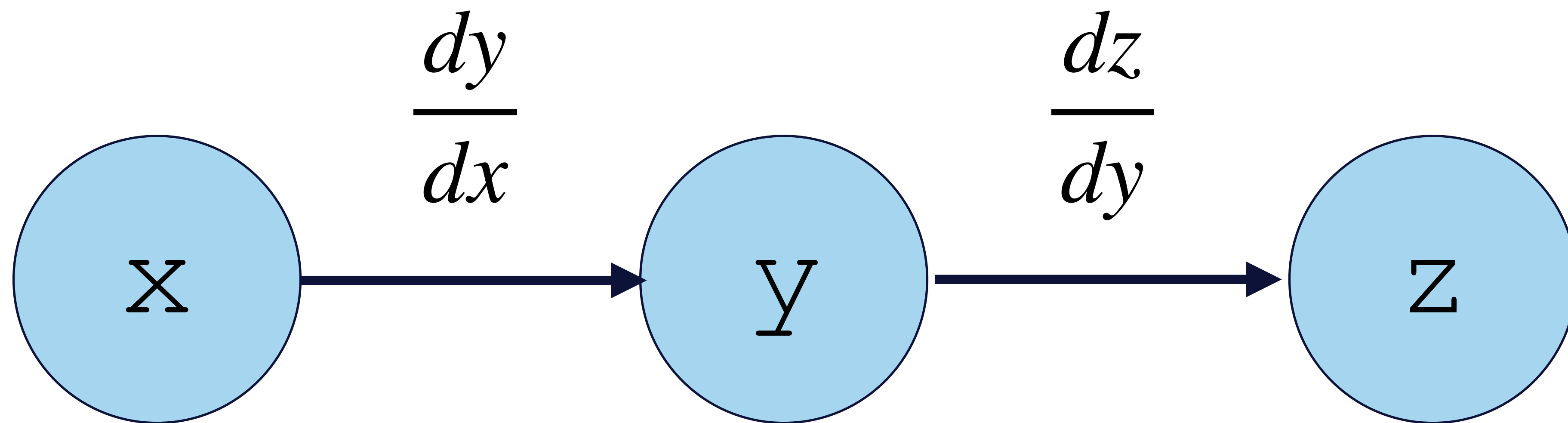
$$z = g(y)$$

- key idea: chain rules, but applied in a smart way

$$\begin{array}{l} y = f(x) \\ z = g(y) \end{array} \quad \frac{dz}{dx} = \frac{dz}{dy} \frac{dy}{dx}$$

$$y = f(x)$$

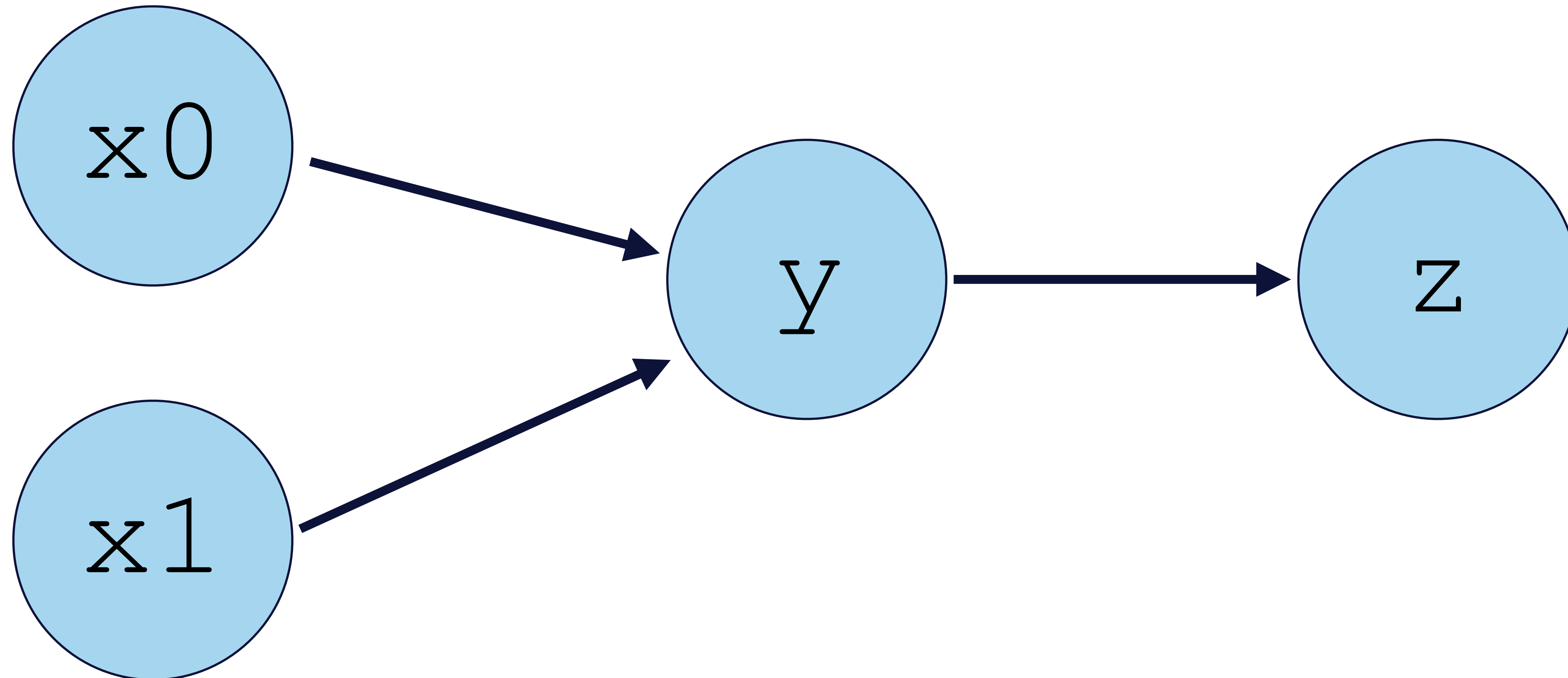
$$z = g(y)$$



MULTIVARIATE EXAMPLE

$$y = f(x_0, x_1)$$

$$z = g(y)$$

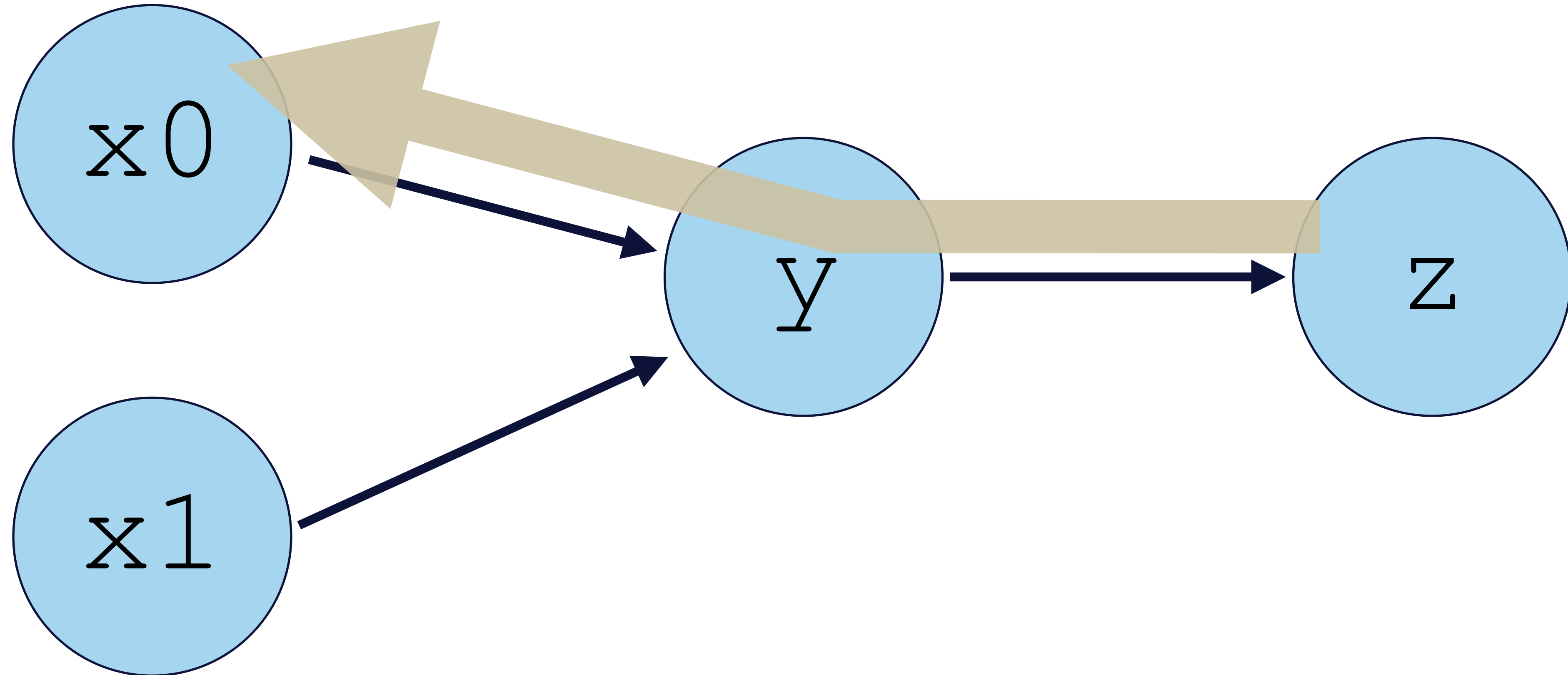


MULTIVARIATE EXAMPLE

$$y = f(x_0, x_1)$$

$$z = g(y)$$

$$\frac{\partial z}{\partial x_0} = \frac{\partial z}{\partial y} \frac{\partial y}{\partial x_0}$$



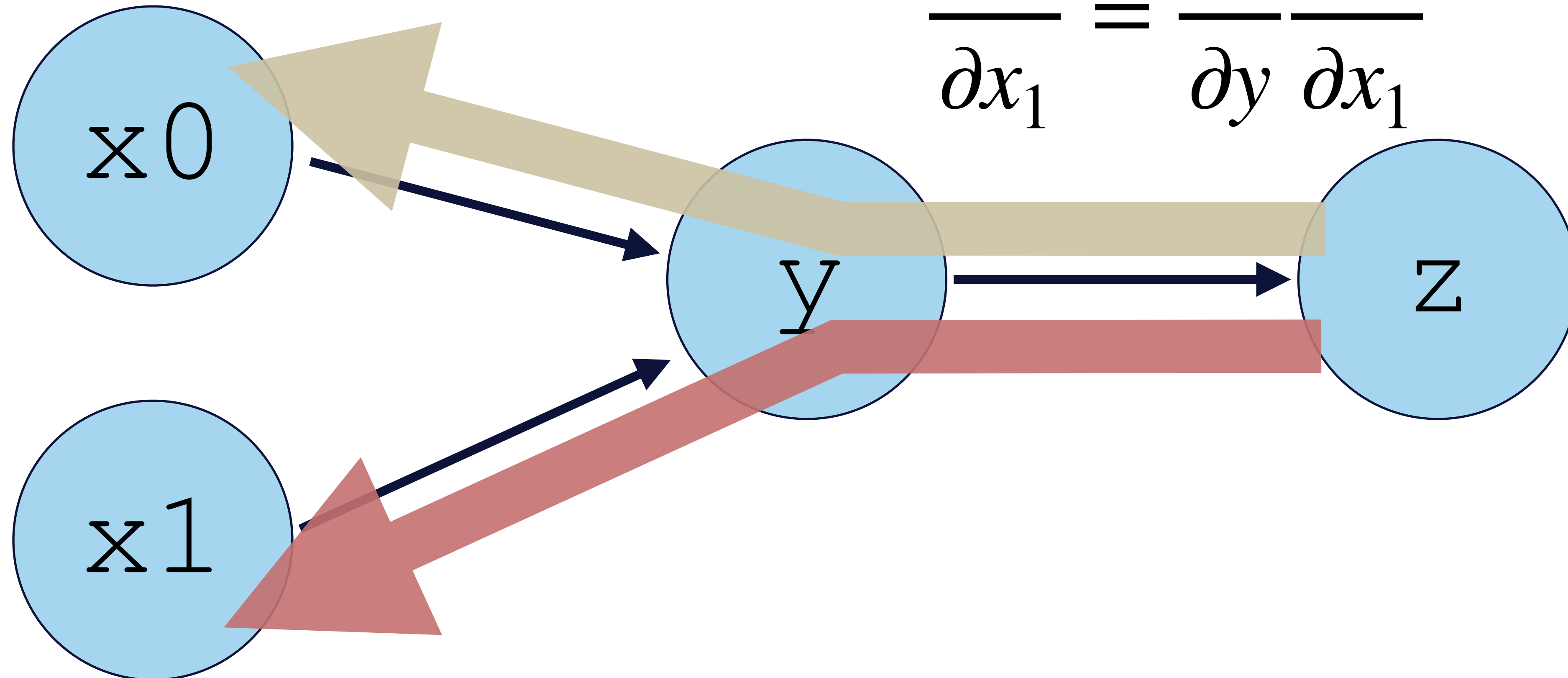
MULTIVARIATE EXAMPLE

$$y = f(x_0, x_1)$$

$$z = g(y)$$

$$\frac{\partial z}{\partial x_0} = \frac{\partial z}{\partial y} \frac{\partial y}{\partial x_0}$$

$$\frac{\partial z}{\partial x_1} = \frac{\partial z}{\partial y} \frac{\partial y}{\partial x_1}$$



MULTIVARIATE EXAMPLE

$$y = f(x_0, x_1)$$

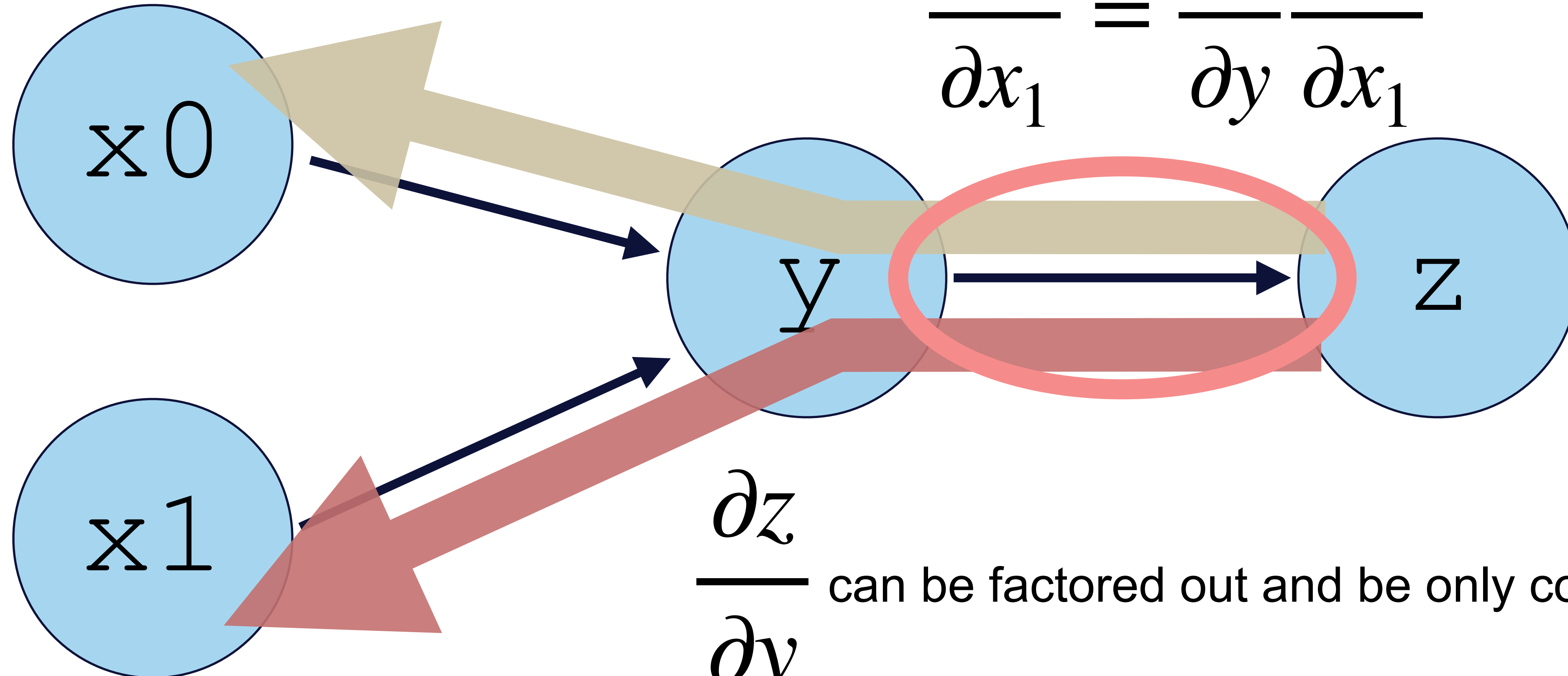
$$z = g(y)$$

$$\frac{\partial z}{\partial x_0} = \frac{\partial z}{\partial y} \frac{\partial y}{\partial x_0}$$

$$\frac{\partial z}{\partial x_1} = \frac{\partial z}{\partial y} \frac{\partial y}{\partial x_1}$$

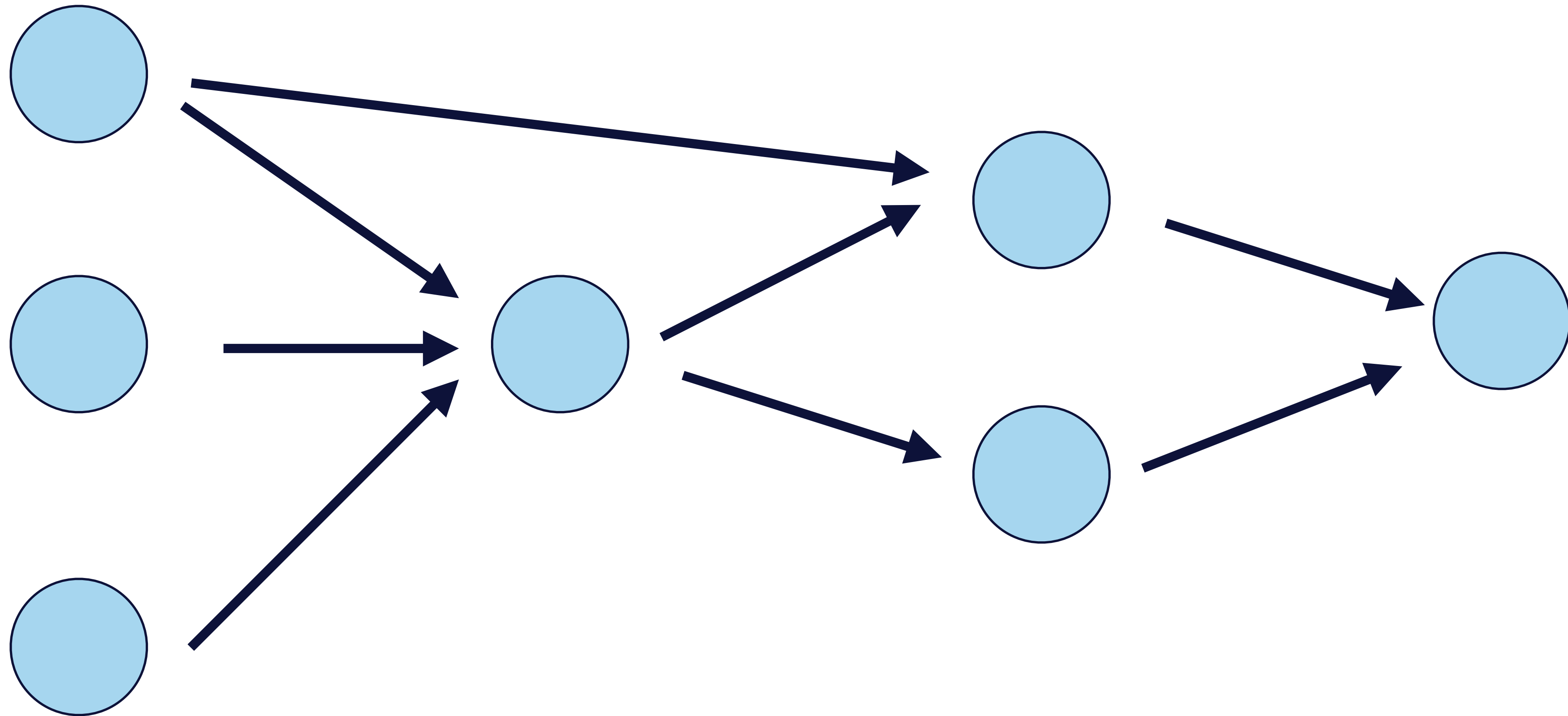
$$\frac{\partial z}{\partial x_0} = \frac{\partial z}{\partial y} \frac{\partial y}{\partial x_0}$$

$$\frac{\partial z}{\partial x_1} = \frac{\partial z}{\partial y} \frac{\partial y}{\partial x_1}$$

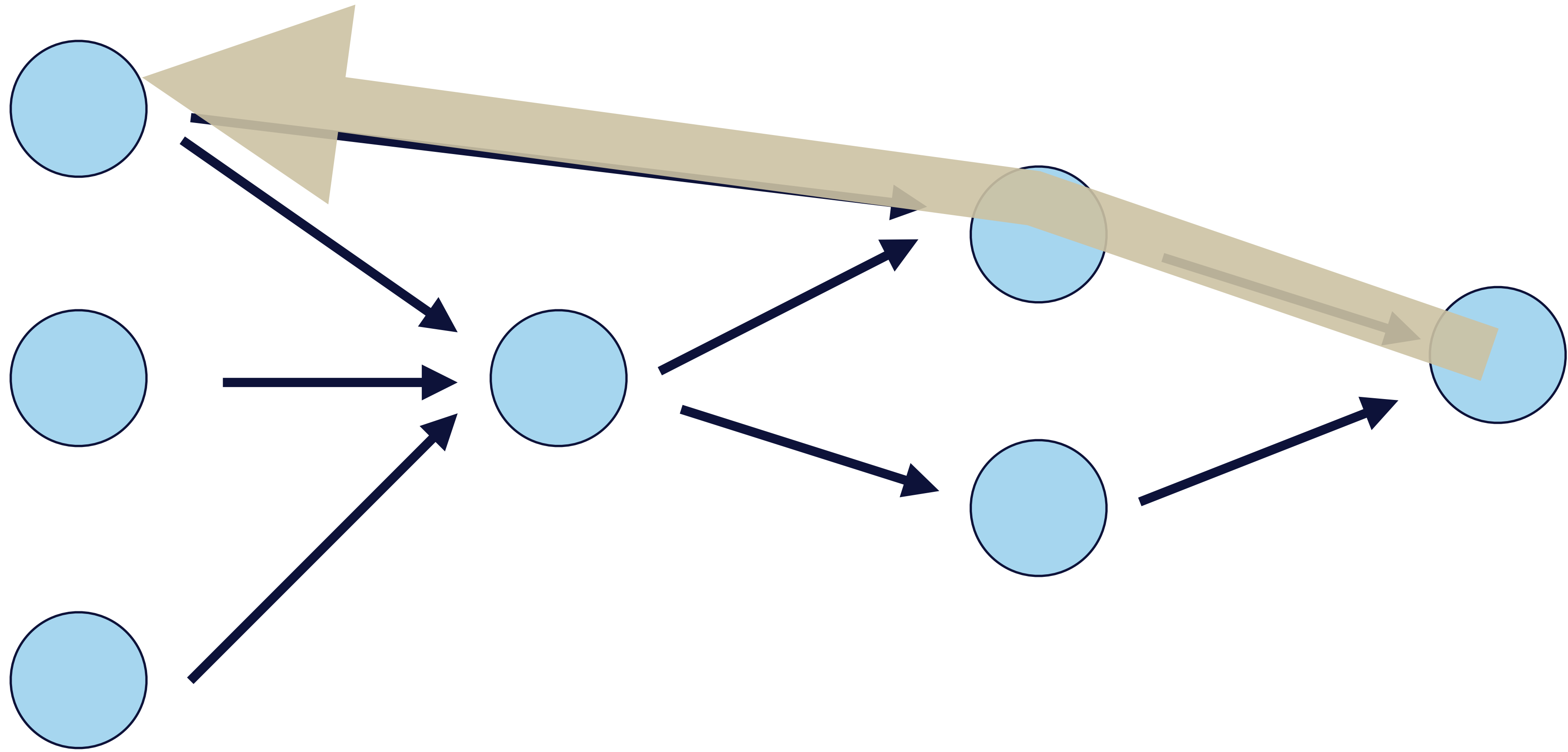


$\frac{\partial z}{\partial y}$ can be factored out and be only computed once!

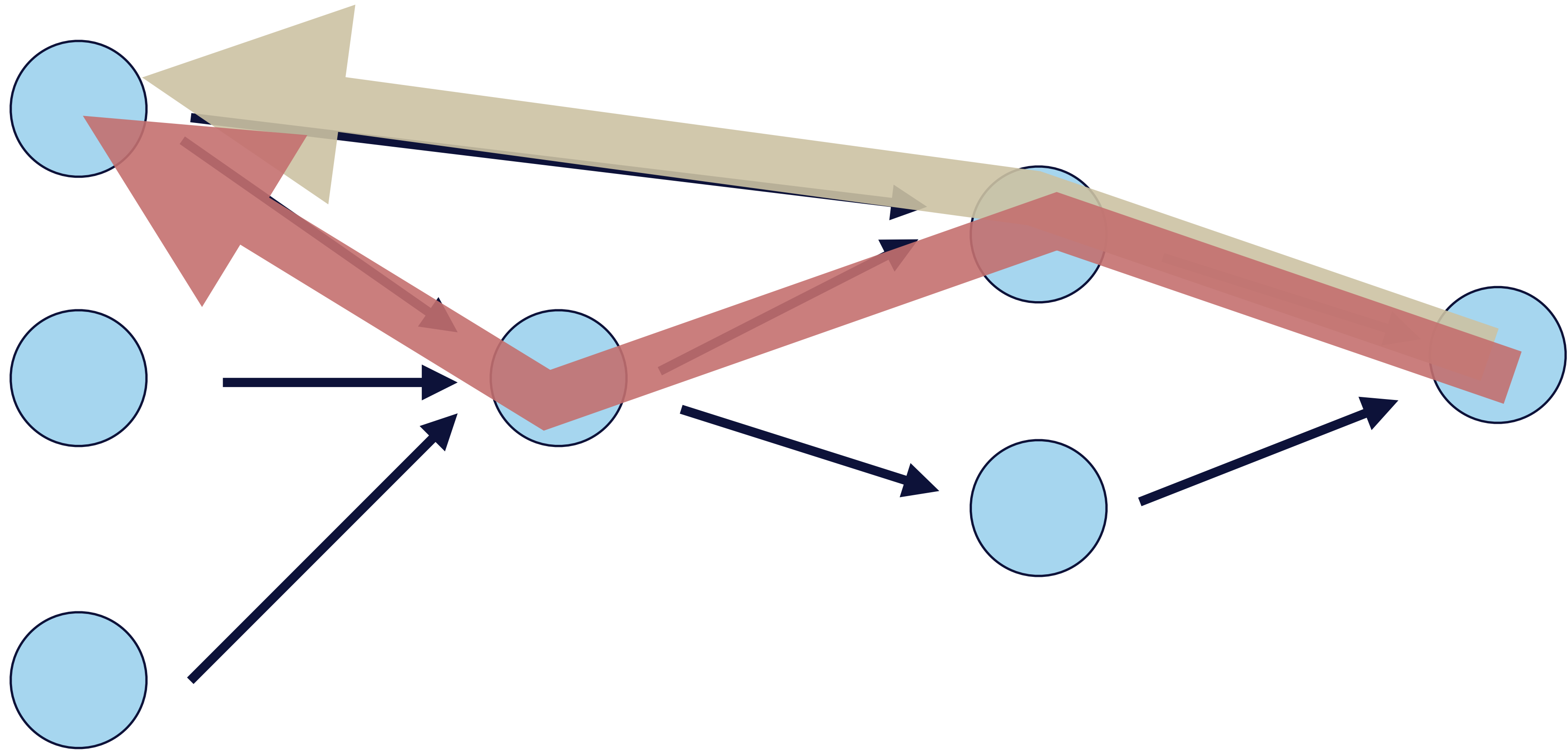
AUTODIFF = A PATH FINDING PROBLEM



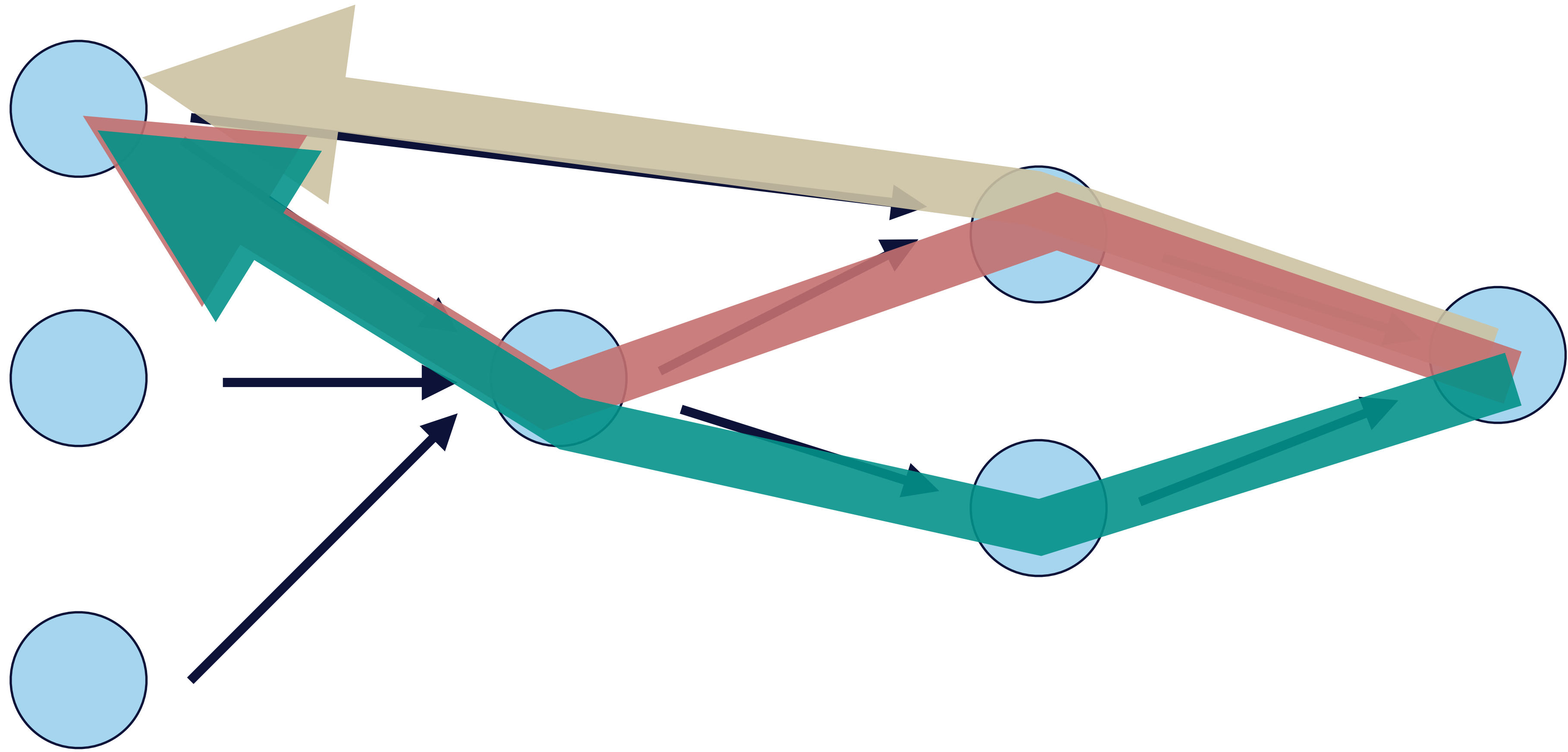
AUTODIFF = A PATH FINDING PROBLEM



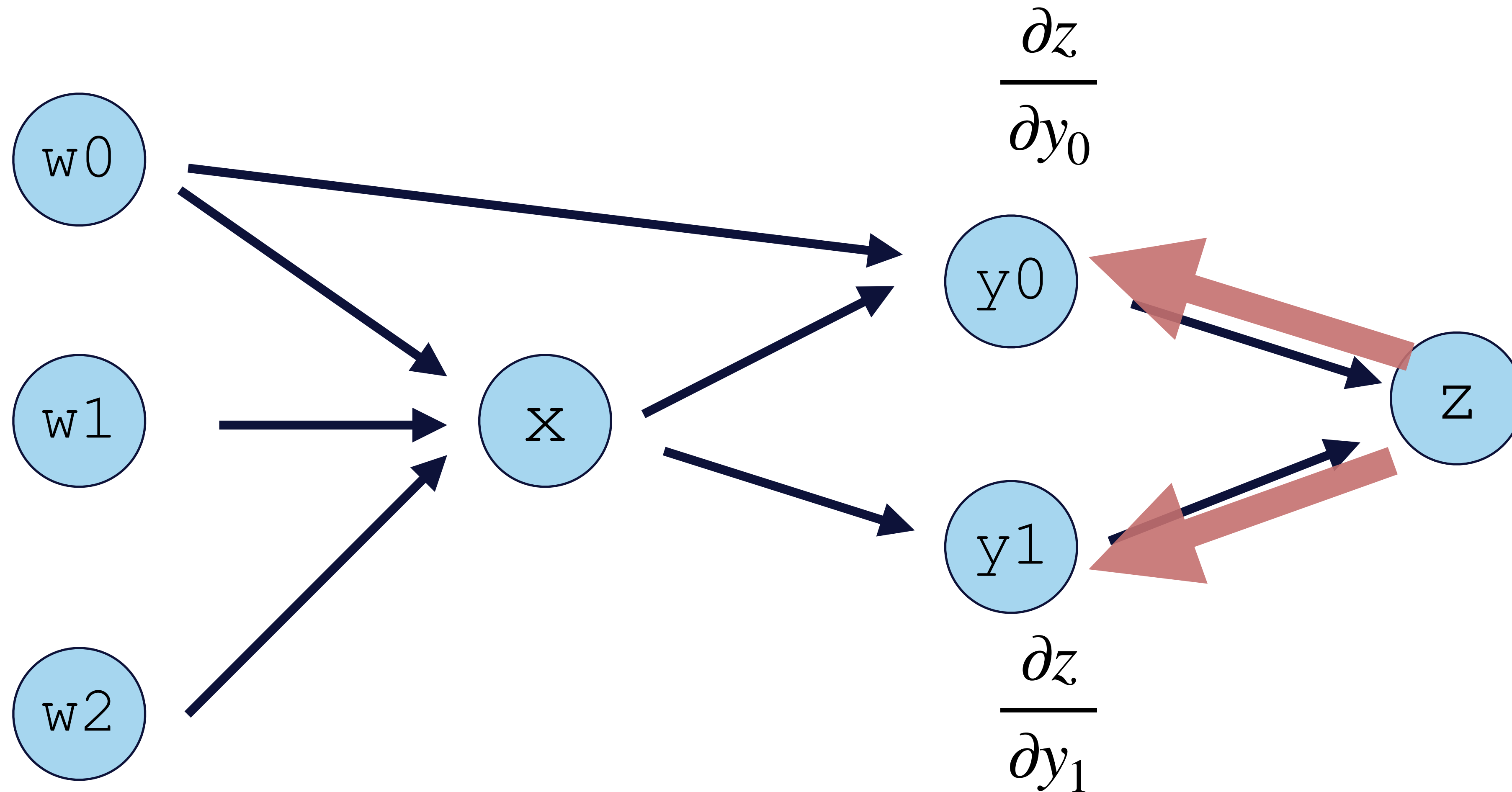
AUTODIFF = A PATH FINDING PROBLEM



AUTODIFF = A PATH FINDING PROBLEM

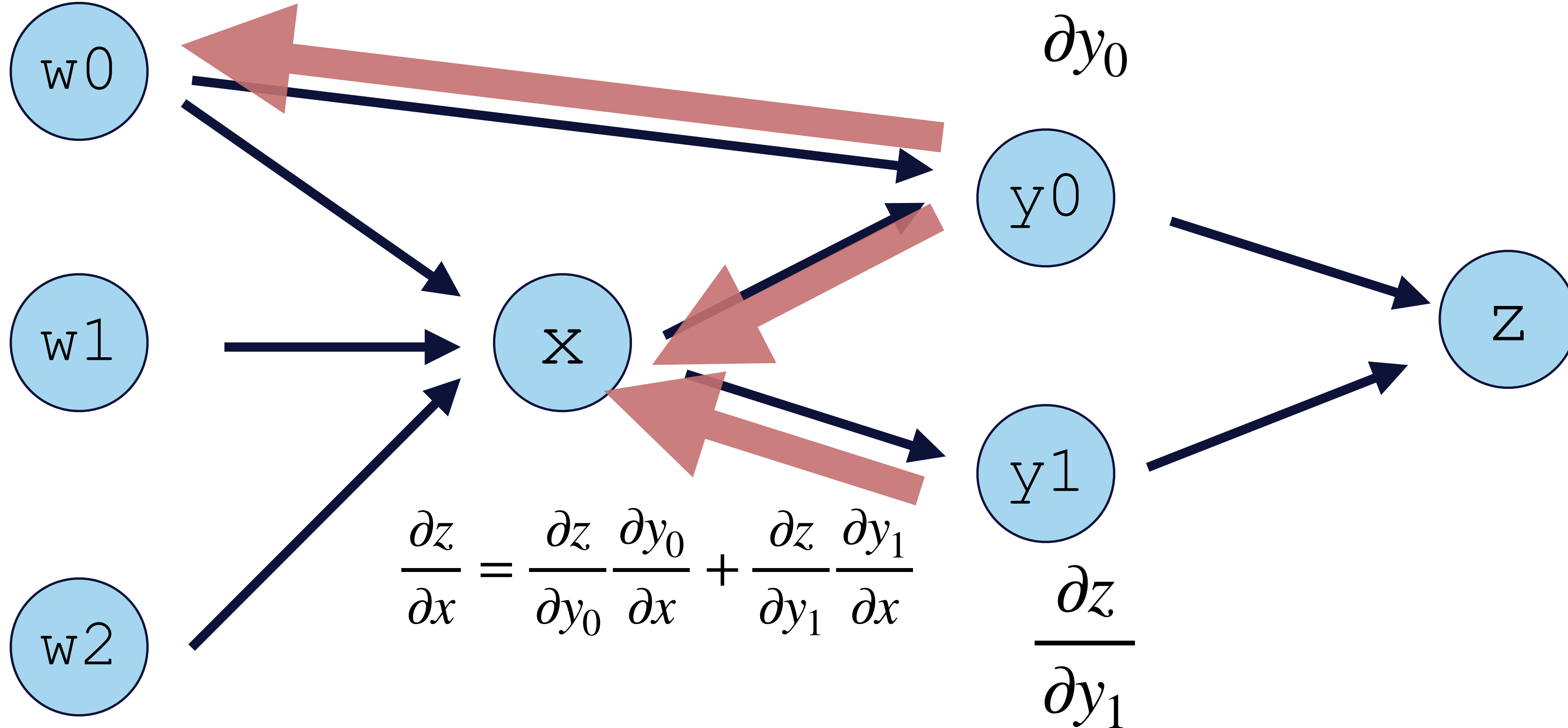


REVERSE-MODE AUTOMATIC DIFFERENTIATION = A GREEDY PATH FACTORIZATION ALGORITHM



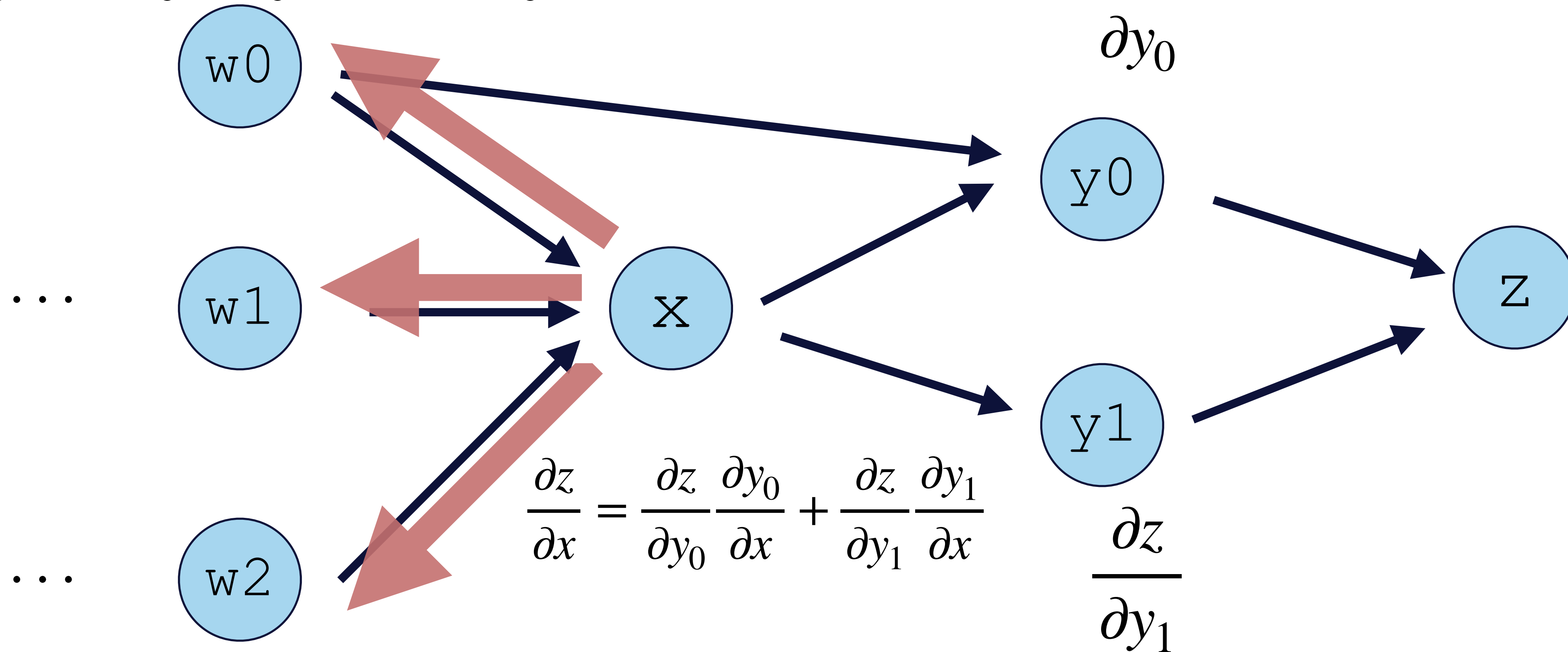
REVERSE-MODE AUTOMATIC DIFFERENTIATION = A GREEDY PATH FACTORIZATION ALGORITHM

$$\frac{\partial z}{\partial w_0} = \frac{\partial z}{\partial y_0} \frac{\partial y_0}{\partial w_0}$$



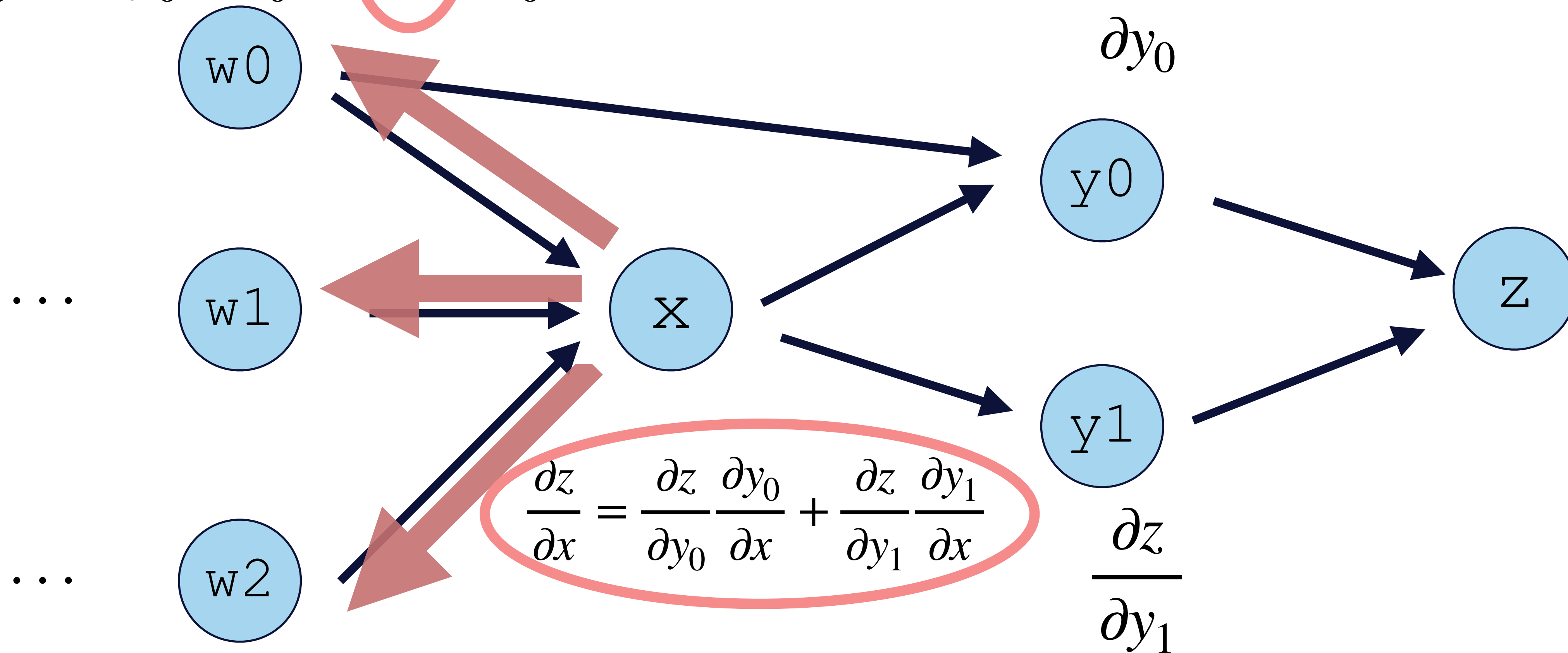
REVERSE-MODE AUTOMATIC DIFFERENTIATION = A GREEDY PATH FACTORIZATION ALGORITHM

$$\frac{\partial z}{\partial w_0} = \frac{\partial z}{\partial y_0} \frac{\partial y_0}{\partial w_0} + \frac{\partial z}{\partial x} \frac{\partial x}{\partial w_0}$$

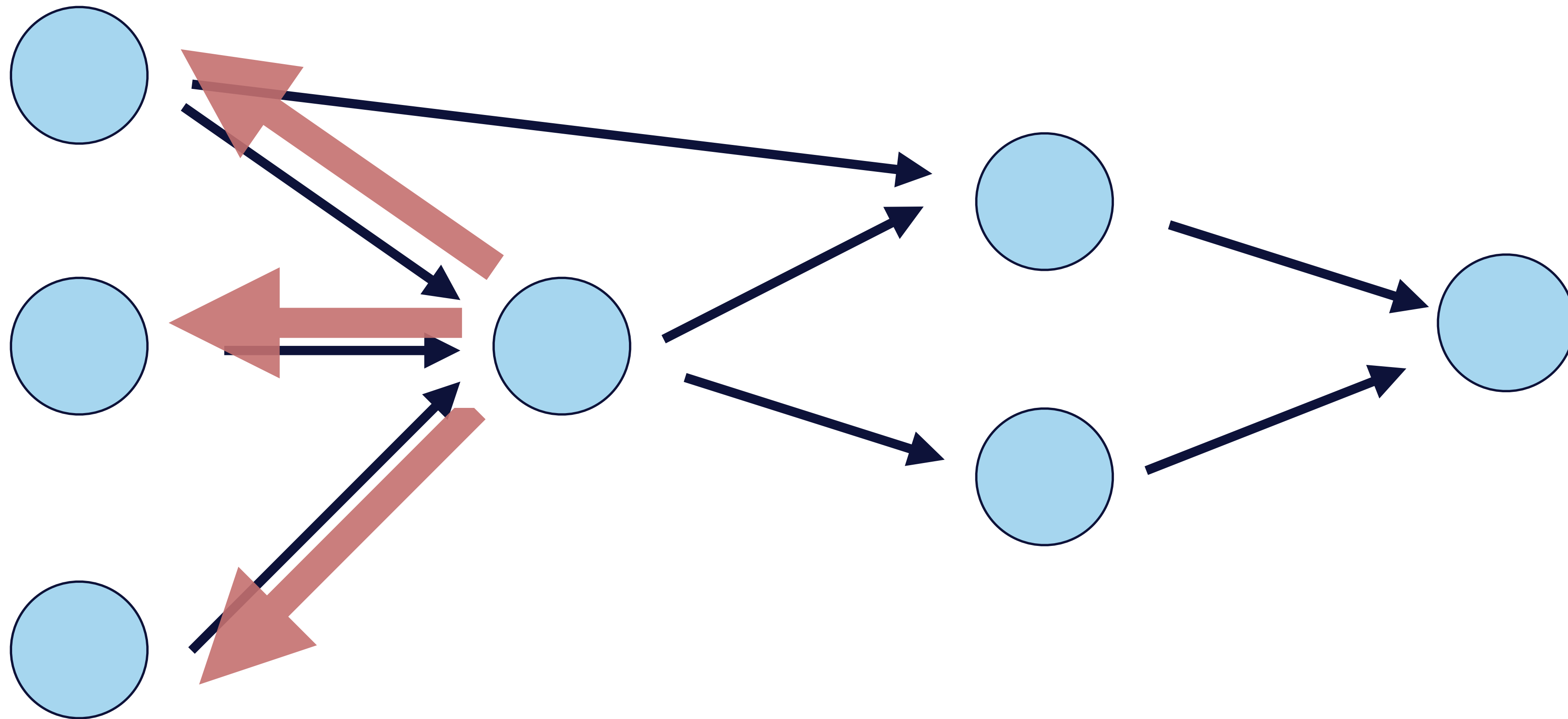


REVERSE-MODE AUTOMATIC DIFFERENTIATION = A GREEDY PATH FACTORIZATION ALGORITHM

$$\frac{\partial z}{\partial w_0} = \frac{\partial z}{\partial y_0} \frac{\partial y_0}{\partial w_0} + \frac{\partial z}{\partial x} \frac{\partial x}{\partial w_0}$$



- gradient complexity: number of edges * constant
 - same as directly computing the function (“*cheap gradient principle*”)



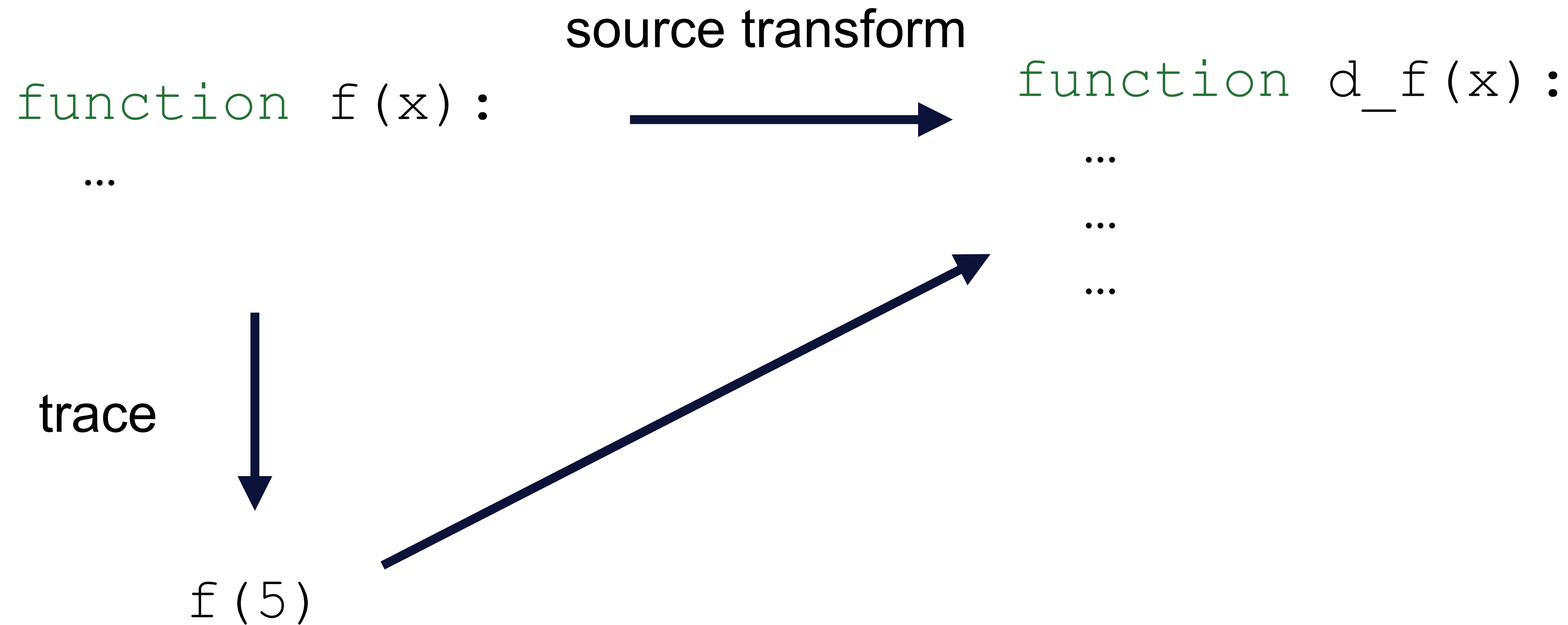
- remember every intermediate values in the forward pass, then run the loop backward
 - also works for recursion
 - unbounded memory usage

```
function f(x):  
    result = x  
    for i = 1 to 8:  
        result = exp(result)  
    return result
```

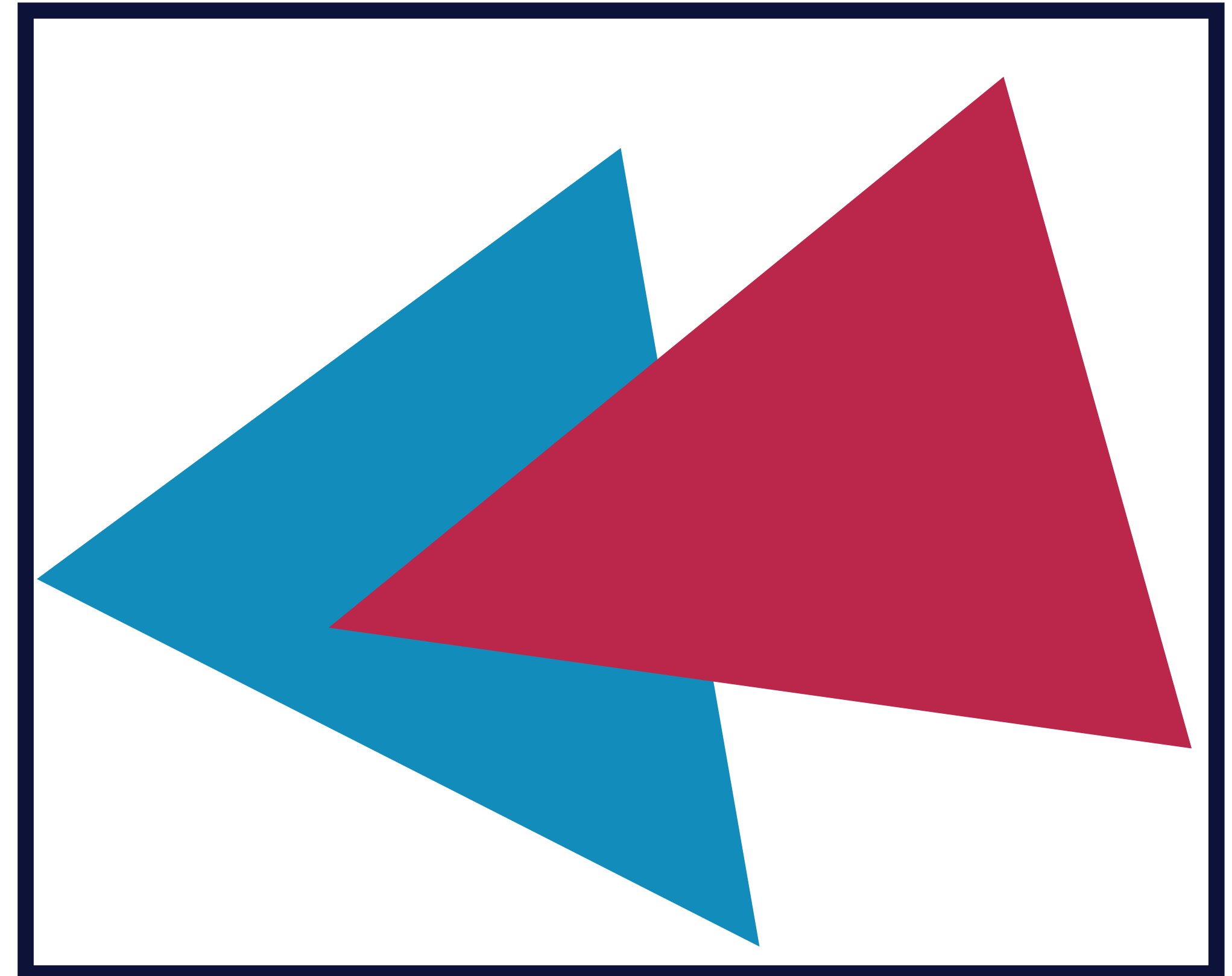


```
function d_f(x):  
    result = x  
    results = []  
    for i = 1 to 8:  
        results.push(result)  
        result = exp(result)  
  
    for i = 8 to 1:  
        d_results = d_result *  
            exp(results[i])  
    return result
```

- a spectrum: how much is done at compile time
 - similar to (tracing) JIT v.s. static compile

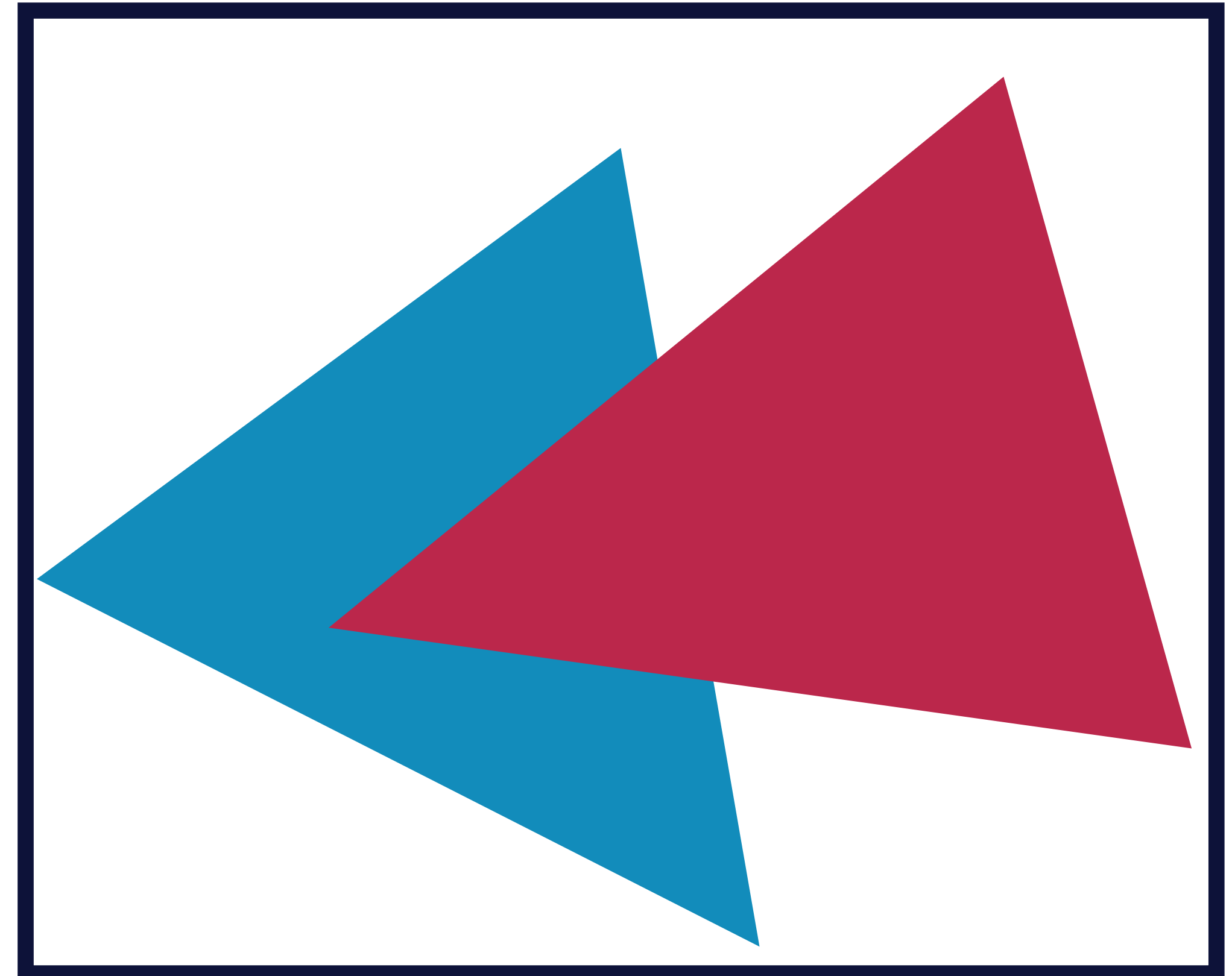



```
if (hit the red triangle)  
    return red  
elif (hit the blue triangle)  
    return blue  
else  
    return white
```



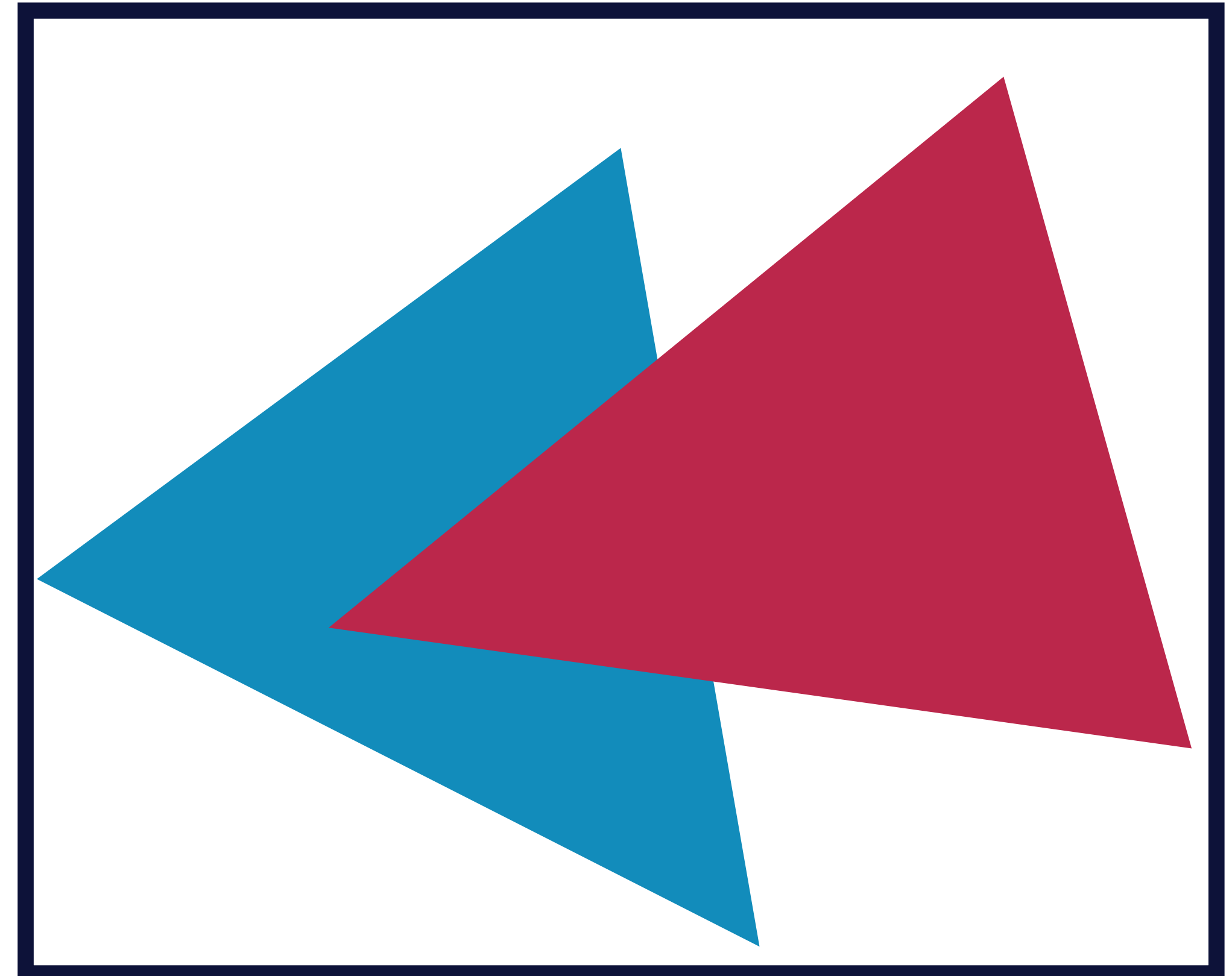
```
if (hit the red triangle)  
    return red  
elif (hit the blue triangle)  
    return blue  
else  
    return white
```

- derivative of color w.r.t. triangle vertex is 0



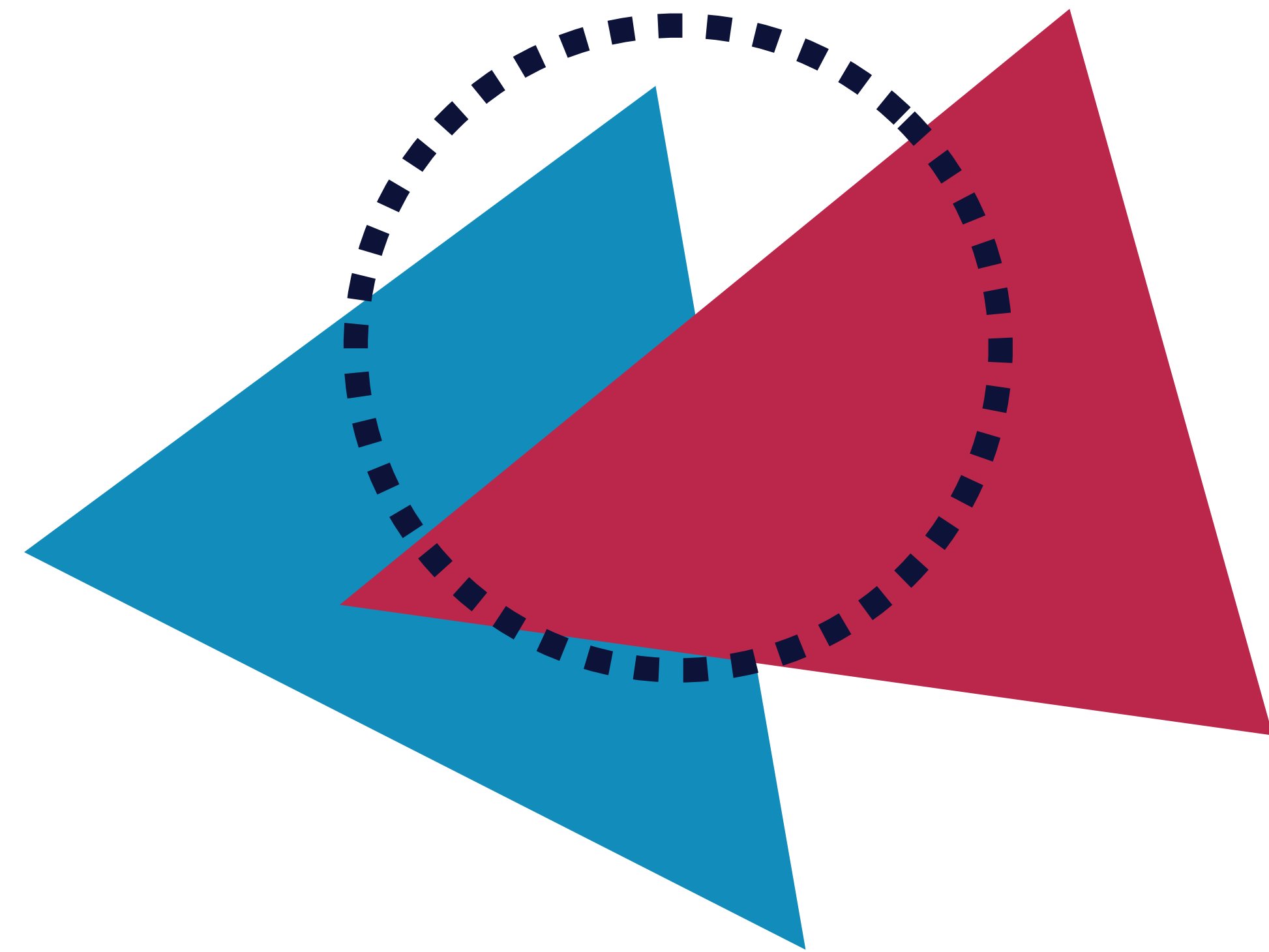

```
if (hit the red triangle)  
    return red  
elif (hit the blue triangle)  
    return blue  
else  
    return white
```

- derivative of color w.r.t. triangle vertex is 0
—or is it?



- pixel color is defined by the average color over an area
 - aka anti-aliasing

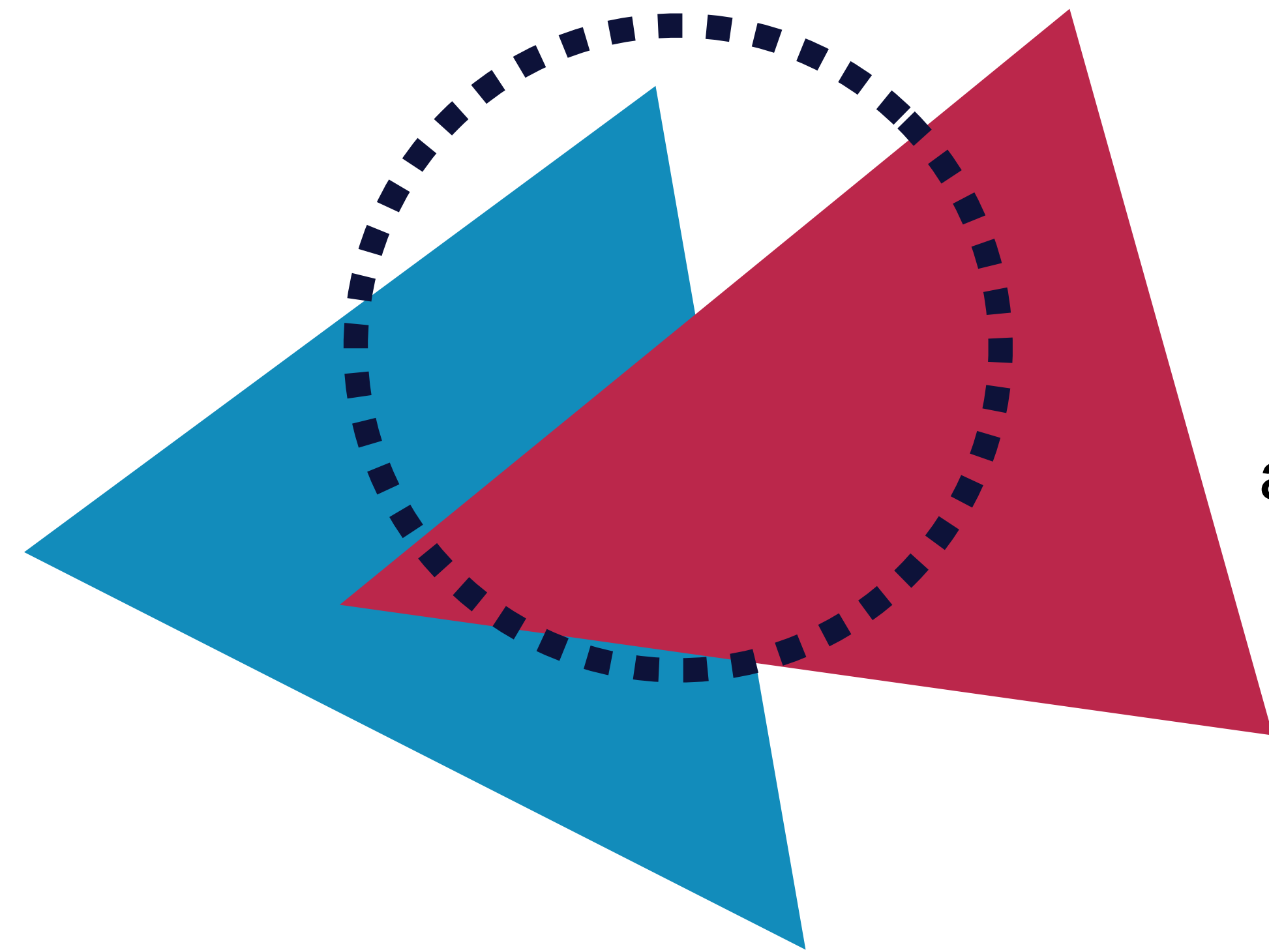
pixel filter support



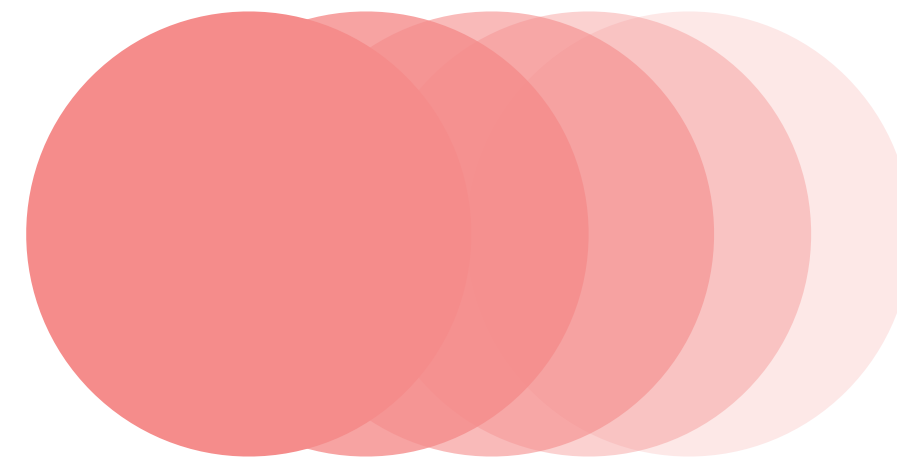
RENDERING = COMPUTING INTEGRALS

- pixel color is defined by the average color over an area
 - aka anti-aliasing

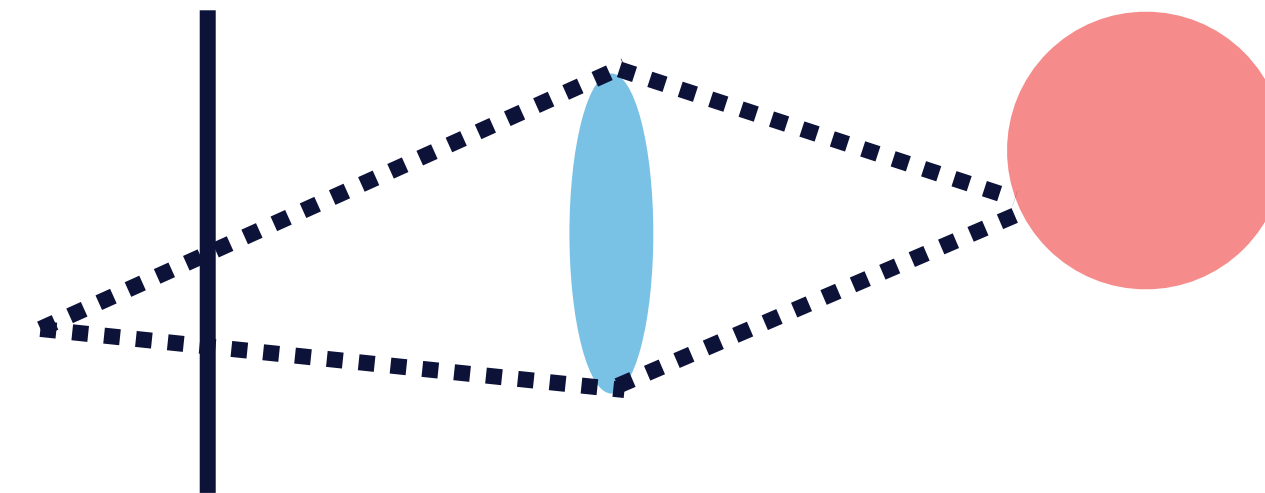
pixel filter support



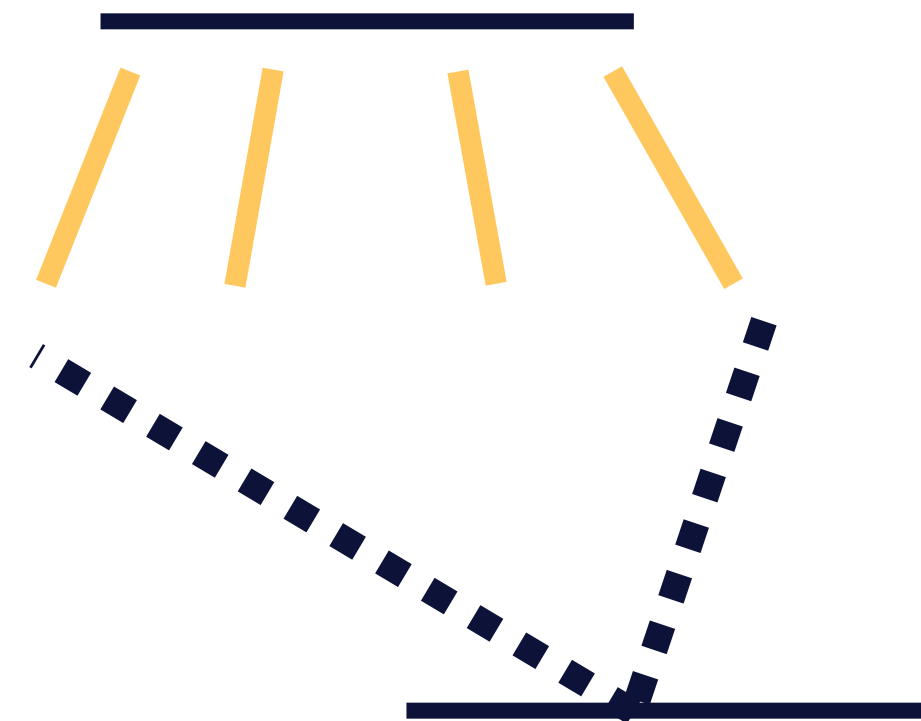
shutter time
(motion blur)



camera aperture
(defocus blur)



area light

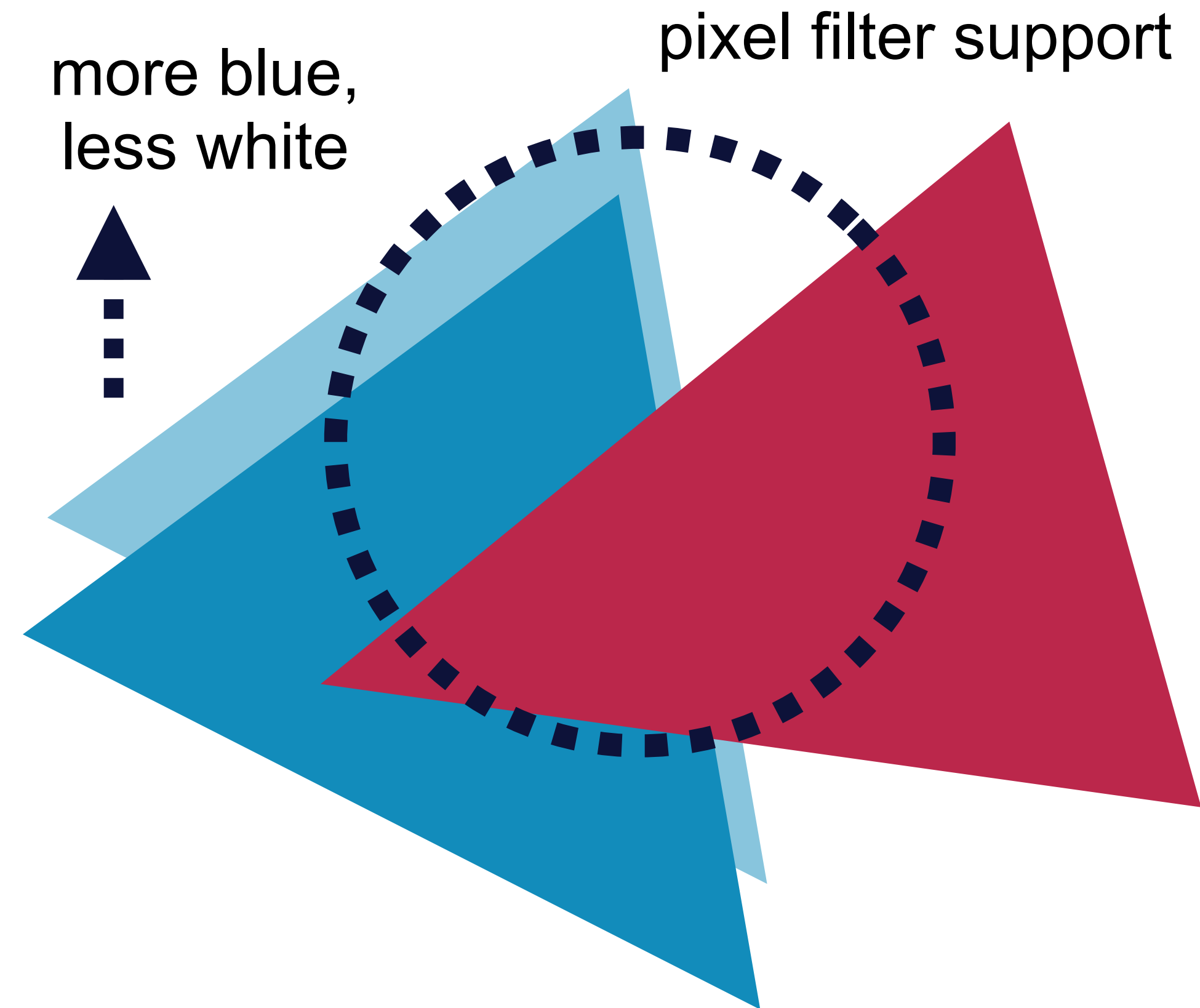


global illumination



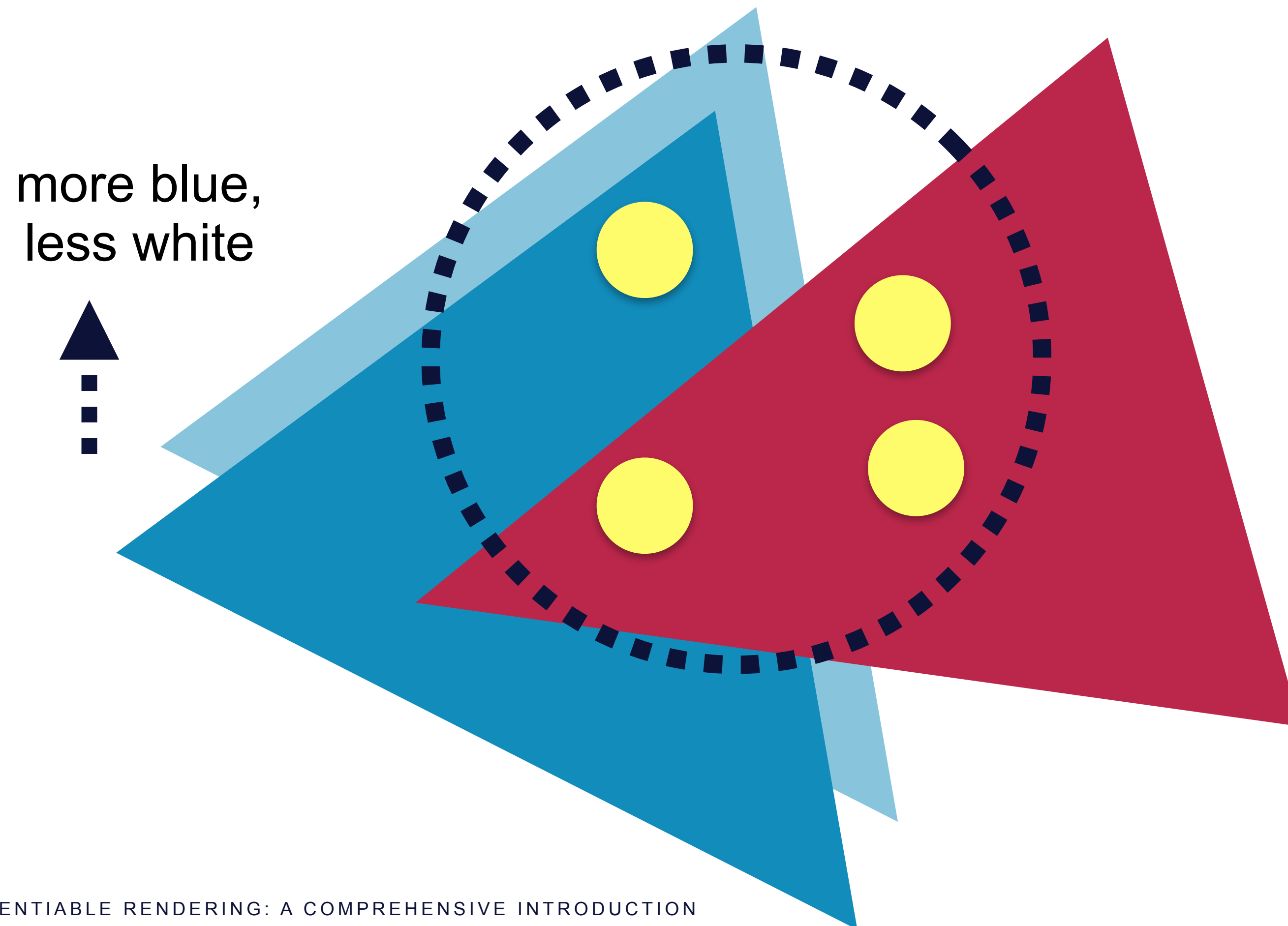
- wavelength
- participating media
- ...
- and more!

- While the *integrand* is discontinuous, the *integral* is differentiable!
 - the average color changes continuously as triangles move



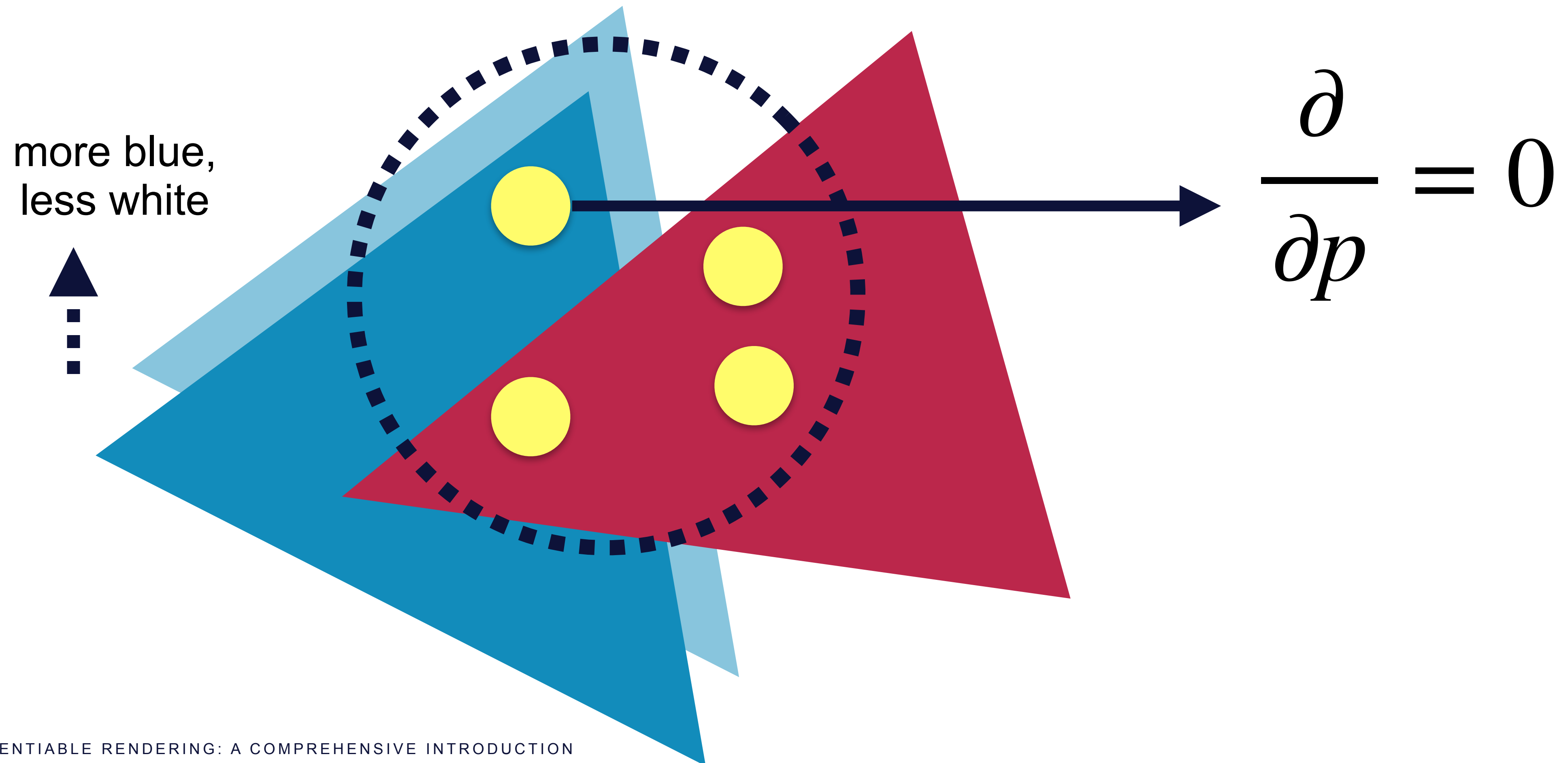
```
if (hit the red triangle)  
    return red  
elif (hit the blue triangle)  
    return blue  
else  
    return white
```


- We evaluate these integrals by sampling them

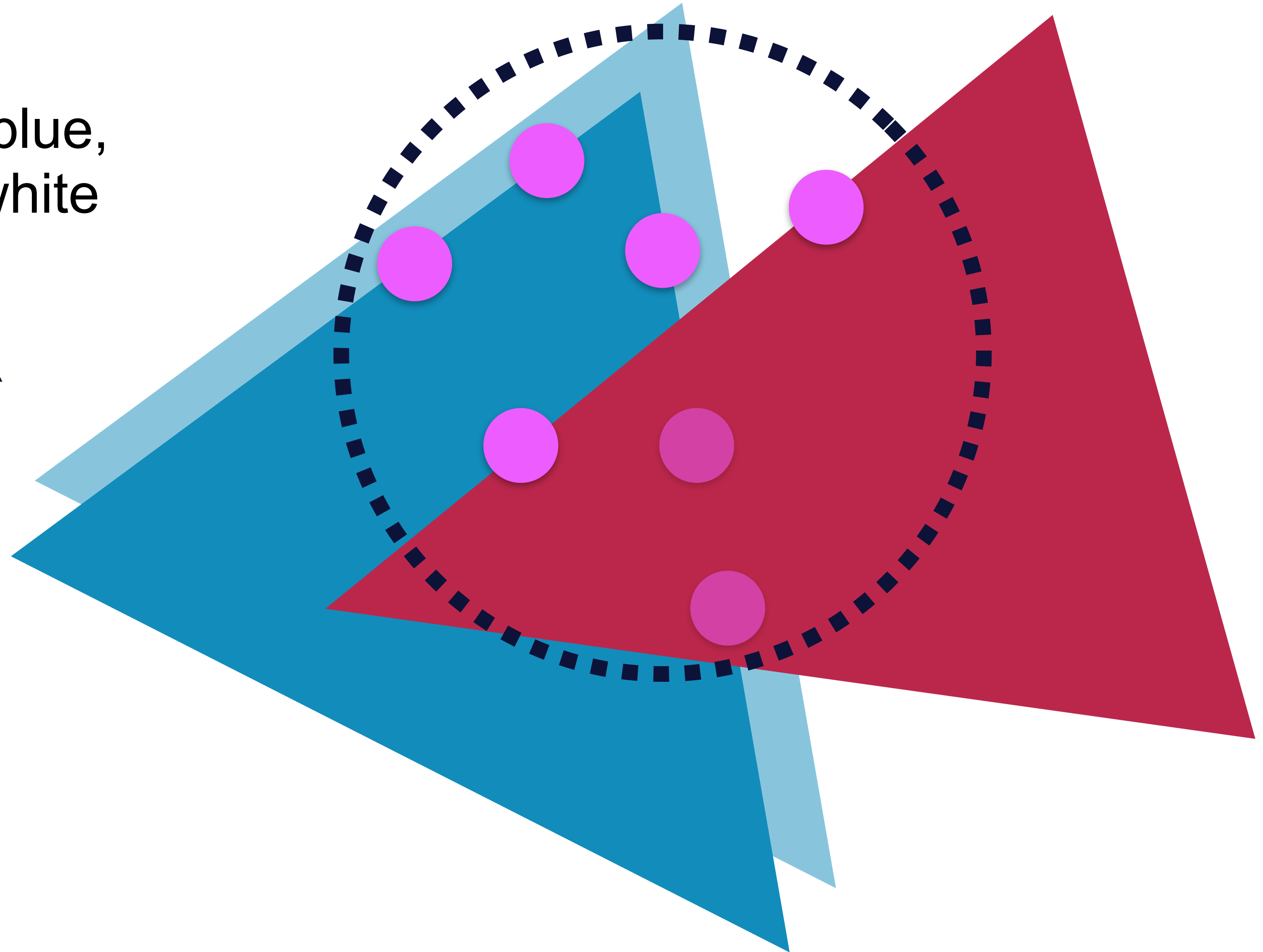


$$\int \dots \approx \sum \dots$$

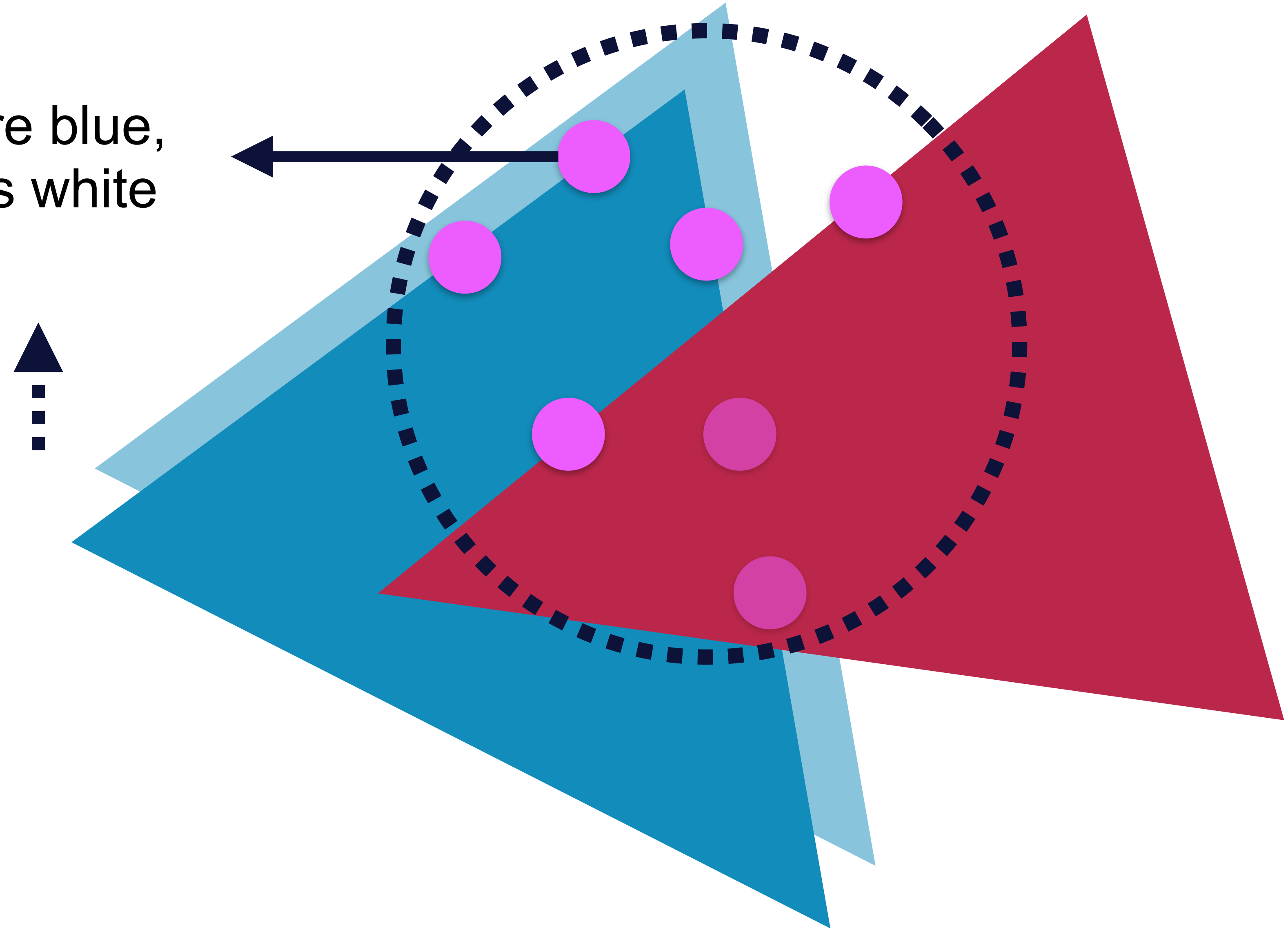
DIFFERENTIATING INTEGRAL SAMPLES GIVES WRONG DERIVATIVES

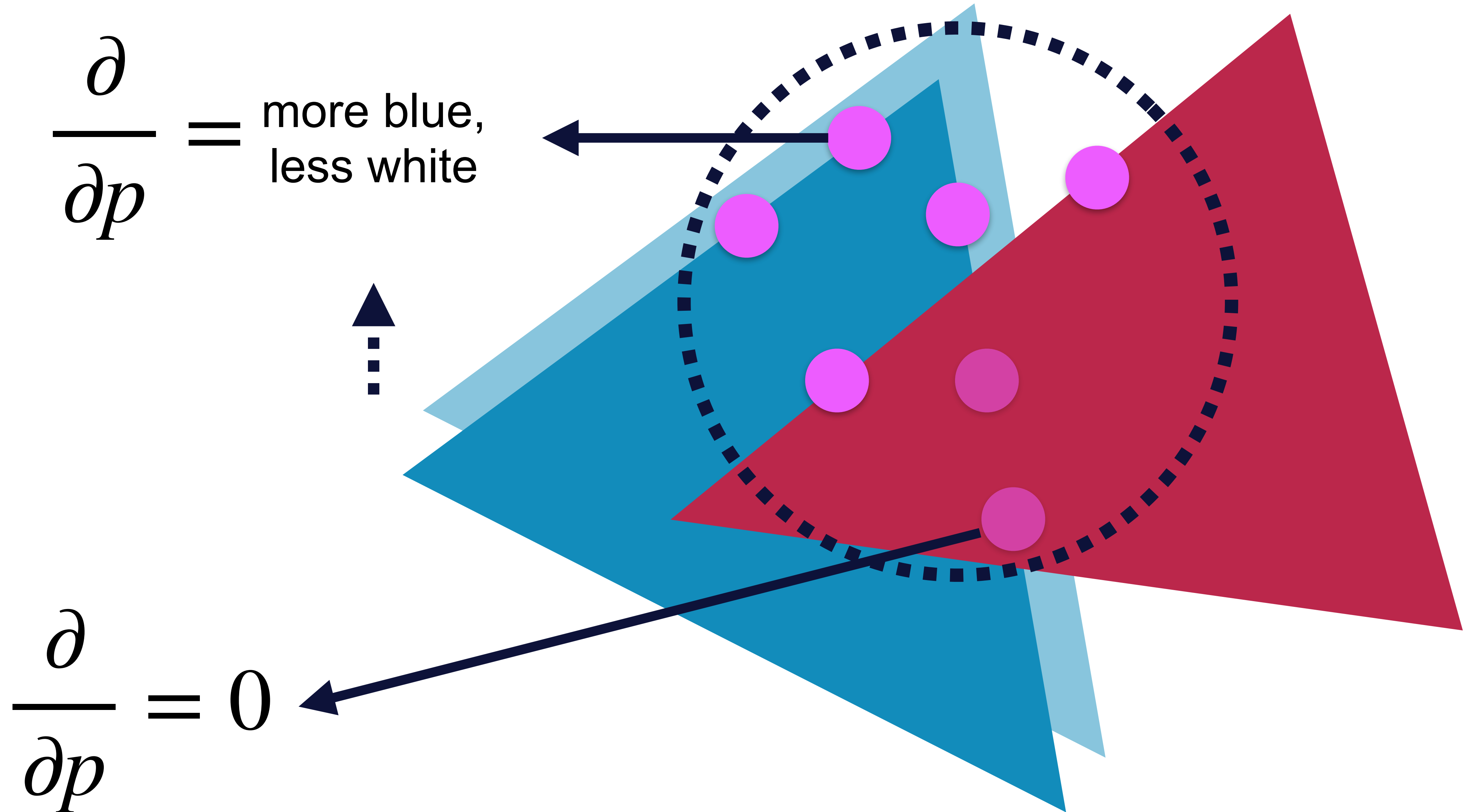


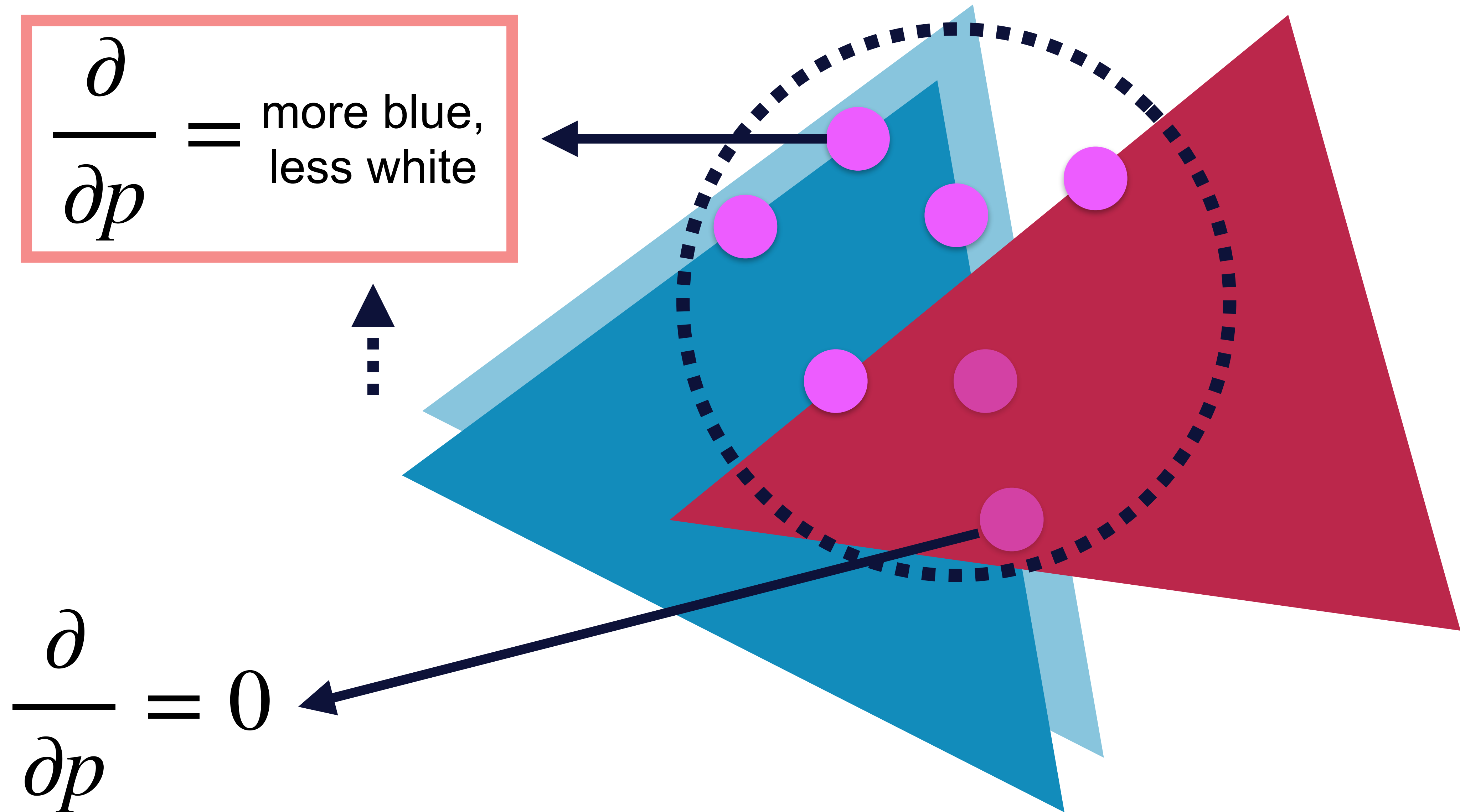
more blue,
less white



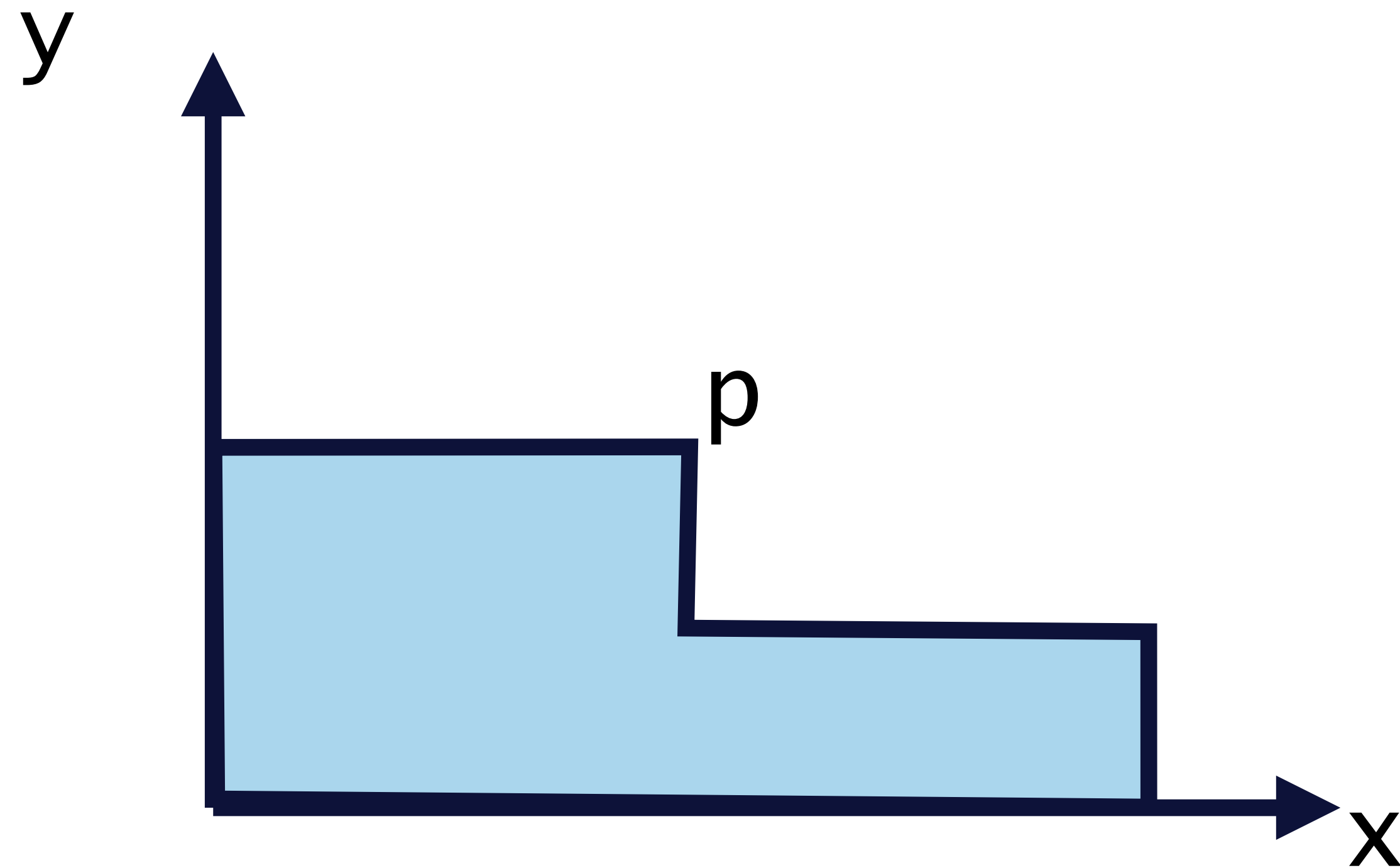
$$\frac{\partial}{\partial p} = \text{more blue, less white}$$







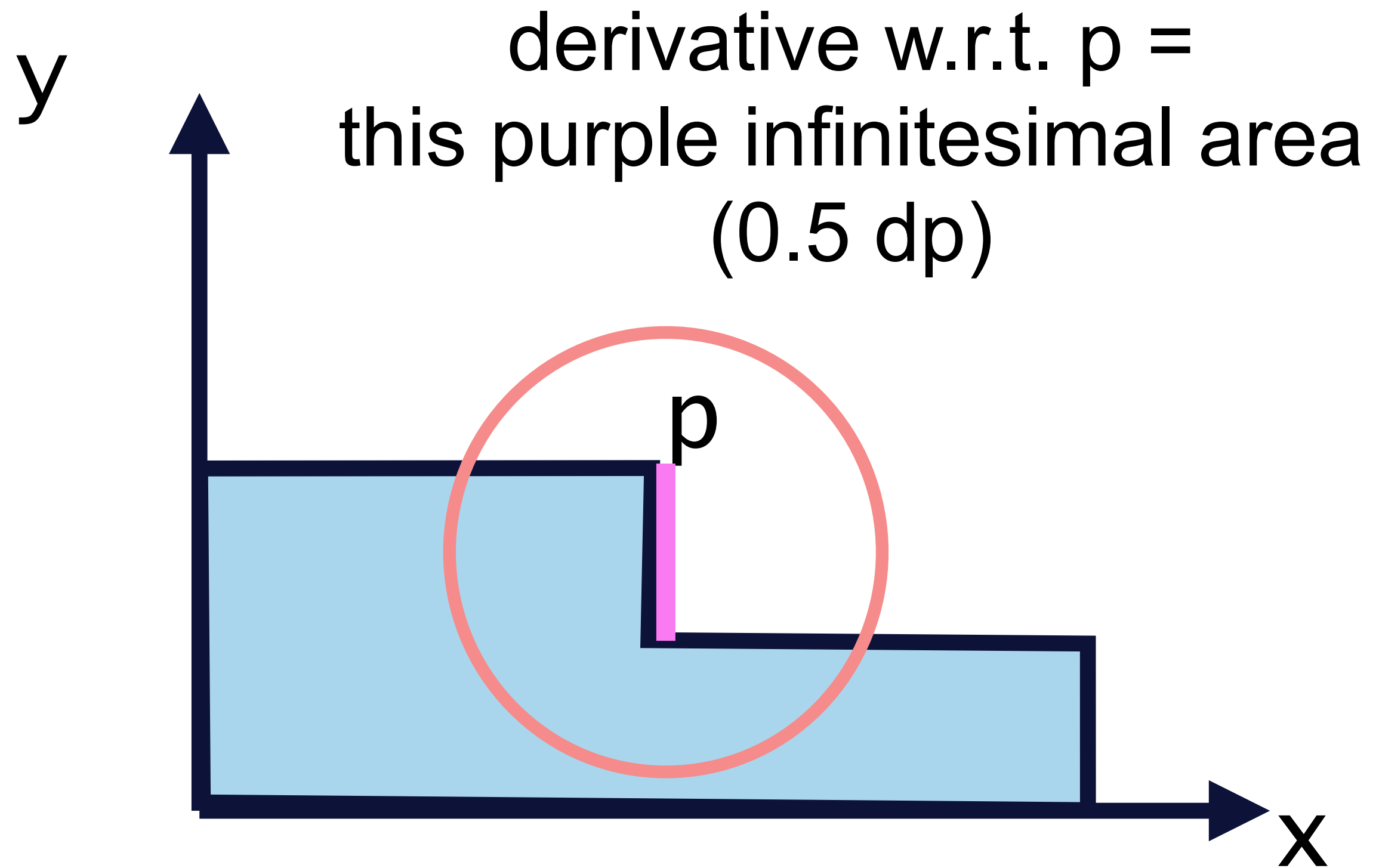
LET'S DERIVE THE DERIVATIVES IN 1D



(the blue area)

$$\int_{x=0}^{x=1} \quad x < p \quad ? \quad 1 : 0.5$$

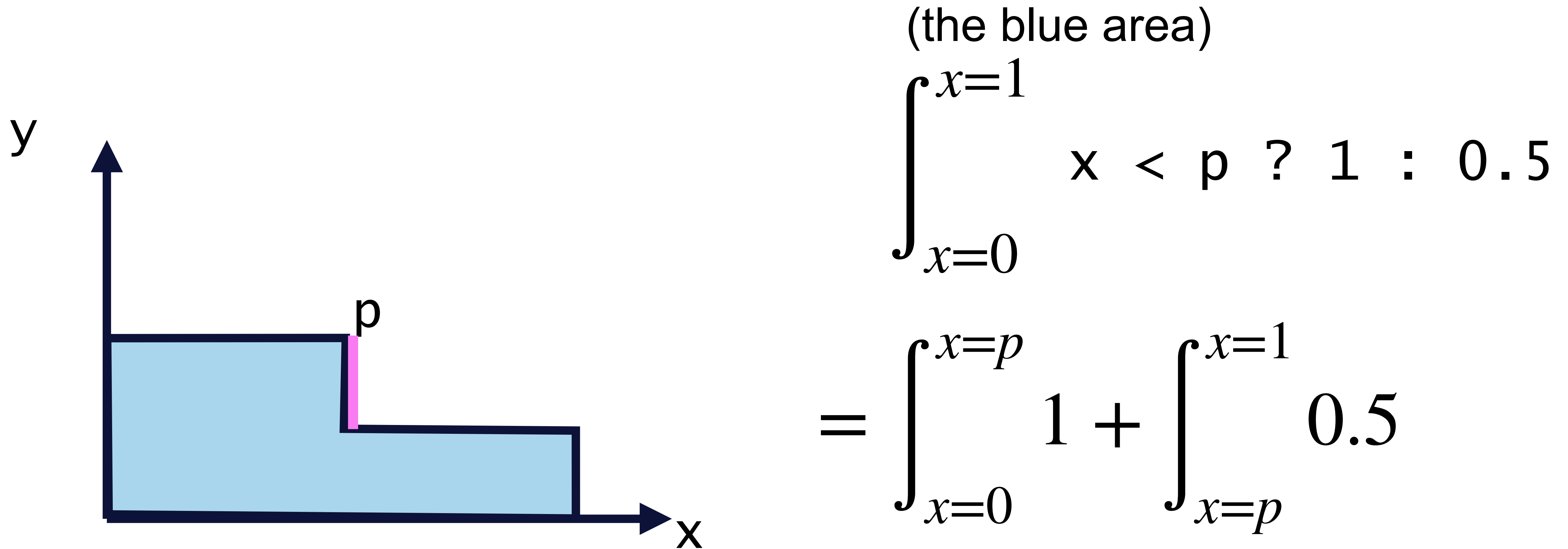
LET'S DERIVE THE DERIVATIVES IN 1D



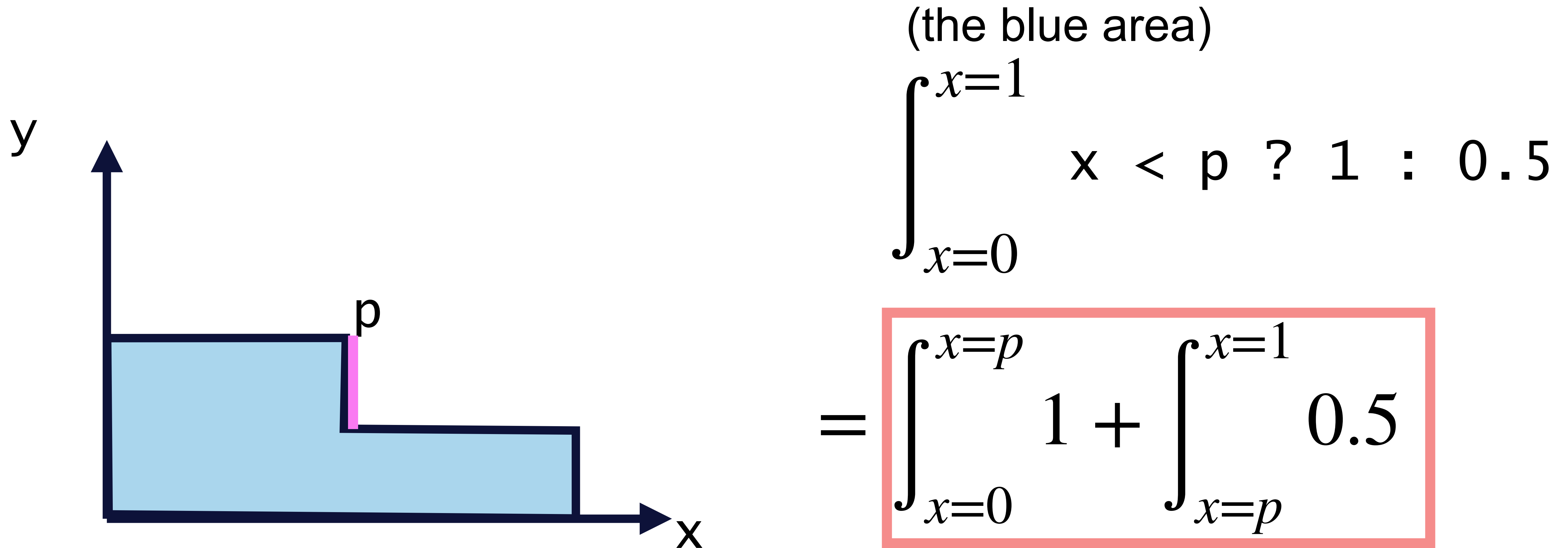
(the blue area)

$$\int_{x=0}^{x=1} x < p ? 1 : 0.5$$

- Trick: move the discontinuities to the integral boundaries

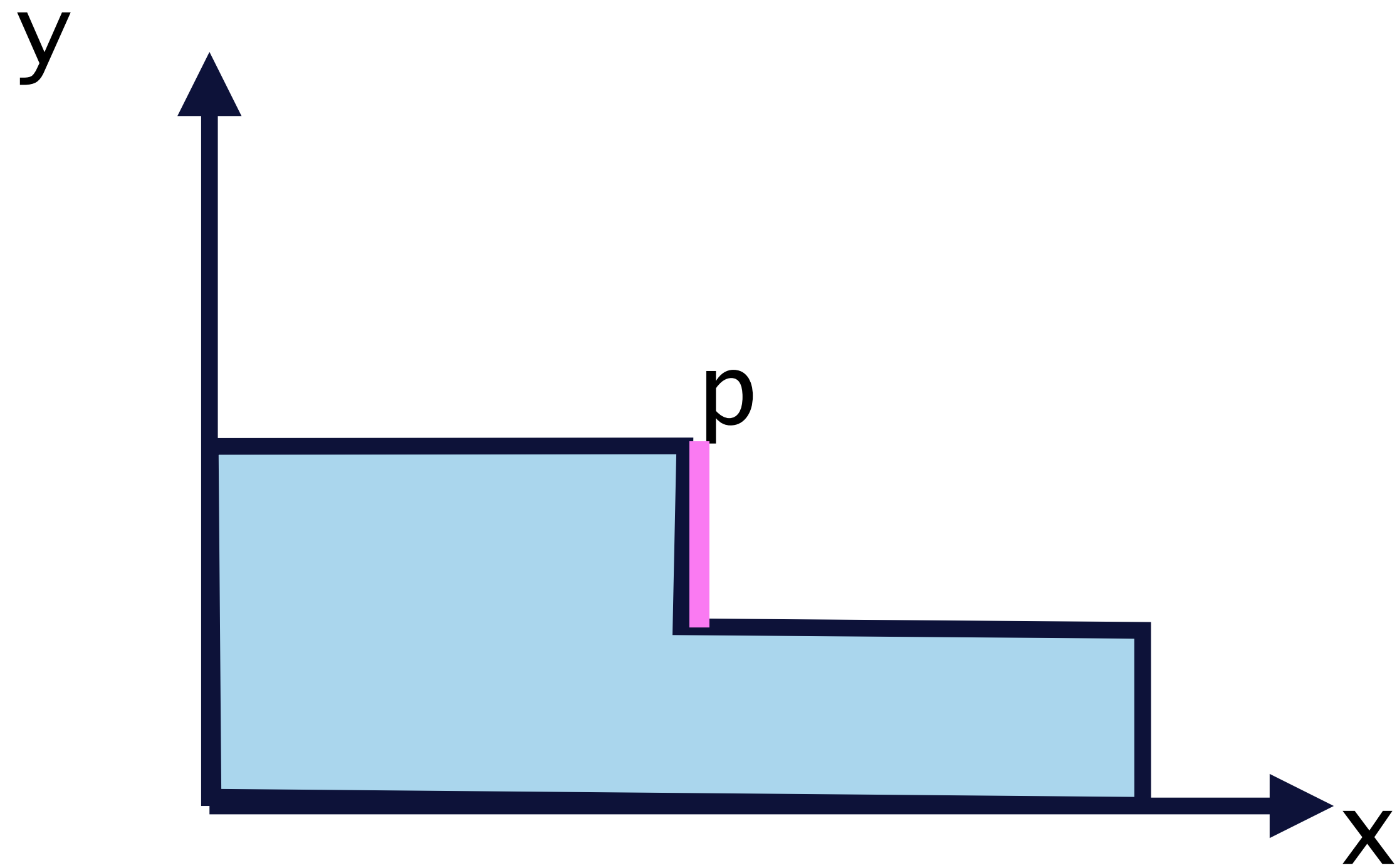


- Trick: move the discontinuities to the integral boundaries



DISCONTINUITY DERIVATIVES = DIFFERENCES AT DISCONTINUITIES

$$\int_{x=0}^{x=1} x < p ? 1 : 0.5$$



(derivative of blue area w.r.t. p)

$$\frac{\partial}{\partial p} \left(\int_{x=0}^{x=p} 1 + \int_{x=p}^{x=1} 0.5 \right) = 1 - 0.5$$

DISCONTINUITY DERIVATIVES = DIFFERENCES AT DISCONTINUITIES

$$\frac{\partial}{\partial p} \int \text{[Graph with discontinuity]} = \int \frac{\partial}{\partial p} \text{[Graph with discontinuity and yellow dots]} +$$

$$\sum \text{[Graph with discontinuity and pink bar]} \quad f_- - f_+$$

“the Leibniz’s integral rule”

DISCONTINUITY DERIVATIVES = DIFFERENCES AT DISCONTINUITIES

interior derivative

$$\frac{\partial}{\partial p} \int \text{[Graph]} = \int \frac{\partial}{\partial p} \text{[Graph]} +$$

“the Leibniz’s integral rule”

$$\Sigma \text{ [Graph]} \quad f_- - f_+$$

boundary derivative

interior derivative

$$\frac{\partial}{\partial p} \iint \text{[Diagram: overlapping triangles with a dashed boundary]} = \iint \frac{\partial}{\partial p} \text{[Diagram: overlapping triangles with interior points and dashed boundary]}$$

Reynolds transport theorem
[Reynolds 1903]

+

$$\int \text{[Diagram: overlapping triangles with boundary points and dashed boundary]}$$

boundary derivative

interior derivative

$$\frac{\partial}{\partial p} \iint \text{[Diagram: overlapping triangles with a dashed boundary]} = \iint \frac{\partial}{\partial p} \text{[Diagram: overlapping triangles with yellow dots inside a dashed boundary]}$$

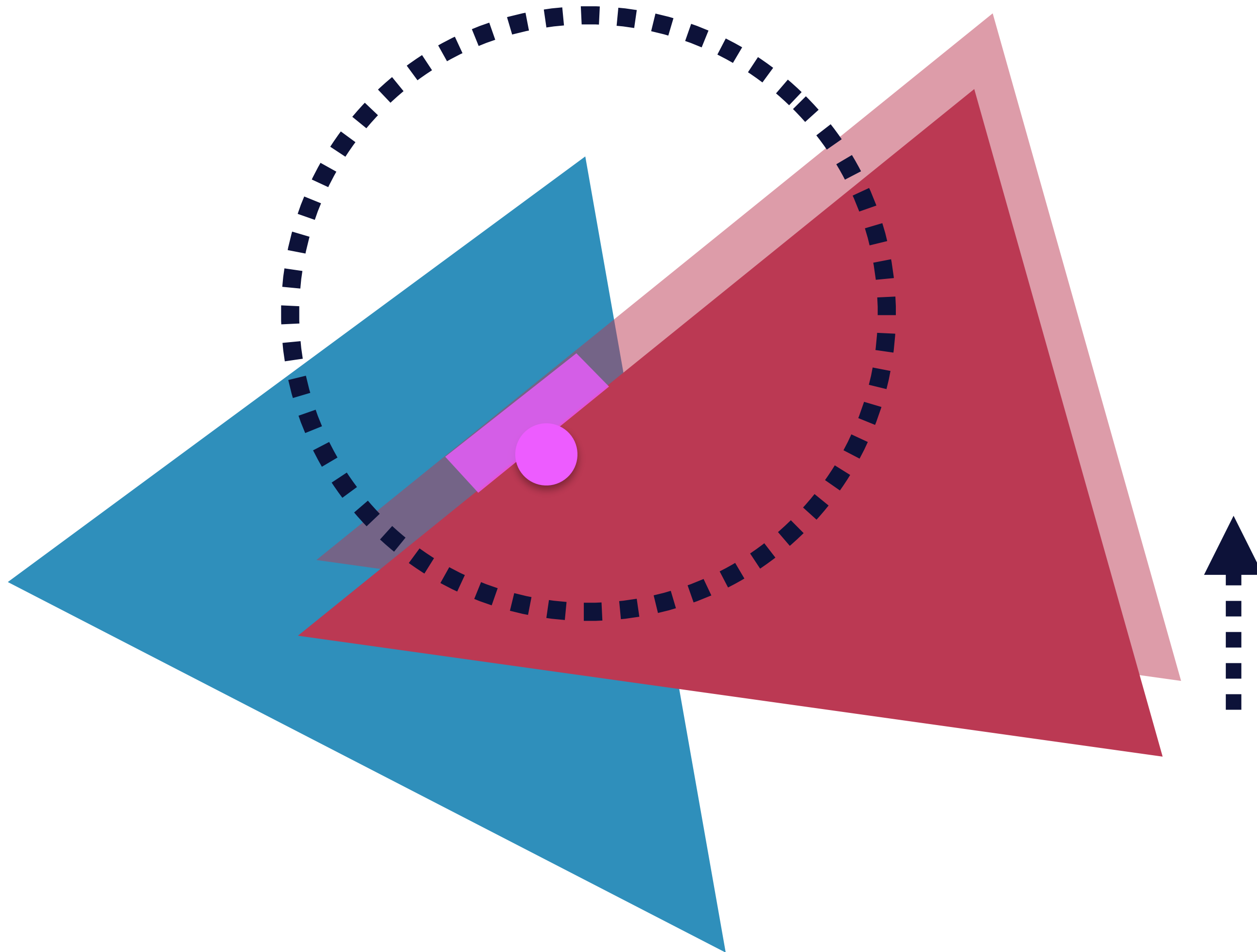
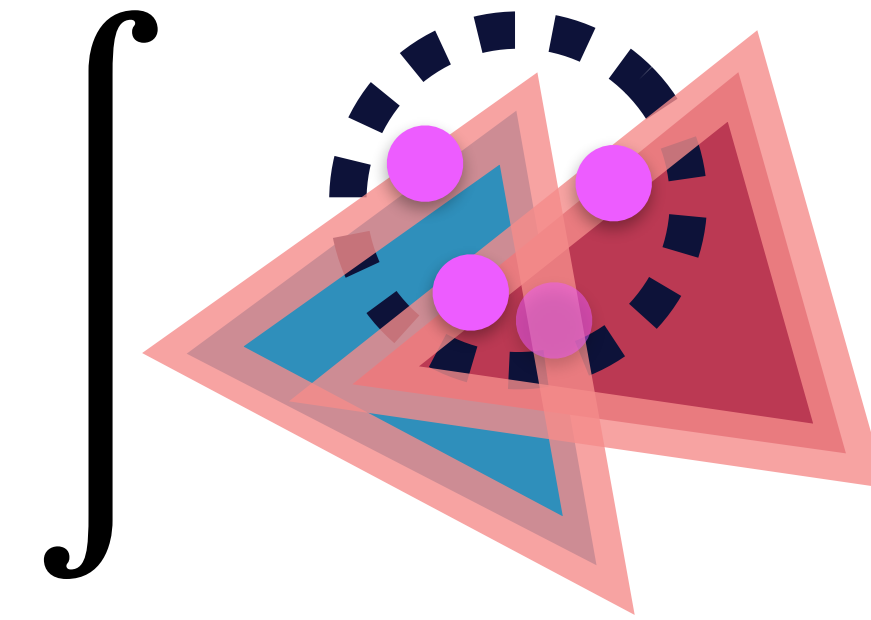
Reynolds transport theorem
[Reynolds 1903]

+

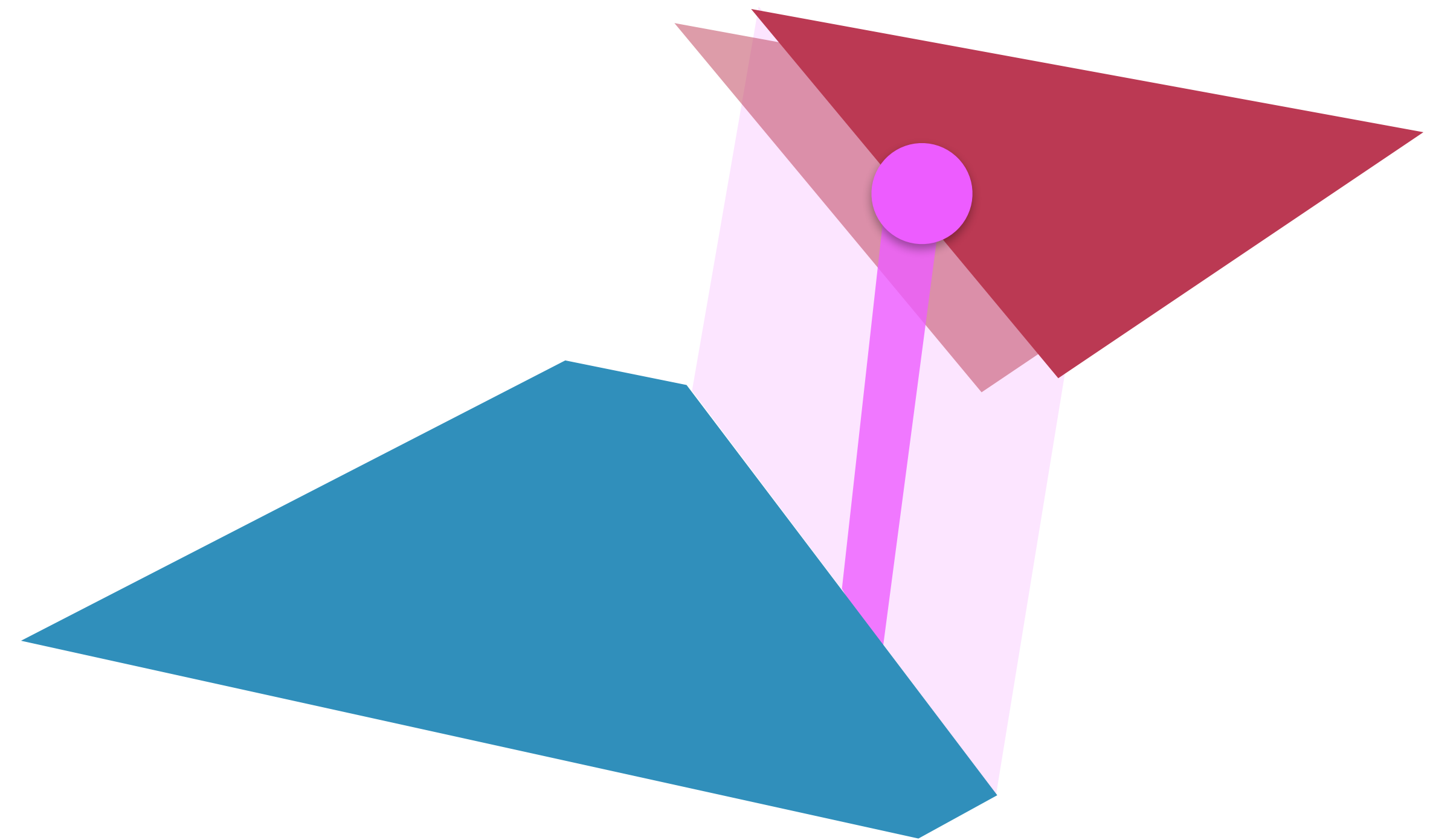
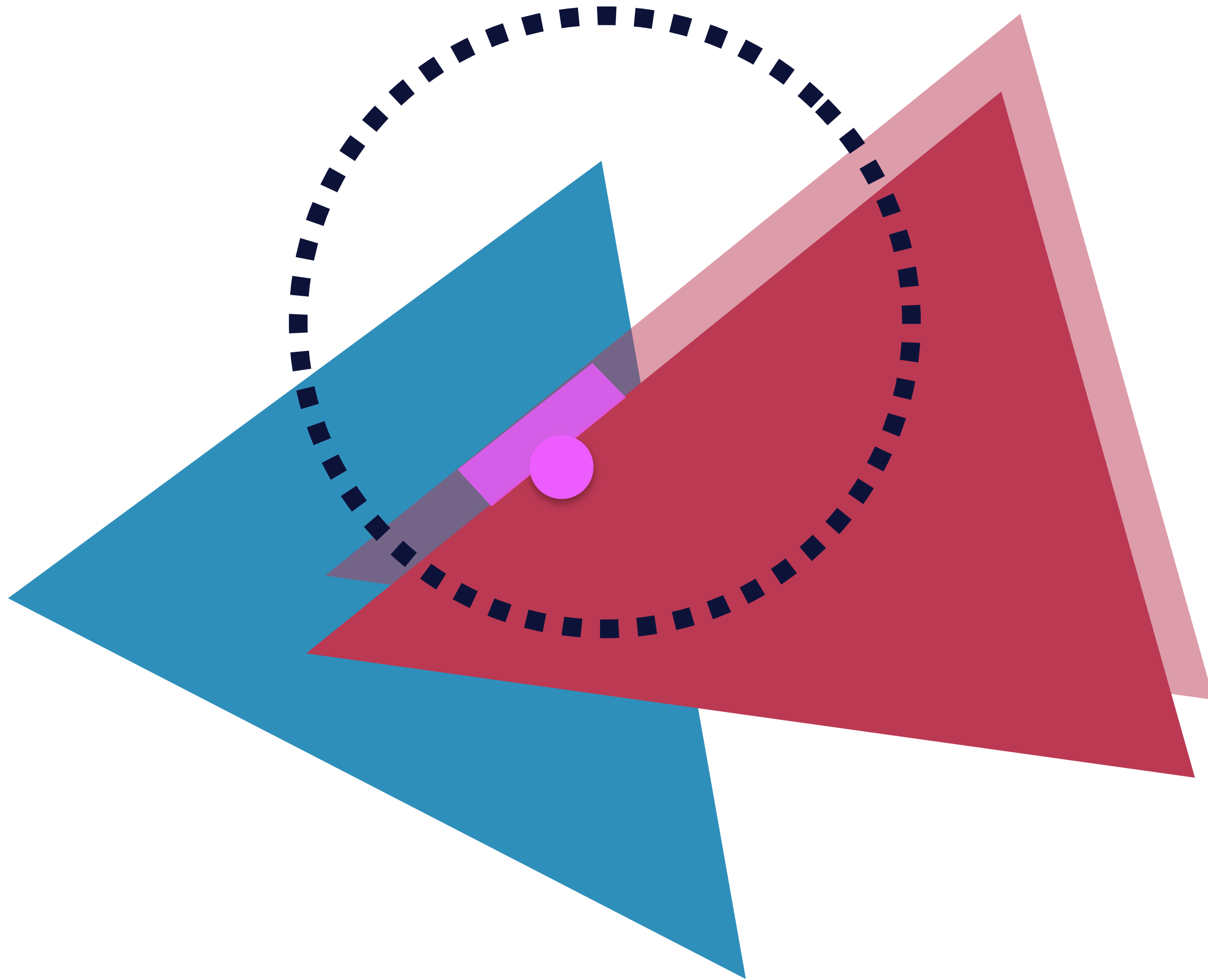
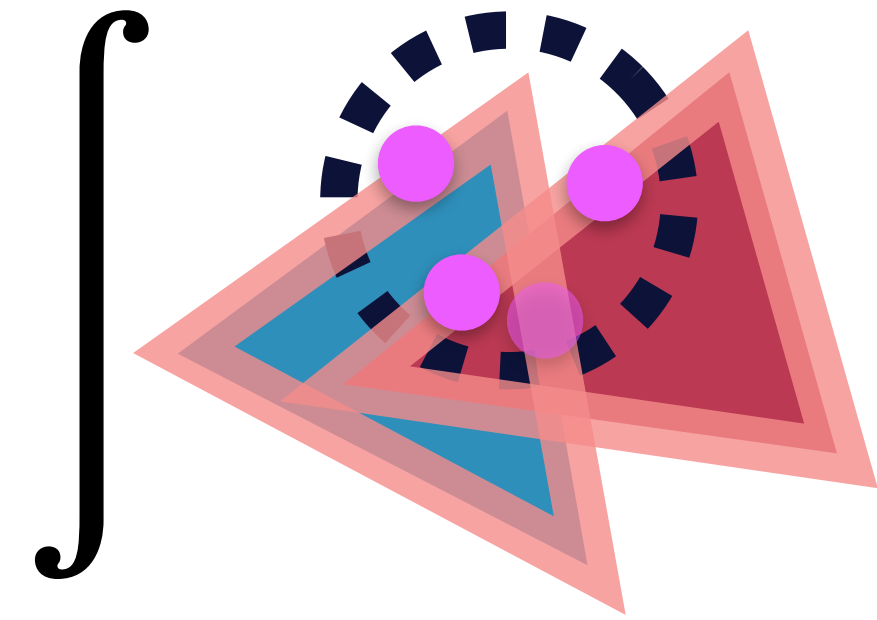
$$\int \text{[Diagram: overlapping triangles with magenta dots on a dashed boundary]}$$

boundary derivative

- boundary derivative = infinitesimal volume change w.r.t. parameter

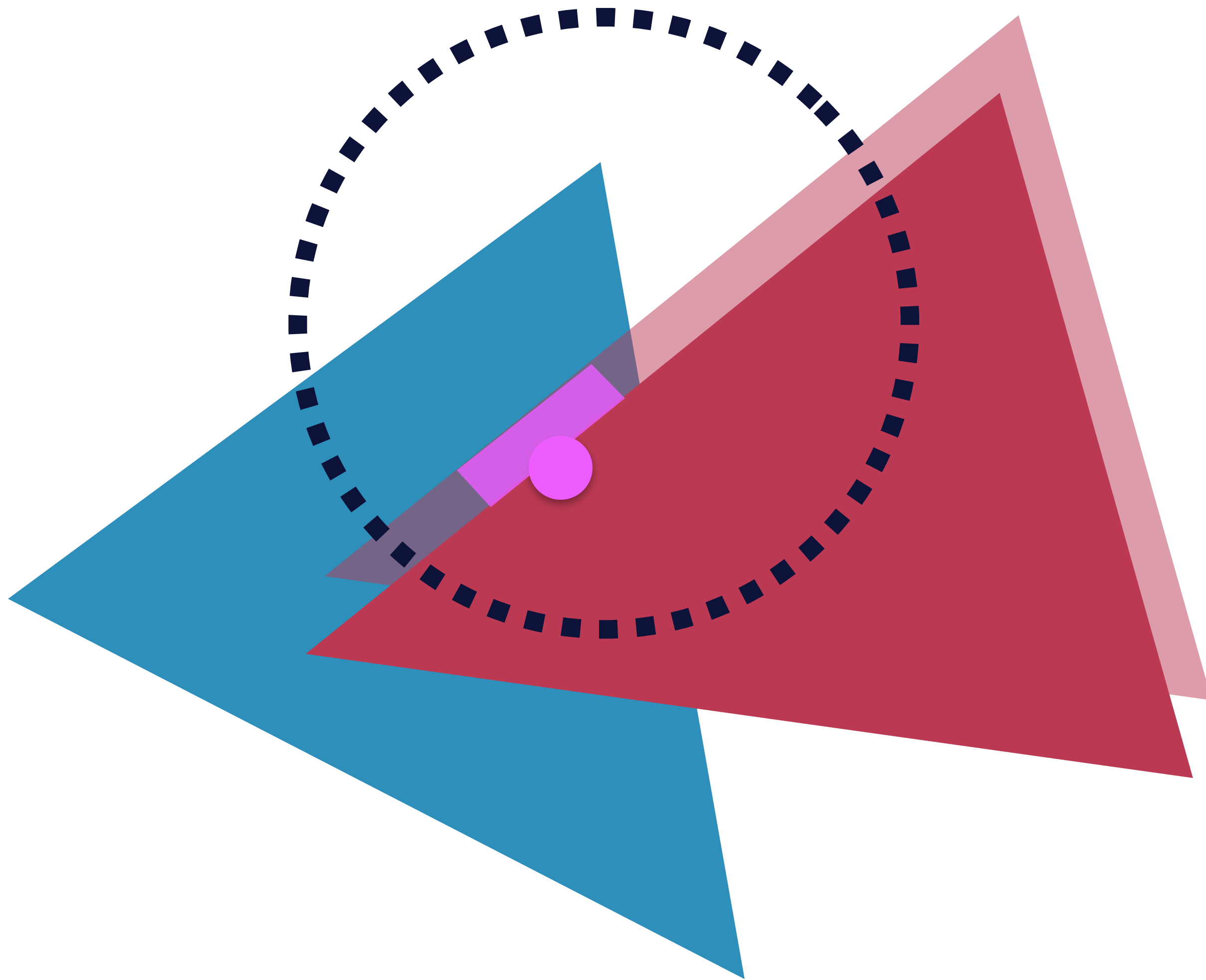
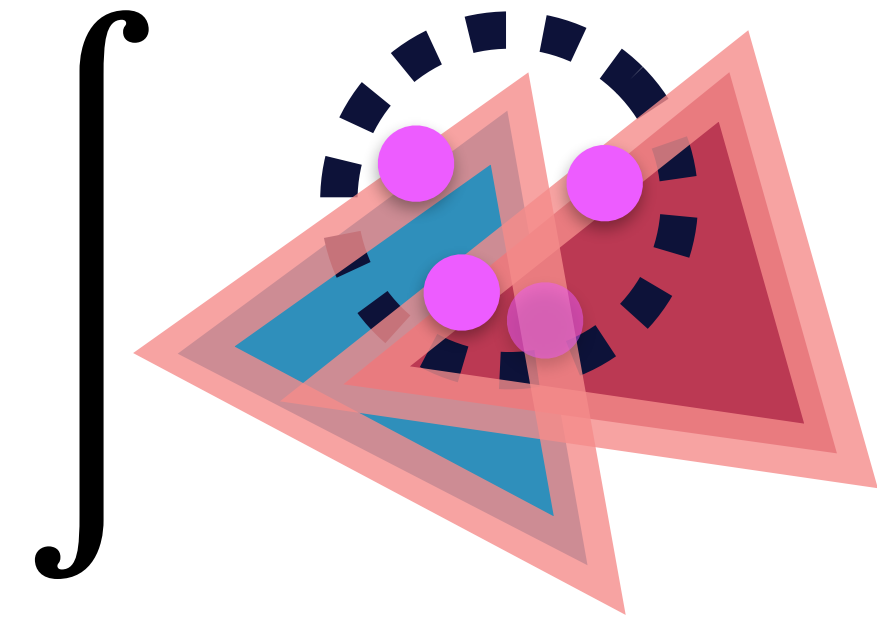


- boundary derivative = infinitesimal volume change w.r.t. parameter

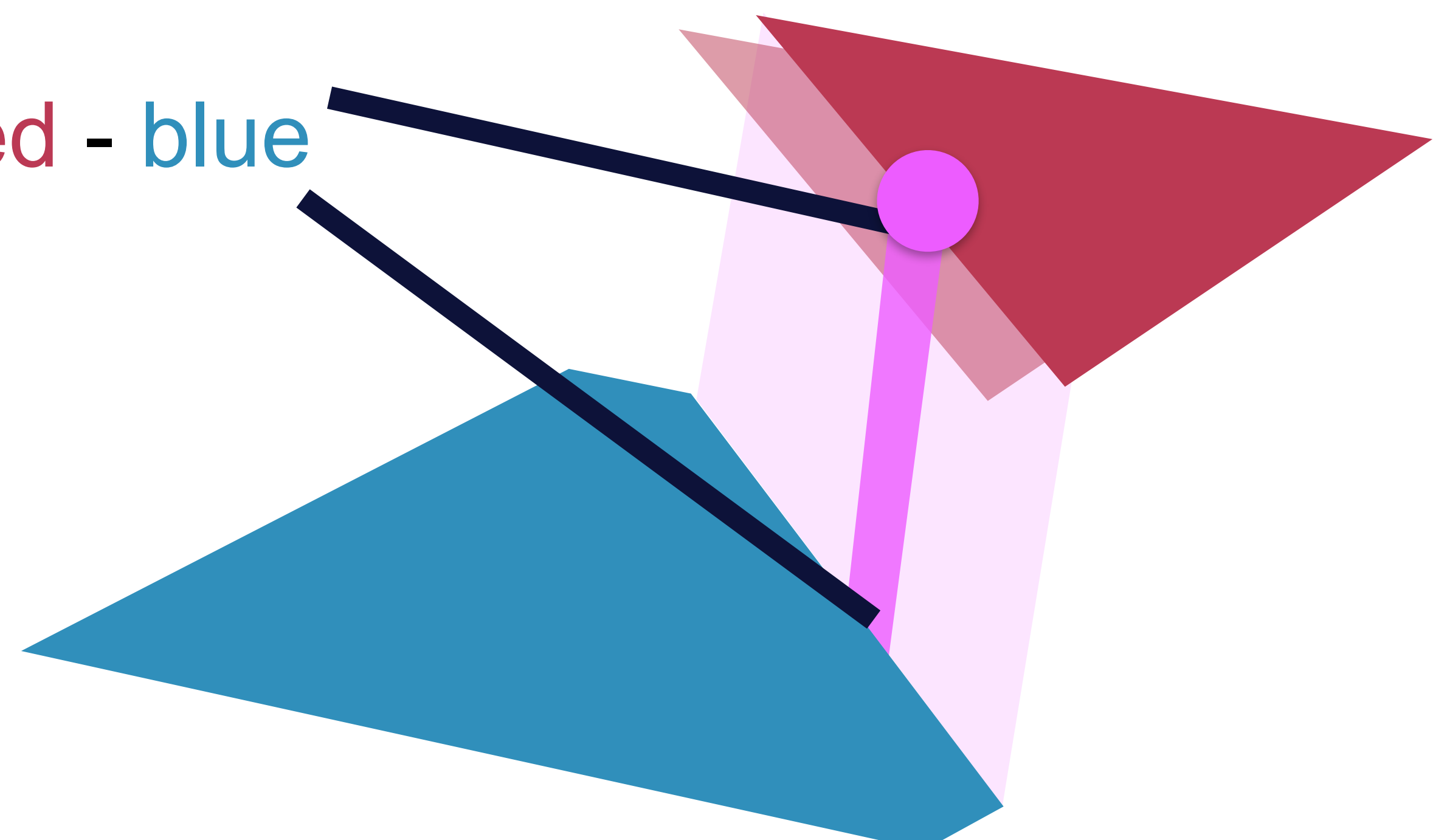


3D view around the purple sample

- boundary derivative = infinitesimal volume change w.r.t. parameter



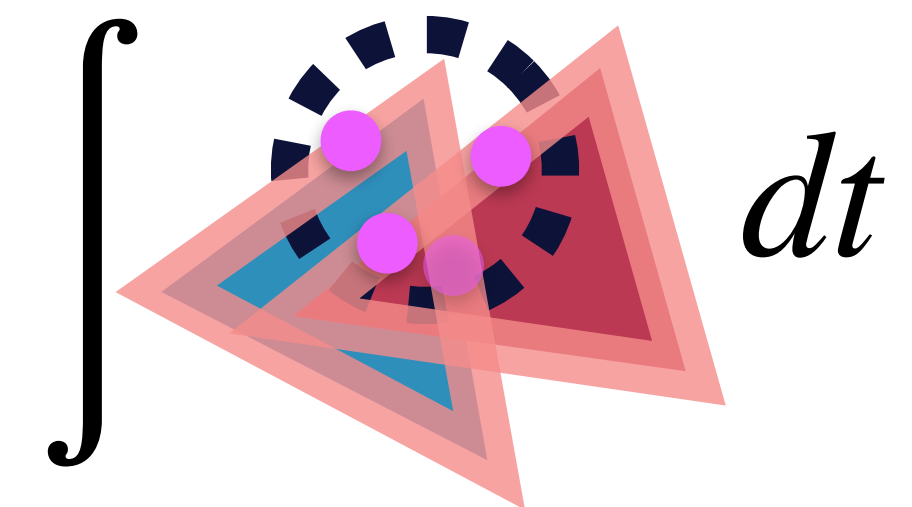
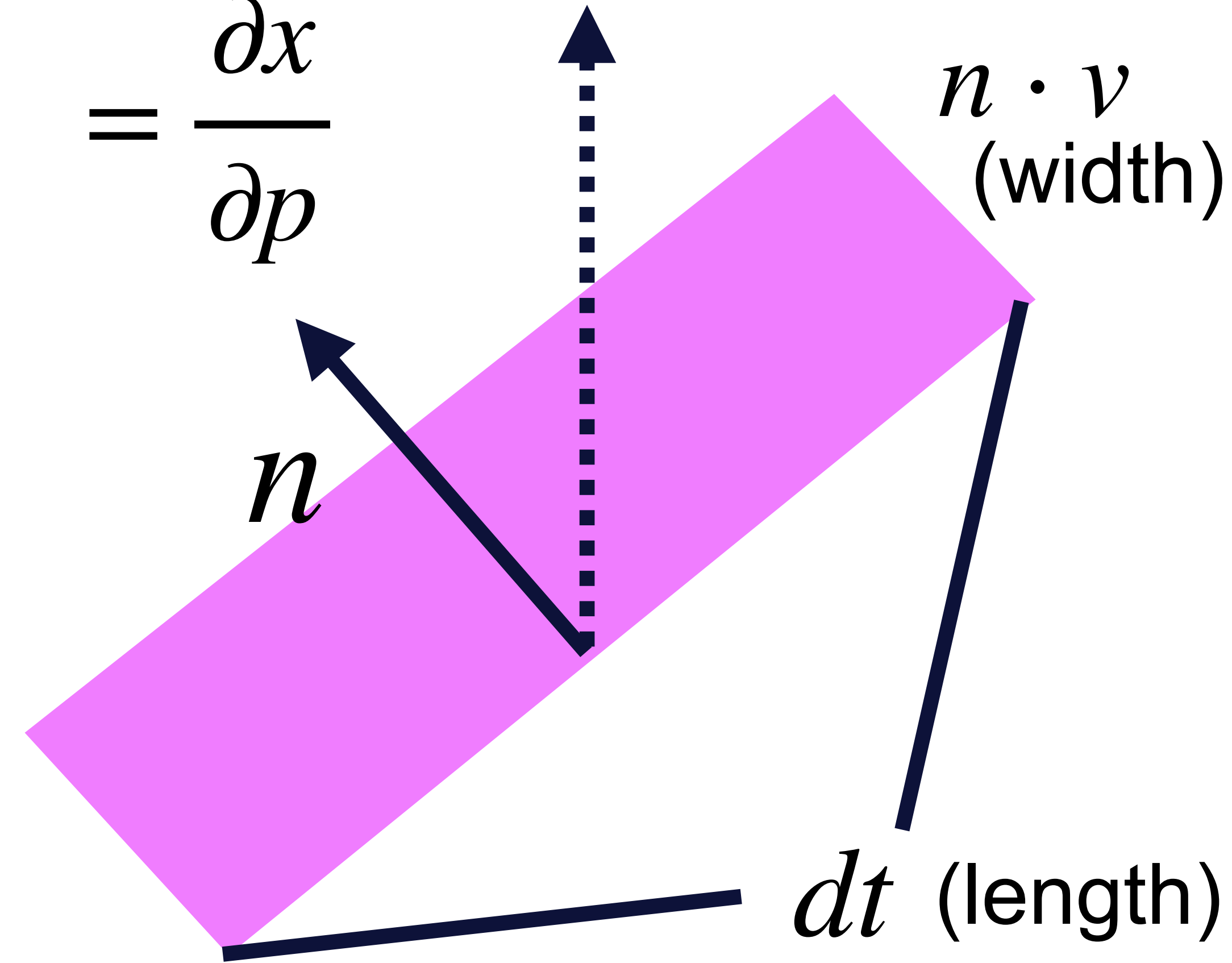
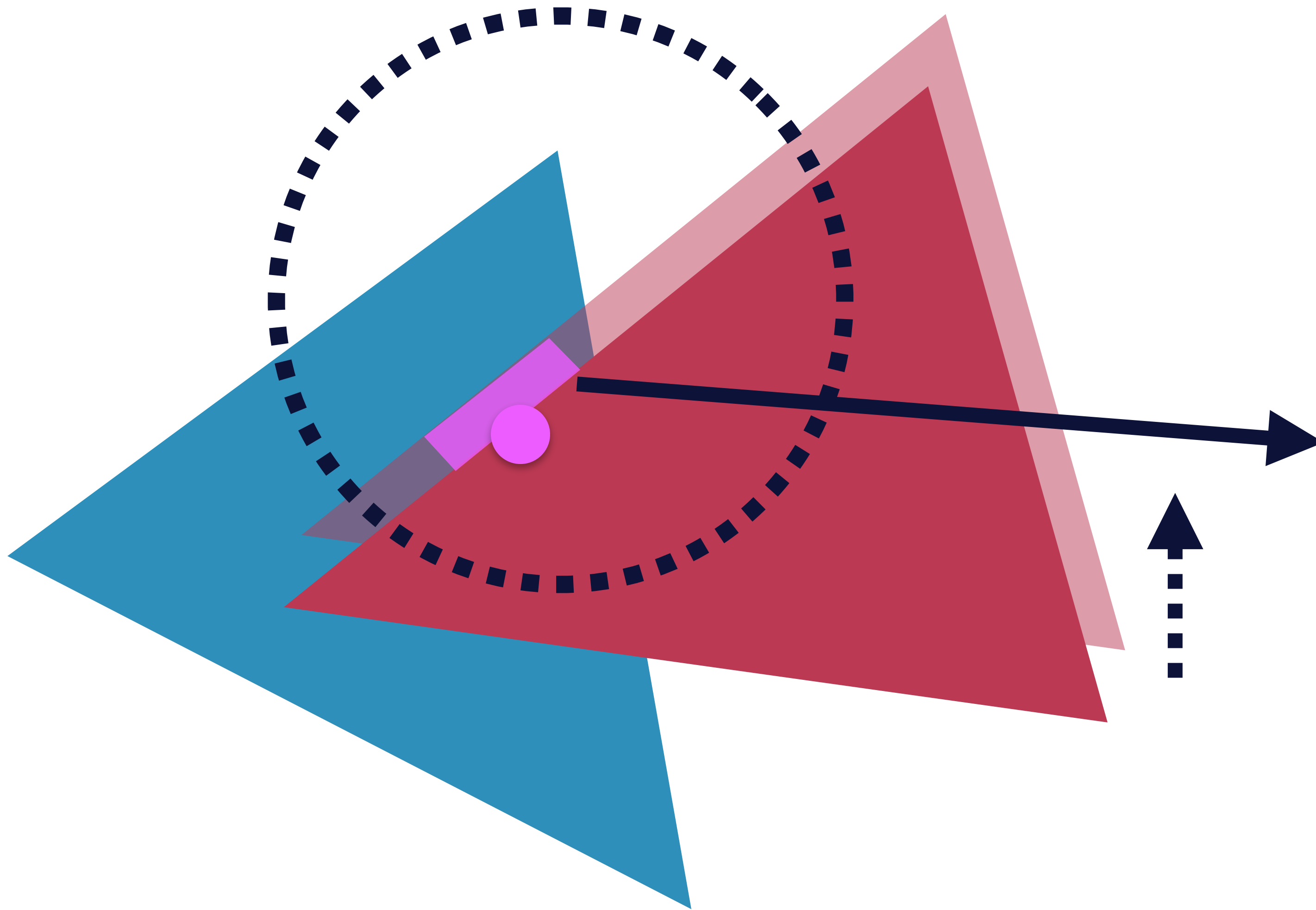
red - blue

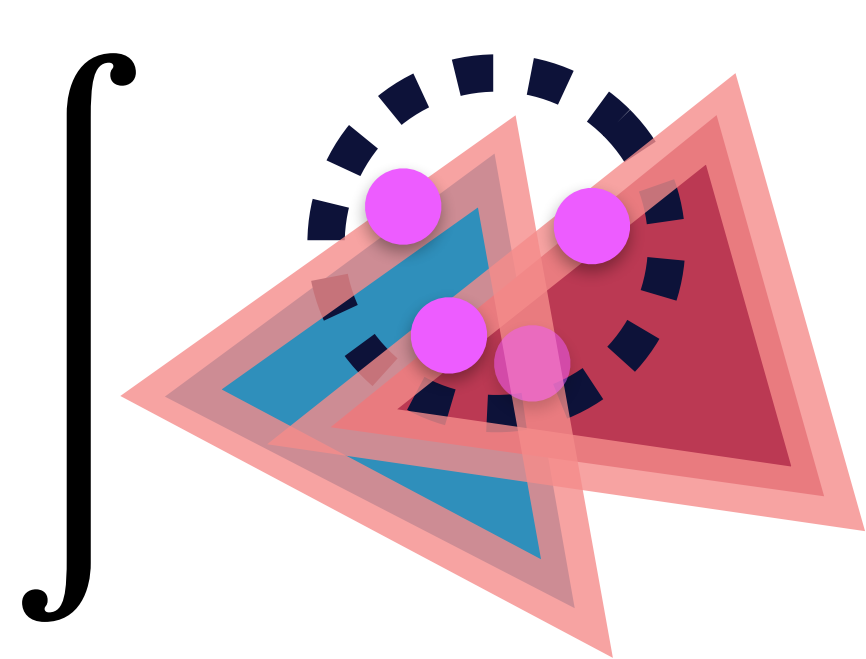


3D view around the purple sample

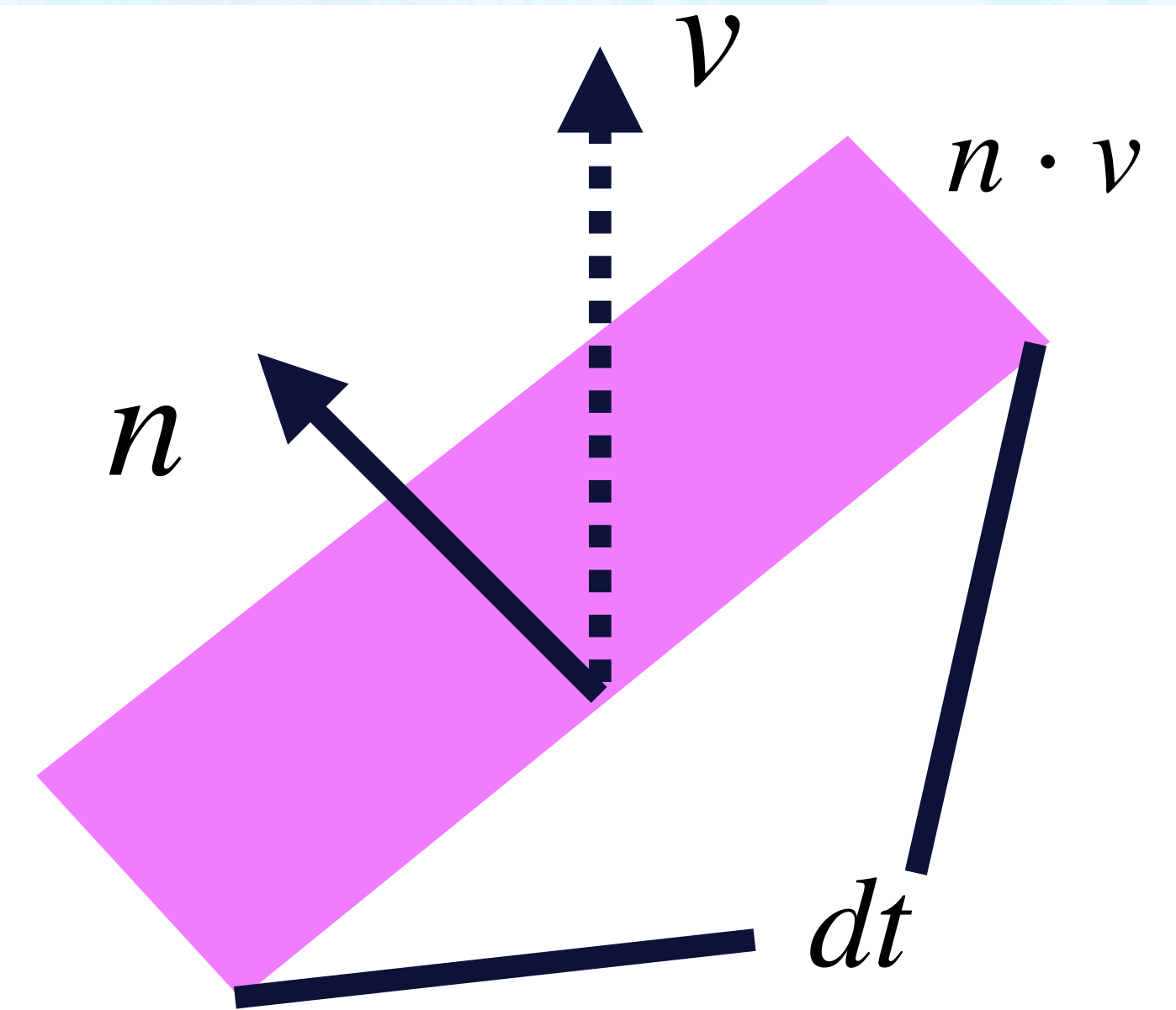
v = boundary movement w.r.t. param

$$= \frac{\partial x}{\partial p}$$

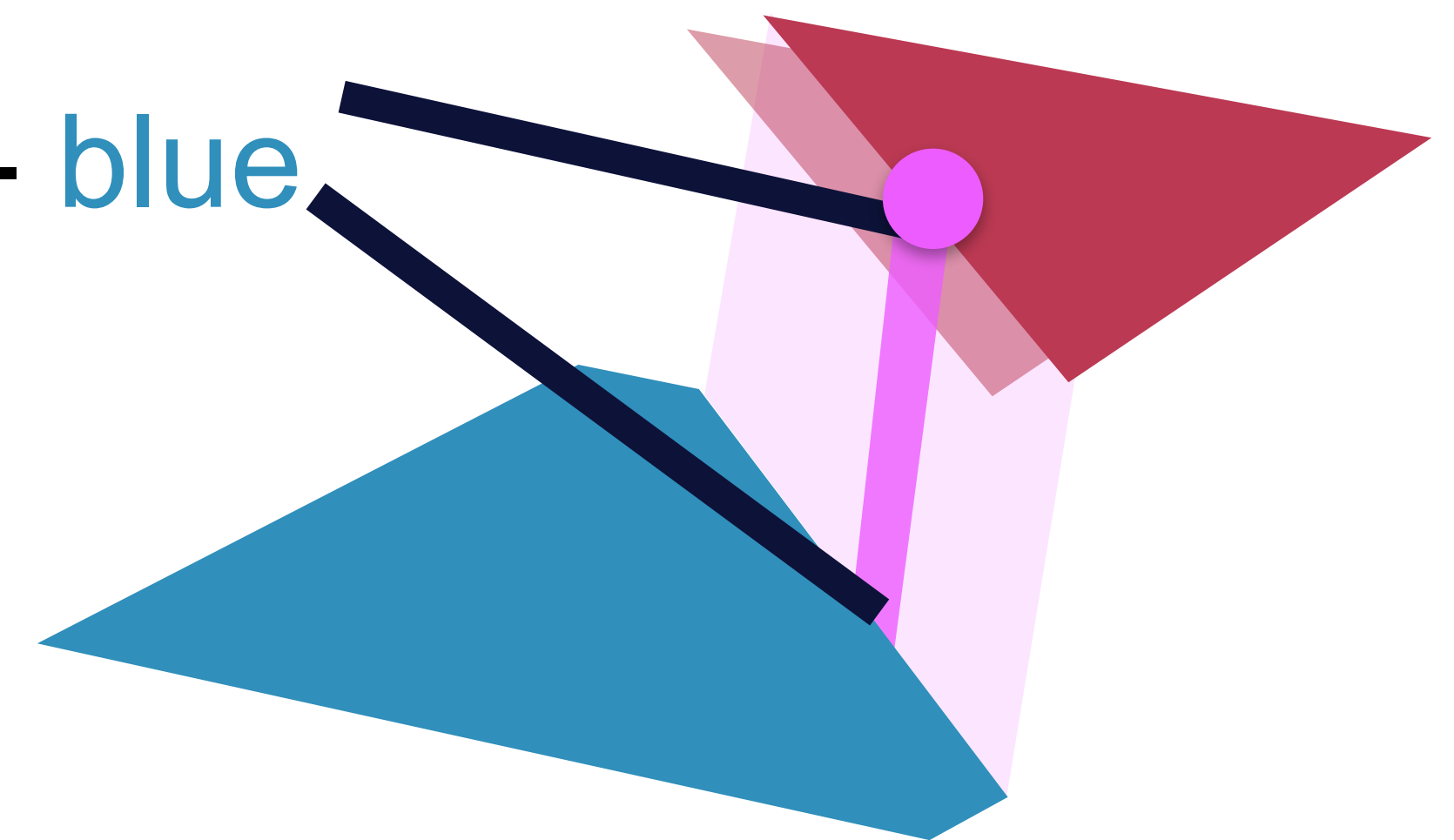




$$\int dt = \int \underbrace{(f_- - f_+)}_{\text{height}} \underbrace{(n \cdot v)}_{\text{width}} \underbrace{dt}_{\text{length}}$$

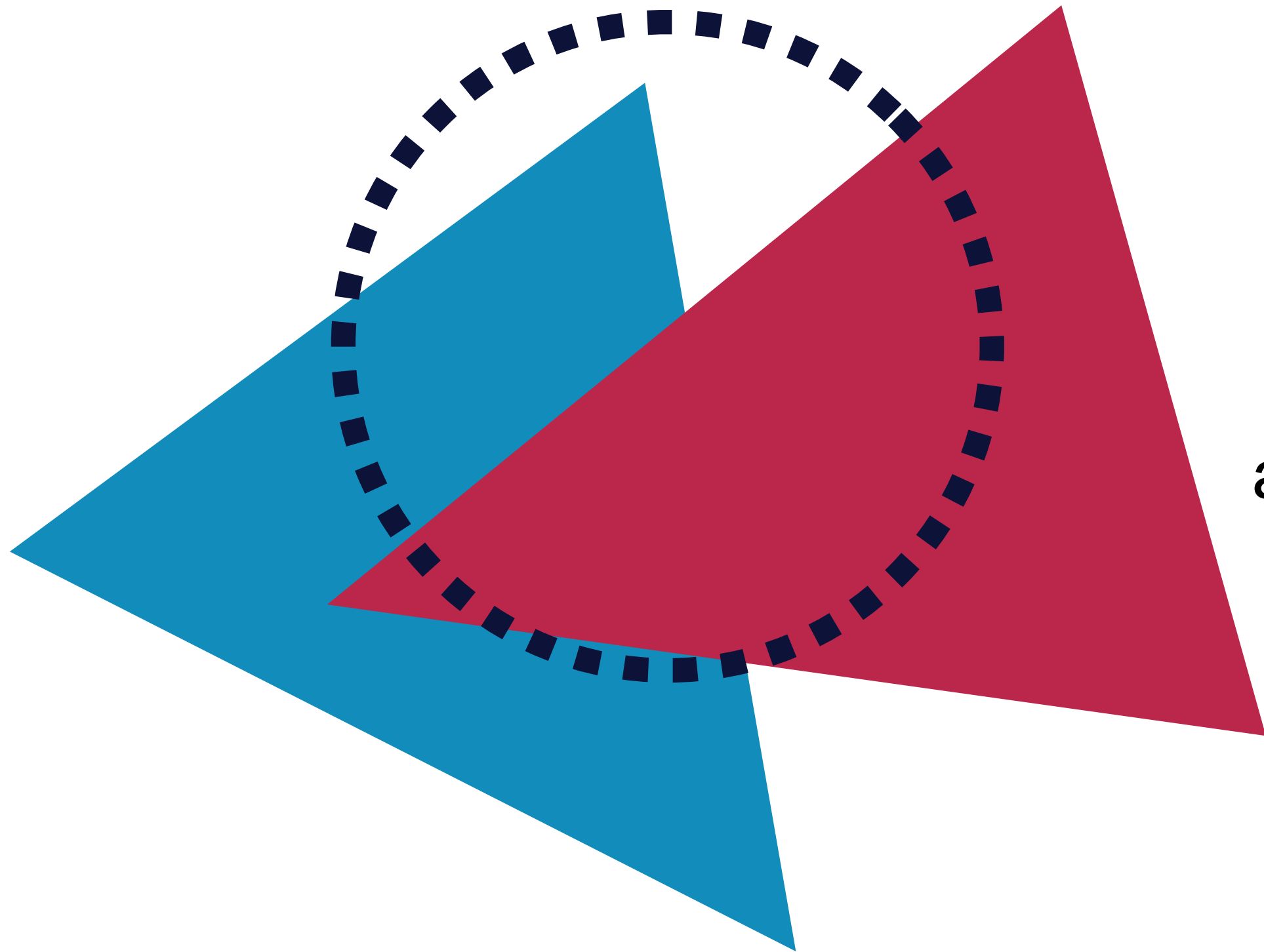


red - blue

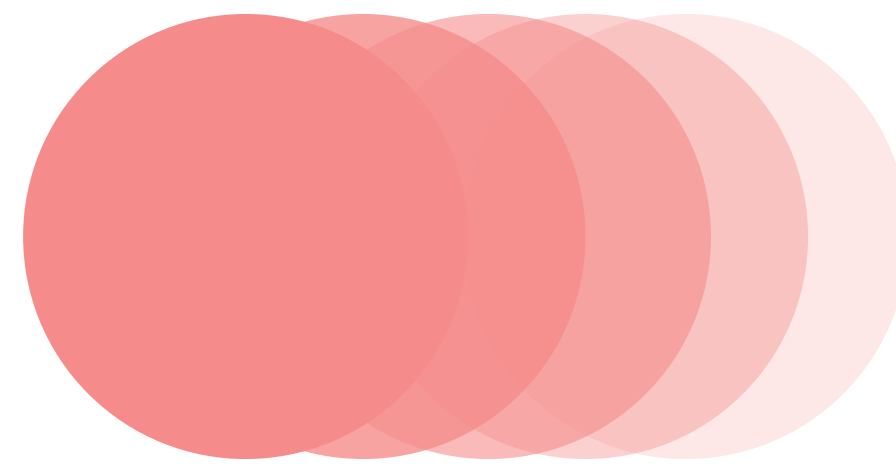


RENDERING = COMPUTING INTEGRALS

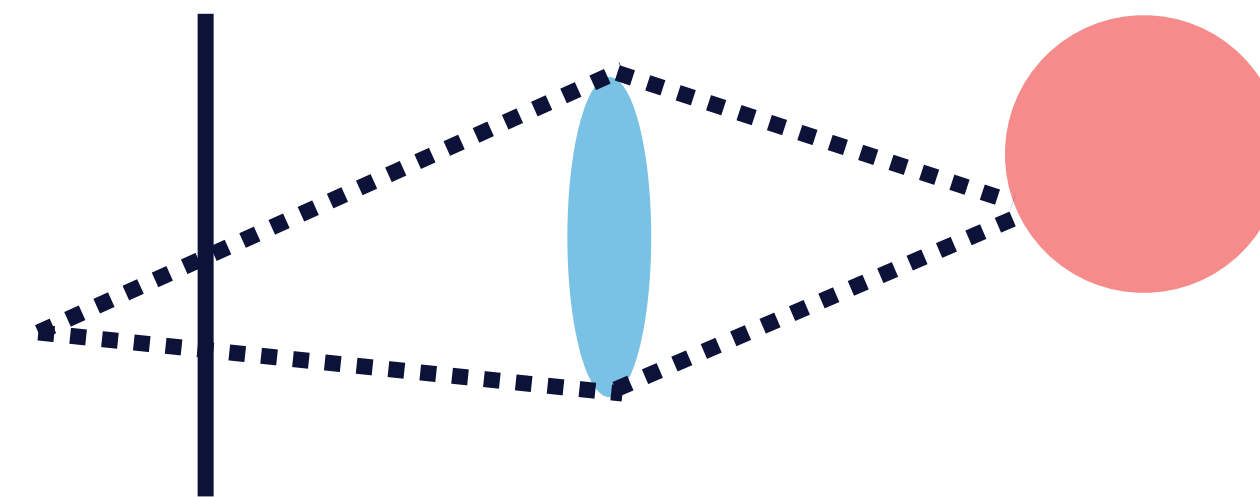
pixel filter support



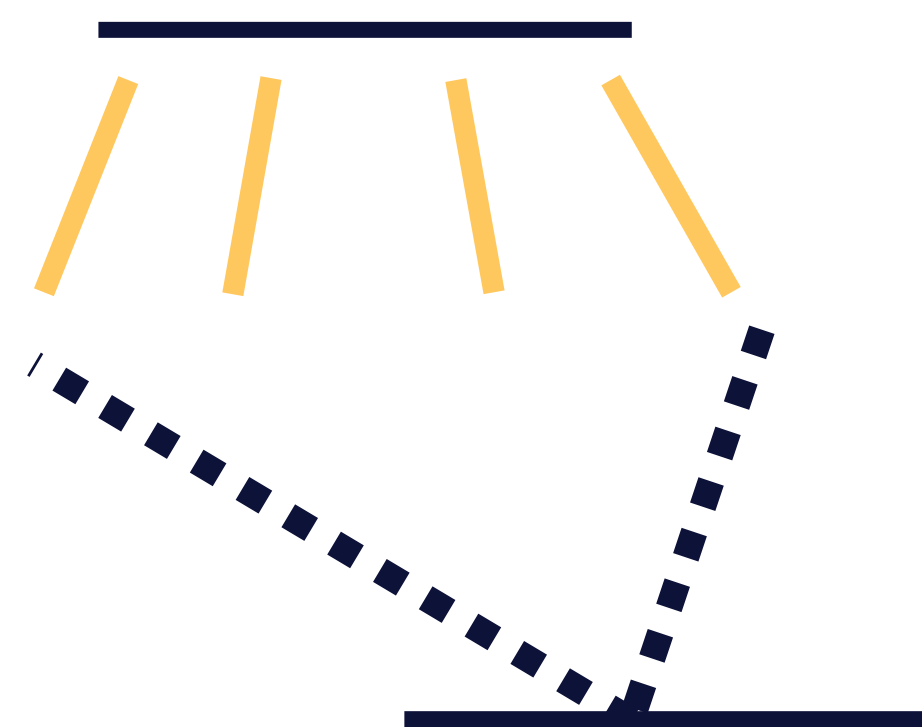
shutter time
(motion blur)



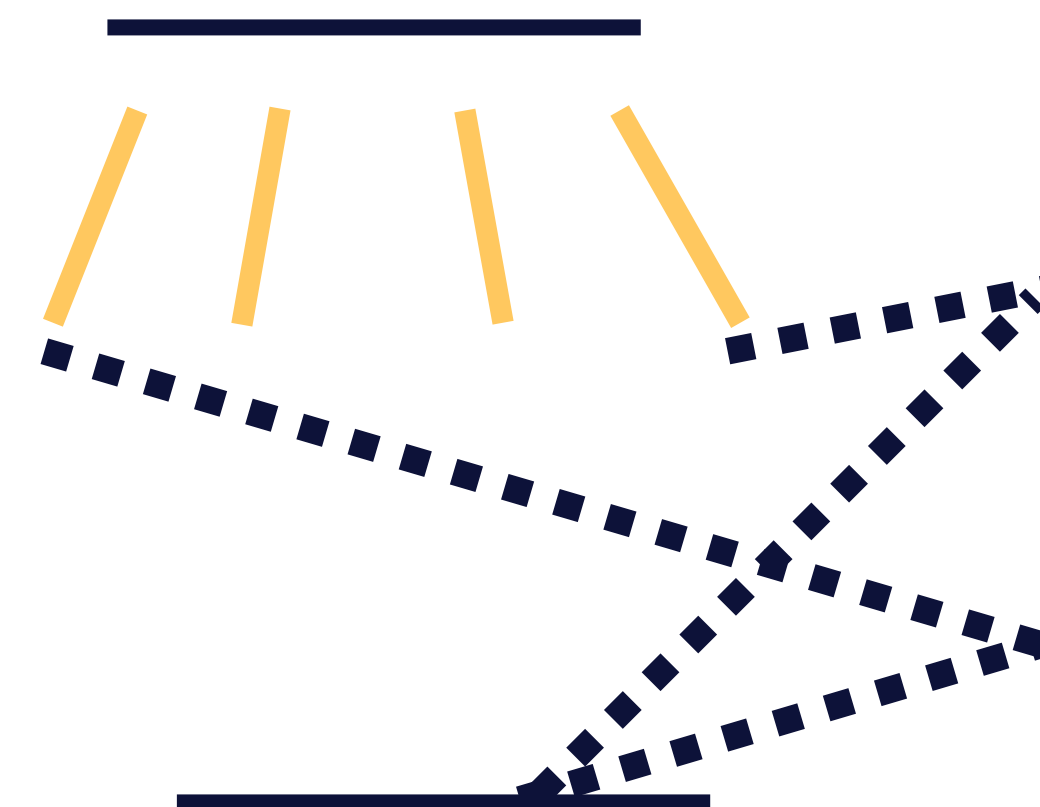
camera aperture
(defocus blur)



area light

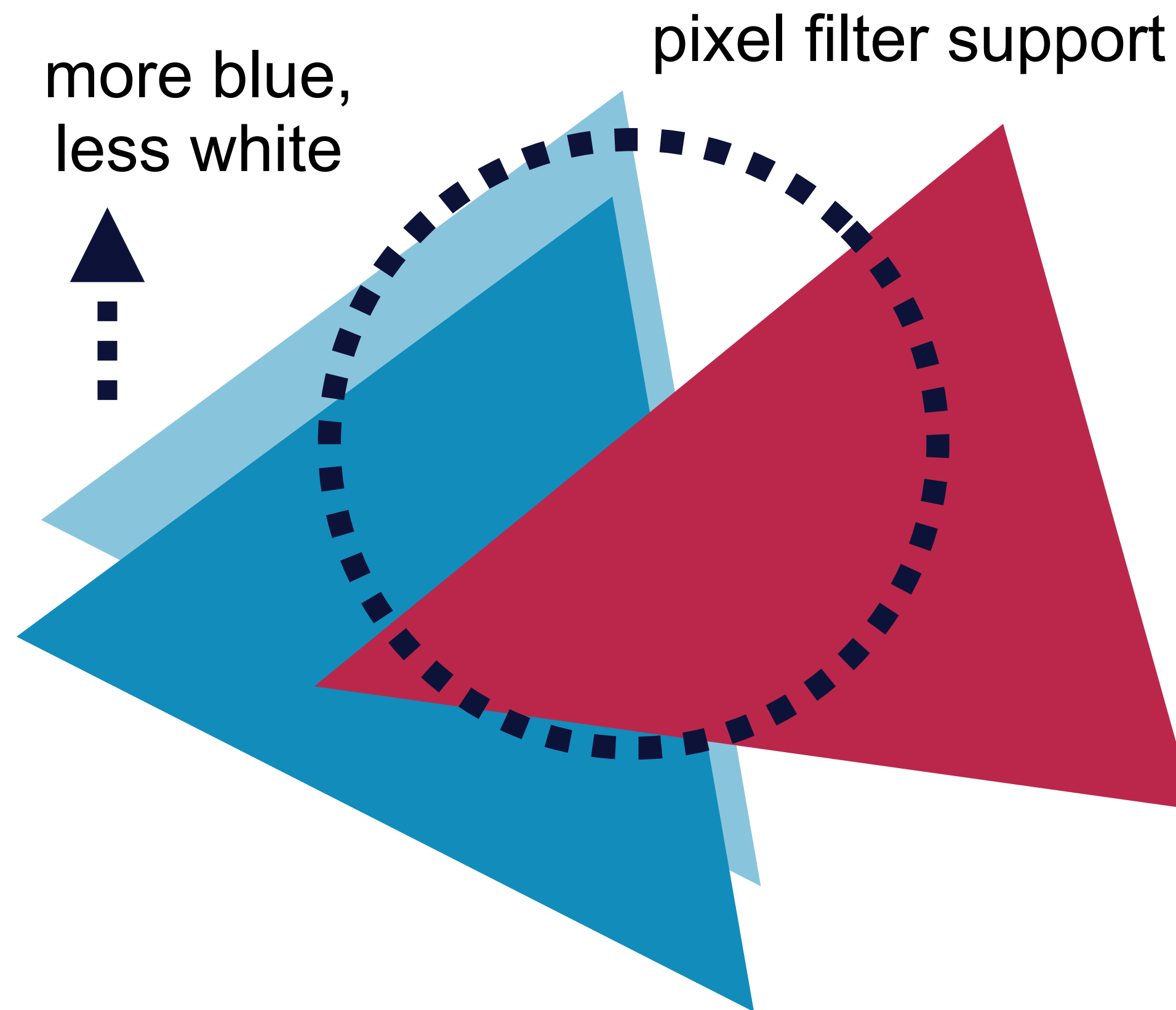


global illumination

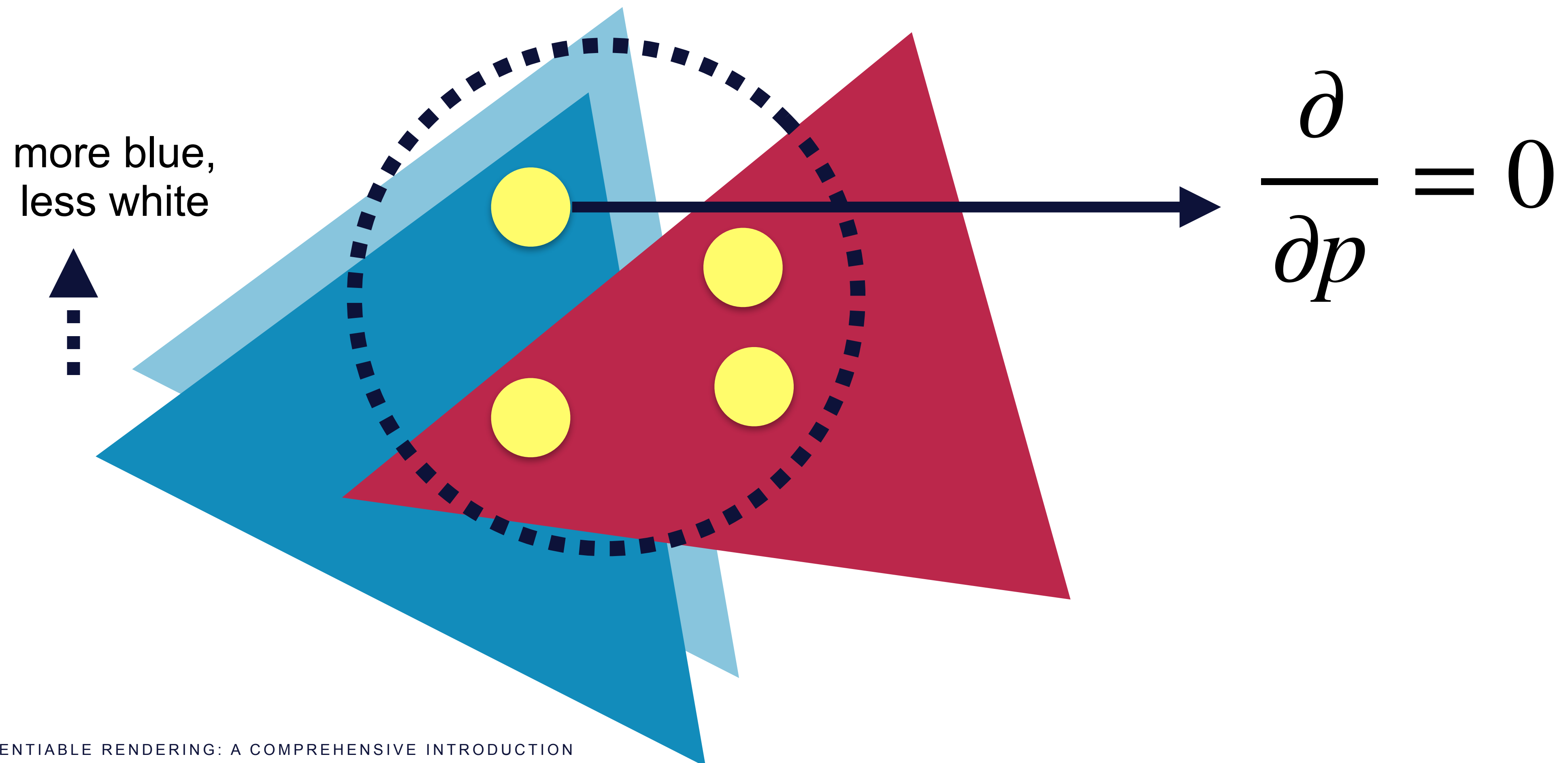


- wavelength
- transmittance
- ...
- and more!

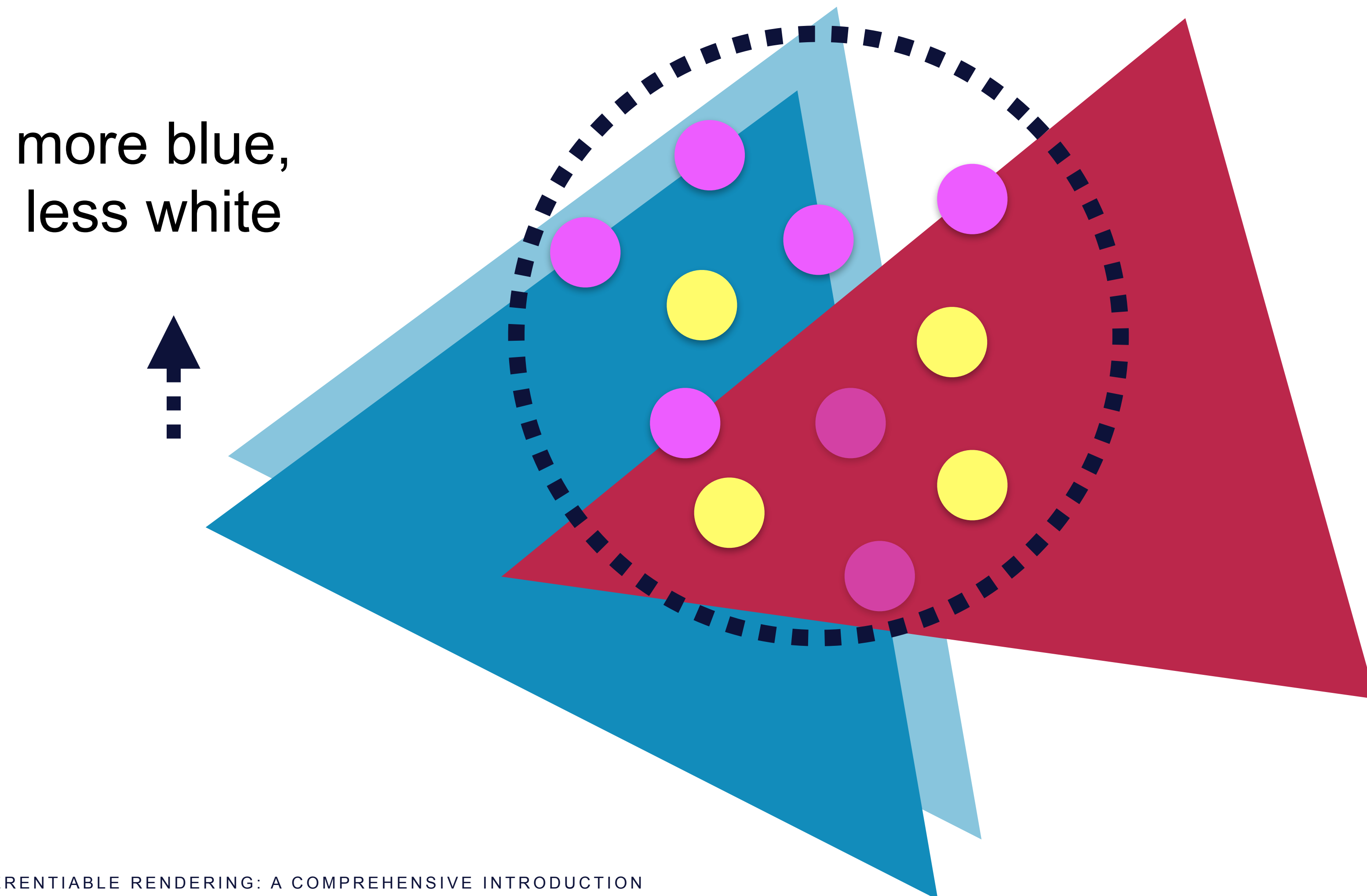
- **While the *integrand* is discontinuous, the *integral* is differentiable!**
 - the average color changes continuously as triangles move



DIFFERENTIATING INTEGRAL SAMPLES GIVES WRONG DERIVATIVES



KEY IDEA: EXPLICITLY INTEGRATE THE BOUNDARIES



interior derivative

$$\frac{\partial}{\partial p} \iint \text{[Diagram: overlapping triangles with dashed boundary]} = \iint \frac{\partial}{\partial p} \text{[Diagram: overlapping triangles with yellow dots inside dashed boundary]}$$

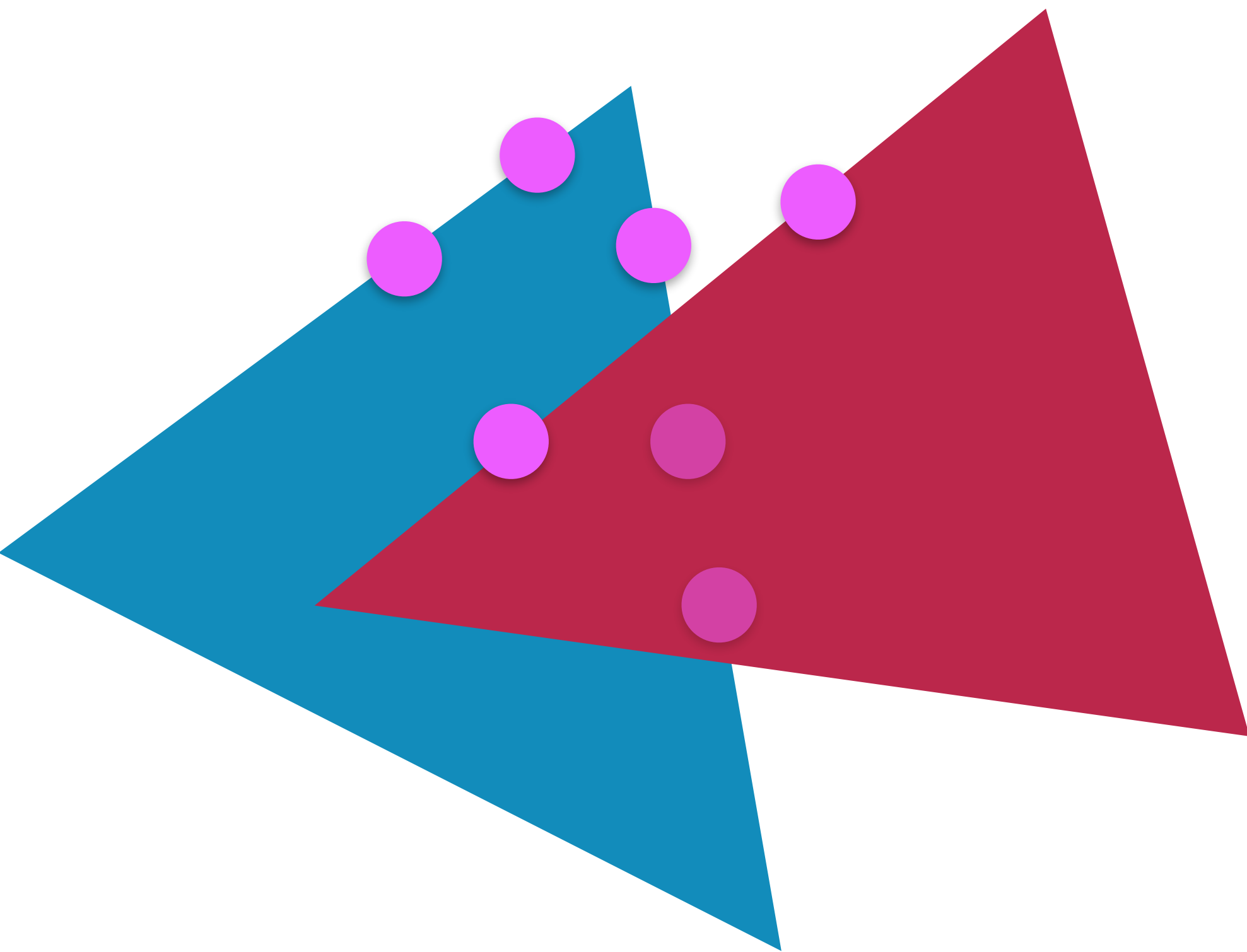
Reynolds transport theorem
[Reynolds 1903]

$$+ \int \text{[Diagram: overlapping triangles with pink dots on dashed boundary]}$$

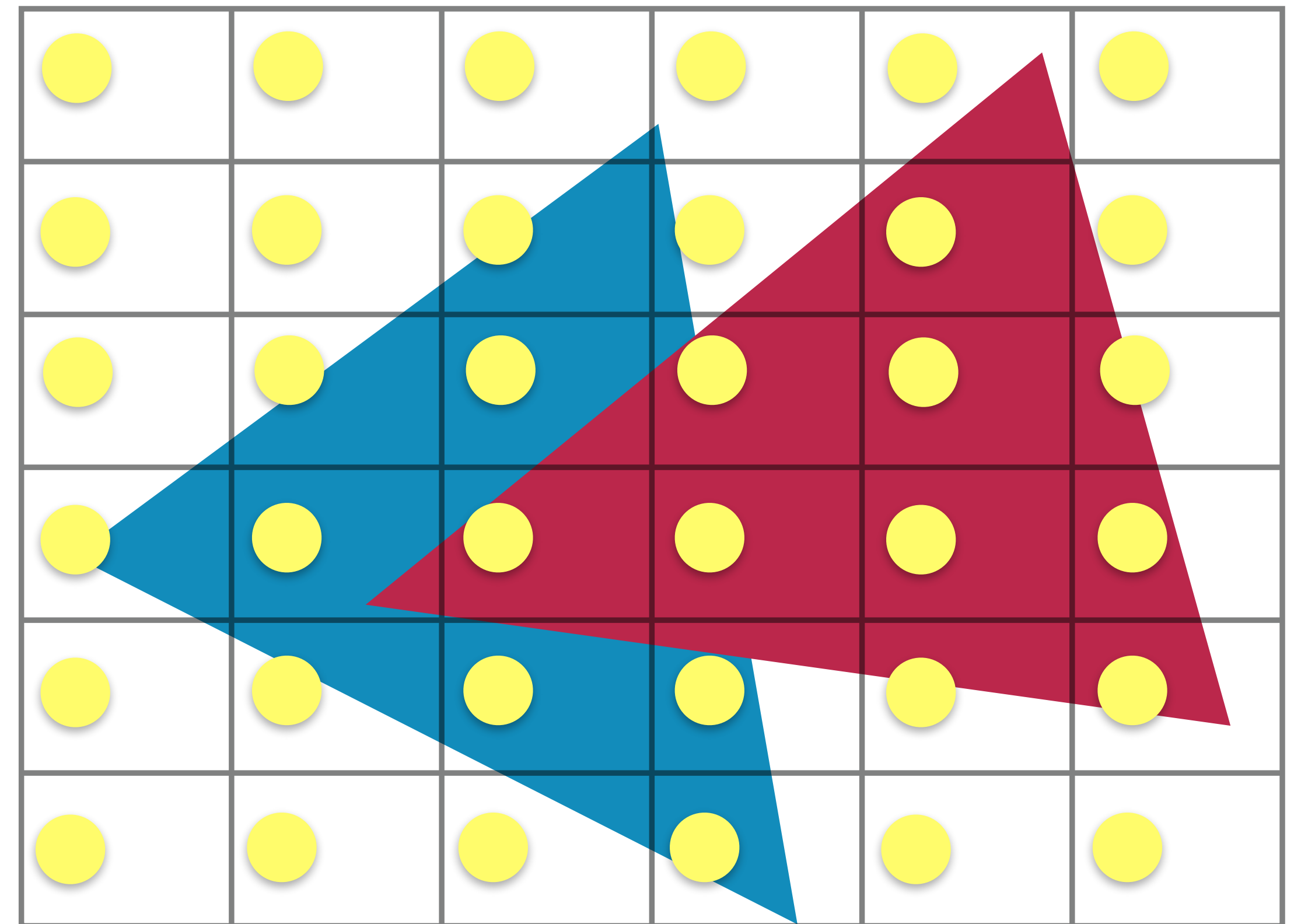
boundary derivative

- Ray tracing vs rasterization
- Approximated solutions
- Geometry representation
- Limitations

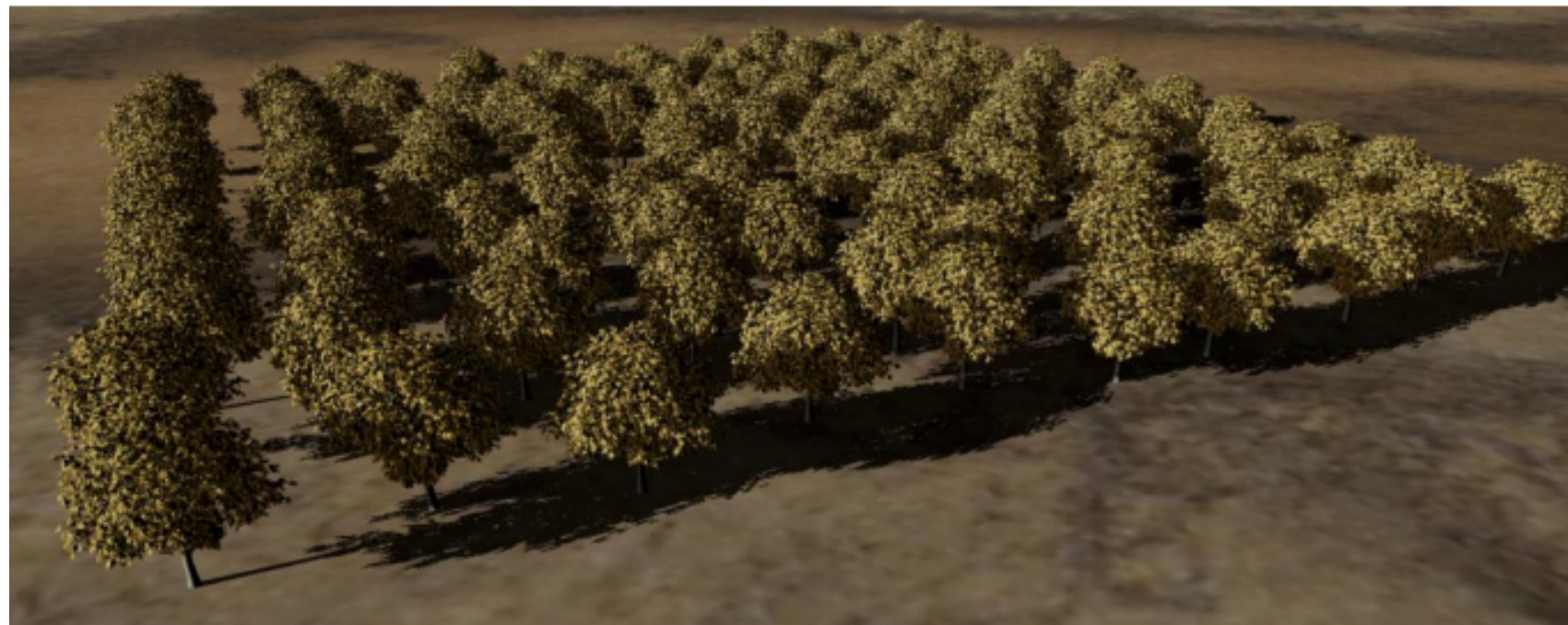
- The boundary sampling is not very compatible with z-buffer rendering



V.S.



- Ray tracing is not significantly slower than rasterization
- The interior derivatives can be computed using rasterization



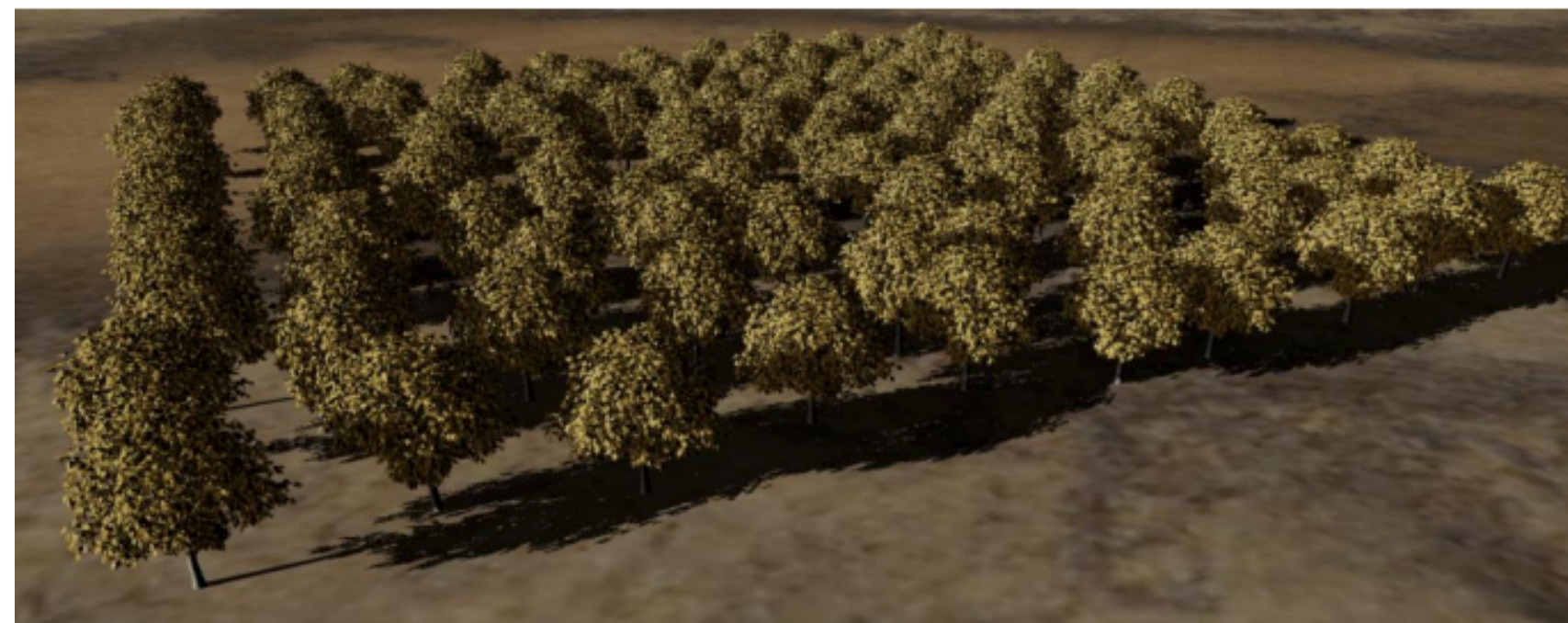
from Gruen 2020

1080p, ~19M triangles

raster: 2.7 ms

raytrace: 8.6 ms (2.5 ms for animation)

- Ray tracing is not significantly slower than rasterization
- The interior derivatives can be computed using rasterization
- Visibility queries may not be the main bottleneck

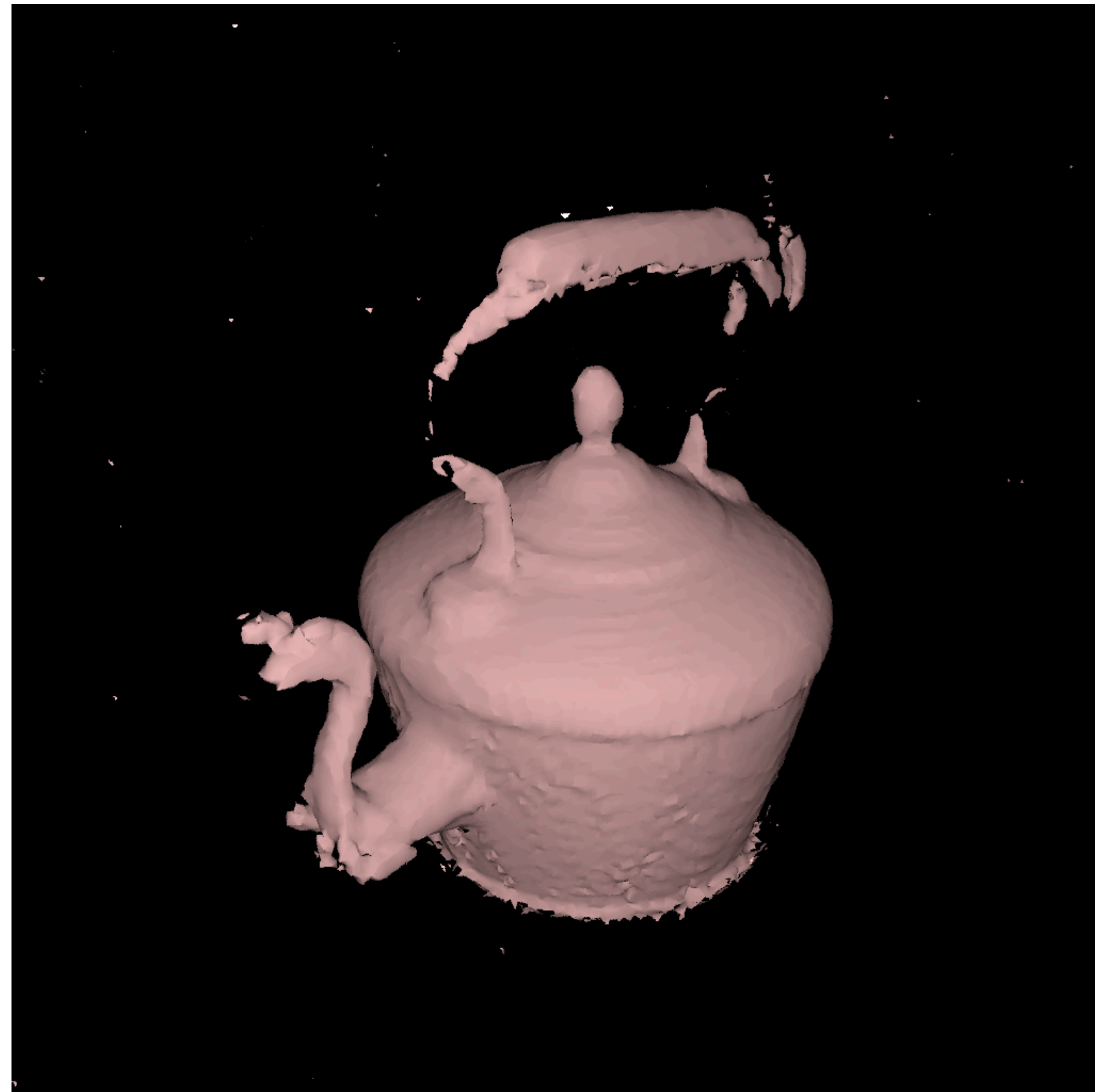


from Gruen 2020
1080p, ~19M triangles
raster: 2.7 ms
raytrace: 8.6 ms (2.5 ms for animation)



~10k faces, 256x256 (Titan Xp)
PyTorch3D (raster) 220ms
redner (raytrace) 60ms
(BVH 20ms, forward 7ms, backward 27ms)

23823 vertices, 44702 faces



initial



target

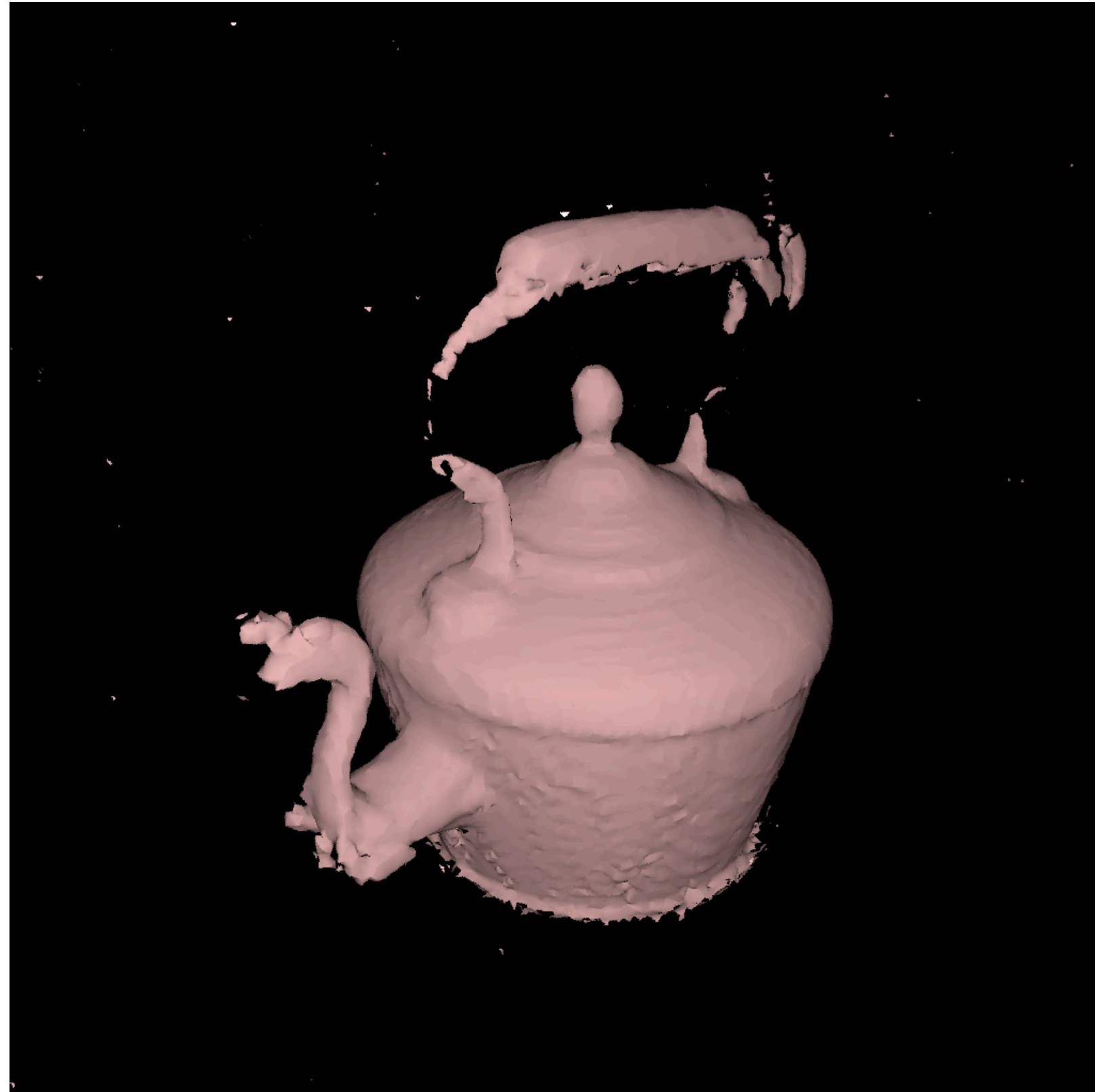
- 1024x1024 at 2 spp (Titan Xp) forward + backward
- Ray tracing + edge sampling: 0.05—0.1 sec
- PyTorch3D: 0.15 sec

RAY TRACING VS RASTERIZATION

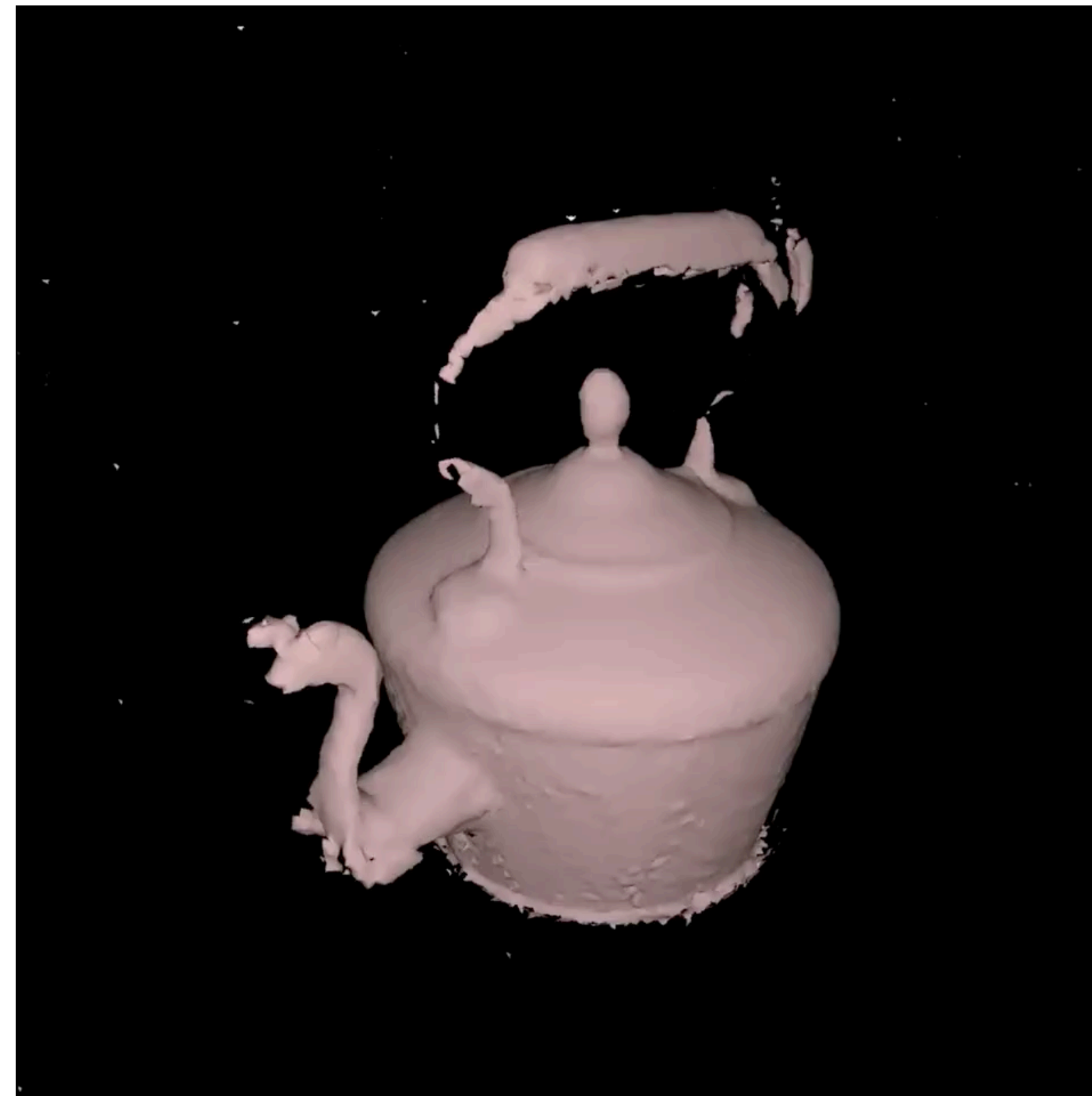
23823 vertices, 44702 faces

Low

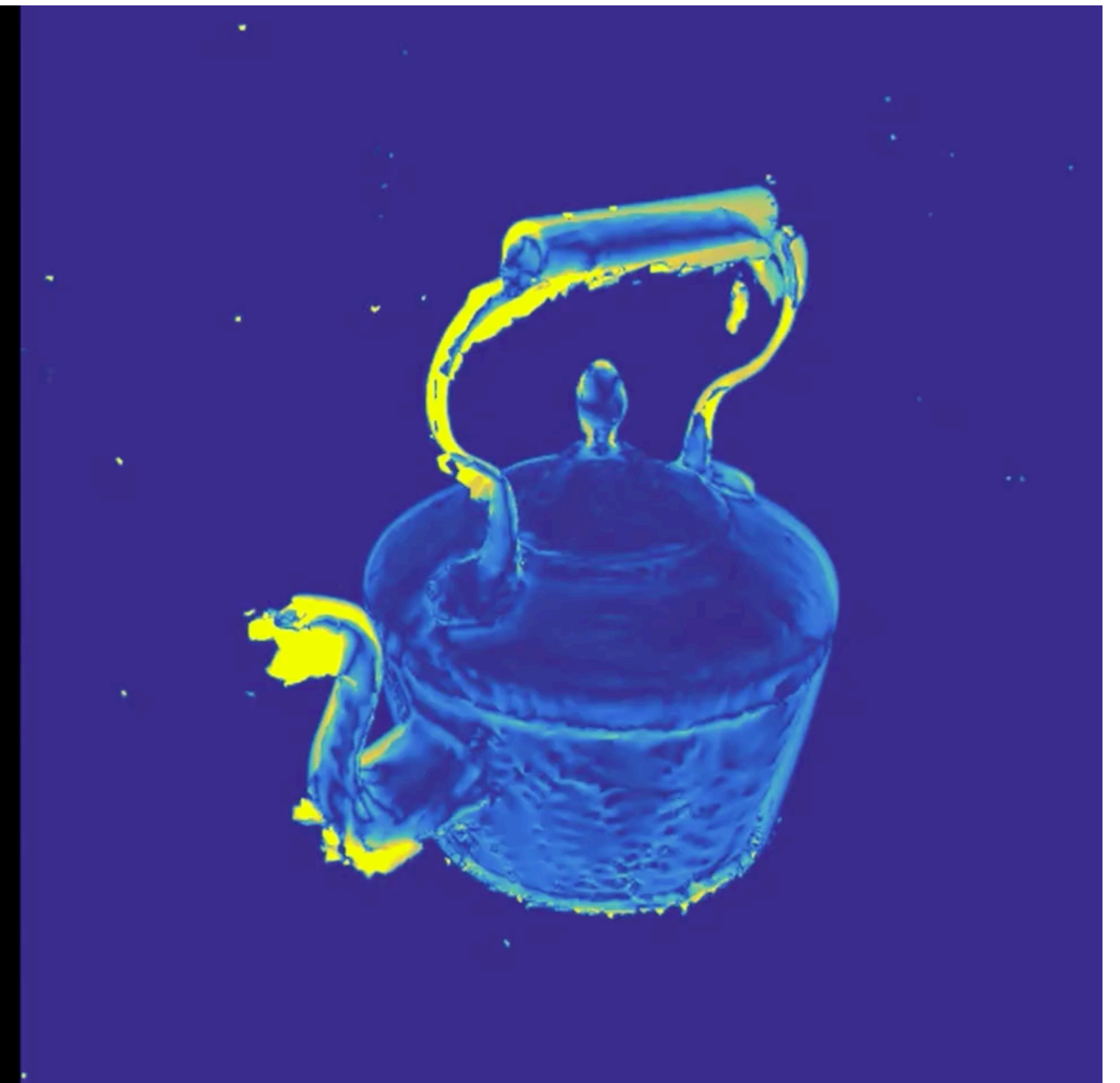
High



initial



edge sampling
optimization video
(1 view over 20)



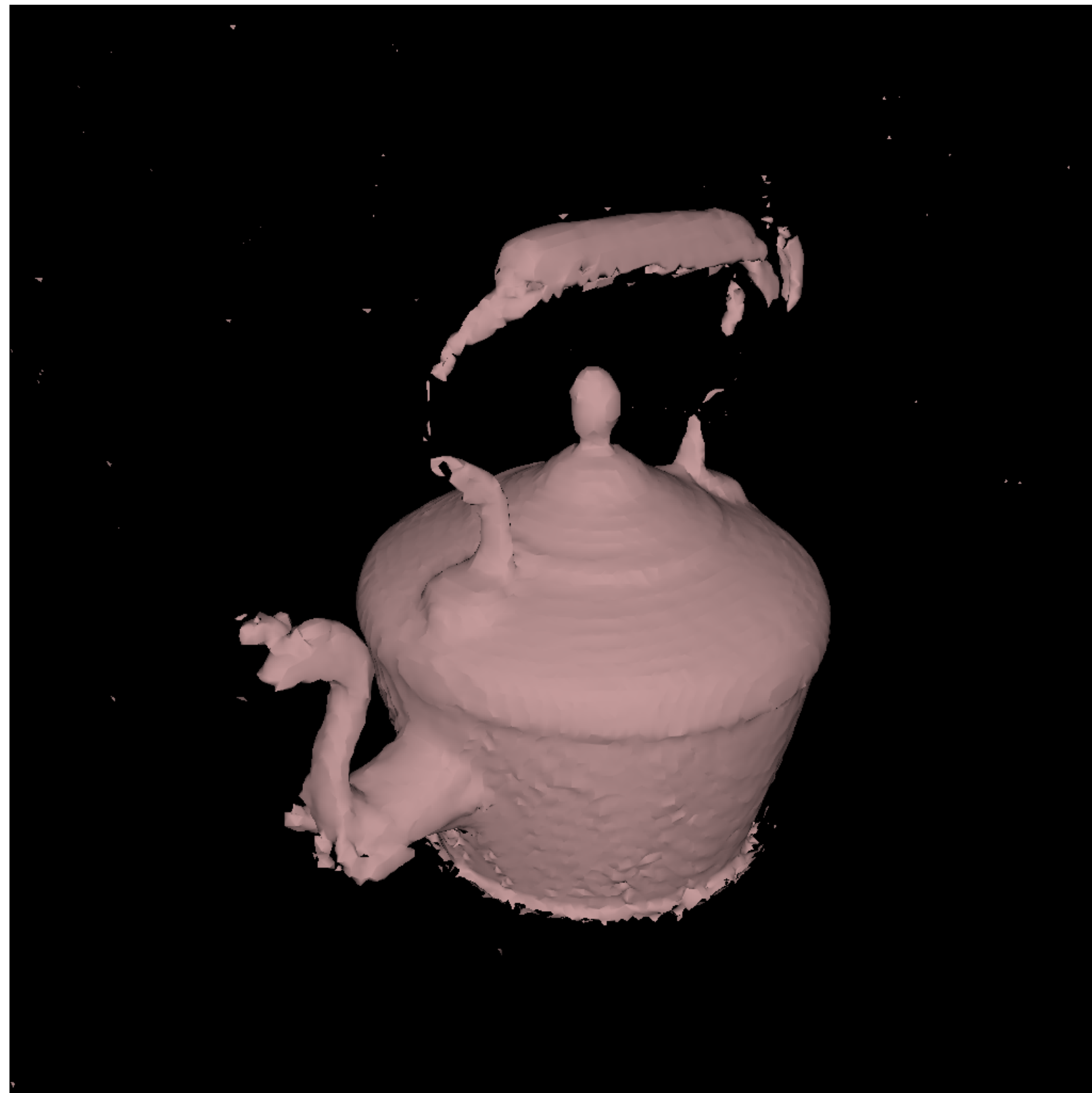
abs. error

RAY TRACING VS RASTERIZATION

23823 vertices, 44702 faces

Low

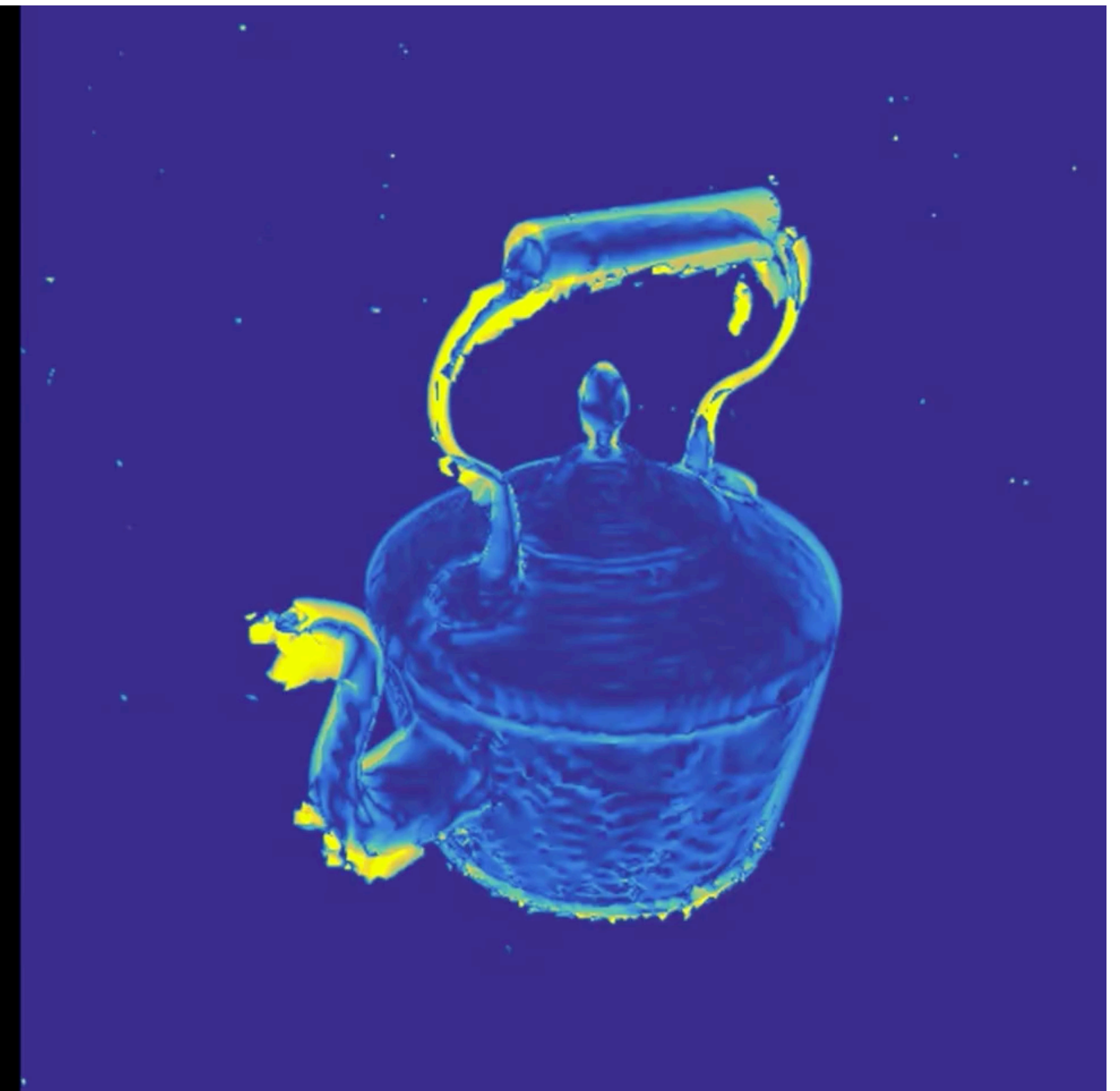
High



initial



PyTorch3D
optimization video
(1 view over 20)



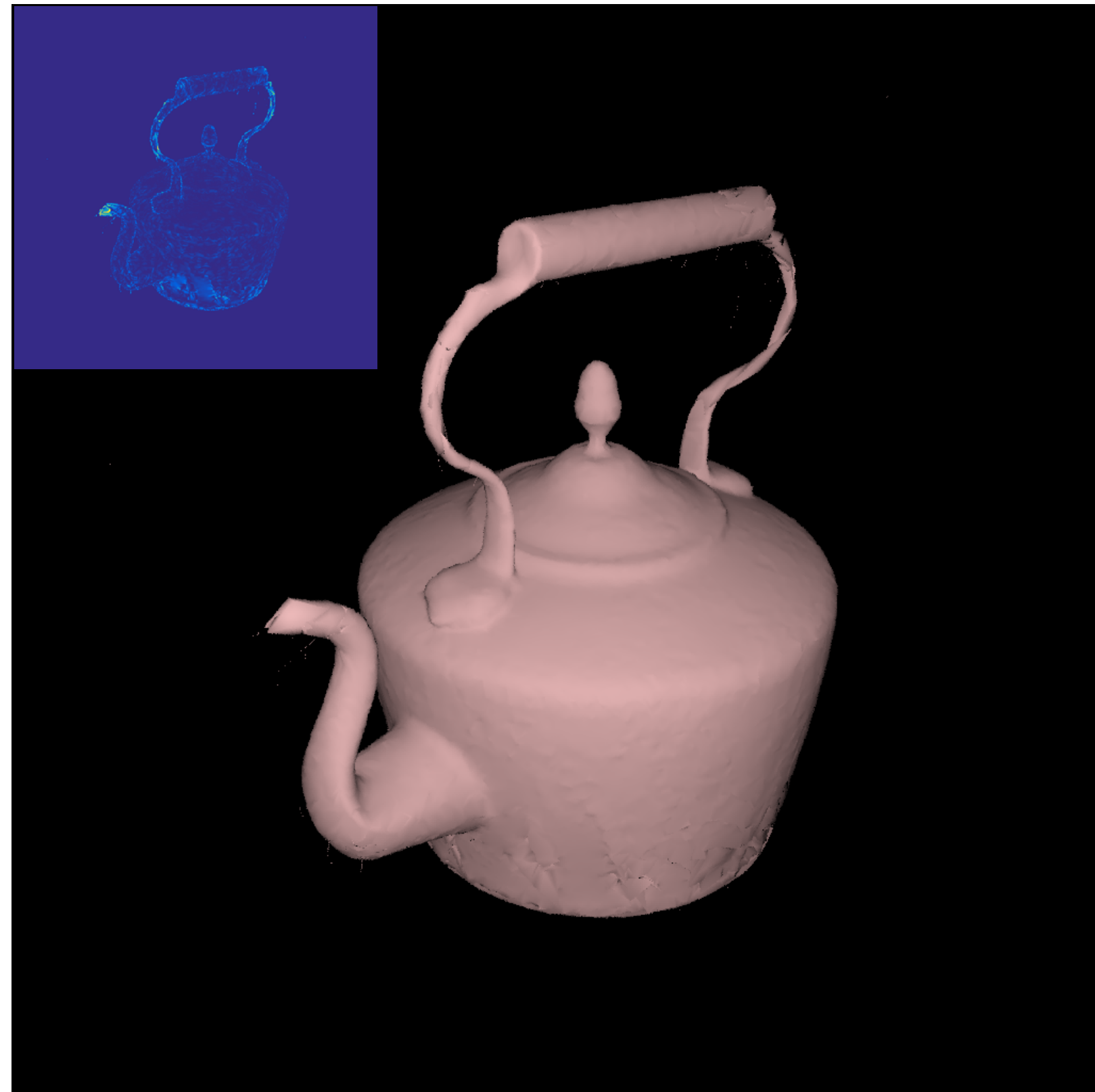
abs. error

RAY TRACING VS RASTERIZATION

Optimization results after 5000 iterations (with identical settings)

Low

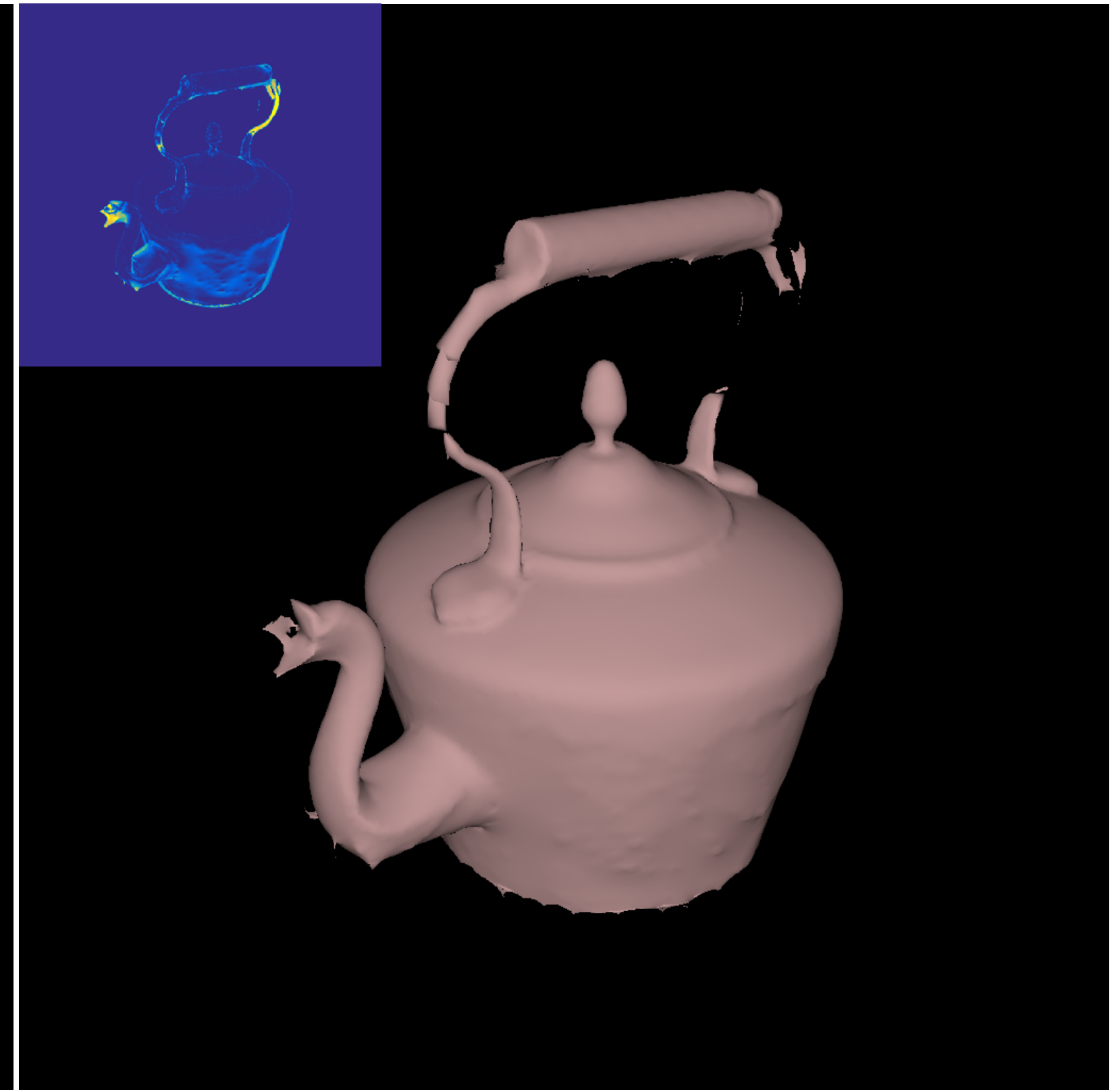
High



optimized (ray tracing)

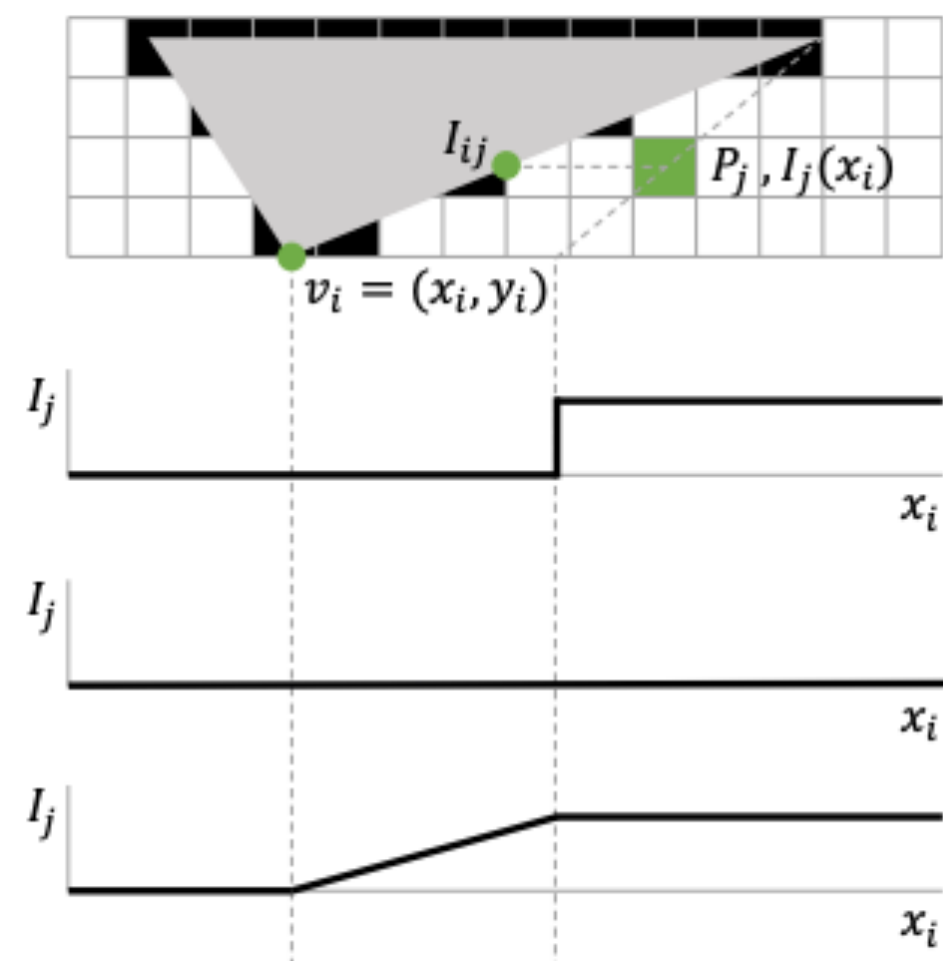


target



optimized (PyTorch3D)

- Our boundary integral is *correct, i.e.*, when the number of samples grows it converges to the integral.
- Two other kinds of approximation:
 - Keep the rendering model, approximate the derivatives (de La Gorce 2011, OpenDR 2014, Kato 2018, ...)
 - Change the rendering model (Rhodin 2015, SoftRas 2019, PyTorch3D 2020...)



Kato 2018



Rhodin 2015

Blend closest K faces in the Z direction

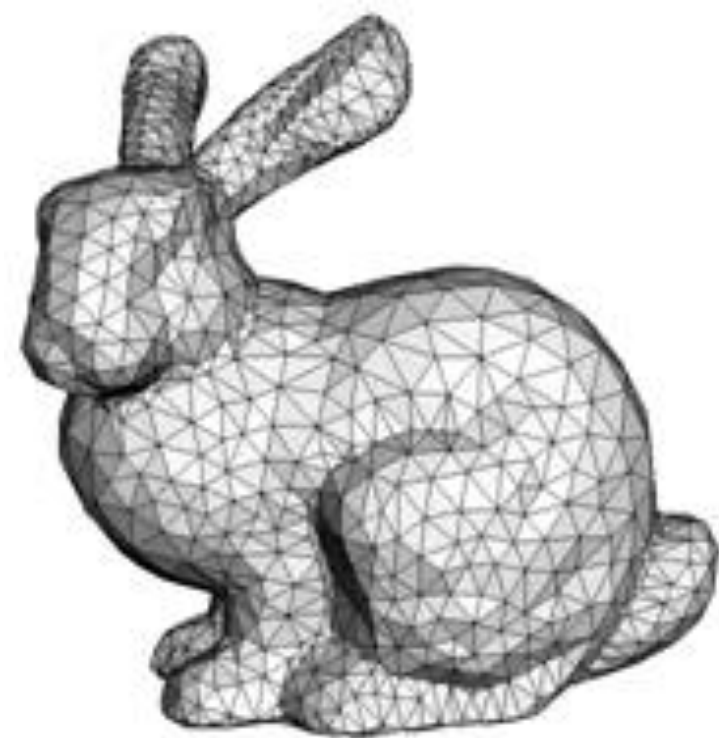


Consider faces which fall within a blur radius

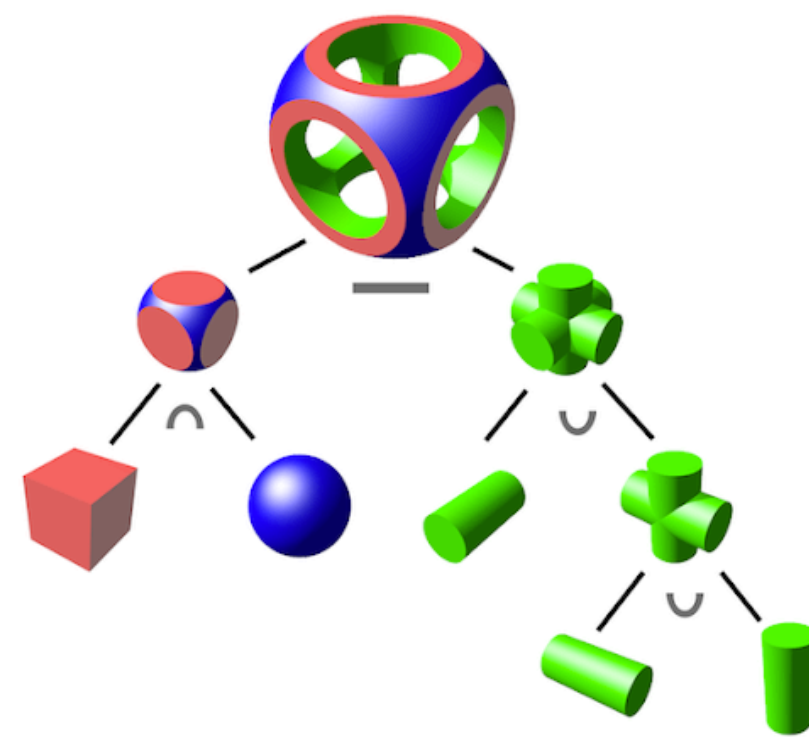


PyTorch3D [Ravi 2020]

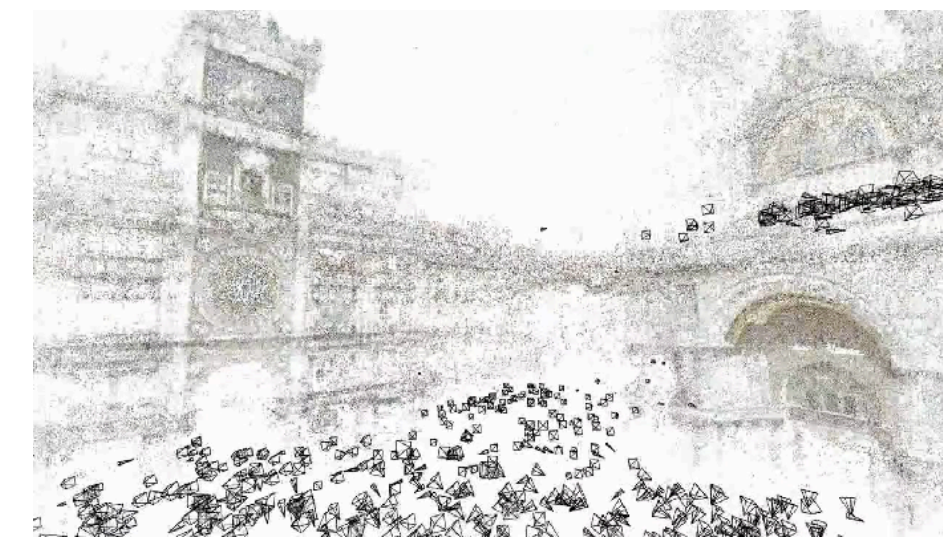
- Need boundary extraction — easier for meshes, harder for implicit representations and fractals



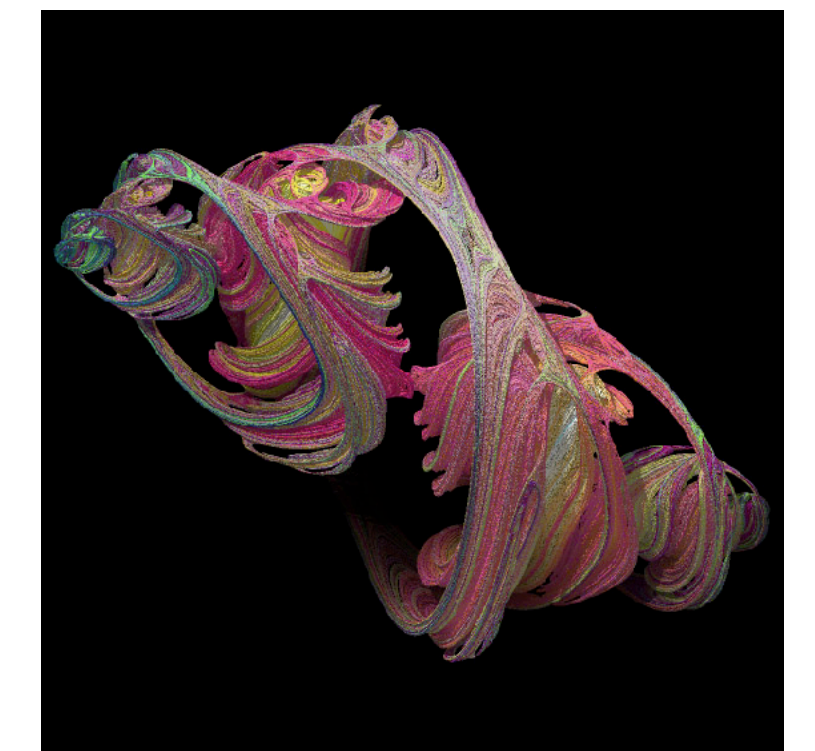
mesh



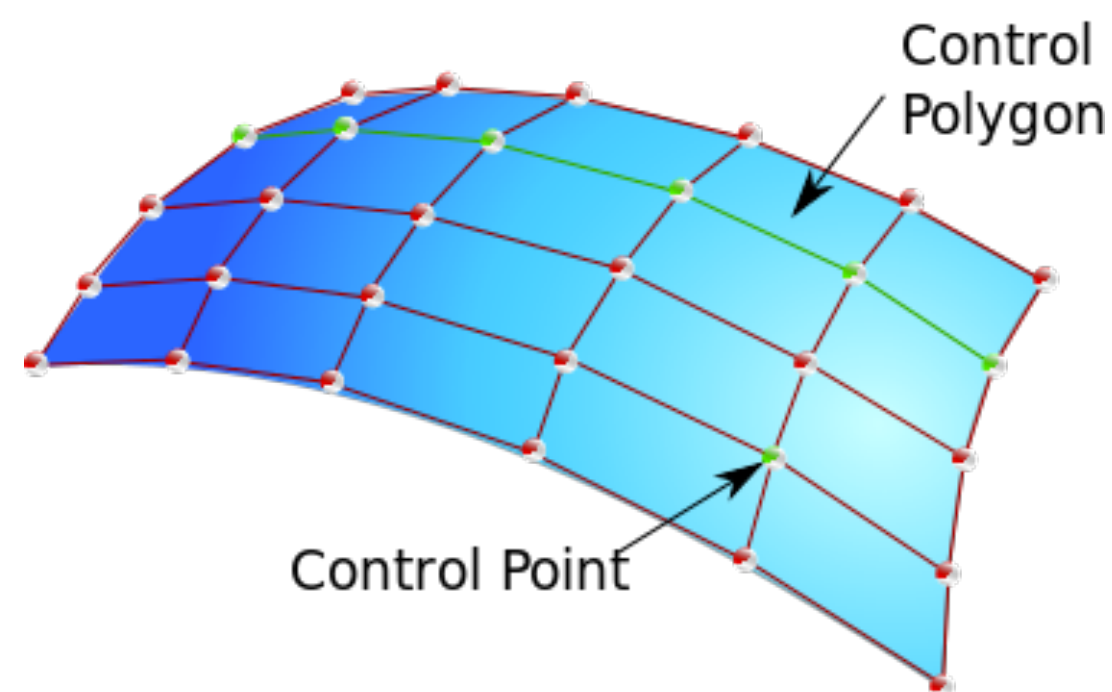
CSG



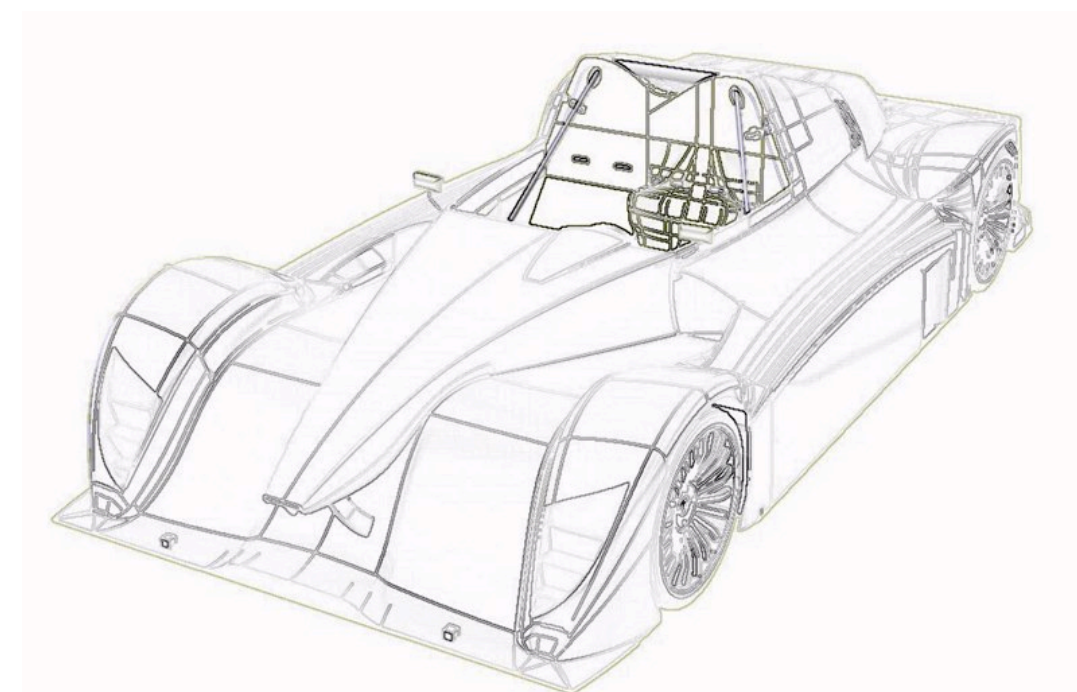
point cloud



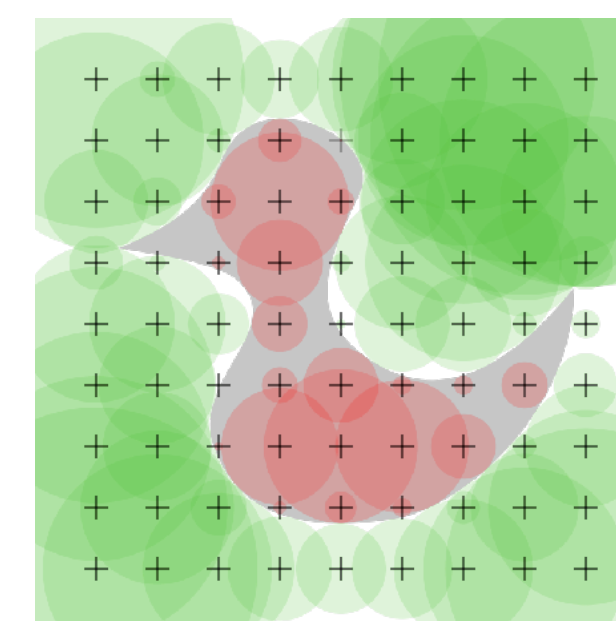
fractal



NURBS



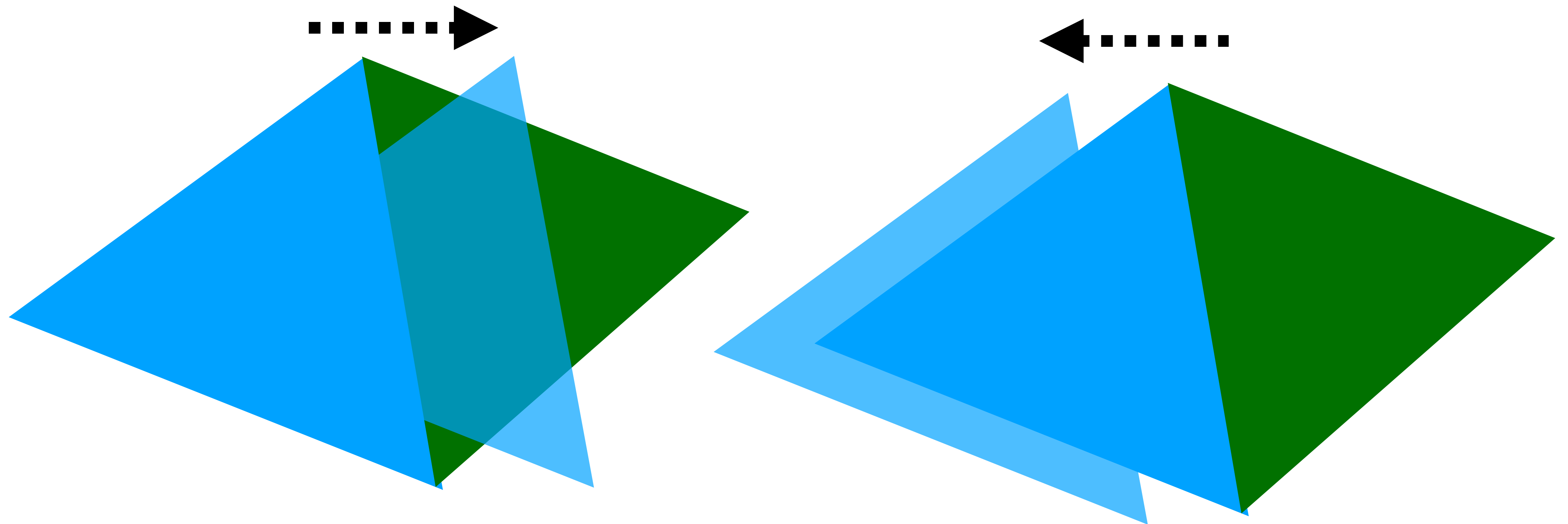
B-rep



SDF

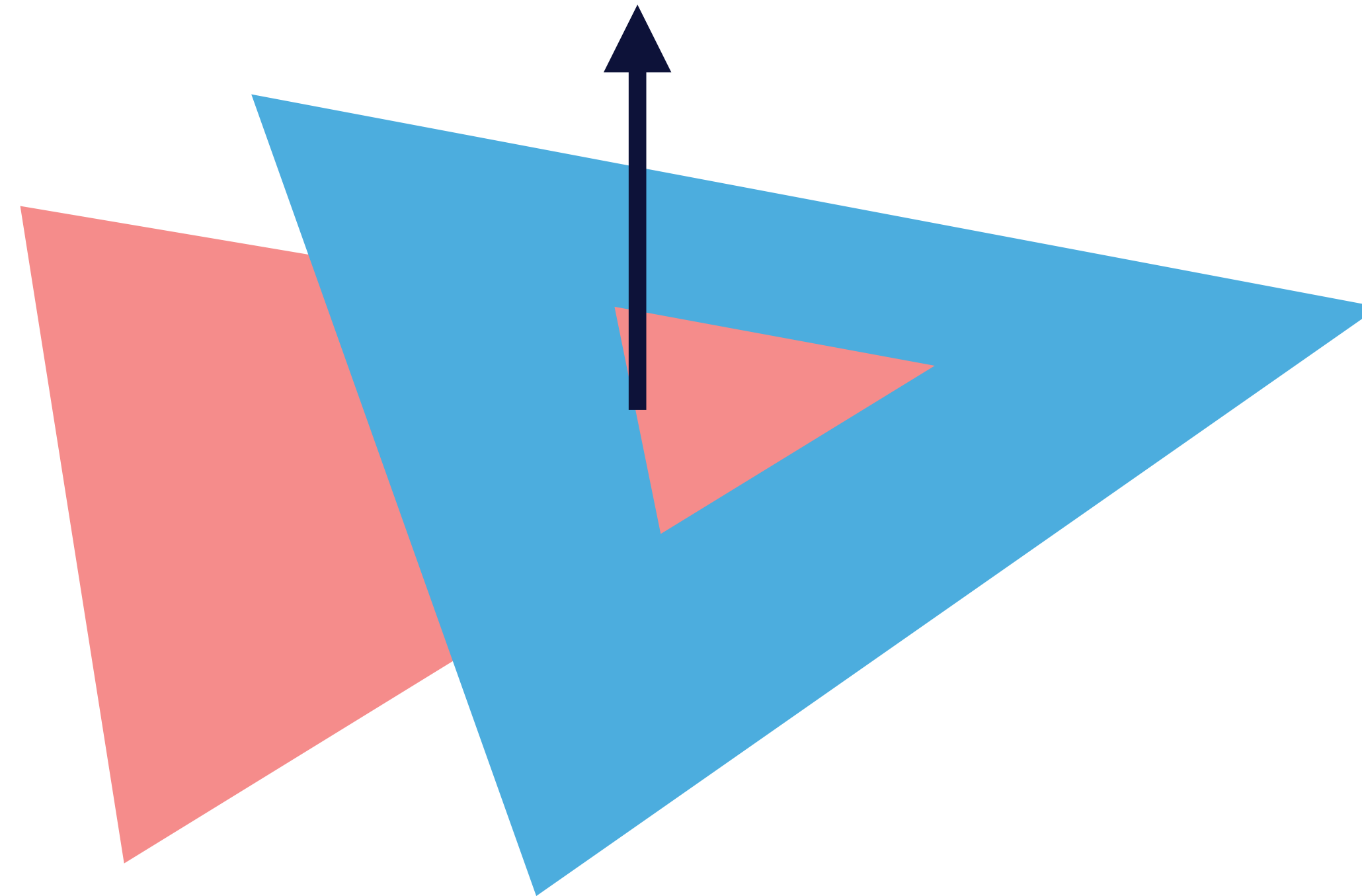
*images courtesy of
Carlson et al., Vladsinger,
Agarwal et al.,
Pso, Solkoll, Zottie,
Drummyfish*

- Non-differentiability of parallel edges of two separate triangles
 - can be resolved by applying a small perturbation to the vertices

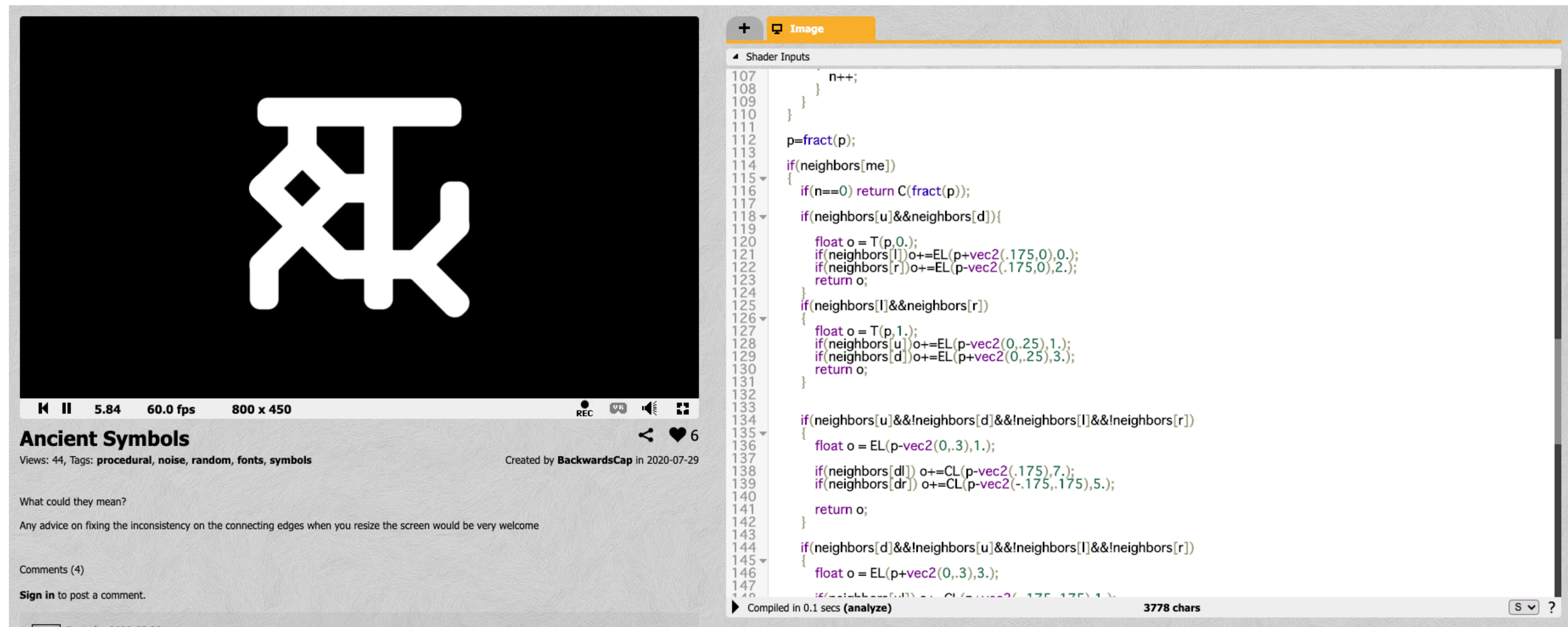


- Non-differentiability of parallel edges of two separate triangles
 - can be resolved by applying a small perturbation to the vertices
- Interpenetration

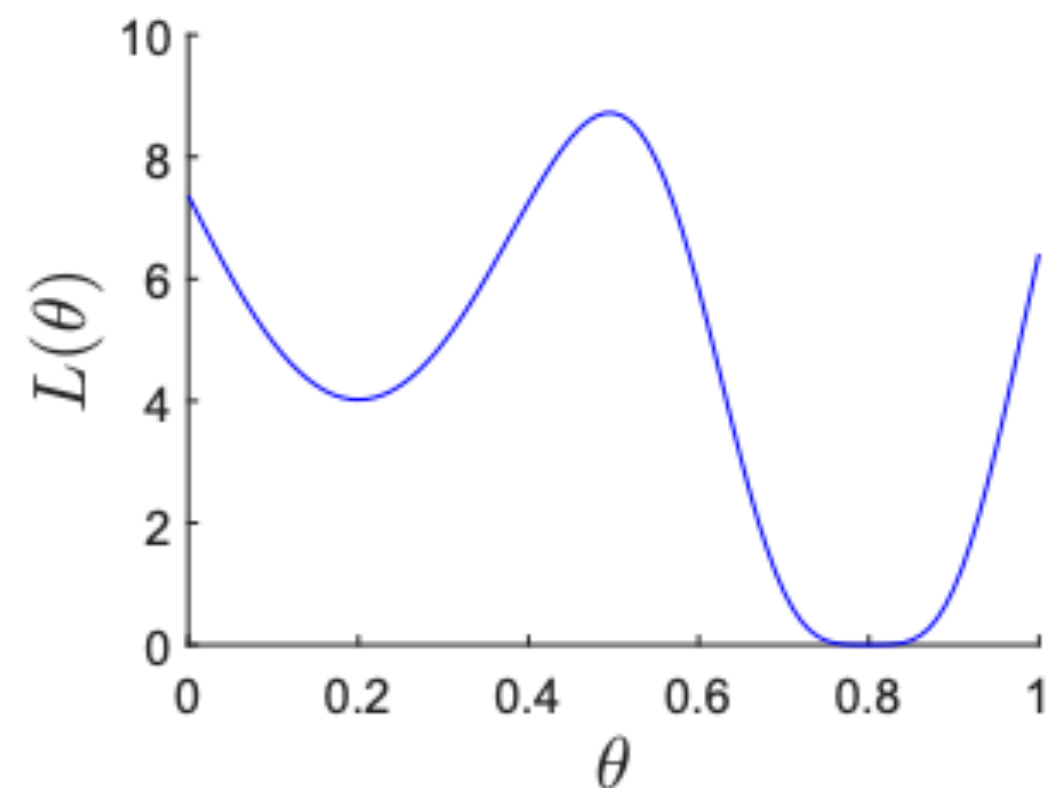
need to extract this edge



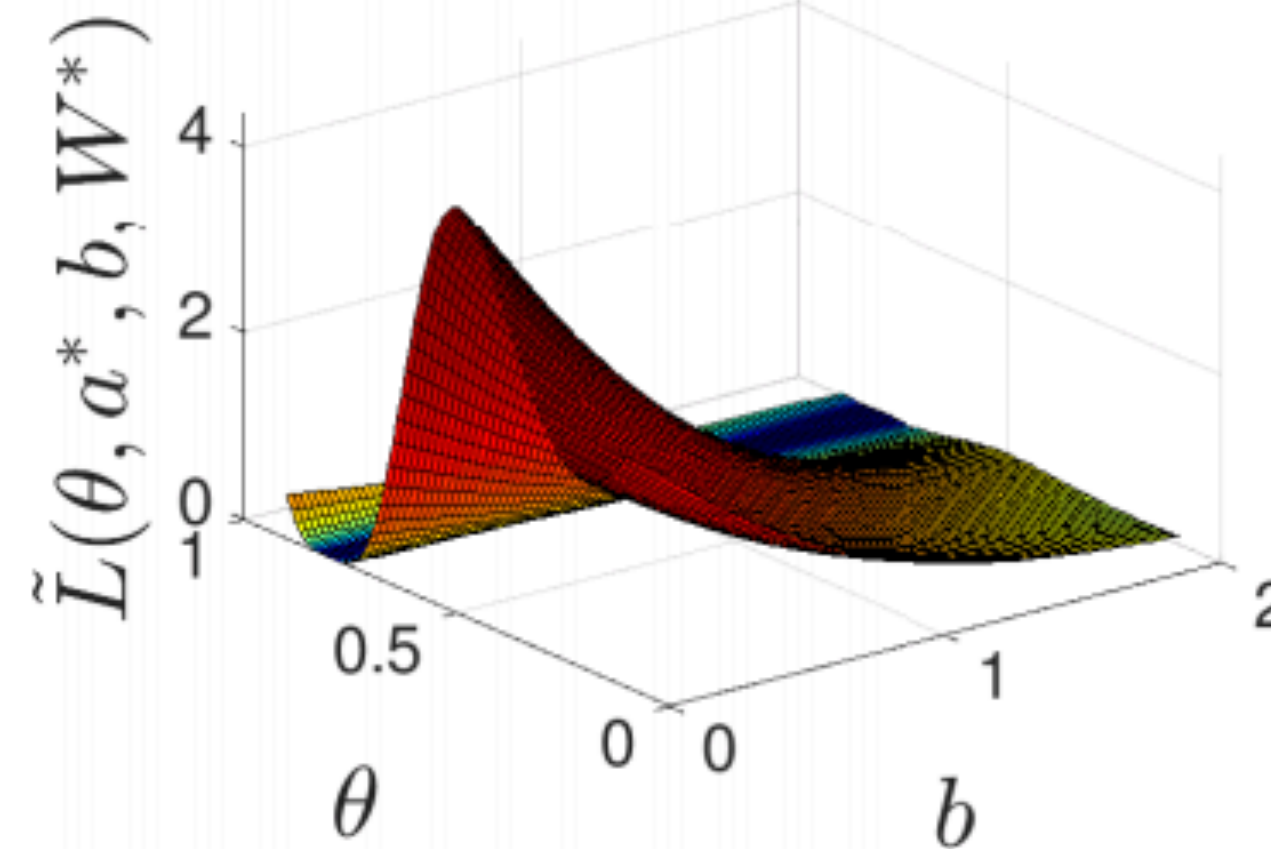
- Non-differentiability of parallel edges of two separate triangles
 - can be resolved by applying a small perturbation to the vertices
- Interpenetration
- If/else conditions in procedural shaders (bitmap texture is 100% fine)



- Non-differentiability of parallel edges of two separate triangles
 - can be resolved by applying a small perturbation to the vertices
- Interpenetration
- If/else conditions in procedural shaders (bitmap texture is 100% fine)
- Local minimum

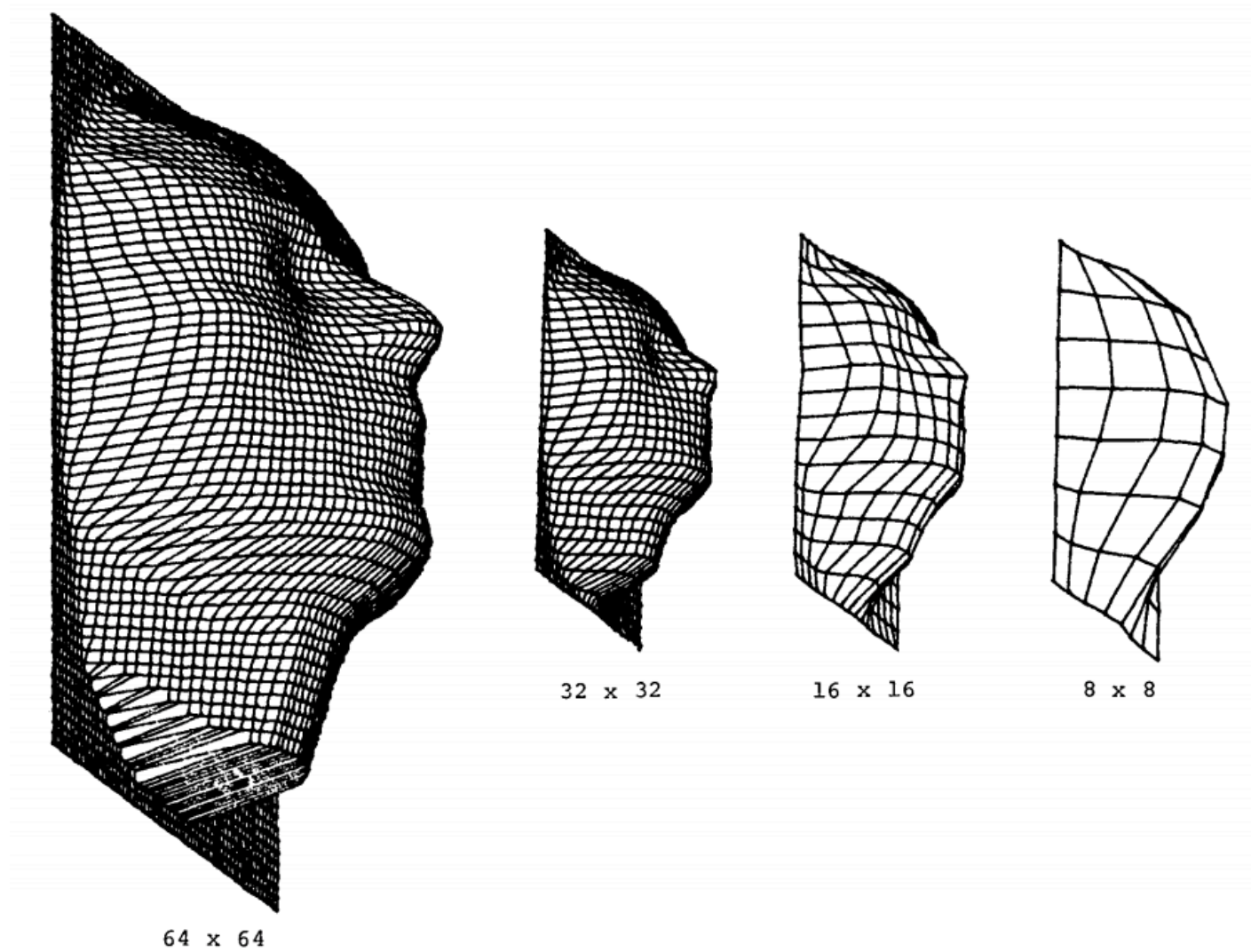


(a) original objective function L



(b) modified objective function \tilde{L}

Kawaguchi and Kaelbling 2019



William 1983

THEORY & ALGORITHMS

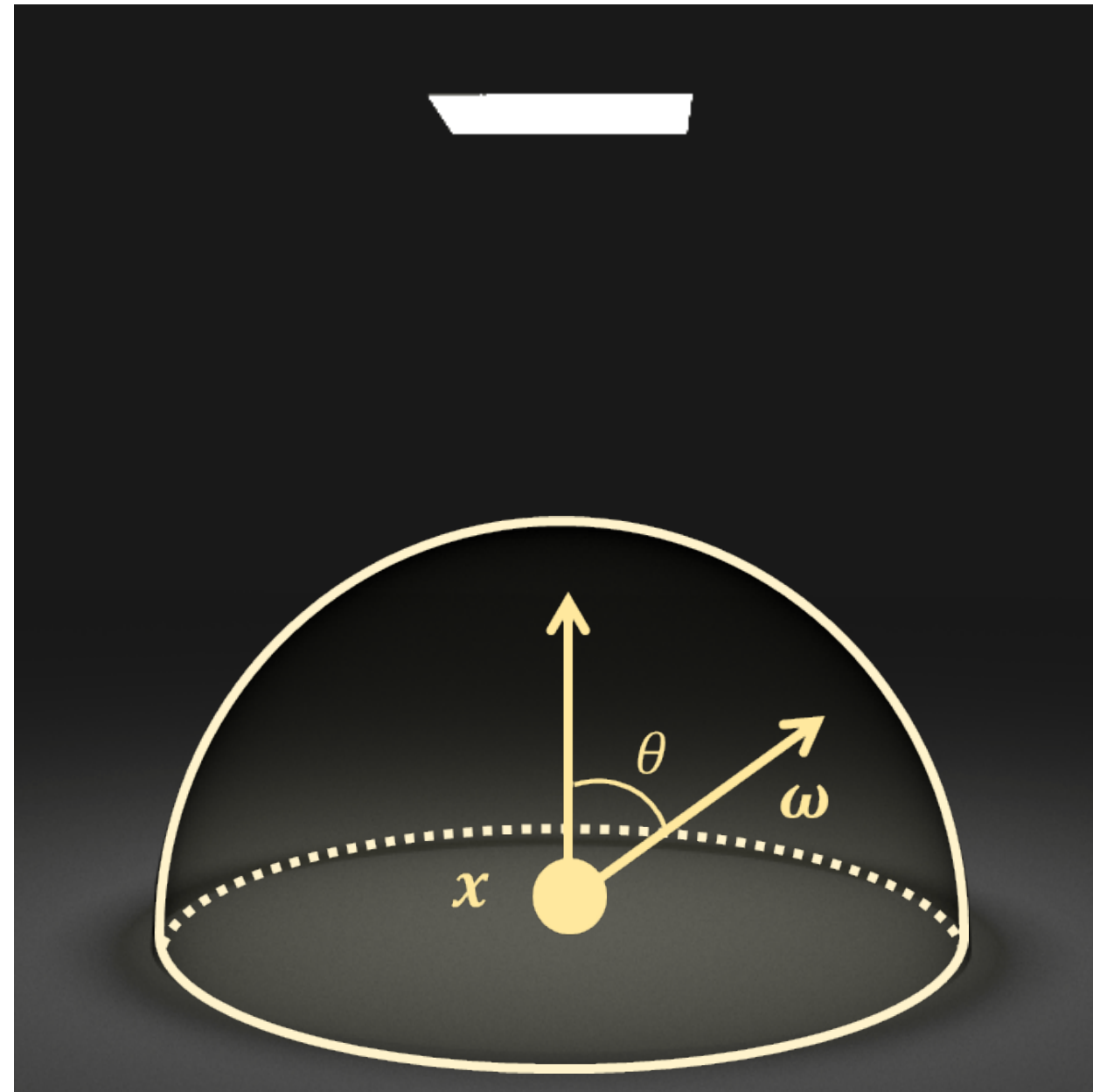
- Warm-up: differential irradiance
- Differentiable path tracing with edge sampling
- Differential radiative transfer
- Another way of dealing with discontinuities
- Radiative backpropagation
- Path-space differentiable rendering

Irradiance at \mathbf{x} :

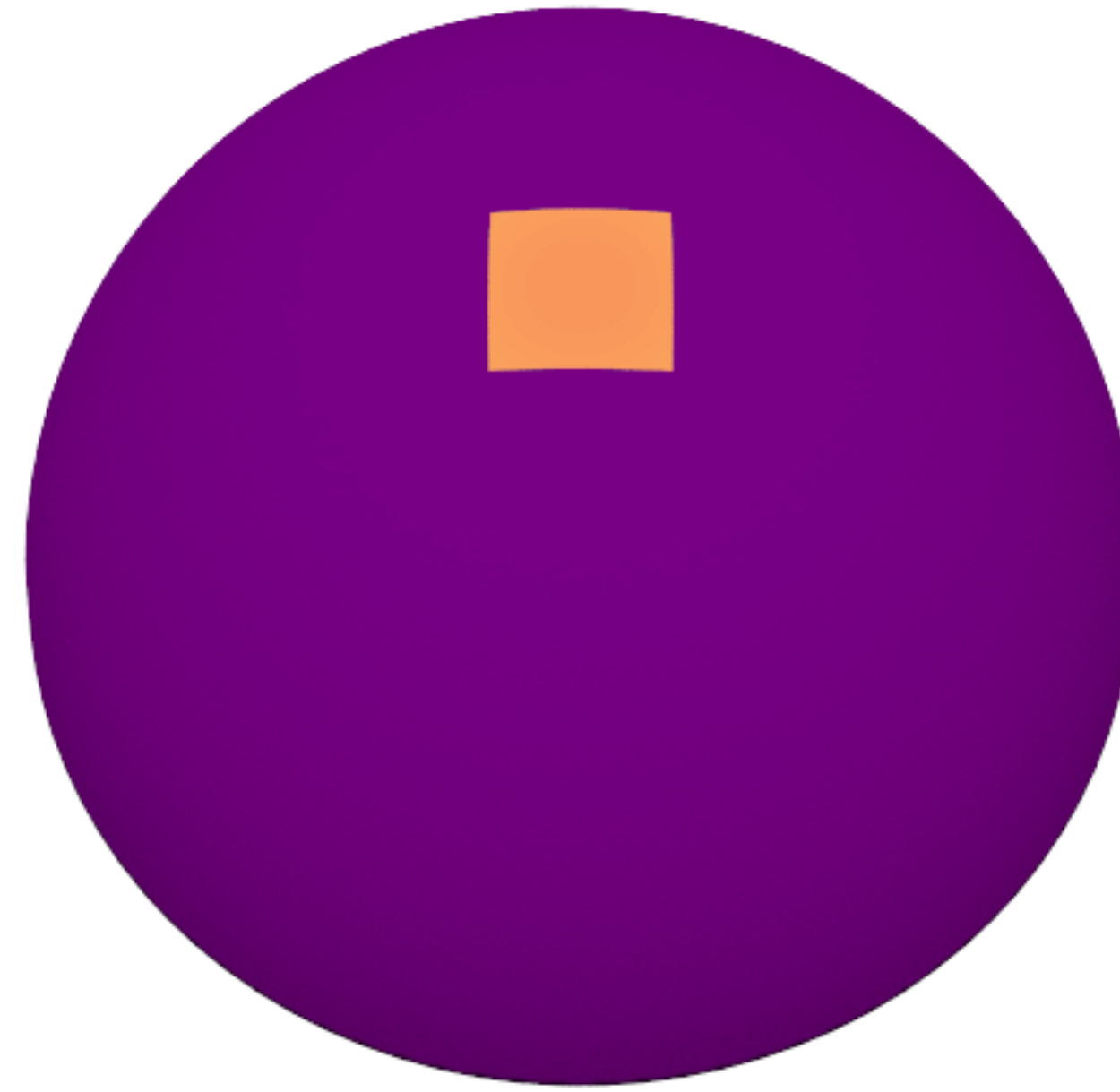
$$E = \int_{\mathbb{H}^2} \overbrace{L_i(\boldsymbol{\omega}) \cos \theta}^{f_E(\boldsymbol{\omega})} d\sigma(\boldsymbol{\omega})$$

WARM-UP: DIFFERENTIAL IRRADIANCE

π : emitter size

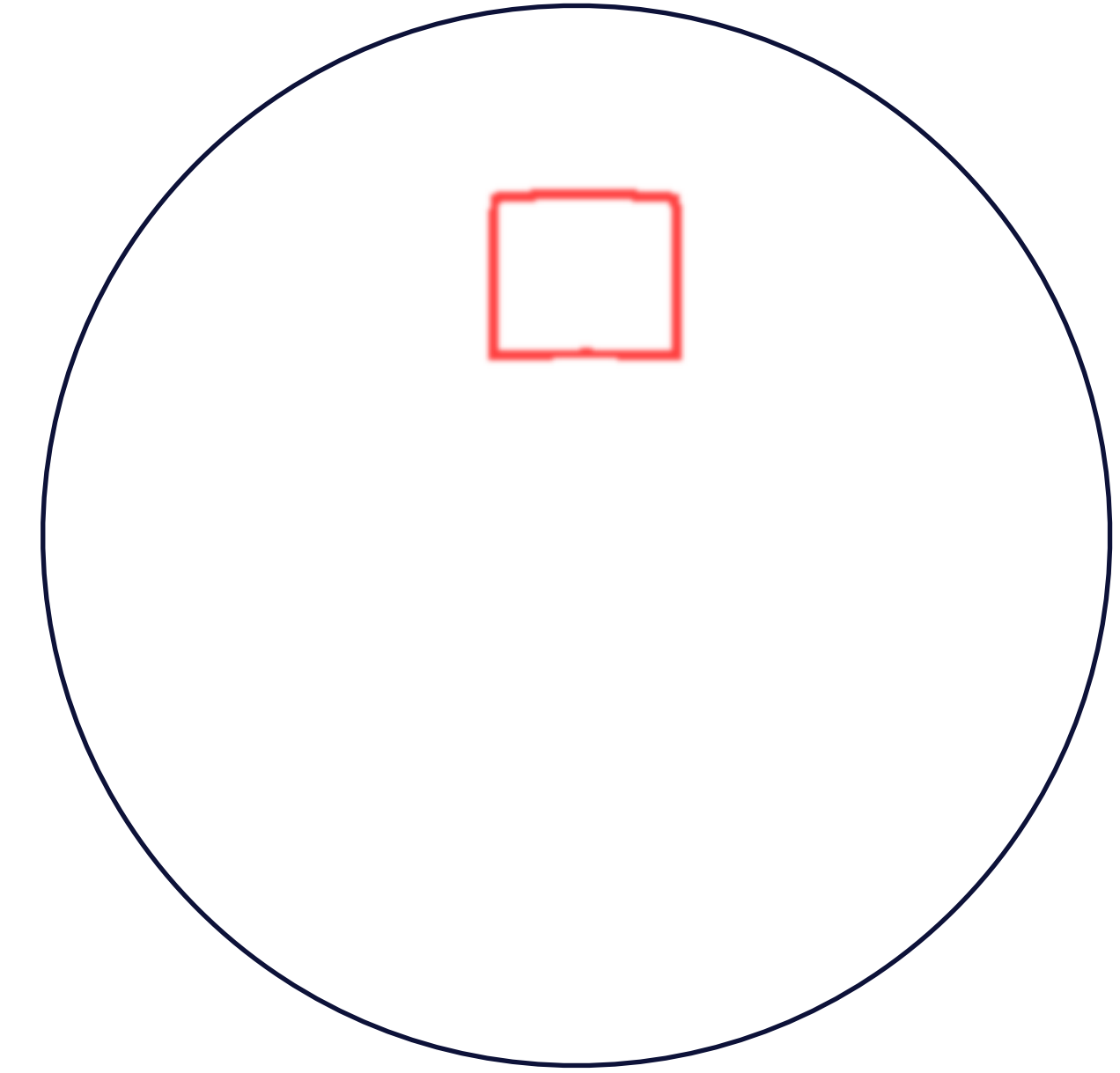


$f_E(\omega)$



Low High

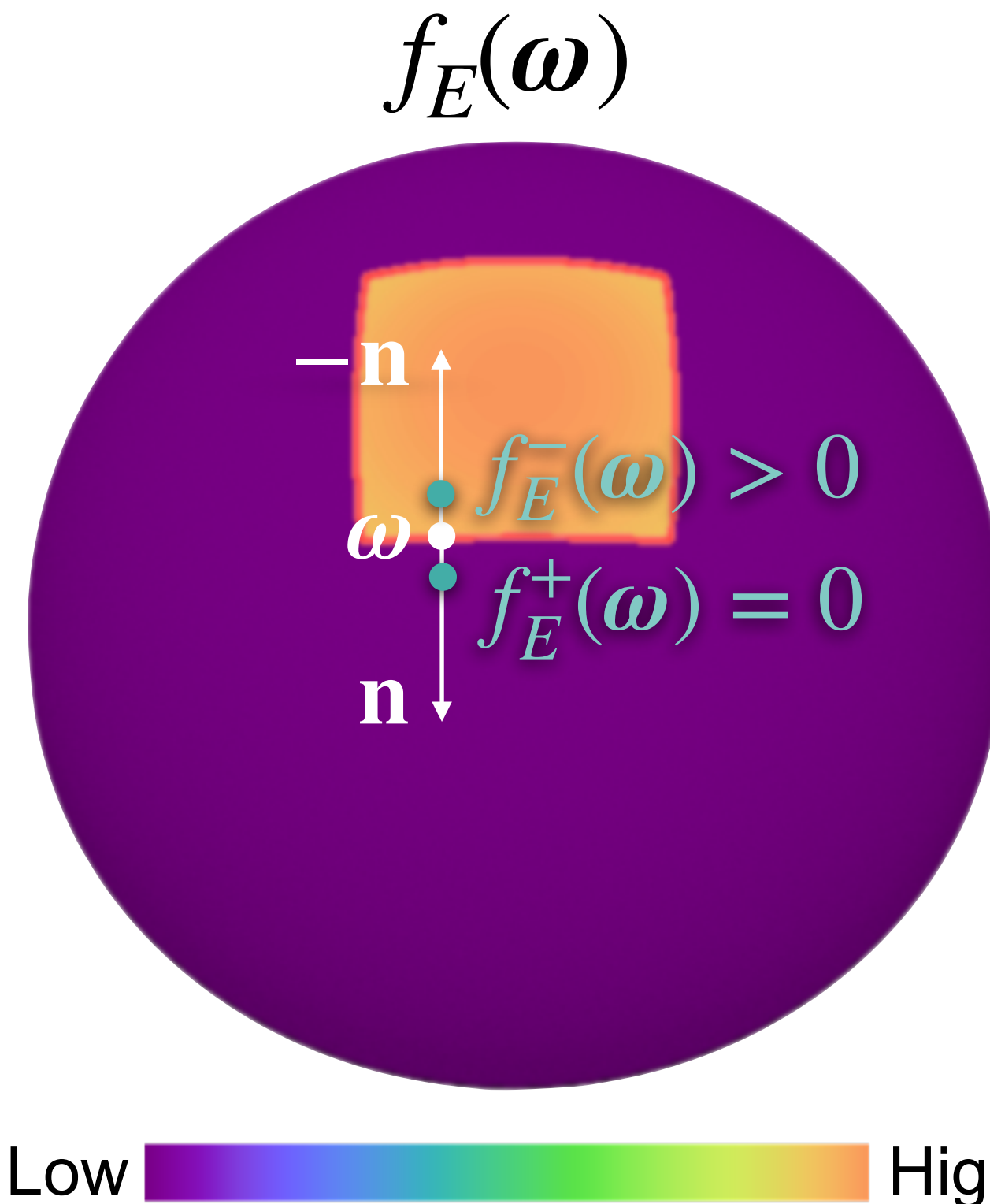
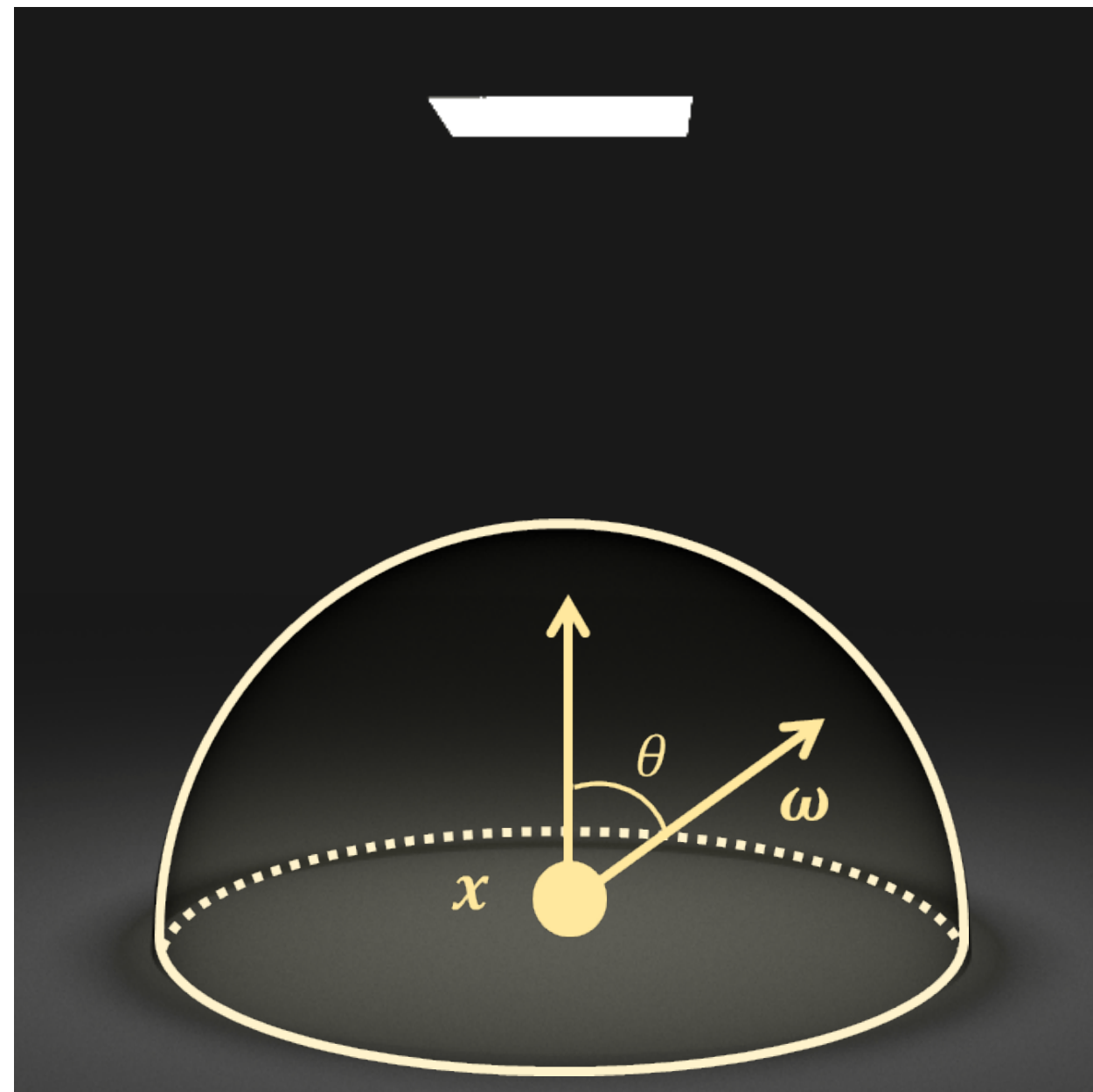
$\partial\mathbb{H}^2$



$$E = \int_{\mathbb{H}^2} \overbrace{L_1(\omega) \cos \theta}^{f_E(\omega)} d\sigma(\omega) \xrightarrow{\text{Reynolds}} \frac{dE}{d\pi} = \int_{\mathbb{H}^2} \frac{df_E}{d\pi}(\omega) d\sigma(\omega) + \int_{\partial\mathbb{H}^2} V_{\partial\mathbb{H}^2}(\omega) \Delta f_E(\omega) d\ell(\omega)$$

Interior integral = 0 Boundary integral

π : emitter size



Scalar normal “velocity” of ω

$$V_{\partial\mathbb{H}^2}(\omega) = \left\langle \mathbf{n}(\omega), \frac{d\omega}{d\pi} \right\rangle$$

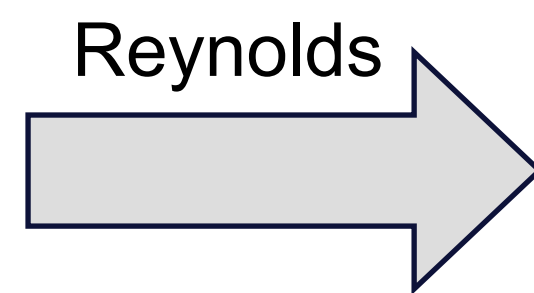
independent of the parameterization of $\partial\mathbb{H}^2$

Difference of the integrand f_E across the boundary

$$\Delta f_E(\omega) = f_E^-(\omega) - f_E^+(\omega)$$

General result

$$E = \int_{\mathbb{H}^2} \overbrace{L_1(\omega) \cos \theta}^{f_E(\omega)} d\sigma(\omega)$$



$$\frac{dE}{d\pi} = \int_{\mathbb{H}^2} \frac{df_E}{d\pi}(\omega) d\sigma(\omega) + \int_{\partial\mathbb{H}^2} V_{\partial\mathbb{H}^2}(\omega) \Delta f_E(\omega) d\ell(\omega)$$

Interior integral Boundary integral

$$E = \int_{\mathbb{H}^2} \overbrace{L_i(\omega) \cos \theta}^{f_E(\omega)} d\sigma(\omega) \xrightarrow{\text{Reynolds}} \frac{dE}{d\pi} = \int_{\mathbb{H}^2} \frac{df_E}{d\pi}(\omega) d\sigma(\omega) + \int_{\partial\mathbb{H}^2} V_{\partial\mathbb{H}^2}(\omega) \Delta f_E(\omega) d\ell(\omega)$$

Interior integral
Boundary integral

This can be generalized easily to obtain the differential rendering equation:

Rendering equation

$$L(\omega_o) = \int_{\mathbb{S}^2} \overbrace{L_i(\omega_i) f_s(\omega_i, \omega_o)}^{f_{RE}(\omega_i)} d\sigma(\omega_i) + L_e(\omega_o)$$

f_s : cosine-weighted BSDF

Interior integral
Boundary integral

Differential rendering equation

$$\frac{d}{d\pi} L(\omega_o) = \int_{\mathbb{S}^2} \frac{d}{d\pi} f_{RE}(\omega_i) d\sigma(\omega_i) + \int_{\partial\mathbb{S}^2} V_{\partial\mathbb{S}^2}(\omega_i) \Delta f_{RE}(\omega_i) d\ell(\omega_i) + \frac{d}{d\pi} L_e(\omega_o)$$

Assumptions:

No **zero-measure** (point and directional) **lights**
(which can create *hard shadow boundaries*)

No **perfectly specular surfaces**
(which can create *virtual images* of other objects)

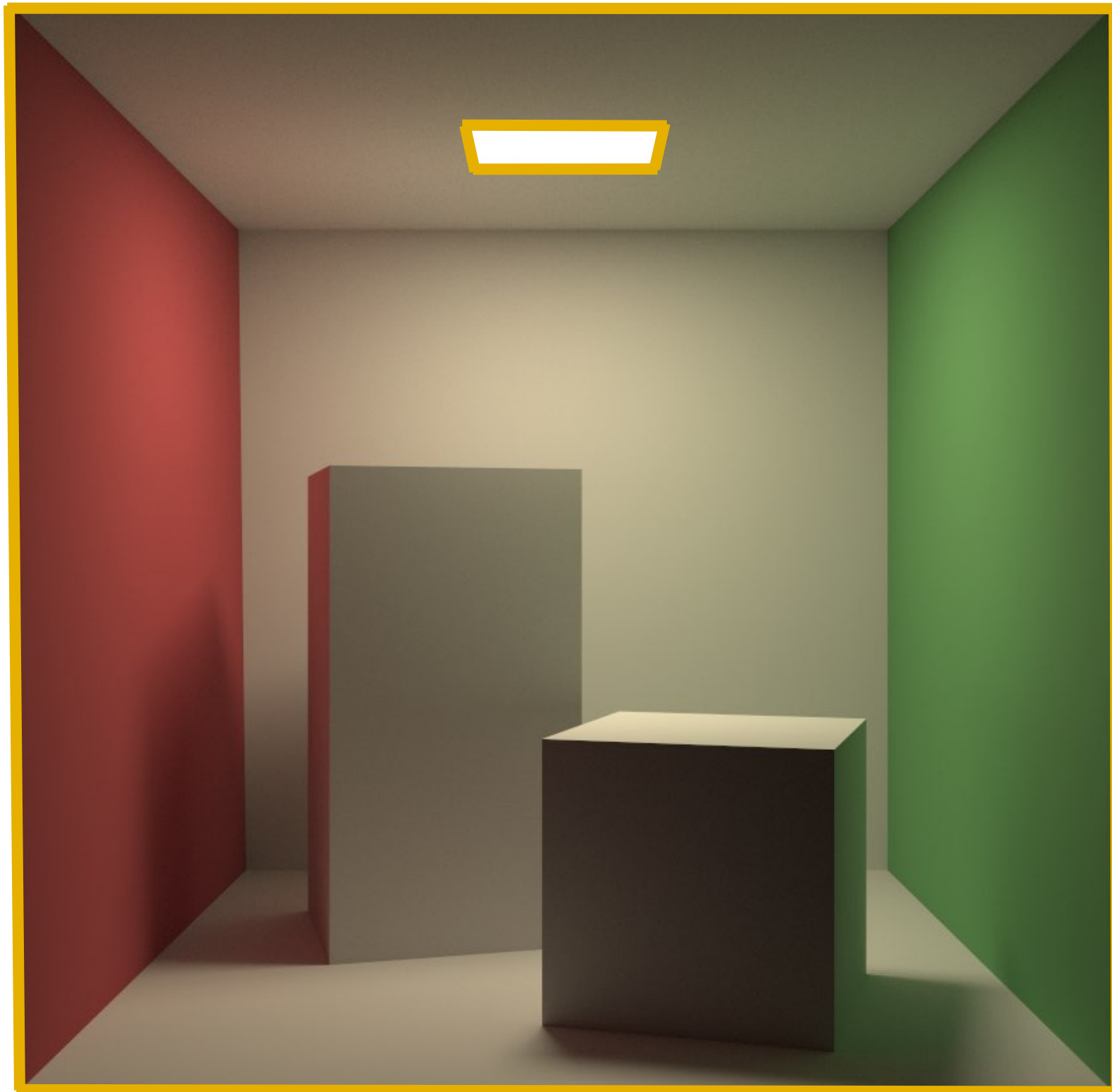
Hard-to-detect
discontinuities



Continuous BSDFs

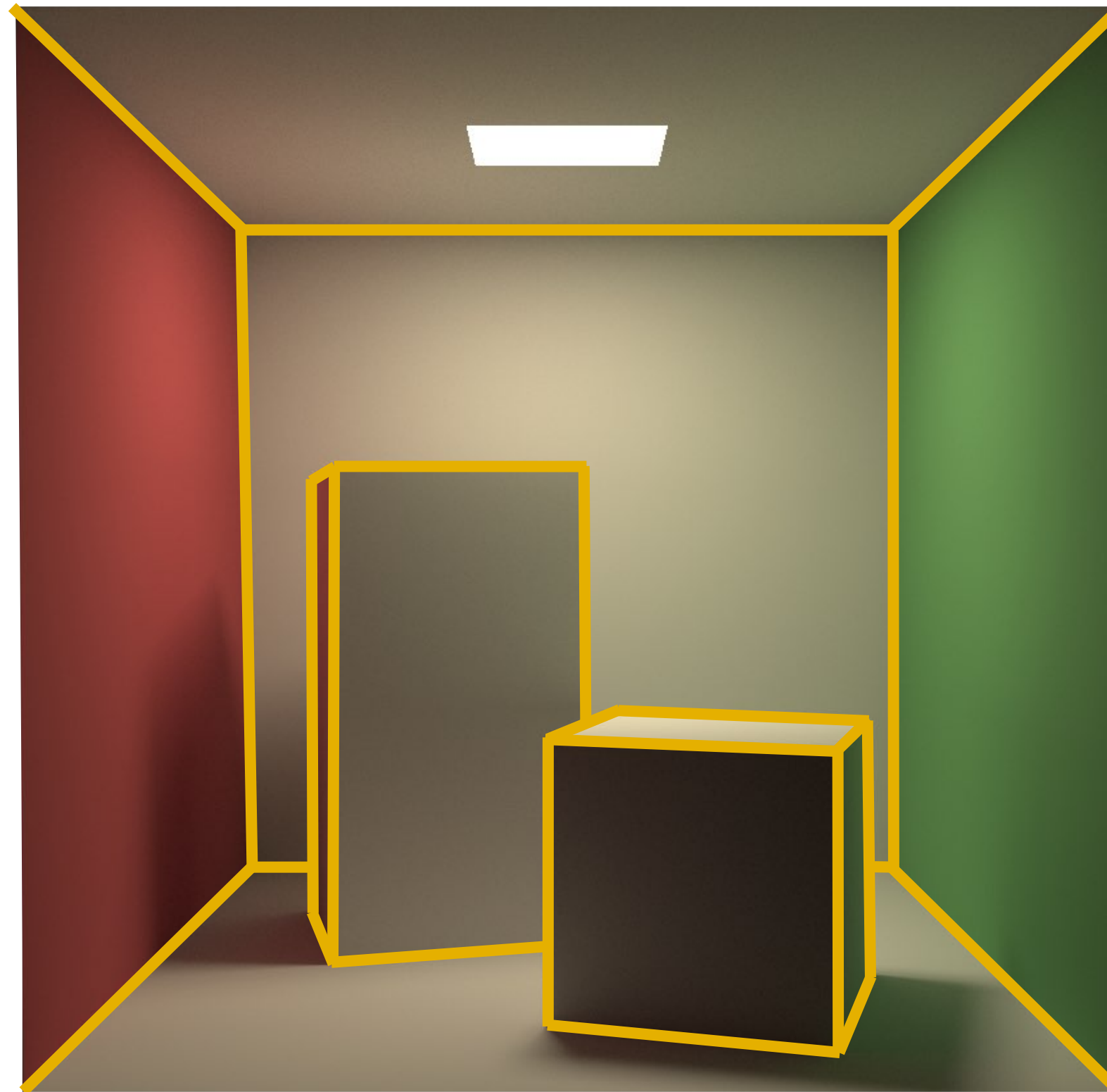
These limitations are largely practical and can be easily mitigated

Boundary edges



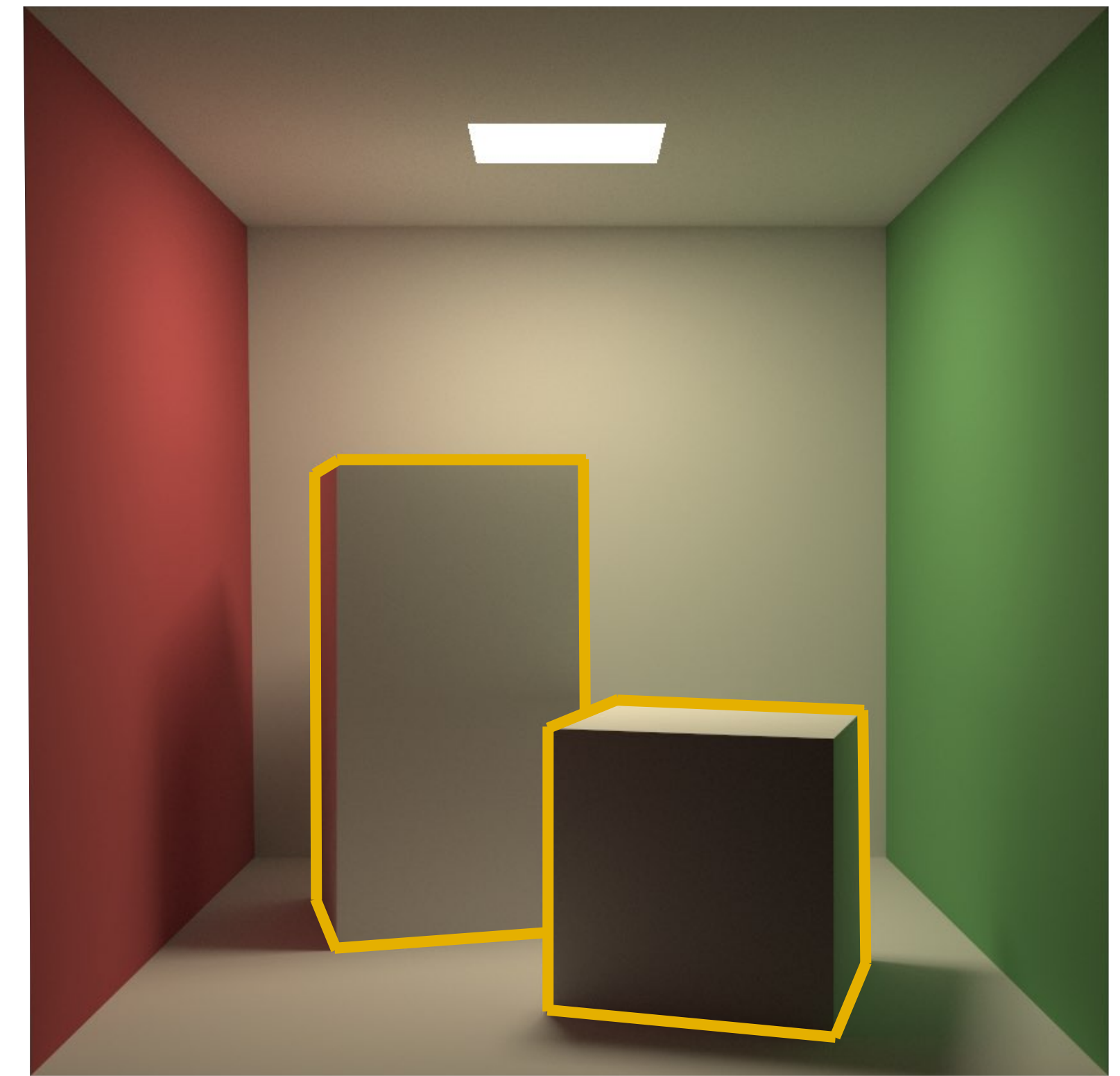
(Topological) boundary of an object

Sharp edges



Surface-normal discontinuities
(e.g., face edges)

Silhouette edges



View-dependent object silhouettes

Path tracing can be generalized to estimate L and $dL/d\pi$ jointly

Rendering equation

$$L(\omega_o) = \int_{\mathbb{S}^2} \overbrace{f_s(\omega_i, \omega_o) L_i(\omega_i)}^{f_{RE}(\omega_i)} d\sigma(\omega_i) + L_e(\omega_o)$$

Differential rendering equation

$$\frac{d}{d\pi} L(\omega_o) = \int_{\mathbb{S}^2} \frac{d}{d\pi} f_{RE}(\omega_i) d\sigma(\omega_i) + \int_{\partial\mathbb{S}^2} V_{\partial\mathbb{S}^2}(\omega_i) \Delta f_{RE}(\omega_i) d\ell(\omega_i) + \frac{d}{d\pi} L_e(\omega_o)$$

Standard path tracing
Edge sampling

Differentiable Monte Carlo Ray Tracing through Edge Sampling

TZU-MAO LI, MIT CSAIL
 MIIKA AITTALA, MIT CSAIL
 FRÉDO DURAND, MIT CSAIL
 JAAKKO LEHTINEN, Aalto University & NVIDIA

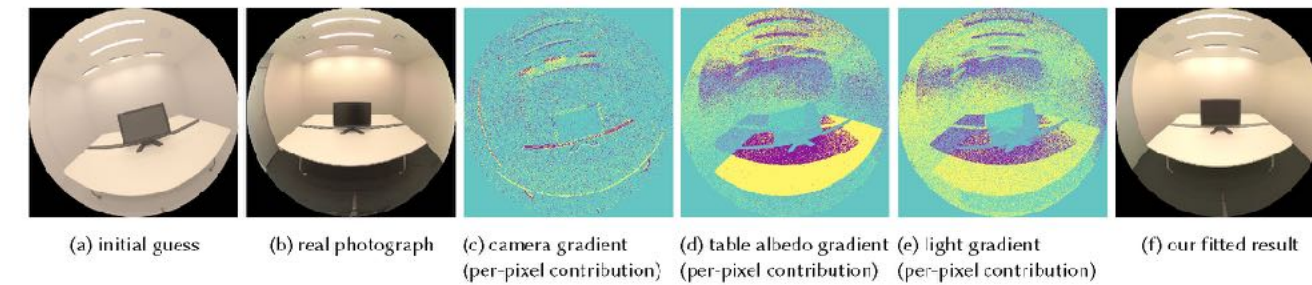


Fig. 1. We develop a general-purpose differentiable renderer that is capable of handling general light transport phenomena. Our method generates gradients with respect to scene parameters, such as camera pose (c), material parameters (d), mesh vertex positions, and lighting parameters (e), from a scalar loss computed from the output image. (c) shows the per-pixel gradient contribution of the L_1 difference with respect to the camera moving into the scene. (d) shows the gradient with respect to the red channel of table albedo. (e) shows the gradient with respect to the green channel of the intensity of one light source. As one of our applications, we use our gradient to perform an inverse rendering task by matching a real photograph (b) starting from an initial configuration (a) with a manual geometric recreation of the scene. The scene contains a fisheye camera with strong indirect illumination and non-Lambertian materials. We optimize for camera pose, material parameters, and light source intensity. Despite slight inaccuracies due to geometry mismatch and lens distortion, our method generates image (f) that almost matches the photo reference.

Gradient-based methods are becoming increasingly important for computer graphics, machine learning, and computer vision. The ability to compute gradients is crucial to optimization, inverse problems, and deep learning. In rendering, the gradient is required with respect to variables such as camera parameters, light sources, scene geometry, or material appearance. However, computing the gradient of rendering is challenging because the rendering integral includes visibility terms that are not differentiable. Previous work on differentiable rendering has focused on approximate solutions. They often do not handle secondary effects such as shadows or global illumination, or they do not provide the gradient with respect to variables other than pixel coordinates.

We introduce a general-purpose differentiable ray tracer, which, to our knowledge, is the first comprehensive solution that is able to compute derivatives of scalar functions over a rendered image with respect to arbitrary scene parameters such as camera pose, scene geometry, materials, and lighting parameters. The key to our method is a novel edge sampling algorithm that directly samples the Dirac delta functions introduced by the derivatives of the discontinuous integrand. We also develop efficient importance sampling methods based on spatial hierarchies. Our method can generate gradients in times running from seconds to minutes depending on scene complexity and desired precision.

Authors' addresses: Tzu-Mao Li, MIT CSAIL, tzumao@mit.edu; Miika Aittala, MIT CSAIL, miika@csail.mit.edu; Frédo Durand, MIT CSAIL, fredod@mit.edu; Jaakko Lehtinen, Aalto University & NVIDIA, jaakko.lehtinen@aalto.fi.

© 2018 Copyright held by the owner(s). This is the author's version of the work. It is posted here for your personal use. Not for redistribution. The definitive version of Record was published in *ACM Transactions on Graphics*. <https://doi.org/10.1145/3272127.3275109>.

We interface our differentiable ray tracer with the deep learning library PyTorch and show prototype applications in inverse rendering and the generation of adversarial examples for neural networks.

CCS Concepts: • Computing methodologies → Ray tracing; Visibility; Reconstruction

Additional Key Words and Phrases: ray tracing, inverse rendering, differentiable programming

ACM Reference Format:

Tzu-Mao Li, Miika Aittala, Frédo Durand, and Jaakko Lehtinen. 2018. Differentiable Monte Carlo Ray Tracing through Edge Sampling. *ACM Trans. Graph.* 37, 6, Article 222 (November 2018), 11 pages. <https://doi.org/10.1145/3272127.3275109>

1 INTRODUCTION

The computation of derivatives is increasingly central to many areas of computer graphics, computer vision, and machine learning. It is critical for the solution of optimization and inverse problems, and plays a major role in deep learning via backpropagation. This creates a need for rendering algorithms that can be differentiated with respect to arbitrary input parameters, such as camera location and direction, scene geometry, lights, material appearance, or texture values. Unfortunately, the rendering integral includes visibility terms that are not differentiable at object boundaries. Whereas the final image function is usually differentiable once radiance has been integrated over pixel prefilters, light source areas, etc., the integrand of rendering algorithms is not. In particular, the derivative of the integrand has Dirac delta terms at occlusion boundaries that cannot be handled by traditional sampling strategies.

ACM Trans. Graph., Vol. 37, No. 6, Article 222. Publication date: November 2018.

Differentiable Monte Carlo Ray Tracing through Edge Sampling

Tzu-Mao Li, Miika Aittala, Frédo Durand, Jaakko Lehtinen

SIGGRAPH Asia 2018

dPT($\mathbf{x}, \boldsymbol{\omega}_0$): # Estimate $L(\mathbf{x}, \boldsymbol{\omega}_0)$ and $\frac{d}{d\pi}[L(\mathbf{x}, \boldsymbol{\omega}_0)]$ jointly

sample $\boldsymbol{\omega}_{i,1} \in \mathbb{S}^2$ with probability $p_{i,1}$

$\mathbf{y} \leftarrow \text{rayIntersect}(\mathbf{x}, \boldsymbol{\omega}_{i,1})$

$(L_i, \dot{L}_i) \leftarrow \text{dPT}(\mathbf{y}, -\boldsymbol{\omega}_{i,1})$

$$L \leftarrow \frac{f_s(\mathbf{x}, \boldsymbol{\omega}_{i,1}, \boldsymbol{\omega}_0) L_i}{p_{i,1}}$$

$$\dot{L} \leftarrow \frac{\frac{d}{d\pi}[f_s(\mathbf{x}, \boldsymbol{\omega}_{i,1}, \boldsymbol{\omega}_0)] L_i + f_s(\mathbf{x}, \boldsymbol{\omega}_{i,1}, \boldsymbol{\omega}_0) \dot{L}_i}{p_{i,1}}$$

Standard PT
w/ symbolic
differentiation

Rendering equation

$$L(\boldsymbol{\omega}_0) = \int_{\mathbb{S}^2} \overbrace{f_s(\boldsymbol{\omega}_i, \boldsymbol{\omega}_0) L_i(\boldsymbol{\omega}_i)}^{f_{\text{RE}}(\boldsymbol{\omega}_i)} d\sigma(\boldsymbol{\omega}_i) + L_e(\boldsymbol{\omega}_0)$$

Differential rendering equation

$$\frac{d}{d\pi} L(\boldsymbol{\omega}_0) = \int_{\mathbb{S}^2} \frac{d}{d\pi} f_{\text{RE}}(\boldsymbol{\omega}_i) d\sigma(\boldsymbol{\omega}_i)$$

sample $\boldsymbol{\omega}_{i,2} \in \partial\mathbb{S}^2$ with probability $p_{i,2}$

$$\dot{L} \leftarrow \dot{L} + \frac{V_{\partial\mathbb{S}^2}(\mathbf{x}, \boldsymbol{\omega}_{i,2}) f_s(\mathbf{x}, \boldsymbol{\omega}_{i,2}, \boldsymbol{\omega}_0) \Delta L_i(\mathbf{x}, \boldsymbol{\omega}_{i,2})}{p_{i,2}}$$

Monte Carlo
edge sampling

return $\left(L + L_e(\mathbf{x}, \boldsymbol{\omega}_0), \dot{L} + \frac{d}{d\pi} L_e(\mathbf{x}, \boldsymbol{\omega}_0) \right)$

$\Delta f_{\text{RE}} = \Delta(f_s L_i) = f_s \Delta L_i$
(assuming f_s to be continuous)

$$+ \int_{\partial\mathbb{S}^2} V_{\partial\mathbb{S}^2}(\boldsymbol{\omega}_i) \Delta f_{\text{RE}}(\boldsymbol{\omega}_i) d\ell(\boldsymbol{\omega}_i) + \frac{d}{d\pi} L_e(\boldsymbol{\omega}_0)$$

dPT($\mathbf{x}, \boldsymbol{\omega}_0$): # Estimate $L(\mathbf{x}, \boldsymbol{\omega}_0)$ and $\frac{d}{d\pi}[L(\mathbf{x}, \boldsymbol{\omega}_0)]$ jointly

sample $\boldsymbol{\omega}_{i,1} \in \mathbb{S}^2$ with probability $p_{i,1}$

$\mathbf{y} \leftarrow \text{rayIntersect}(\mathbf{x}, \boldsymbol{\omega}_{i,1})$

$(L_i, \dot{L}_i) \leftarrow \text{dPT}(\mathbf{y}, -\boldsymbol{\omega}_{i,1})$

$$L \leftarrow \frac{f_s(\mathbf{x}, \boldsymbol{\omega}_{i,1}, \boldsymbol{\omega}_0) L_i}{p_{i,1}}$$

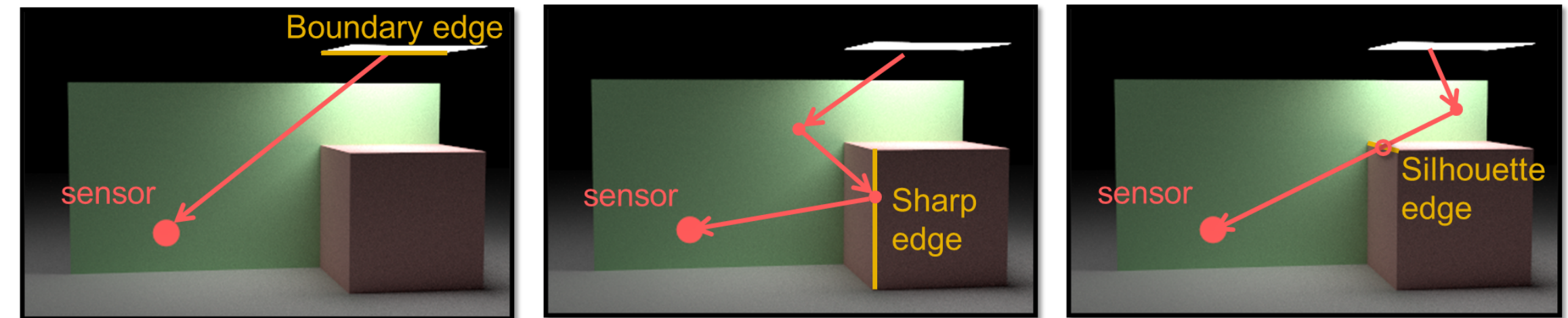
$$\dot{L} \leftarrow \frac{\frac{d}{d\pi}[f_s(\mathbf{x}, \boldsymbol{\omega}_{i,1}, \boldsymbol{\omega}_0)] L_i + f_s(\mathbf{x}, \boldsymbol{\omega}_{i,1}, \boldsymbol{\omega}_0) \dot{L}_i}{p_{i,1}}$$

sample $\boldsymbol{\omega}_{i,2} \in \partial\mathbb{S}^2$ with probability $p_{i,2}$

$$\dot{L} \leftarrow \dot{L} + \frac{V_{\partial\mathbb{S}^2}(\mathbf{x}, \boldsymbol{\omega}_{i,2}) f_s(\mathbf{x}, \boldsymbol{\omega}_{i,2}, \boldsymbol{\omega}_0) \Delta L_i(\mathbf{x}, \boldsymbol{\omega}_{i,2})}{p_{i,2}}$$

return $\left(L + L_e(\mathbf{x}, \boldsymbol{\omega}_0), \dot{L} + \frac{d}{d\pi} L_e(\mathbf{x}, \boldsymbol{\omega}_0) \right)$

- A new sampling procedure introduced by Li et al. [2018]
- **Key:** determining $\partial\mathbb{S}^2$, the discontinuity points of ΔL_i (w.r.t. incident direction $\boldsymbol{\omega}_i$)



- For polygonal meshes, $\partial\mathbb{S}^2$ can involve:
 - Boundary edges (associated with only one face)
 - Face edges (when not using smooth shading)
 - Silhouette edges (shared by a front and a back face)
 - Requires traversing a 6D BVH
 - Expensive for complex scenes
 - To be addressed later!

dPT($\mathbf{x}, \boldsymbol{\omega}_0$): # Estimate $L(\mathbf{x}, \boldsymbol{\omega}_0)$ and $\frac{d}{d\pi}[L(\mathbf{x}, \boldsymbol{\omega}_0)]$ jointly

sample $\boldsymbol{\omega}_{i,1} \in \mathbb{S}^2$ with probability $p_{i,1}$

$\mathbf{y} \leftarrow \text{rayIntersect}(\mathbf{x}, \boldsymbol{\omega}_{i,1})$

$(L_i, \dot{L}_i) \leftarrow \text{dPT}(\mathbf{y}, -\boldsymbol{\omega}_{i,1})$

$$L \leftarrow \frac{f_s(\mathbf{x}, \boldsymbol{\omega}_{i,1}, \boldsymbol{\omega}_0) L_i}{p_{i,1}}$$

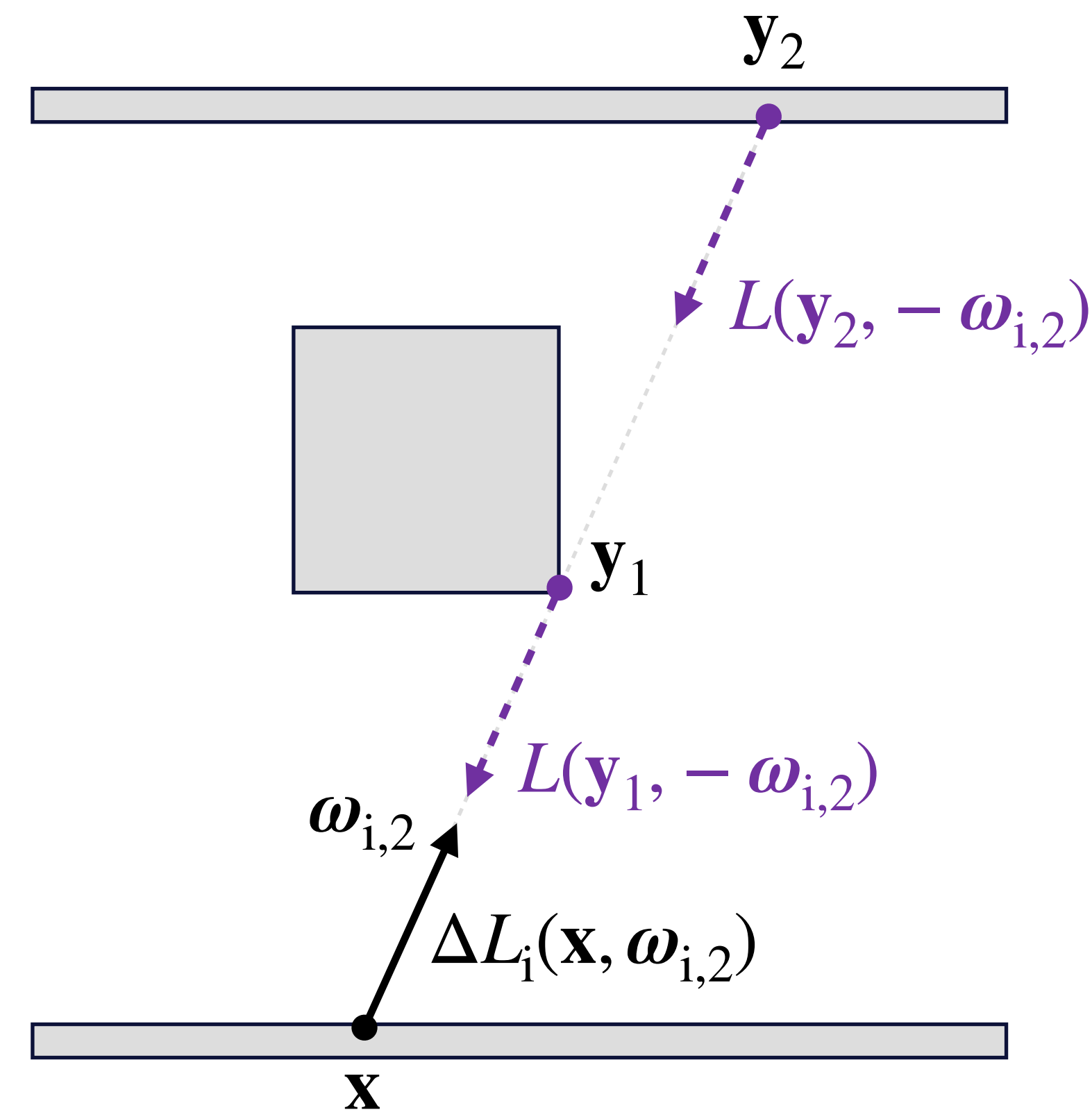
$$\dot{L} \leftarrow \frac{\frac{d}{d\pi}[f_s(\mathbf{x}, \boldsymbol{\omega}_{i,1}, \boldsymbol{\omega}_0)] L_i + f_s(\mathbf{x}, \boldsymbol{\omega}_{i,1}, \boldsymbol{\omega}_0) \dot{L}_i}{p_{i,1}}$$

sample $\boldsymbol{\omega}_{i,2} \in \partial\mathbb{S}^2$ with probability $p_{i,2}$

$$\dot{L} \leftarrow \dot{L} + \frac{V_{\partial\mathbb{S}^2}(\mathbf{x}, \boldsymbol{\omega}_{i,2}) f_s(\mathbf{x}, \boldsymbol{\omega}_{i,2}, \boldsymbol{\omega}_0) \Delta L_i(\mathbf{x}, \boldsymbol{\omega}_{i,2})}{p_{i,2}}$$

return $\left(L + L_e(\mathbf{x}, \boldsymbol{\omega}_0), \dot{L} + \frac{d}{d\pi} L_e(\mathbf{x}, \boldsymbol{\omega}_0) \right)$

Monte Carlo
edge sampling



$$\Delta L_i(\mathbf{x}, \boldsymbol{\omega}_{i,2}) = \pm \left[L(\mathbf{y}_1, -\boldsymbol{\omega}_{i,2}) - L(\mathbf{y}_2, -\boldsymbol{\omega}_{i,2}) \right]$$

Radiance values $L(\mathbf{y}_1, -\boldsymbol{\omega}_{i,2})$ and $L(\mathbf{y}_2, -\boldsymbol{\omega}_{i,2})$ can be computed by tracing additional “side” paths

$dPT(\mathbf{x}, \boldsymbol{\omega}_0)$: # Estimate $L(\mathbf{x}, \boldsymbol{\omega}_0)$ and $\frac{d}{d\pi}[L(\mathbf{x}, \boldsymbol{\omega}_0)]$ jointly

sample $\boldsymbol{\omega}_{i,1} \in S^2$ with probability $p_{i,1}$

$\mathbf{y} \leftarrow \text{rayIntersect}(\mathbf{x}, \boldsymbol{\omega}_{i,1})$

$(L_i, \dot{L}_i) \leftarrow dPT(\mathbf{y}, -\boldsymbol{\omega}_{i,1})$

$$L \leftarrow \frac{f_s(\mathbf{x}, \boldsymbol{\omega}_{i,1}, \boldsymbol{\omega}_0) L_i}{p_{i,1}}$$

$$\dot{L} \leftarrow \frac{\frac{d}{d\pi}[f_s(\mathbf{x}, \boldsymbol{\omega}_{i,1}, \boldsymbol{\omega}_0)] L_i + f_s(\mathbf{x}, \boldsymbol{\omega}_{i,1}, \boldsymbol{\omega}_0) \dot{L}_i}{p_{i,1}}$$

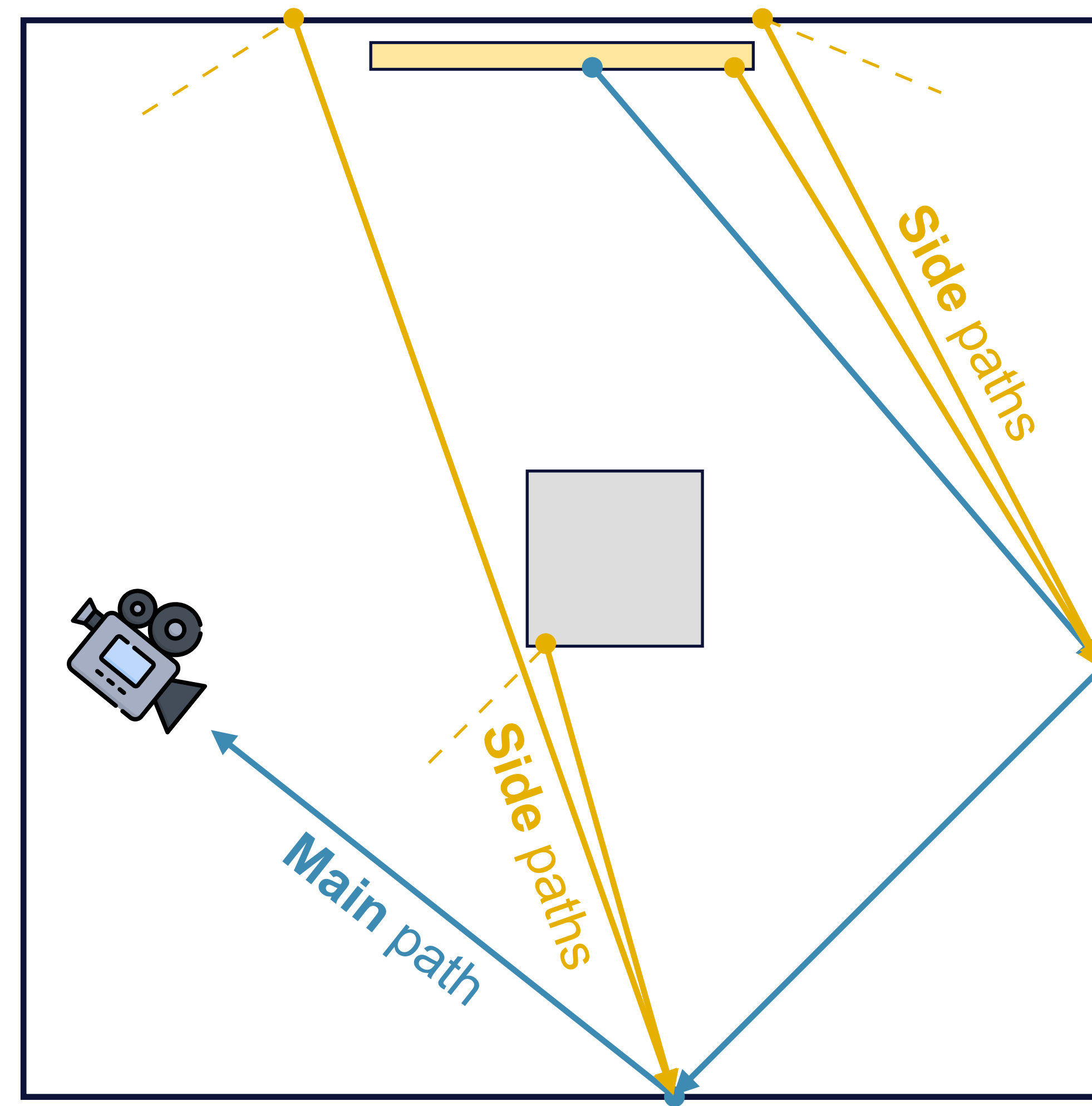
sample $\boldsymbol{\omega}_{i,2} \in \partial S^2$ with probability $p_{i,2}$

$$\dot{L} \leftarrow \dot{L} + \frac{V_{\partial S^2}(\mathbf{x}, \boldsymbol{\omega}_{i,2}) f_s(\mathbf{x}, \boldsymbol{\omega}_{i,2}, \boldsymbol{\omega}_0) \Delta L_i(\mathbf{x}, \boldsymbol{\omega}_{i,2})}{p_{i,2}}$$

return $\left(L + L_e(\mathbf{x}, \boldsymbol{\omega}_0), \dot{L} + \frac{d}{d\pi} L_e(\mathbf{x}, \boldsymbol{\omega}_0) \right)$

Standard PT
w/ symbolic
differentiation

Monte Carlo
edge sampling



A Differential Theory of Radiative Transfer

CHENG ZHANG, University of California, Irvine
LIFAN WU, University of California, San Diego
CHIANGXI ZHENG, Columbia University
IOANNIS GKIIOULEKAS, Carnegie Mellon University
RAVI RAMAMOORTHY, University of California, San Diego
SHUANG ZHAO, University of California, Irvine

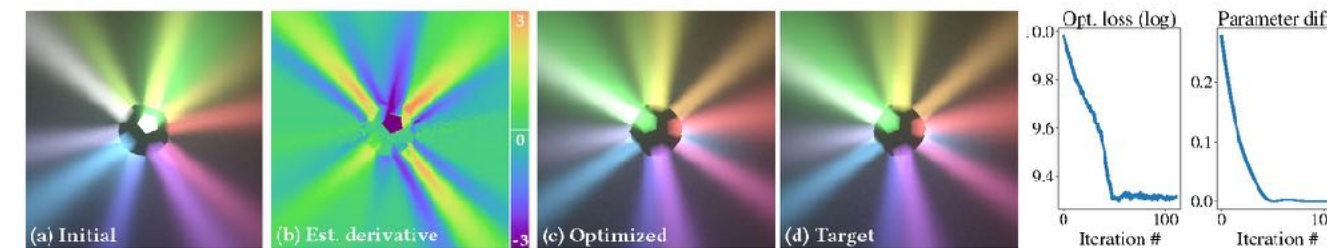


Fig. 1. We introduce a new differential theory of radiative transfer, which lays the foundation for computing the derivatives of radiometric measures with respect to arbitrary scene parameterizations (e.g., material properties and object geometries). The ability to evaluate these derivatives can facilitate gradient-based optimization for many diverse applications. As an example, here we optimize the pose of a dodecahedron emitting colored beams inside a participating medium. Given a target image (d) and an initial configuration (a), the optimization uses derivatives estimated by our method (b) to find parameters that produce rendered images (c) closely matching the target. Per-iteration optimization loss and difference between true and estimated parameters (both measured in L_2) are plotted on the right.

Physics-based differentiable rendering is the task of estimating the derivatives of radiometric measures with respect to scene parameters. The ability to compute these derivatives is necessary for enabling gradient-based optimization in a diverse array of applications: from solving analysis-by-synthesis problems to training machine learning pipelines incorporating forward rendering processes. Unfortunately, physics-based differentiable rendering remains challenging, due to the complex and typically nonlinear relation between pixel intensities and scene parameters.

We introduce a differential theory of radiative transfer, which shows how individual components of the radiative transfer equation (RTE) can be differentiated with respect to arbitrary differentiable changes of a scene. Our theory encompasses the same generality as the standard RTE, allowing differentiation while accurately handling a large range of light transport phenomena such as volumetric absorption and scattering, anisotropic phase functions, and heterogeneity. To numerically estimate the derivatives given by our theory, we introduce an unbiased Monte Carlo estimator supporting arbitrary surface and volumetric configurations. Our technique differentiates

Authors' addresses: Cheng Zhang, University of California, Irvine, chengz20@uci.edu; Lifan Wu, University of California, San Diego, lwt056@eng.ucsd.edu; Changxi Zheng, Columbia University, czx@cs.columbia.edu; Ioannis Gkioulekas, Carnegie Mellon University, igkioule@andrew.cmu.edu; Ravi Ramamoorthi, University of California, San Diego, ravir@cs.ucsd.edu; Shuang Zhao, University of California, Irvine, sz2@ics.uci.edu.

Permission to make digital or hard copies of all or part of this work for personal or classroom use is granted without fee provided that copies are not made or distributed for profit or commercial advantage and that copies bear this notice and the full citation on the first page. Copyrights for components of this work owned by others than the author(s) must be honored. Abstracting with credit is permitted. To copy otherwise, to republish, to post on servers or to redistribute to lists, requires prior specific permission and/or a fee. Request permissions from permissions.acm.org.
© 2019 Copyright held by the owner/author(s). Publication rights licensed to ACM. 0730-0301/2019/11-ART227 \$15.00
<https://doi.org/10.1145/3355089.3356522>

path contributions symbolically and uses additional boundary integrals to capture geometric discontinuities such as visibility changes.

We validate our method by comparing our derivative estimations to those generated using the finite-difference method. Furthermore, we use a few synthetic examples inspired by real-world applications in inverse rendering, non line of sight (NLOS) and biomedical imaging, and design, to demonstrate the practical usefulness of our technique.

CCS Concepts • Computing methodologies → Rendering.

Additional Key Words and Phrases radiative transfer, differentiable rendering, Monte Carlo path tracing

ACM Reference Format:

Cheng Zhang, Lifan Wu, Changxi Zheng, Ioannis Gkioulekas, Ravi Ramamoorthi, and Shuang Zhao. 2019. A Differential Theory of Radiative Transfer. *ACM Trans. Graph.* 38, 6, Article 227 (November 2019), 16 pages. <https://doi.org/10.1145/3355089.3356522>

1 INTRODUCTION

A fundamental task of physics-based light transport simulation is to compute the radiant power (generally measured using radiance) at certain 3D locations and directions in a virtual scene, e.g., those corresponding to radiometric sensors. Such *forward* evaluations of light transport have been a focus of research efforts in computer graphics since the field's inception. These efforts have resulted in mature forward rendering algorithms, including Monte Carlo techniques, that can efficiently and accurately simulate complex light transport effects such as interreflections and subsurface scattering.

Mathematically, it is convenient to be capable of evaluating not only a given function but also its various transformations. One such

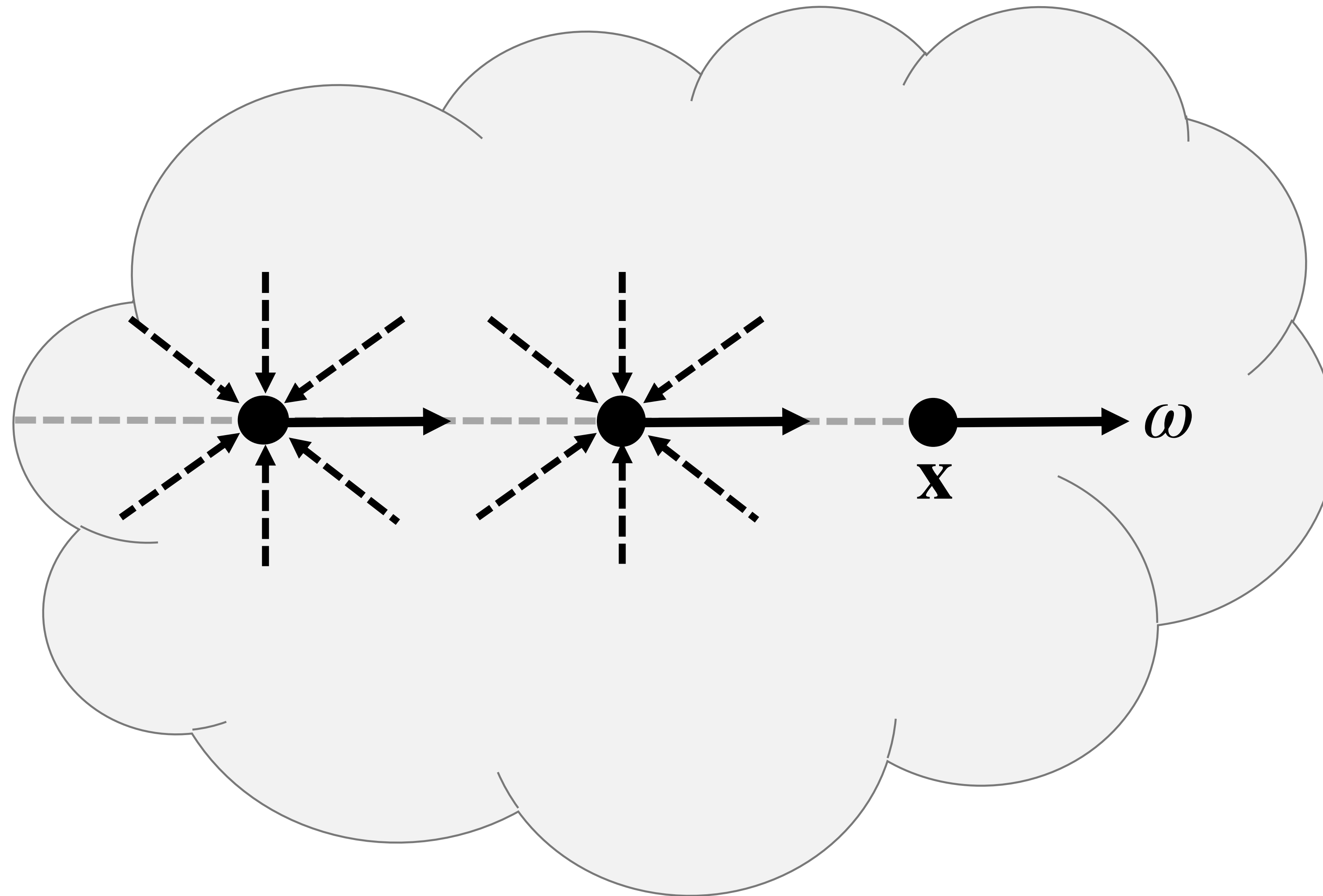
ACM Trans. Graph., Vol. 38, No. 5, Article 227. Publication date: November 2019.

A Differential Theory of Radiative Transfer

Cheng Zhang, Lifan Wu, Changxi Zheng, Ioannis Gkioulekas, Ravi Ramamoorthi, Shuang Zhao

SIGGRAPH Asia 2019

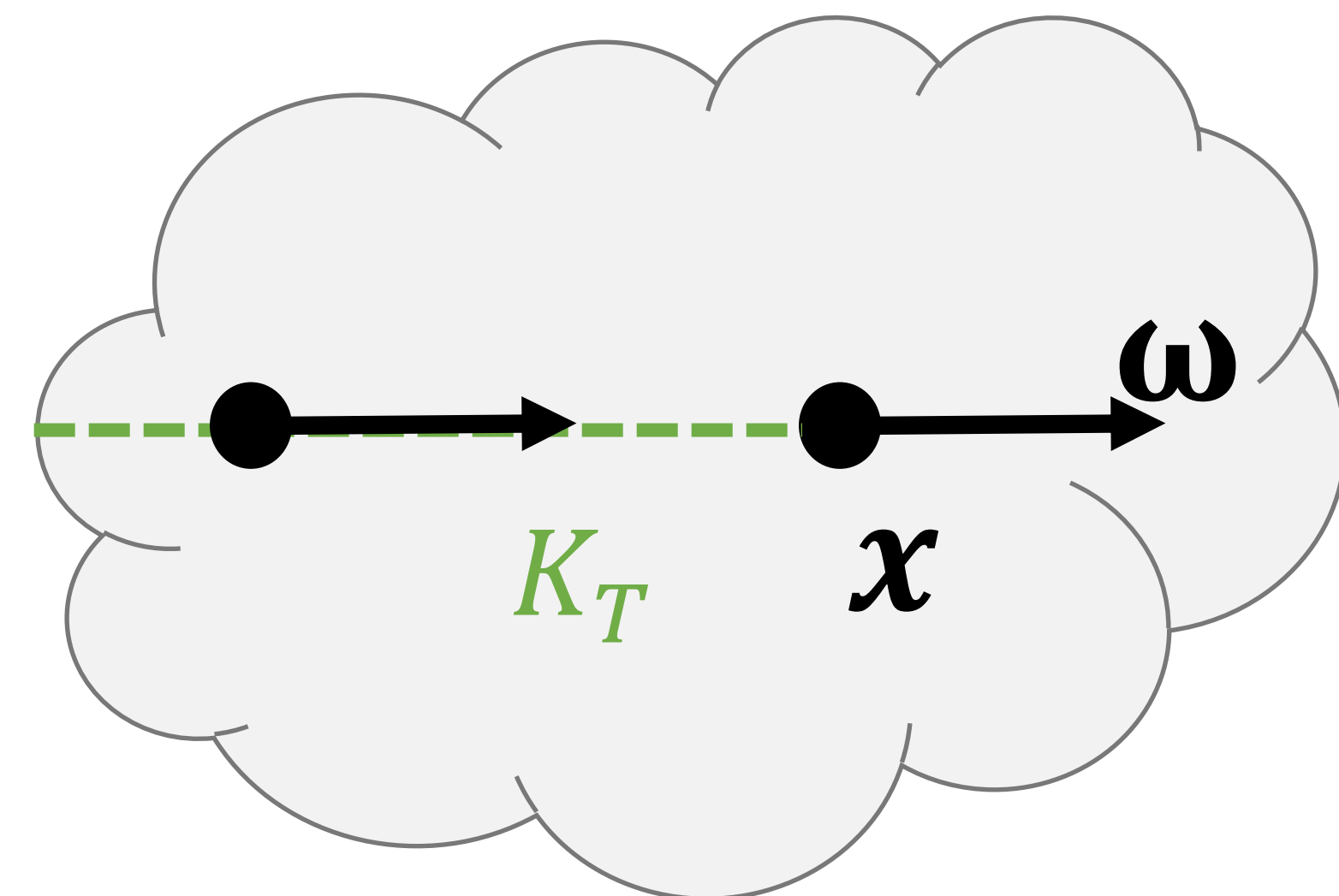
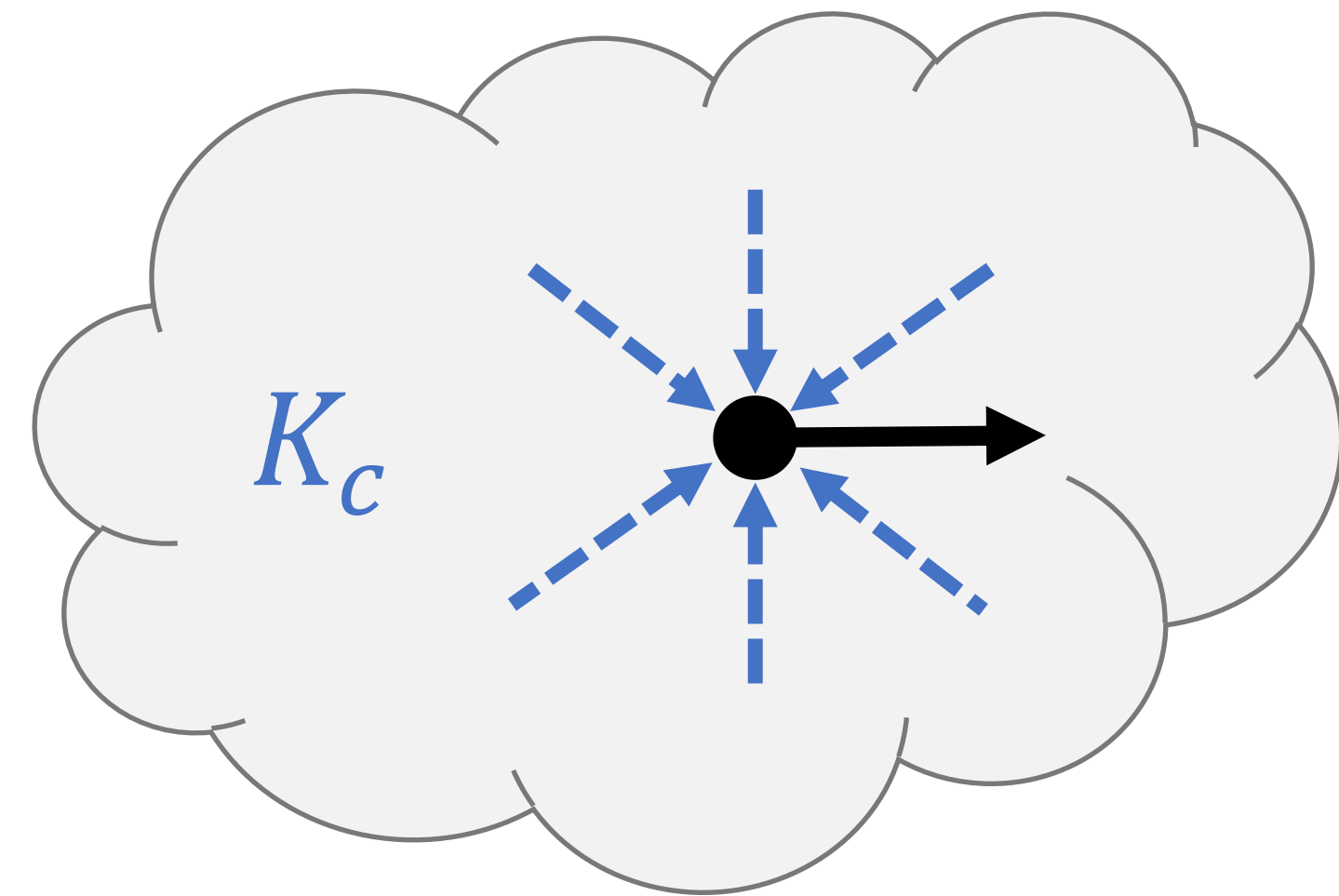
RECAP: RADIATIVE TRANSFER THEORY



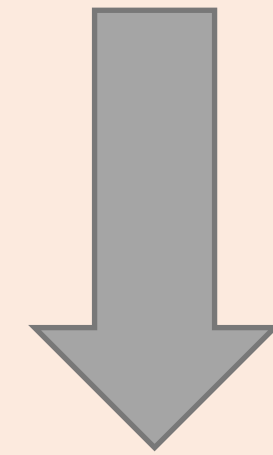
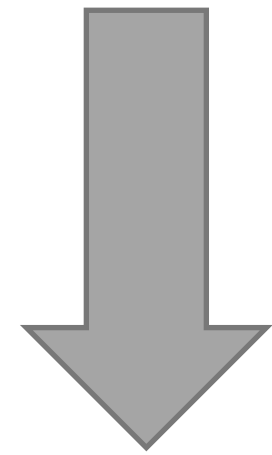
Transport operator Collision operator Source

$$L = K_T K_c L + Q$$

Radiative transfer equation (RTE)
in operator form



$$L = K_T K_c L + Q$$



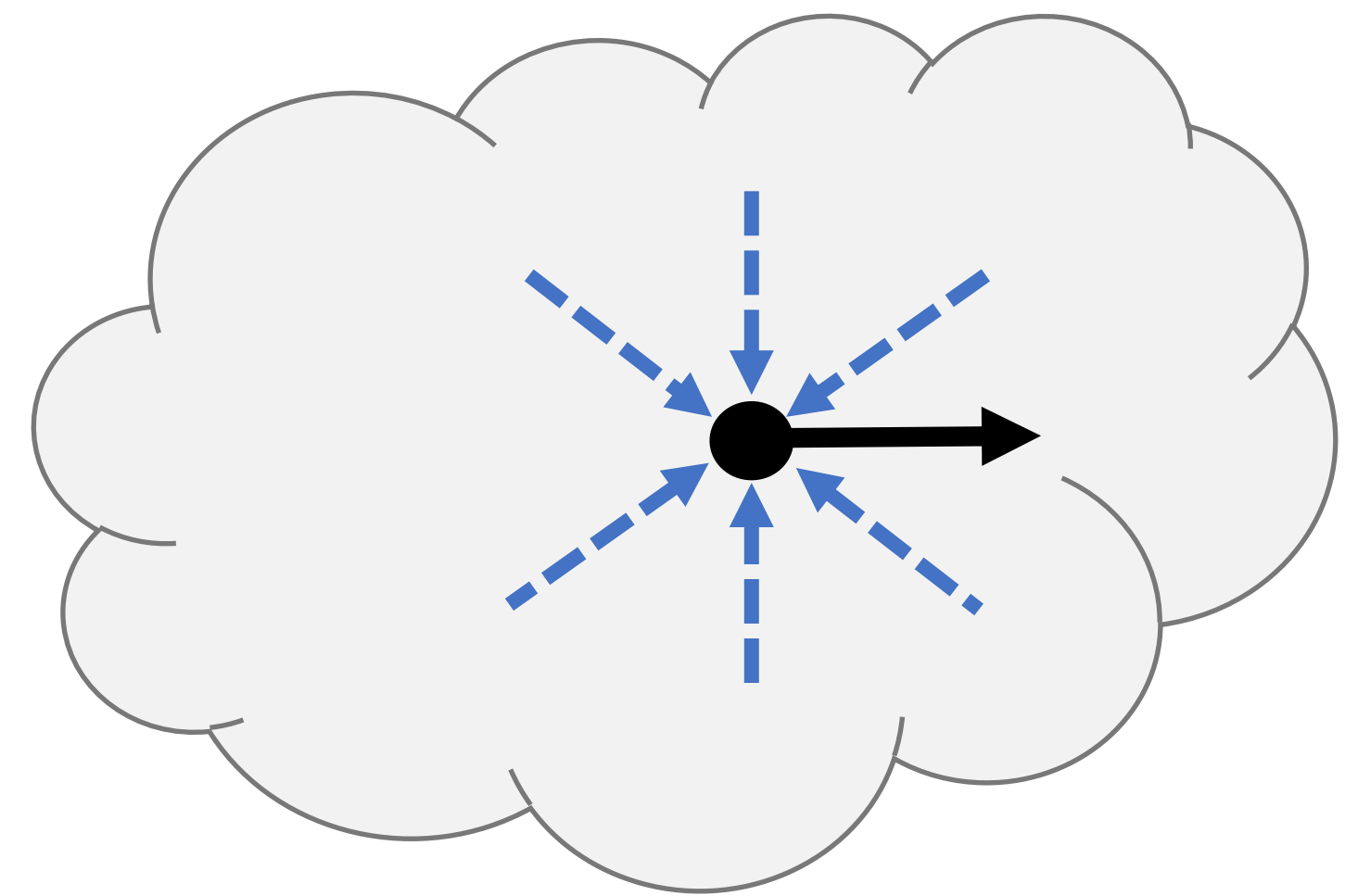
$$\partial_{\pi} L = \partial_{\pi} (K_T K_c L) + \partial_{\pi} Q$$

Differentiating individual operators

$$\text{RTE: } L = K_T K_c L + Q$$

(\mathbf{x} omitted for notational simplicity)

$$(K_c L)(\boldsymbol{\omega}) = \underbrace{\sigma_s}_{\text{Scattering coefficient}} \int_{S^2} \underbrace{f_p(\boldsymbol{\omega}_i, \boldsymbol{\omega})}_{\text{Phase function}} \underbrace{L(\boldsymbol{\omega}_i)}_{f(\boldsymbol{\omega}_i)} d\boldsymbol{\omega}_i$$



$$\partial_{\pi} \int_{S^2} f(\boldsymbol{\omega}_i) d\boldsymbol{\omega}_i = ?$$

Requires differentiating a spherical integral

$$(KcL)(\omega) = \sigma_s \int_{S^2} \overbrace{f_p(\omega_i, \omega) L(\omega_i)}^{f(\omega_i)} d\omega_i$$

$$\partial_\pi \int_{S^2} f(\omega_i) d\omega_i = \underbrace{\int_{S^2} \partial_\pi f(\omega_i) d\omega_i}_{\text{Interior integral}} + \underbrace{\int_{\partial S^2} \left\langle \mathbf{n}, \frac{\partial \omega_i}{\partial \pi} \right\rangle \Delta f(\omega_i) d\omega_i}_{\text{Boundary integral}}$$

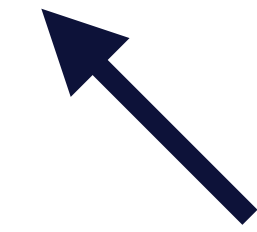
By applying Reynolds transport theorem
(largely identical to the differentiation of the rendering equation)

$$L = K_T K_c L + Q$$

Transport operator (can be differentiated using Leibniz's rule)

$$(K_T K_c L)(x, \omega) = \int_0^D T(x', x) (K_c L)(x', \omega) d\tau$$

Transmittance



Source

$$Q = T(x_0, x) L_s(x_0, \omega)$$

$$\dot{L}(\mathbf{x}, \omega) = \int_0^D T(\mathbf{x}', \mathbf{x}) \left[\sigma_s(\mathbf{x}') \dot{L}^{ins}(\mathbf{x}', \omega) + (\dot{\sigma}_s(\mathbf{x}') - \Sigma_t(\mathbf{x}, \omega, \tau) \sigma_s(\mathbf{x}')) \dot{L}^{ins}(\mathbf{x}', \omega) \right] d\tau$$

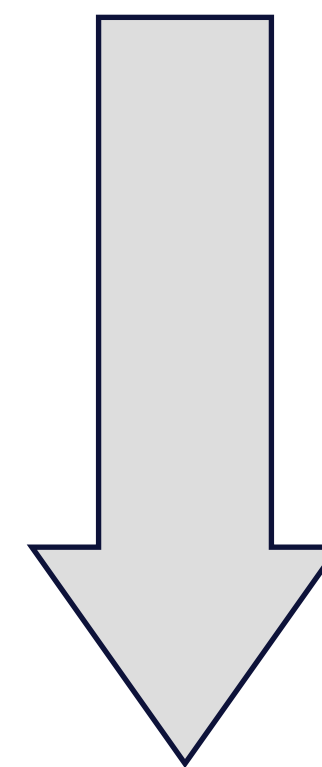
$$+ T(\mathbf{x}_0, \mathbf{x}) \left[- (\Sigma_t(\mathbf{x}, \omega, D) + \dot{D} \sigma_t(\mathbf{x}_0)) L_s(\mathbf{x}_0, \omega) + \dot{L}_s(\mathbf{x}_0, \omega) + \dot{D} \sigma_s(\mathbf{x}_0) \dot{L}^{ins}(\mathbf{x}_0, \omega) \right],$$

where Σ_t is defined in Eq. (17), \dot{L}^{ins} follows Eq. (22), and $\dot{L}_s = \dot{L}_s^r + \dot{L}_s^e$ with \dot{L}_s^r given by Eq. (29)

This is Eq. (32) of the work by Zhang et al. [2019]

$$L = K_T K_c L + Q$$

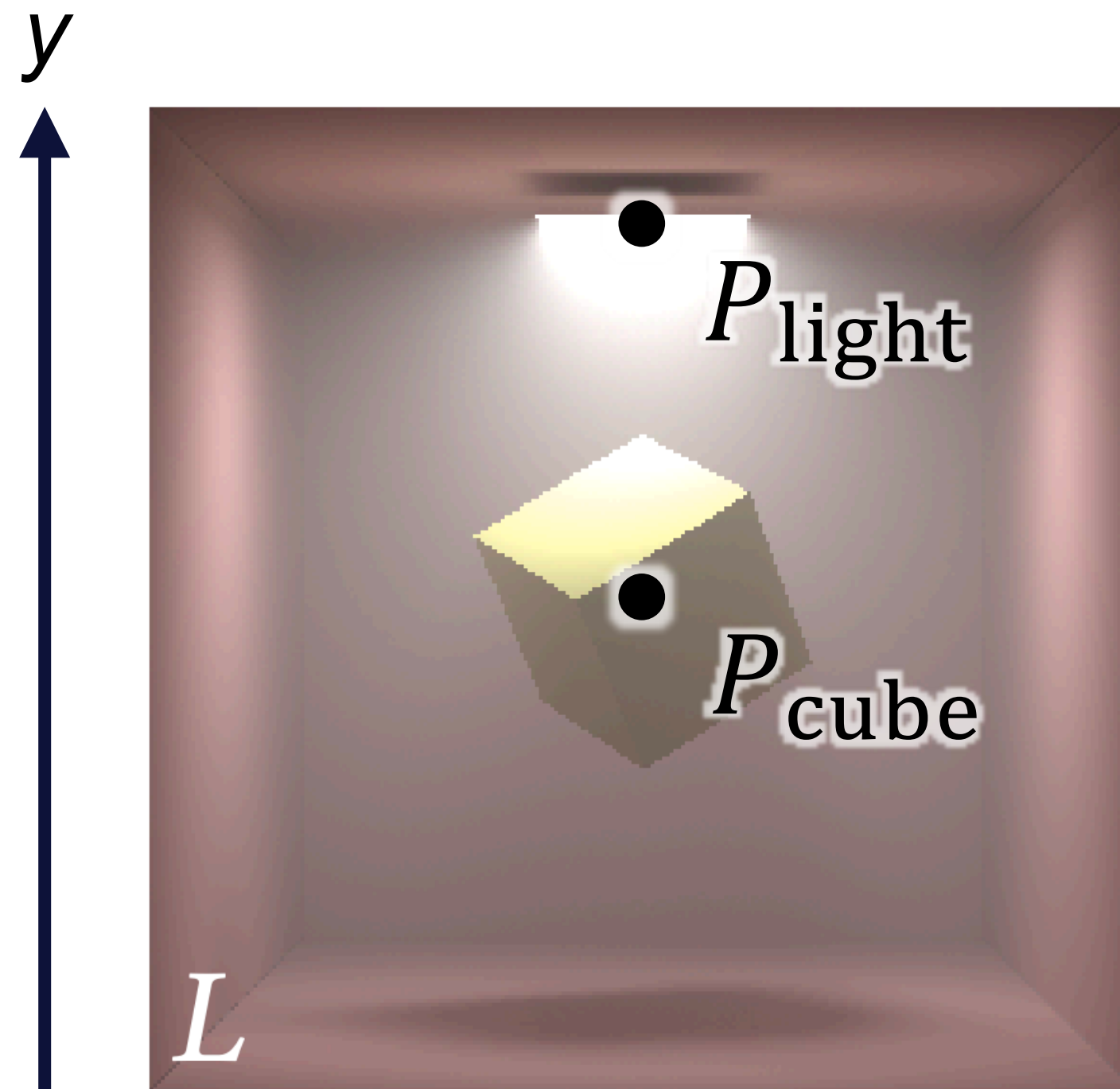
$$\partial_\pi L = \partial_\pi (K_T K_c L) + \partial_\pi Q$$



Captures the boundary integrals

$$\begin{pmatrix} \partial_\pi L \\ L \end{pmatrix} = \begin{pmatrix} K_T K_c & K_* \\ 0 & K_T K_c \end{pmatrix} \begin{pmatrix} \partial_\pi L \\ L \end{pmatrix} + \begin{pmatrix} \partial_\pi Q \\ Q \end{pmatrix}$$

Differential radiative transfer equation



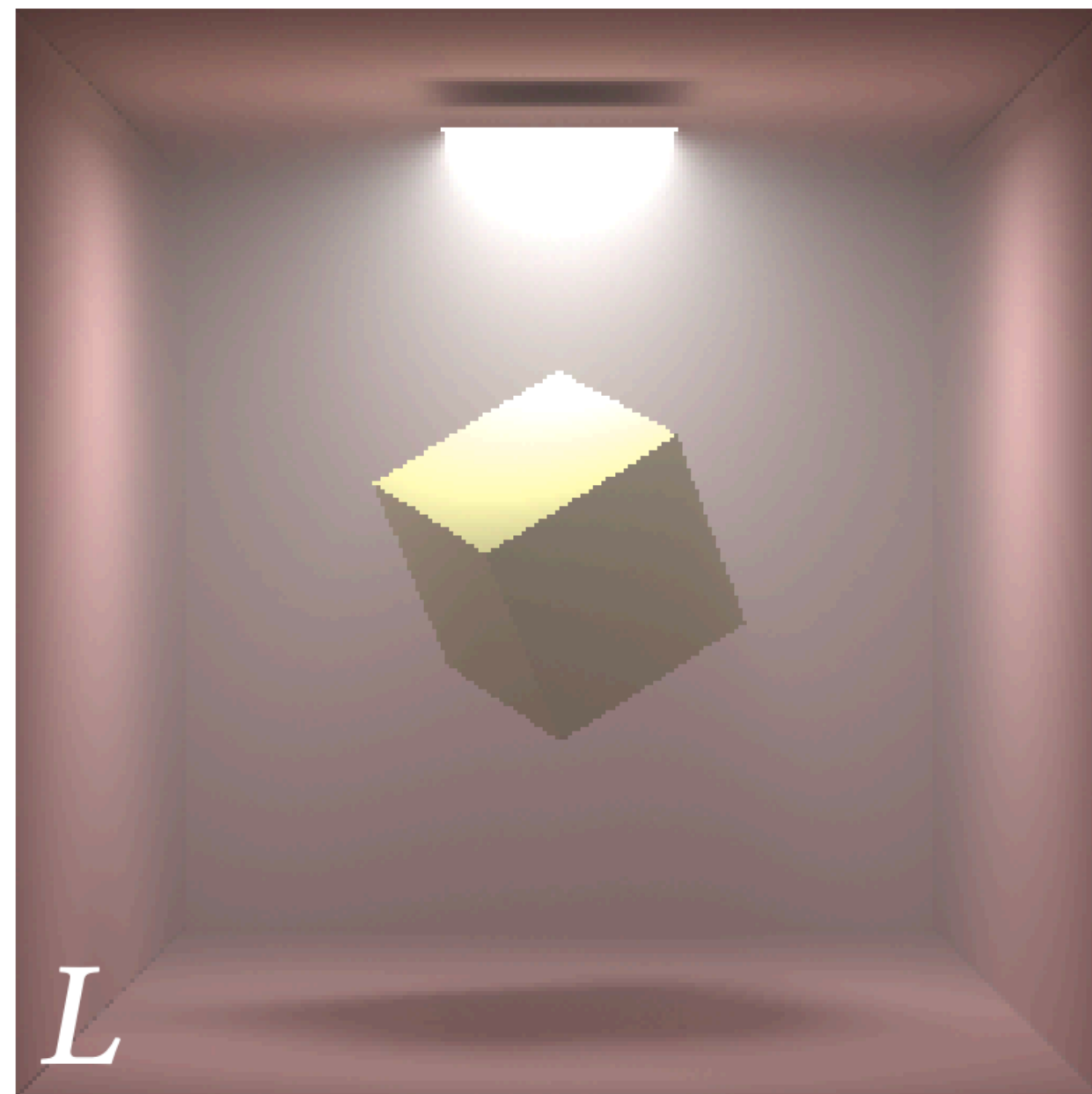
Original image

$$\mathbf{P}_{\text{light}}(\pi) = \mathbf{P}_0 + \begin{pmatrix} 0 \\ \pi \\ 0 \end{pmatrix}$$

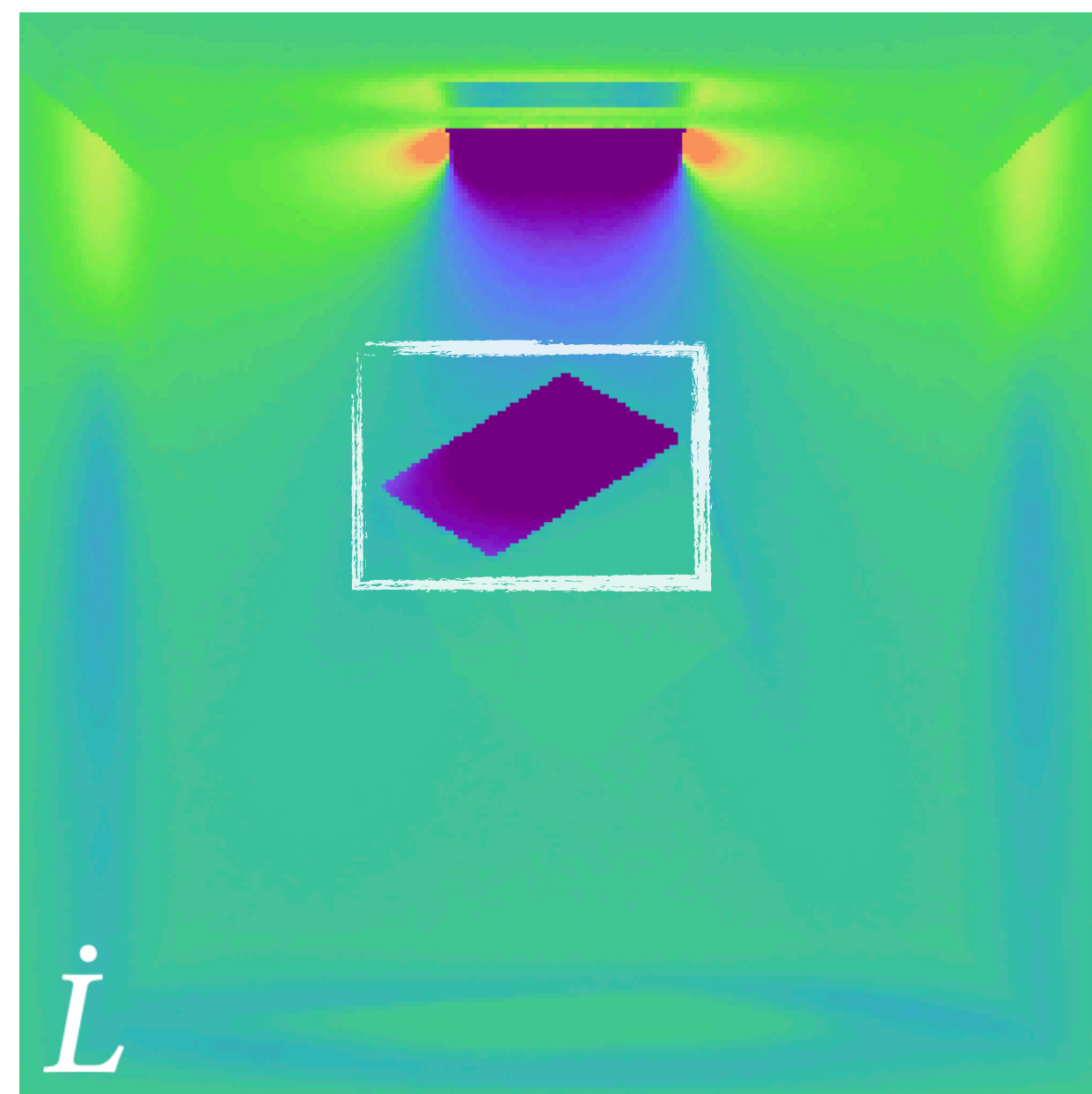
$$\mathbf{P}_{\text{cube}}(\pi) = \mathbf{P}_1 + \begin{pmatrix} 0 \\ \pi \\ 0 \end{pmatrix}$$

Constant
initial positions

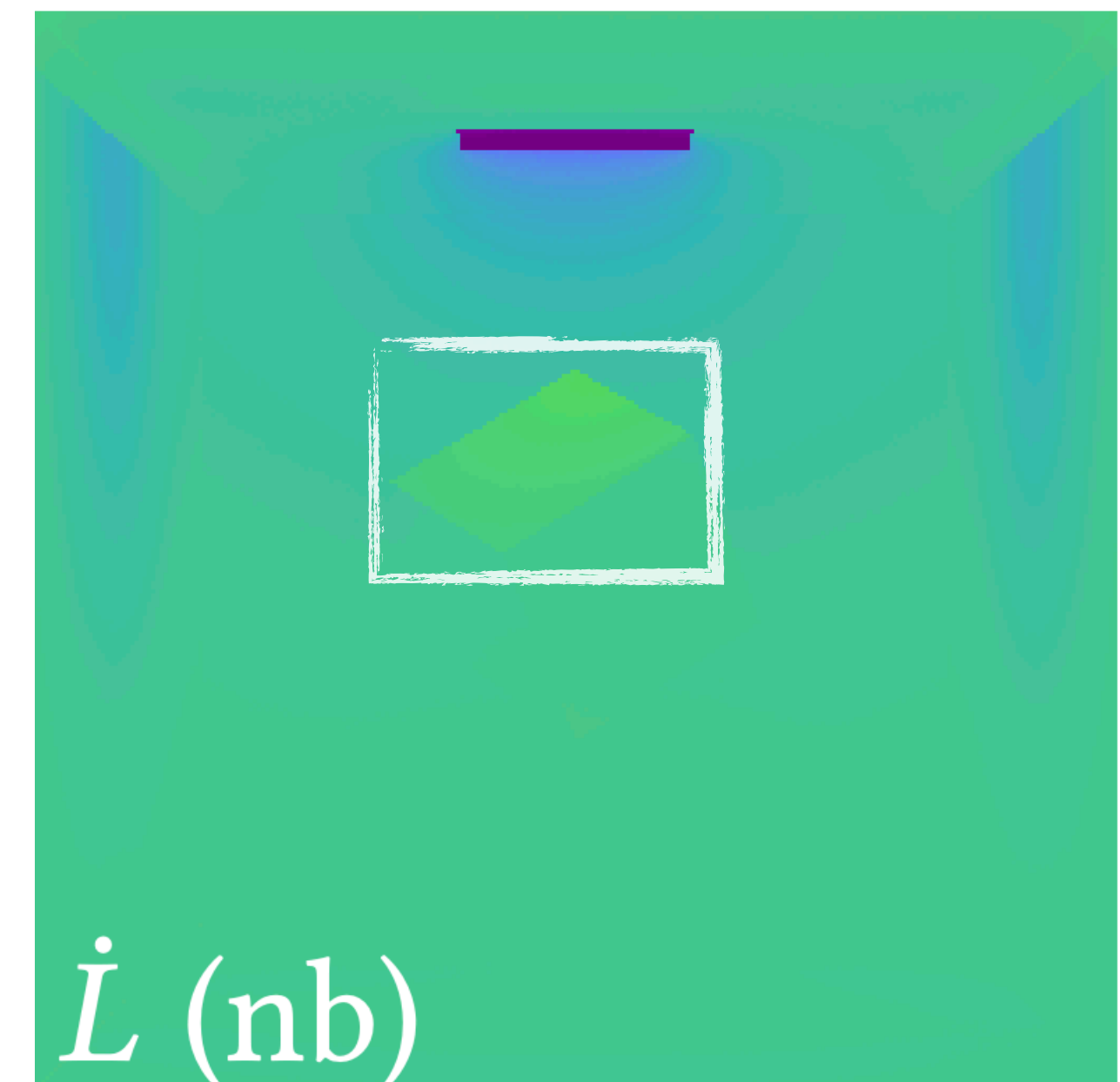
Negative  Zero Positive



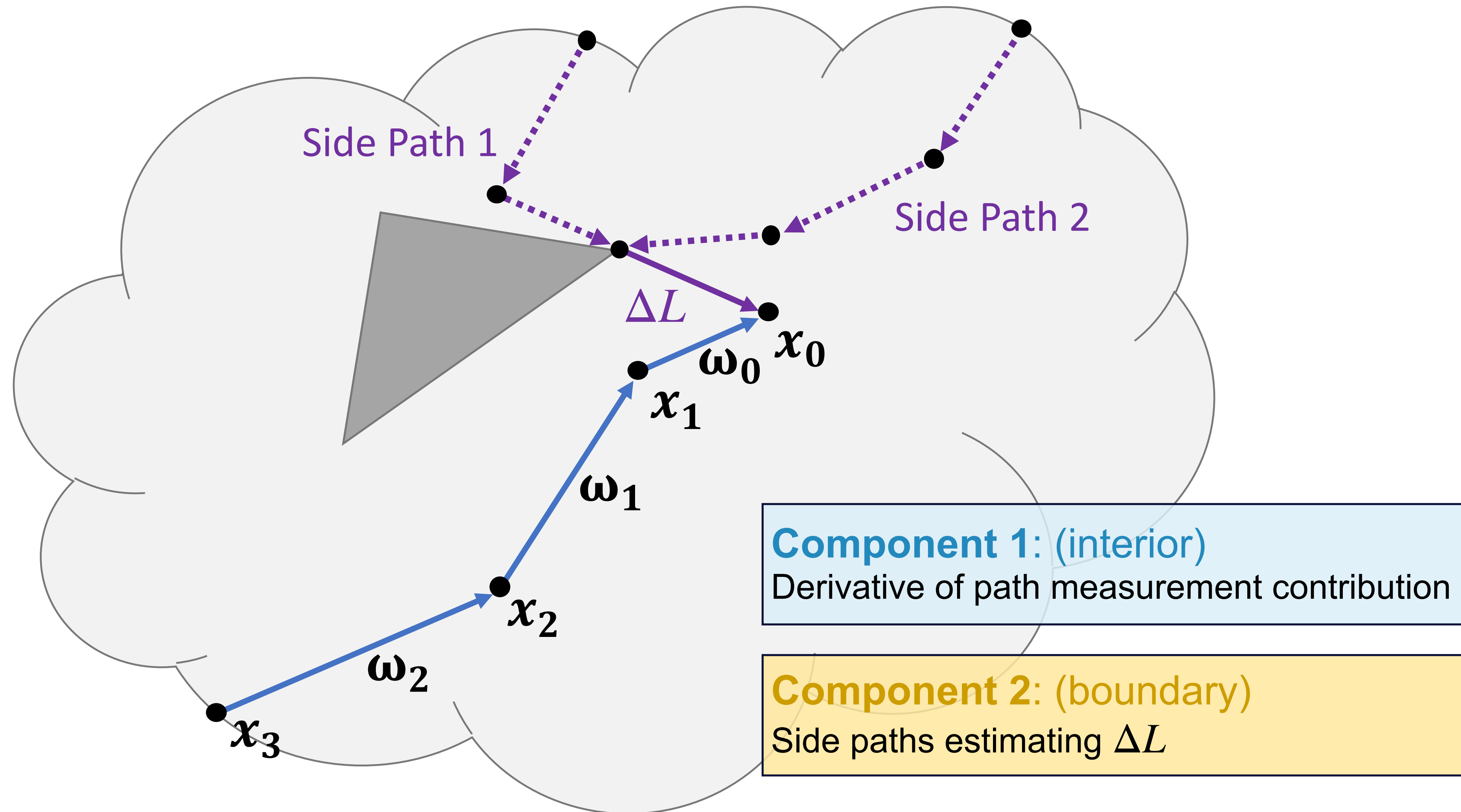
Original image



Derivative image



Derivative image
(w/o boundary integral)

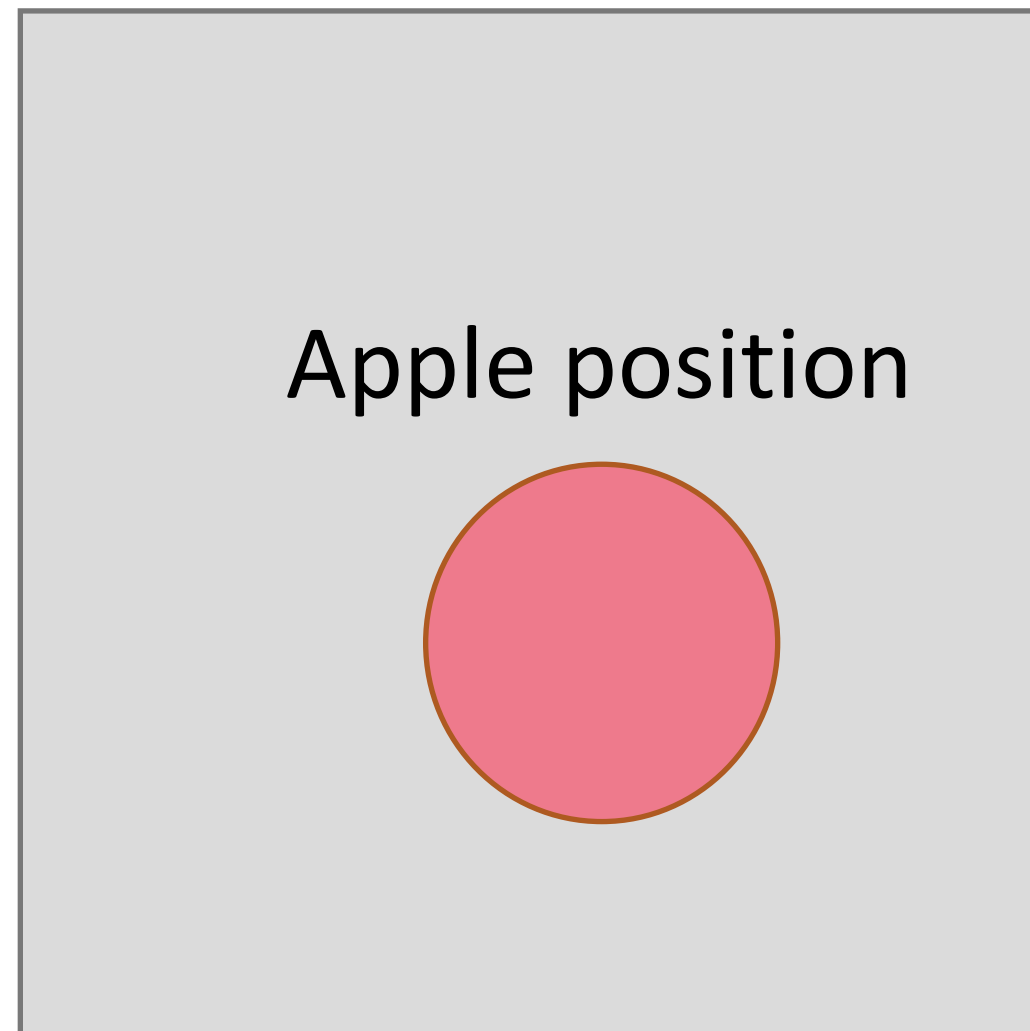


INVERSE-RENDERING RESULTS

- Scene configurations
 - Participating media
 - Changing geometry
- Optimization
 - Using only image loss (L2)

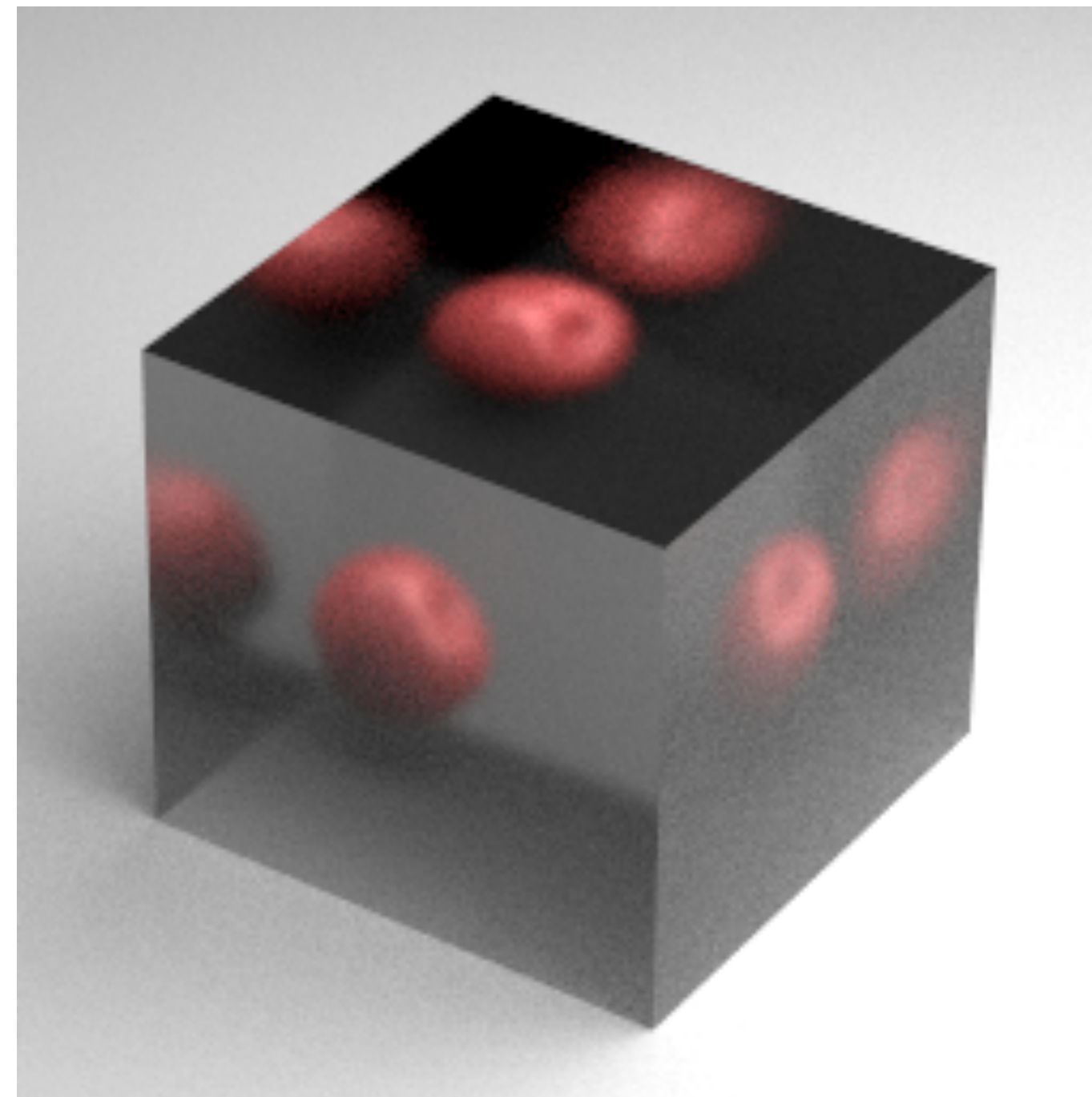
Apple in a box

Parameters

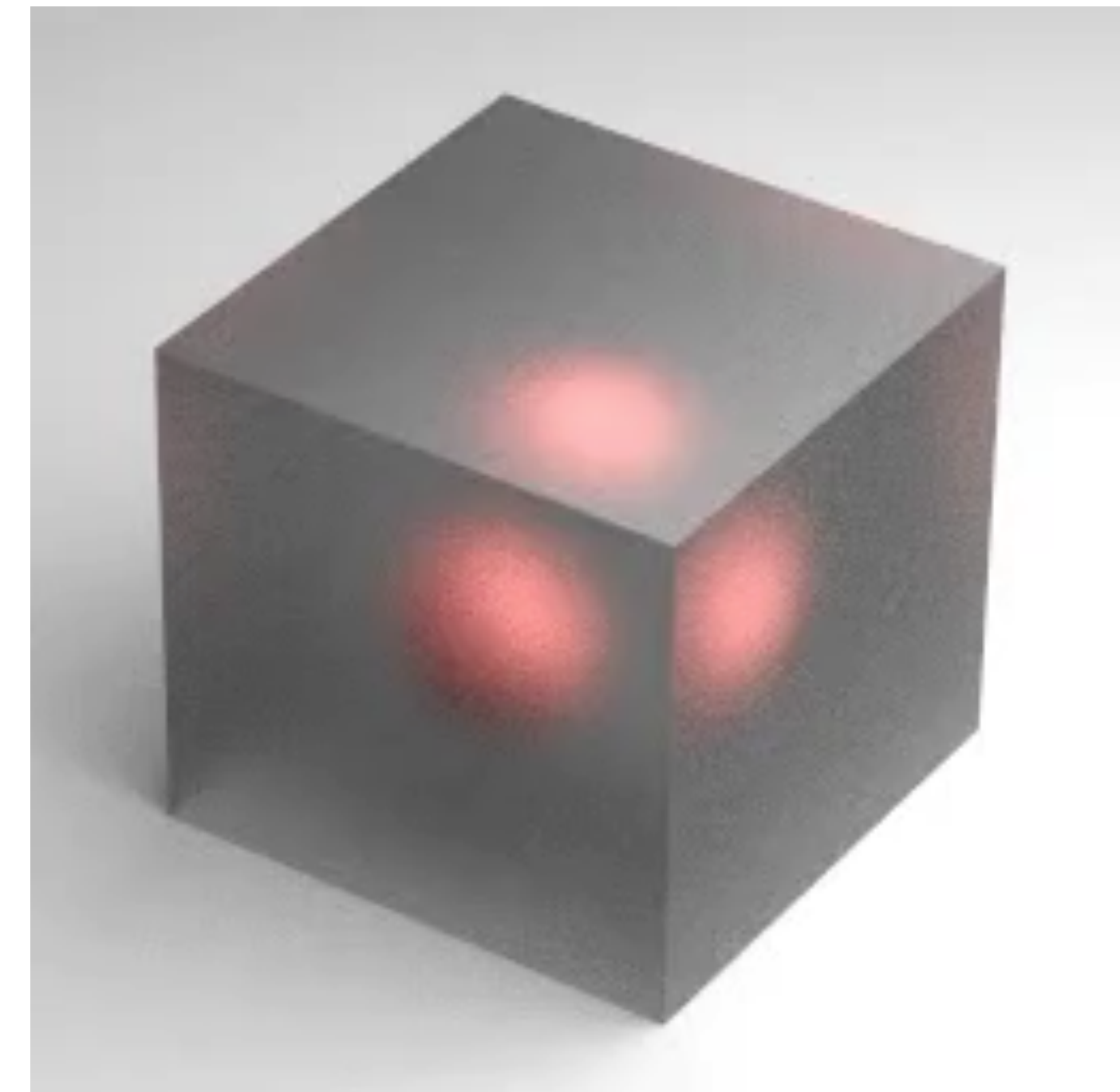


Cube roughness

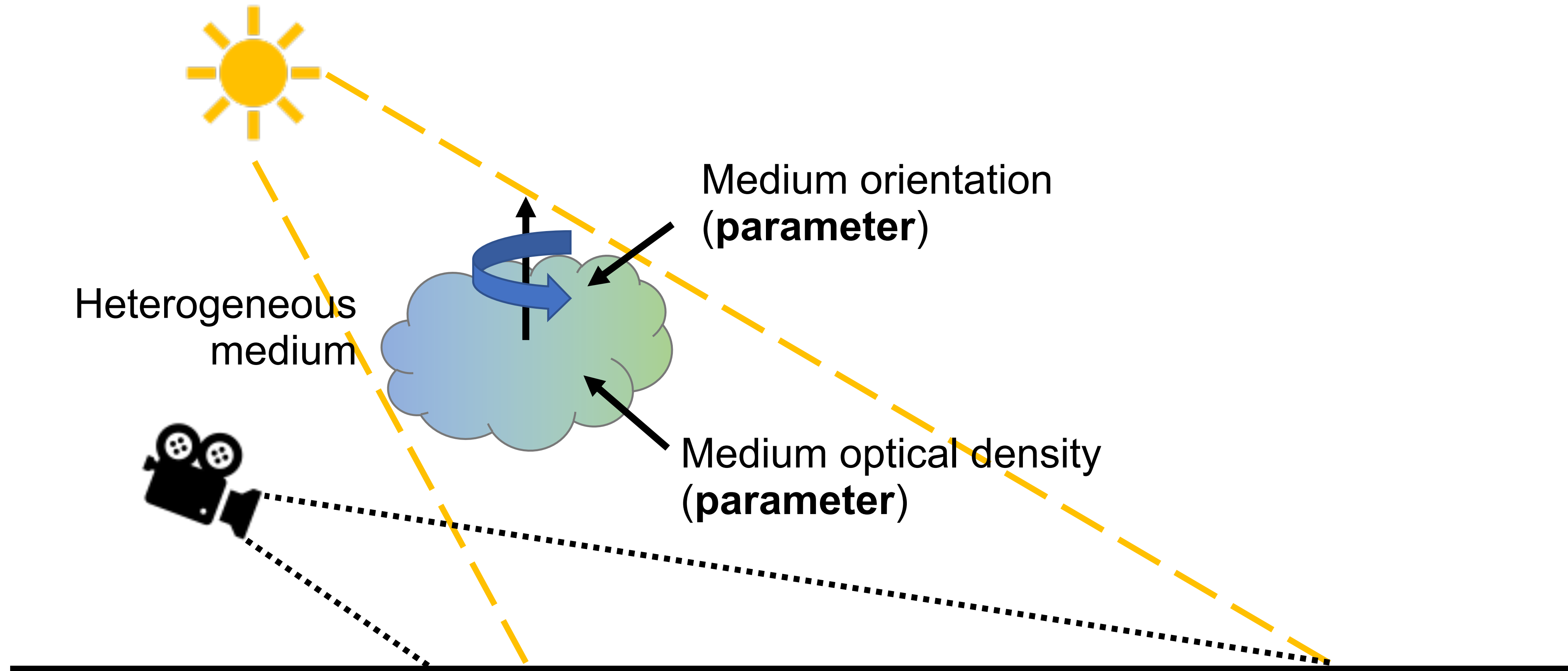
Target



Optimization process



Non-line-of-sight inverse rendering



Non-line-of-sight inverse rendering

Target



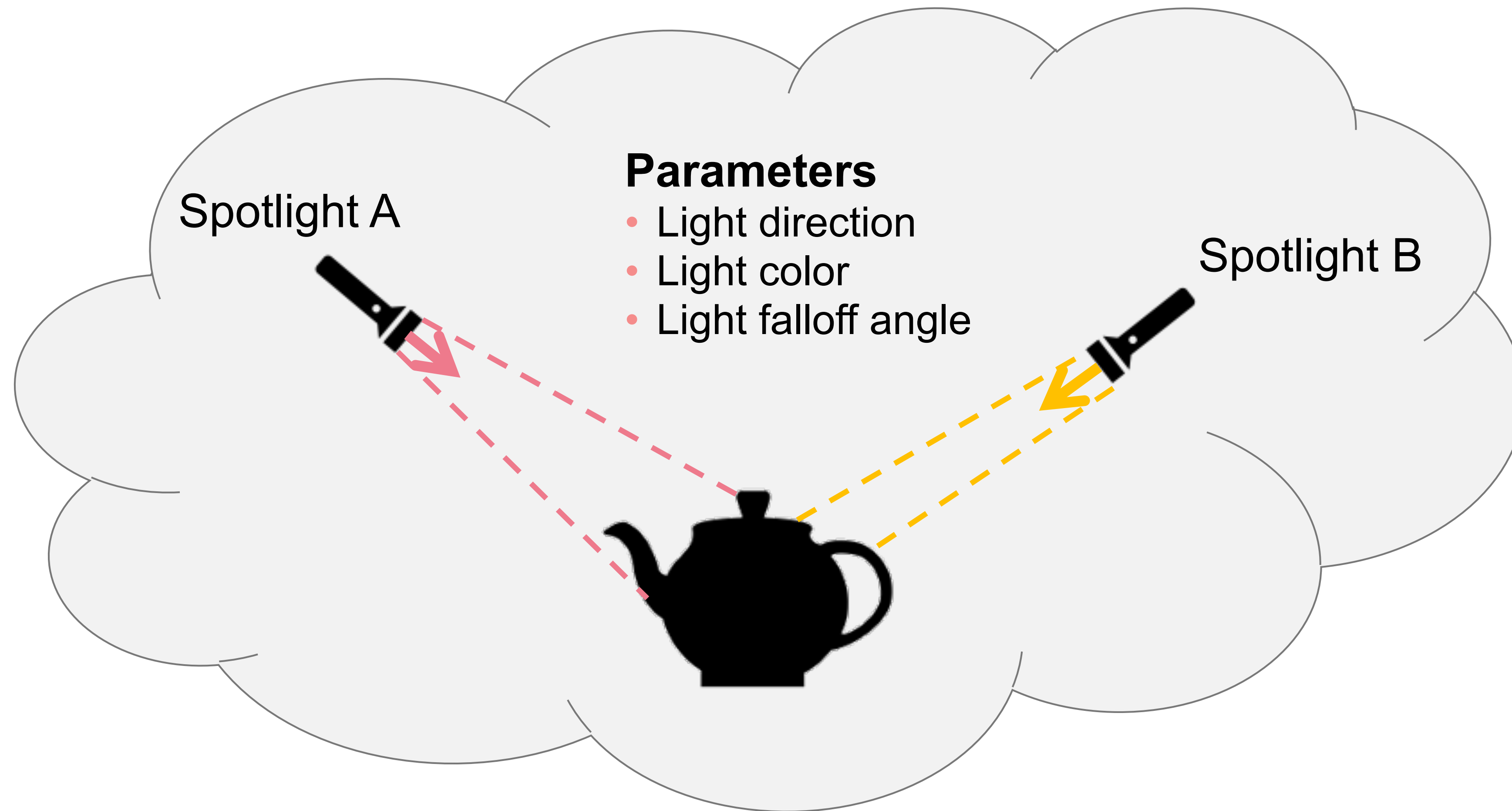
Optimization process



Different view



Design-inspired inverse rendering

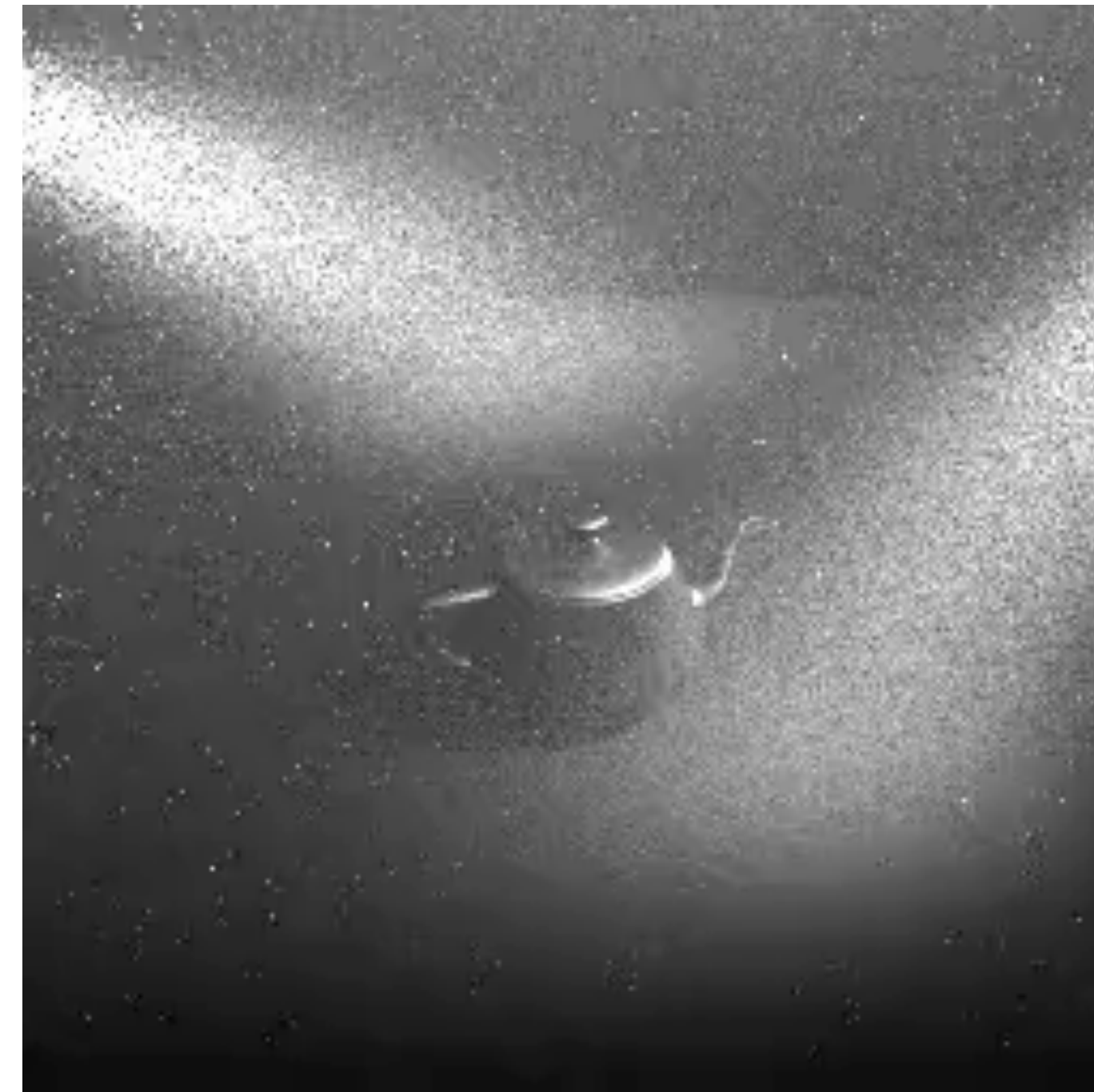


Design-inspired inverse rendering

Target



Optimization process



Reparameterizing Discontinuous Integrands for Differentiable Rendering

GUILLAUME LOUBET, École Polytechnique Fédérale de Lausanne (EPFL)
NICOLAS HOLZSCHUCH, Inria, Univ. Grenoble-Alpes, CNRS, LJK
WENZEL JAKOB, École Polytechnique Fédérale de Lausanne (EPFL)

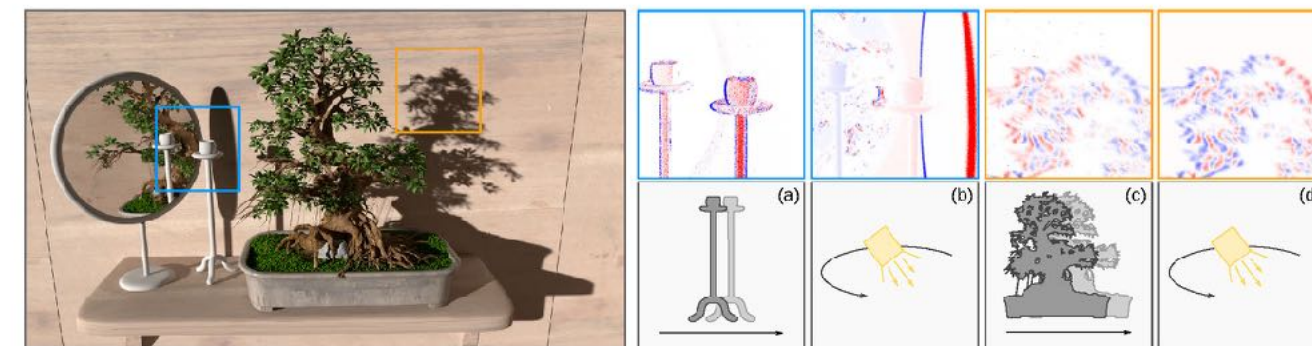


Fig. 1. The solution of inverse rendering problems using gradient-based optimization requires estimates of pixel derivatives with respect to arbitrary scene parameters. We focus on the problem of computing such derivatives for parameters that affect visibility, such as the position and shape of scene geometry (a, c) and light sources (b, d). Our renderer re-parameterizes integrals so that their gradients can be estimated using standard Monte Carlo integration and automatic differentiation—even when visibility changes would normally make the integrands non-differentiable. Our technique produces high-quality gradients at low sample counts (64 spp in these examples) for changes in both direct and indirect visibility, such as glossy reflections (a, b) and shadows (c, d).

Differentiable rendering has recently opened the door to a number of challenging inverse problems involving photorealistic images, such as computational material design and scattering-aware reconstruction of geometry and materials from photographs. Differentiable rendering algorithms strive to estimate partial derivatives of pixels in a rendered image with respect to scene parameters, which is difficult because visibility changes are inherently non-differentiable.

We propose a new technique for differentiating path-traced images with respect to scene parameters that affect visibility, including the position of cameras, light sources, and vertices in triangle meshes. Our algorithm computes the gradients of illumination integrals by applying changes of variables that remove or strongly reduce the dependence of the position of discontinuities on differentiable scene parameters. The underlying parameterization is created on the fly for each integral and enables accurate gradient estimates using standard Monte Carlo sampling in conjunction with automatic differentiation. Importantly, our approach does not rely on sampling silhouette edges, which has been a bottleneck in previous work and tends to produce high-variance gradients when important edges are found with insufficient

probability in scenes with complex visibility and high-resolution geometry. We show that our method only requires a few samples to produce gradients with low bias and variance for challenging cases such as glossy reflections and shadows. Finally, we use our differentiable path tracer to reconstruct the 3D geometry and materials of several real-world objects from a set of reference photographs.

CCS Concepts: • Computing methodologies → Rendering; Ray tracing.

Additional Key Words and Phrases: differentiable rendering, inverse rendering, stochastic gradient descent, discontinuous integrands, path tracing

ACM Reference Format:

Guillaume Loubet, Nicolas Holzschuch, Wenzel Jakob, and . 2019. Reparameterizing Discontinuous Integrands for Differentiable Rendering. *ACM Trans. Graph.* 38, 6, Article 228 (November 2019), 14 pages. <https://doi.org/10.1145/3355085.3355510>

1 INTRODUCTION

Physically based rendering algorithms generate photorealistic images by simulating the flow of light through a detailed mathematical representation of a virtual scene. Historically a one-way transformation from scene to rendered image, the emergence of a new class of differentiable rendering algorithms has enabled the use of rendering in an inverse sense, to find a scene that maximizes a user-specified objective function. One particular choice of objective leads to *inverse rendering*, whose goal is the acquisition of 3D shape and material properties from photographs of real-world objects, alleviating the tedious task of modeling photorealistic content by hand. Other kinds of objective functions hold significant untapped potential in areas

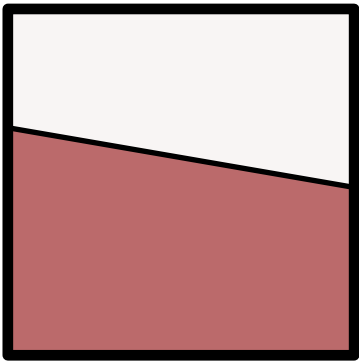
ACM Trans. Graph., Vol. 38, No. 5, Article 228. Publication date: November 2019.


Reparameterizing Discontinuous Integrals for Differentiable Rendering

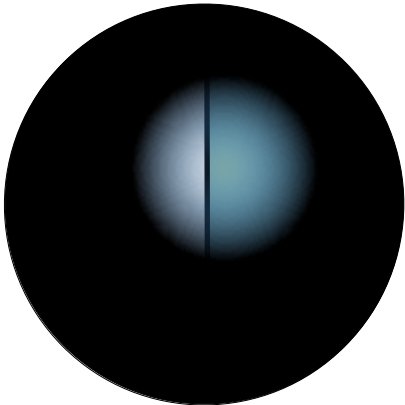
Guillaume Loubet, Nicolas Holzschuch, Wenzel Jakob

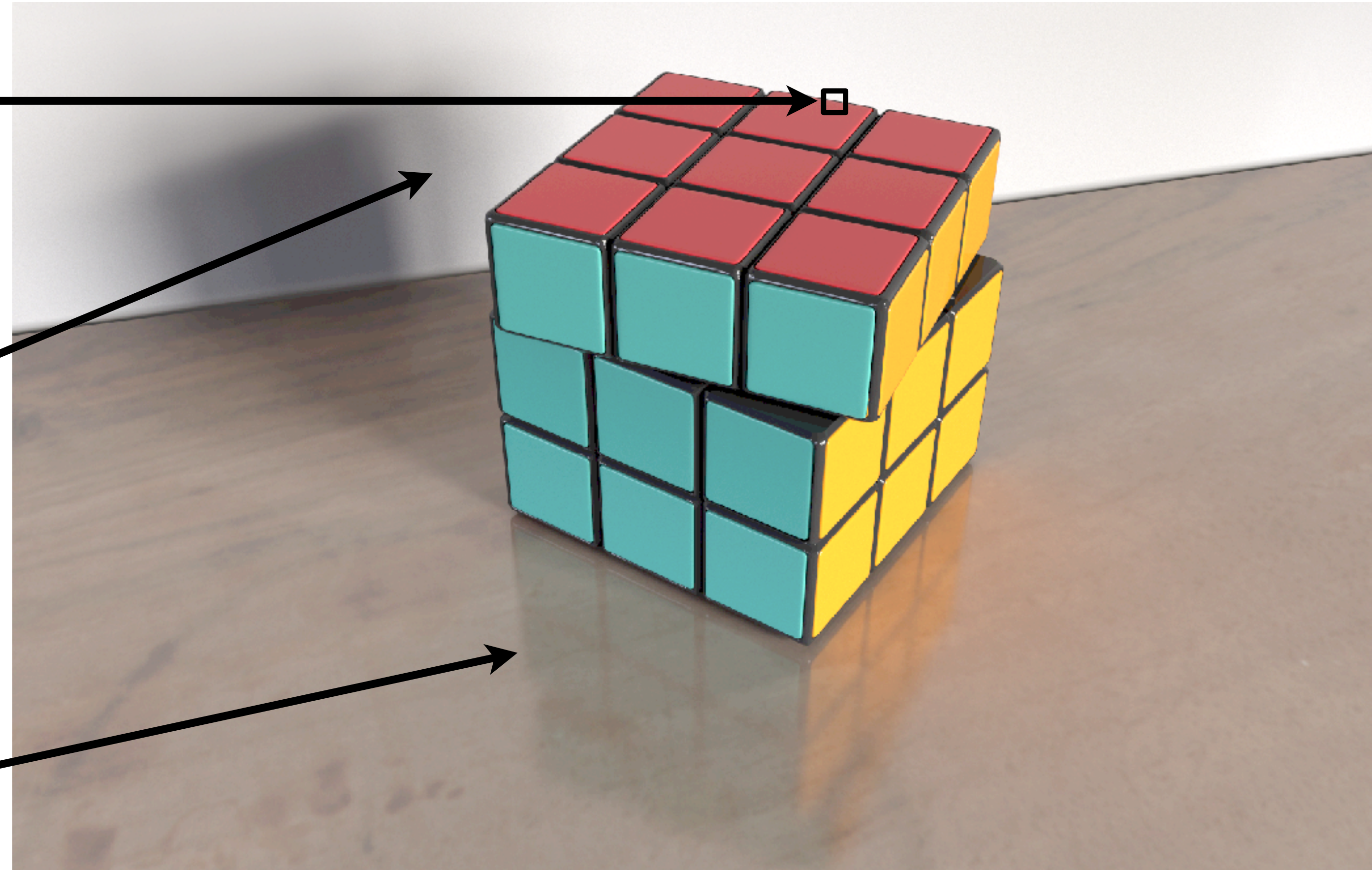
SIGGRAPH Asia 2019

MOVING DISCONTINUITIES

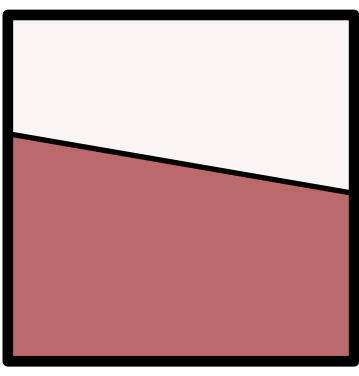
Pixel integrals \iint  $dx dy$


Light integrals \int  $d\omega$

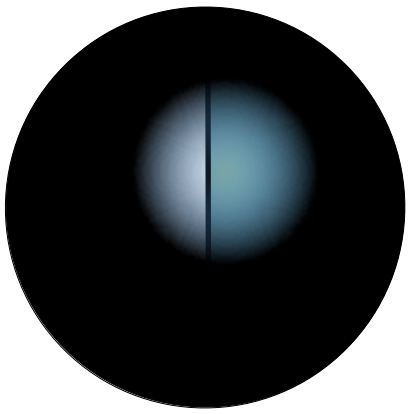
BSDF integrals \int  $d\omega$

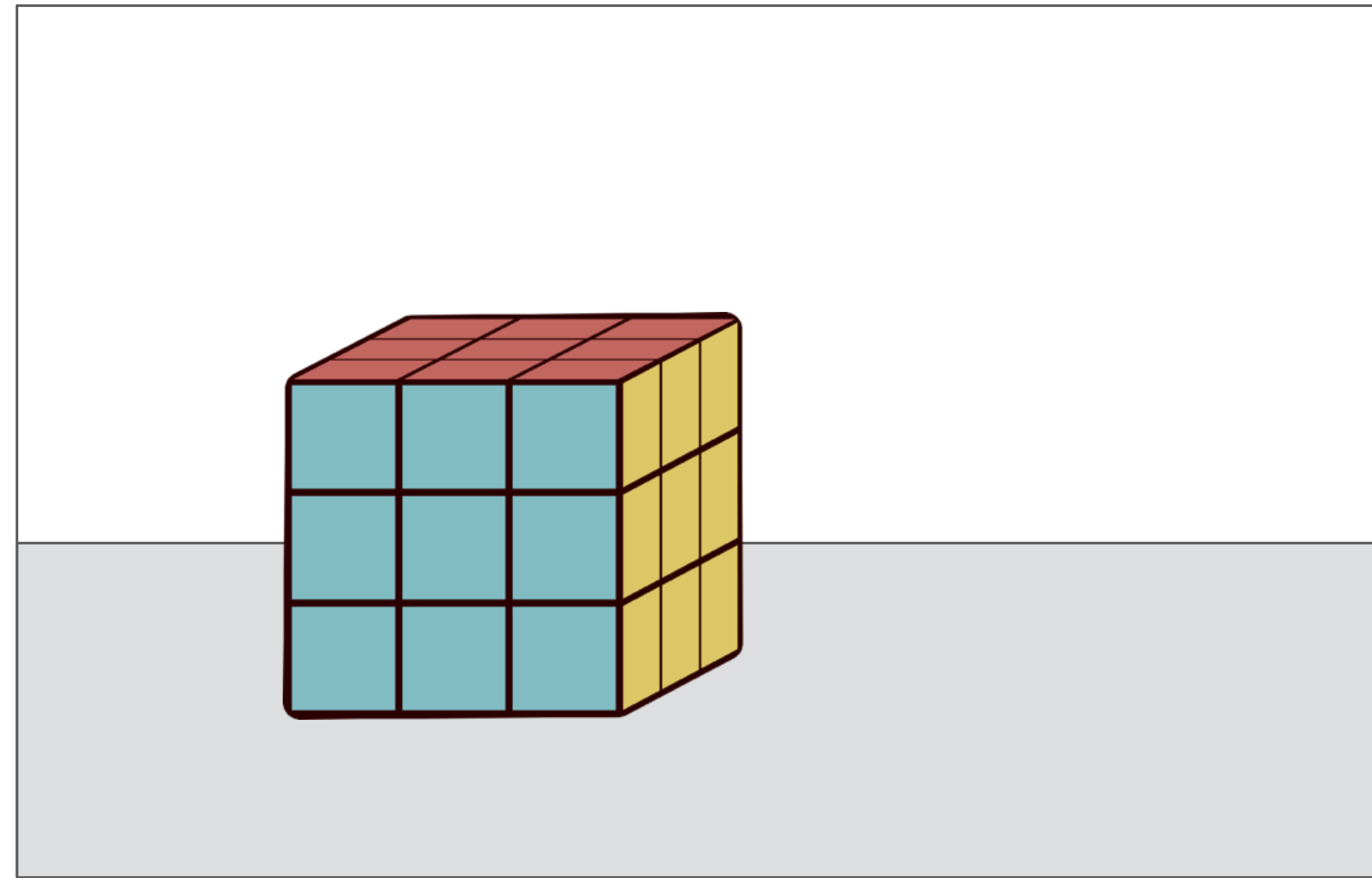


MOVING DISCONTINUITIES

Pixel integrals \iint  $dx dy$

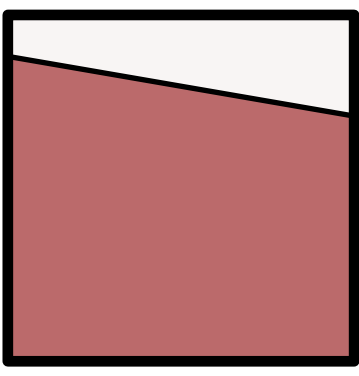
Light integrals \int  $d\omega$

BSDF integrals \int  $d\omega$

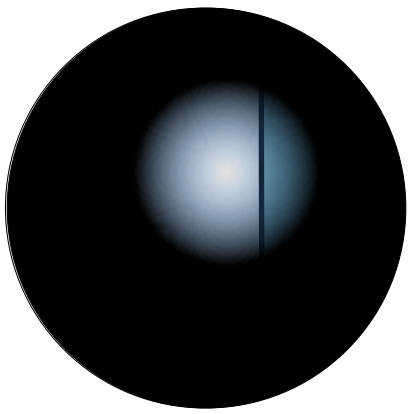


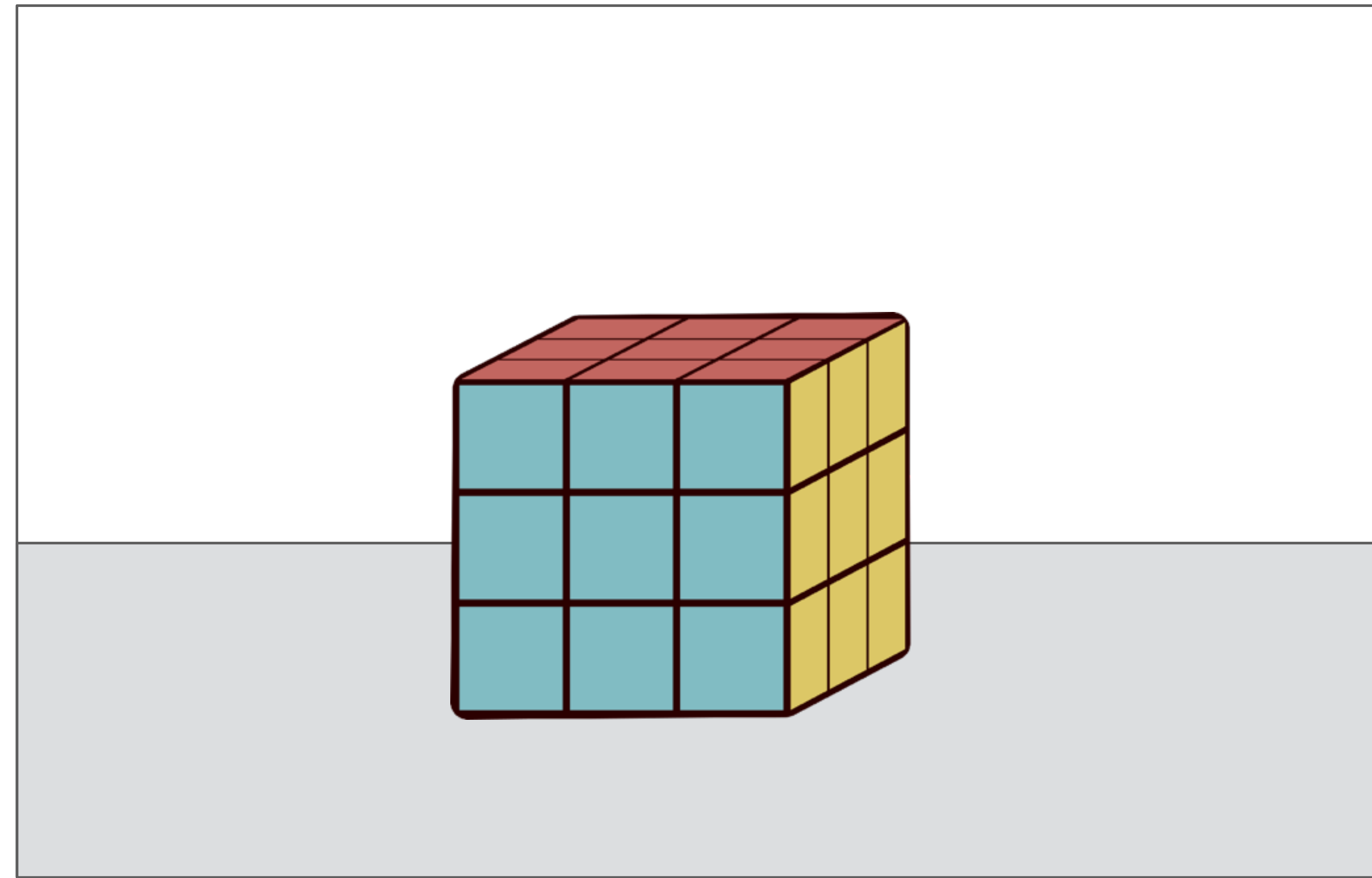
Scene parameter x_i 

MOVING DISCONTINUITIES

Pixel integrals \iint  $dx dy$

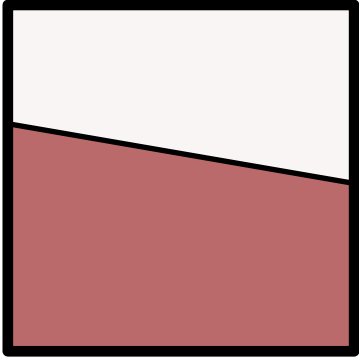
Light integrals \int  $d\omega$


BSDF integrals \int  $d\omega$

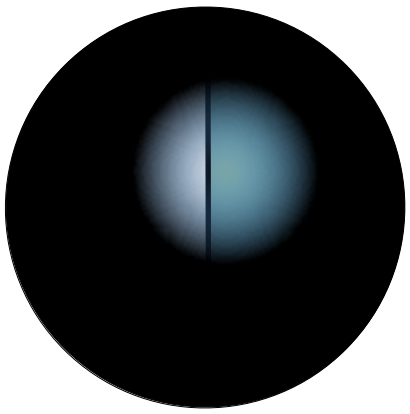


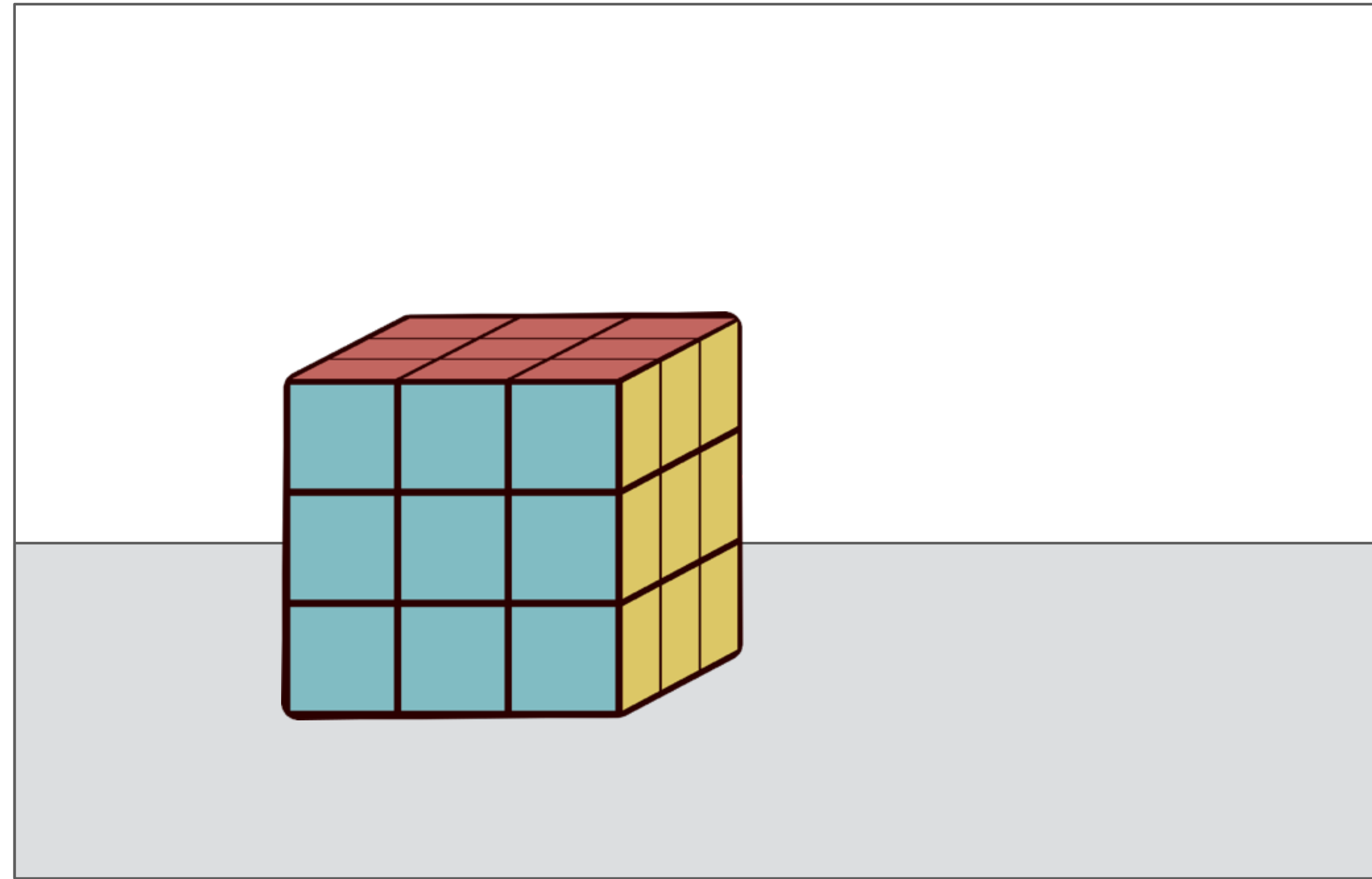
Scene parameter x_i 

MOVING DISCONTINUITIES

Pixel integrals \iint  $dx dy$

Light integrals \int  $d\omega$

BSDF integrals \int  $d\omega$



Scene parameter x_i 

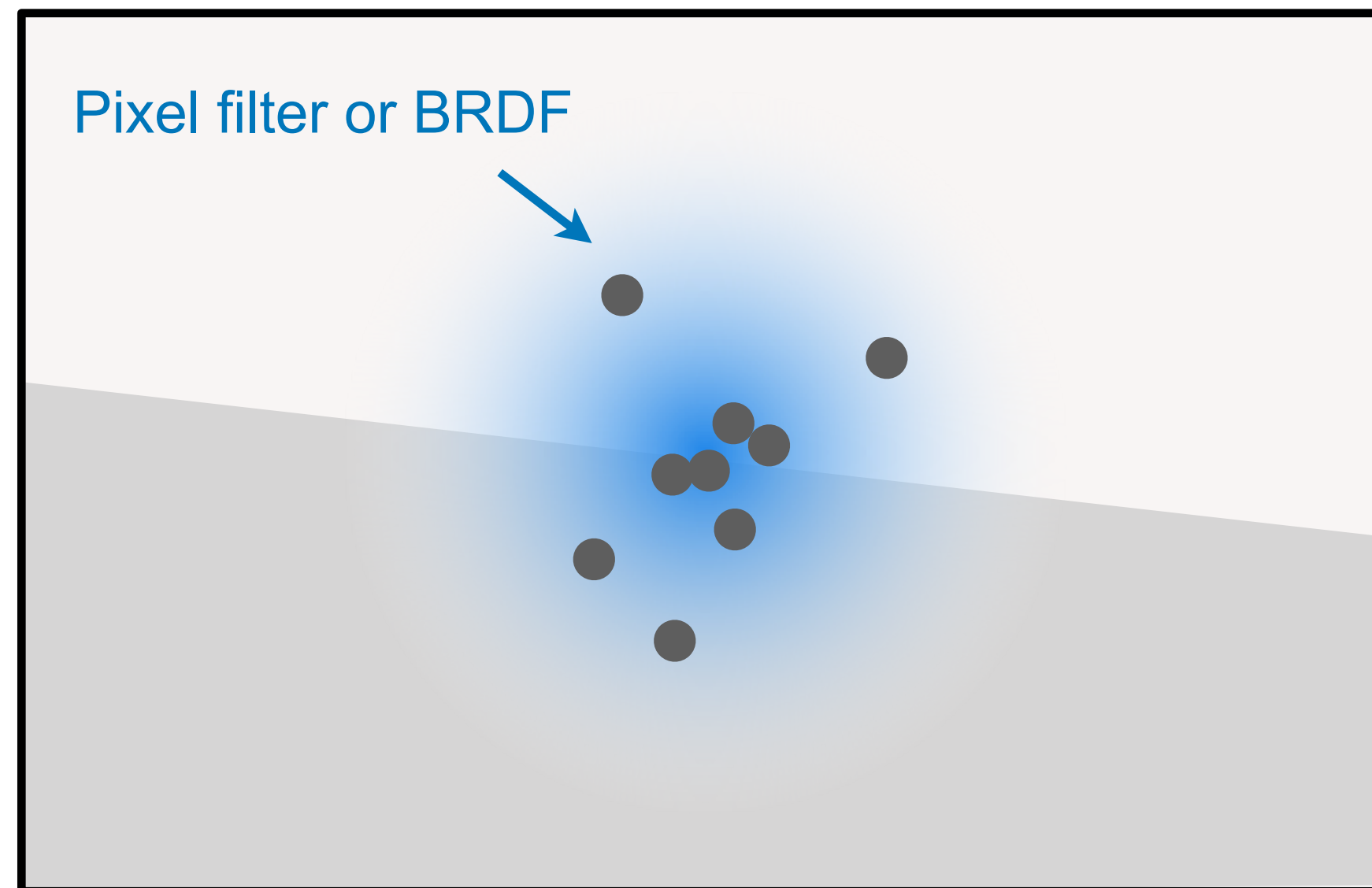
Cannot differentiate standard Monte Carlo estimates



We currently don't have good acceleration data structures for this operation.

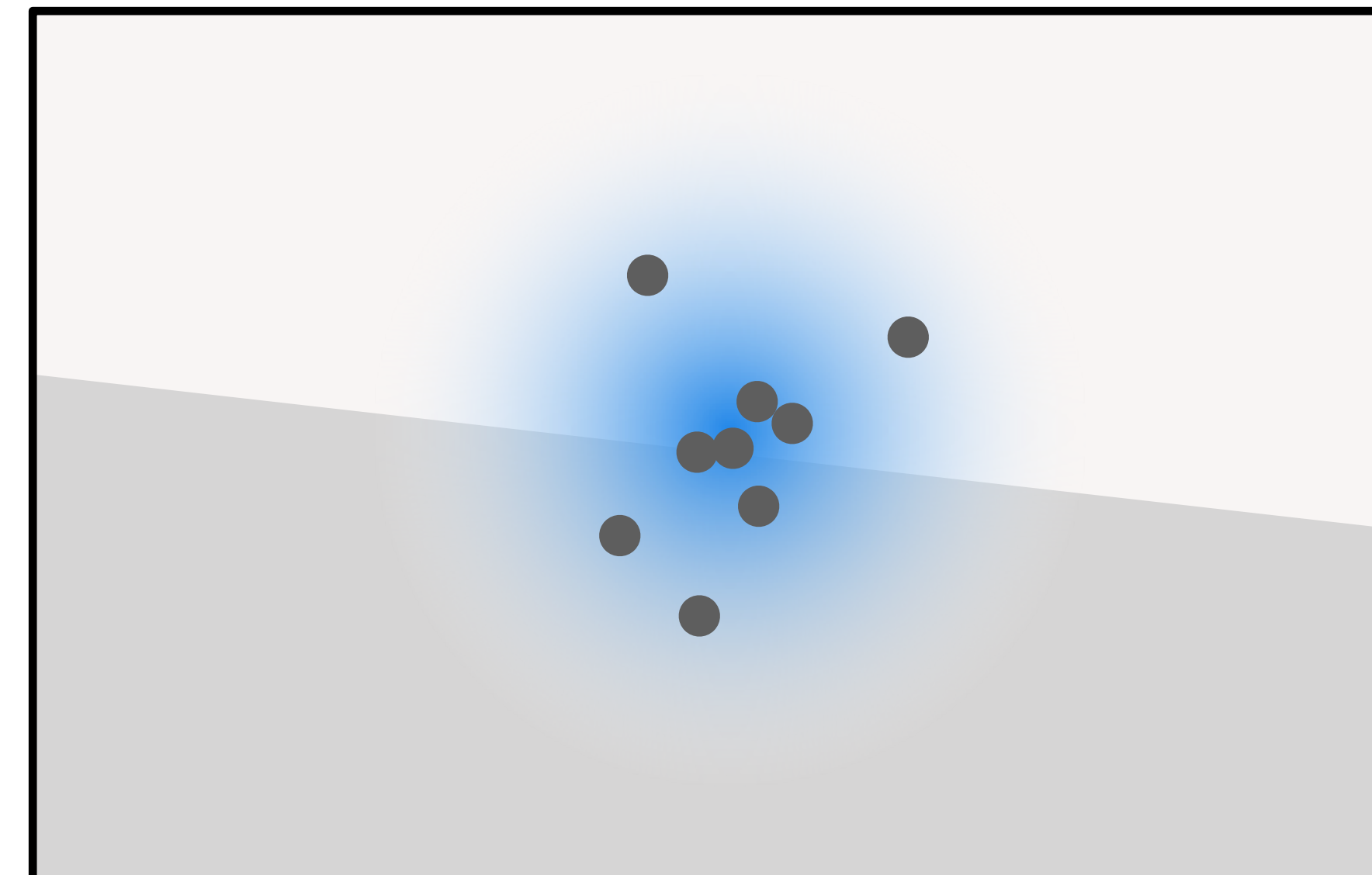
REPARAMETERIZE INTEGRALS?

Non-differentiable Monte Carlo estimates



x_i ————●—————

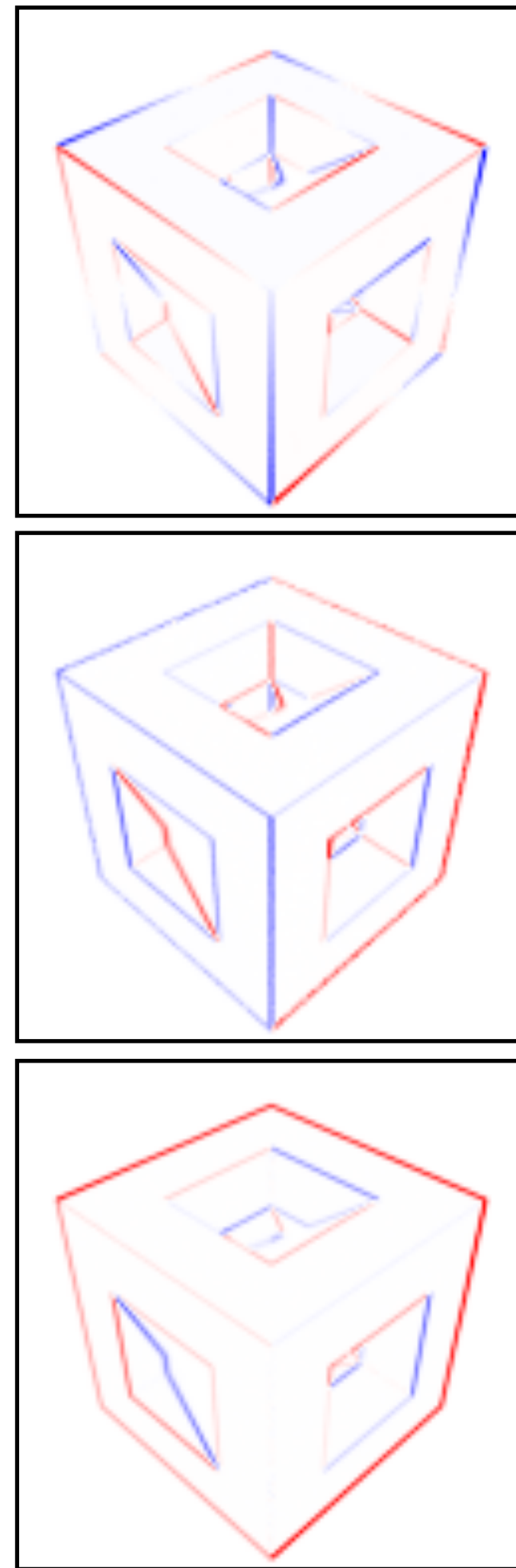
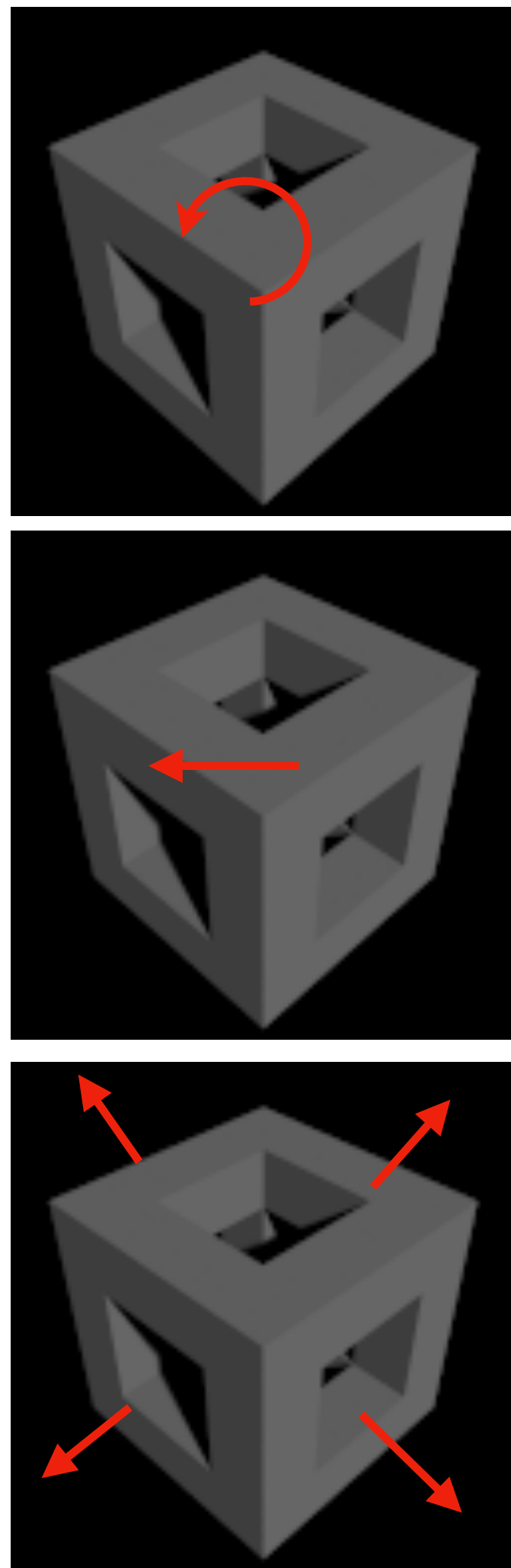
Differentiable Monte Carlo estimates



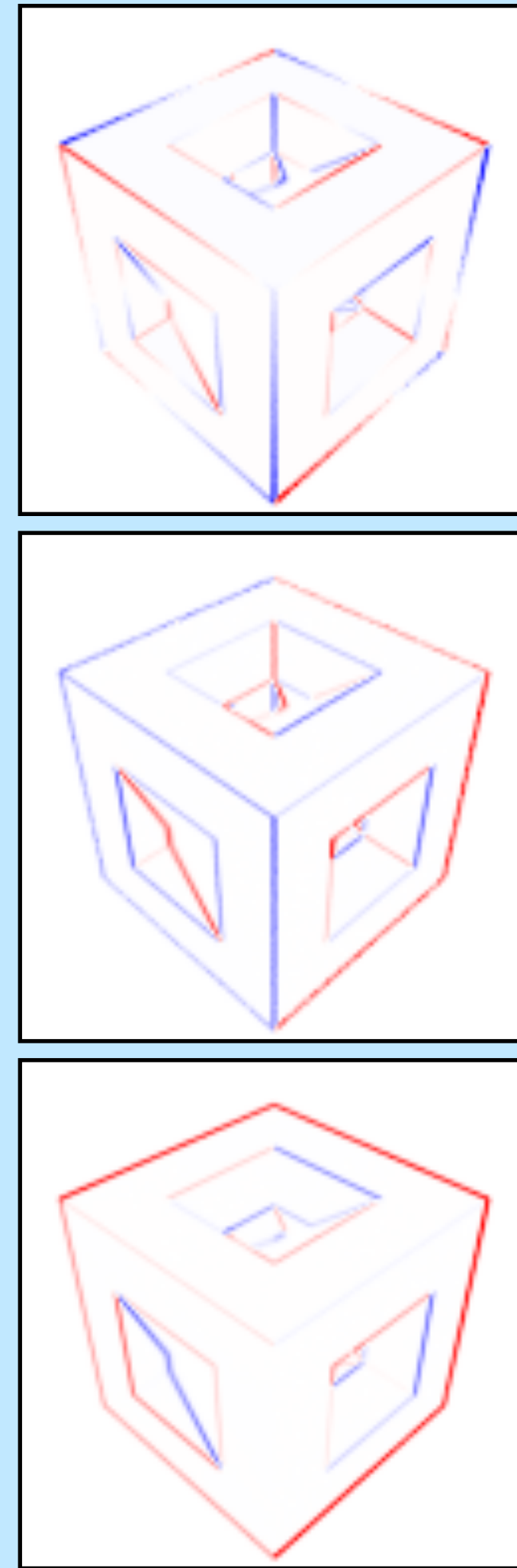
x_i ————●—————

Change of variables

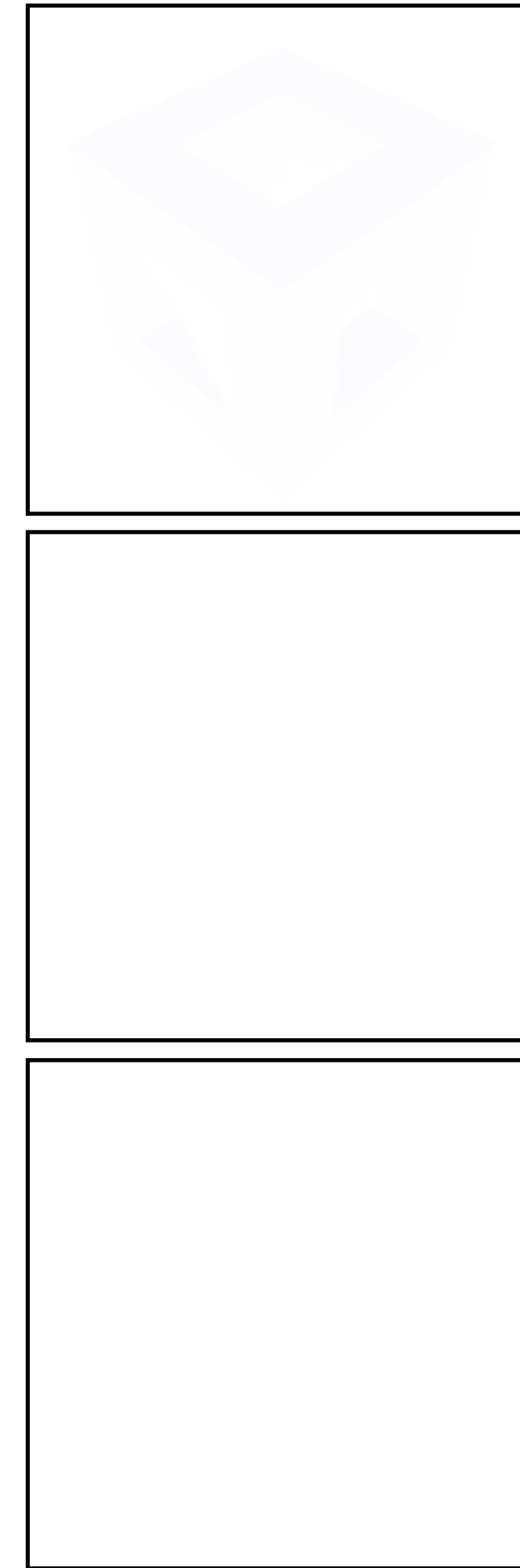
RESULTS



Ours



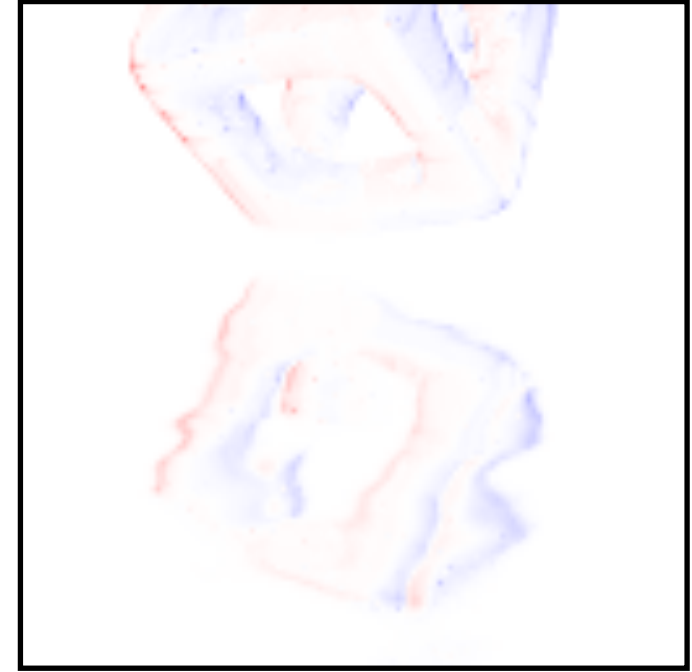
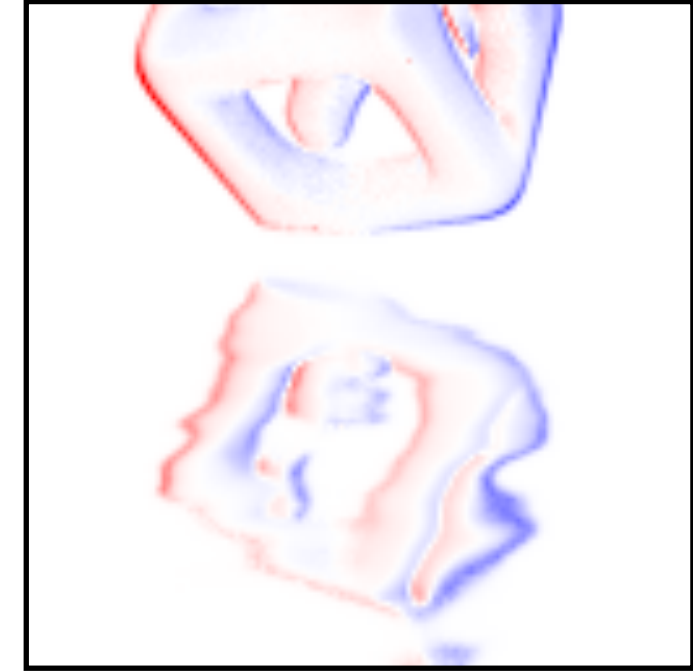
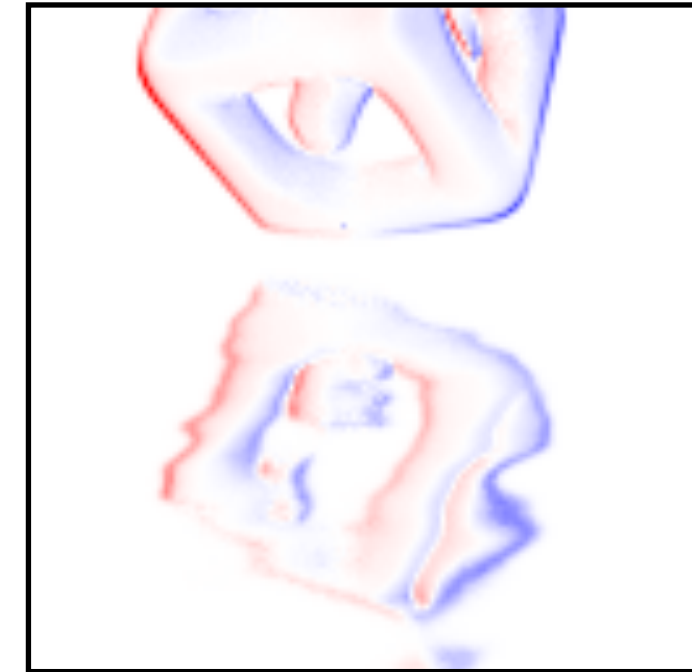
Reference
(Finite differences)



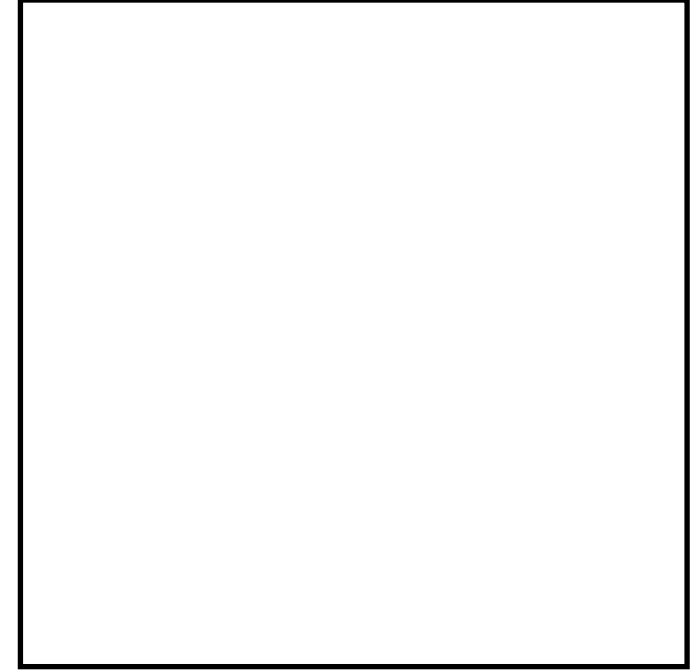
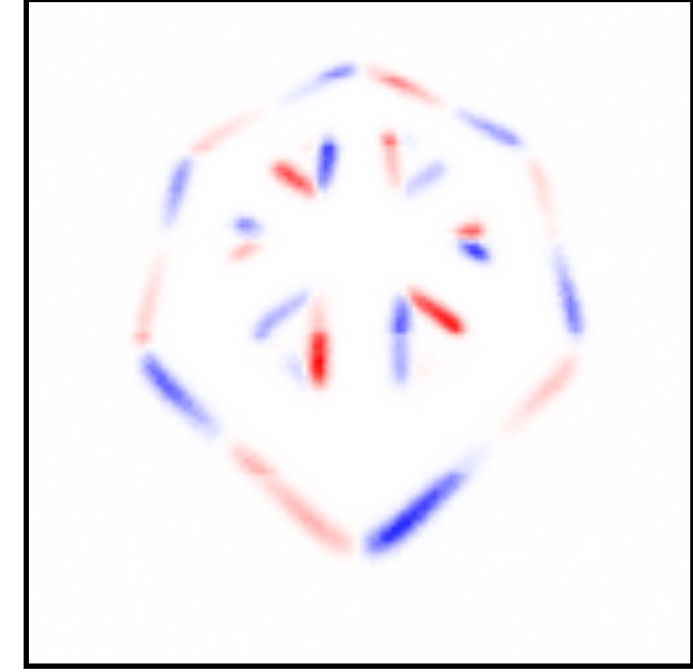
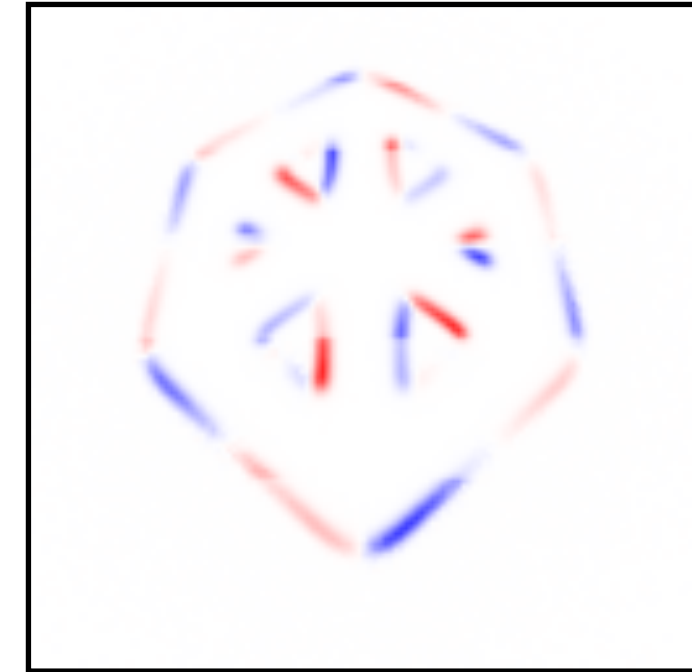
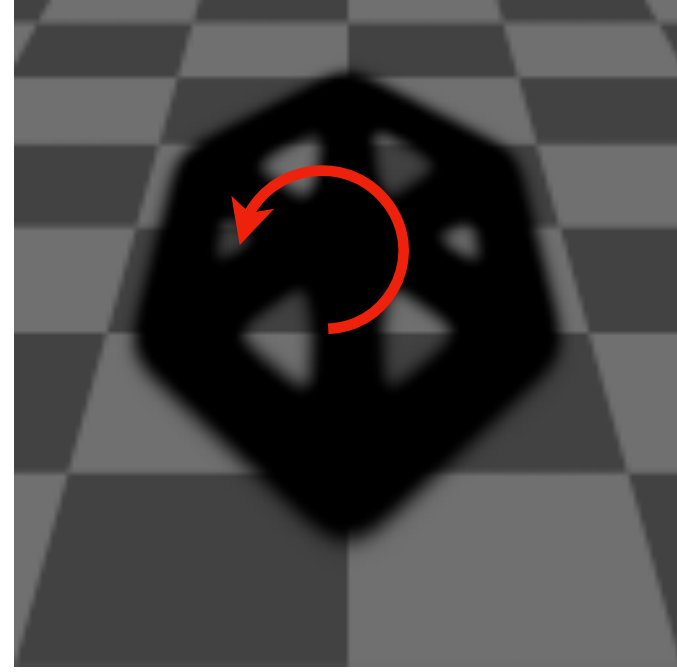
Without
changes of variables

RESULTS

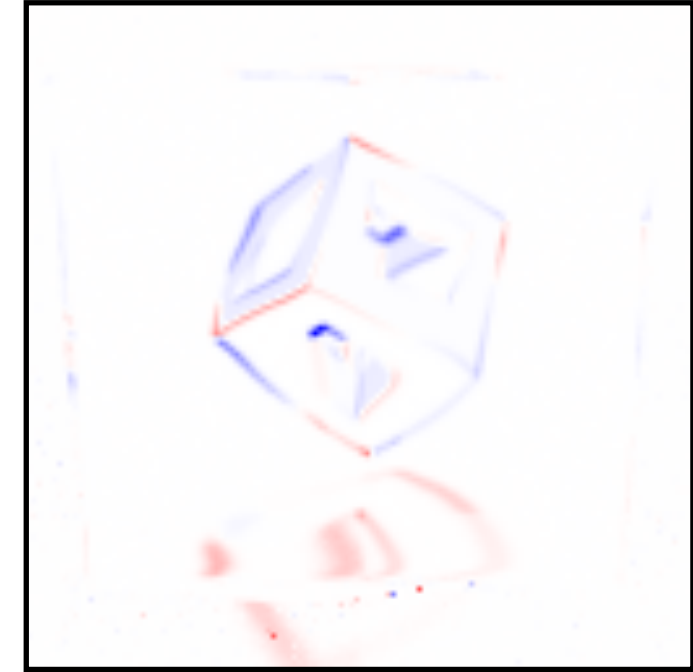
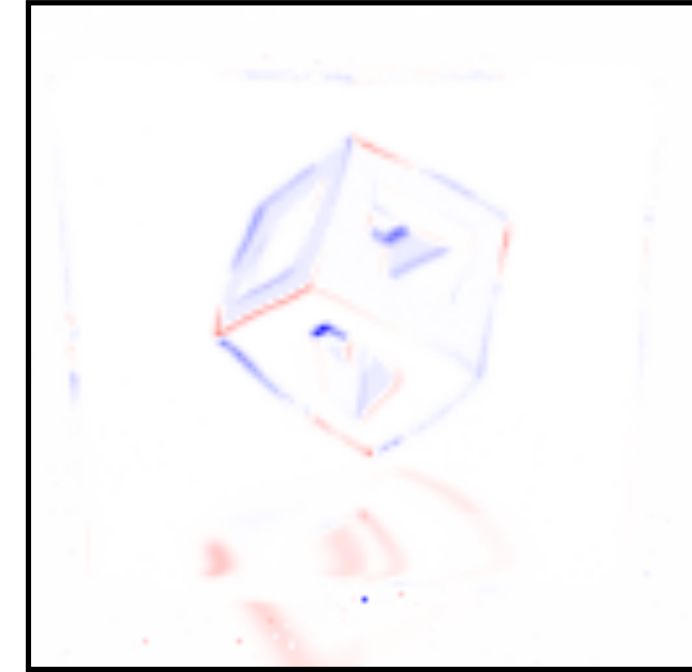
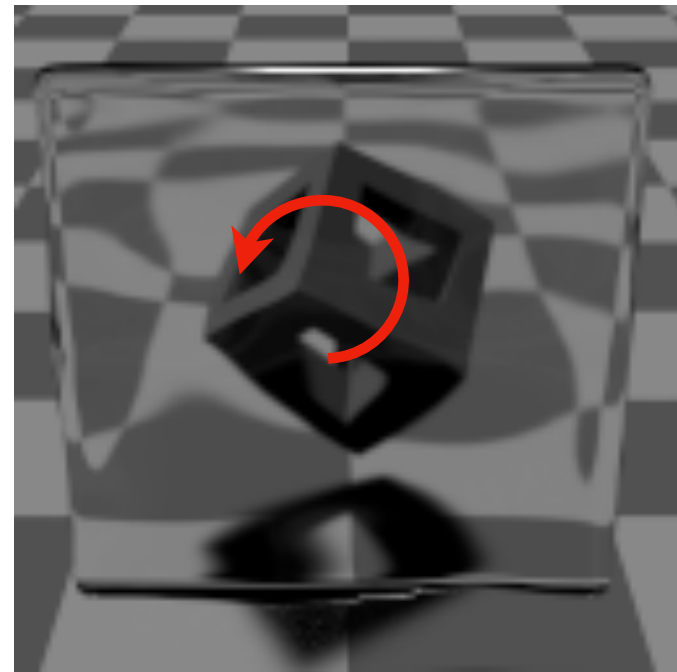
Glossy reflection



Shadows



Refraction



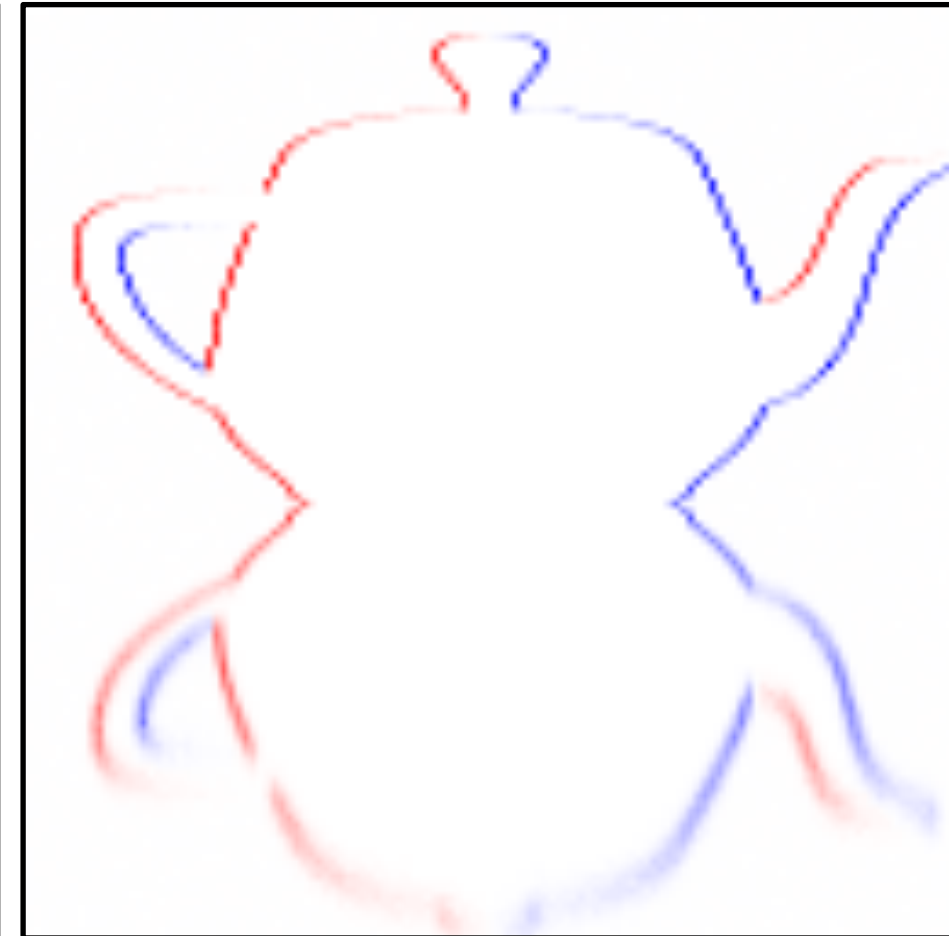
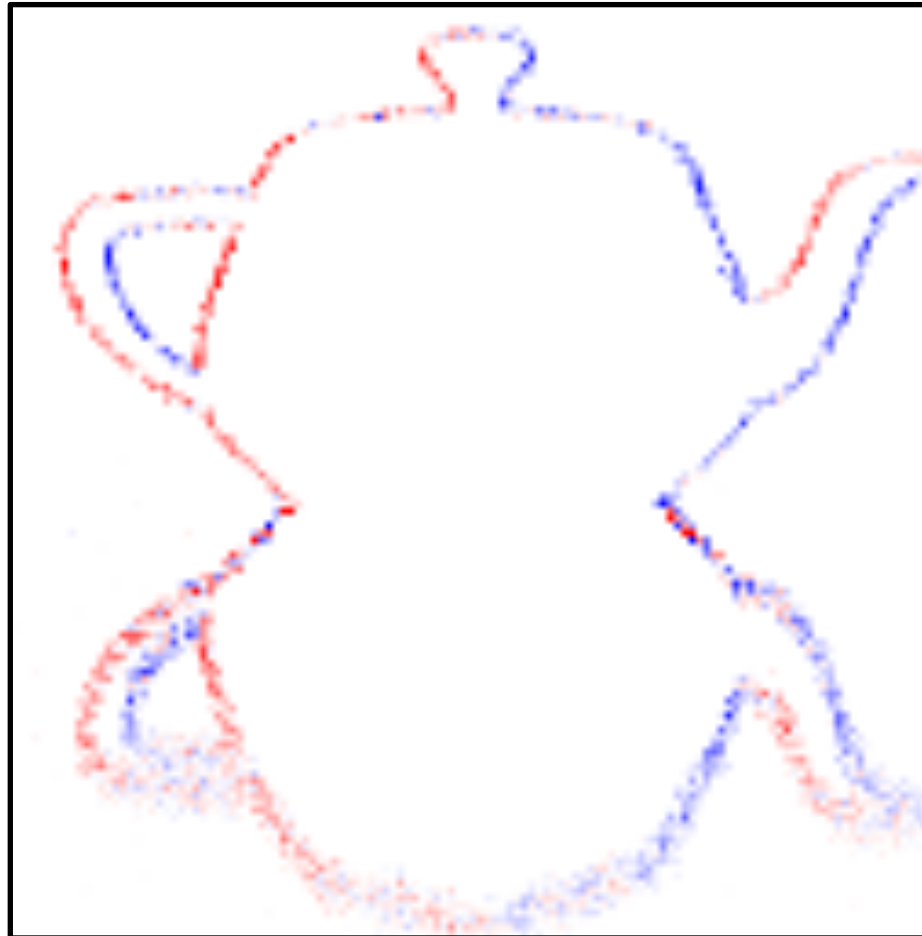
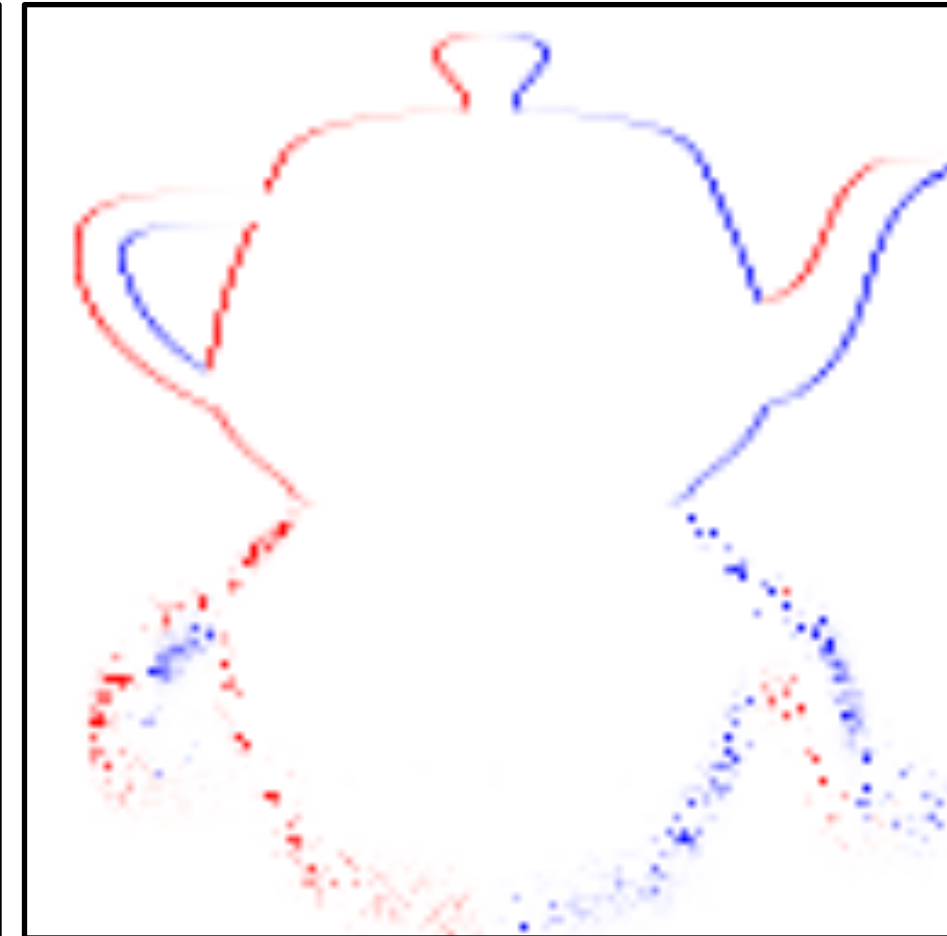
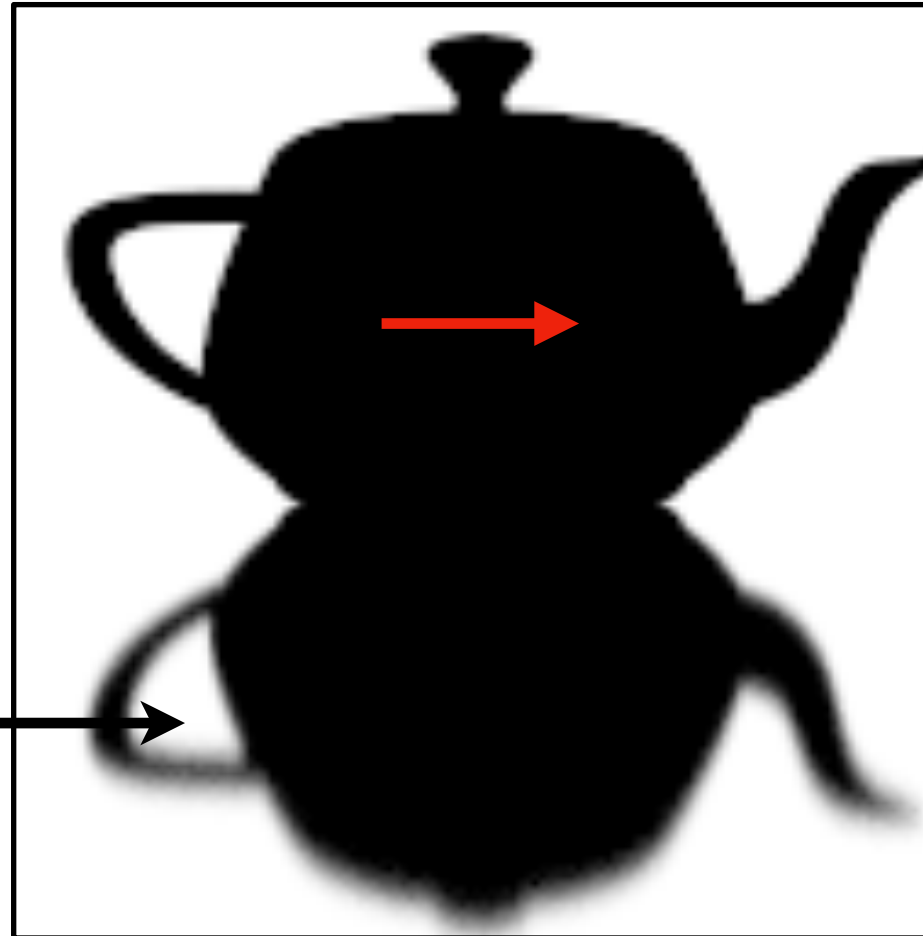
Ours

**Reference
(Finite differences)**

**Without
changes of variables**

RESULTS

Glossy reflection

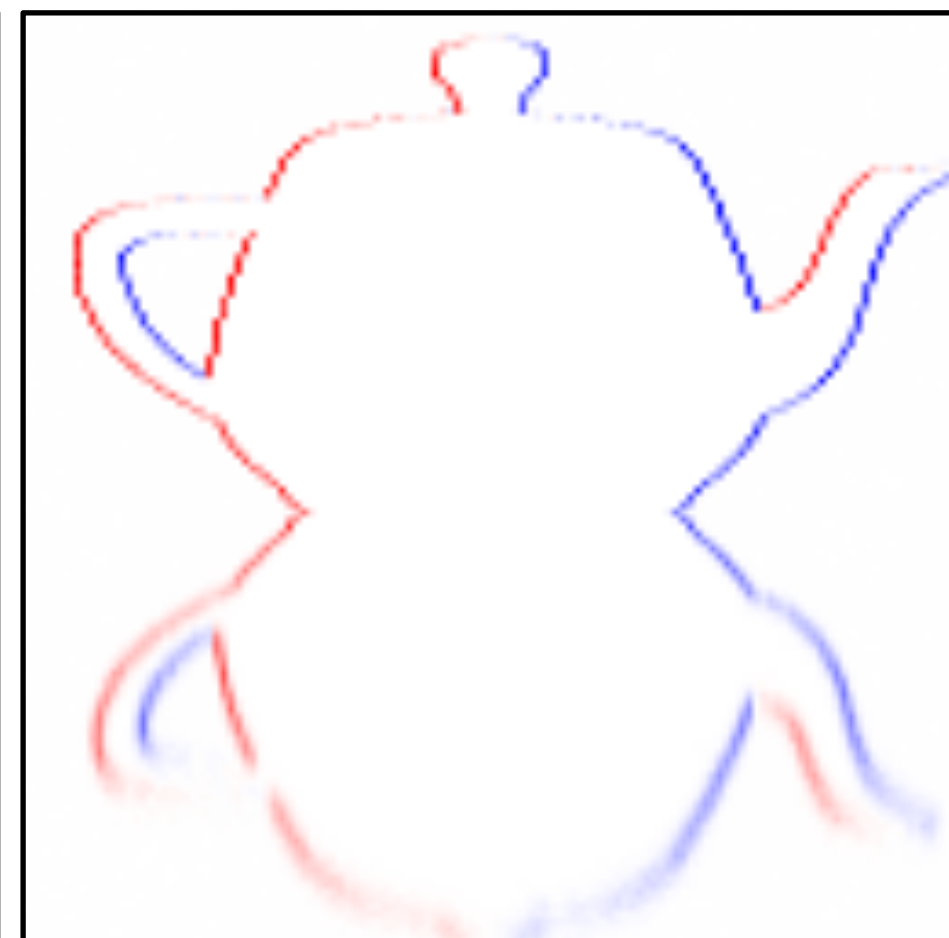
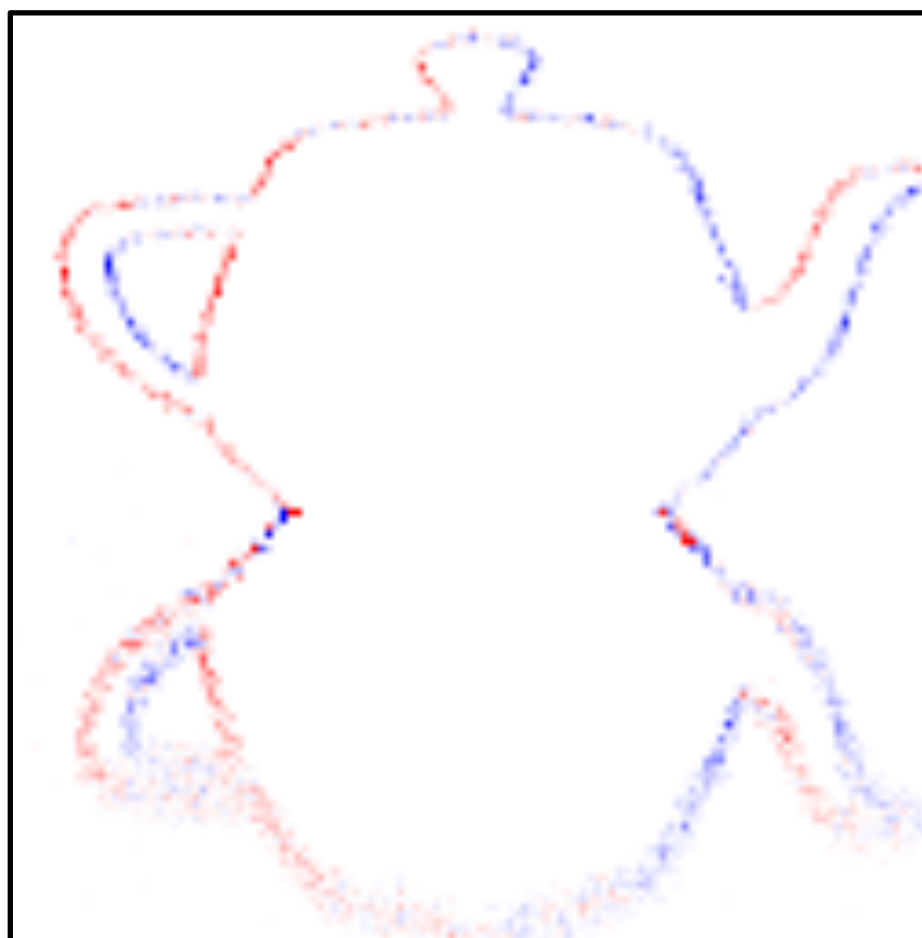
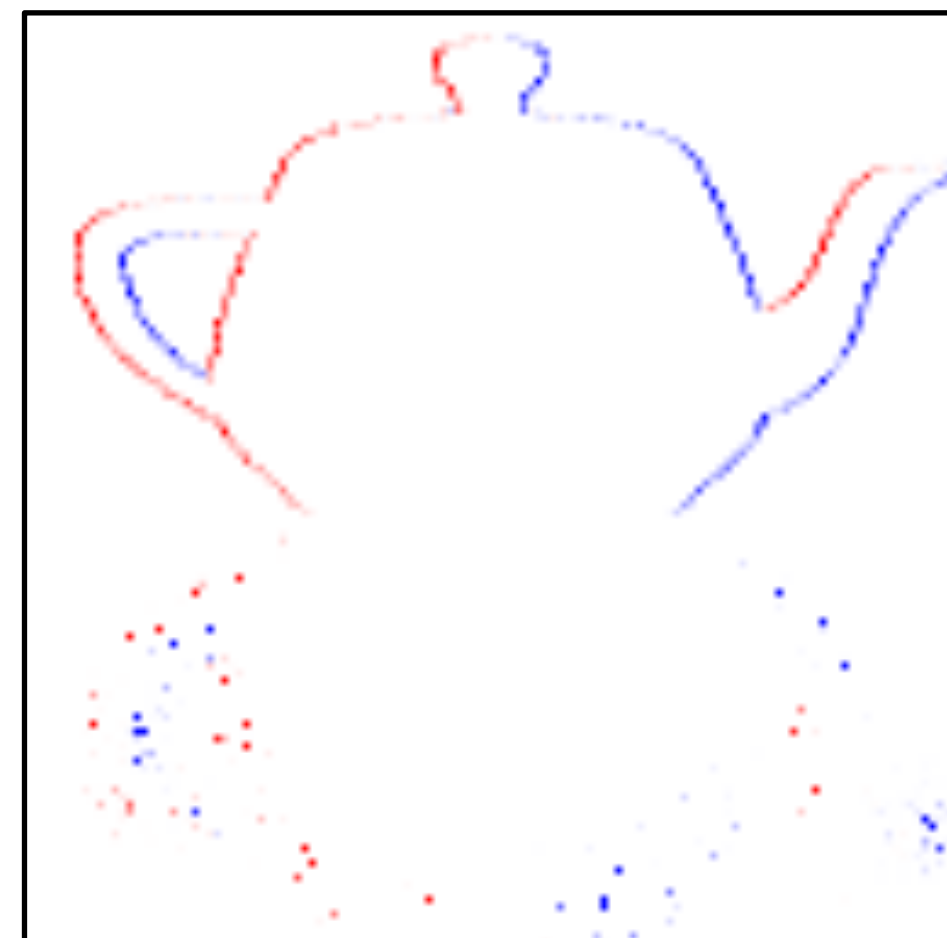


Edge sampling
[Li et al. 2018]

Reparameterization

Reference
Finite differences

Mesh subdivision



Dealing with discontinuities is not enough.

Want to propagate derivative information through complex simulations with **millions** of differentiable parameters.

“Monte-Carlo calculation of derivatives of functionals from the solution of the transfer equation according to the parameters of the system”

G. A. Mikhailov, Novosibirsk, **July 1966**

“Monte Carlo Analysis of Reactivity Coefficients in Fast Reactors, General Theory and Applications”

L.B. Miller, Argonne Natl. Laboratory,
March 1967

**ВЫЧИСЛЕНИЕ МЕТОДОМ МОНТЕ-КАРЛО ПРОИЗВОДНЫХ ФУНКЦИОНАЛОВ
ОТ РЕШЕНИЯ УРАВНЕНИЯ ПЕРЕНОСА ПО ПАРАМЕТРАМ СИСТЕМ**

Г. А. МИХАЙЛОВ

(Новосибирск)

**§ 1. Оценка функционалов от решения уравнения переноса
методом Монте-Карло. Метод зависимых испытаний**

Интегральное уравнение переноса (см., например, [1]) можно записать в виде

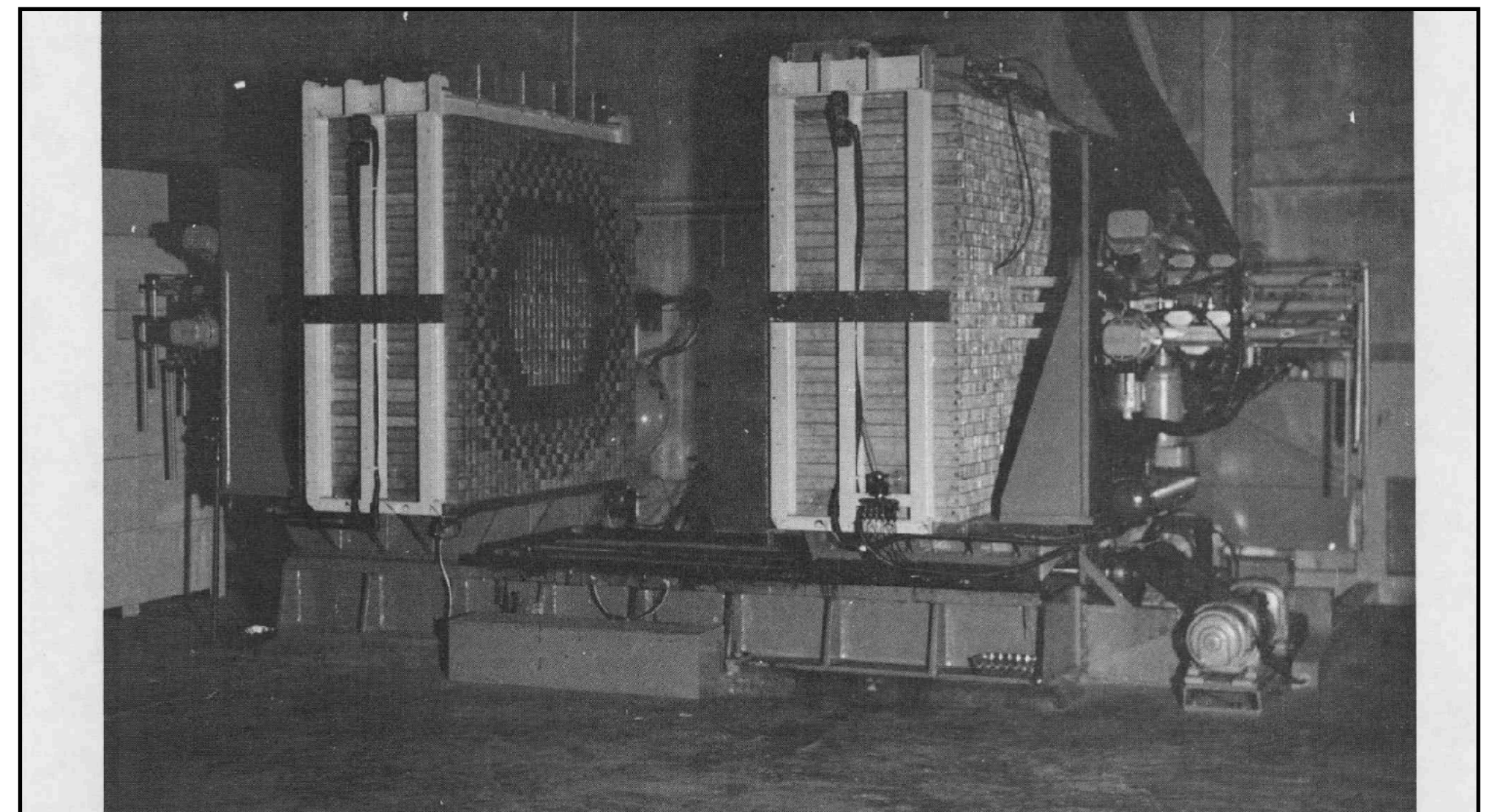
$$F(x) = \int_x k(x' \rightarrow x) F(x') dx' + f(x), \quad (1)$$

или

$$F = KF + f,$$

где X — фазовое пространство координат и скоростей, $F(x)$ — плотность столкновений в точке $x \in X$; $k(x' \rightarrow x)$ — плотность «первичных» столкновений в точке x от «одного» столкновения в точке x' ; $x, x' \in X$, $f(x)$ — плотность источников.

Мы будем предполагать, что решение уравнения (1) можно представить в виде ряда Неймана



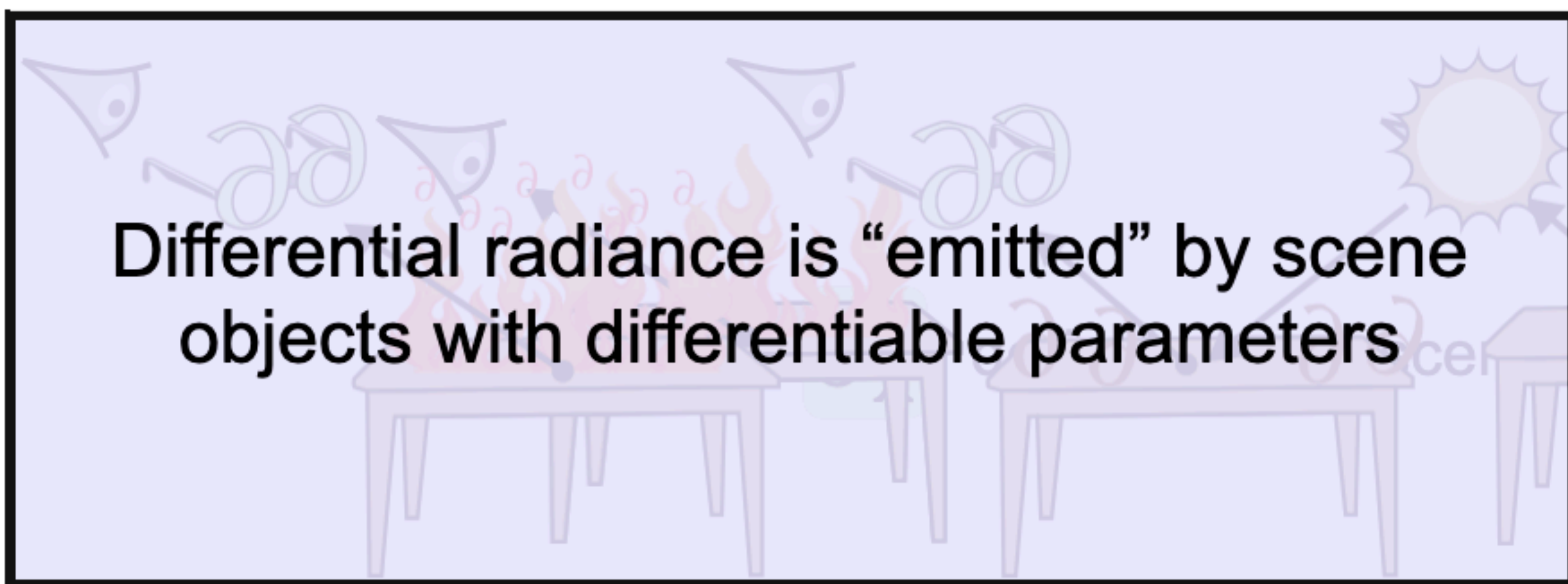
103-298

Fig. 2. ZPR-3 Critical Facility

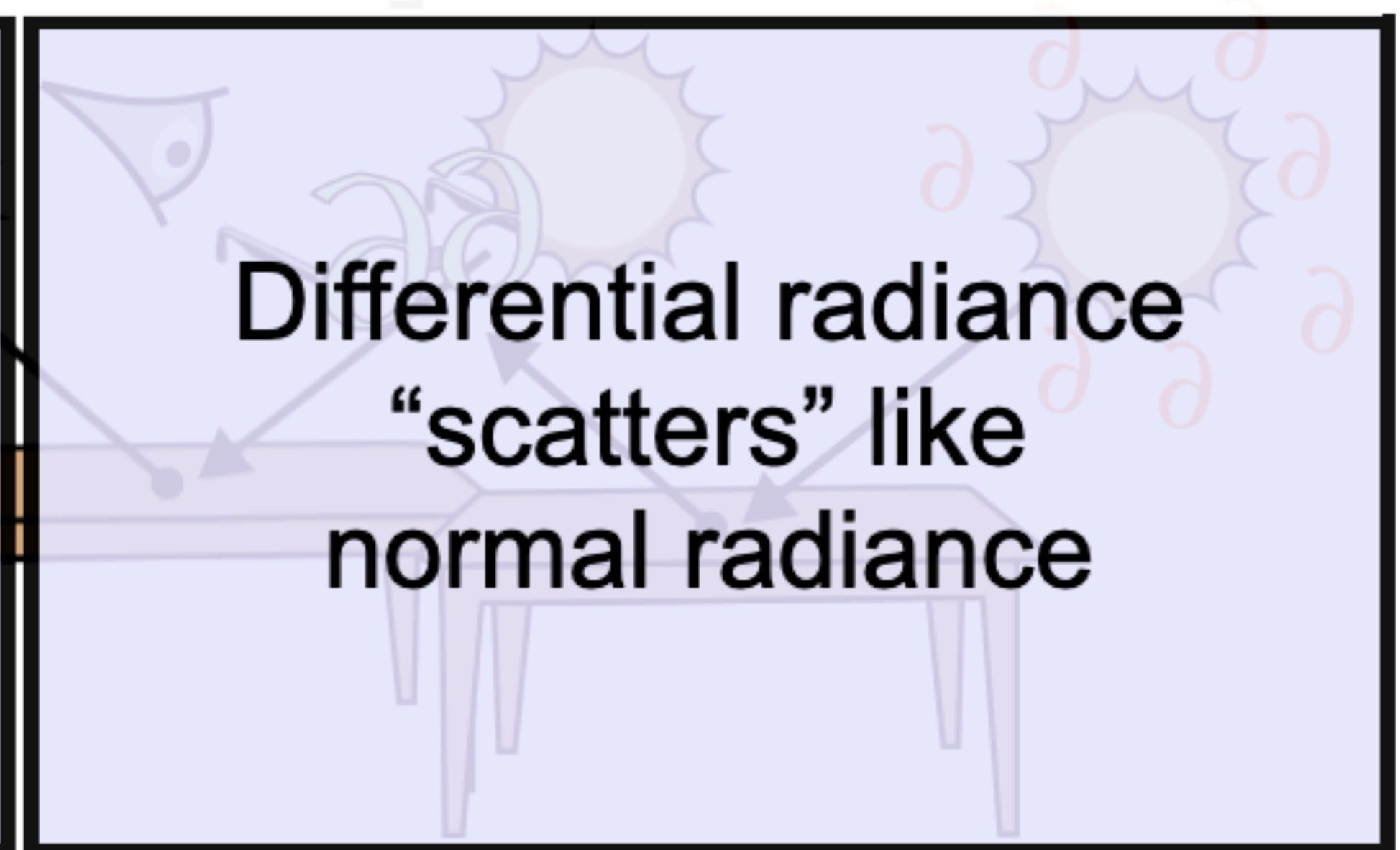
$$\partial_{\mathbf{x}} L_o(\mathbf{x}, \omega) = \partial_{\mathbf{x}}(e(\mathbf{x}, \omega) + \int_{\Omega} f_r(\mathbf{x}, \omega, \omega') L_i(\mathbf{x}, \omega') f_s(\mathbf{x}, \omega, \omega') \cos \theta d\omega')$$

TL;DR

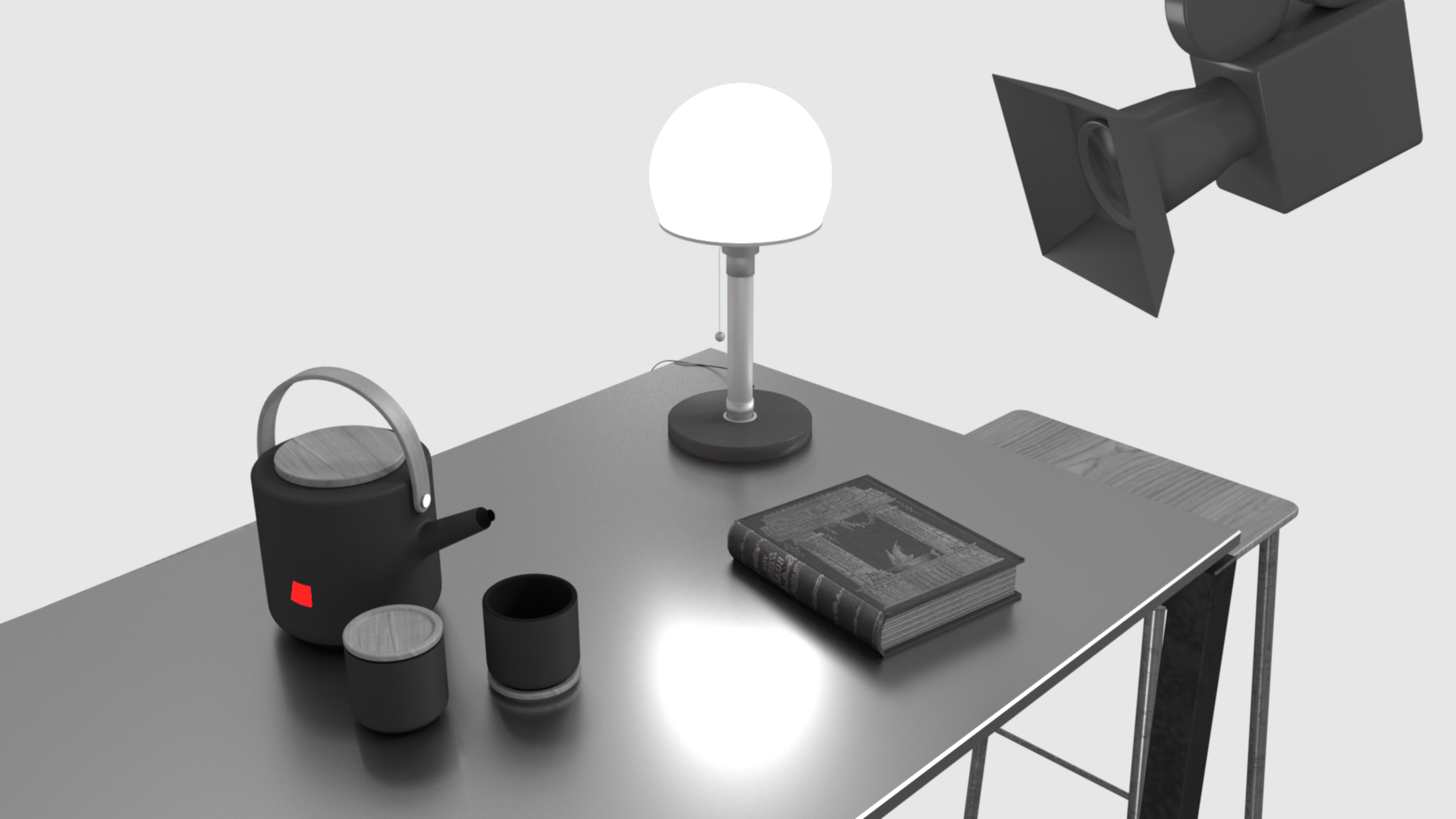
$$+ \partial_{\mathbf{x}} L_i(\mathbf{x}, \omega') f_s(\mathbf{x}, \omega, \omega') \cos \theta d\omega'$$



Differential radiance is “emitted” by scene objects with differentiable parameters

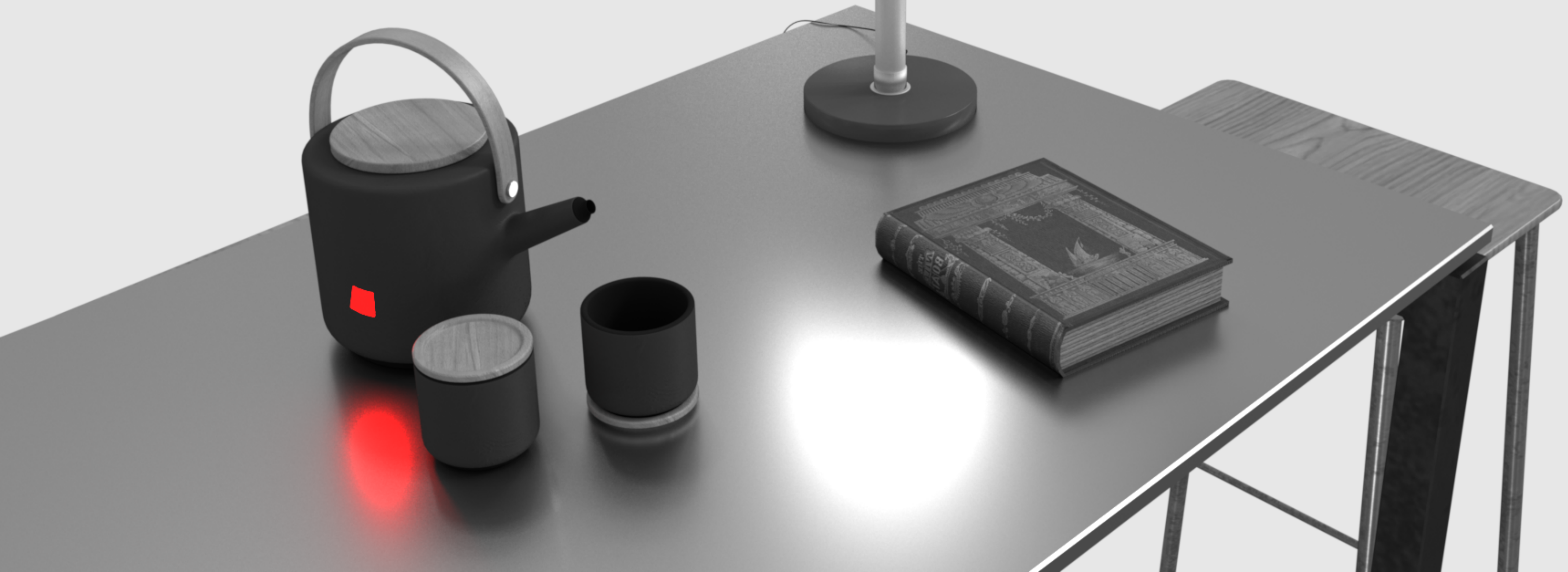
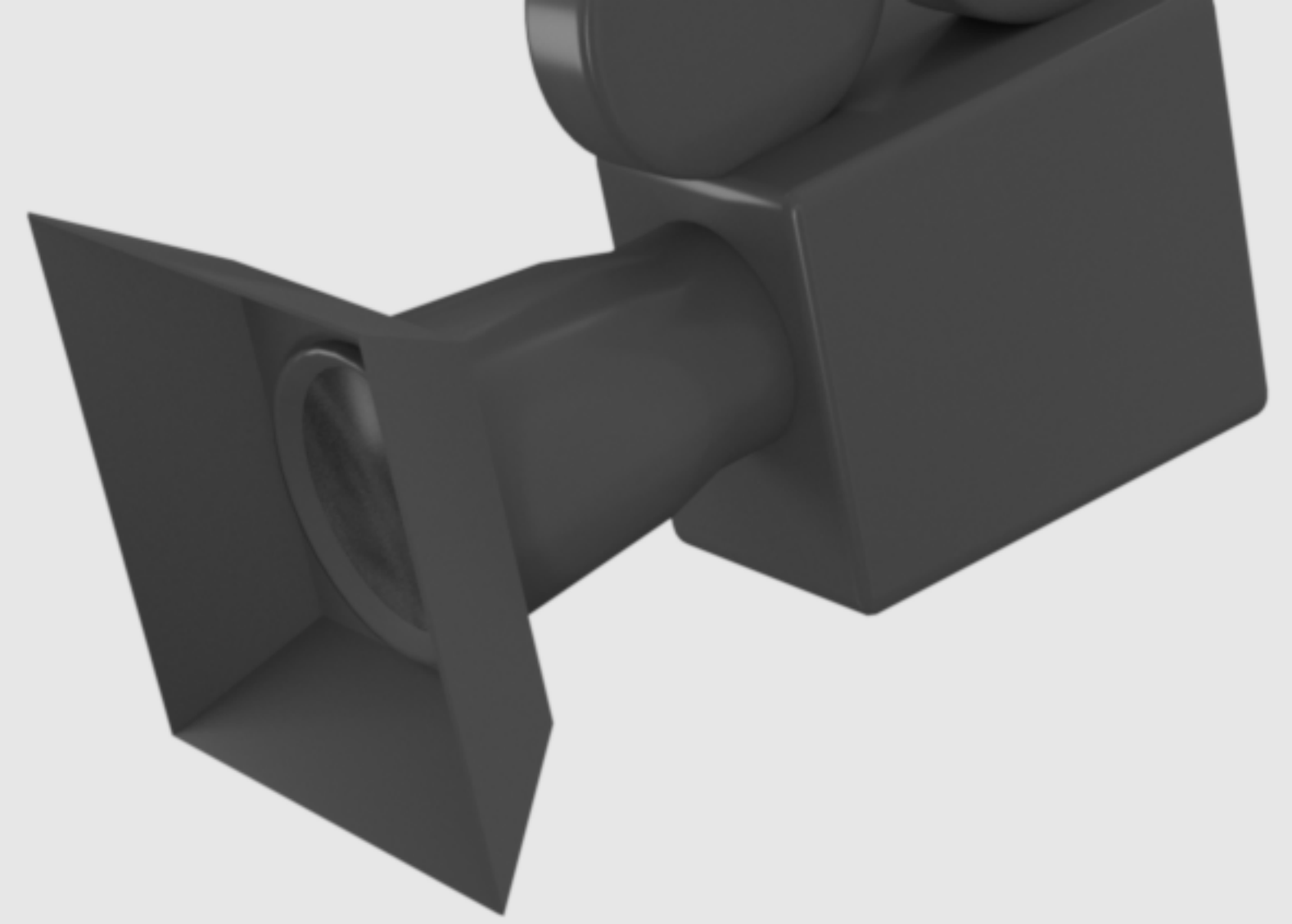
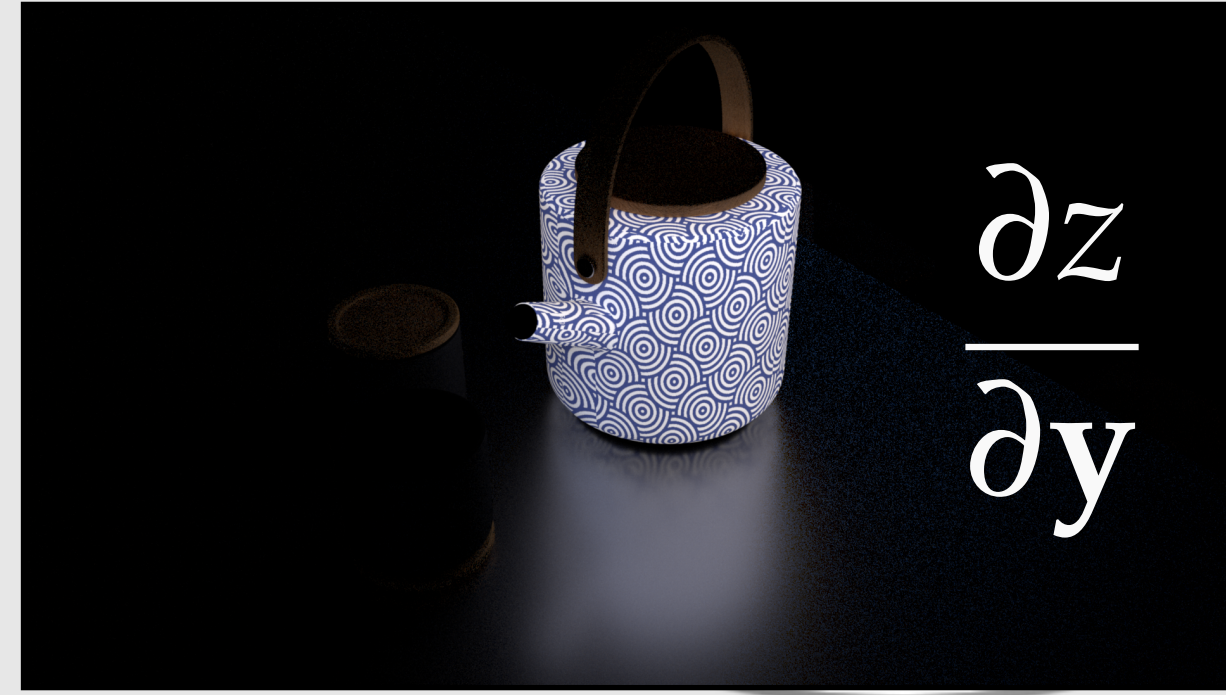


Differential radiance “scatters” like normal radiance

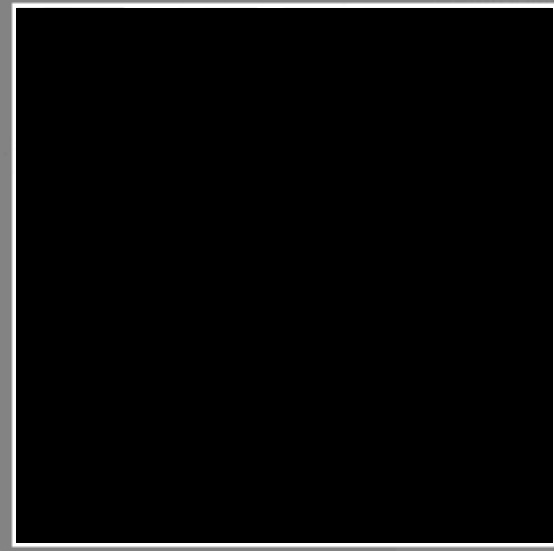




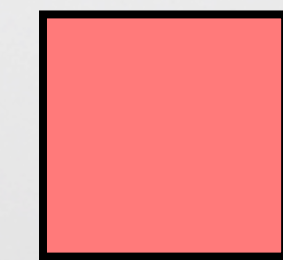
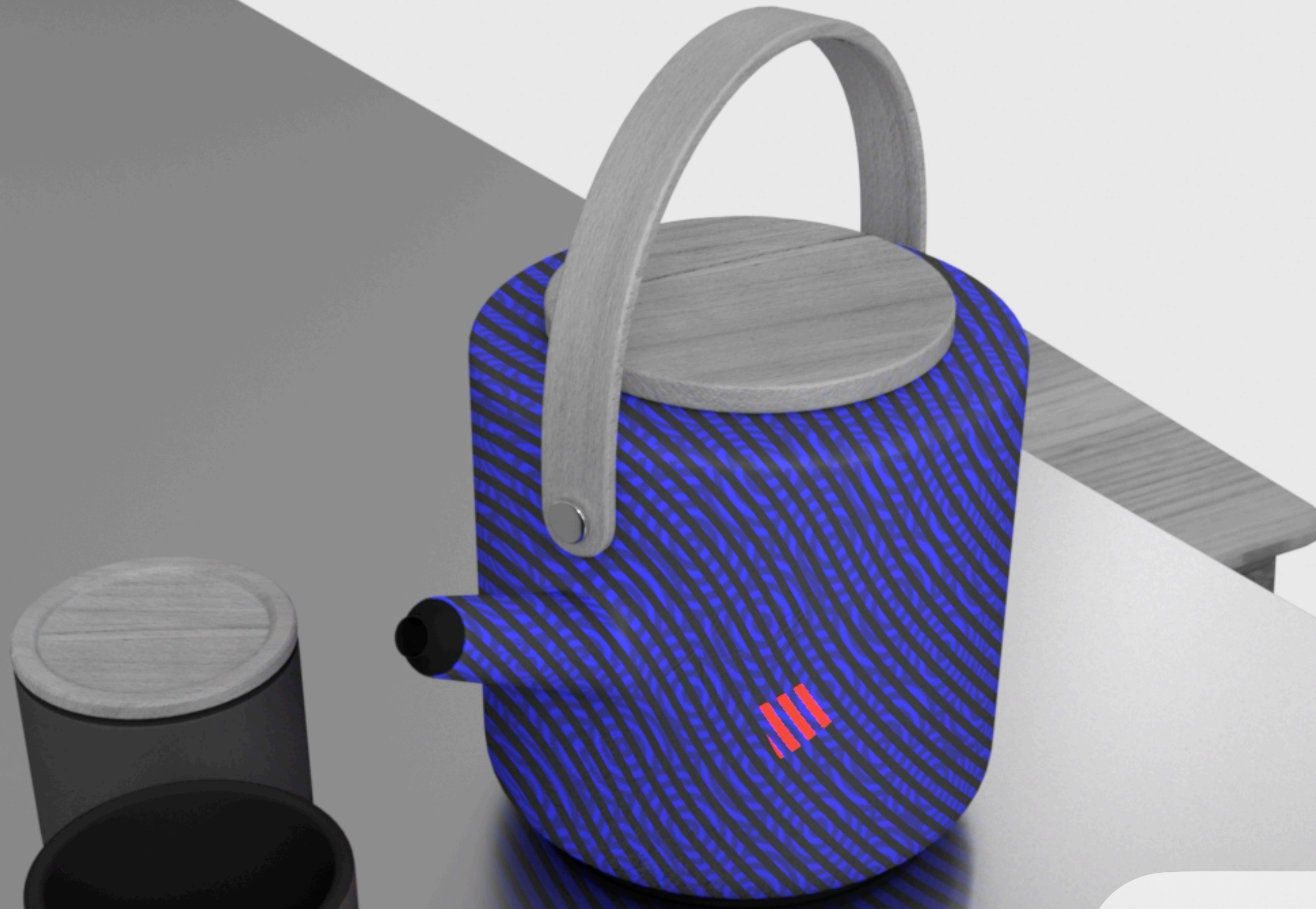
$$\frac{\partial z}{\partial x} = \frac{\partial z}{\partial y} \cdot \frac{\partial y}{\partial x}$$



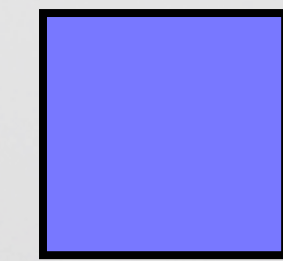




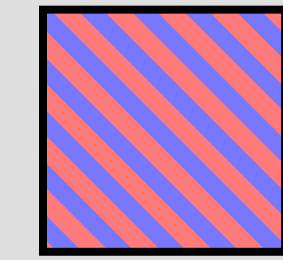
Gradients



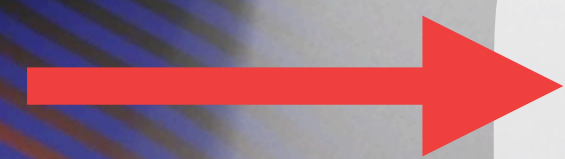
Derivative wrt. parameters

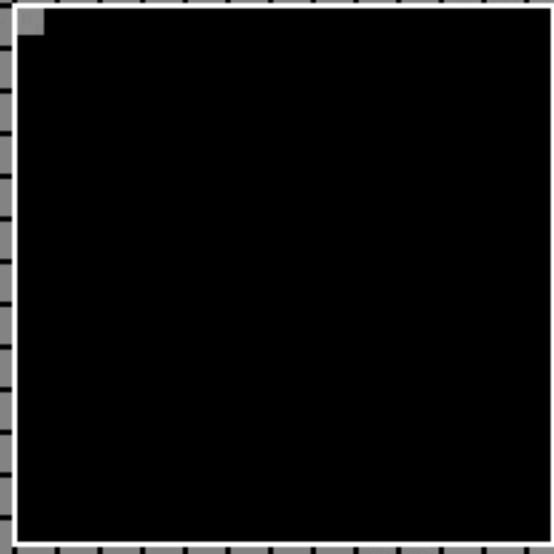


Derivative wrt. objective

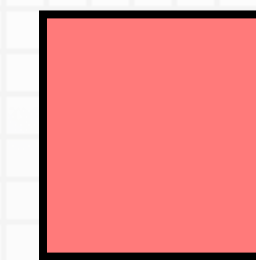
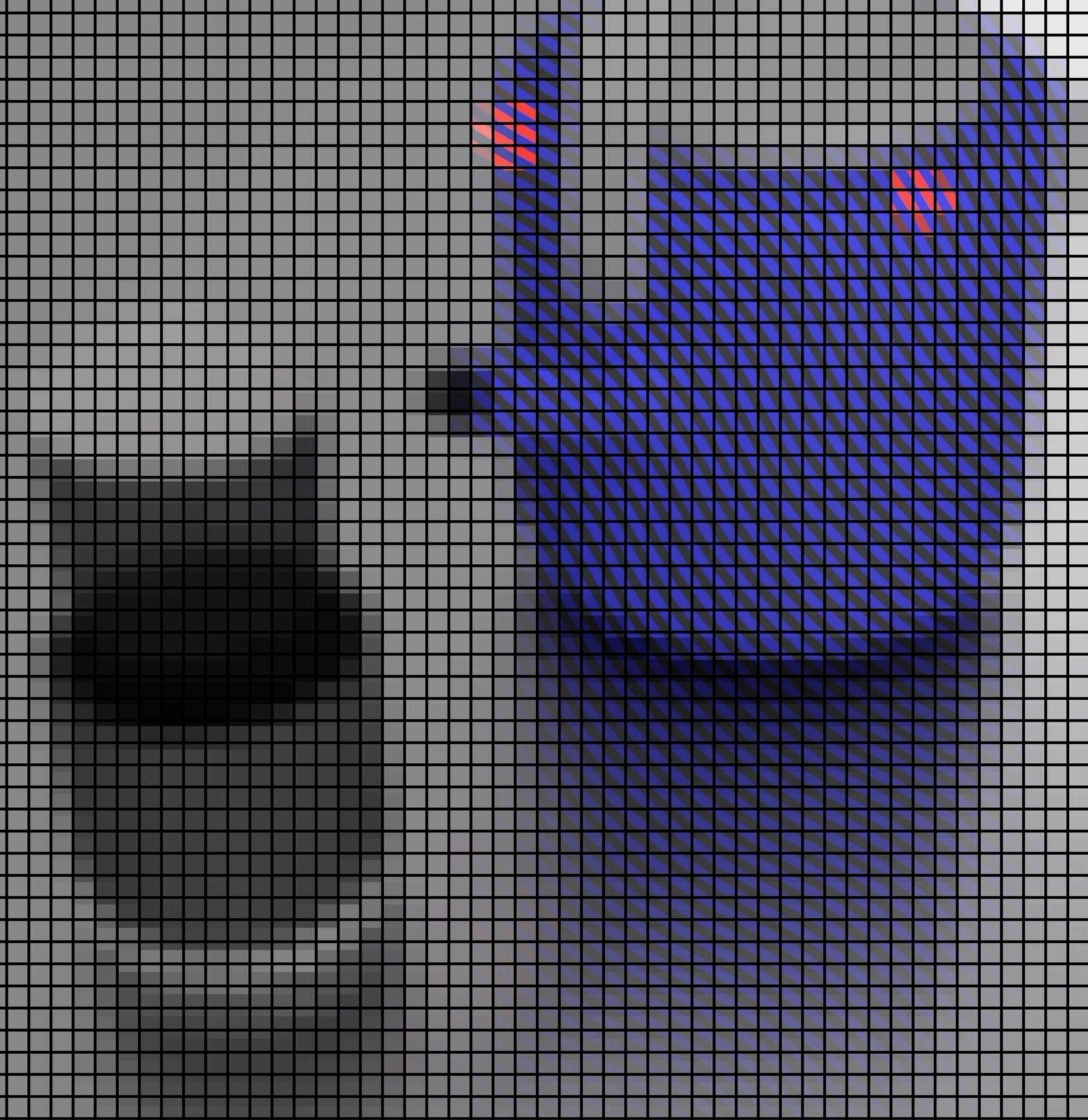


Dot product (discrete)

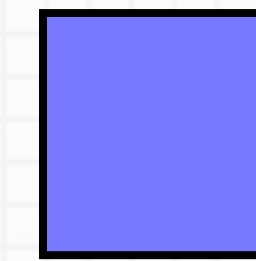




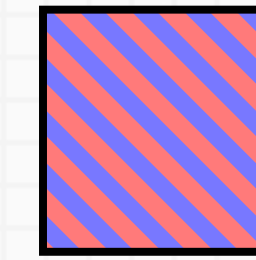
Gradients



Derivative wrt. parameters



Derivative wrt. objective



Dot product (discrete)

1MPix rendering &
1M parameters:

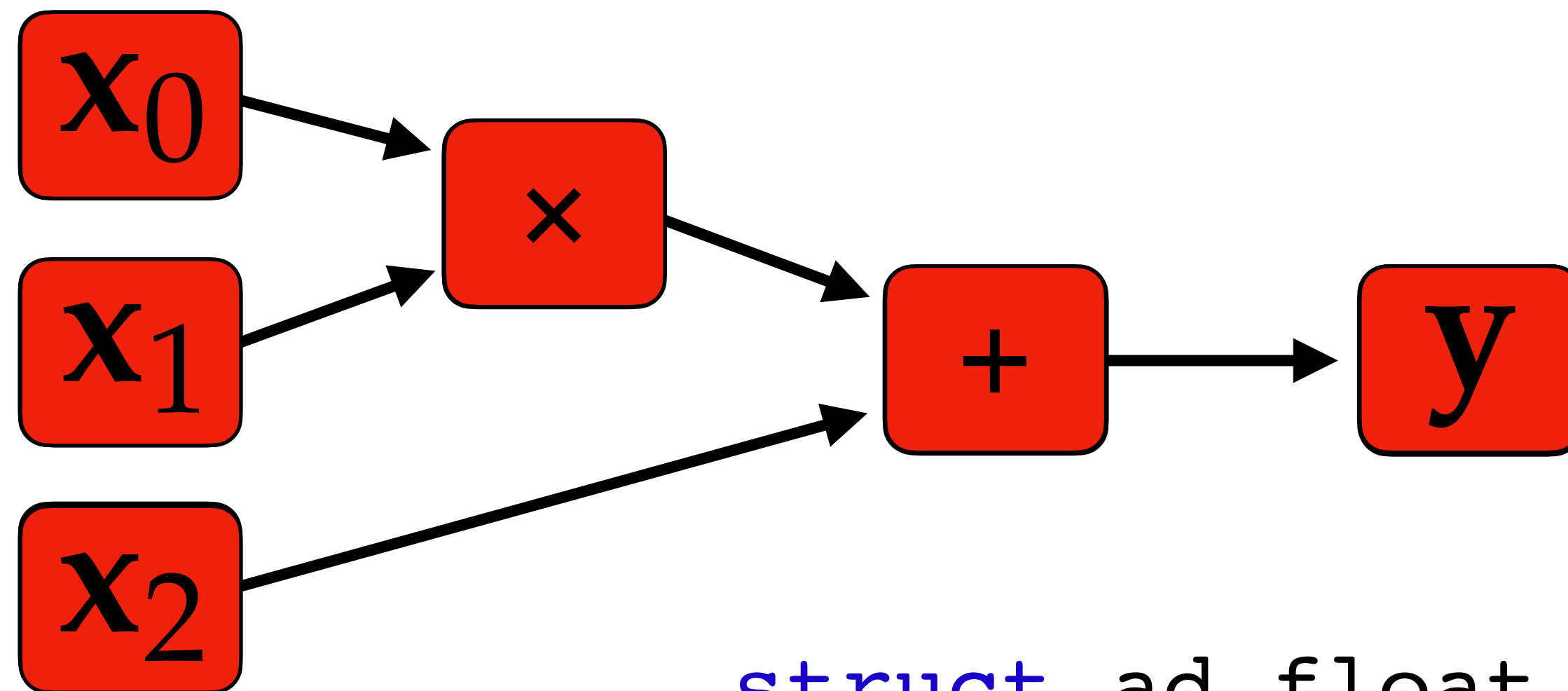
$$\frac{\partial y}{\partial x} \in \mathbb{R}^{1000000 \times 1000000}$$

(~3.6 TiB)

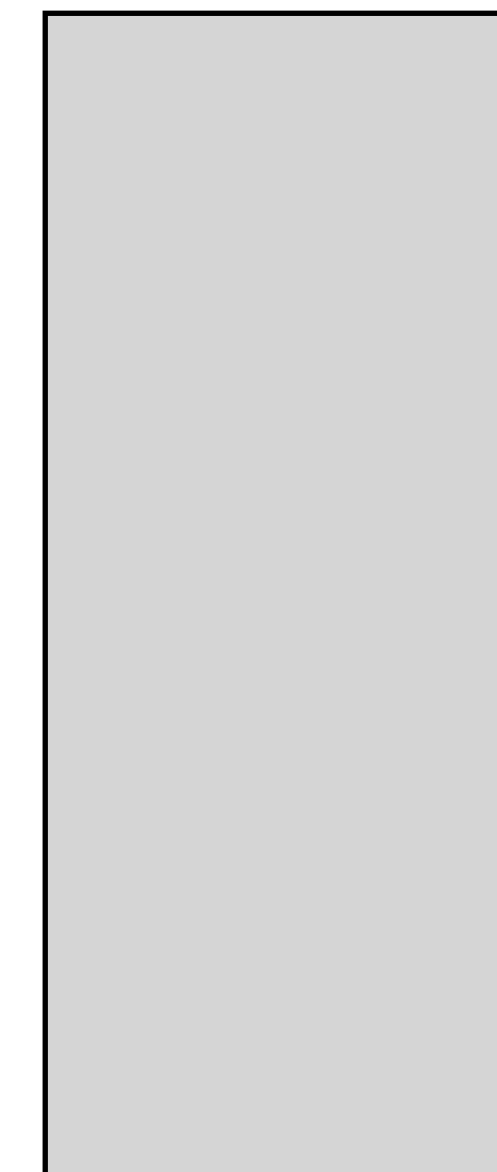


Forward mode

$$y = x_0 \cdot x_1 + x_2$$



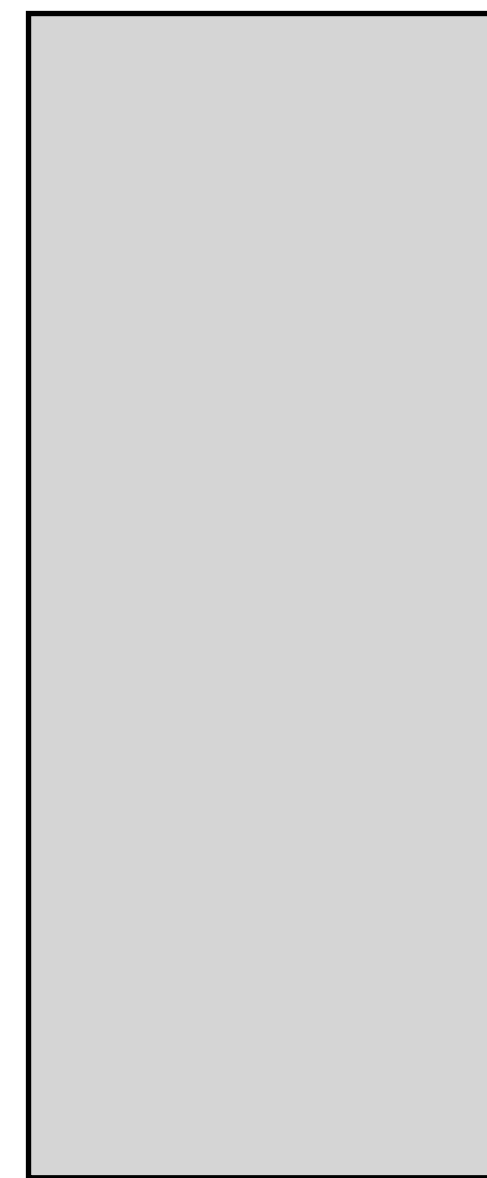
```
struct ad_float {  
    float value;  
    float derivative;  
};
```



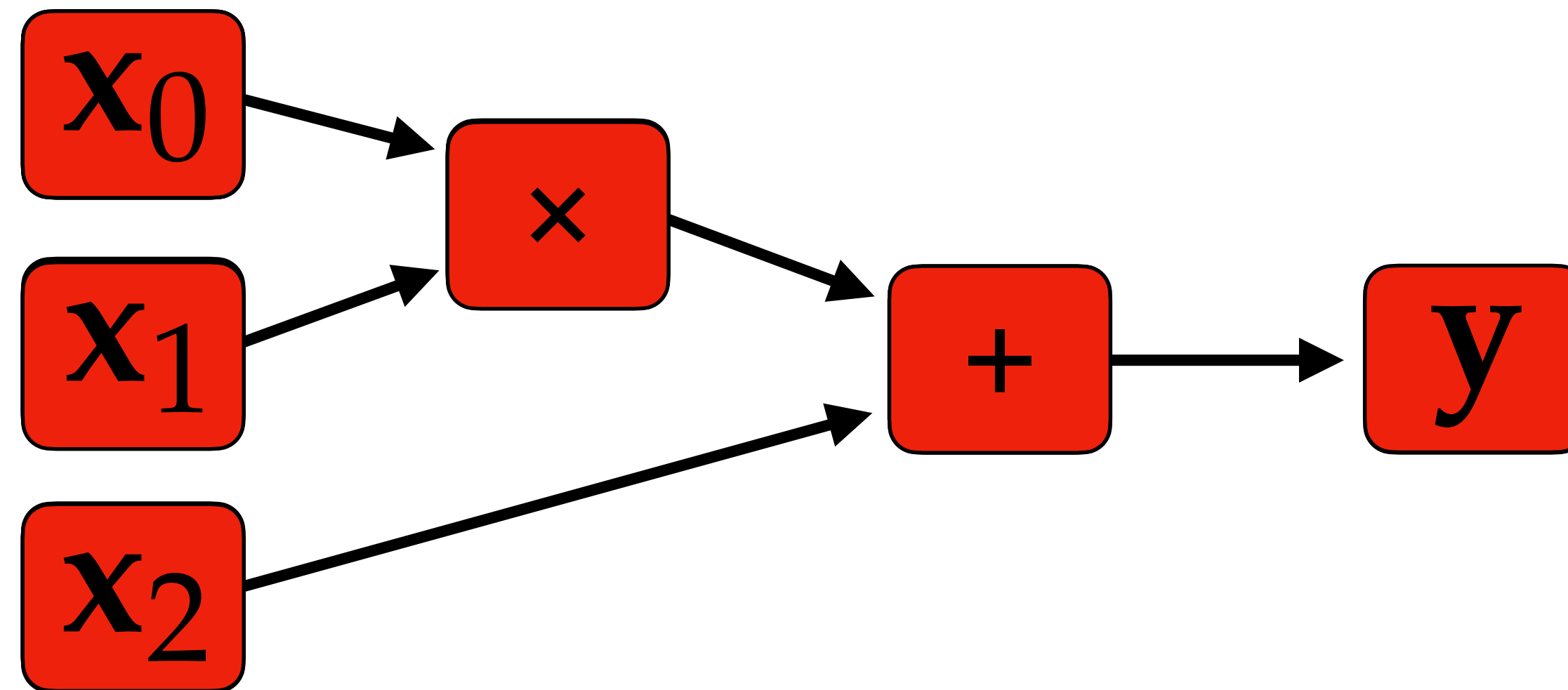
Gradient

Reverse mode

$$y = x_0 \cdot x_1 + x_2$$



Gradient



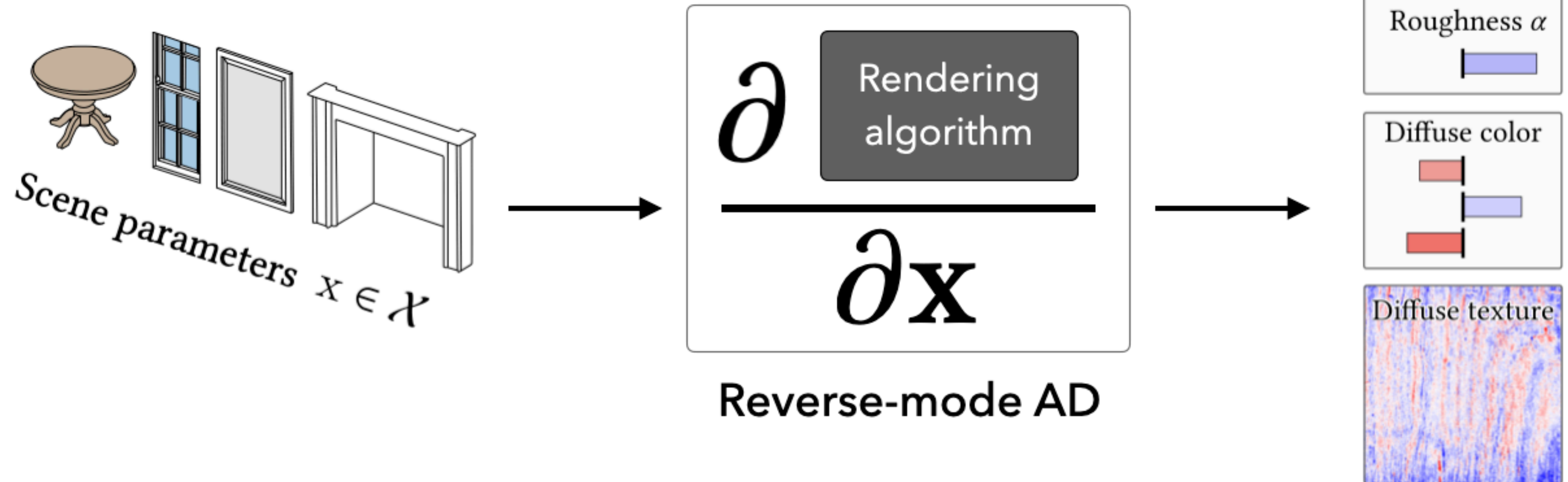
Program execution



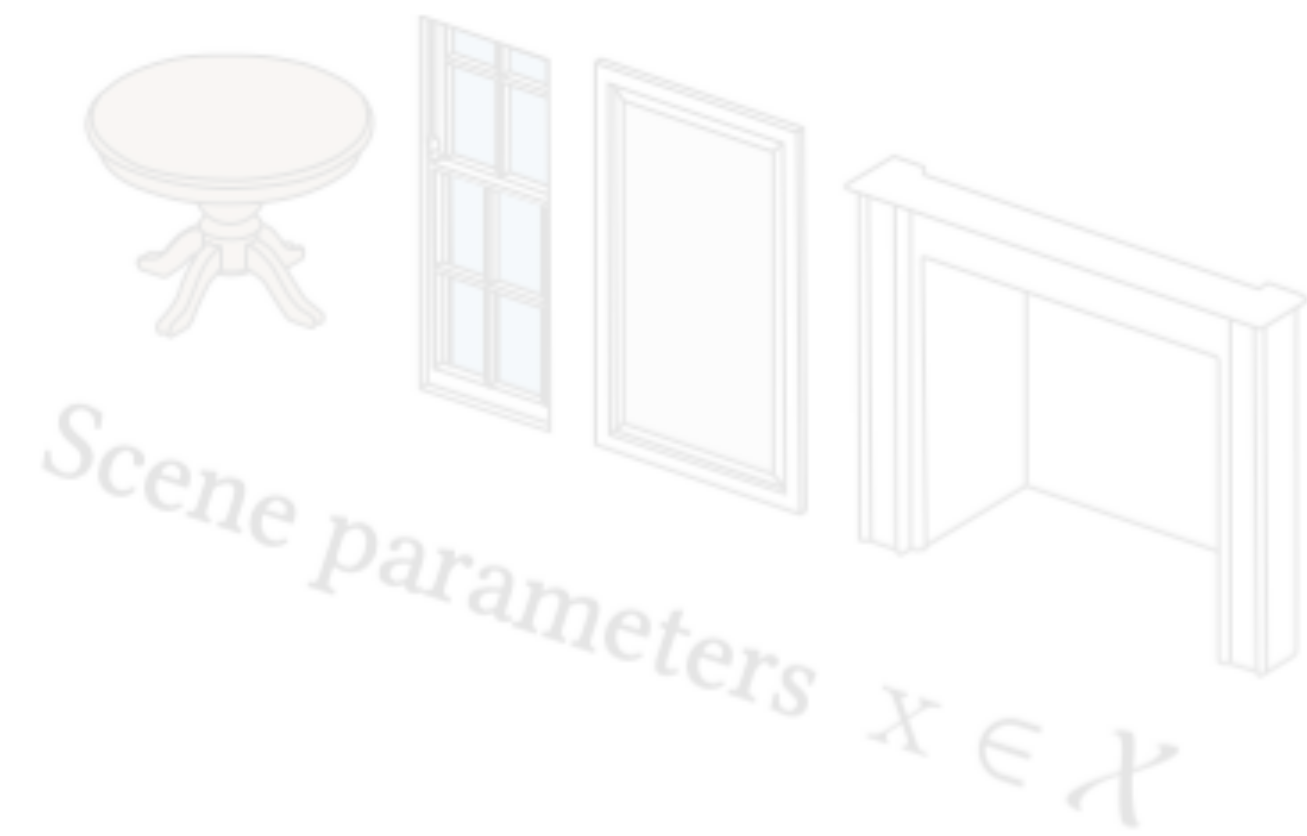
Differentiation



Autodiff-based differentiable rendering



Autodiff-based differentiable rendering



OUT OF MEMORY

Gradients

Shininess α

Diffuse color

Diffuse texture

Reverse mode AD

Radiative Backpropagation: An Adjoint Method for Lightning-Fast Differentiable Rendering

MERLIN NIMIER-DAVID, École Polytechnique Fédérale de Lausanne (EPFL)
SÉBASTIEN SPEIERER, École Polytechnique Fédérale de Lausanne (EPFL)
BENOÎT RUIZ, École Polytechnique Fédérale de Lausanne (EPFL)
WENZEL JAKOB, École Polytechnique Fédérale de Lausanne (EPFL)

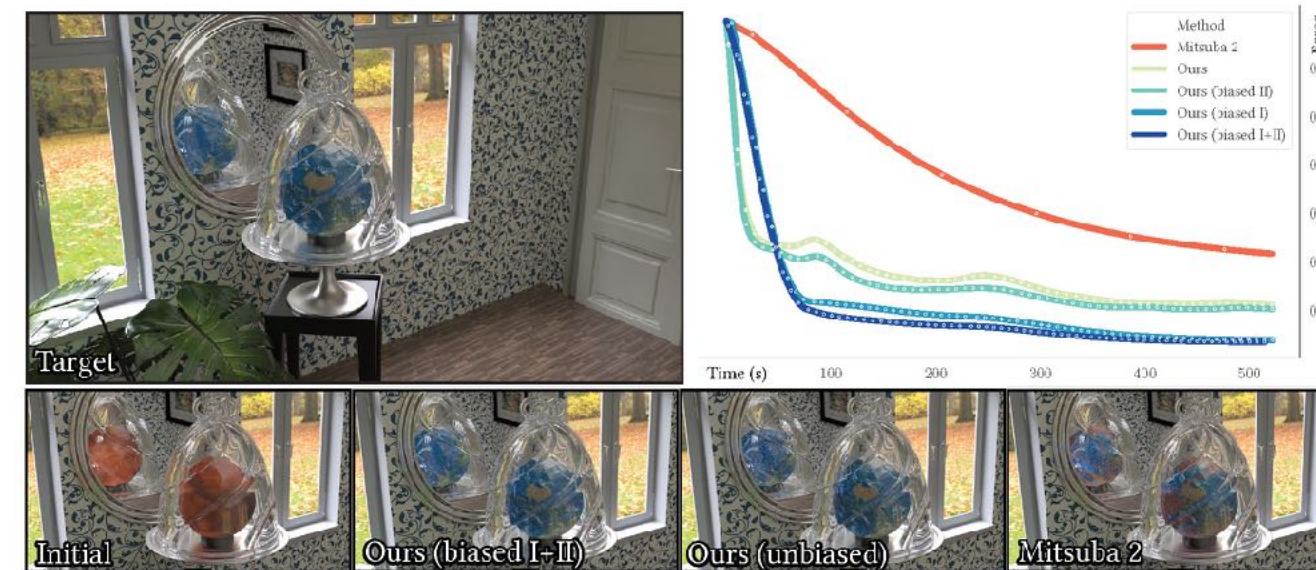


Fig. 1. GLOBE: Our method is able to reconstruct the texture of a globe seen through a bell jar in this interior scene with complex materials and interreflection. Starting from a different initialization (Mars), it attempts to match a reference rendering by differentiating scene parameters with respect to L_2 image distance. The plot on the right shows convergence over time for prior work [Nimier-David et al. 2019] and multiple variants of radiative backpropagation. Our method removes the severe overheads of differentiation compared to ordinary rendering, and we demonstrate speedups of up to $\sim 1000\times$ compared to prior work.

Physically based differentiable rendering has recently evolved into a powerful tool for solving inverse problems involving light. Methods in this area perform a differentiable simulation of the physical process of light transport and scattering to estimate partial derivatives relating scene parameters to pixels in the rendered image. Together with gradient-based optimization, such algorithms have interesting applications in diverse disciplines, e.g., to improve the reconstruction of 3D scenes, while accounting for interreflection and transparency, or to design meta-materials with specified optical properties.

Authors' addresses: Merlin Nimier-David, École Polytechnique Fédérale de Lausanne (EPFL), merlin.nimier-david@epfl.ch; Sébastien Speierer, École Polytechnique Fédérale de Lausanne (EPFL), sebastien.speierer@epfl.ch; Benoît Ruiz, École Polytechnique Fédérale de Lausanne (EPFL), benoit.ruiz@epfl.ch; Wenzel Jakob, École Polytechnique Fédérale de Lausanne (EPFL), wenzel.jakob@epfl.ch.

Permission to make digital or hard copies of all or part of this work for personal or classroom use is granted without fee provided that copies are not made or distributed for profit or commercial advantage and that copies bear this notice and the full citation on the first page. Copyrights for components of this work owned by others than the author(s) must be honored. Abstracting with credit is permitted. To copy otherwise, to republish, to post on servers or to redistribute to lists, requires prior specific permission and/or a fee. Request permissions from permissions.acm.org.
© 2020 Copyright held by the owner/author(s). Publication rights licensed to ACM.
0730-0301/2020/7-ART146 \$15.00
<https://doi.org/10.1145/3386569.3392406>

The most versatile differentiable rendering algorithms rely on reverse-mode differentiation to compute all requested derivatives at once, enabling optimization of scene descriptions with millions of free parameters. However, a severe limitation of the reverse-mode approach is that it requires a detailed transcript of the computation that is subsequently replayed to back-propagate derivatives to the scene parameters. The transcript of typical renderings is extremely large, exceeding the available system memory by many orders of magnitude, hence current methods are limited to simple scenes rendered at low resolutions and sample counts.

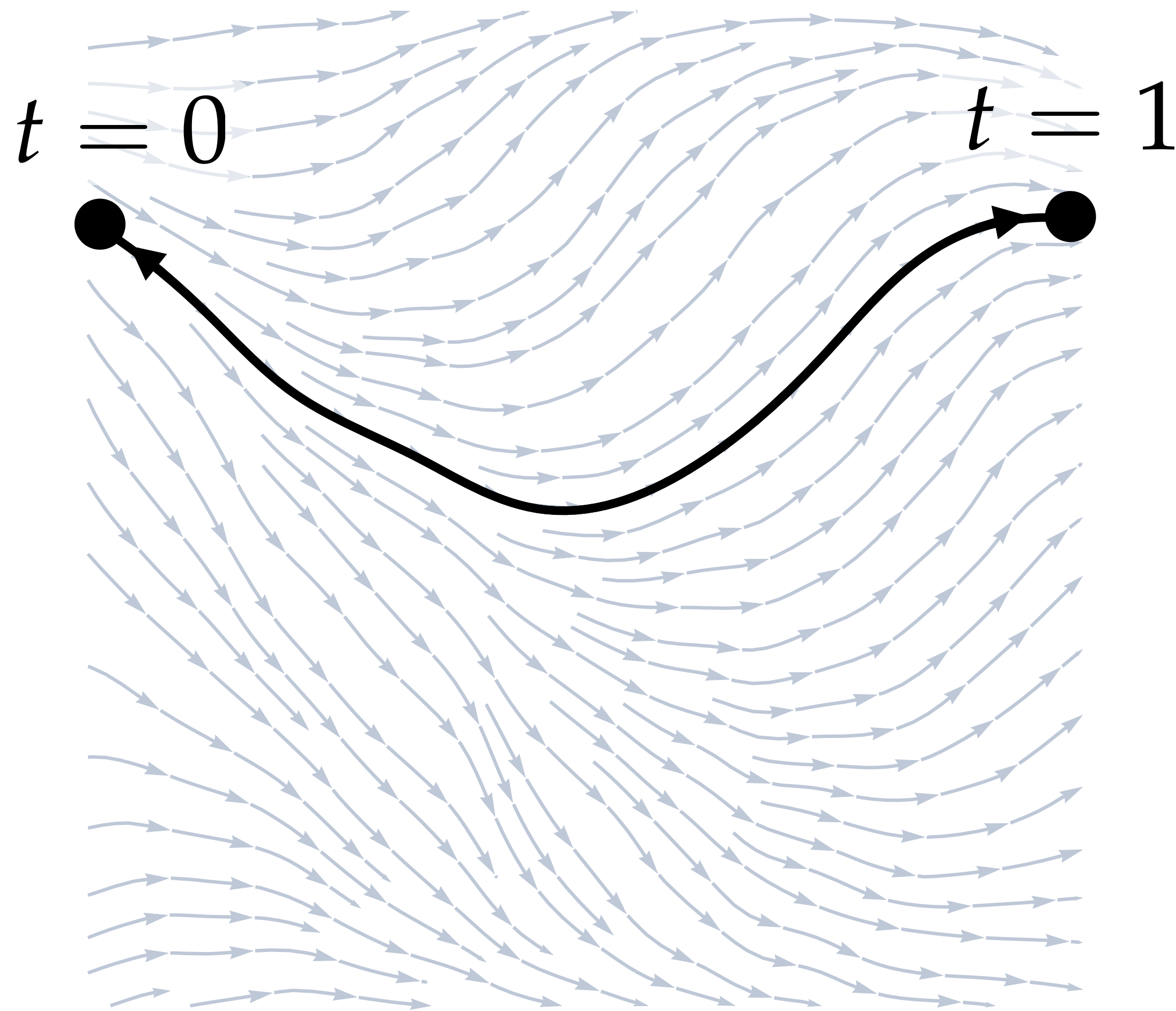
We introduce *radiative backpropagation*, a fundamentally different approach to differentiable rendering that does not require a transcript, greatly improving its scalability and efficiency. Our main insight is that reverse-mode propagation through a rendering algorithm can be interpreted as the solution of a continuous transport problem involving the partial derivative of radiance with respect to the optimization objective. This quantity is “emitted” by sensors, “scattered” by the scene, and eventually “received” by objects with differentiable parameters. Differentiable rendering then decomposes into two separate primal and adjoint simulation steps that scale to complex scenes rendered at high resolutions. We also investigated biased variants of this algorithm and find that they considerably improve both runtime and convergence speed. We showcase an efficient GPU implementation of radiative backpropagation and compare its performance and the quality of its gradients to prior work.

ACM Trans. Graph., Vol. 39, No. 4, Article 146. Publication date: July 2020.

Radiative Backpropagation: An Adjoint Method for Lightning-Fast Differentiable Rendering

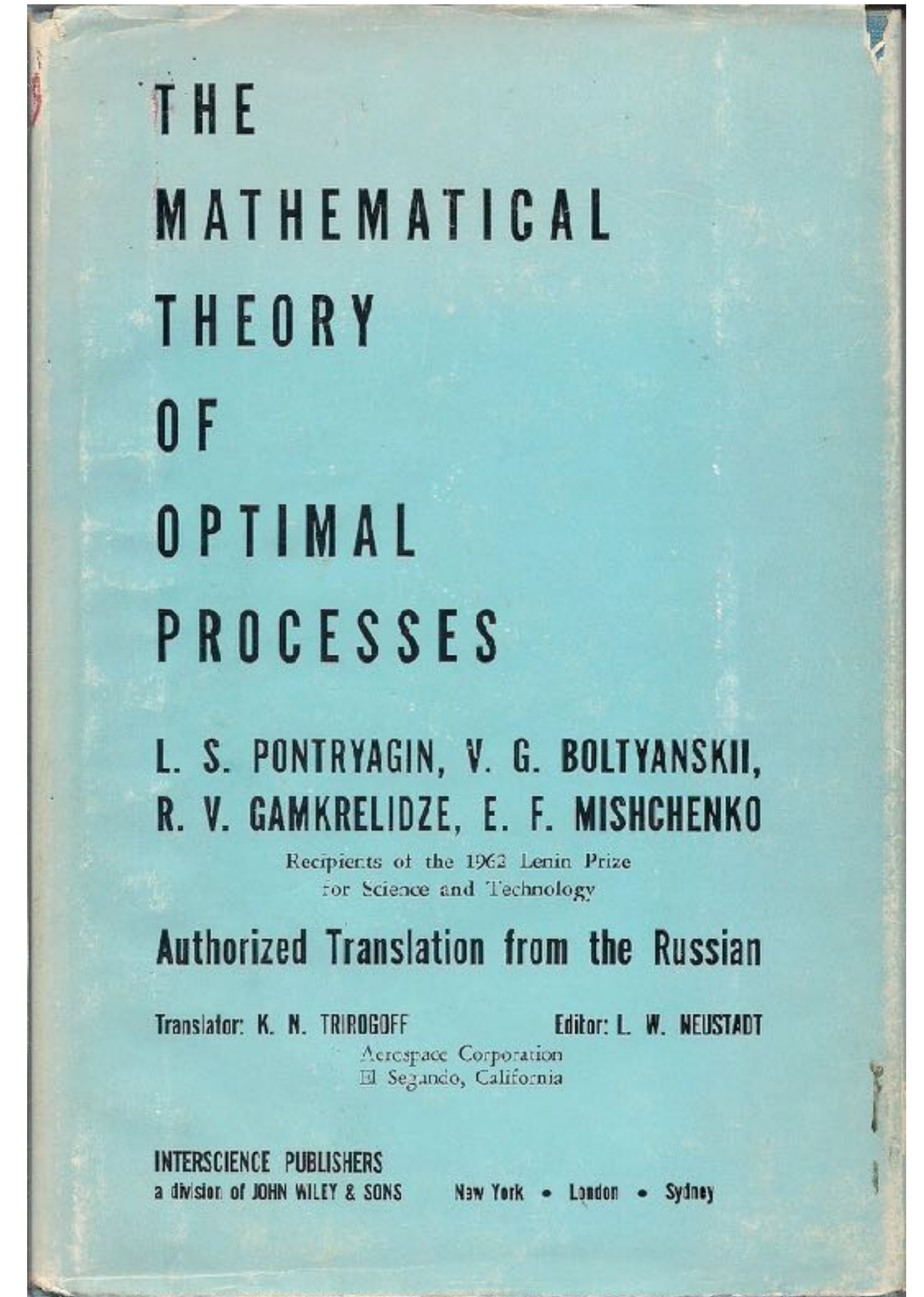
Merlin Nimier-David, Sébastien Speierer, Benoit Ruïz, Wenzel Jakob

SIGGRAPH 2020

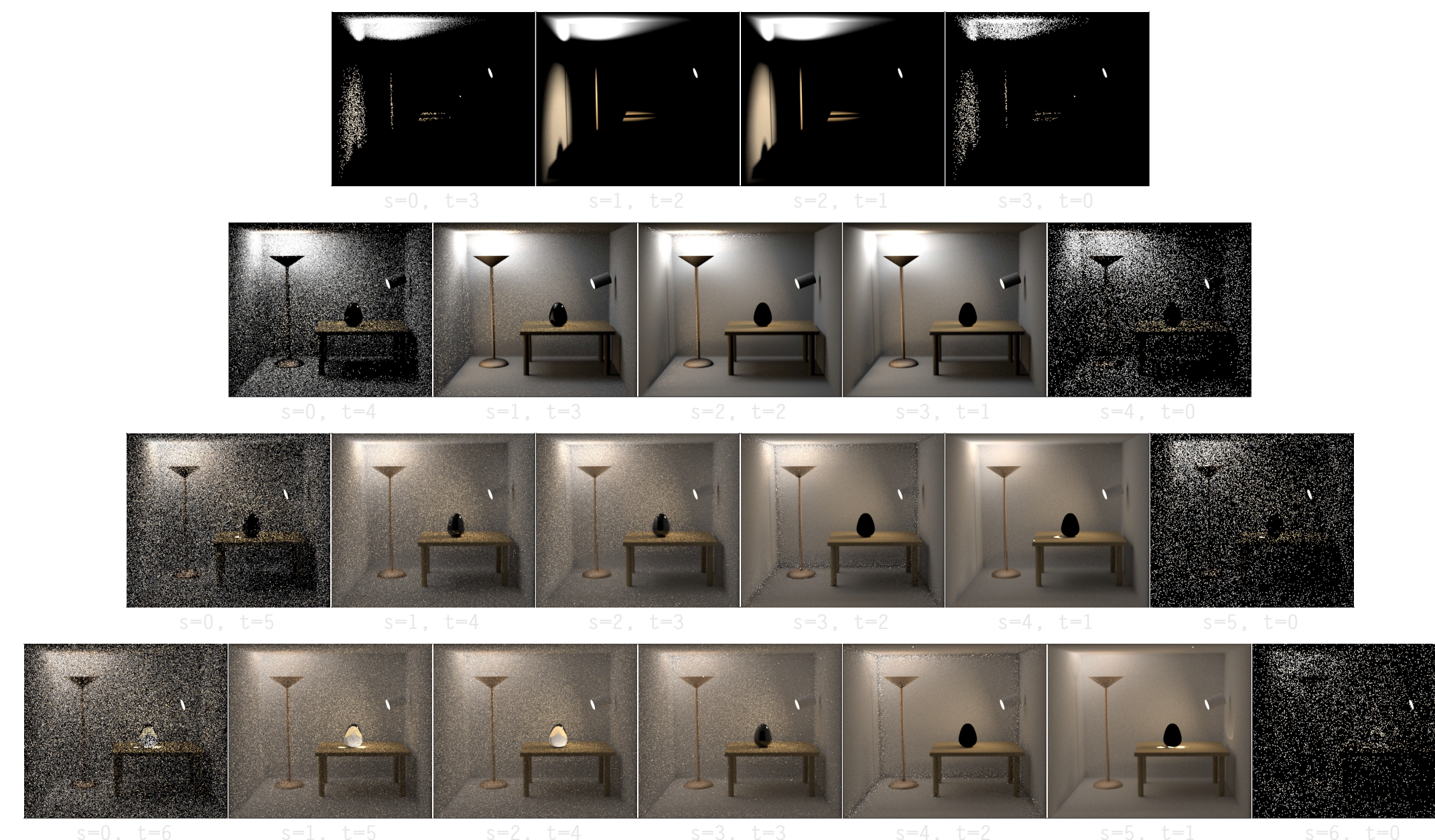
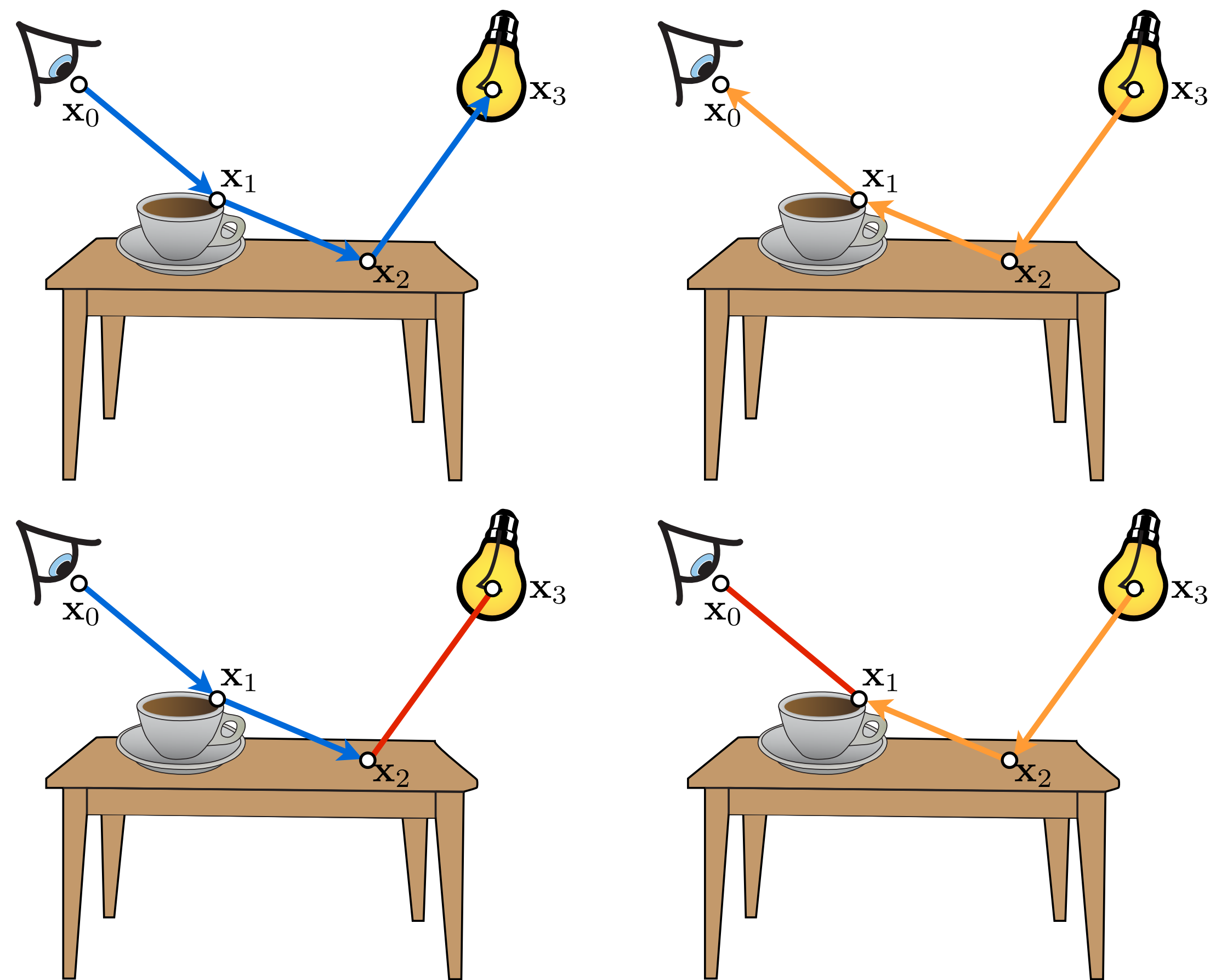


For problems with
a time dimension
(ODEs, ..)

Pontryagin et al.
1962



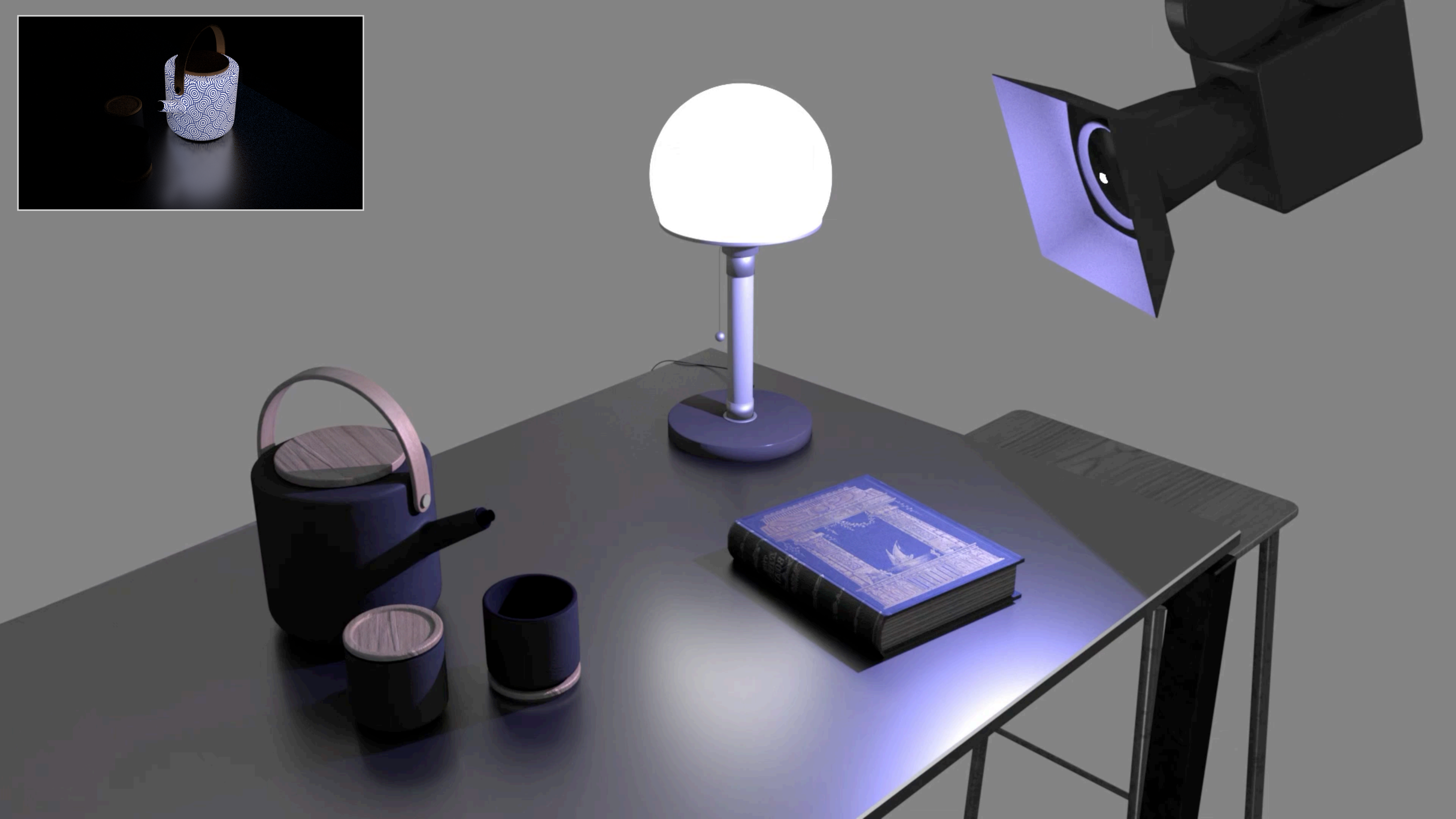
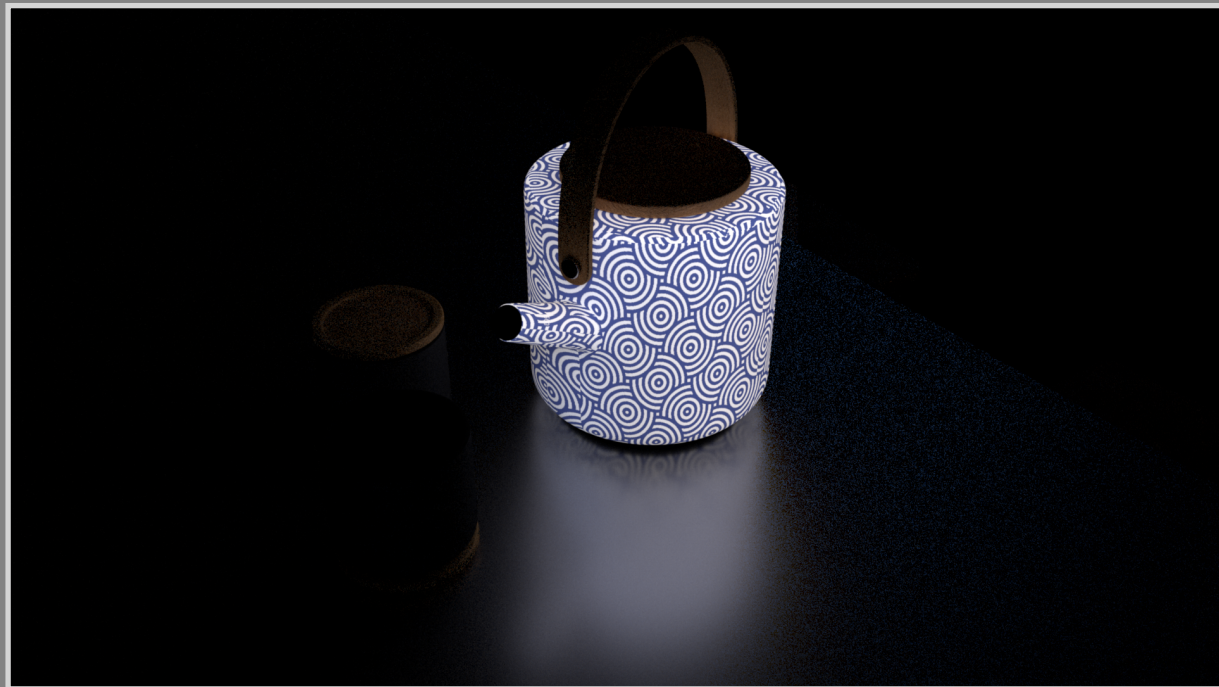
"ADJOINT" – THAT SOUNDS FAMILIAR!



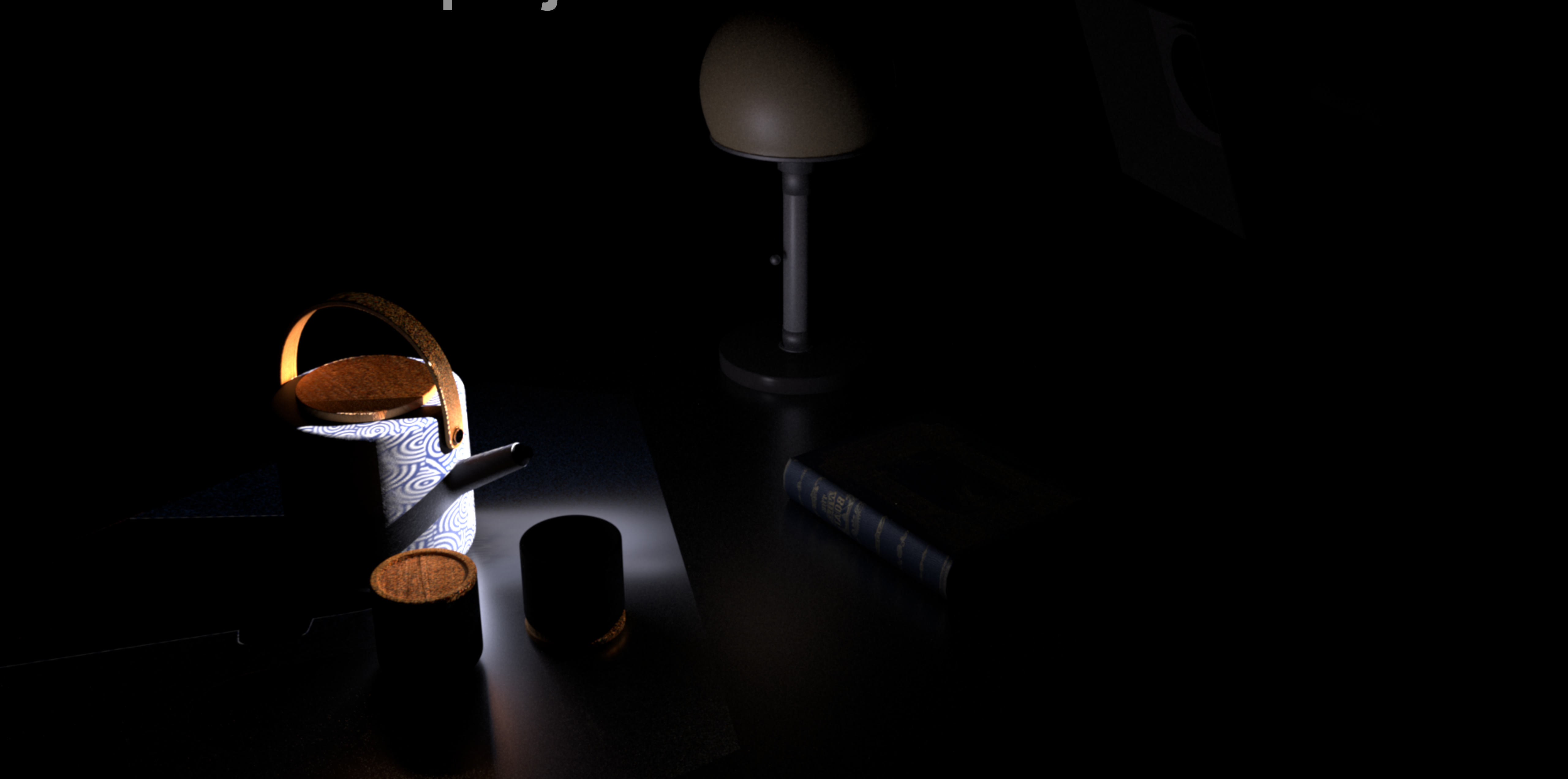
Bidirectional Estimators for Light Transport
Veach & Guibas, 1994

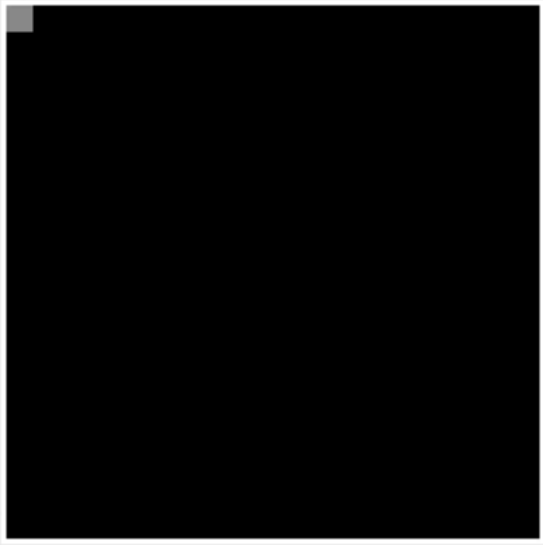
$$\langle Oa, b \rangle = \langle a, Ob \rangle$$

(Underlying principle: self-adjoint operators)

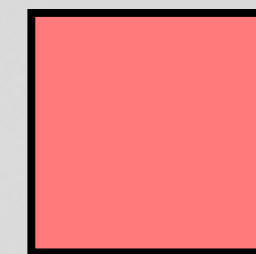
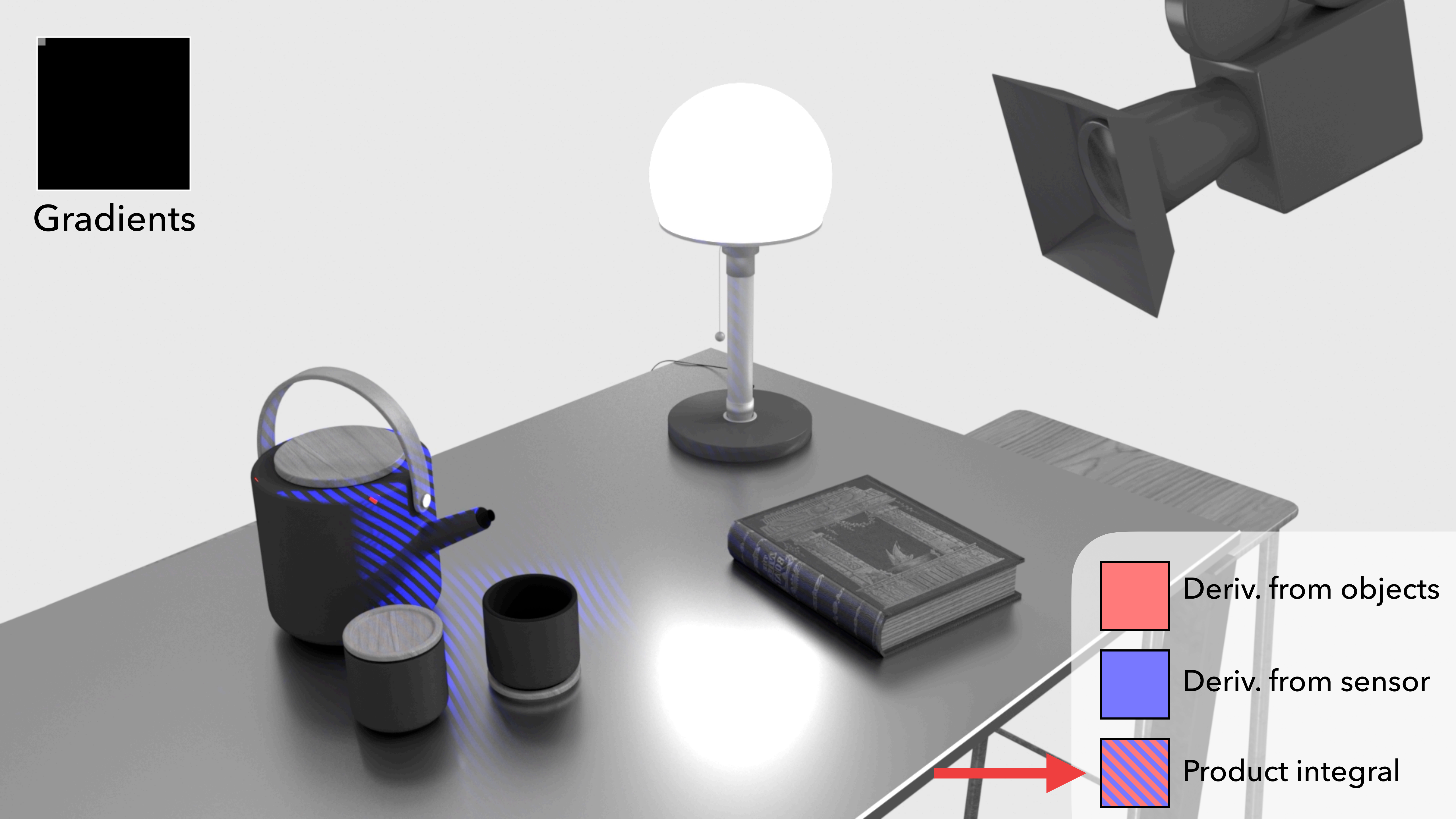


Derivatives projected into the scene

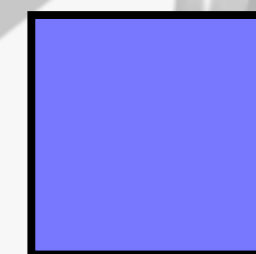




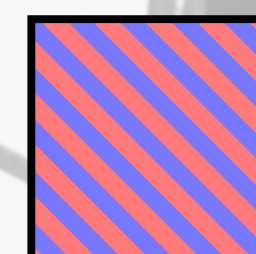
Gradients



Deriv. from objects



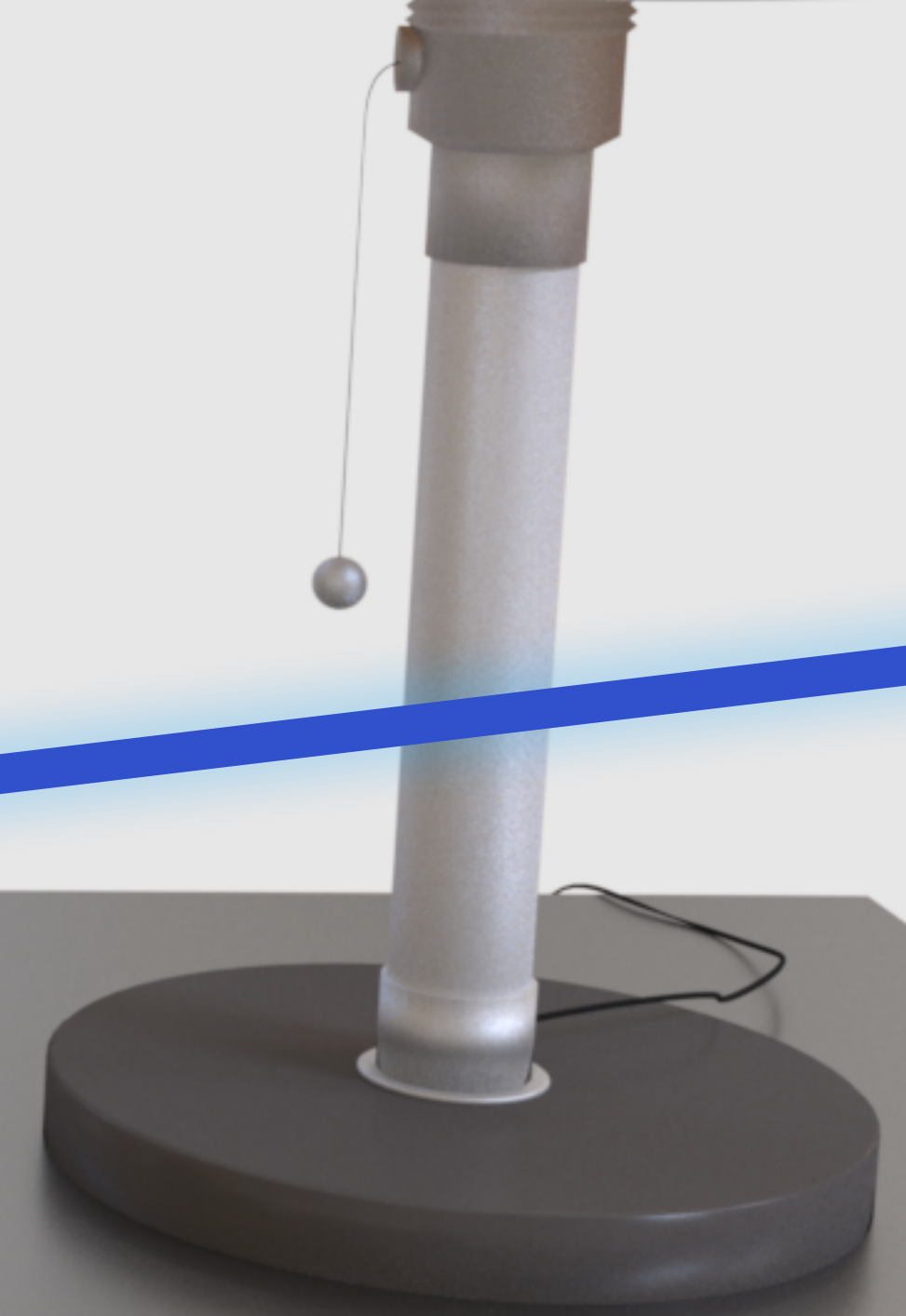
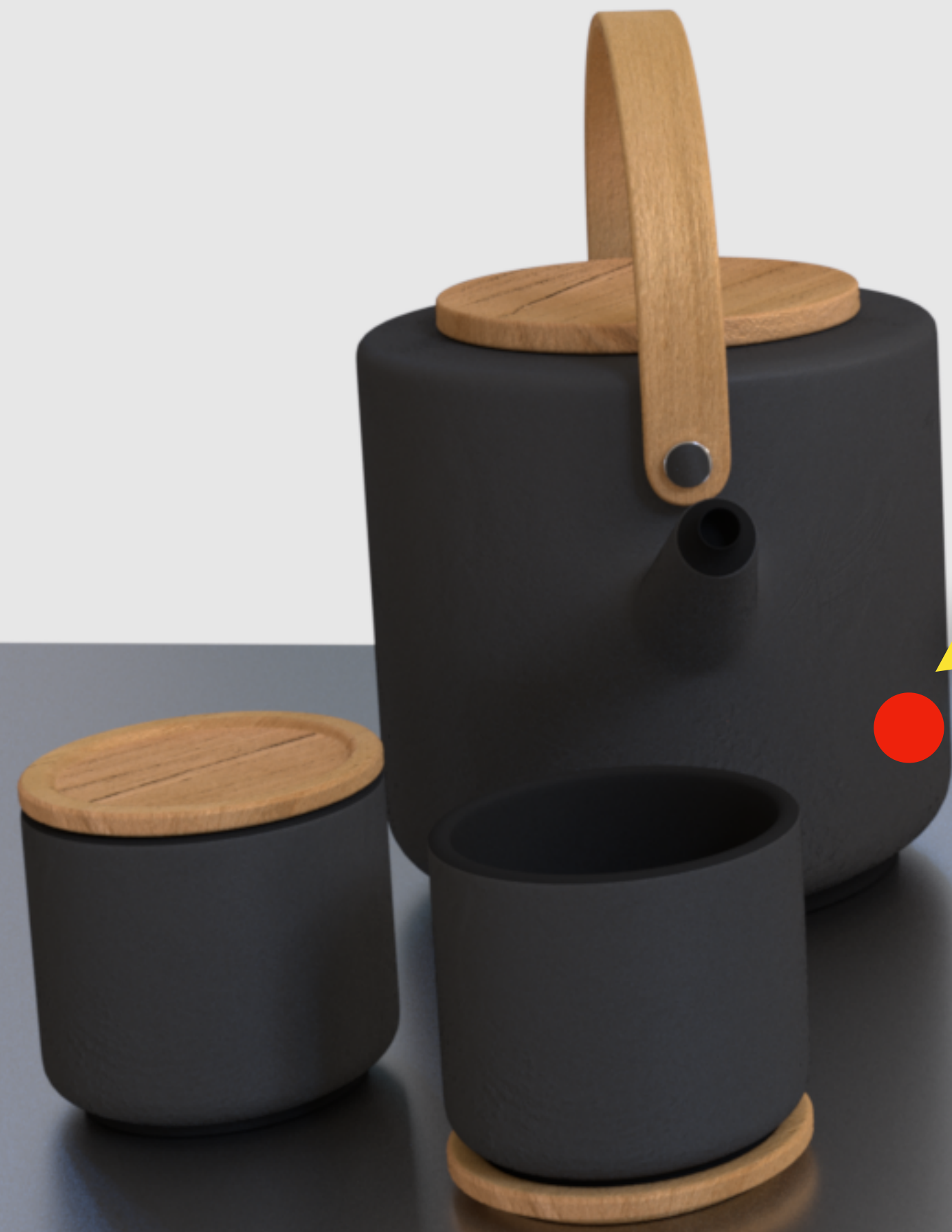
Deriv. from sensor



Product integral

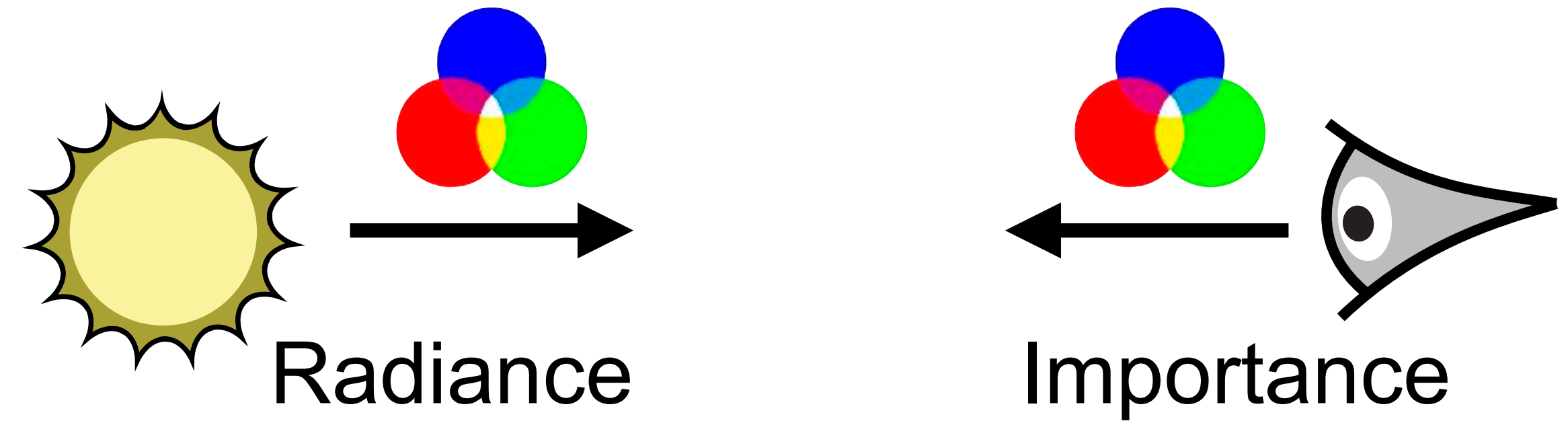


$$f_s : (\omega_i, \omega_0, \underbrace{x_1, x_2, \dots}_{\text{parameters}}) \mapsto \mathbb{R}$$



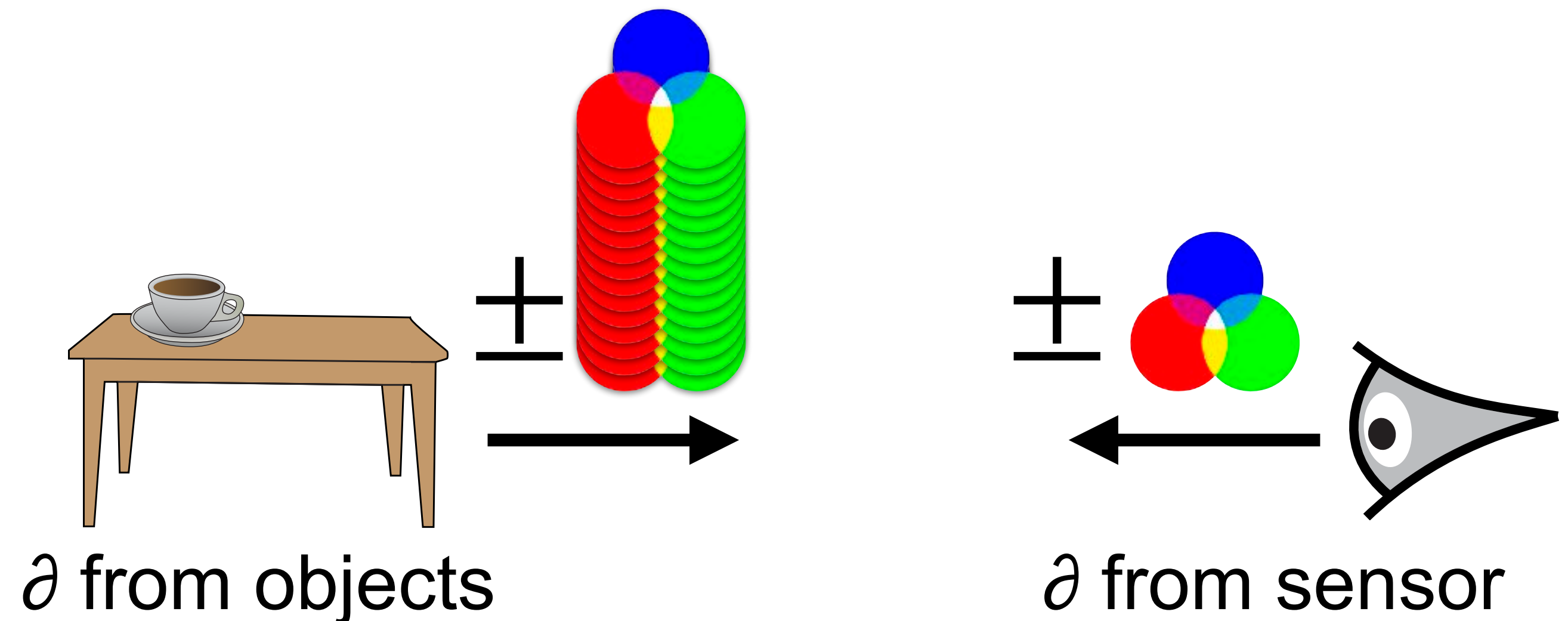
Normal rendering

- Transporting from sensor/light may yield lower variance.



Differentiable rendering

- Transporting from objects is **completely impractical**.



Surface texture optimization



Initial state

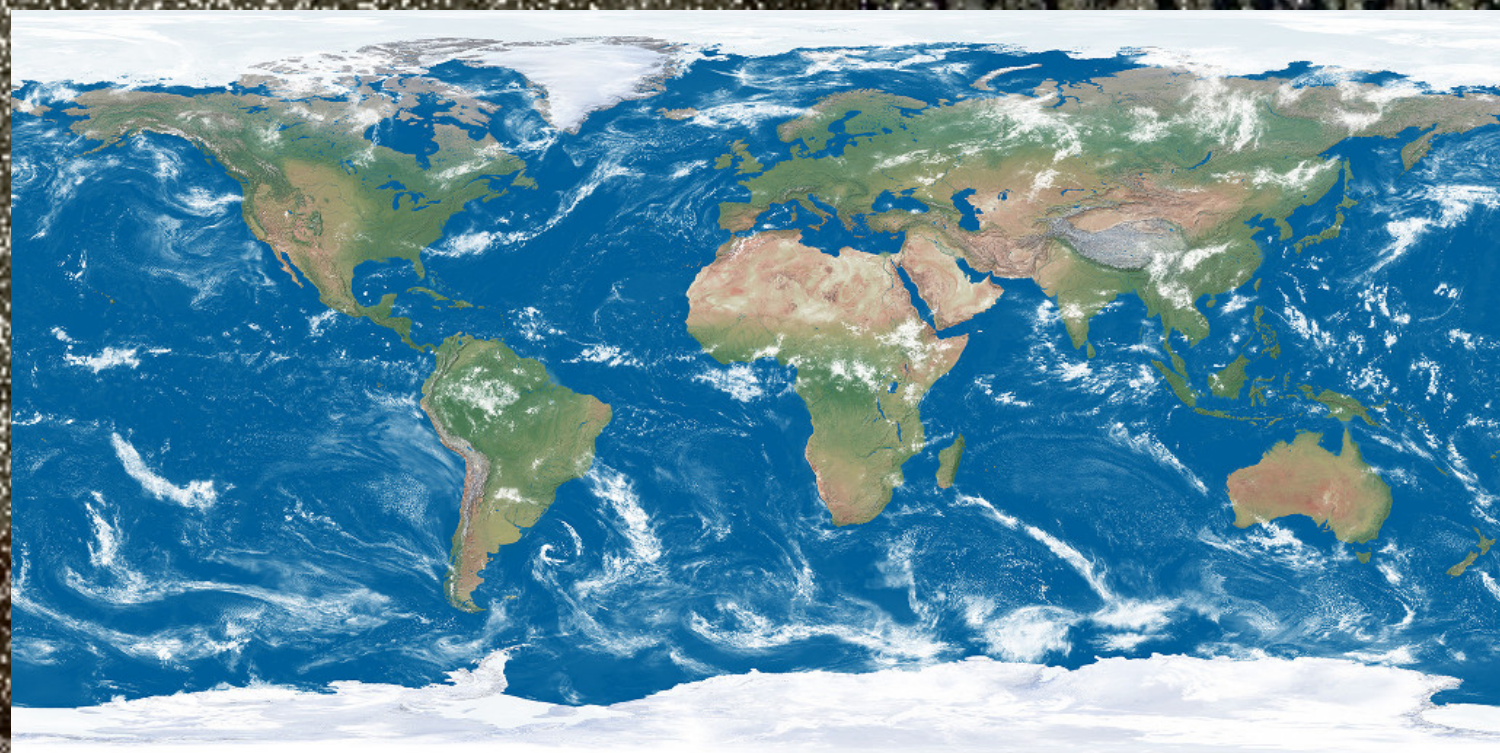


Target state

Optimized texture

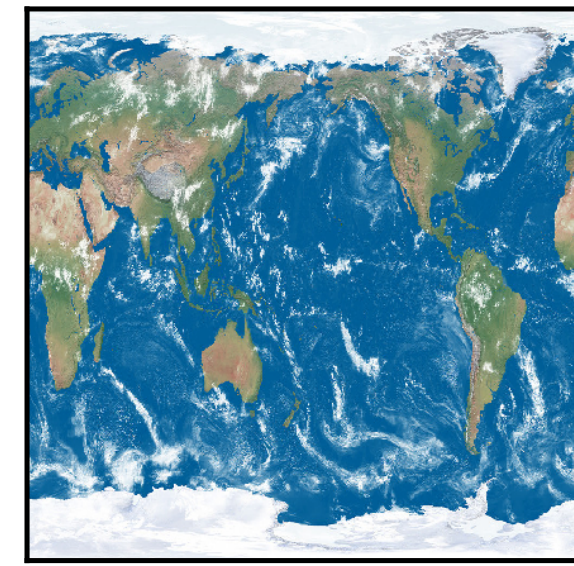


Target

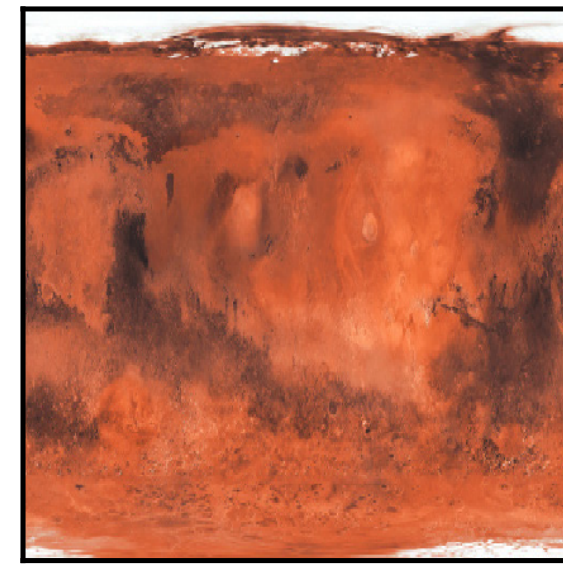




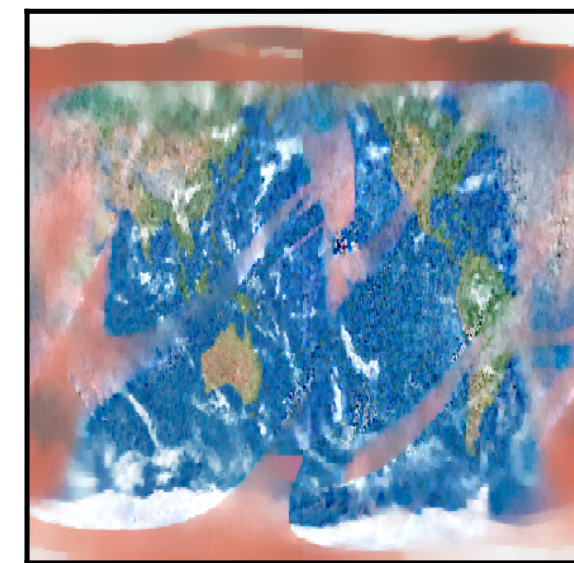
Surface BSDF optimization



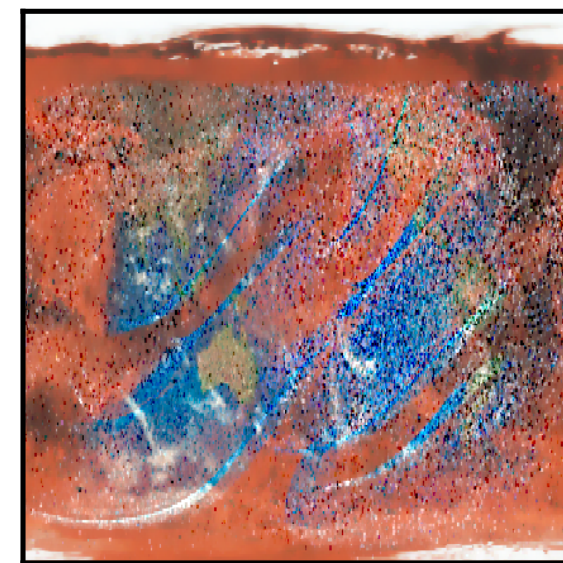
Reference



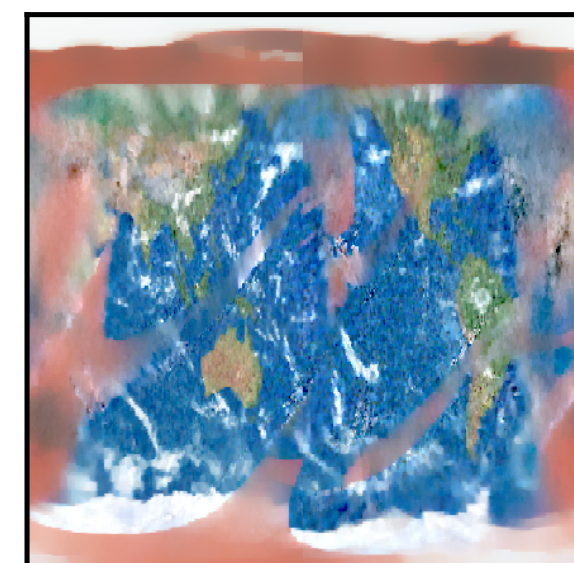
Initial state



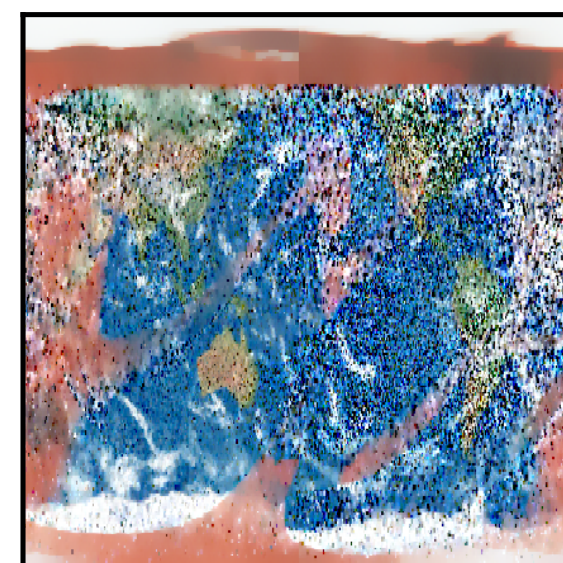
Ours (biased I)



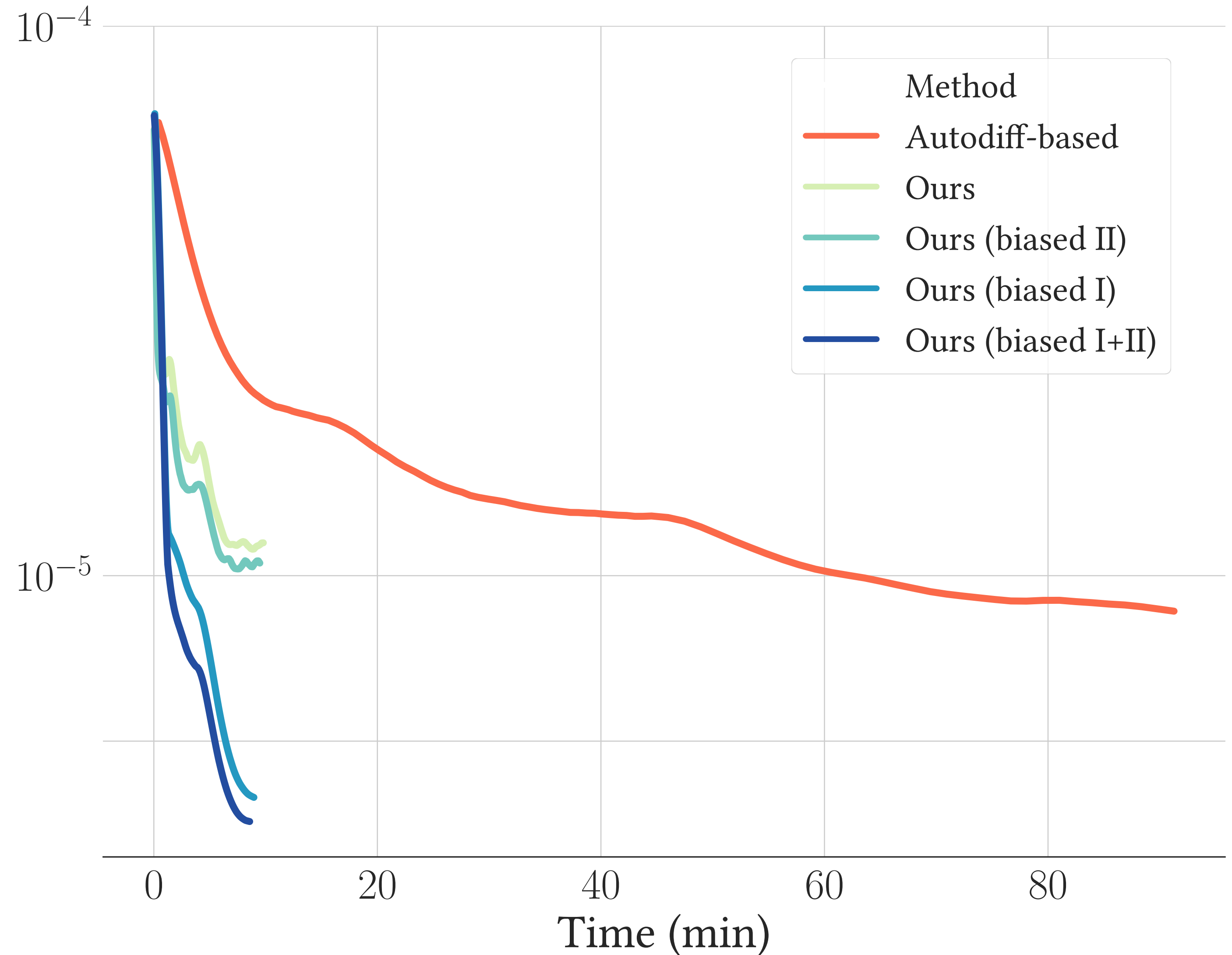
Autodiff-based



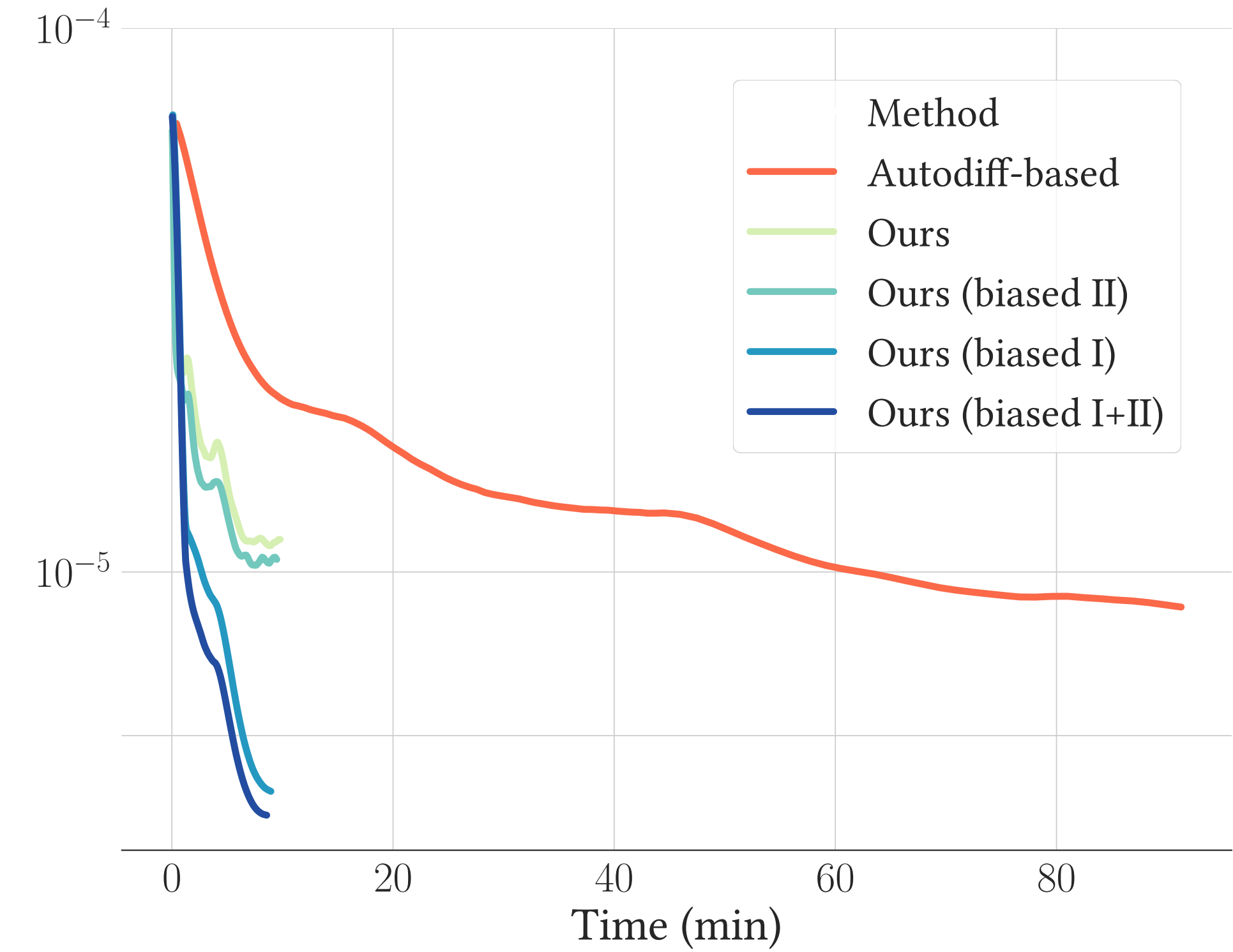
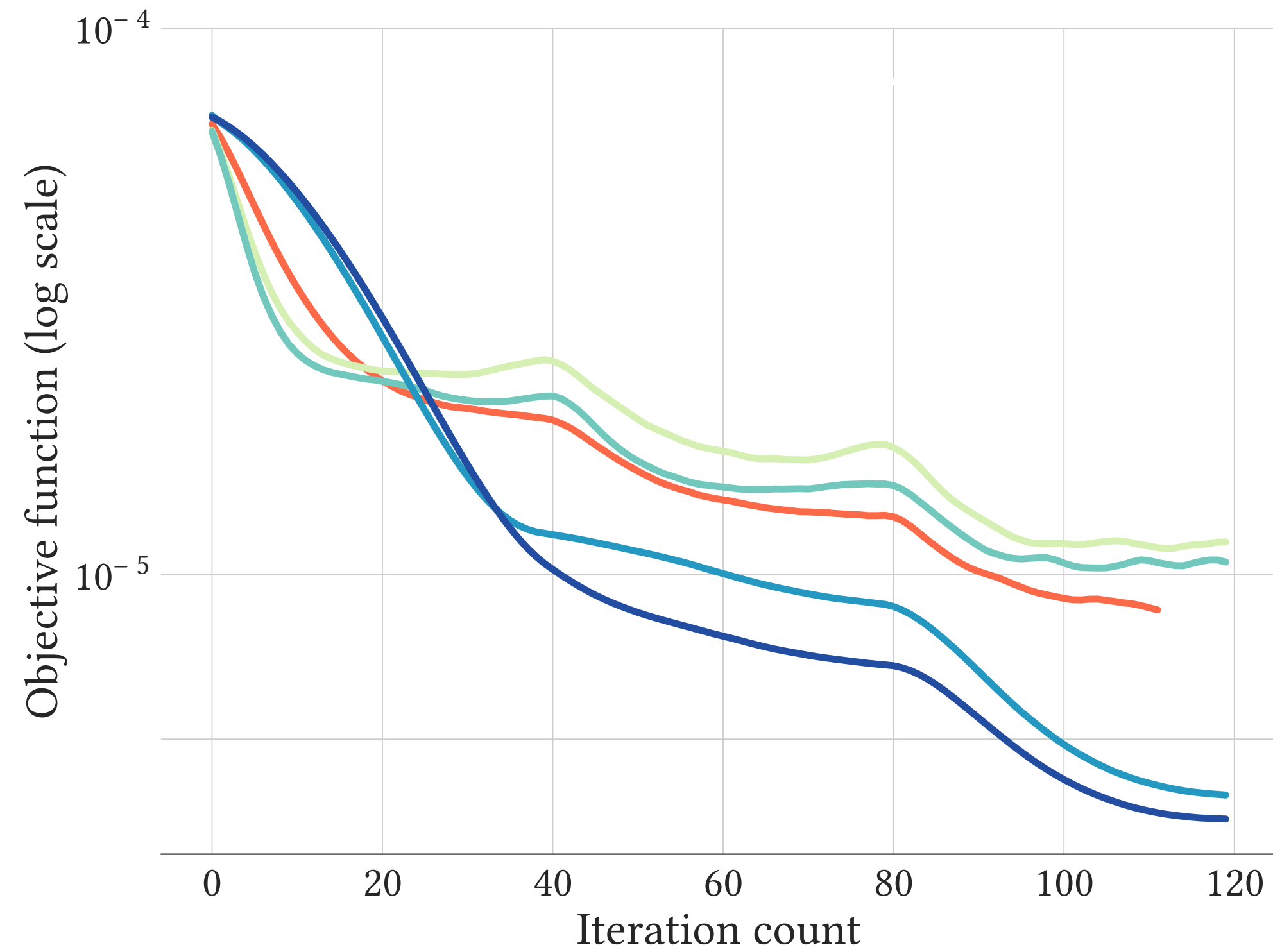
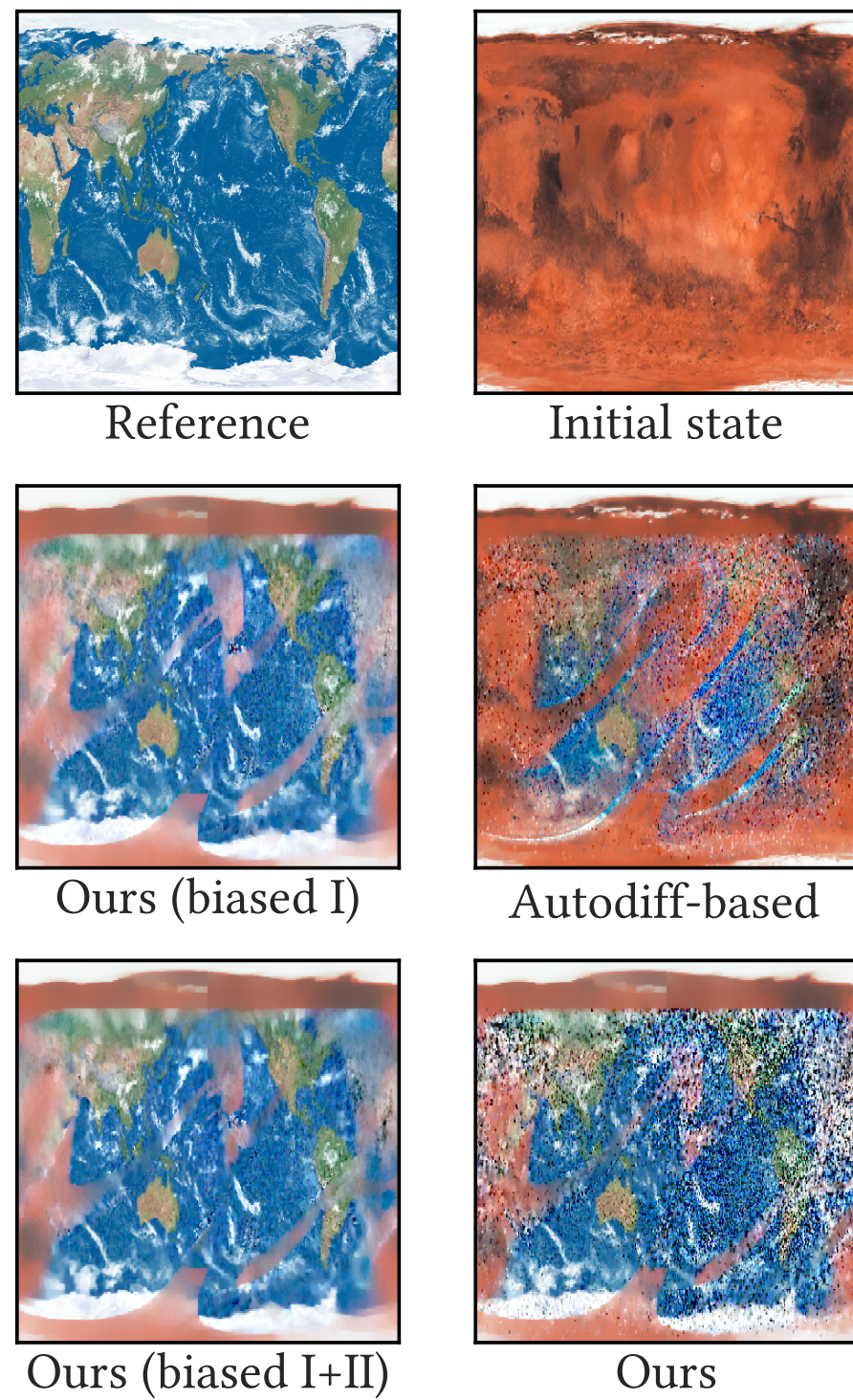
Ours (biased I+II)

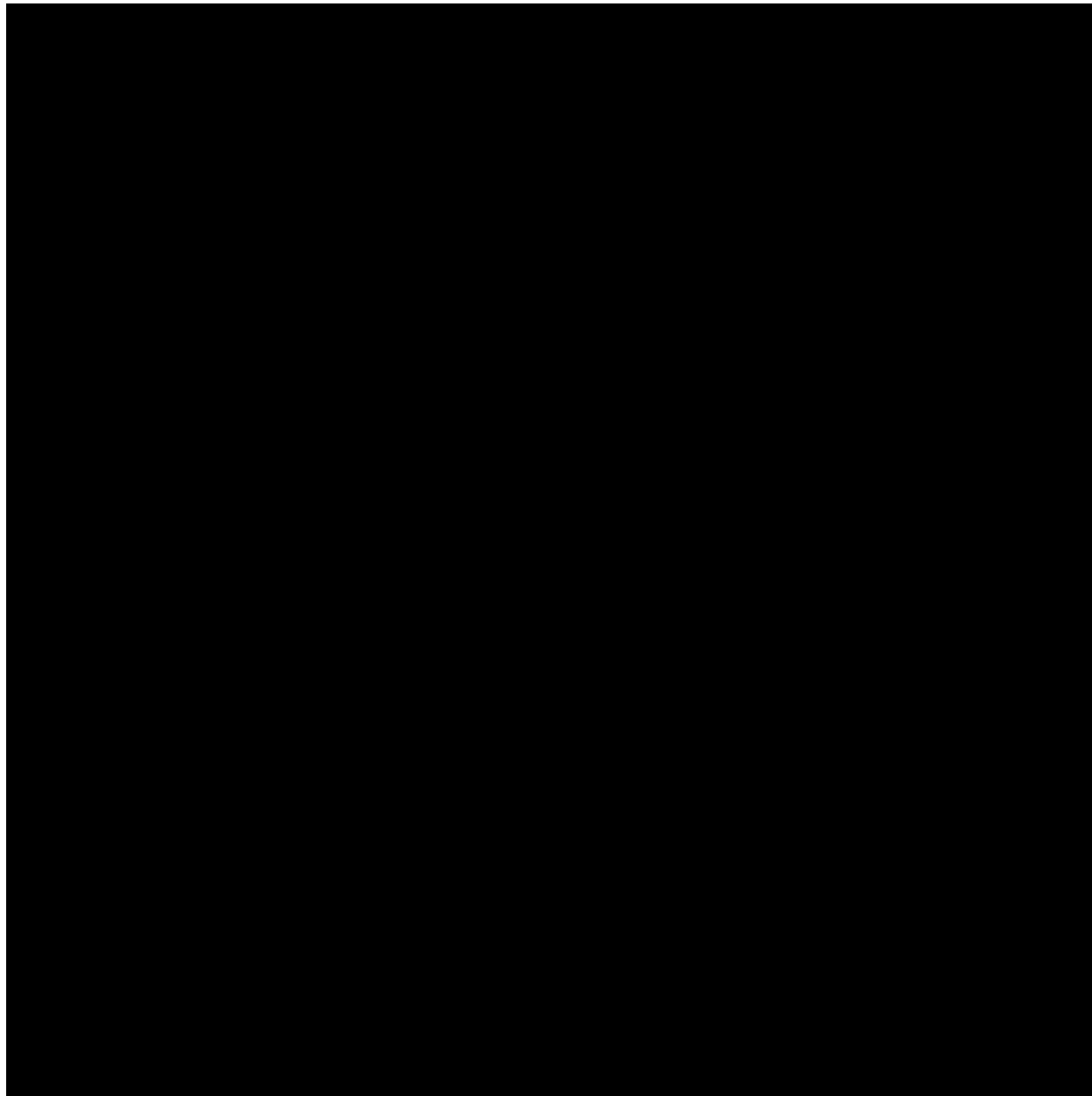


Ours



Surface BSDF optimization

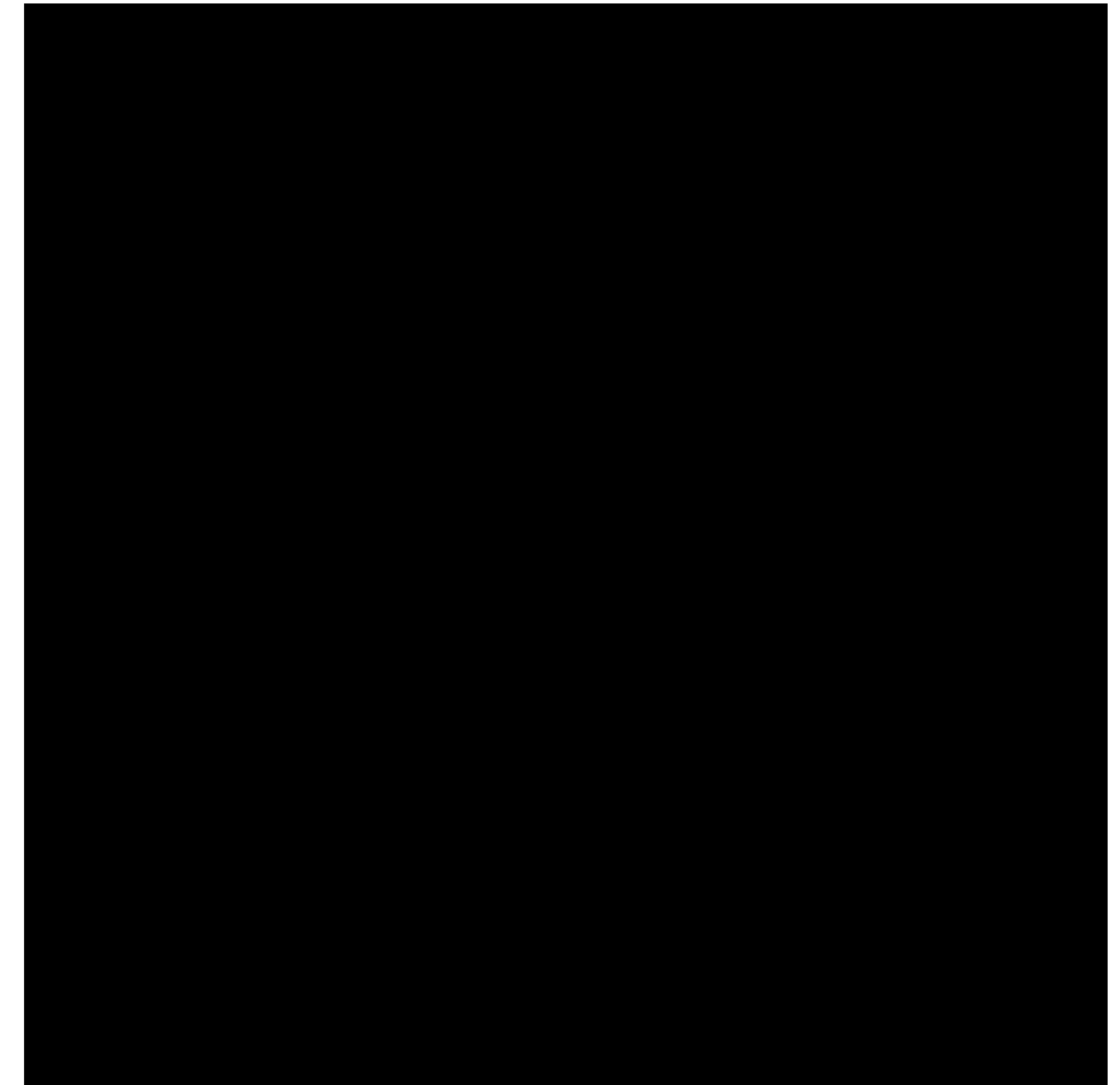




Mitsuba 2 (AD-based)



Radiative Backprop.
(biased I + II)



Target

Volume density optimization



Reference



Initial state



Ours (biased I)



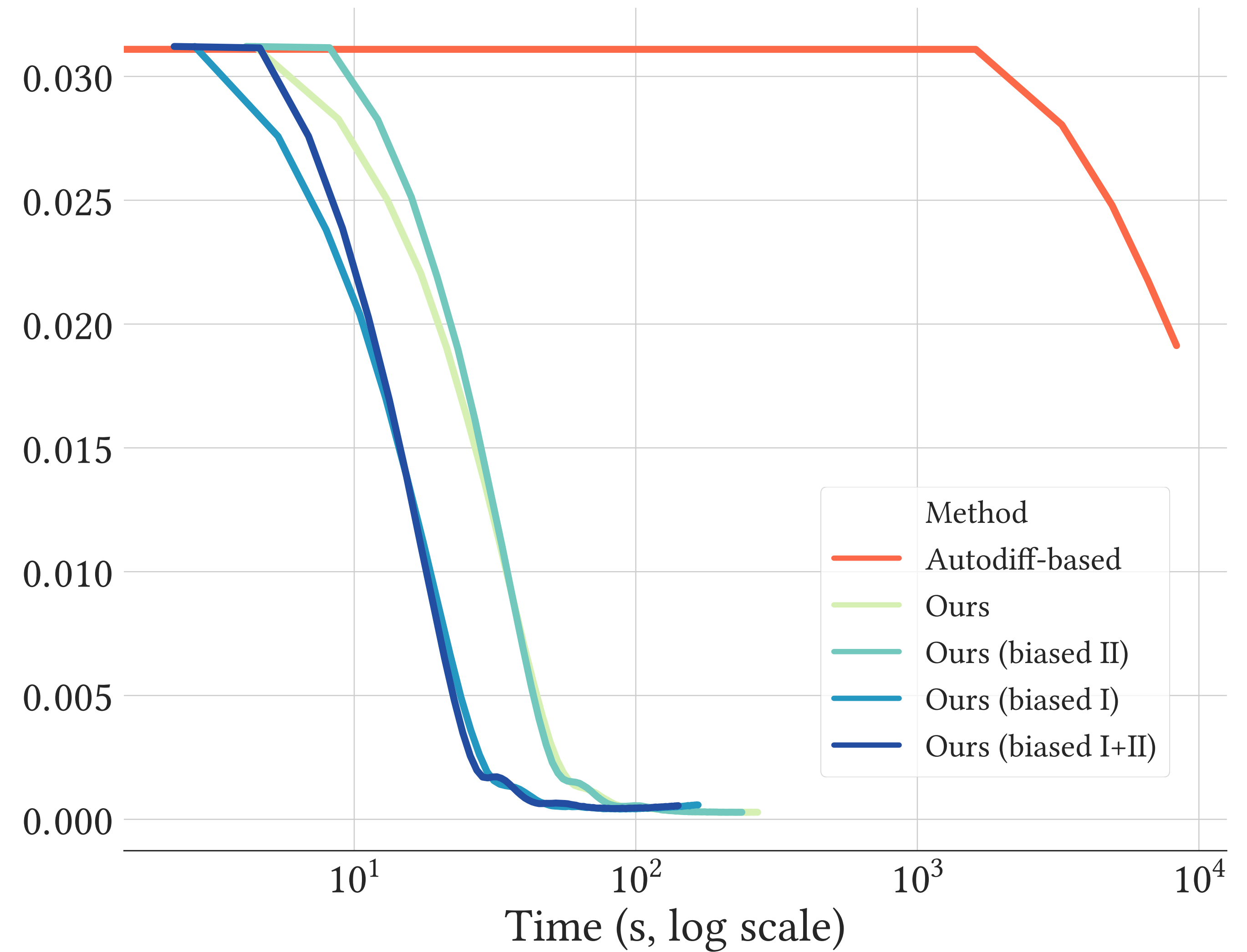
Autodiff-based



Ours (biased I+II)

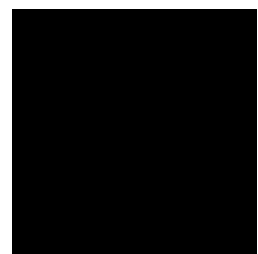
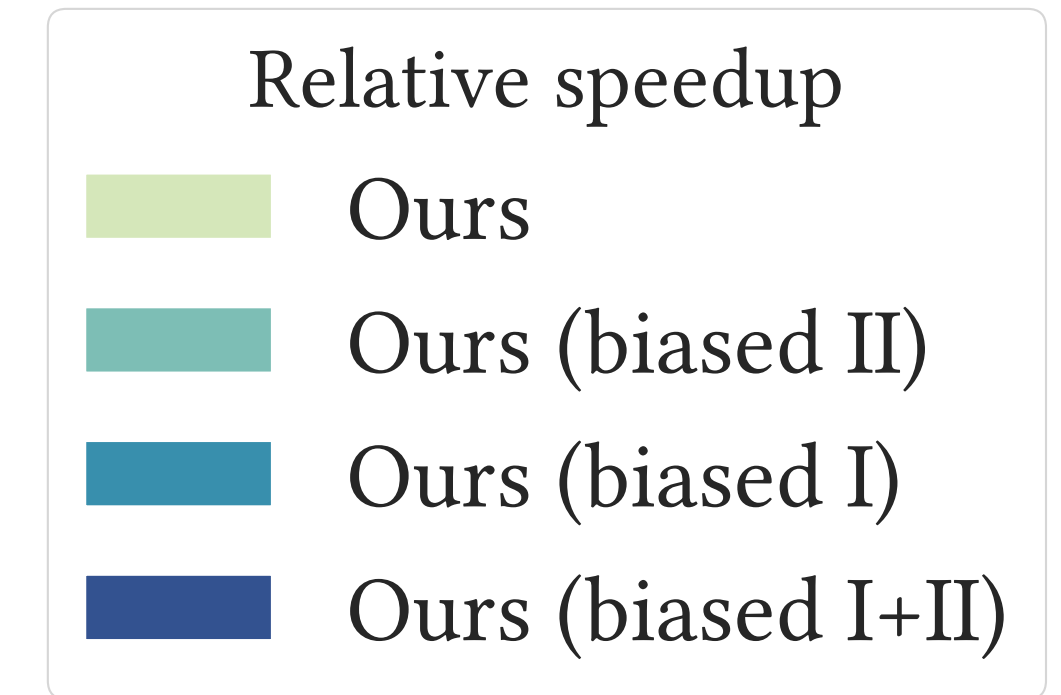
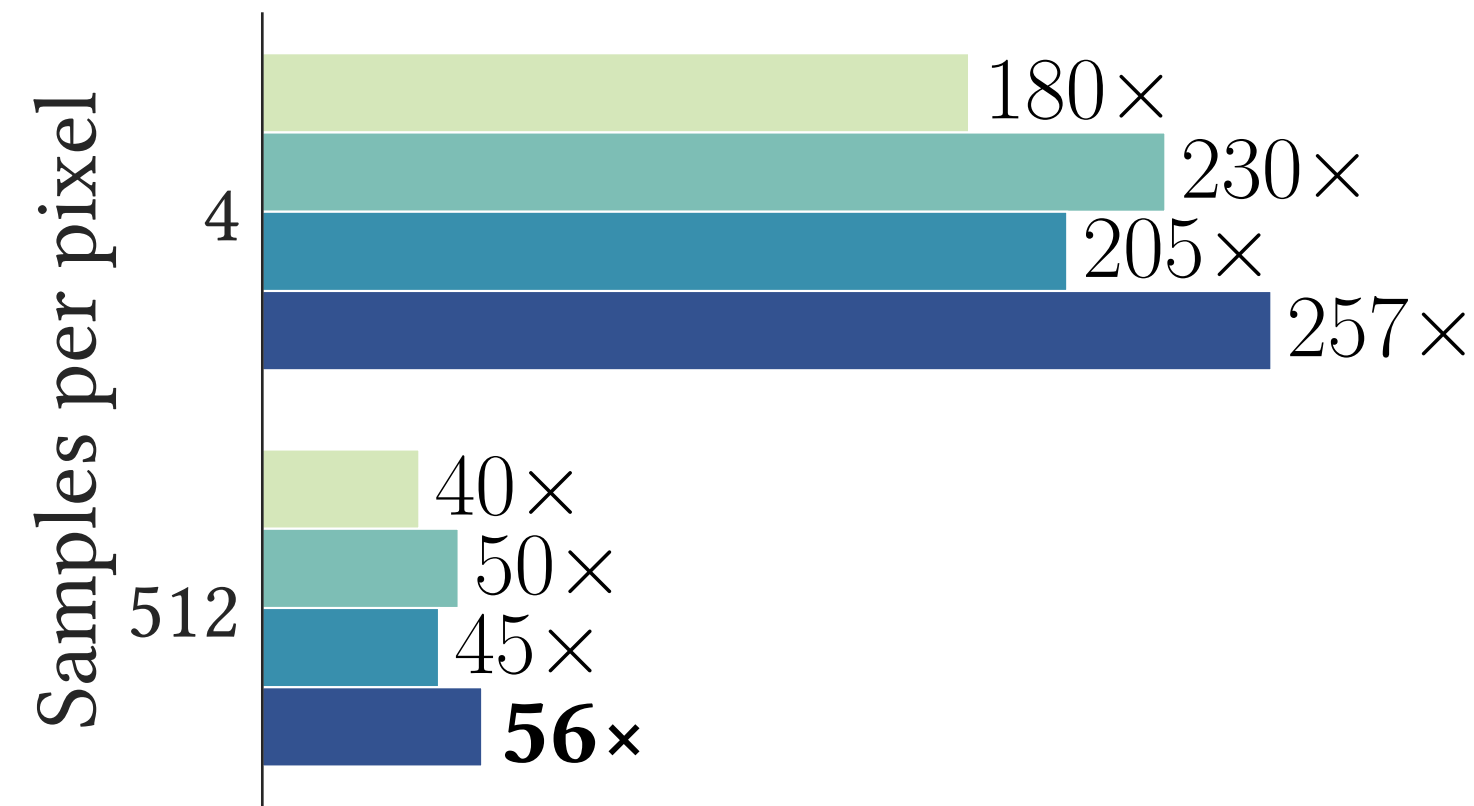


Ours

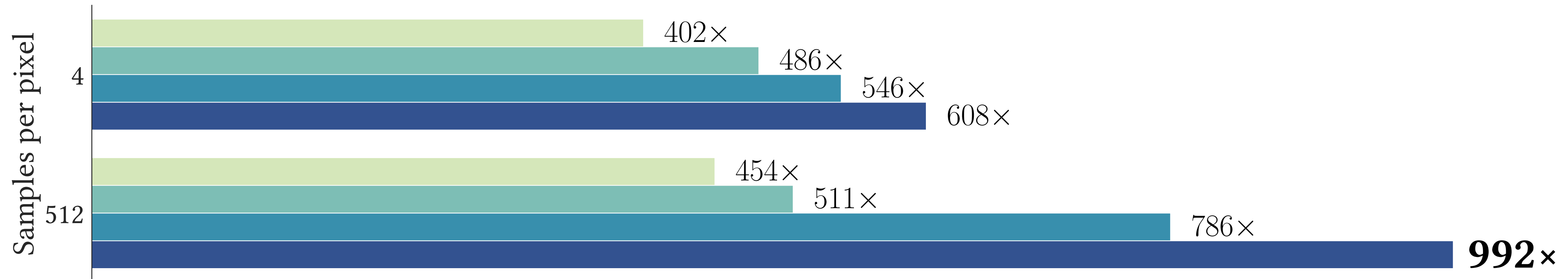




Surface texture optimization



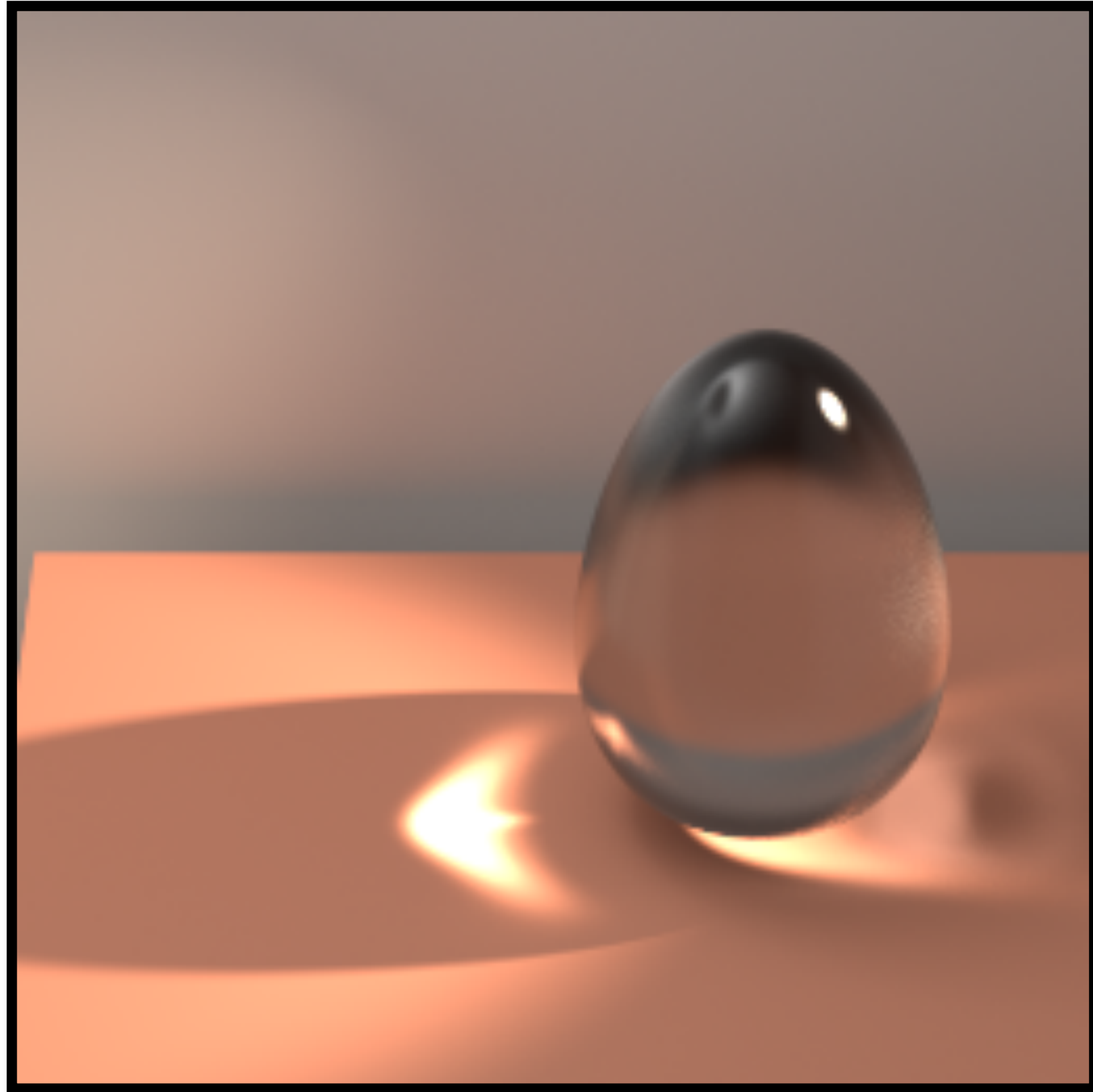
Volume density optimization



- Radiative Backpropagation is **“just” another kind** of light transport simulation with weird sensors and emitters.
 - Orders of magnitude faster (up to $\sim 1000\times$ in our experiments)
 - Lifts memory limitations entirely
 - Only need to differentiate BSDFs etc. (“easy”)
 - Can build on decades of research targeting such problems!



CHALLENGES REMAIN



Complex light transport

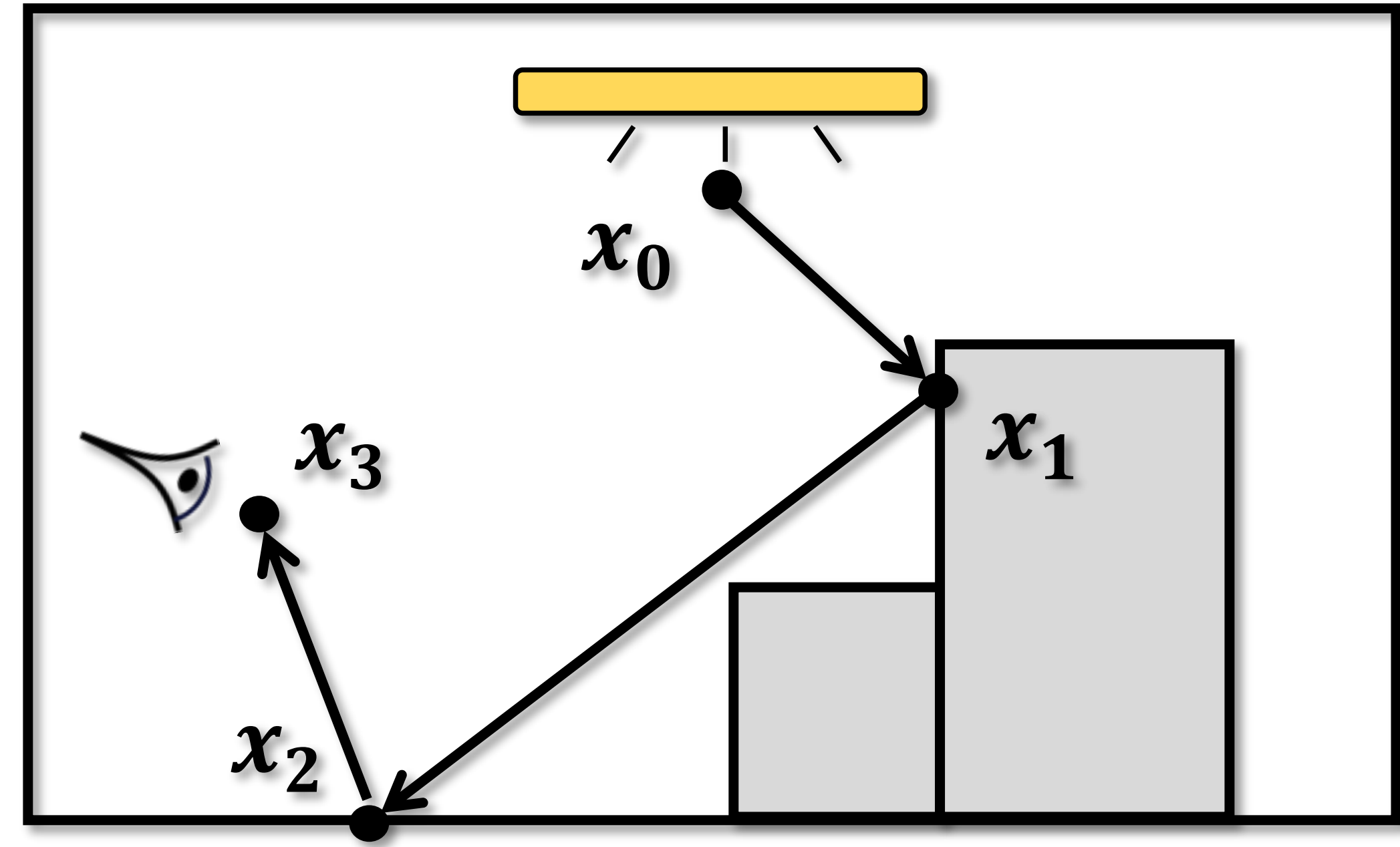


Complex geometry & motion

$$I = \int_{\Omega} f(\bar{x}) d\mu(\bar{x})$$

Measurement contribution function $f(\bar{x})$
Path space Ω
Area-product measure $d\mu(\bar{x})$

- Introduced by Veach [1997]
- Foundation of sophisticated Monte Carlo algorithms (e.g., BDPT, MCMC rendering)



Light path $\bar{x} = (x_0, x_1, x_2, x_3)$

Can we have something similar for **differentiable rendering**?

Path-Space Differentiable Rendering

CHENG ZHANG, University of California, Irvine
BAILEY MILLER, Carnegie Mellon University
KAI YAN, University of California, Irvine
IOANNIS GKIIOULEKAS, Carnegie Mellon University
SHUANG ZHAO, University of California, Irvine

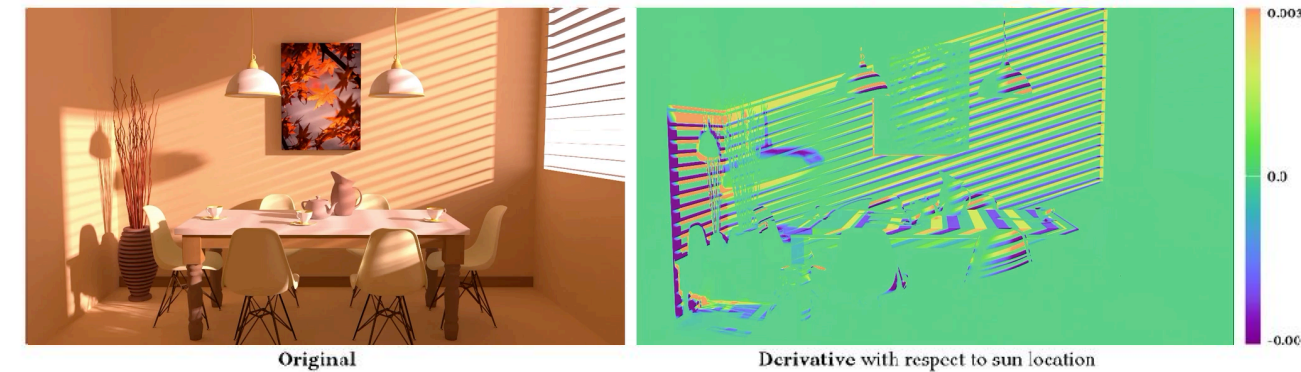


Fig. 1. We introduce **path-space differentiable rendering**, a new theoretical framework to estimate derivatives of radiometric measurements with respect to arbitrary scene parameters (e.g., material properties and object geometries). By directly differentiating full path integrals, we derive the *differential path integral* framework, enabling the design of new unbiased Monte Carlo methods capable of efficiently estimating derivatives in virtual scenes with complex geometry and light transport effects. This example shows a dining room scene lit by the sun from outside the window. On the right, we show the corresponding derivative image with respect to the vertical location of the sun. (Please use Adobe Acrobat to view the teaser images to see them animated.)

Physics-based differentiable rendering, the estimation of derivatives of radiometric measures with respect to arbitrary scene parameters, has a diverse array of applications from solving analysis-by-synthesis problems to training machine learning pipelines incorporating forward rendering processes. Unfortunately, general-purpose differentiable rendering remains challenging due to the lack of efficient estimators as well as the need to identify and handle complex discontinuities such as visibility boundaries.

In this paper, we show how path integrals can be differentiated with respect to arbitrary differentiable changes of a scene. We provide a detailed theoretical analysis of this process and establish new differentiable rendering formulations based on the resulting differential path integrals. Our path-space differentiable rendering formulation allows the design of new Monte Carlo estimators that offer significantly better efficiency than state-of-the-art methods in handling complex geometric discontinuities and light transport phenomena such as caustics.

Authors' addresses: Cheng Zhang, University of California, Irvine, chengz20@uci.edu; Bailey Miller, Carnegie Mellon University, baileymark.miller@gmail.com; Kai Yan, University of California, Irvine, kyan@uci.edu; Ioannis Gkioulekas, Carnegie Mellon University, igkioule@andrew.cmu.edu; Shuang Zhao, University of California, Irvine, sz2@ics.uci.edu.

Permission to make digital or hard copies of all or part of this work for personal or classroom use is granted without fee provided that copies are not made or distributed for profit or commercial advantage and that copies bear this notice and the full citation on the first page. Copyrights for components of this work owned by others than the author(s) must be honored. Abstracting with credit is permitted. To copy otherwise, to republish, to post on servers or to redistribute to lists, requires prior specific permission and/or a fee. Request permissions from permissions.siggraph.org.
© 2020 Copyright held by the owner/authors(s). Publication rights licensed to ACM. 0730-0301/2020/7-ART143 \$15.00
<https://doi.org/10.1145/3386569.3392383>

We validate our method by comparing our derivative estimates to those generated using the finite-difference method. To demonstrate the effectiveness of our technique, we compare inverse-rendering performance with a few state-of-the-art differentiable rendering methods.

CCS Concepts • **Computing methodologies** → **Rendering**.

Additional Key Words and Phrases: Differentiable rendering, path integral, Monte Carlo rendering

ACM Reference Format:

Cheng Zhang, Bailey Miller, Kai Yan, Ioannis Gkioulekas, and Shuang Zhao. 2020. Path-Space Differentiable Rendering. *ACM Trans. Graph.* 39, 4, Article 143 (July 2020), 19 pages. <https://doi.org/10.1145/3386569.3392383>

1 INTRODUCTION

Physics-based light transport simulation, a core research topic in computer graphics since the field's inception, focuses on numerically estimating radiometric sensor responses in fully specified virtual scenes. Previous research efforts have led to mature *forward rendering* algorithms that can efficiently and accurately simulate light transport in virtual environments with high complexities.

Differentiable rendering computes the derivatives of radiometric measurements with respect to differential changes of such environments. These techniques can enable, for example: (i) *gradient-based optimization* when solving *inverse-rendering* problems; and (ii) efficient integration of physics-based light transport simulation in *machine learning* and *probabilistic inference* pipelines.

ACM Trans. Graph., Vol. 39, No. 4, Article 143. Publication date: July 2020.

Path-Space Differentiable Rendering

Cheng Zhang, Bailey Miller, Kai Yan, Ioannis Gkioulekas, Shuang Zhao

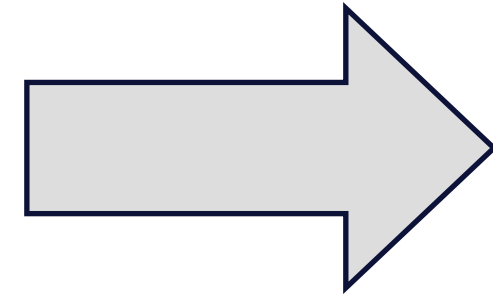
SIGGRAPH 2020

Path integral

$$I = \int_{\Omega} f(\bar{\mathbf{x}}) d\mu(\bar{\mathbf{x}}) \quad \longrightarrow \quad \frac{dI}{d\pi} = ?$$

Path integral

$$I = \int_{\Omega} f(\bar{\mathbf{x}}) d\mu(\bar{\mathbf{x}})$$



$$\frac{dI}{d\pi} = \int_{\Omega} \frac{d}{d\pi} f(\bar{\mathbf{x}}) d\mu(\bar{\mathbf{x}}) + \int_{\partial\Omega} g(\bar{\mathbf{x}}) d\mu'(\bar{\mathbf{x}})$$

Interior integral

Boundary integral

Differential path integral (for meshes)

We now derive $\partial I_N / \partial \pi$ in Eq. (25) using the recursive relations provided by Eqs. (21) and (24). Let

$$h_n^{(0)} := \left[\prod_{n'=n+1}^N g(\mathbf{x}_{n'}; \mathbf{x}_{n'-2}, \mathbf{x}_{n'-1}) \right] W_e(\mathbf{x}_N \rightarrow \mathbf{x}_{N-1}), \quad (52)$$

$$h_n^{(1)} := \sum_{n'=n+1}^N \kappa(\mathbf{x}_{n'}) V(\mathbf{x}_{n'}), \quad (53)$$

$$\Delta h_{n,n'}^{(0)} := h_n^{(0)} \Delta g(\mathbf{x}_{n'}; \mathbf{x}_{n'-2}, \mathbf{x}_{n'-1}) / g(\mathbf{x}_{n'}; \mathbf{x}_{n'-2}, \mathbf{x}_{n'-1}), \quad (54)$$

for $0 \leq n < n' \leq N$. We omit the dependencies of $h_n^{(0)}$, $h_n^{(1)}$, and $\Delta h_{n,n'}^{(0)}$ on $\mathbf{x}_{n+1}, \dots, \mathbf{x}_N$ for notational convenience.

We now show that, for all $0 \leq n < N$, it holds that

$$h_n(\mathbf{x}_n; \mathbf{x}_{n-1}) = \int_{\mathcal{M}^{N-n}} h_n^{(0)} \prod_{n'=n+1}^N dA(\mathbf{x}_{n'}), \quad (55)$$

and

$$\begin{aligned} \dot{h}_n(\mathbf{x}_n; \mathbf{x}_{n-1}) &= \int_{\mathcal{M}^{N-n}} \left[\left(h_n^{(0)} \right)' - h_n^{(0)} h_n^{(1)} \right] \prod_{\substack{n' = n+1 \\ i \neq n'}}^N dA(\mathbf{x}_{n'}) \\ &+ \sum_{n'=n+1}^N \int \Delta h_{n,n'}^{(0)} V_{\partial \mathcal{M}_{n'}}(\mathbf{x}_{n'}) d\ell(\mathbf{x}_{n'}) \prod_{\substack{n' = n+1 \\ i \neq n'}}^N dA(\mathbf{x}_i), \quad (56) \end{aligned}$$

where the integral domain of the second term on the right-hand side, which is omitted for notational clarity, is $\mathcal{M}(\pi)$ for each \mathbf{x}_i with $i \neq n'$ and $\partial \mathcal{M}_{n'}(\pi)$, which depends on $\mathbf{x}_{n'-1}$, for $\mathbf{x}_{n'}$.

It is easy to verify that Eqs. (55) and (56) hold for $n = N - 1$. We now show that, if they hold for some $0 < n < N$, then it is also the case for $n - 1$. Let $g_{n-1} := g(\mathbf{x}_n; \mathbf{x}_{n-2}, \mathbf{x}_{n-1})$ for all $0 < n \leq N$. Then,

$$\begin{aligned} h_{n-1}(\mathbf{x}_{n-1}; \mathbf{x}_{n-2}) &= \int_{\mathcal{M}} g_{n-1} \int_{\mathcal{M}^{N-n}} h_n^{(0)} \prod_{n'=n+1}^N dA(\mathbf{x}_{n'}) dA(\mathbf{x}_n) \\ &= \int_{\mathcal{M}^{N-n+1}} h_{n-1}^{(0)} \prod_{n'=n}^N dA(\mathbf{x}_{n'}), \quad (57) \end{aligned}$$

and

$$\begin{aligned} \dot{h}_{n-1}(\mathbf{x}_{n-1}; \mathbf{x}_{n-2}) &= \int_{\mathcal{M}} \left[\dot{g}_{n-1} h_n + g_{n-1} (\dot{h}_n - h_n \kappa(\mathbf{x}_n) V(\mathbf{x}_n)) \right] dA(\mathbf{x}_n) \\ &+ \int_{\partial \mathcal{M}_n} \Delta g_{n-1} h_n V_{\partial \mathcal{M}_n} d\ell(\mathbf{x}_n) \\ &= \int_{\mathcal{M}^{N-n+1}} \left\{ \dot{g}_{n-1} h_n^{(0)} + g_{n-1} \left[\left(h_n^{(0)} \right)' - h_n^{(0)} h_n^{(1)} \right] \right\} \prod_{n'=k}^N dA(\mathbf{x}_{n'}) \\ &+ \sum_{n'=n+1}^N \int g_{n-1} \Delta h_{n,n'}^{(0)} V_{\partial \mathcal{M}_{n'}}(\mathbf{x}_{n'}) d\ell(\mathbf{x}_{n'}) \prod_{\substack{n' = n+1 \\ i \neq n'}}^N dA(\mathbf{x}_i) \\ &+ \int \Delta g_{n-1} h_n^{(0)} V_{\partial \mathcal{M}_n} d\ell(\mathbf{x}_n) \prod_{n'=n+1}^N dA(\mathbf{x}_{n'}) \\ &= \int_{\mathcal{M}^{N-n+1}} \left[\left(h_{n-1}^{(0)} \right)' - h_{n-1}^{(0)} h_{n-1}^{(1)} \right] \prod_{n'=n}^N dA(\mathbf{x}_{n'}) \\ &+ \sum_{n'=n}^N \int \Delta h_{n-1,n'}^{(0)} V_{\partial \mathcal{M}_{n'}}(\mathbf{x}_{n'}) d\ell(\mathbf{x}_{n'}) \prod_{\substack{n' = n \\ i \neq n'}}^N dA(\mathbf{x}_i). \quad (58) \end{aligned}$$

Thus, using mathematical induction, we know that Eqs. (55) and (56) hold for all $0 \leq n < N$.

Notice that $h_0^{(0)} = f$ and $\Delta h_{0,n'}^{(0)} = \Delta f_{n'}$, where $\Delta f_{n'}$ follows the definition in Eq. (28). Letting $n = 0$ in Eq. (56) yields

$$\begin{aligned} \dot{h}_0(\mathbf{x}_0) &= \int_{\mathcal{M}^N} \left[\dot{f}(\bar{\mathbf{x}}) - f(\bar{\mathbf{x}}) \sum_{n'=1}^N \kappa(\mathbf{x}_{n'}) V(\mathbf{x}_{n'}) \right] \prod_{n'=1}^N dA(\mathbf{x}_{n'}) \\ &+ \sum_{n'=1}^N \int \Delta f_{n'}(\bar{\mathbf{x}}) V_{\partial \mathcal{M}_{n'}} d\ell(\mathbf{x}_{n'}) \prod_{\substack{0 < i \leq N \\ i \neq n'}}^N dA(\mathbf{x}_i). \quad (59) \end{aligned}$$

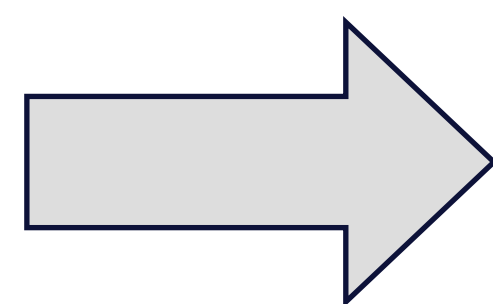
Lastly, based on the assumption that h_0 is continuous in \mathbf{x}_0 , Eq. (25) can be obtained by differentiating Eq. (23):

$$\begin{aligned} \frac{\partial I_N}{\partial \pi} &= \frac{\partial}{\partial \pi} \int_{\mathcal{M}} h_0(\mathbf{x}_0) dA(\mathbf{x}_0) \\ &= \int_{\mathcal{M}} \left[\dot{h}_0(\mathbf{x}_0) - h_0(\mathbf{x}_0) \kappa(\mathbf{x}_0) V(\mathbf{x}_0) \right] dA(\mathbf{x}_0) \\ &+ \int_{\partial \mathcal{M}_0} h_0(\mathbf{x}_0) V_{\partial \mathcal{M}_0}(\mathbf{x}_0) d\ell(\mathbf{x}_0) \quad (60) \\ &= \int_{\Omega_N} \left[\dot{f}(\bar{\mathbf{x}}) - f(\bar{\mathbf{x}}) \sum_{K=0}^N \kappa(\mathbf{x}_K) V(\mathbf{x}_K) \right] d\mu(\bar{\mathbf{x}}) \\ &+ \sum_{K=0}^N \int_{\Omega_{N,K}} \Delta f_K(\bar{\mathbf{x}}) V_{\partial \mathcal{M}_K} d\mu'_{N,K}(\bar{\mathbf{x}}). \end{aligned}$$

Full derivation in the paper [Zhang et al. 2020]

Path integral

$$I = \int_{\Omega} f(\bar{x}) d\mu(\bar{x})$$



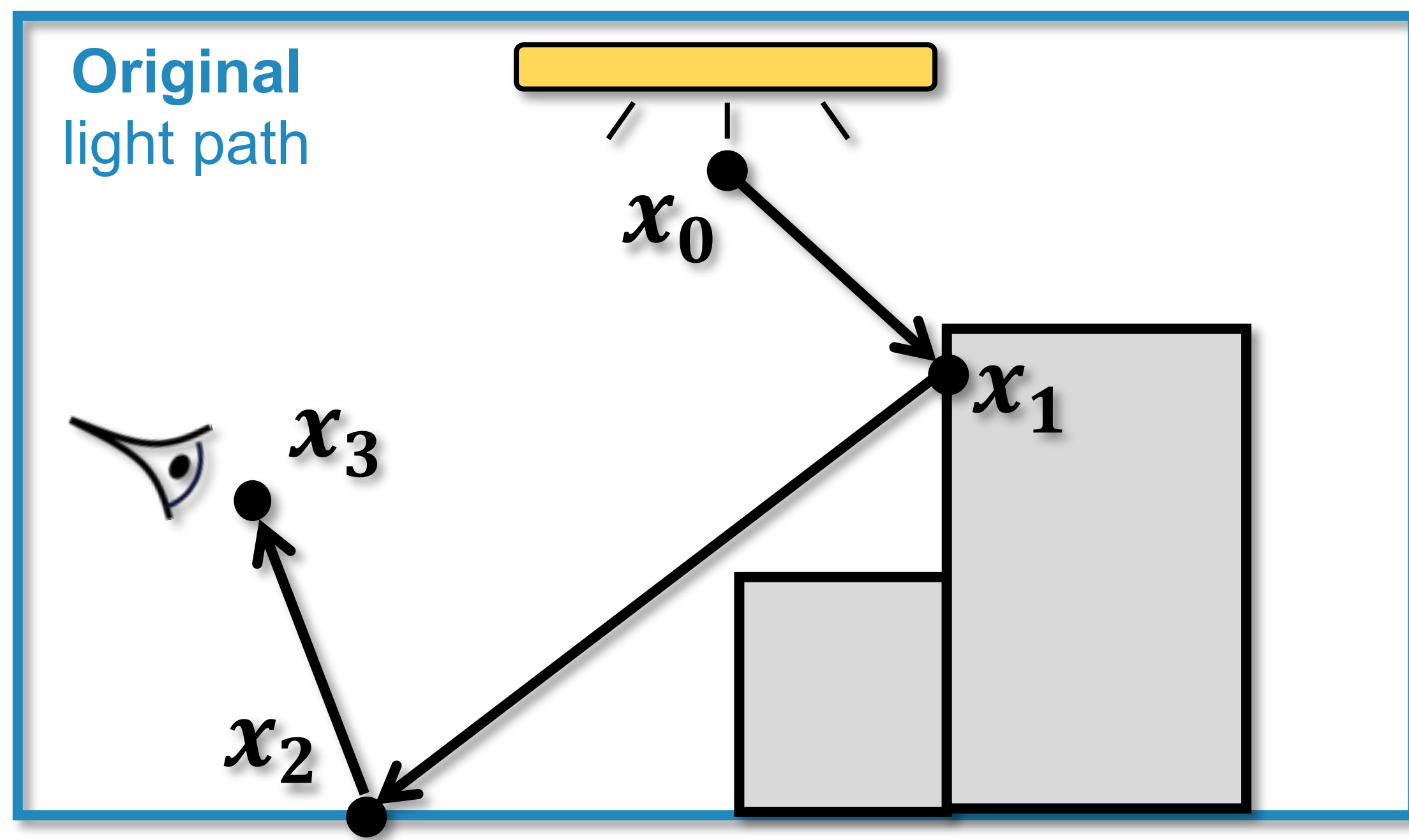
Differential path integral (for meshes)

$$\frac{dI}{d\pi} = \int_{\Omega} \frac{d}{d\pi} f(\bar{x}) d\mu(\bar{x}) + \int_{\partial\Omega} g(\bar{x}) d\mu'(\bar{x})$$

Path space

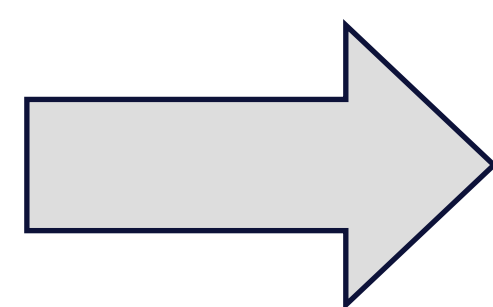
Path space

Interior integral



Path integral

$$I = \int_{\Omega} f(\bar{x}) d\mu(\bar{x})$$

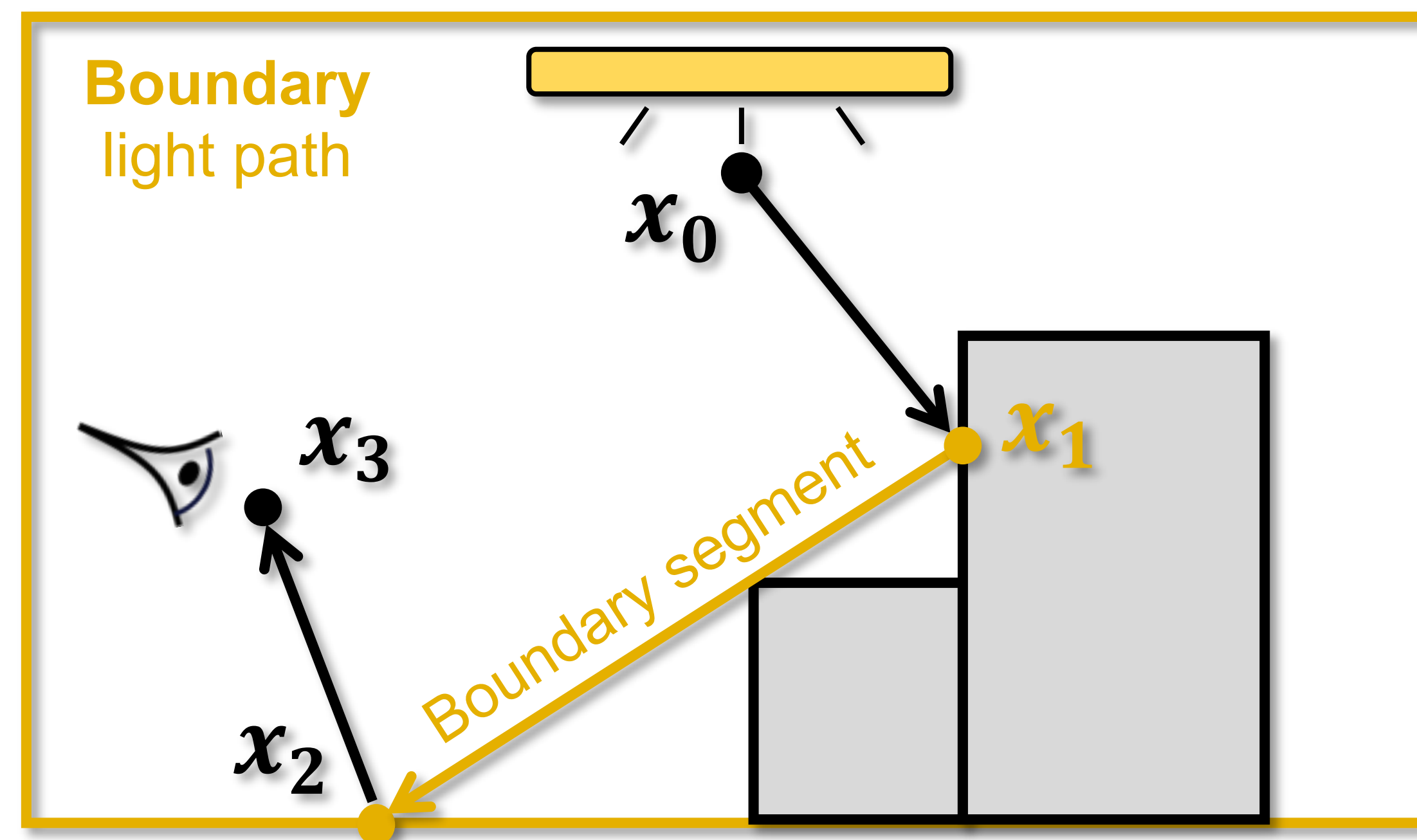
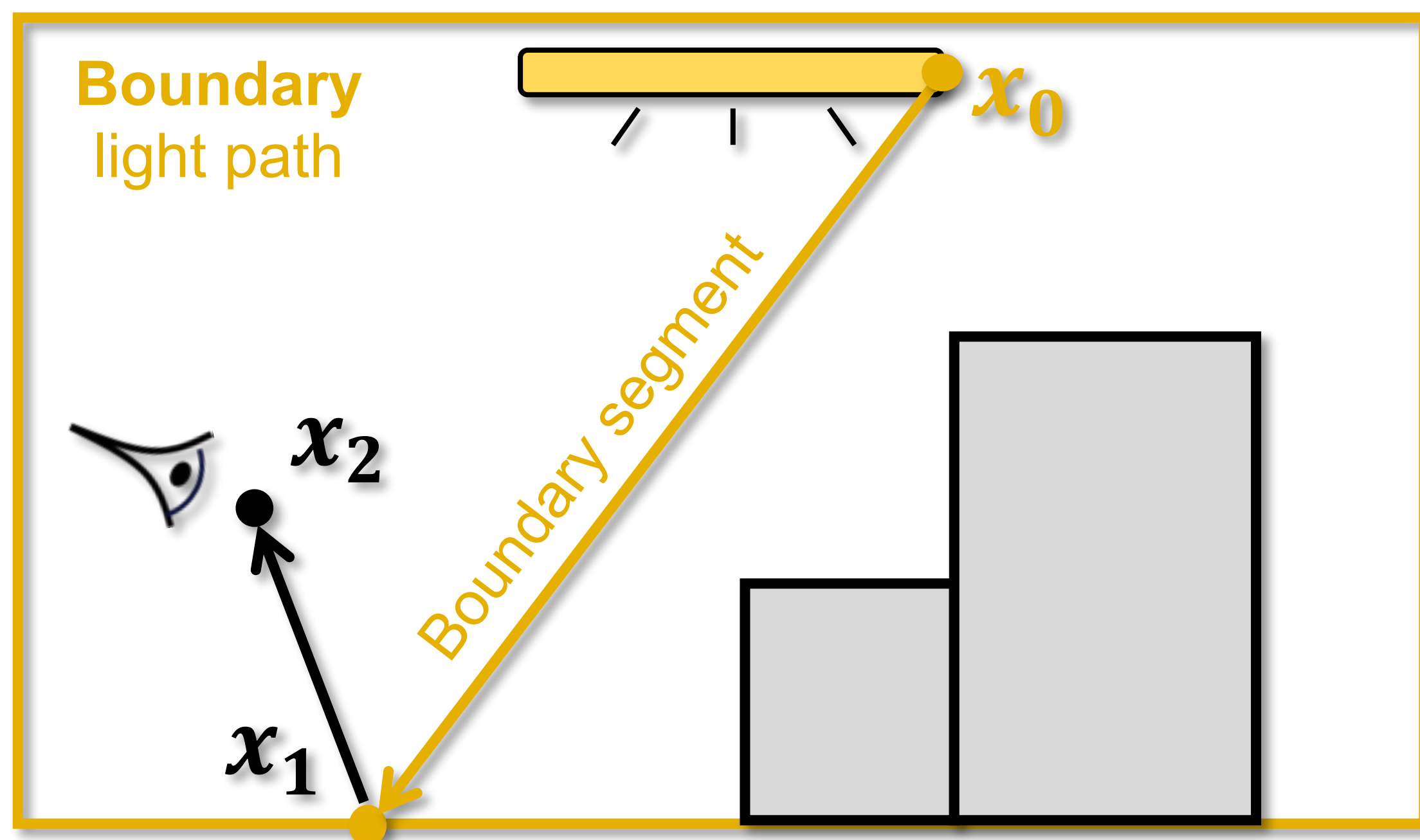


Differential path integral (for meshes)

$$\frac{dI}{d\pi} = \int_{\Omega} \frac{d}{d\pi} f(\bar{x}) d\mu(\bar{x}) + \int_{\partial\Omega} g(\bar{x}) d\mu'(\bar{x})$$

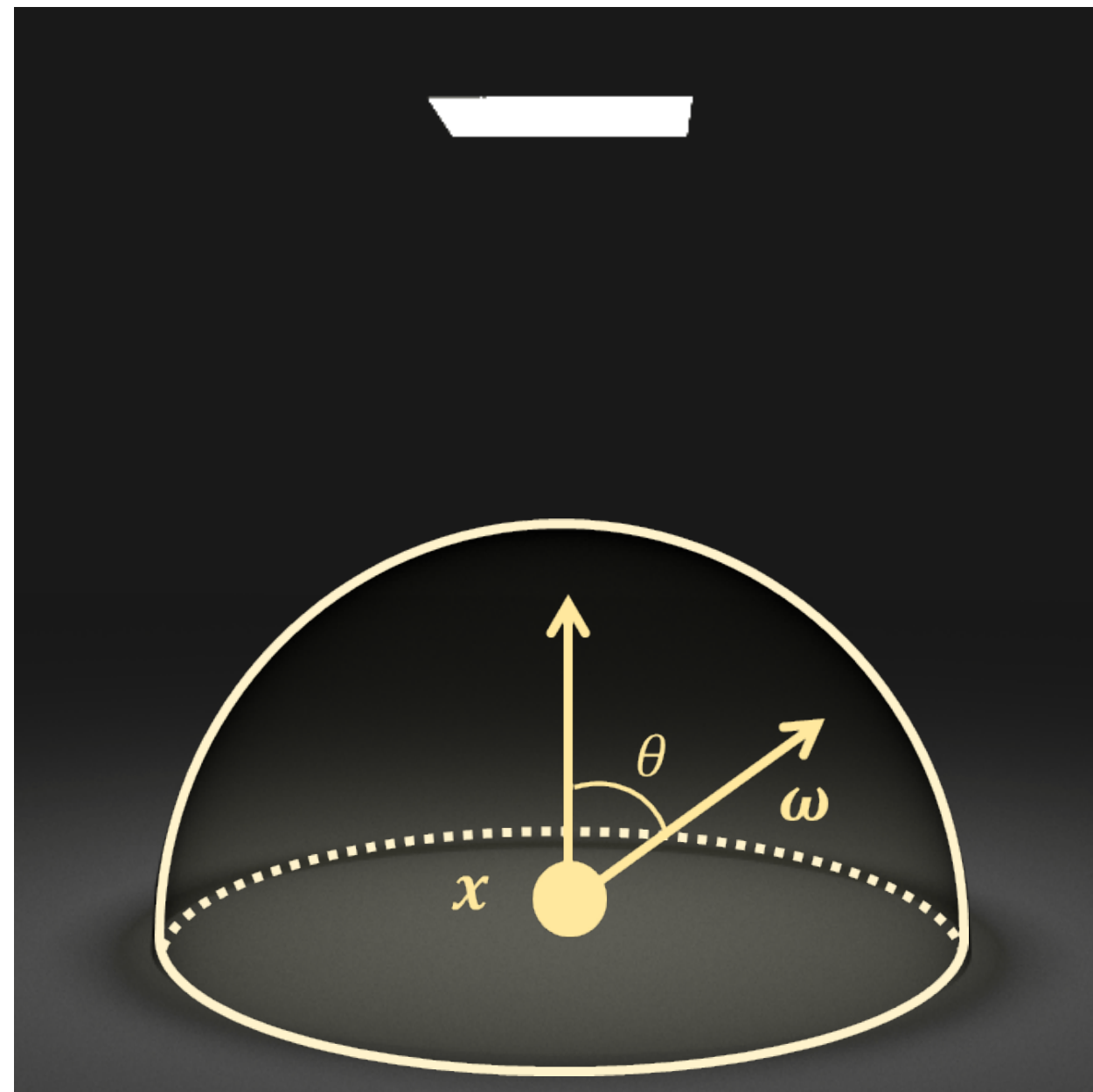
Boundary path space \nearrow Boundary integral

Boundary light path: same as original light path except having exactly one boundary segment

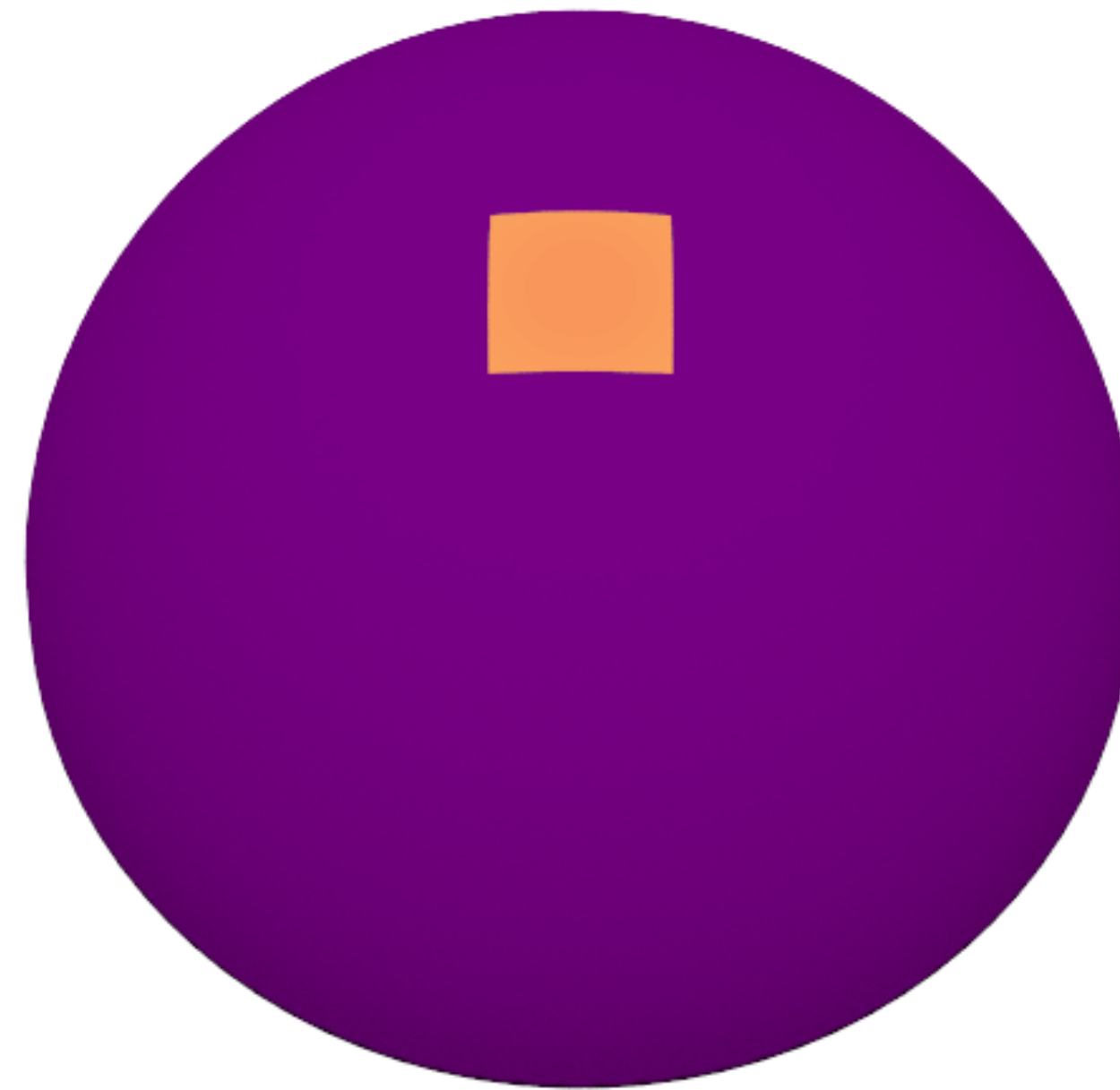


RECAP: DIFFERENTIAL IRRADIANCE

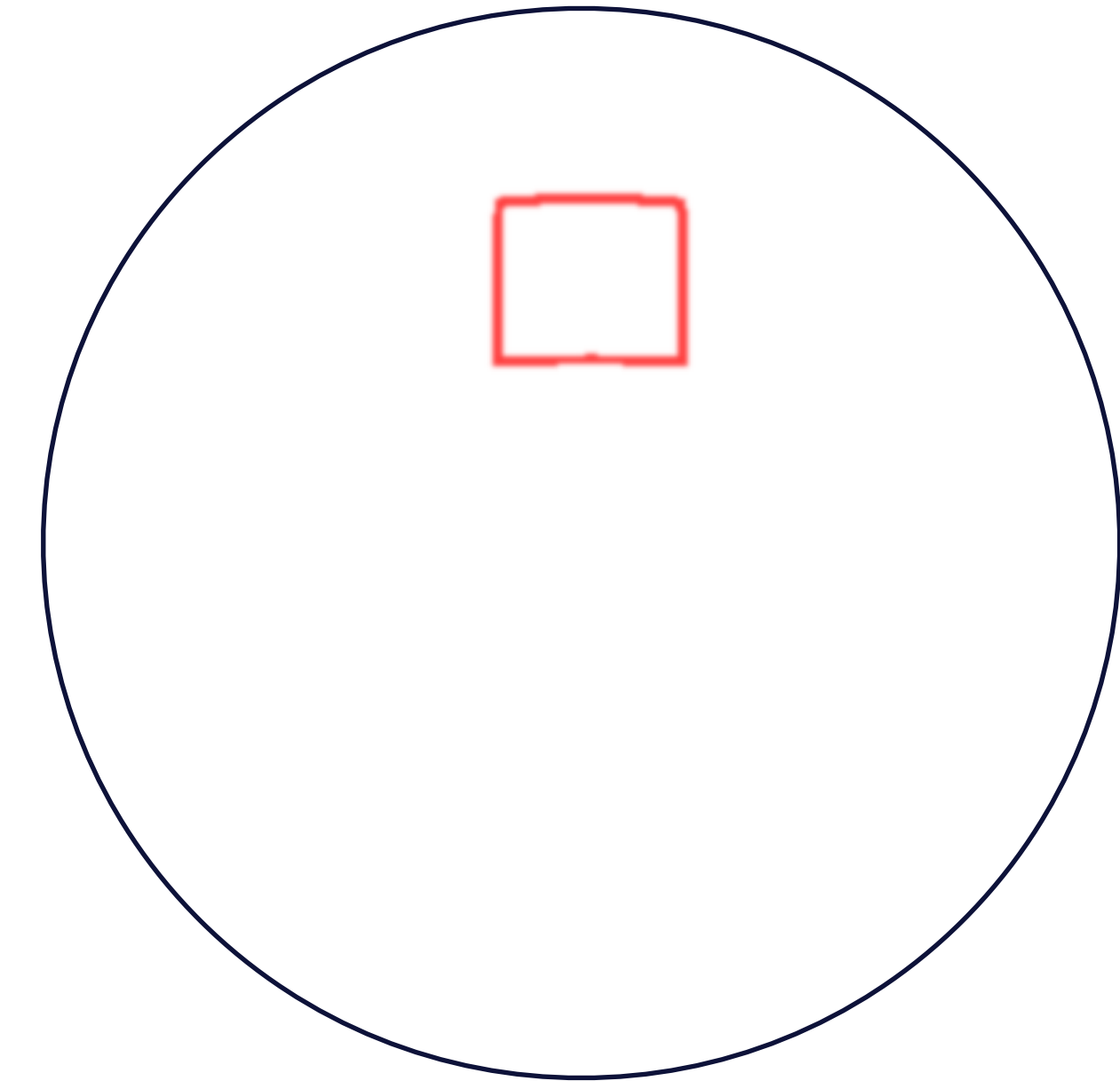
π : emitter size



$f_E(\omega)$



$\partial\mathbb{H}^2$

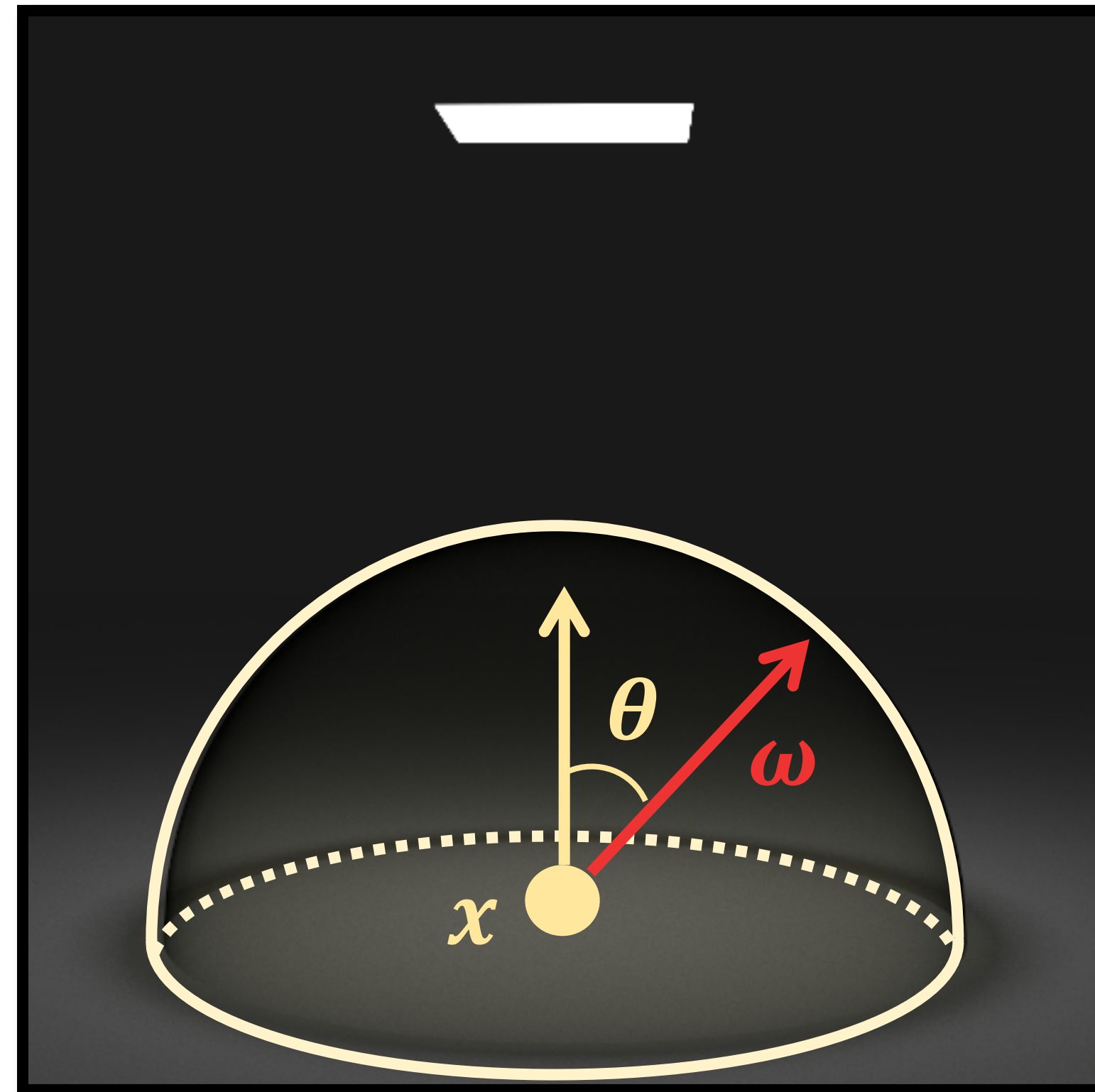


Low High

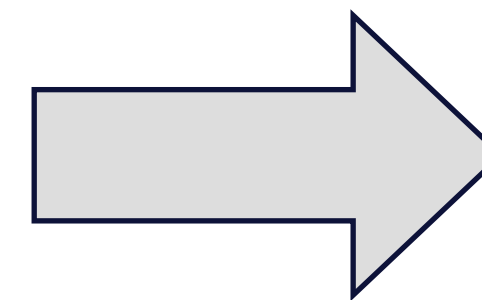
$$E = \int_{\mathbb{H}^2} \overbrace{L_i(\omega) \cos \theta}^{f_E(\omega)} d\sigma(\omega) \xrightarrow{\text{Reynolds}} \frac{dE}{d\pi} = \int_{\mathbb{H}^2} \frac{df_E}{d\pi}(\omega) d\sigma(\omega) + \int_{\partial\mathbb{H}^2} V_{\partial\mathbb{H}^2}(\omega) \Delta f_E(\omega) d\ell(\omega)$$

Interior integral = 0
Boundary integral

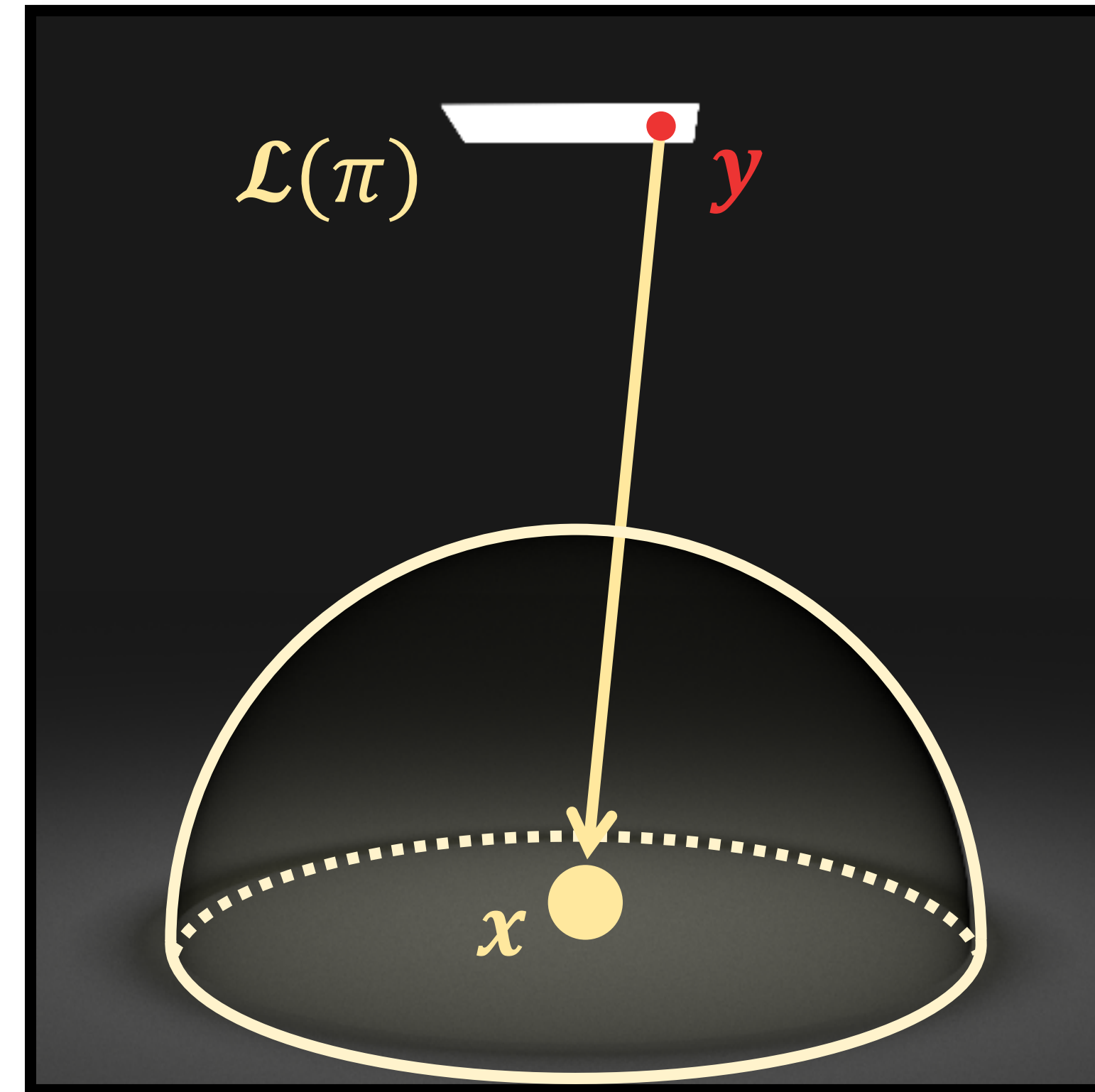
Spherical integral



$$E = \int_{\mathbb{H}^2} L_i(\boldsymbol{\omega}) \cos \theta \, d\sigma(\boldsymbol{\omega})$$

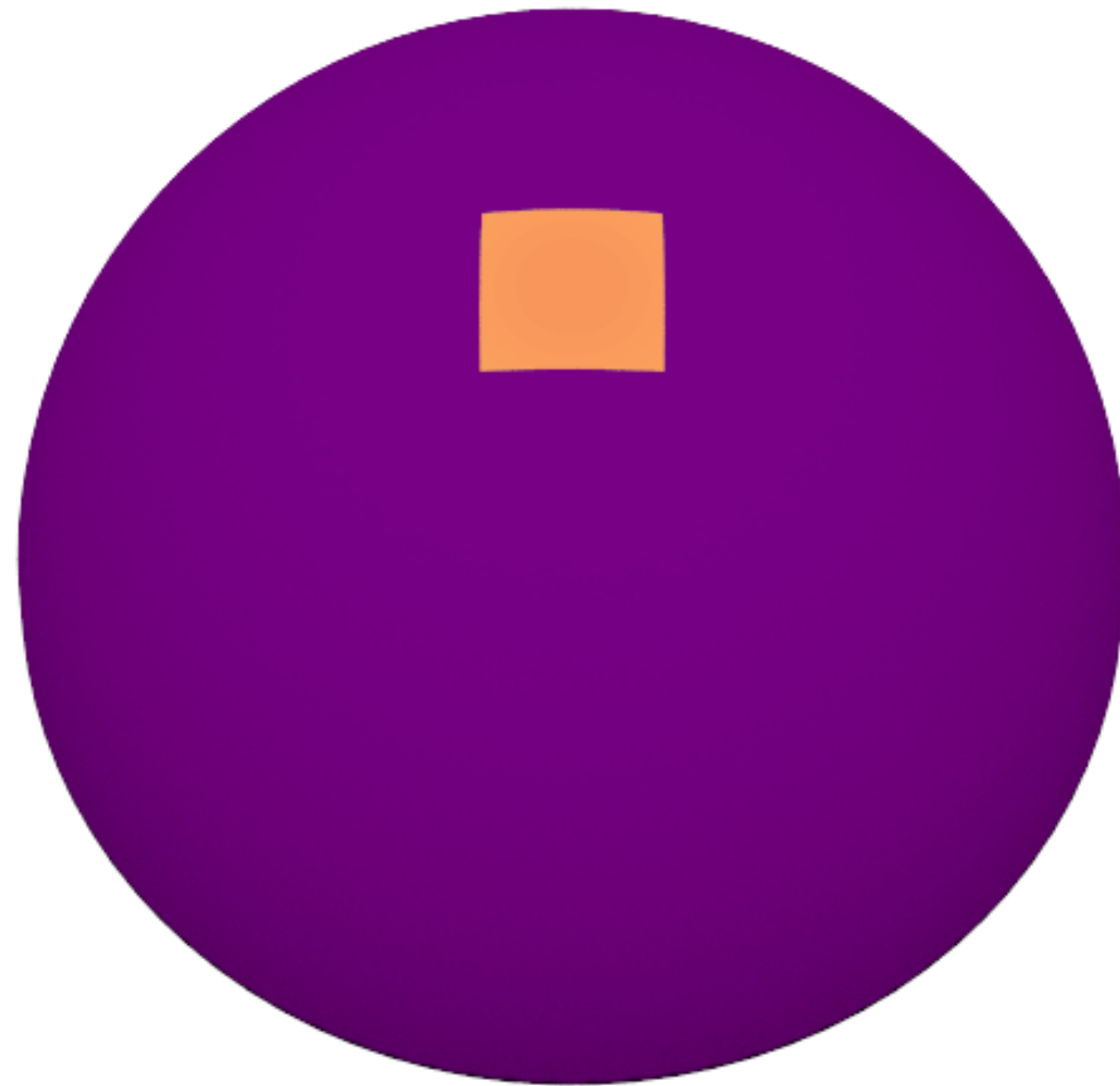


Surface integral



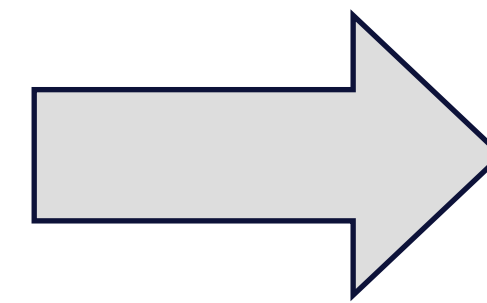
$$E = \int_{\mathcal{L}(\pi)} L_e(\mathbf{y} \rightarrow \mathbf{x}) G(\mathbf{x} \leftrightarrow \mathbf{y}) \, dA(\mathbf{y})$$

Spherical integral



$$E = \int_{\mathbb{H}^2} \overset{\text{Discontinuous}}{L_i(\boldsymbol{\omega}) \cos \theta} d\sigma(\boldsymbol{\omega})$$

Constant domain



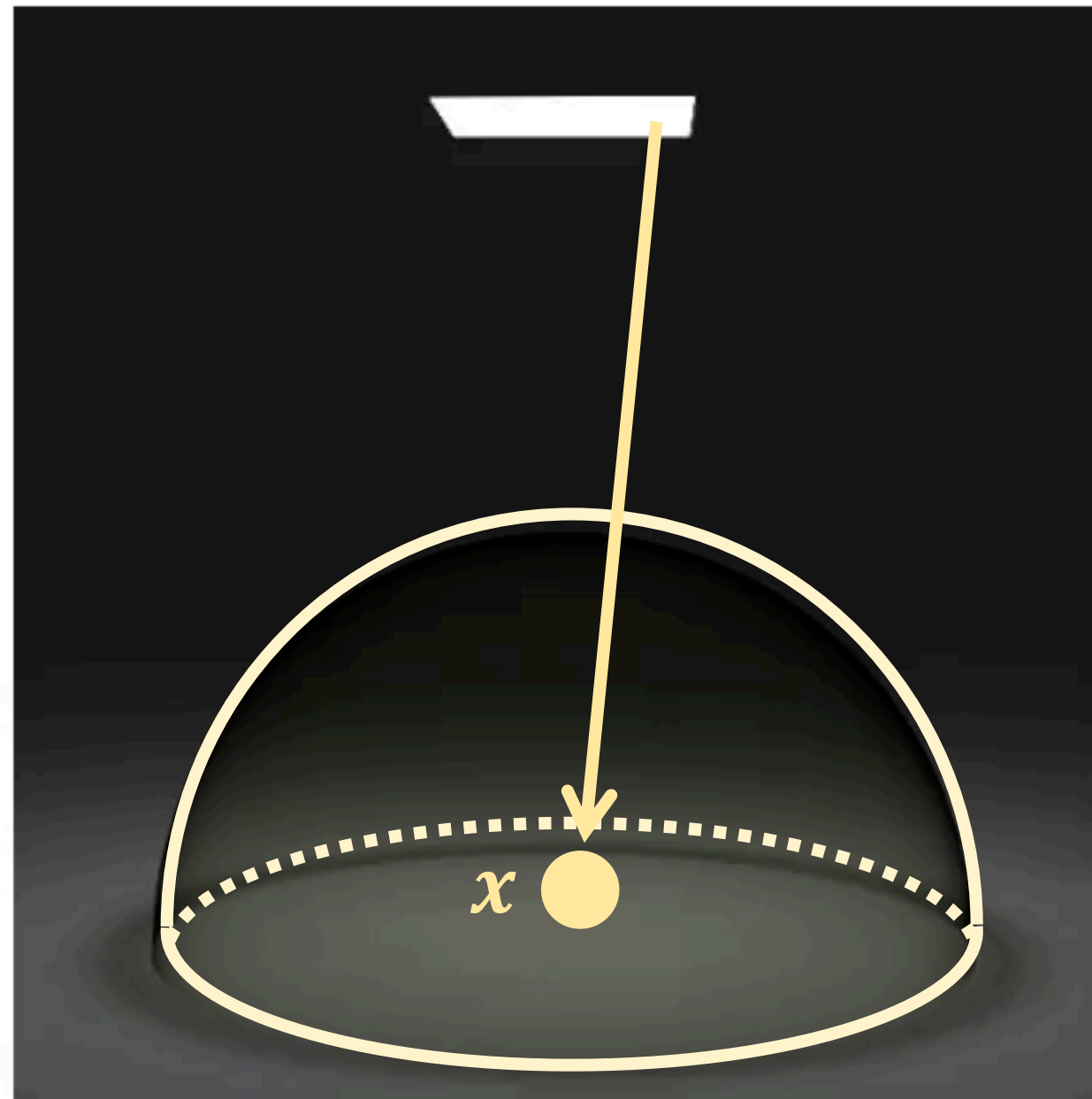
Surface integral



$$E = \int_{\mathcal{L}(\pi)} \overset{\text{Continuous}}{L_e(\mathbf{y} \rightarrow \mathbf{x}) G(\mathbf{x} \leftrightarrow \mathbf{y})} dA(\mathbf{y})$$

Evolving domain

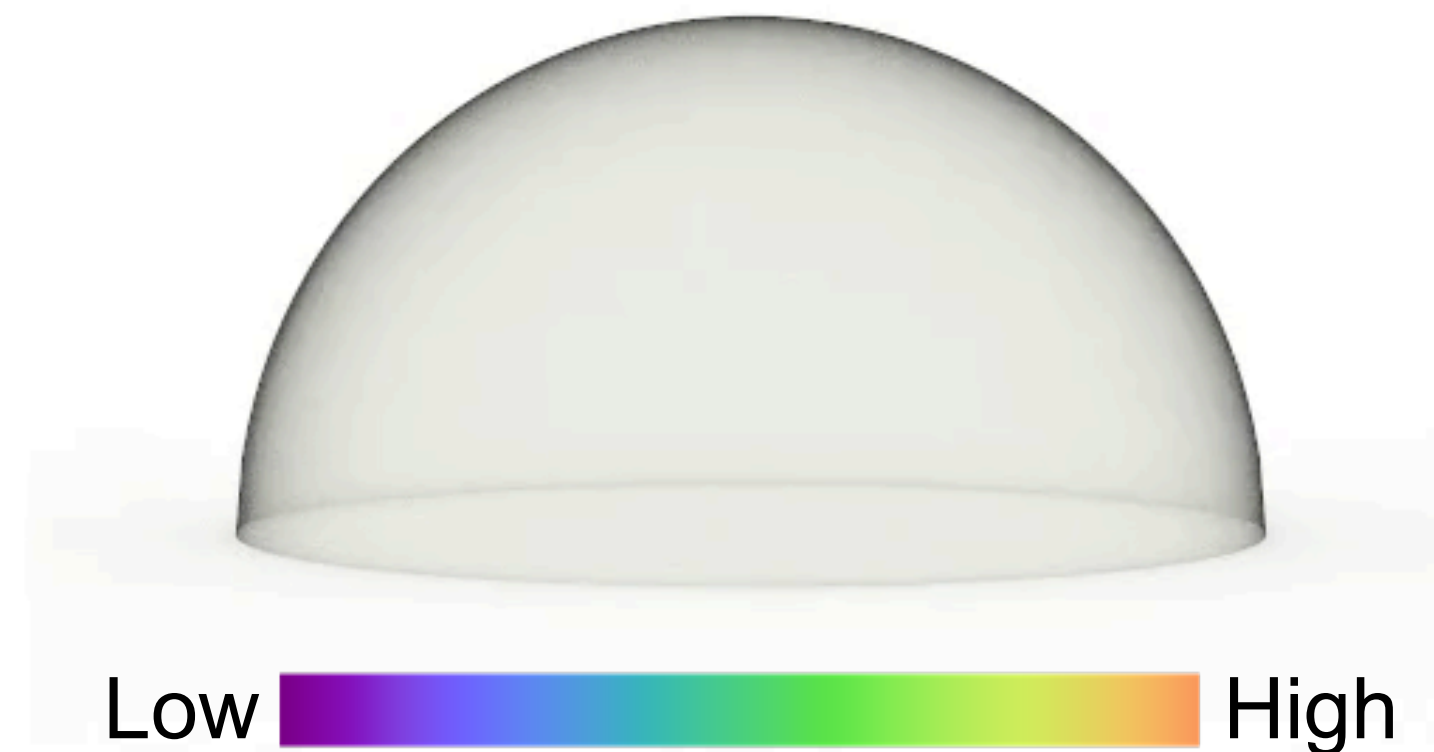
π : emitter size



$f_E(\mathbf{y})$



$\partial\mathcal{L}(\pi)$

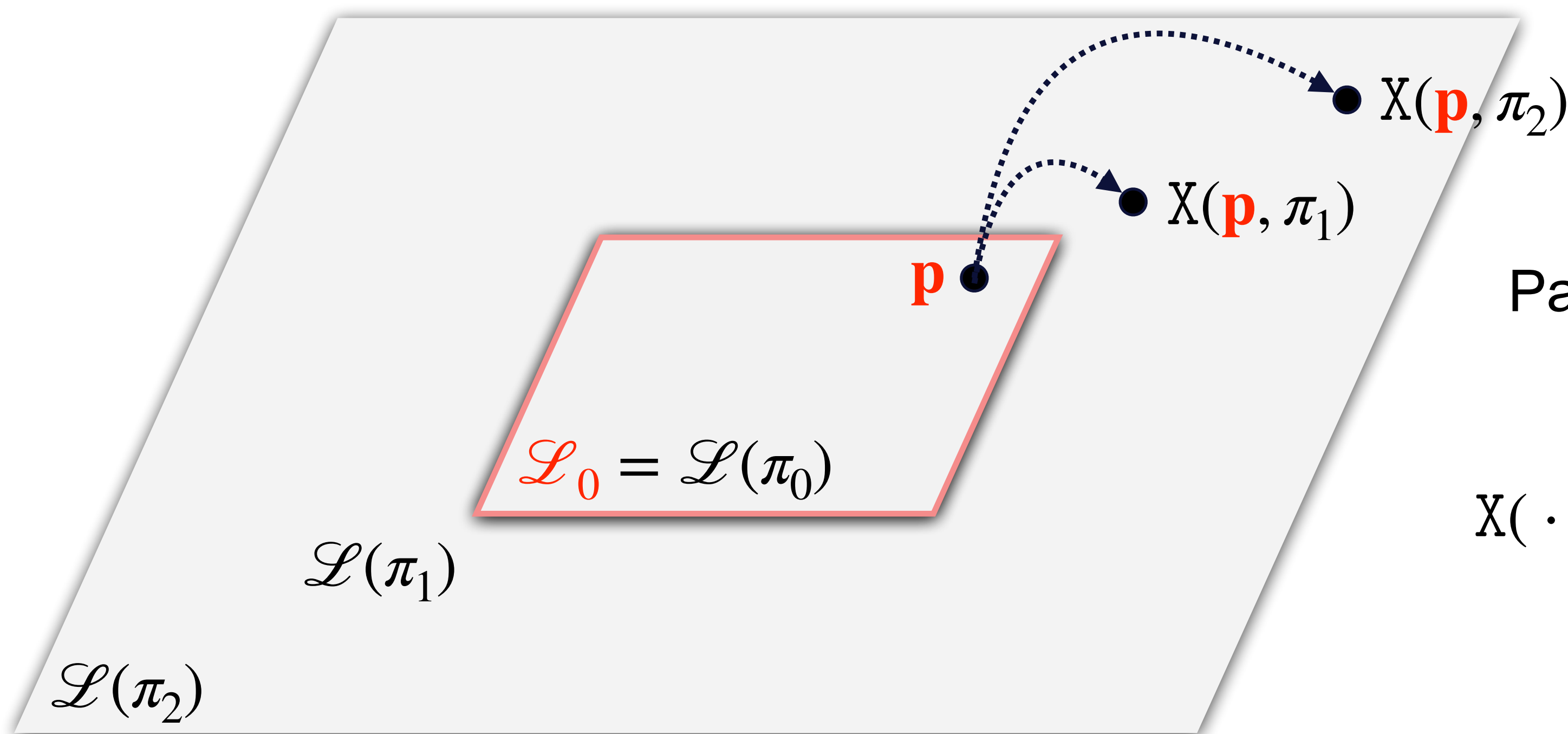


$$E = \int_{\mathcal{L}(\pi)} \overbrace{L_e(\mathbf{y} \rightarrow \mathbf{x}) G(\mathbf{x} \leftrightarrow \mathbf{y})}^{f_E(\mathbf{y})} dA(\mathbf{y}) \xrightarrow{\text{when } \mathcal{L}(\pi) \text{ is flat}} \frac{dE}{d\pi} = \int_{\mathcal{L}(\pi)} \frac{df_E}{d\pi}(\mathbf{y}) dA(\mathbf{y}) + \int_{\partial\mathcal{L}(\pi)} V_{\partial\mathcal{L}(\pi)}(\mathbf{y}) \Delta f_E(\mathbf{y}) d\ell(\mathbf{y})$$

Interior integral
Boundary integral $\neq 0$

Before
reparameterization

$$E = \int_{\mathcal{L}(\pi)} L_e(\mathbf{y} \rightarrow \mathbf{x}) G(\mathbf{x} \leftrightarrow \mathbf{y}) dA(\mathbf{y})$$



Parameterize $\mathcal{L}(\pi)$ using fixed \mathcal{L}_0 :
 $\mathbf{y} = X(\mathbf{p}, \pi)$

$X(\cdot, \pi)$ is **one-to-one** and **continuous**

Reparameterization
with $\mathbf{y} = X(\mathbf{p}, \pi)$

$$E = \int_{\mathcal{L}_0} L_e(\mathbf{y} \rightarrow \mathbf{x}) G(\mathbf{x} \leftrightarrow \mathbf{y}) \left| \frac{dA(\mathbf{y})}{dA(\mathbf{p})} \right| dA(\mathbf{p})$$



↓ $\mathbf{y} = X(\mathbf{p}, \pi)$



$$E = \int_{\mathcal{L}(\pi)} \overbrace{L_e(\mathbf{y} \rightarrow \mathbf{x}) G(\mathbf{x} \leftrightarrow \mathbf{y})}^{f_E(\mathbf{y})} dA(\mathbf{y})$$

Interior integral = 0

Boundary integral $\neq 0$

$$\frac{dE}{d\pi} = \int_{\mathcal{L}(\pi)} \frac{df_E}{d\pi}(\mathbf{y}) dA(\mathbf{y}) + \int_{\partial\mathcal{L}(\pi)} V_{\partial\mathcal{L}(\pi)}(\mathbf{y}) \Delta f_E(\mathbf{y}) d\ell(\mathbf{y})$$

$$E = \int_{\mathcal{L}_0} \overbrace{L_e(\mathbf{y} \rightarrow \mathbf{x}) G(\mathbf{x} \leftrightarrow \mathbf{y})}^{f_E(\mathbf{p})} \left| \frac{dA(\mathbf{y})}{dA(\mathbf{p})} \right| dA(\mathbf{p})$$

← π -dependent

Interior integral $\neq 0$

Boundary integral = 0

$$\frac{dE}{d\pi} = \int_{\mathcal{L}_0} \frac{df_E}{d\pi}(\mathbf{p}) dA(\mathbf{p}) + \int_{\partial\mathcal{L}_0} V_{\partial\mathcal{L}_0}(\mathbf{p}) \Delta f_E(\mathbf{p}) d\ell(\mathbf{p})$$

Reparameterization for irradiance

$$E = \int_{\mathcal{L}(\pi)} L_e(\mathbf{y} \rightarrow \mathbf{x}) G(\mathbf{x} \leftrightarrow \mathbf{y}) dA(\mathbf{y}) \xrightarrow{\mathbf{y} = X(\mathbf{p}, \pi)} E = \int_{\mathcal{L}_0} L_e(\mathbf{y} \rightarrow \mathbf{x}) G(\mathbf{x} \leftrightarrow \mathbf{y}) \left| \frac{dA(\mathbf{y})}{dA(\mathbf{p})} \right| dA(\mathbf{p})$$

\uparrow
 fixed surface

Reparameterization for path integral

Spatial form $I = \int_{\Omega(\pi)} f(\bar{\mathbf{x}}) d\mu(\bar{\mathbf{x}}) \xrightarrow{\bar{\mathbf{x}} = X(\bar{\mathbf{p}}, \pi)} I = \int_{\Omega_0} f(\bar{\mathbf{x}}) \left| \frac{d\mu(\bar{\mathbf{x}})}{d\mu(\bar{\mathbf{p}})} \right| d\mu(\bar{\mathbf{p}})$ Material form

\uparrow
 fixed path space

\parallel
 $\prod_i \left| \frac{dA(\mathbf{x}_i)}{dA(\mathbf{p}_i)} \right|$

Path integrals

Spatial form $I = \int_{\Omega(\pi)} f(\bar{\mathbf{x}}) d\mu(\bar{\mathbf{x}})$ $\xrightarrow{\bar{\mathbf{x}} = X(\bar{\mathbf{p}}, \pi)}$ $I = \int_{\Omega_0} f(\bar{\mathbf{x}}) \left| \frac{d\mu(\bar{\mathbf{x}})}{d\mu(\bar{\mathbf{p}})} \right| d\mu(\bar{\mathbf{p}})$ **Material form**

Differential path integrals

$$\frac{dI}{d\pi} = \int_{\Omega(\pi)} \frac{df}{d\pi}(\bar{\mathbf{x}}) d\mu(\bar{\mathbf{x}}) + \int_{\partial\Omega(\pi)} g(\bar{\mathbf{x}}) d\mu'(\bar{\mathbf{x}}) \quad \frac{dI}{d\pi} = \int_{\Omega_0} \frac{d}{d\pi} \left(f(\bar{\mathbf{x}}) \left| \frac{d\mu(\bar{\mathbf{x}})}{d\mu(\bar{\mathbf{p}})} \right| \right) d\mu(\bar{\mathbf{p}}) + \int_{\partial\Omega_0} g(\bar{\mathbf{p}}) d\mu'(\bar{\mathbf{p}})$$

Pro: no global parameterization required

Con: more types of discontinuities

Pro: fewer types of discontinuities

Con: requires global parameterization X

Spatial form

$$\frac{dI}{d\pi} = \int_{\Omega(\pi)} \frac{df}{d\pi}(\bar{\mathbf{x}}) d\mu(\bar{\mathbf{x}}) + \int_{\partial\Omega(\pi)} g(\bar{\mathbf{x}}) d\mu'(\bar{\mathbf{x}})$$

Differential path integrals

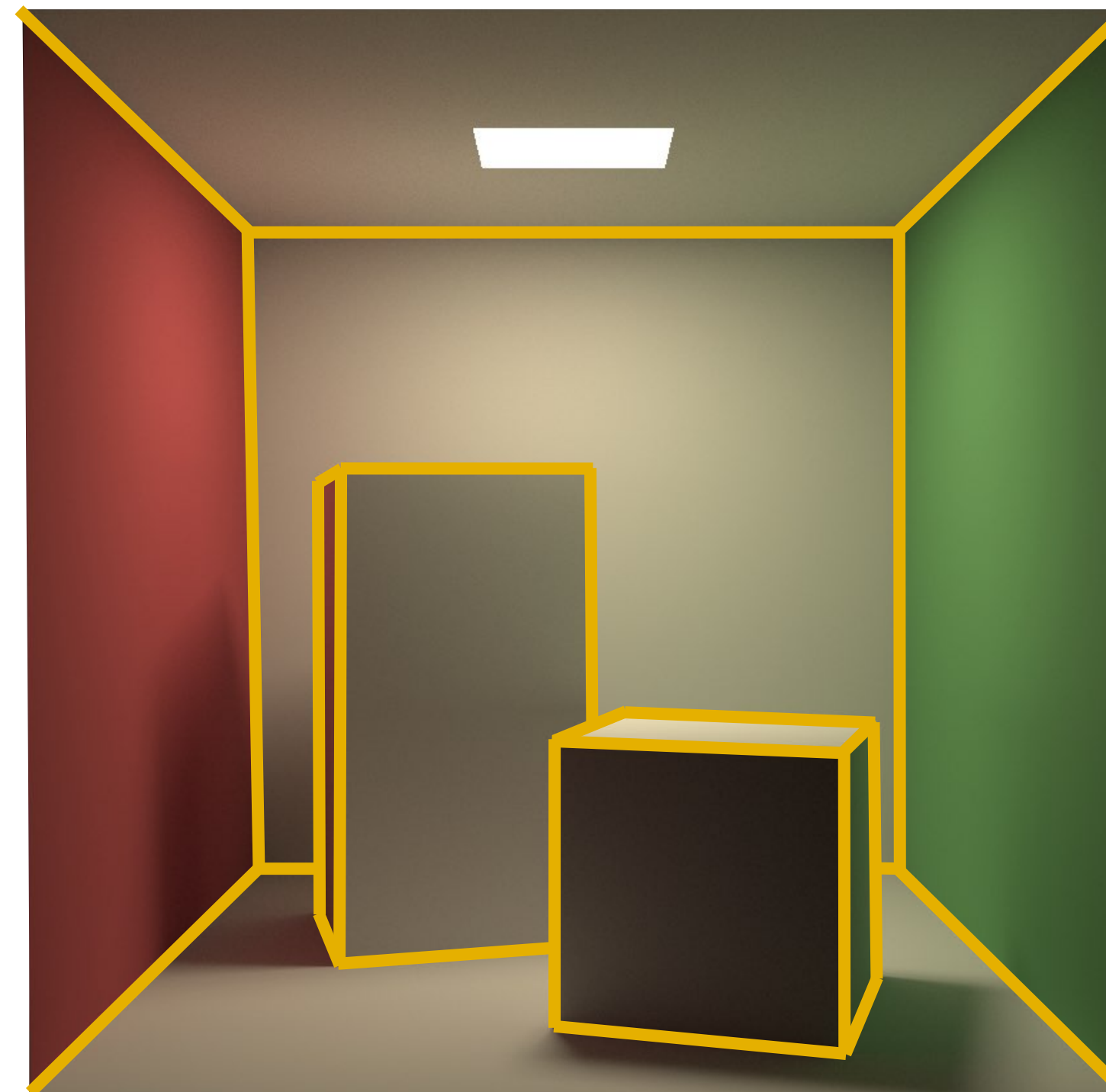
$$\frac{dI}{d\pi} = \int_{\Omega_0} \frac{d}{d\pi} \left(f(\bar{\mathbf{x}}) \left| \frac{d\mu(\bar{\mathbf{x}})}{d\mu(\bar{\mathbf{p}})} \right| \right) d\mu(\bar{\mathbf{p}}) + \int_{\partial\Omega_0} g(\bar{\mathbf{p}}) d\mu'(\bar{\mathbf{p}})$$

Material form

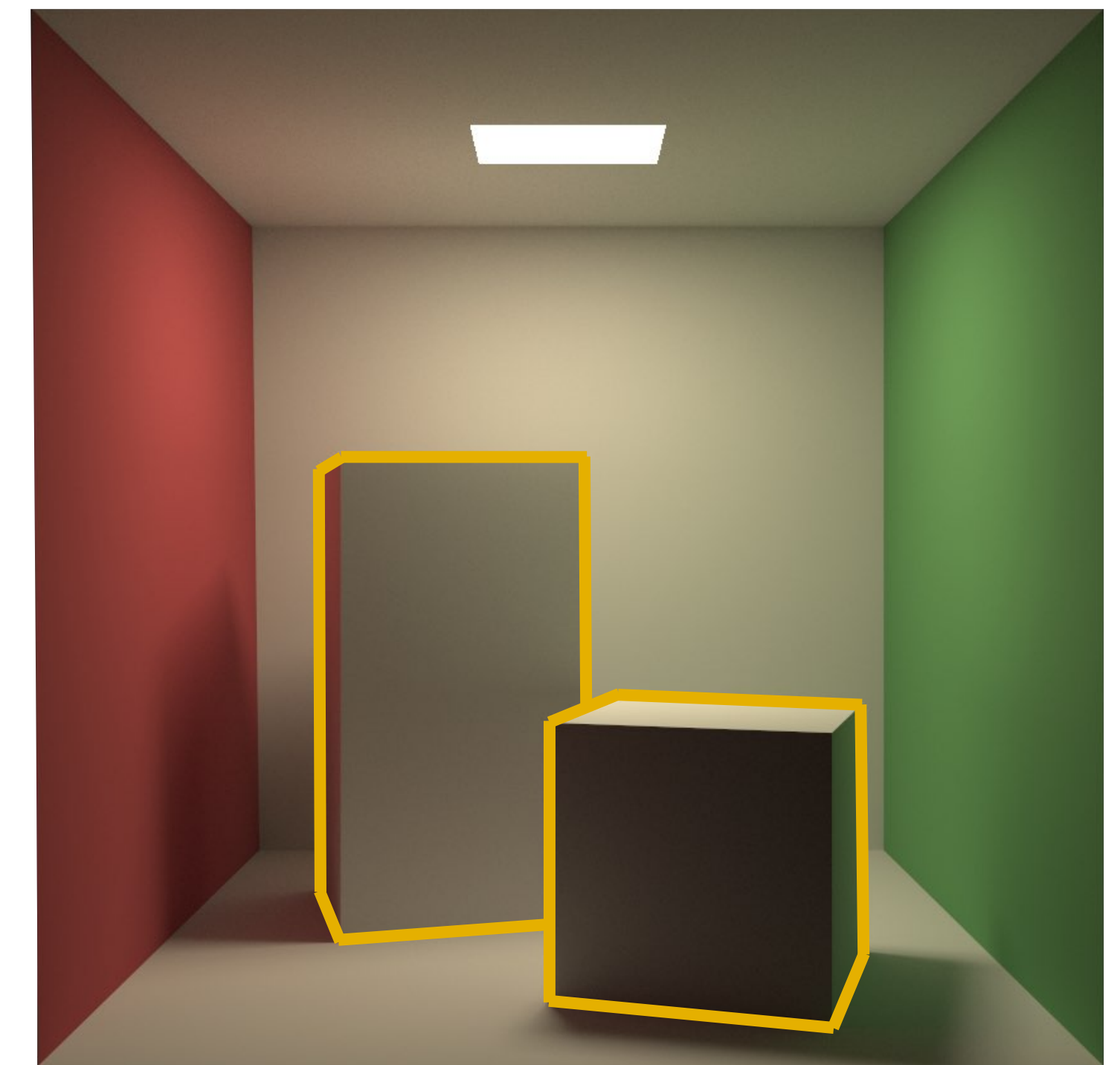
Boundary edges



Sharp edges



Silhouette edges



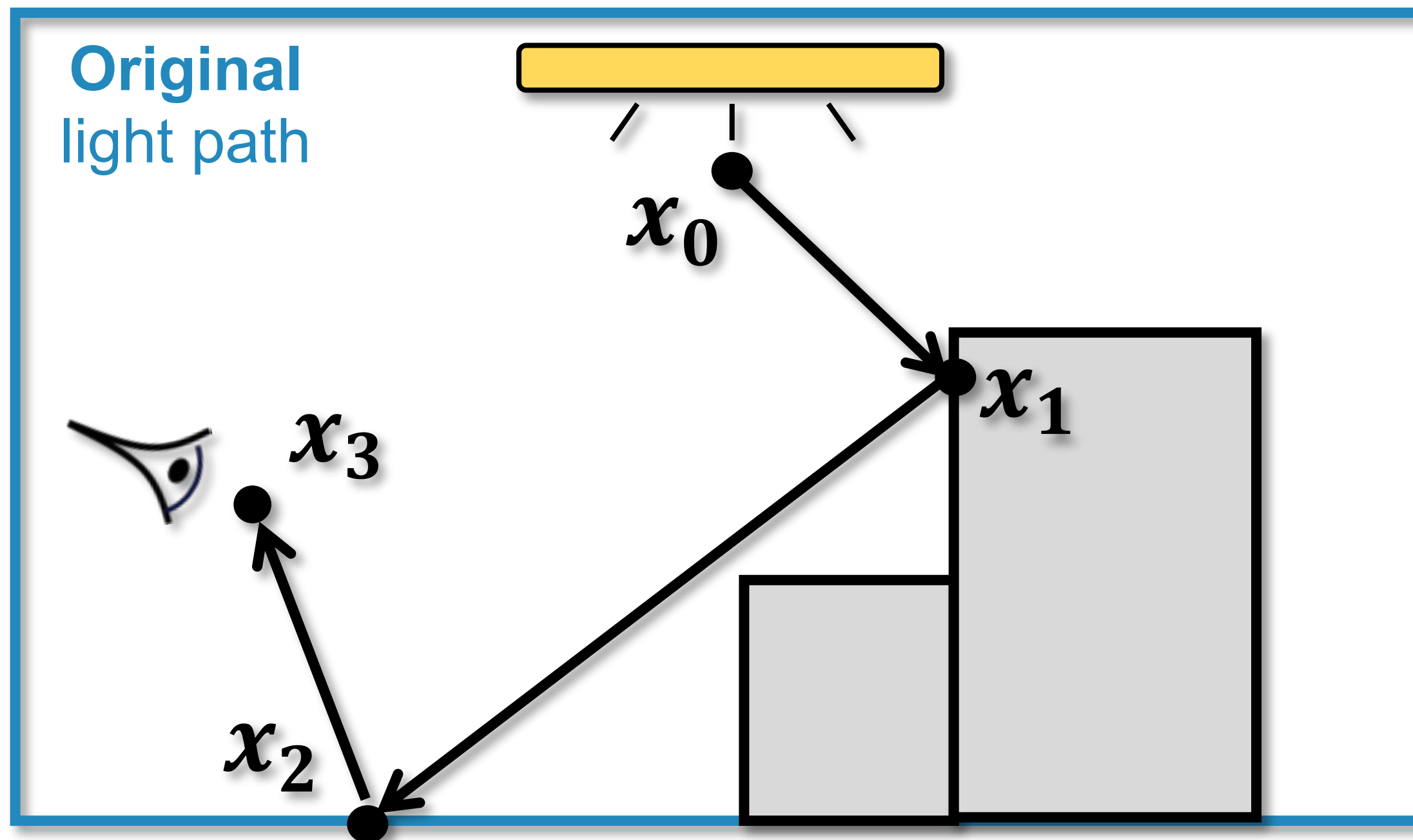
(material-form)
Differential path integral

$$\frac{dI}{d\pi} = \int_{\Omega_0} \frac{d}{d\pi} \left(f(\bar{\mathbf{x}}) \left| \frac{d\mu(\bar{\mathbf{x}})}{d\mu(\bar{\mathbf{p}})} \right| \right) d\mu(\bar{\mathbf{p}}) + \int_{\partial\Omega_0} g(\bar{\mathbf{p}}) d\mu'(\bar{\mathbf{p}})$$

Interior integral

Boundary integral

Estimated
separately



Can be estimated using identical path sampling strategies as forward rendering

- Unidirectional path tracing
- Bidirectional path tracing
- ...

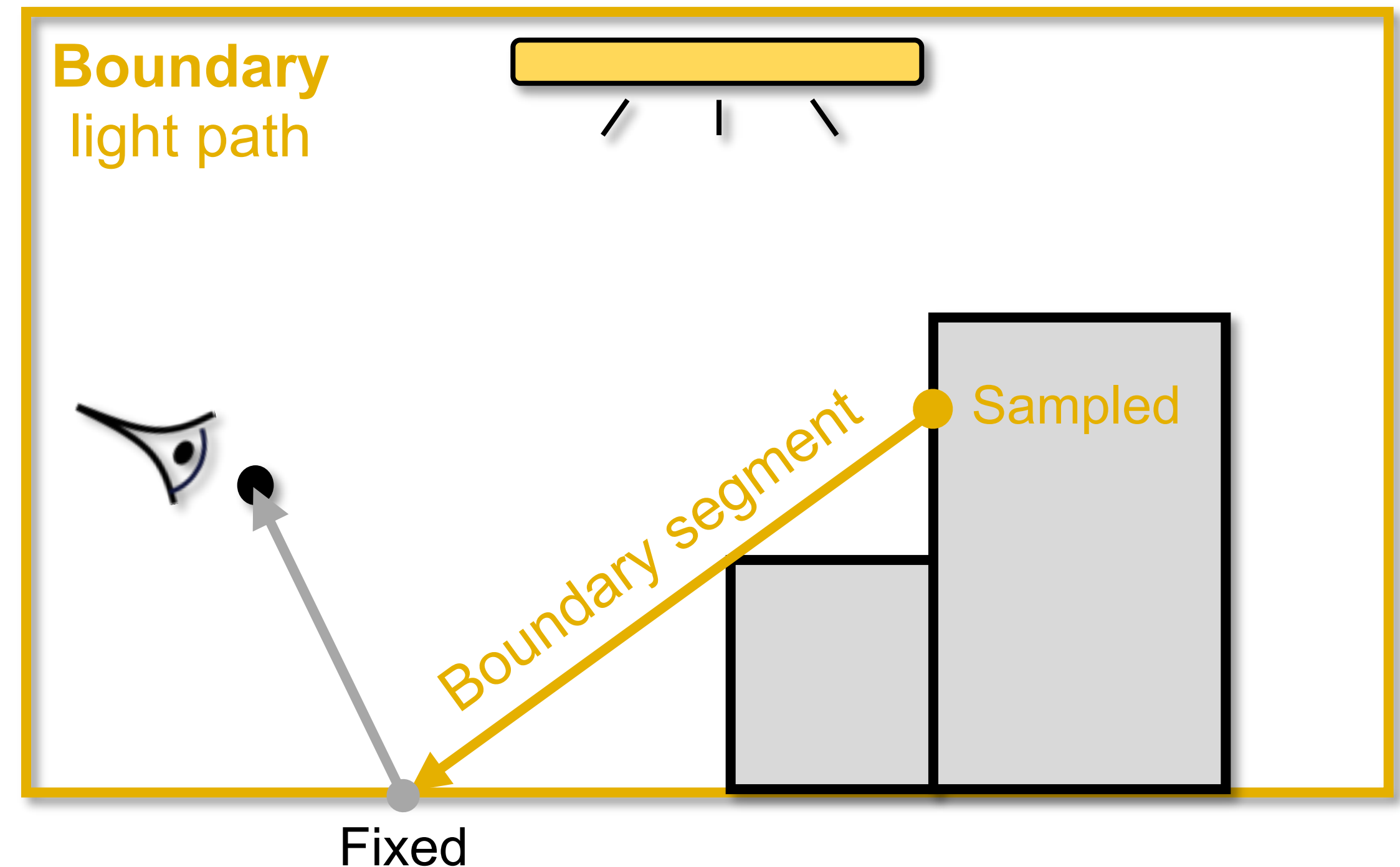
(material-form)
Differential path integral

$$\frac{dI}{d\pi} = \int_{\Omega_0} \frac{d}{d\pi} \left(f(\bar{\mathbf{x}}) \left| \frac{d\mu(\bar{\mathbf{x}})}{d\mu(\bar{\mathbf{p}})} \right| \right) d\mu(\bar{\mathbf{p}}) + \int_{\partial\Omega_0} g(\bar{\mathbf{p}}) d\mu'(\bar{\mathbf{p}})$$

Boundary integral

Unidirectional sampling:

- Construct the **boundary path** from the eye
- Draw the **boundary segment** by fixing one endpoint and sampling the other
- Problems
 - Requires expensive silhouette detection



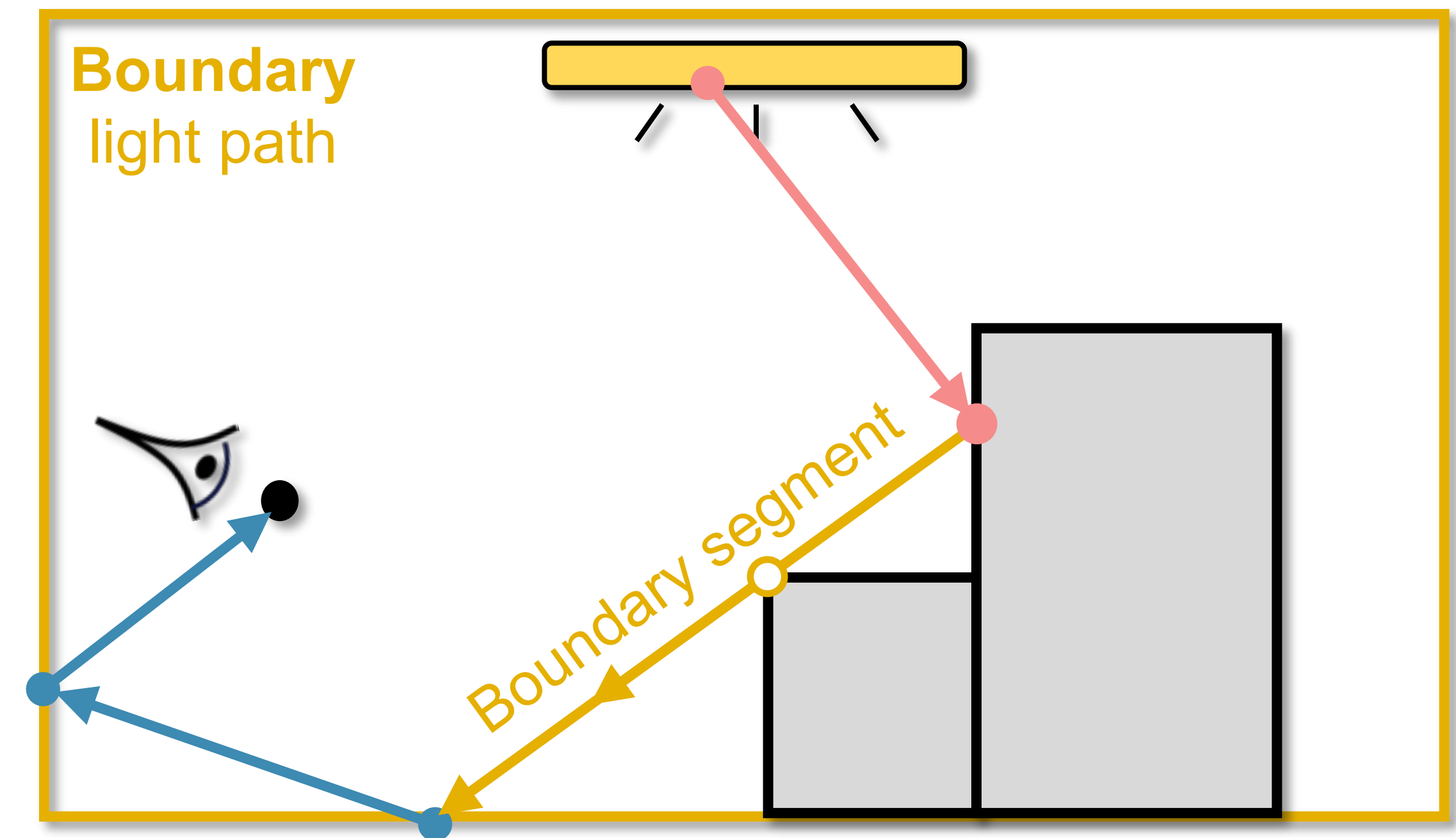
(material-form)
Differential path integral

$$\frac{dI}{d\pi} = \int_{\Omega_0} \frac{d}{d\pi} \left(f(\bar{\mathbf{x}}) \left| \frac{d\mu(\bar{\mathbf{x}})}{d\mu(\bar{\mathbf{p}})} \right| \right) d\mu(\bar{\mathbf{p}}) + \int_{\partial\Omega_0} g(\bar{\mathbf{p}}) d\mu'(\bar{\mathbf{p}})$$

Boundary integral

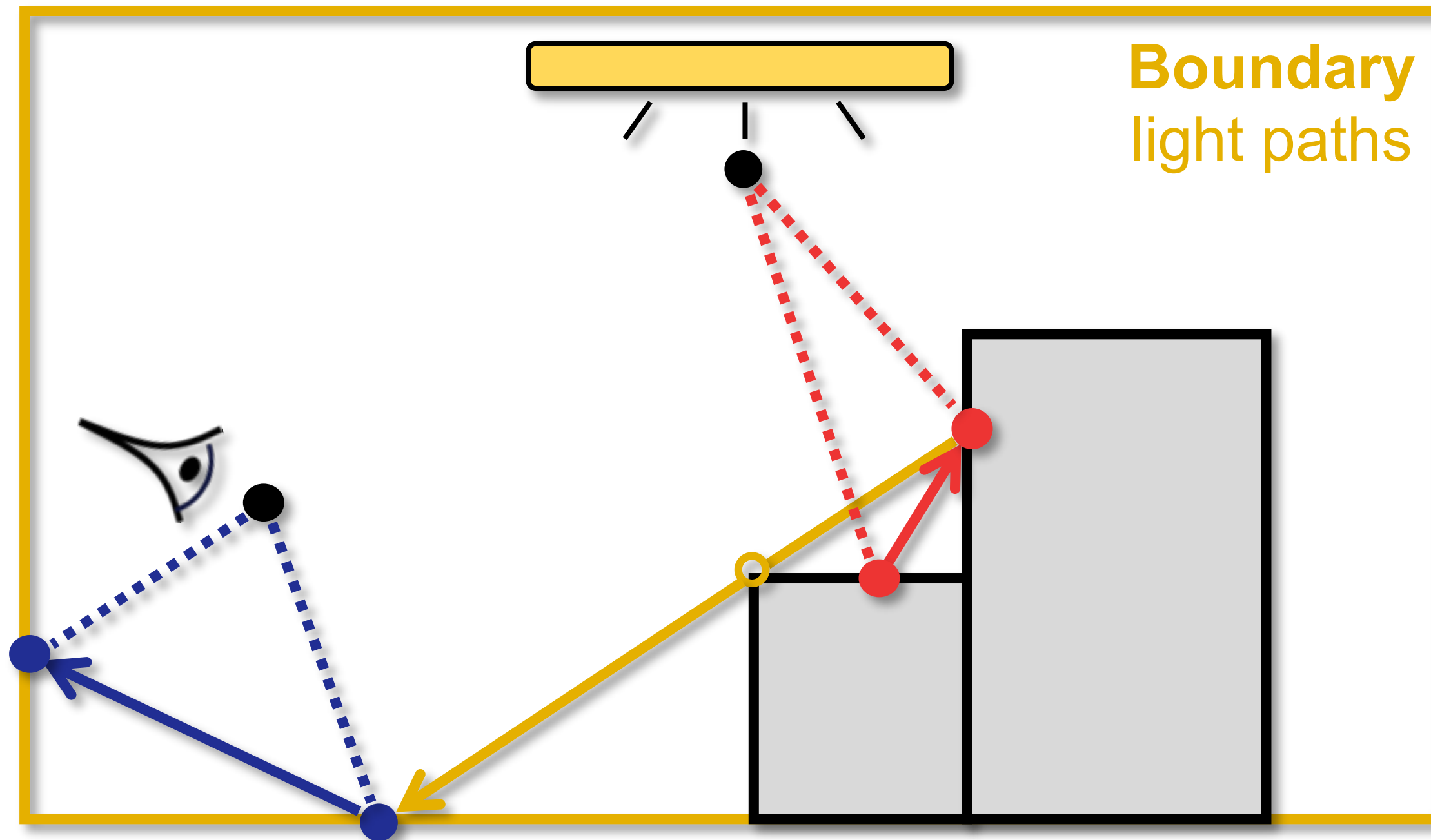
Multi-directional sampling:

- Construct the **boundary segment** from the middle
- Construct **source** and **sensor** subpaths
- To further improve efficiency
 - Next-event estimation
 - Importance sampling boundary segments



Unidirectional estimator

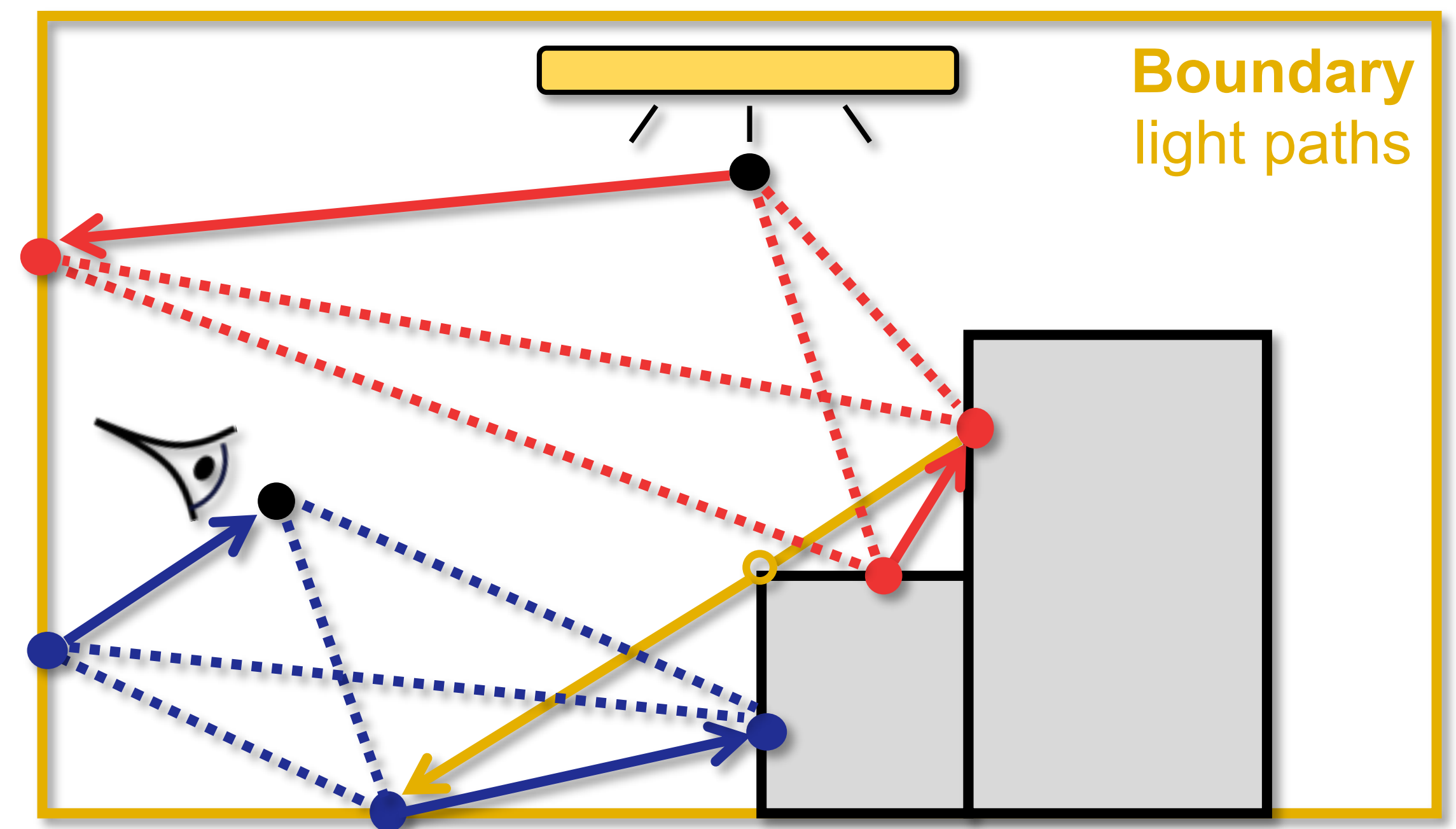
- **Interior:** unidirectional path tracing
- **Boundary:** unidirectional sampling of subpaths



Unidirectional path tracing + NEE

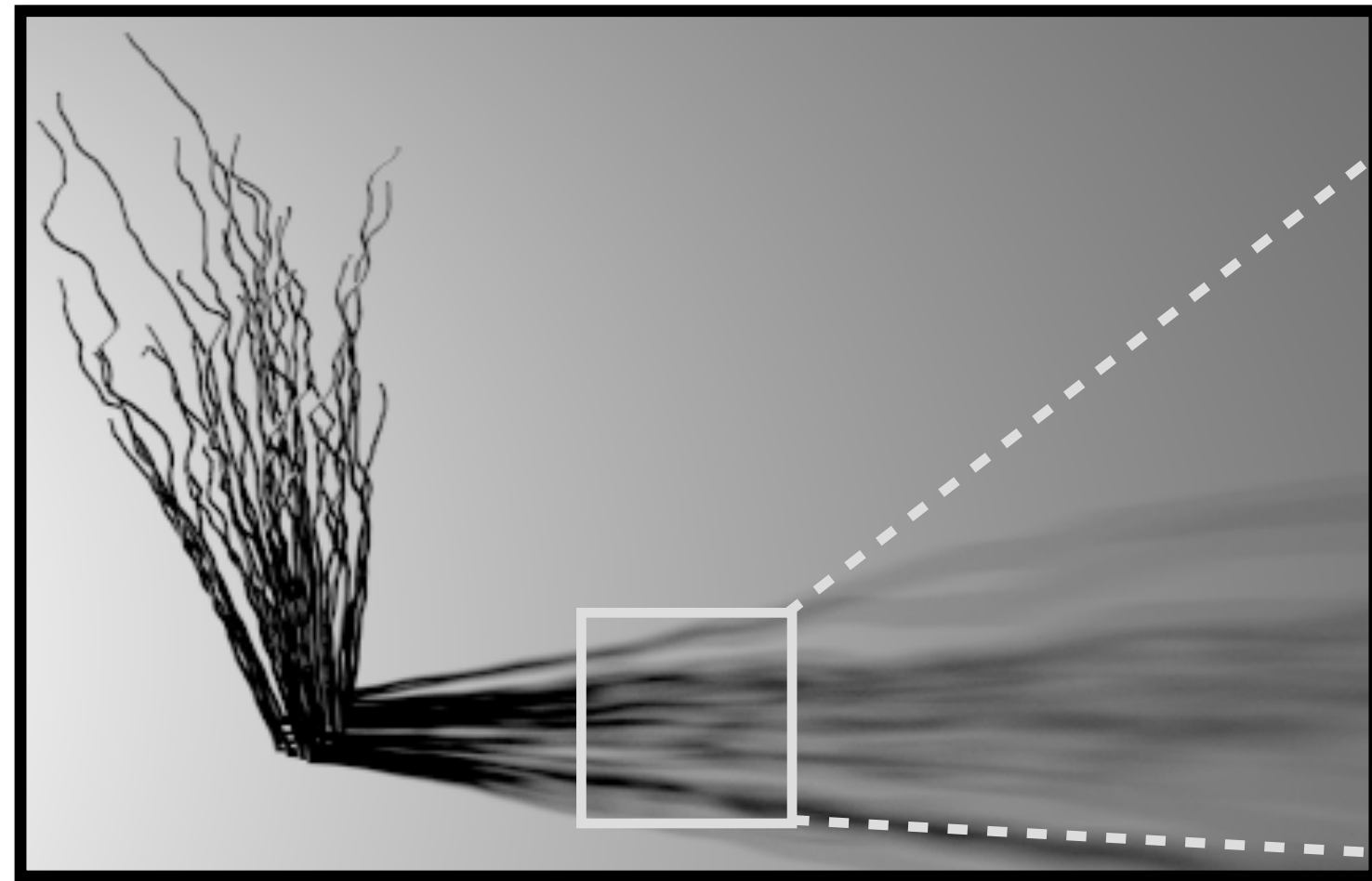
Bidirectional estimator

- **Interior:** bidirectional path tracing
- **Boundary:** bidirectional sampling of subpaths

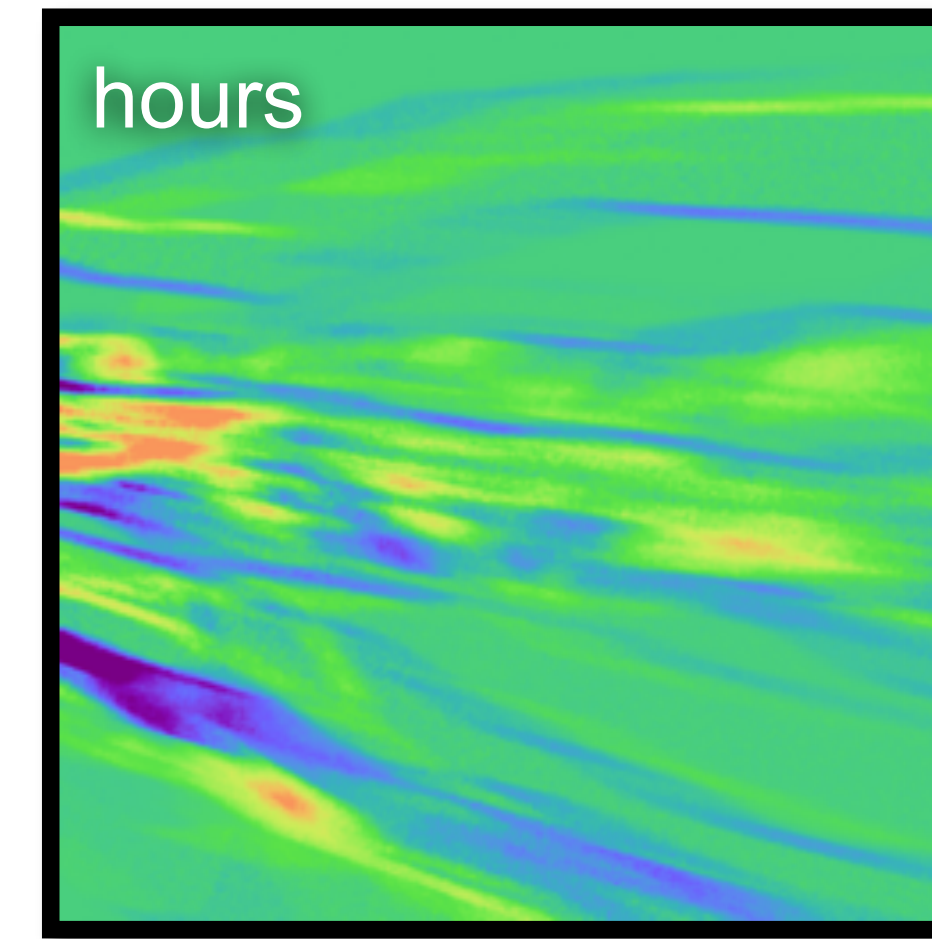
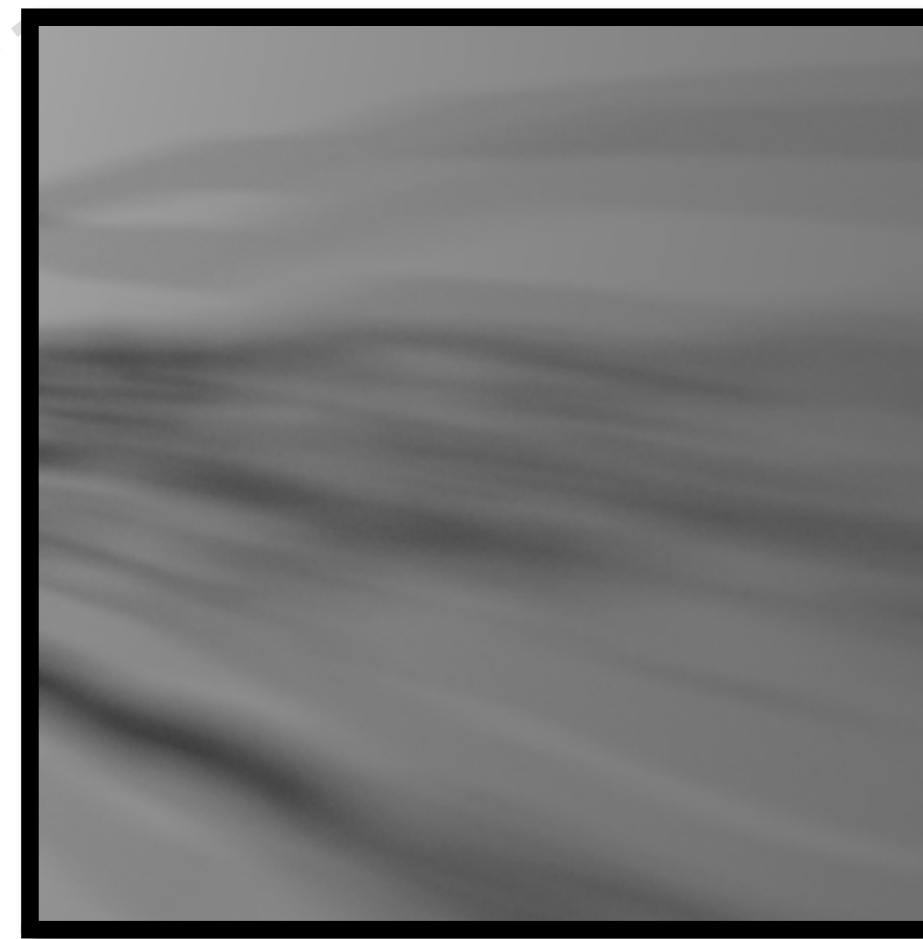


Bidirectional path tracing

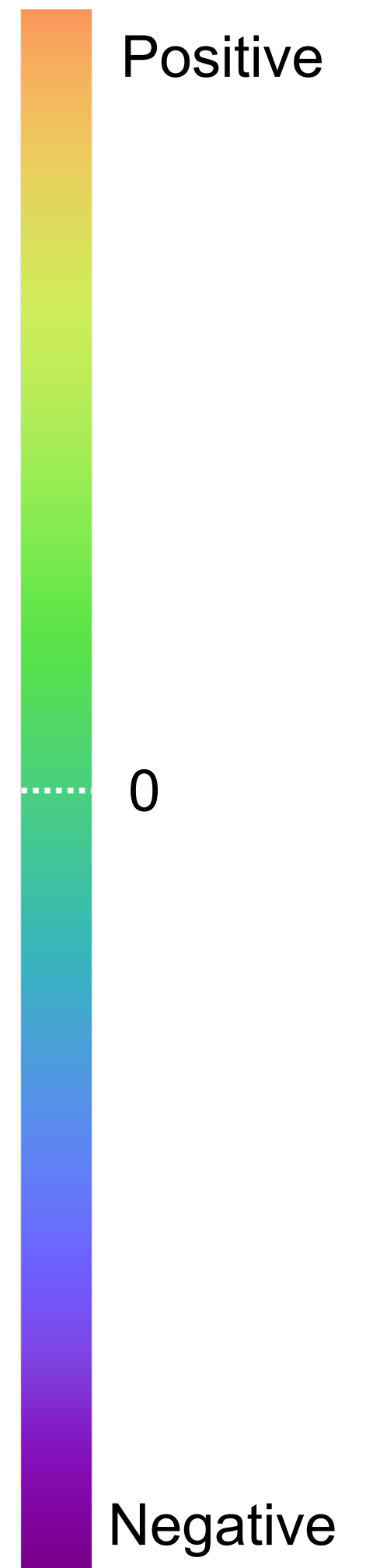
RESULT: COMPLEX GEOMETRY & MOTION



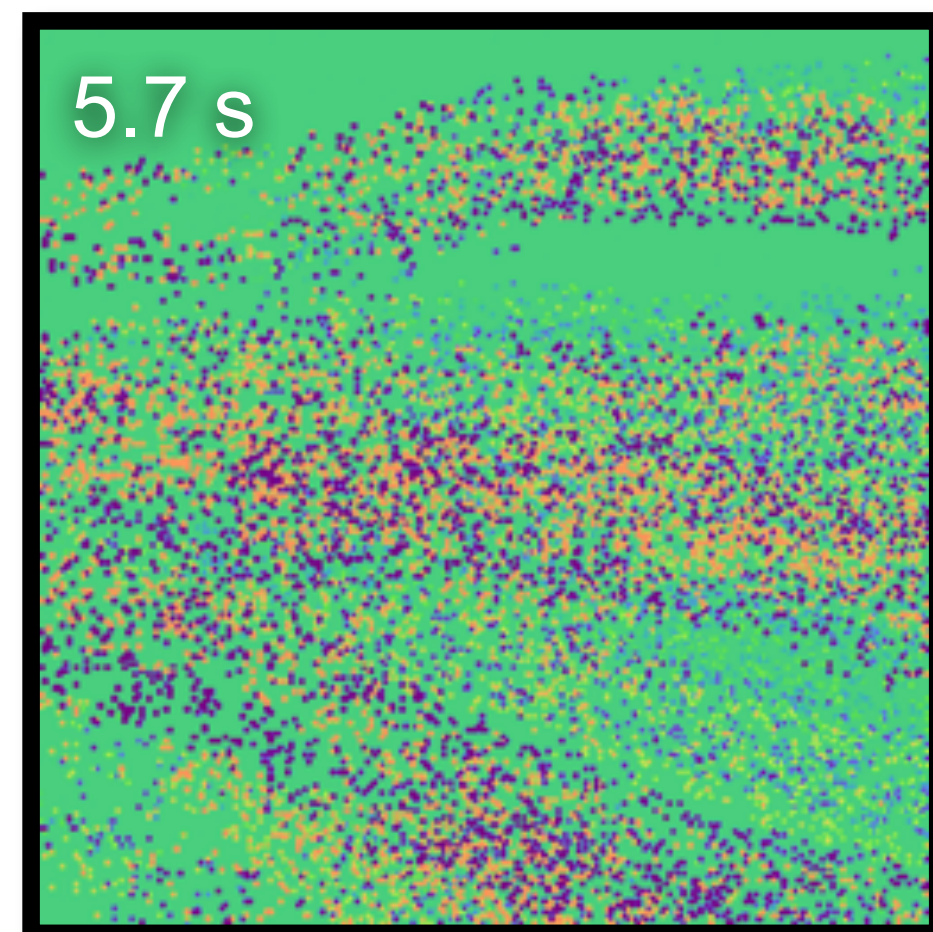
Parameter: rotation angle of the object



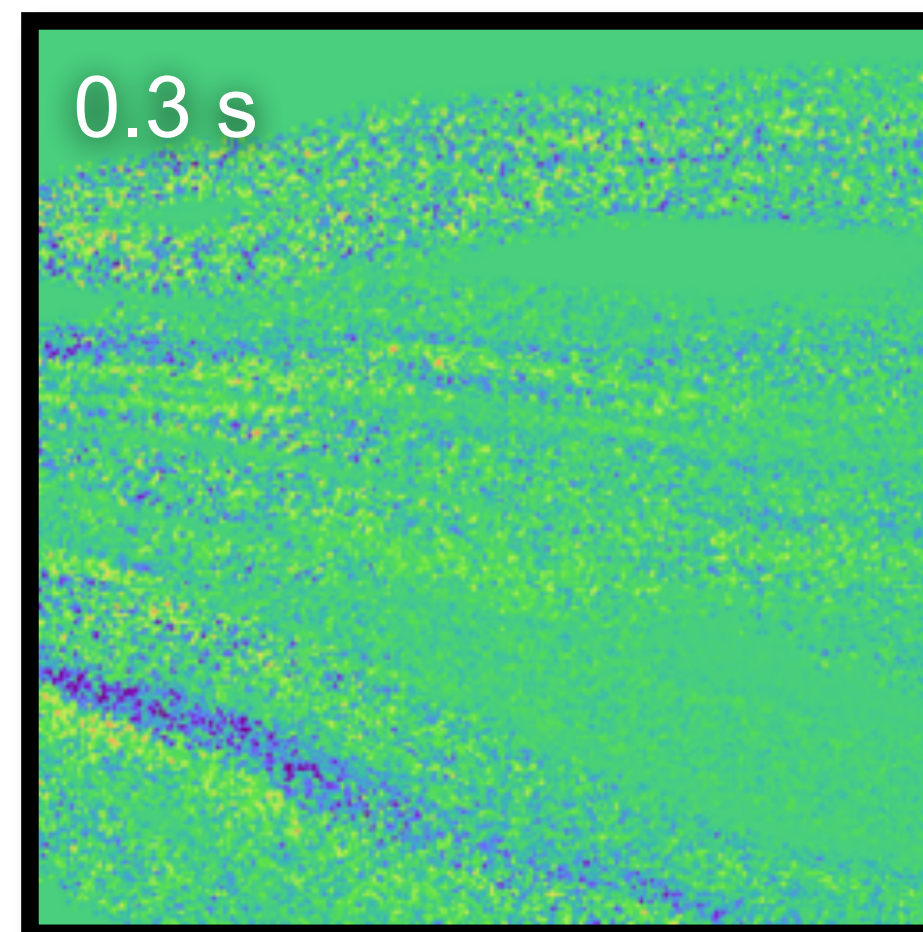
Reference



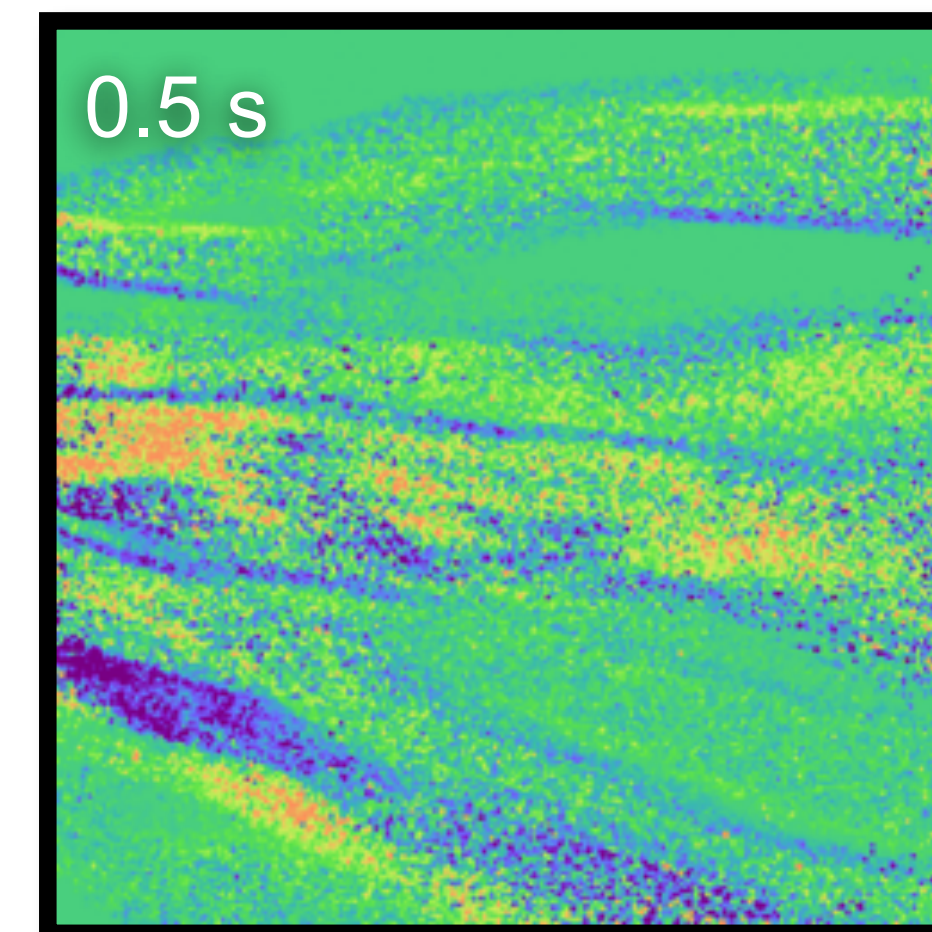
Equal-sample comparison



Path tracing w/ edge sampling
[Li et al. 2018, Zhang et al. 2019]



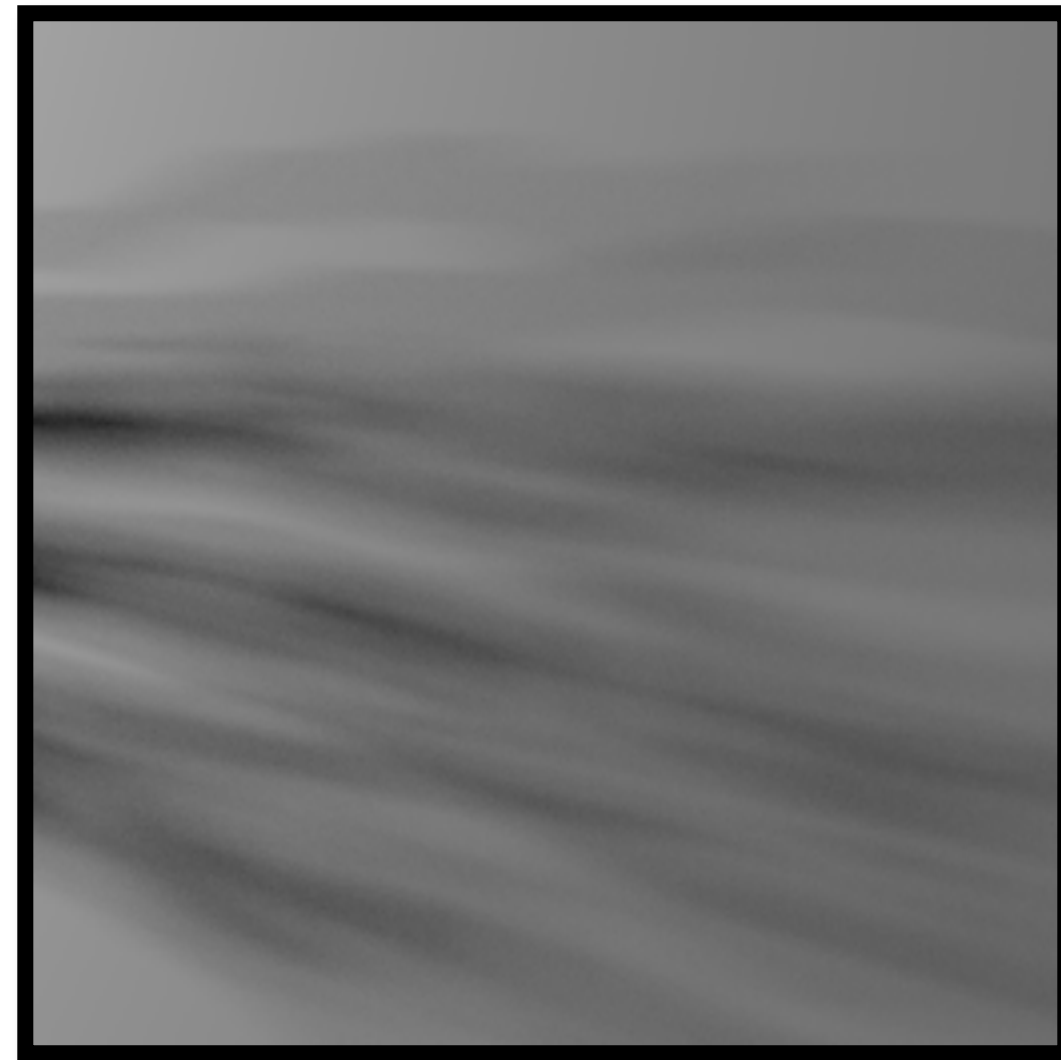
Reparameterization
[Loubet et al. 2019]



Path-space, unidir.
[Zhang et al. 2020]

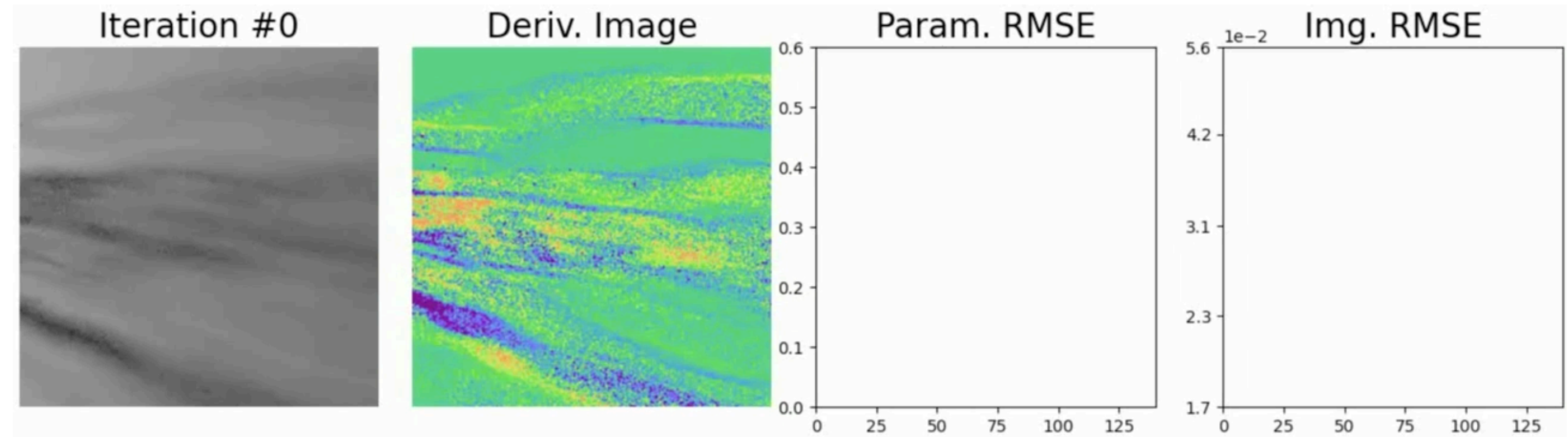
RESULT: COMPLEX LIGHT-TRANSPORT EFFECT

Target image

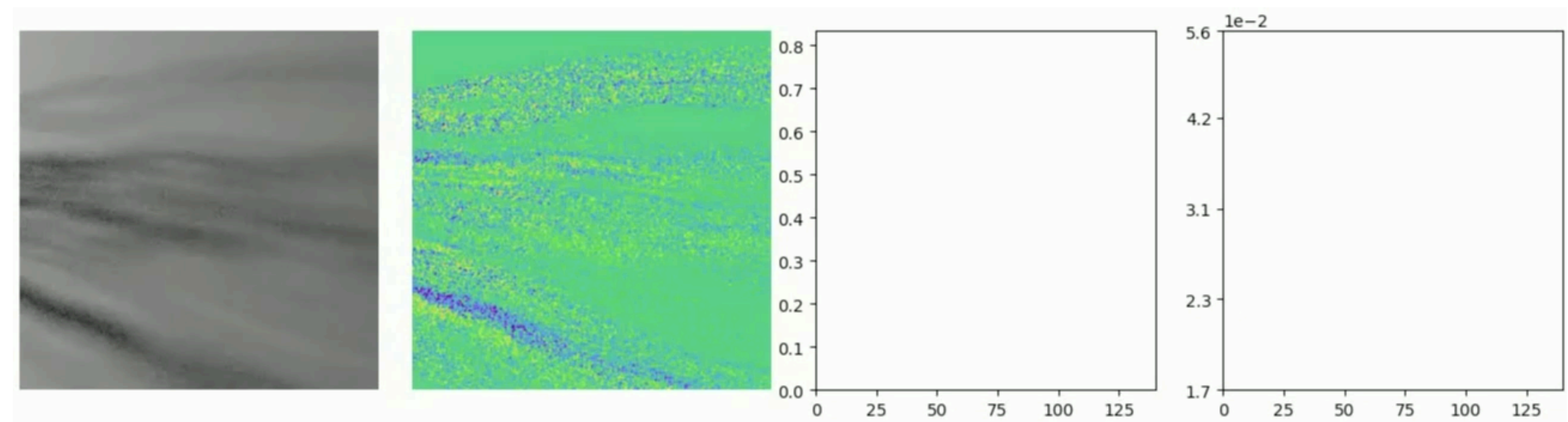


- Optimizing
 - Object rotation angle
- **Equal-sample** per iteration
- **Identical** optimization settings
 - Learning rate (Adam)
 - Initializations

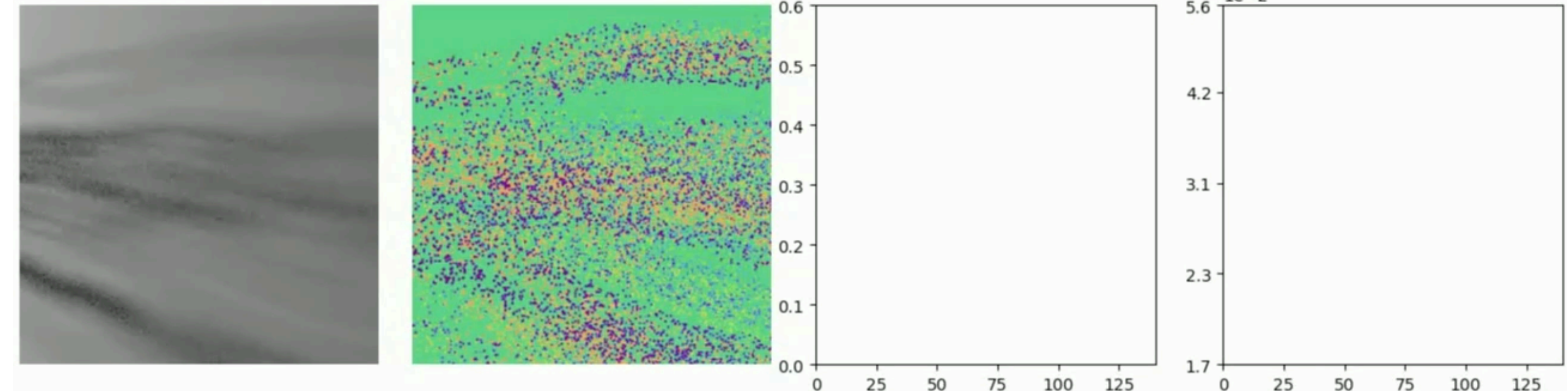
Path-space



Reparameterization
[Loubet 2019]

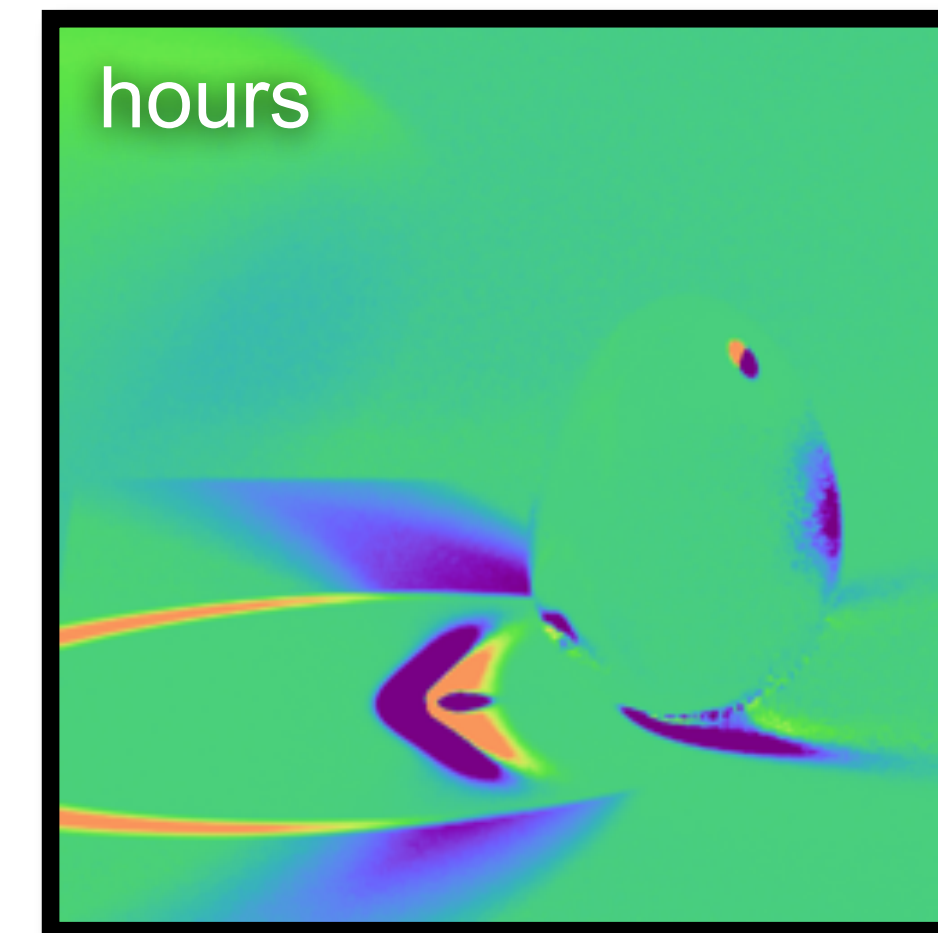
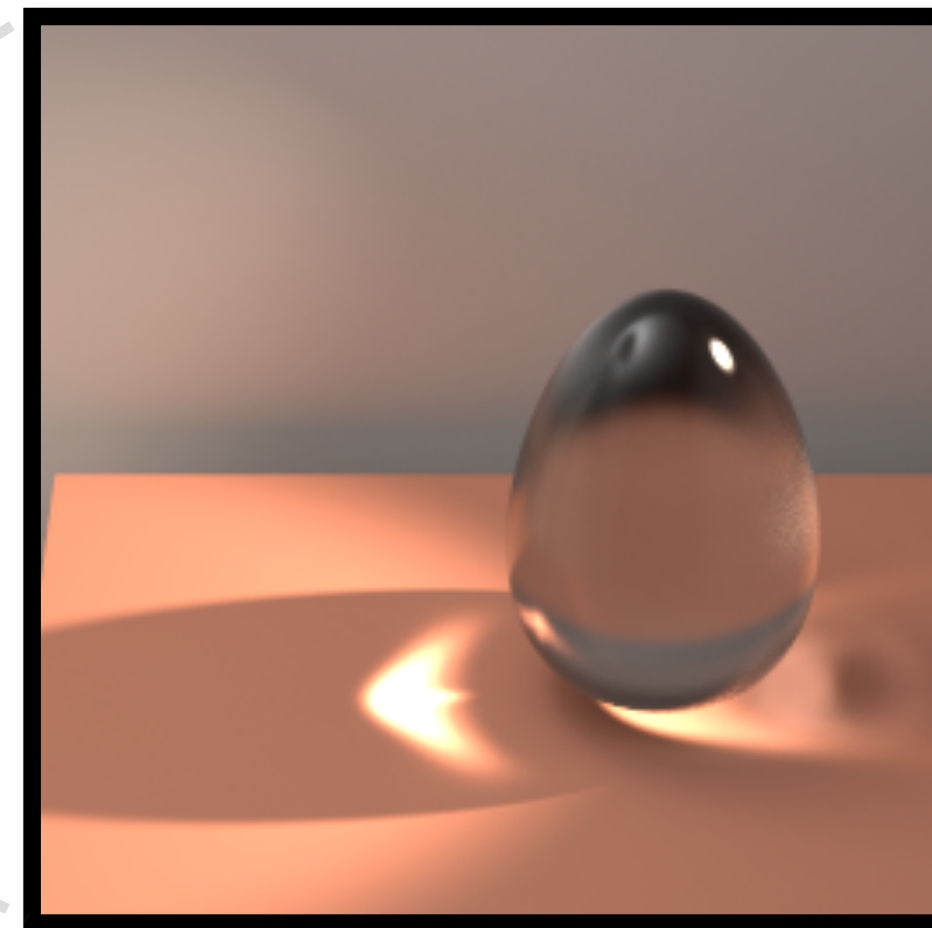
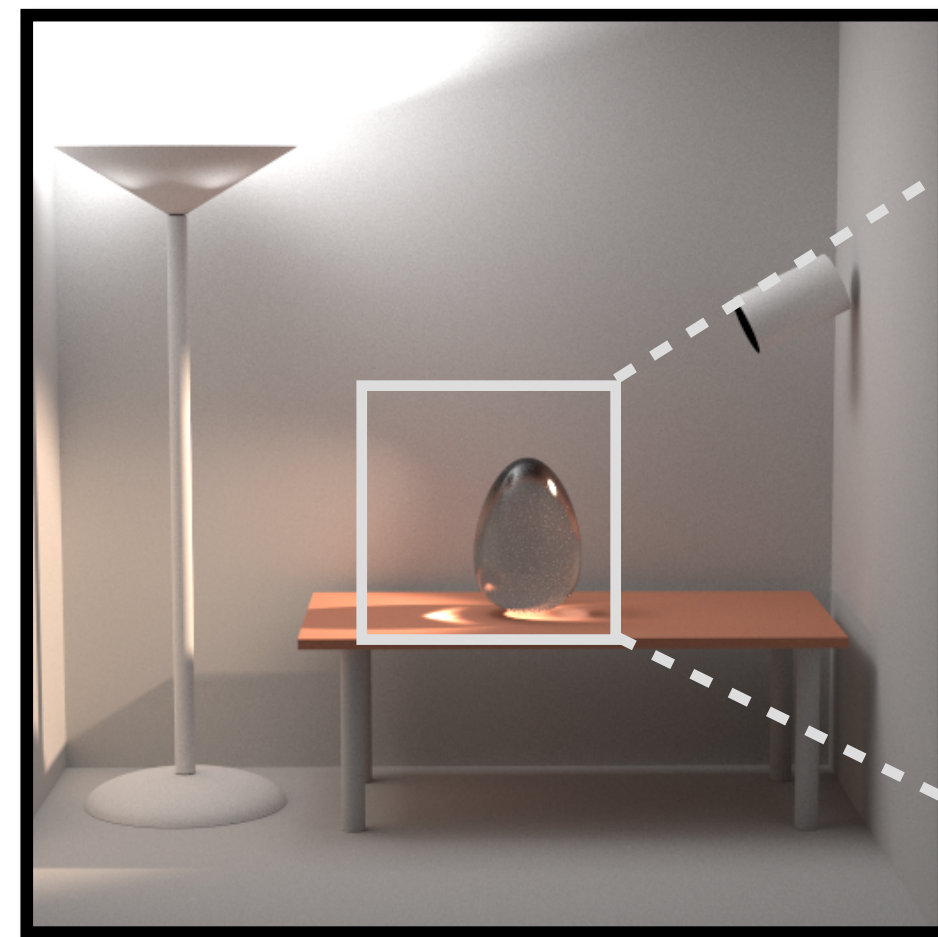


Edge sampling
[Li 18, Zhang 19]

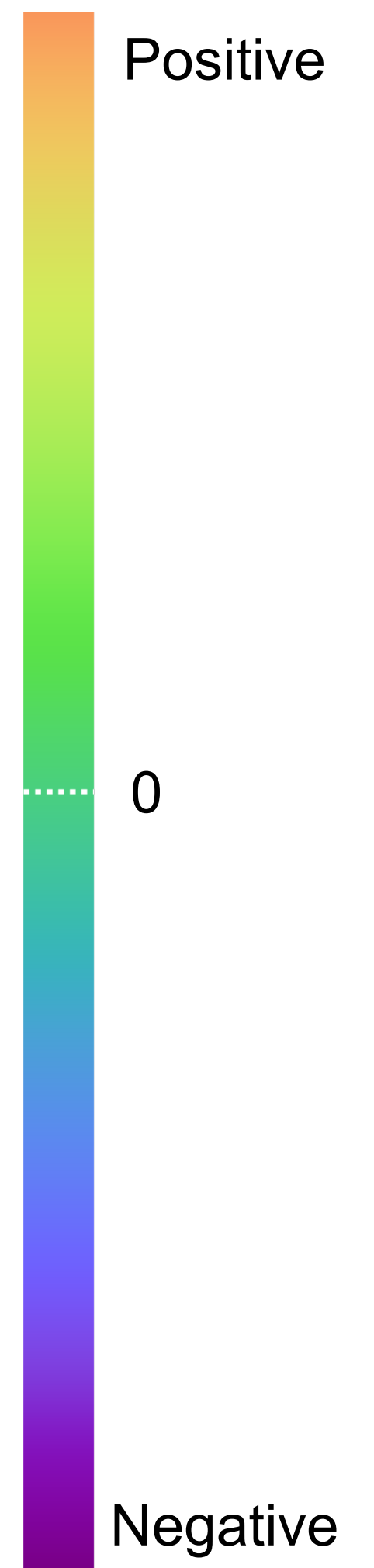


RESULT: COMPLEX LIGHT-TRANSPORT EFFECT

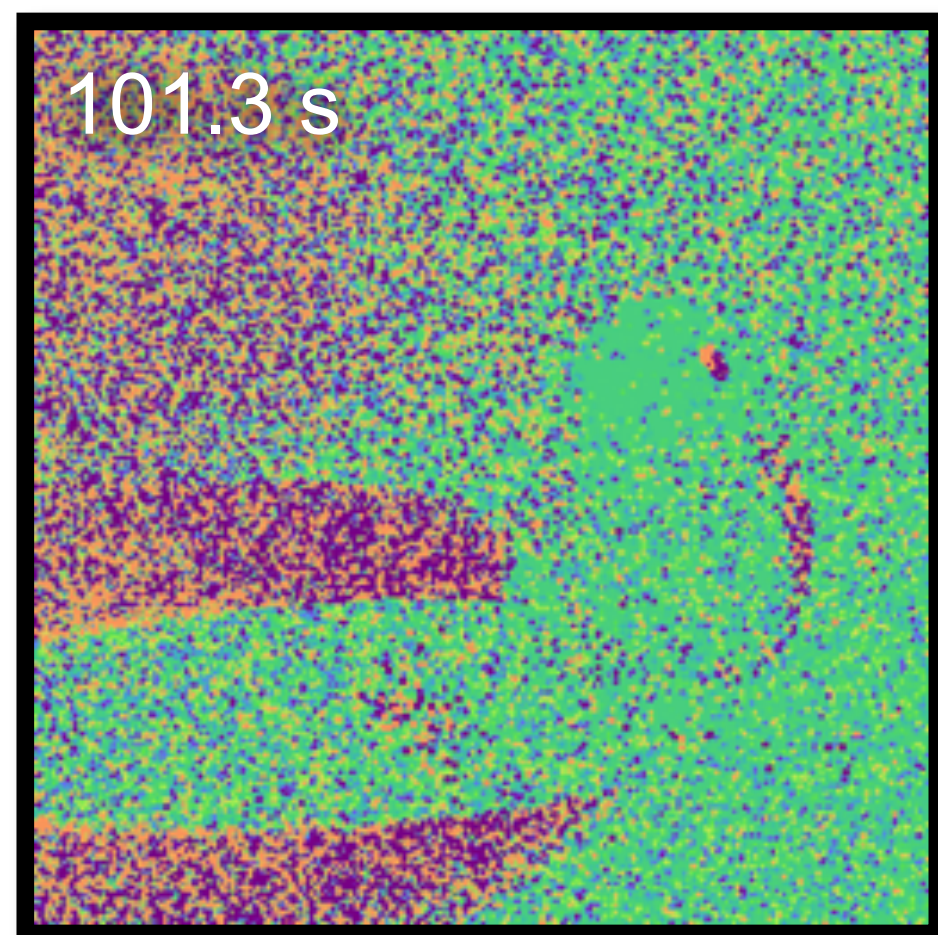
Parameter:
vertical position
of the spot light



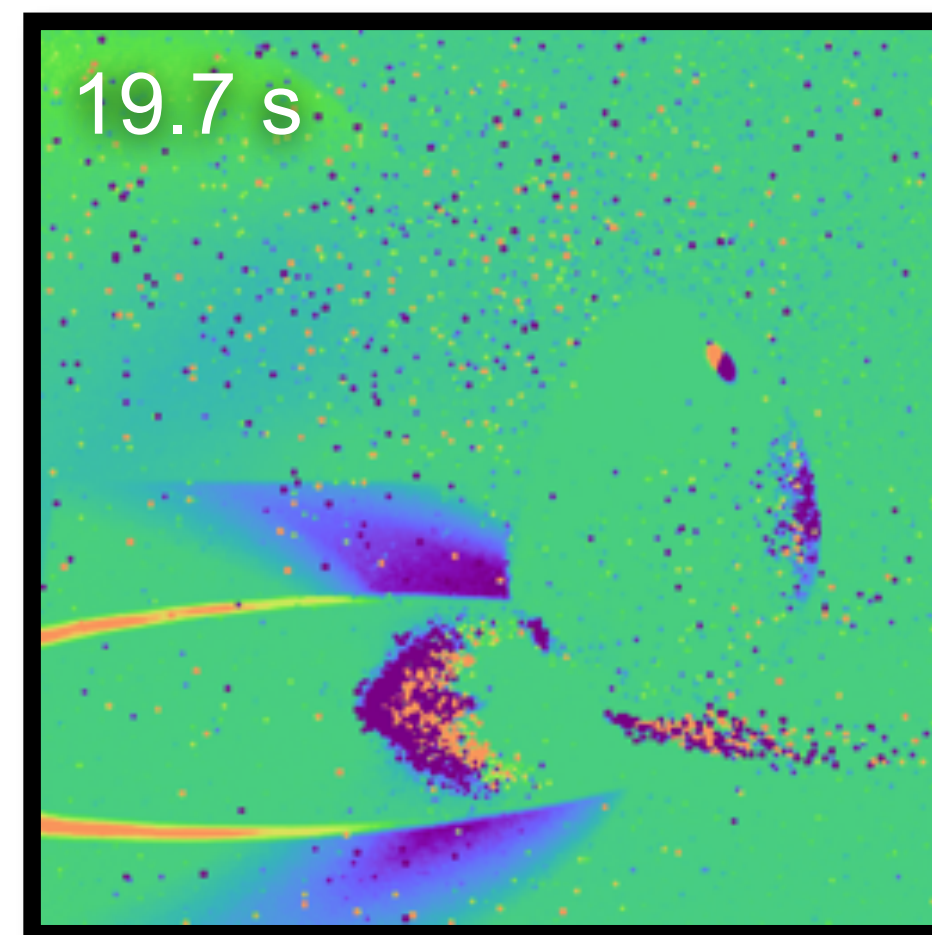
Reference



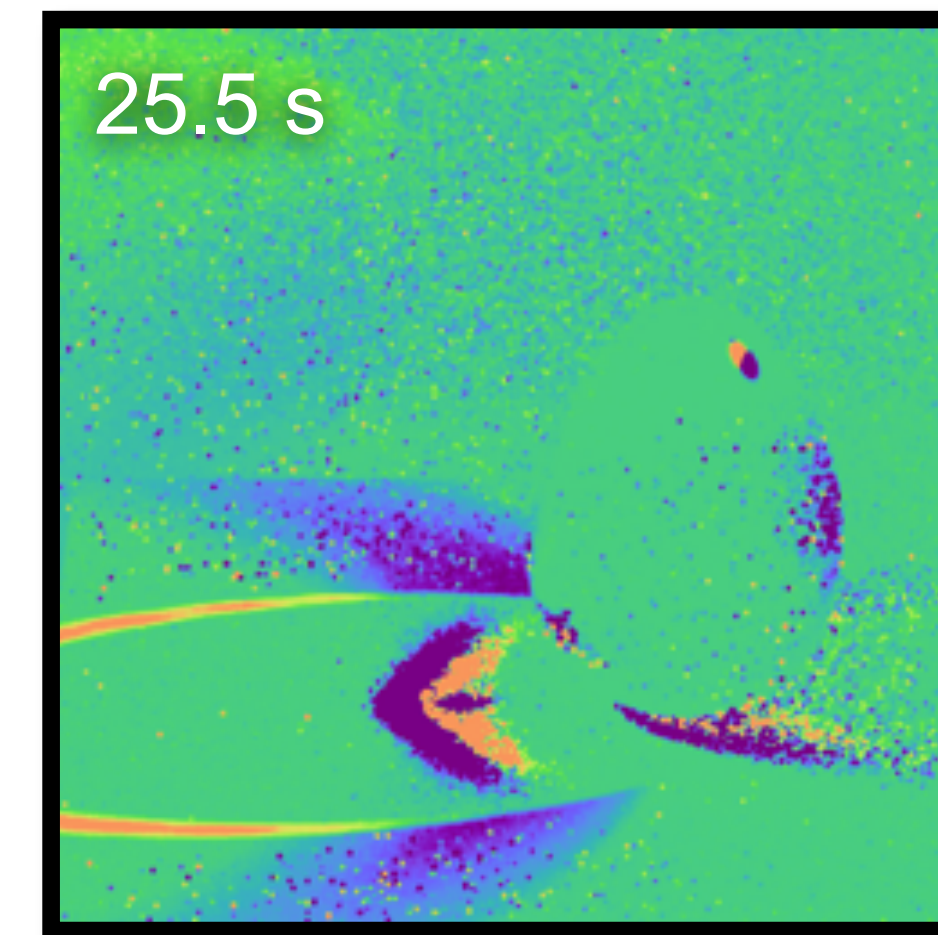
**Equal-sample
comparison**



Path tracing w/ edge sampling
[Li et al. 2018, Zhang et al. 2019]



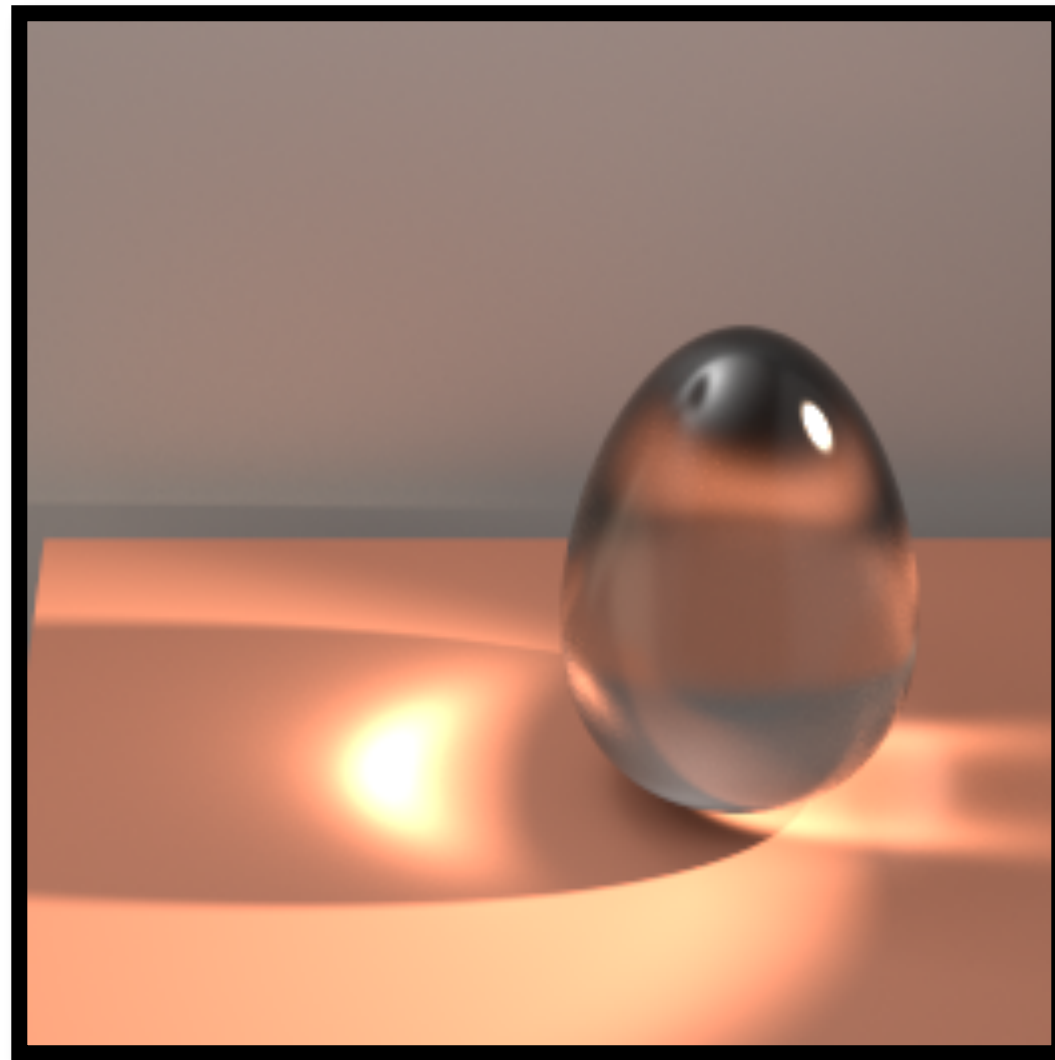
Path-space, unidirectional
[Zhang et al. 2020]



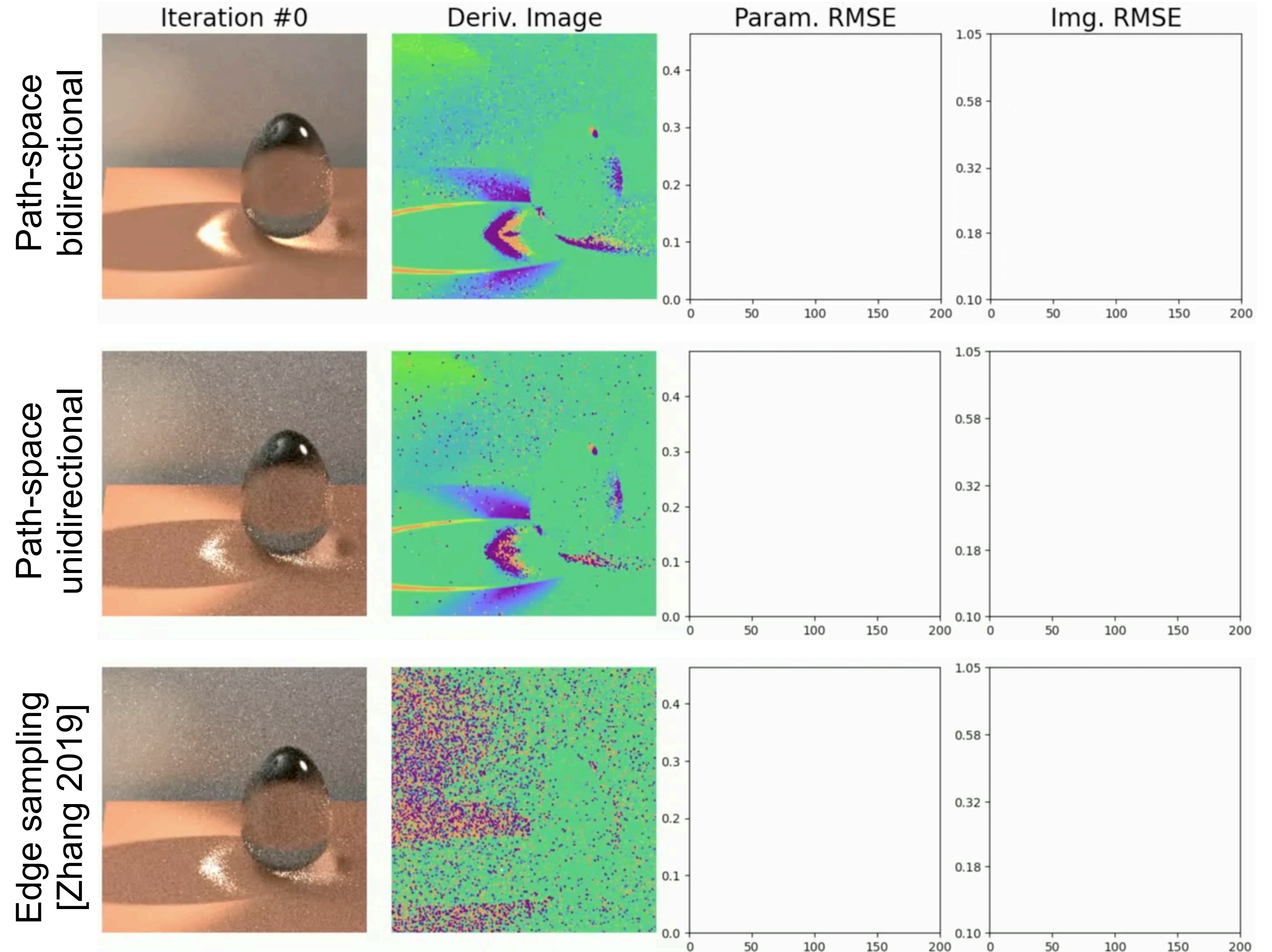
Path-space, bidirectional
[Zhang et al. 2020]

RESULT: COMPLEX LIGHT-TRANSPORT EFFECT

Target image

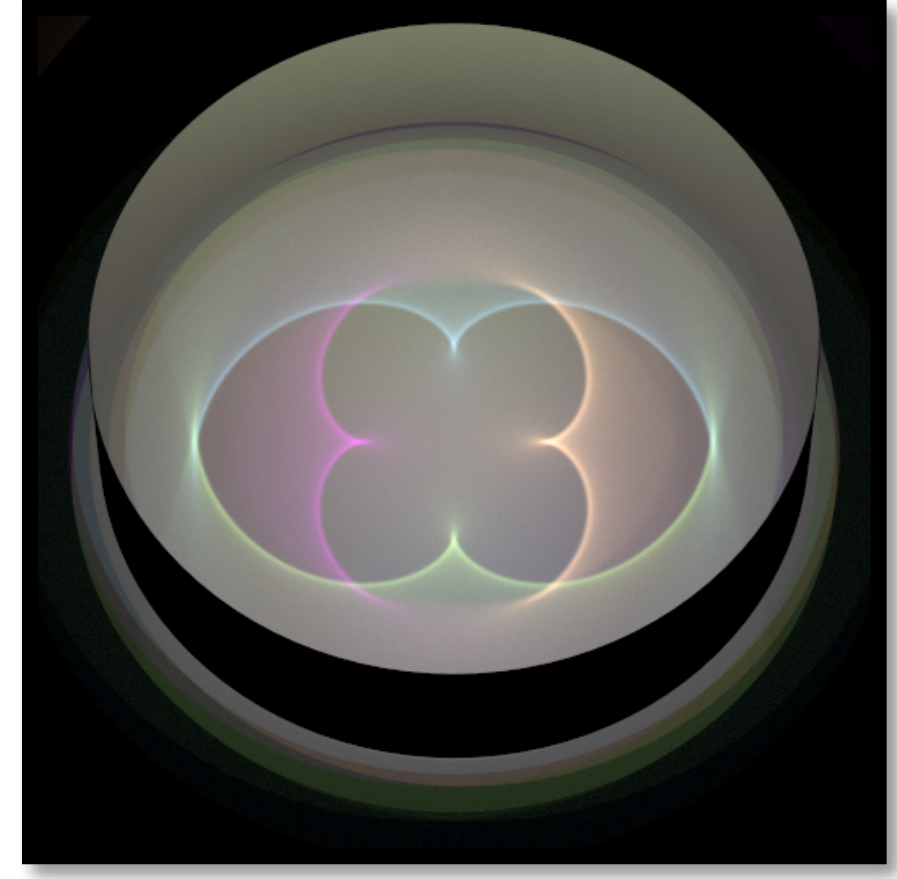


- Optimizing
 - Glass IOR
 - Spotlight position
- **Equal-time** per iteration
- **Identical** optimization settings
 - Learning rate (Adam)
 - Initializations

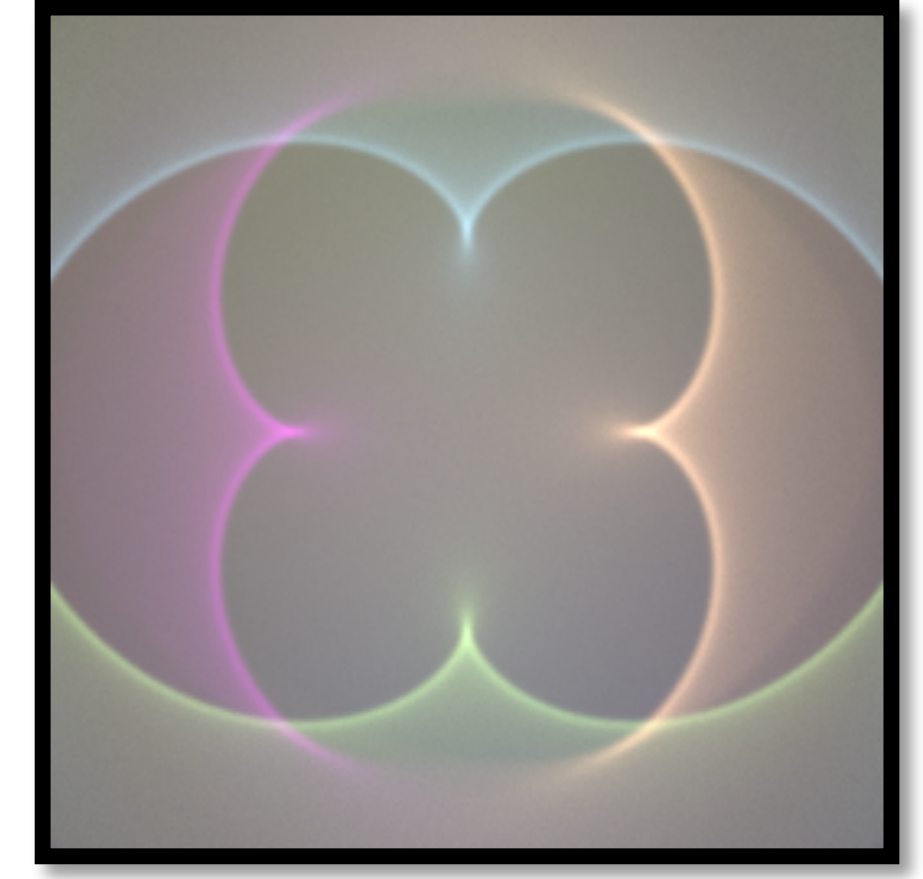


RESULT: COMPLEX LIGHT-TRANSPORT EFFECT

Config.

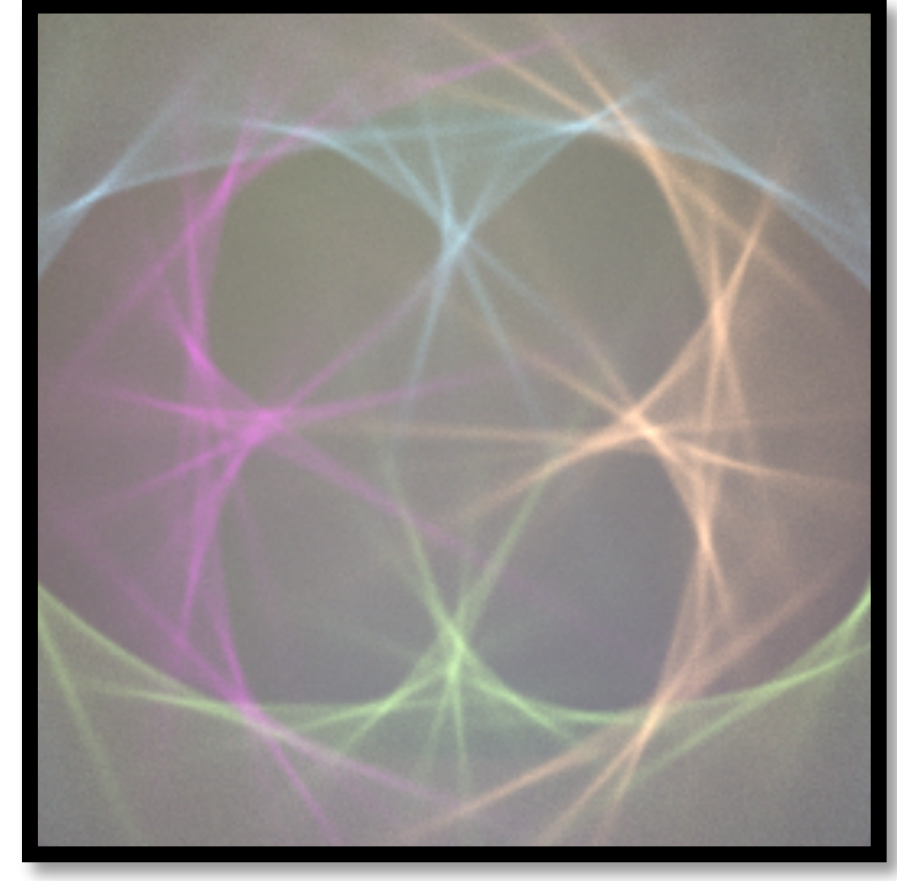


Initial

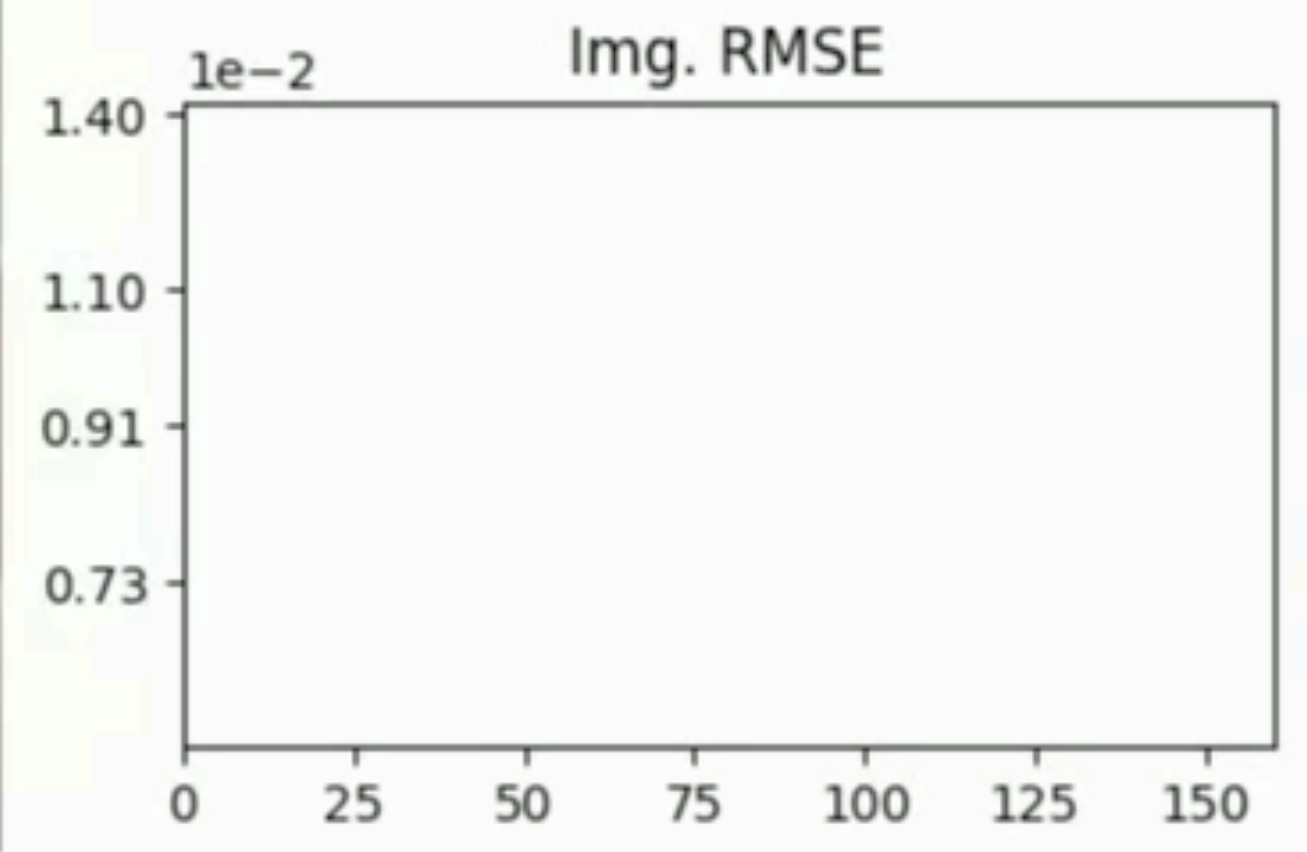
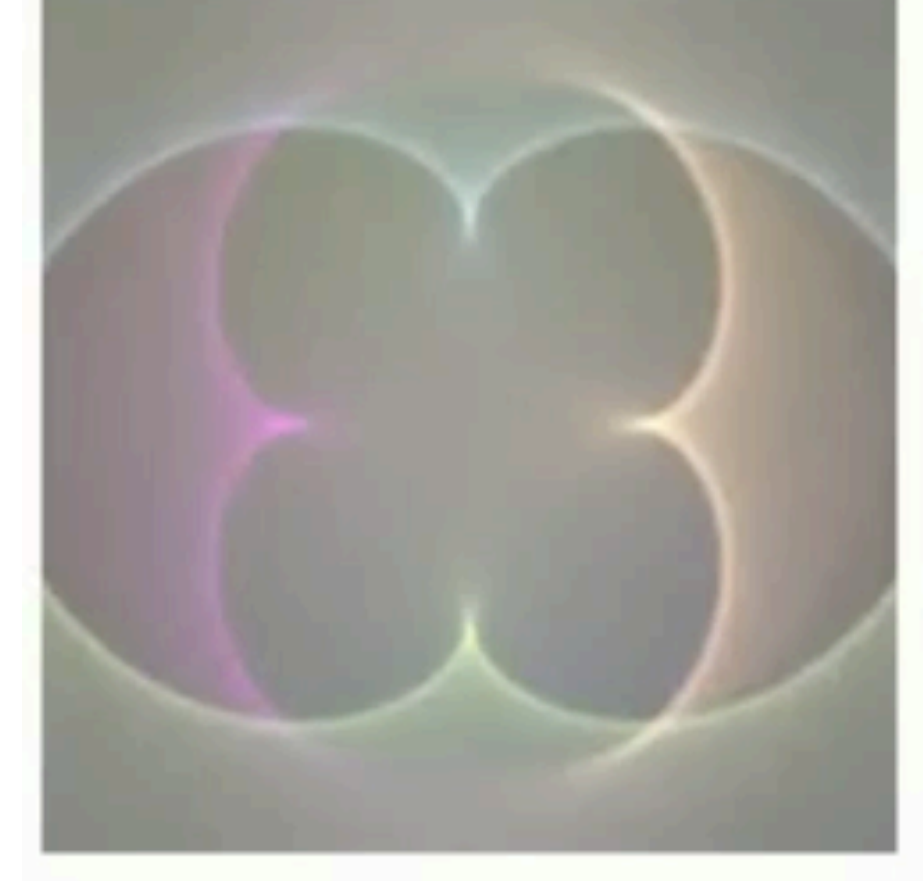


- Scene configuration:
 - A glossy ring lit by four colored light sources
- Optimizing:
 - **Cross-sectional shape** of the ring

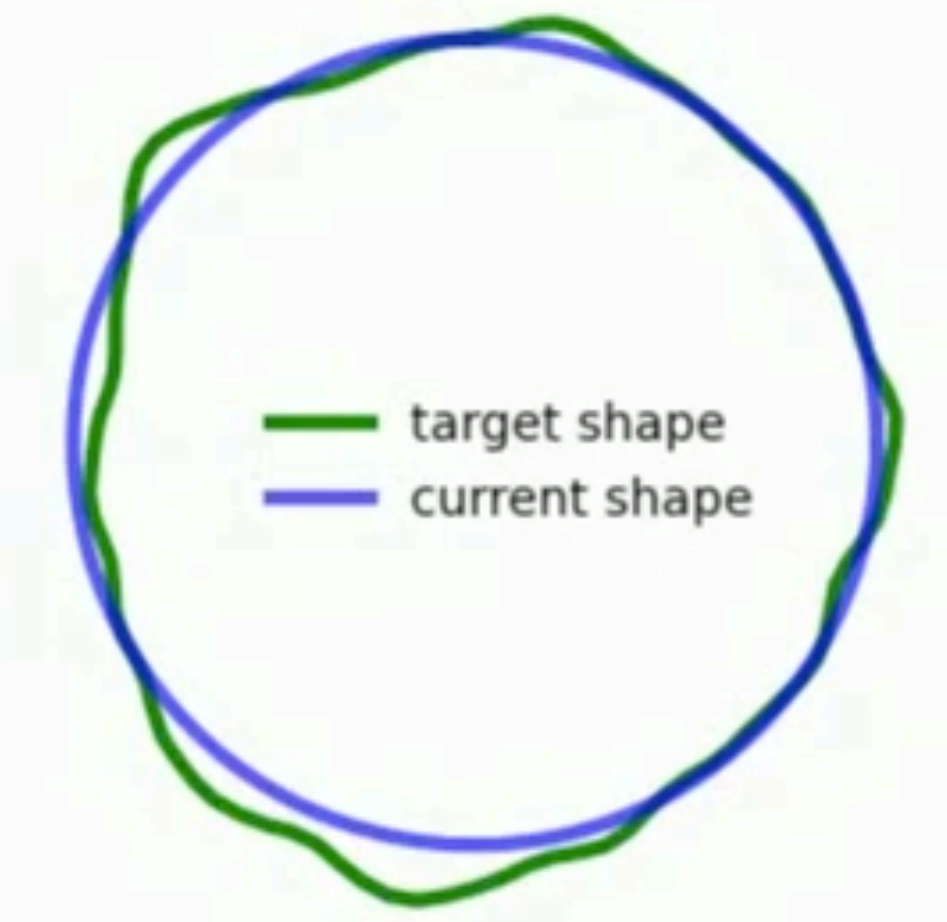
Target



Iter #0

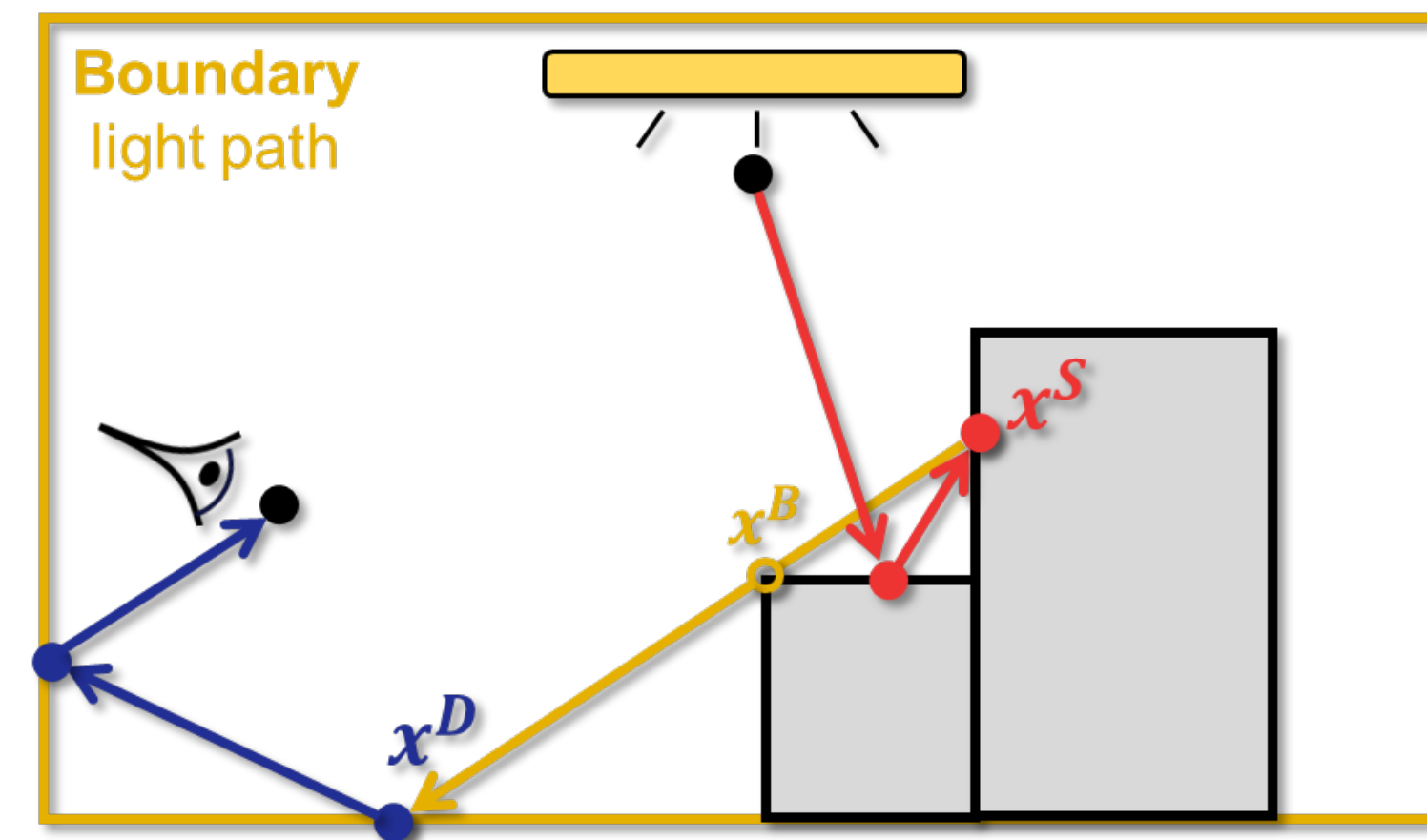
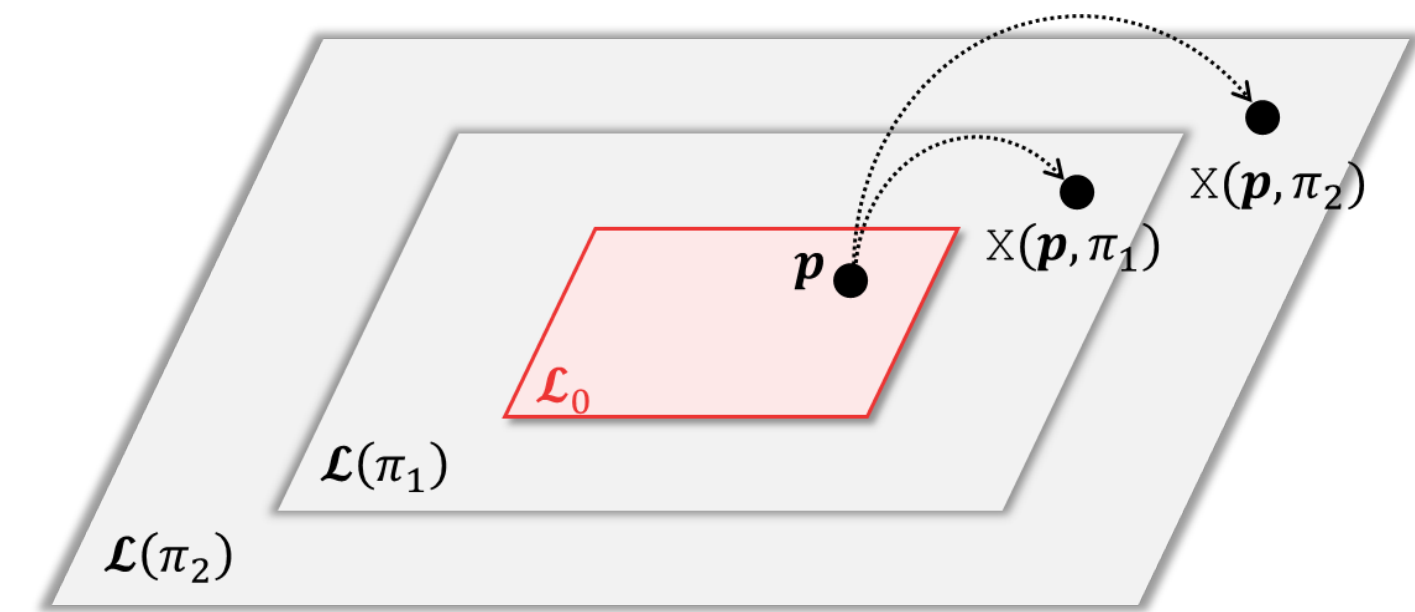


Cross-sectional shape (displacement x 20)



- **Differential path integral**
 - Separated interior and boundary components
- **Reparameterization**
 - Only need to consider silhouette edges
- **Unbiased Monte Carlo methods**
 - Unidirectional and bidirectional algorithms
 - No silhouette detection is needed

$$\frac{d}{d\pi} \int_{\Omega} f d\mu = \underbrace{\int_{\Omega} \frac{df}{d\pi} d\mu}_{\text{Interior}} + \underbrace{\int_{\partial\Omega} g d\mu'}_{\text{Boundary}}$$



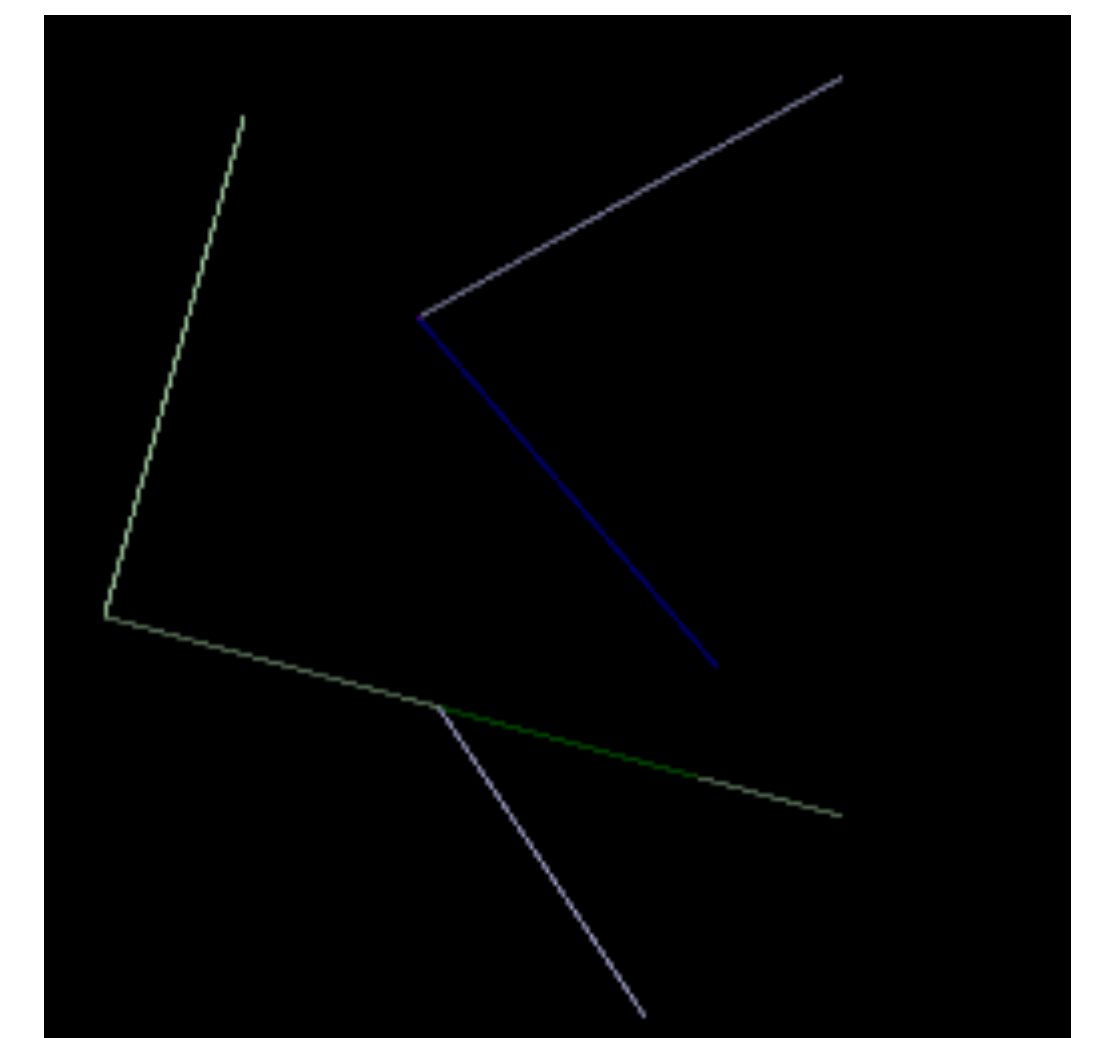
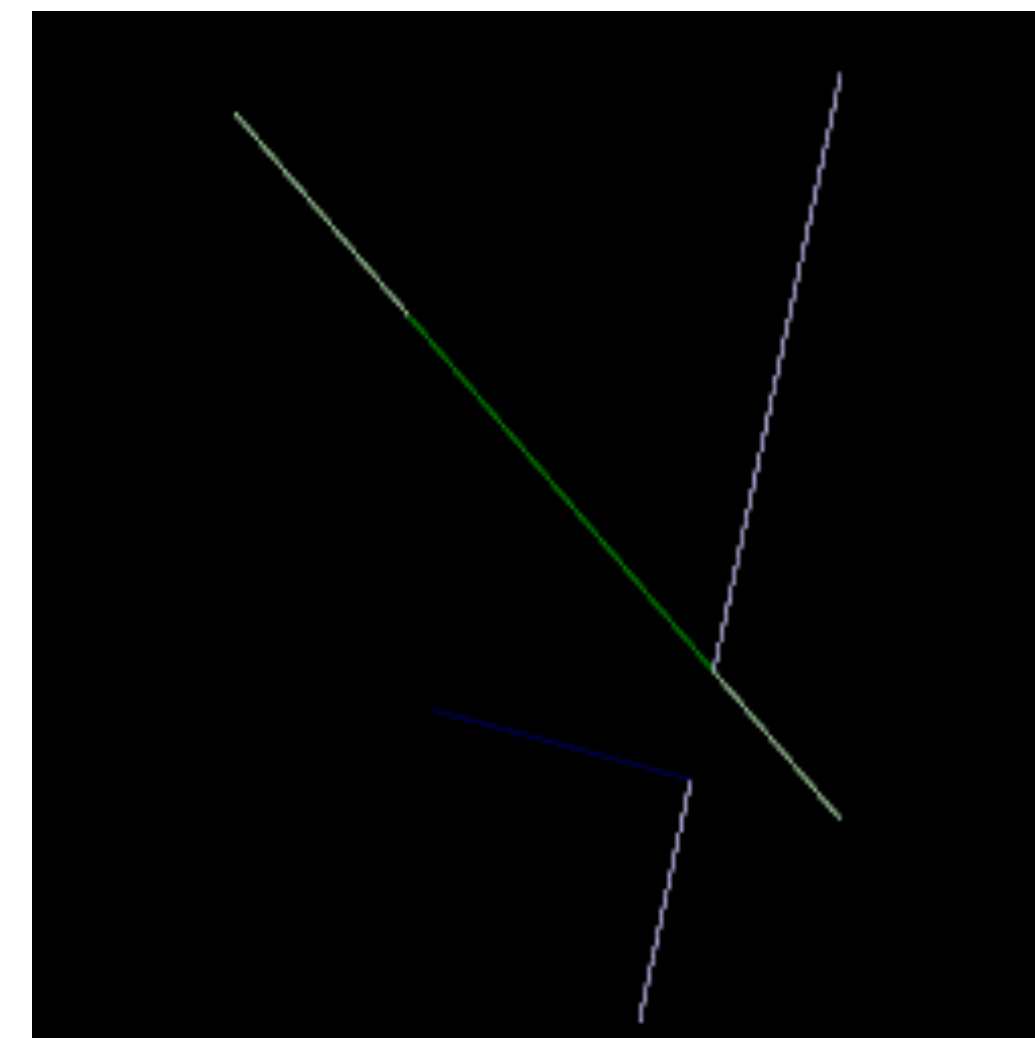
IMPLEMENTATION DETAILS

- C++11, single thread, ~300 lines
- render images of 2D triangles, their screen coordinates derivatives, and compute gradients w.r.t. vertex positions & color



“talk is cheap, show me the code!”

https://github.com/BachiLi/diffrender_tutorials




```
template <typename T>
struct Vec2 {
    T x, y;
    Vec2(T x = 0, T y = 0) : x(x), y(y) {}
};
template <typename T>
struct Vec3 {
    T x, y, z;
    Vec3(T x = 0, T y = 0, T z = 0) : x(x), y(y), z(z) {}
};
using Vec2f = Vec2<Real>;
using Vec3i = Vec3<int>;
using Vec3f = Vec3<Real>;

// some basic vector operations
// ...
```

```
struct TriangleMesh {
    vector<Vec2f> vertices;
    vector<Vec3i> indices;
    vector<Vec3f> colors; // defined for each face
};

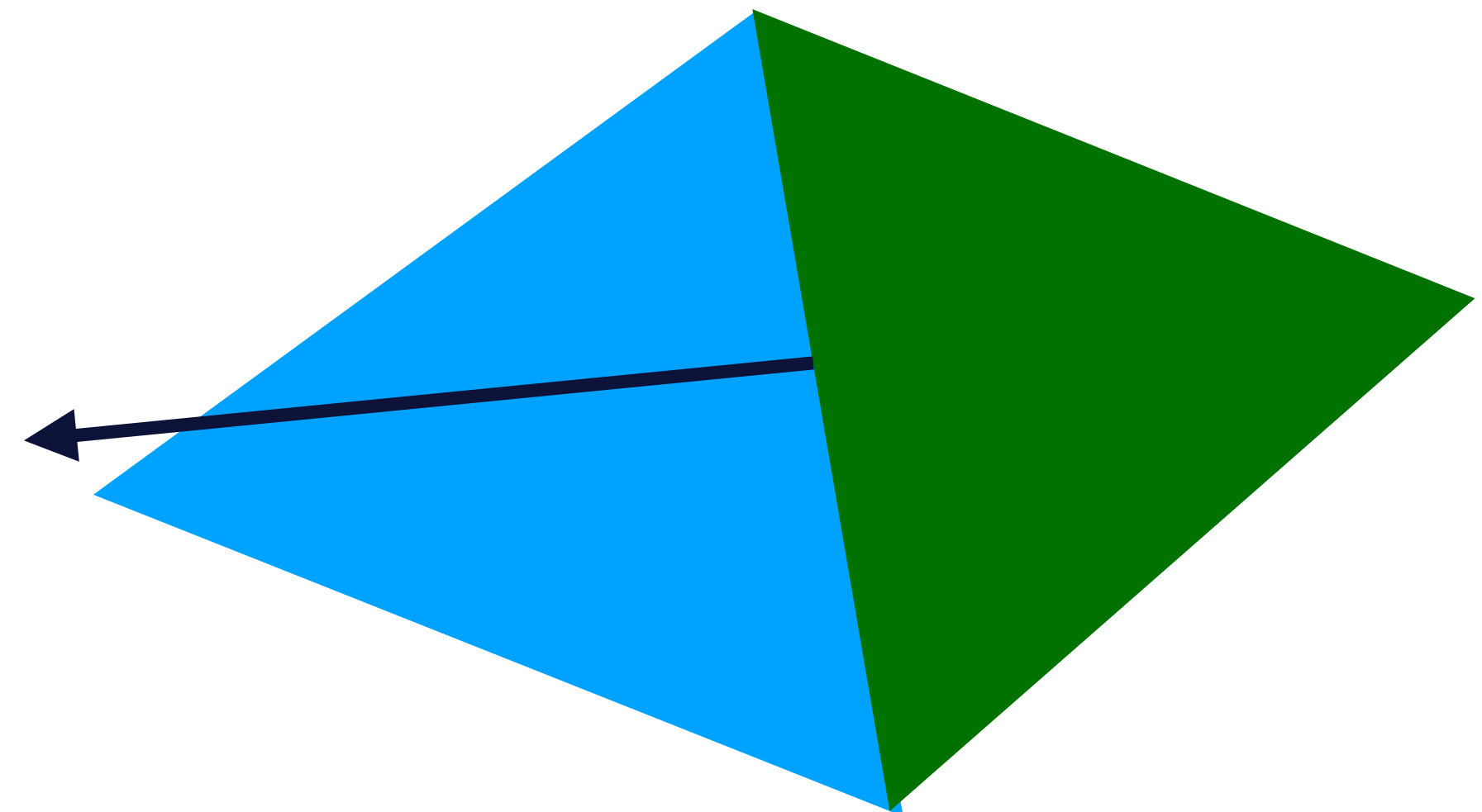
// stores the gradients w.r.t. a triangle mesh
struct DTriangleMesh {
    DTriangleMesh(int num_vertices, int num_colors) {
        vertices.resize(num_vertices, Vec2f{0, 0});
        colors.resize(num_colors, Vec3f{0, 0, 0});
    }

    vector<Vec2f> vertices;
    vector<Vec3f> colors;
};
```



```
struct Edge {  
    int v0, v1; // vertex ID, v0 < v1  
  
    Edge(int v0, int v1) : v0(min(v0, v1)), v1(max(v0, v1)) {}  
  
    // for sorting edges  
    bool operator<(const Edge &e) const {  
        return this->v0 != e.v0 ? this->v0 < e.v0 :  
            this->v1 < e.v1;  
    }  
};
```

need to avoid double count this edge



```
// for sampling edges with inverse transform sampling
struct Sampler {
    vector<Real> pmf, cdf;
};

// binary search for inverting the CDF in the sampler
int sample(const Sampler &sampler, const Real u) {
    auto cdf = sampler.cdf;
    return clamp<int>(upper_bound(
        cdf.begin(), cdf.end(), u) - cdf.begin() - 1,
        0, cdf.size() - 2);
}
```



```
struct Img {  
    Img(int width, int height,  
        const Vec3f &val = Vec3f{0, 0, 0}) :  
        width(width), height(height) {  
        color.resize(width * height, val);  
    }  
  
    vector<Vec3f> color;  
    int width;  
    int height;  
};
```

SETUP: THE MAIN() FUNCTION

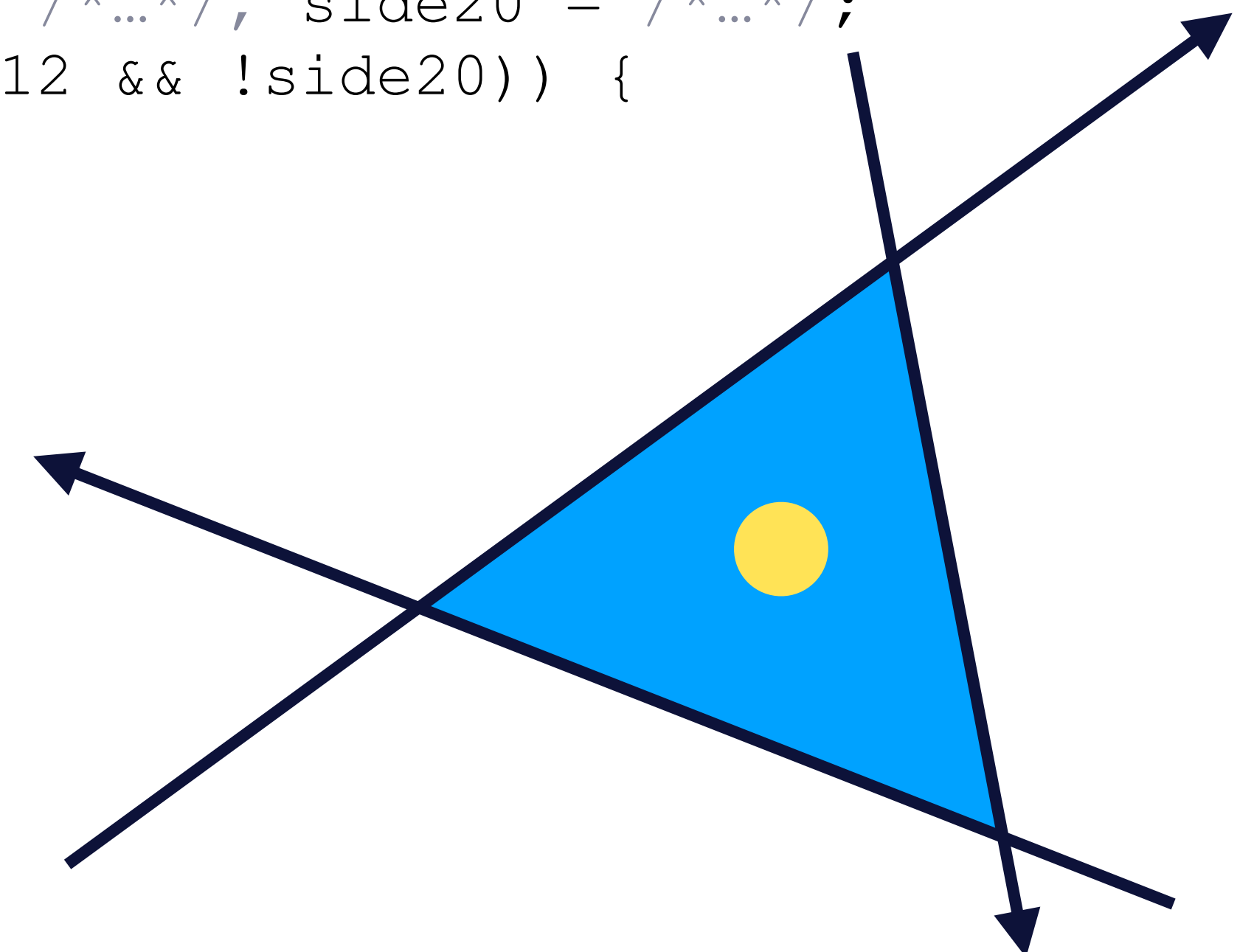
```
int main(int argc, char *argv[]) {
    TriangleMesh mesh{
        {{50.0, 25.0}, {200.0, 200.0}, {15.0, 150.0}, // vertices
         {200.0, 15.0}, {150.0, 250.0}, {50.0, 100.0}},
        {{0, 1, 2}, {3, 4, 5}}, // indices
        {{0.3, 0.5, 0.3}, {0.3, 0.3, 0.5}} // color
    };
    Img img(256, 256);
    mt19937 rng(1234);
    render(/*...*/);
    save_img(img, "render.ppm");
    // compute derivatives
    // adjoint is the gradient of some scalar loss w.r.t. image
    Img adjoint(img.width, img.height, Vec3f{1, 1, 1});
    Img dx(img.width, img.height), dy(img.width, img.height);
    DTriangleMesh d_mesh(mesh.vertices.size(), mesh.colors.size());
    d_render(/*...*/);
    // save derivative images
    // ...
    return 0;
}
```



```
void render(/*...*/) {  
    // ...  
    for (int y = 0; y < img.height; y++) { // for each pixel  
        for (int x = 0; x < img.width; x++) {  
            for (int dy = 0; dy < sqrt_num_samples; dy++) { // for each subpixel  
                for (int dx = 0; dx < sqrt_num_samples; dx++) {  
                    // ...  
                    auto color = raytrace(mesh, screen_pos);  
                    img.color[y * img.width + x] += color / samples_per_pixel;  
                }  
            }  
        }  
    }  
}
```

“RAY TRACE”

```
Vec3f raytrace(const TriangleMesh &mesh, const Vec2f &screen_pos, int *hit_index = nullptr) {  
    // loop over all triangles in the mesh, return the first one that hits  
    for (int i = 0; i < (int)mesh.indices.size(); i++) {  
        // retrieve the three vertices of a triangle  
        auto index = mesh.indices[i];  
        auto v0 = mesh.vertices[index.x], v1 = mesh.vertices[index.y],  
            v2 = mesh.vertices[index.z];  
        // form three half-planes: v1-v0, v2-v1, v0-v2  
        // if a point is on the same side of all three half-planes, it's inside the triangle  
        auto n01 = normal(v1 - v0), n12 = normal(v2 - v1), n20 = normal(v0 - v2);  
        auto side01 = dot(screen_pos - v0, n01) > 0, side12 = /*...*/, side20 = /*...*/;  
        if ((side01 && side12 && side20) || (!side01 && !side12 && !side20)) {  
            if (hit_index != nullptr) {  
                *hit_index = i;  
            }  
            return mesh.colors[i];  
        }  
    }  
    // return background  
    // ...  
}
```



RENDERING: DONE!



```
void d_render ( /*...*/ ) {  
    compute_interior_derivatives ( /*...*/ );  
    auto edges = collect_edges ( mesh );  
    auto edge_sampler = build_edge_sampler ( mesh, edges );  
    compute_edge_derivatives ( /*...*/ );  
}
```

interior derivative

$$\frac{\partial}{\partial p} \iint \text{[triangle diagram]} = \iint \frac{\partial}{\partial p} \text{[triangle diagram with yellow dots]}$$

Reynolds transport theorem
[Reynolds 1903]

$$+ \int \text{[triangle diagram with pink dots]} \text{ boundary derivative}$$


```
void d_render ( /*...*/ ) {  
    compute_interior_derivatives ( /*...*/ );  
    auto edges = collect_edges ( mesh );  
    auto edge_sampler = build_edge_sampler ( mesh, edges );  
    compute_edge_derivatives ( /*...*/ );  
}
```

interior derivative

$$\frac{\partial}{\partial p} \iint \text{[triangle diagram]} = \iint \frac{\partial}{\partial p} \text{[triangle diagram with yellow dots]}$$

Reynolds transport theorem
[Reynolds 1903]

$$+ \int \text{[triangle diagram with pink dots]} \text{ boundary derivative}$$

```
void compute_interior_derivatives(/*...*/) {
    // ...
    for (int y = 0; y < adjoint.height; y++) { // for each pixel
        for (int x = 0; x < adjoint.width; x++) {
            for (int dy = 0; dy < sqrt_num_samples; dy++) { // for each subpixel
                for (int dx = 0; dx < sqrt_num_samples; dx++) {
                    // ...
                    int hit_index = -1;
                    raytrace(mesh, screen_pos, &hit_index);
                    if (hit_index != -1) {
                        // scatter to the gradient buffer
                        d_colors[hit_index] +=
                            adjoint.color[y * adjoint.width + x] / samples_per_pixel;
                    }
                }
            }
        }
    }
}
```



```
void compute_interior_derivatives(/*...*/) {
    // ...
    for (int y = 0; y < adjoint.height; y++) { // for each pixel
        for (int x = 0; x < adjoint.width; x++) {
            for (int dy = 0; dy < sqrt_num_samples; dy++) { // for each subpixel
                for (int dx = 0; dx < sqrt_num_samples; dx++) {
                    // ...
                    int hit_index = -1;
                    raytrace(mesh, screen_pos, &hit_index);
                    if (hit_index != -1) {
                        // scatter to the gradient buffer
                        d_colors[hit_index] +=
                            adjoint.color[y * adjoint.width + x] / samples_per_pixel;
                    }
                }
            }
        }
    }
}
```

- automatic differentiation of a standard renderer
- can be replaced by radiative backpropagation

```
void d_render ( /*...*/ ) {  
    compute_interior_derivatives ( /*...*/ );  
    auto edges = collect_edges ( mesh );  
    auto edge_sampler = build_edge_sampler ( mesh, edges );  
    compute_edge_derivatives ( /*...*/ );  
}
```

interior derivative

$$\frac{\partial}{\partial p} \iint \text{[triangle diagram]} = \iint \frac{\partial}{\partial p} \text{[triangle diagram with yellow dots]}$$

Reynolds transport theorem
[Reynolds 1903]

$$+ \int \text{[triangle diagram with pink dots]} \text{ boundary derivative}$$


```
vector<Edge> collect_edges(const TriangleMesh &mesh) {  
    set<Edge> edges;  
    for (auto index : mesh.indices) {  
        edges.insert(Edge(index.x, index.y));  
        edges.insert(Edge(index.y, index.z));  
        edges.insert(Edge(index.z, index.x));  
    }  
    return vector<Edge>(edges.begin(), edges.end());  
}
```

- can be parallelized using parallel sorting + parallel stream compaction

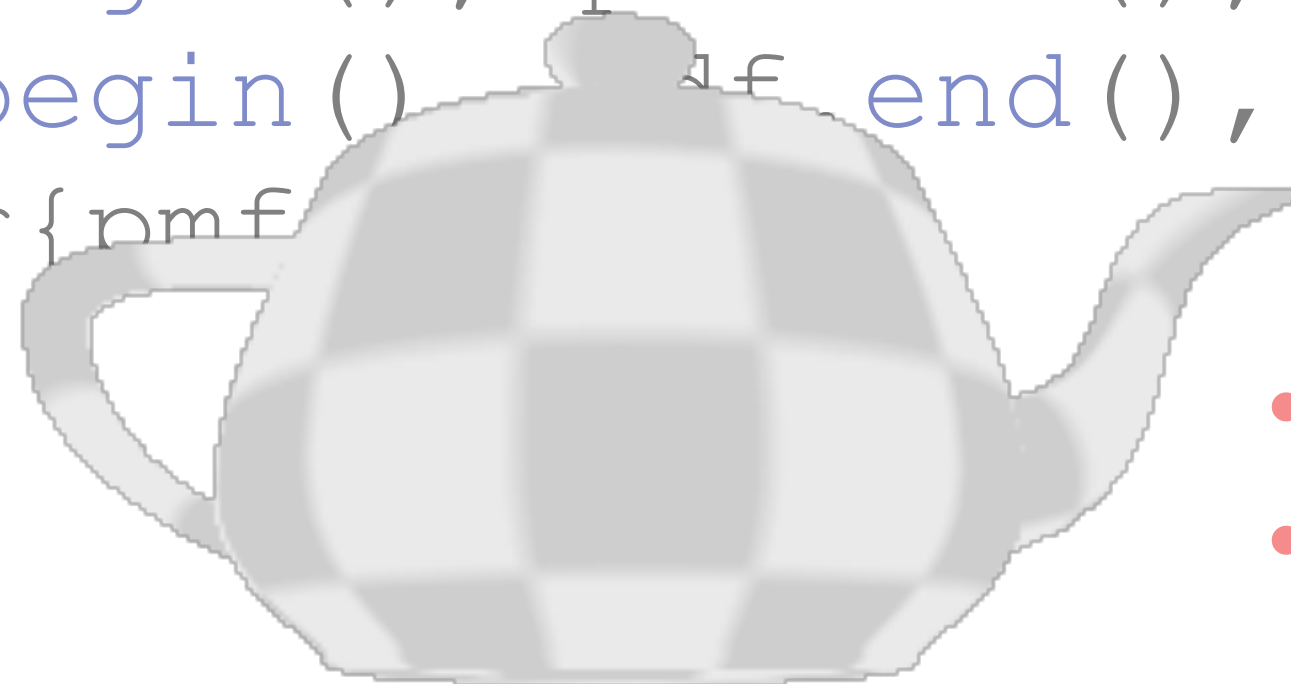
BUILD EDGE SAMPLER

```
// build a discrete CDF using edge length
Sampler build_edge_sampler(const TriangleMesh &mesh,
                          const vector<Edge> &edges) {
    vector<Real> pmf, cdf;
    pmf.reserve(edges.size()); cdf.reserve(edges.size() + 1);
    cdf.push_back(0);
    for (auto edge : edges) {
        auto v0 = mesh.vertices[edge.v0], v1 = mesh.vertices[edge.v1];
        pmf.push_back(length(v1 - v0));
        cdf.push_back(pmf.back() + cdf.back());
    }
    auto length_sum = cdf.back(); // normalize pmf/cdf
    for_each(pmf.begin(), pmf.end(), [&](Real &p) {p /= length_sum;});
    for_each(cdf.begin(), cdf.end(), [&](Real &p) {p /= length_sum;});
    return Sampler{pmf, cdf};
}
```


BUILD EDGE SAMPLER

```
// build a discrete CDF using edge length
```

```
Sampler build_edge_sampler(const TriangleMesh &mesh,  
                           const vector<Edge> &edges) {  
    vector<Real> pmf, cdf;  
    pmf.reserve(edges.size()); cdf.reserve(edges.size() + 1);  
    cdf.push_back(0);  
    for (auto edge : edges) {  
        auto v0 = mesh.vertices[edge.v0], v1 = mesh.vertices[edge.v1];  
        pmf.push_back(length(v1 - v0));  
        cdf.push_back(pmf.back() + cdf.back());  
    }  
    auto length_sum = cdf.back(); // normalize pmf/cdf  
    for_each(pmf.begin(), pmf.end(), [&](Real &p) {p /= length_sum;});  
    for_each(cdf.begin(), cdf.end(), [&](Real &p) {p /= length_sum;});  
    return Sampler{pmf,  
                  }  
}
```



- can exclude non-silhouette edges here
- can be parallelized using parallel scans

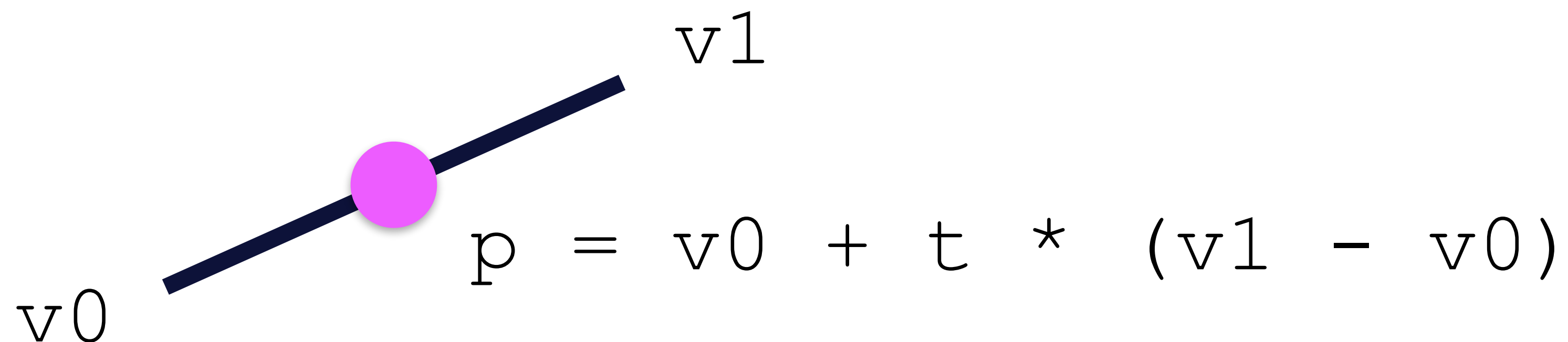
EDGE SAMPLING!

```
void compute_edge_derivatives (/*...*/) {  
    for (int i = 0; i < num_edge_samples; i++) {  
        // pick an edge  
        // ...  
        // pick a point p on the edge  
        // ...  
        // compute the colors at the two sides of p  
        // ...  
        // compute the weights using the PDF and adjoint image  
        // ...  
        // compute the derivatives using the Reynolds transport theorem  
        // ...  
    }  
}
```


EDGE SAMPLING — PICKING EDGES

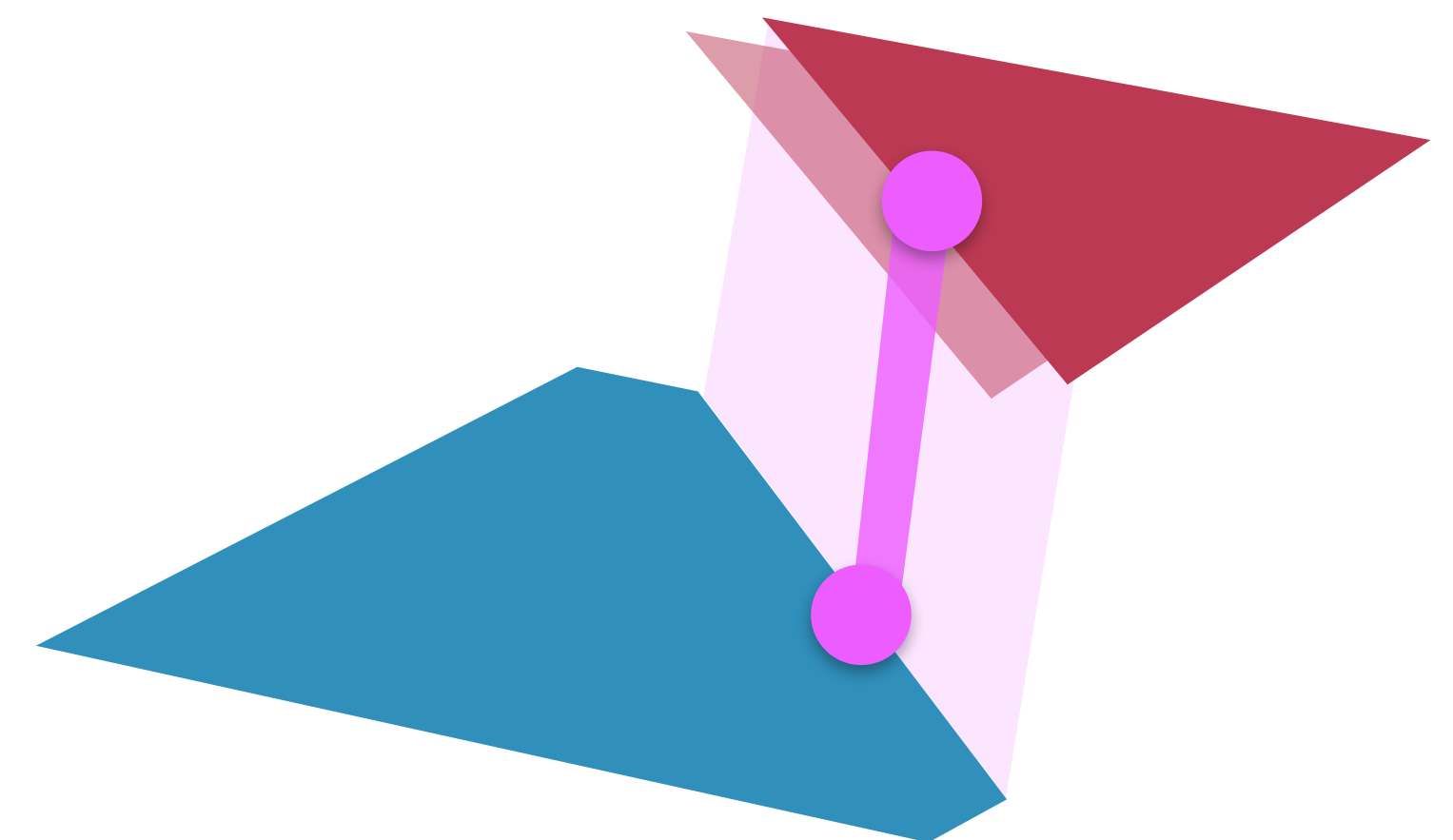
```
void compute_edge_derivatives (/*...*/) {  
    for (int i = 0; i < num_edge_samples; i++) {  
        // pick an edge  
        // ...  
        // pick a point p on the edge  
        // ...  
        // compute the colors at the two sides of p  
        // ...  
        // compute the weights using the PDF and adjoint image  
        // ...  
        // compute the derivatives using the Reynolds transport theorem  
        // ...  
    }  
}
```

```
// pick an edge  
auto edge_id = sample(edge_sampler, uni_dist(rng));  
auto edge = edges[edge_id];  
// pick a point p on the edge  
auto v0 = mesh.vertices[edge.v0], v1 = mesh.vertices[edge.v1];  
auto t = uni_dist(rng);  
auto p = v0 + t * (v1 - v0);  
auto xi = (int)p.x; auto yi = (int)p.y; // integer coordinates  
if (xi < 0 || yi < 0 || xi >= adjoint.width || yi >= adjoint.height) continue;
```




```
void compute_edge_derivatives (/*...*/) {  
    for (int i = 0; i < num_edge_samples; i++) {  
        // pick an edge  
        // ...  
        // pick a point p on the edge  
        //  
        // compute the colors at the two sides of p  
        //  
        // compute the weights using the PDF and adjoint image  
        // ...  
        // compute the derivatives using the Reynolds transport theorem  
        // ...  
    }  
}
```

```
// ...  
// compute the colors at the two sides of the selected edge  
auto n = normal((v1 - v0) / length(v1 - v0));  
auto color_in = raytrace(mesh, p - 1e-3f * n),  
        color_out = raytrace(mesh, p + 1e-3f * n);  
// ...
```



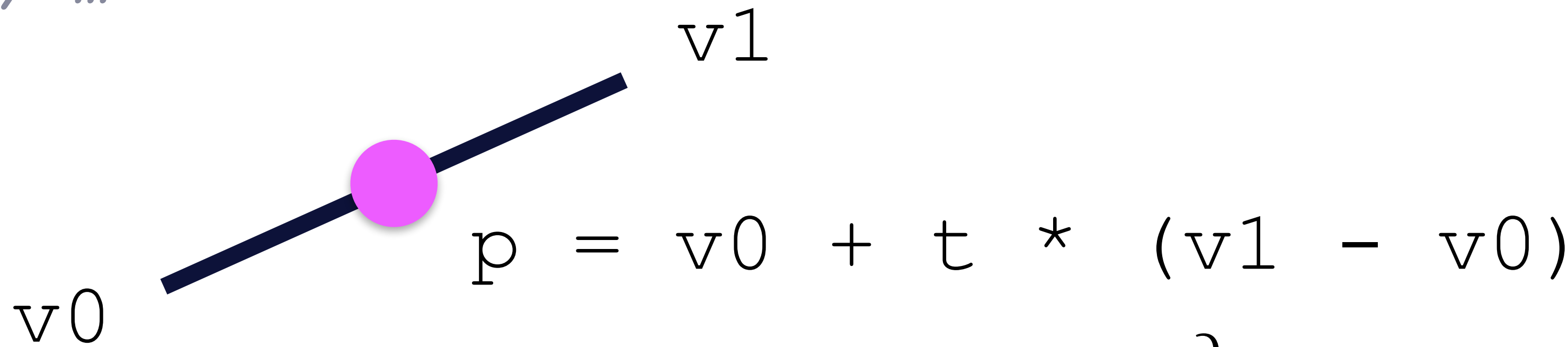

```
void compute_edge_derivatives (/*...*/) {  
    for (int i = 0; i < num_edge_samples; i++) {  
        // pick an edge  
        // ...  
        // pick a point p on the edge  
        // ...  
        // sample the two sides of p  
        //  
        // compute the weights using the PDF and adjoint image  
        // ...  
        // compute the derivatives using the Reynolds transport theorem  
        // ...  
    }  
}
```

```
// ...  
// compute the weights using the PDF and adjoint image  
auto pmf = edge_sampler.pmf[edge_id];  
auto pdf = pmf / (length(v1 - v0));  
auto weight = Real(1 / (pdf * Real(num_edge_samples)));  
auto adj = dot(color_in - color_out,  
               adjoint.color[yi * adjoint.width + xi]);  
  
// ...
```

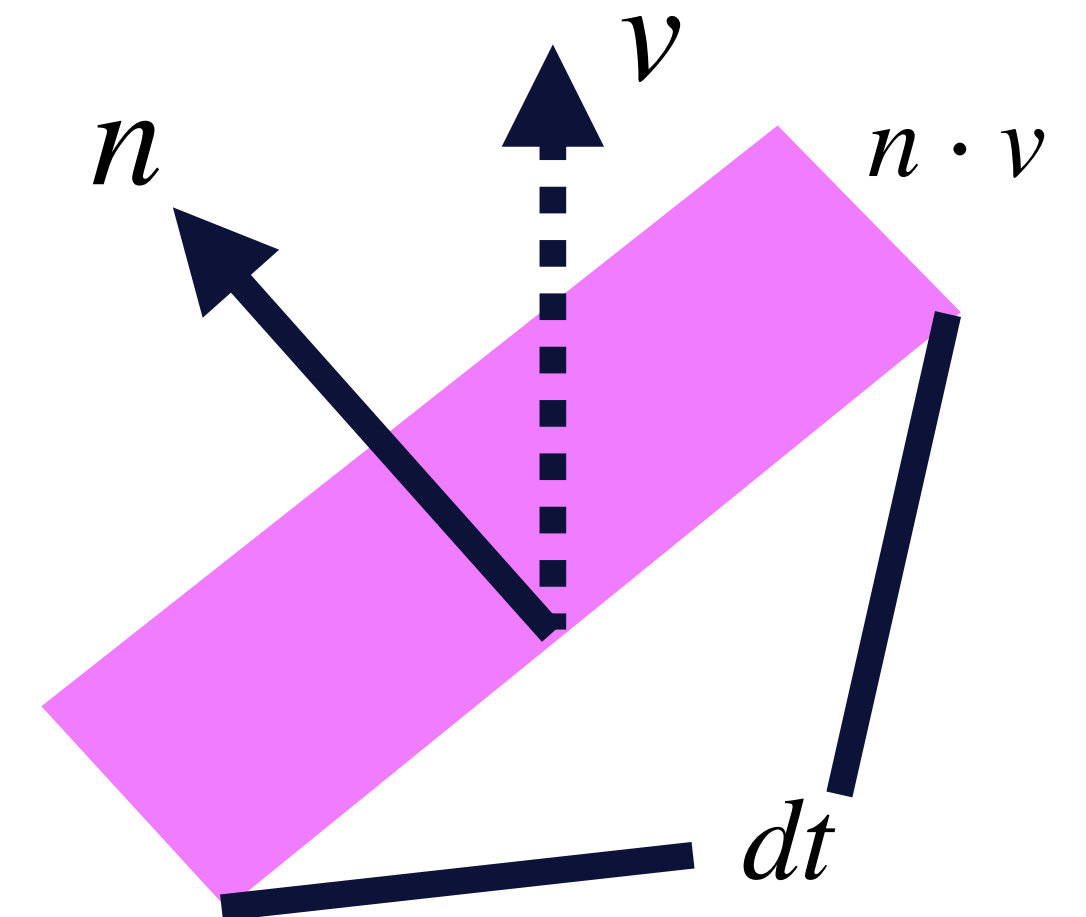


```
void compute_edge_derivatives (/*...*/) {  
    for (int i = 0; i < num_edge_samples; i++) {  
        // pick an edge  
        // ...  
        // pick a point p on the edge  
        // ...  
        // sample the two sides of p  
        // ...  
        // compute the weights using the PDF and adjoint image  
        // ...  
        // compute the derivatives using the Reynolds transport theorem  
        // ...  
    }  
}
```

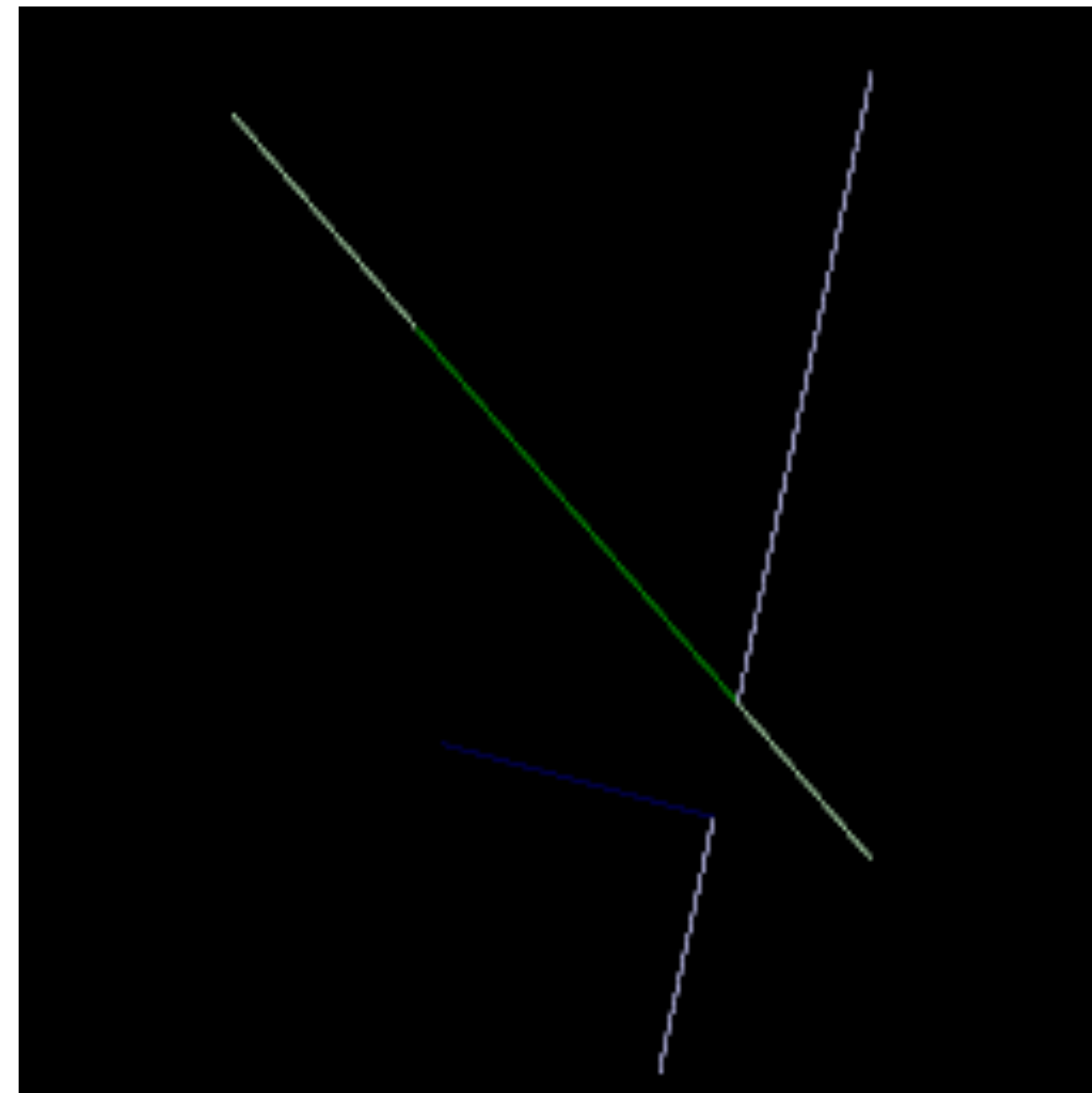
```
// ...
// compute the derivatives using Reynolds transport theorem
auto d_v0 = Vec2f{ (1 - t) * n.x, (1 - t) * n.y } * adj * weight;
auto d_v1 = Vec2f{      t * n.x,      t * n.y } * adj * weight;
// screen coordinate derivatives ignore the adjoint
auto dx = -n.x * (color_in - color_out) * weight;
auto dy = -n.y * (color_in - color_out) * weight;
// scatter gradients to buffers
// ...
```



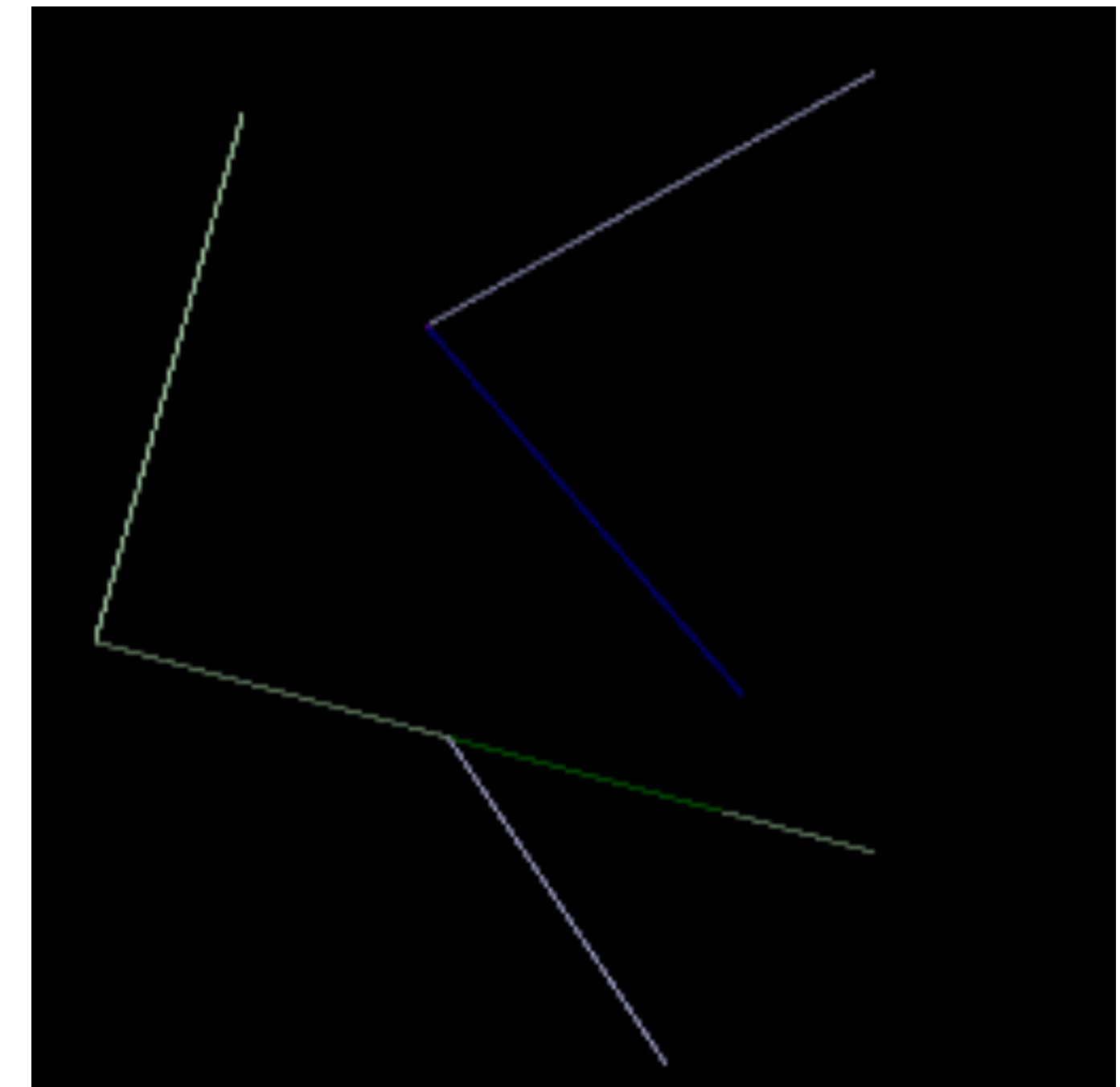
$$v = \frac{\partial p}{\partial \text{param}}$$



$$\int (f_- - f_+) (n \cdot v) dt$$

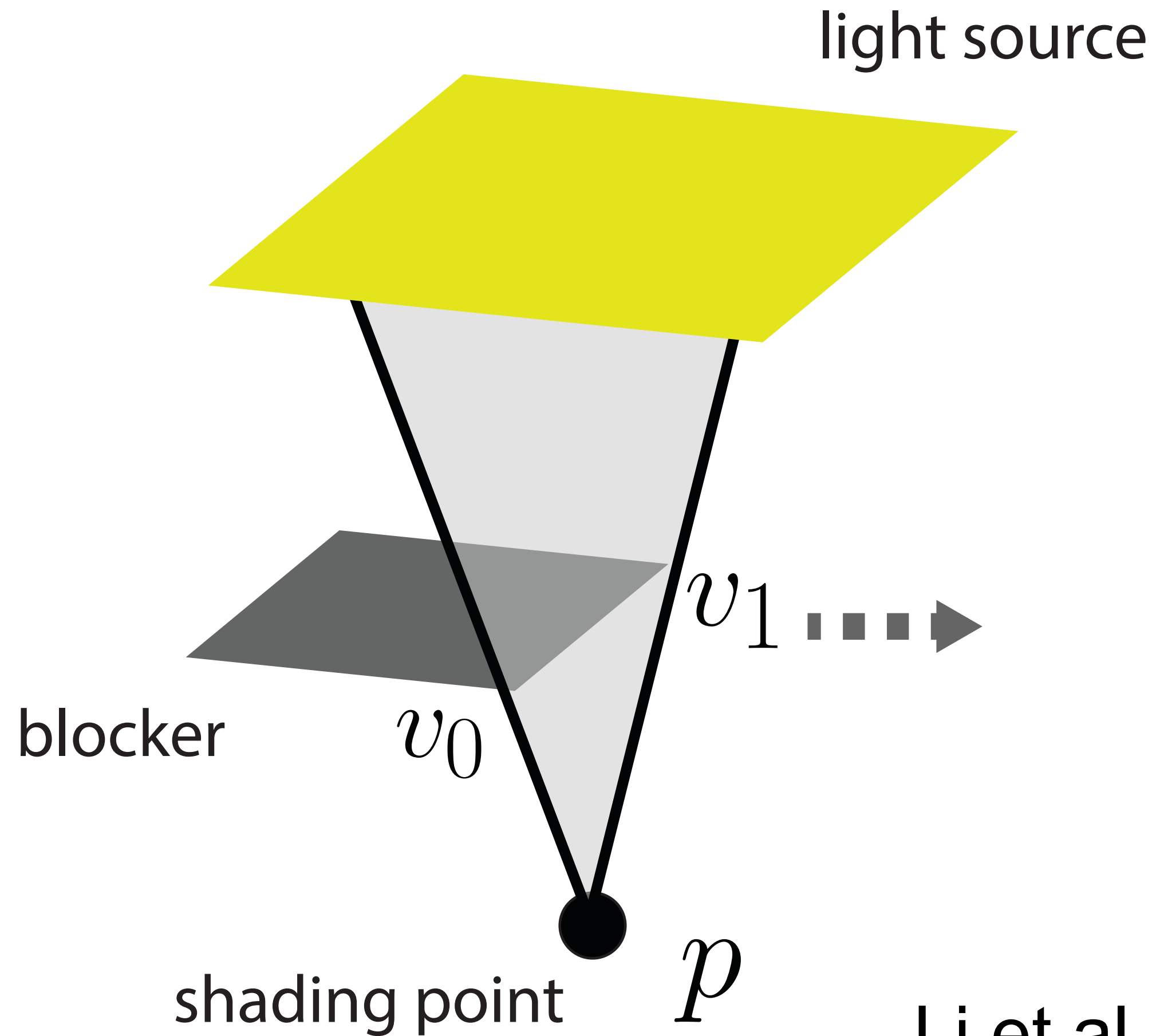


negative dx



positive dx

- 3D ray tracing and edge sampling
- camera
- spatially-varying shading
- differentiating PDFs in interior derivatives
- stratification



$$\int (f_- - f_+) (n \cdot v) dt$$

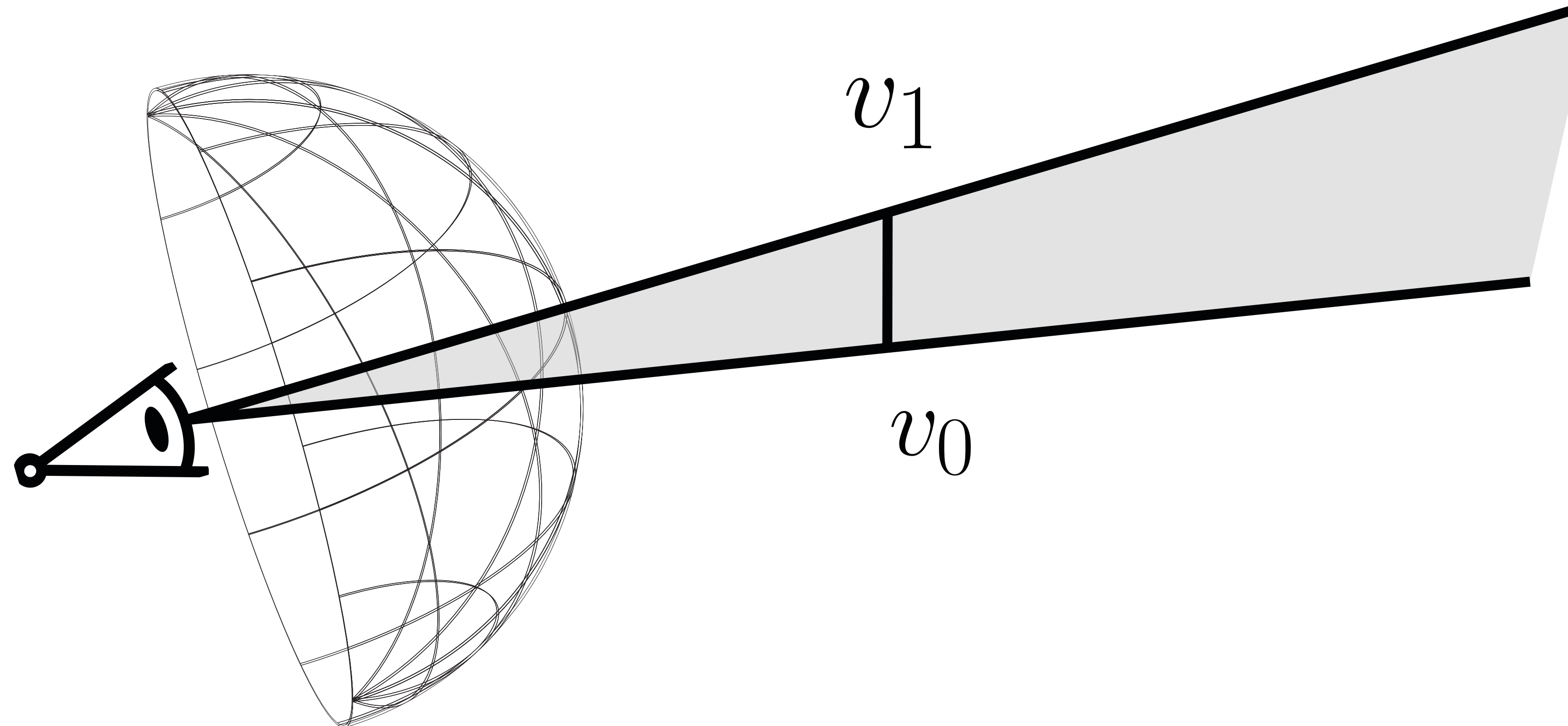
what are these?

Li et al. 2018 & Zhang et al. 2019 derived the equations

implementation at

https://github.com/BachiLi/diffrender_tutorials

- linear projective cameras: a preprocessing pass
- other cameras: use the 3D formula and backprop to camera parameters
 - also works for defocus blur



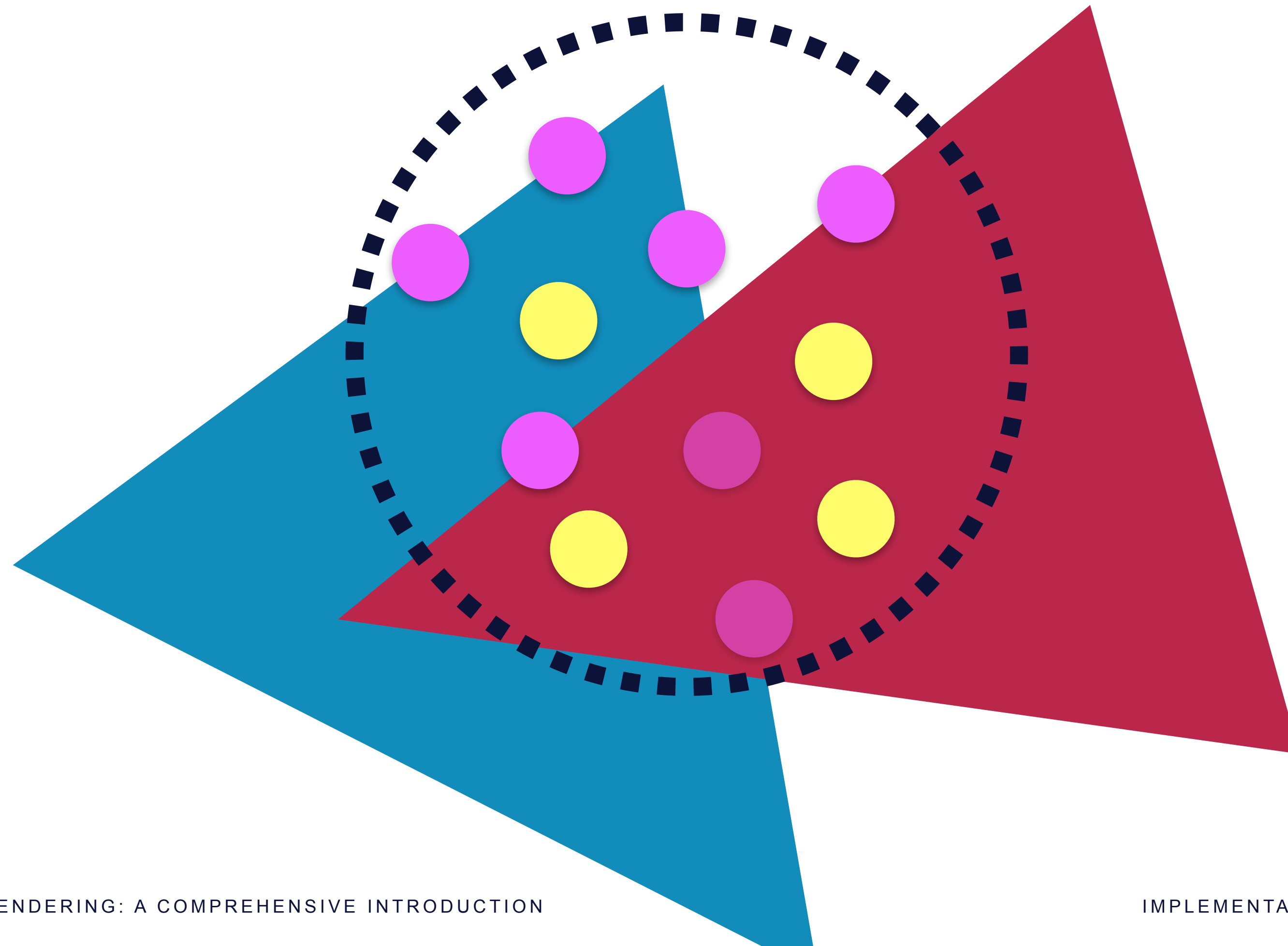
- Should be handled in the interior derivatives
- Use a smooth texture reconstruction filter (e.g., trilinear interpolation)
 - mipmapping is extremely important for variance reduction

```
void compute_interior_derivatives(/*...*/) {  
    // ...  
    for (int y = 0; y < adjoint.height; y++) { // for each pixel  
        for (int x = 0; x < adjoint.width; x++) {  
            for (int dy = 0; dy < sqrt_num_samples; dy++) { // for each subpixel  
                for (int dx = 0; dx < sqrt_num_samples; dx++) {  
                    // ...  
                    int hit_index = -1;  
                    raytrace(mesh, screen_pos, &hit_index);  
                    if (hit_index != -1) {  
                        // scatter to the gradient buffer  
                        d_colors[hit_index] +=  
                            adjoint.color[y * adjoint.width + x] / samples_per_pixel;  
                    }  
                }  
            }  
        }  
    }  
}
```

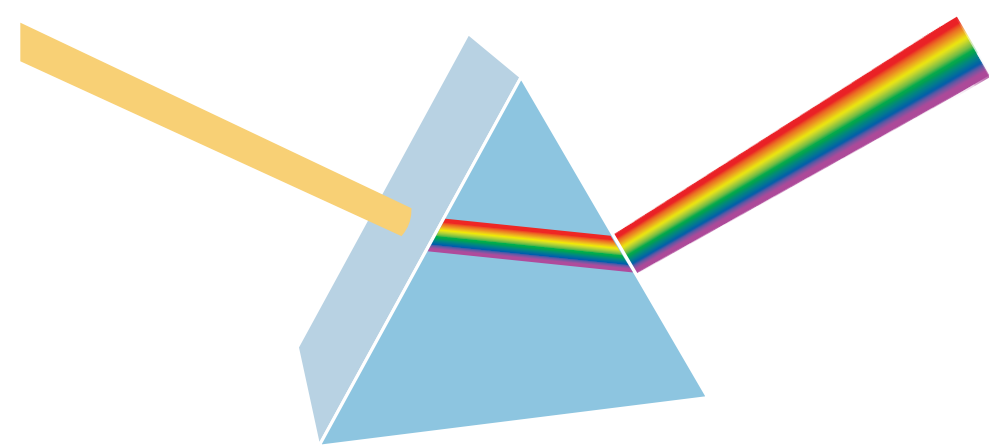
- PDF in importance sampling = Jacobian for reparametrization
- The Monte Carlo estimator is correct whether you backprop through the PDF or not
 - unclear which one has lower variance, pick the one that is more computationally convenient

$$\int \nabla_{\theta} f(x; \theta) dx \quad x = g(y)$$
$$= \int \left(\nabla_{\theta} f(x; \theta) \right) \Big|_{x \rightarrow g(y)} \frac{dx}{dy} dy \quad \textit{differentiate} \rightarrow \textit{reparametrize}$$
$$= \int \nabla_{\theta} \left(f(x; \theta) \Big|_{x \rightarrow g(y)} \frac{dx}{dy} \right) dy \quad \textit{reparametrize} \rightarrow \textit{differentiate}$$

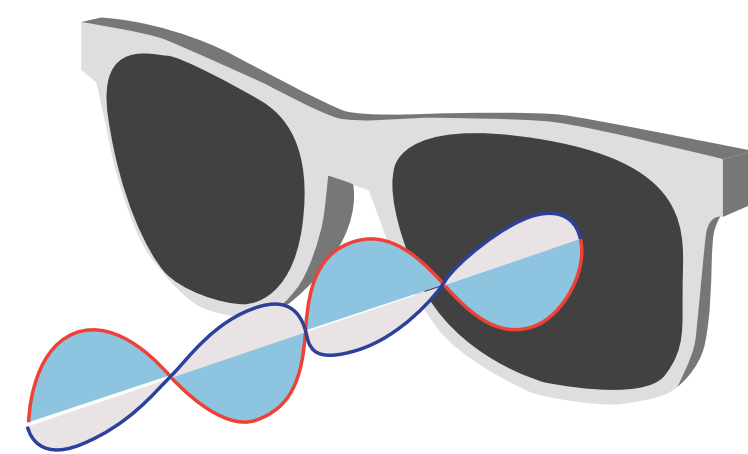
- low discrepancy samples, stratified sampling, etc can all be used
- stratifying differentiable rendering is an unsolved problem



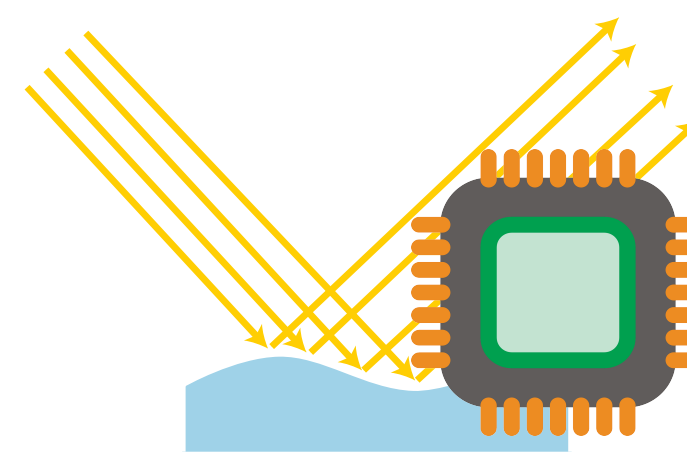
- **Mitsuba** is an open source physically-based rendering system
 - Common platform for rendering research (many papers at SIGGRAPH (Asia), EG, EGSR, etc., build on it)
 - ~ 120 plugins (highly modular architecture)
 - ~ 180'000 lines of C++ code
- **BUT:** did *not* provide a number of key features:



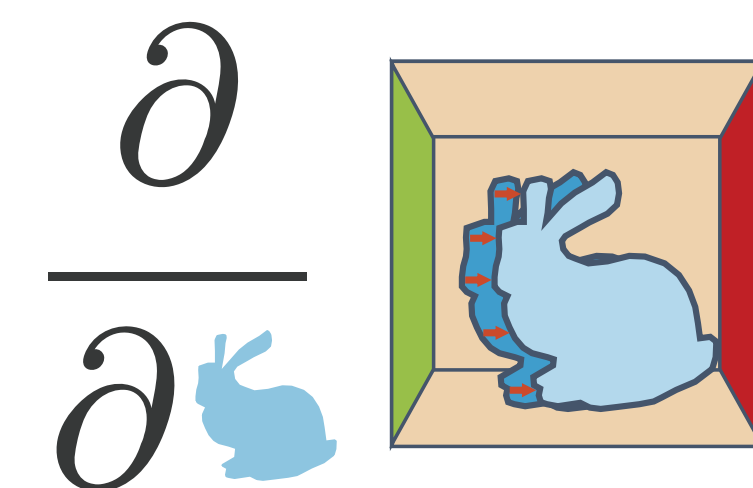
Spectral rendering



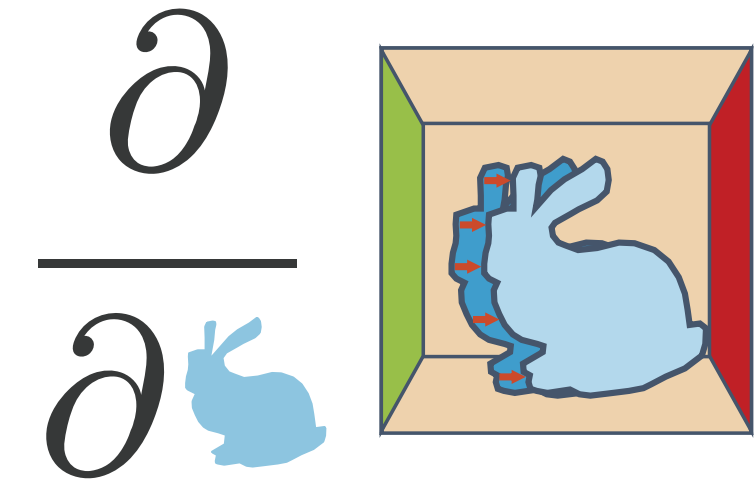
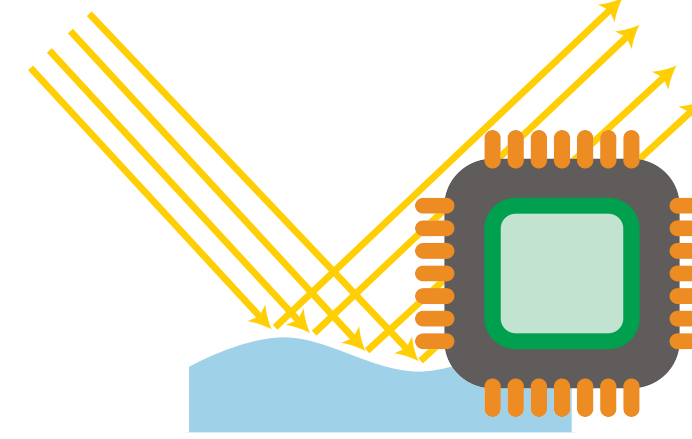
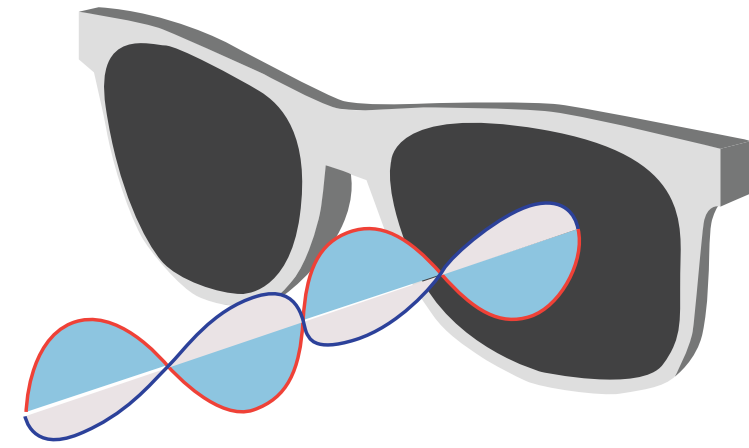
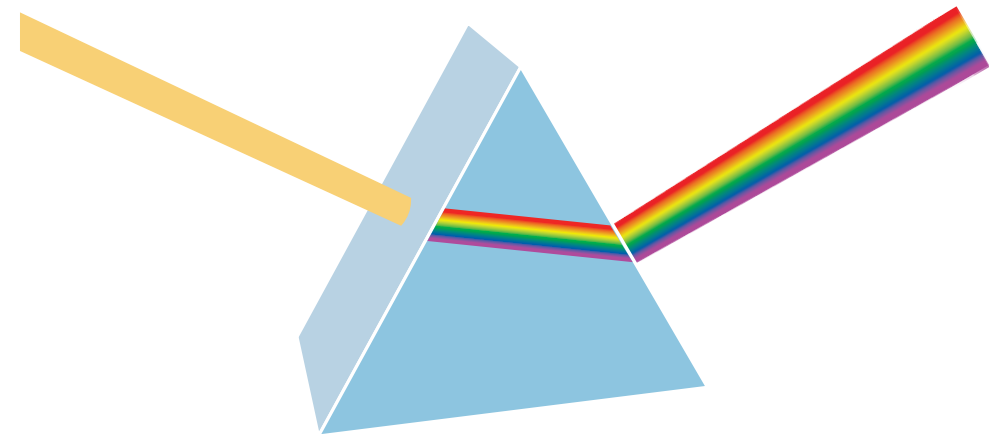
Polarization



Vectorization



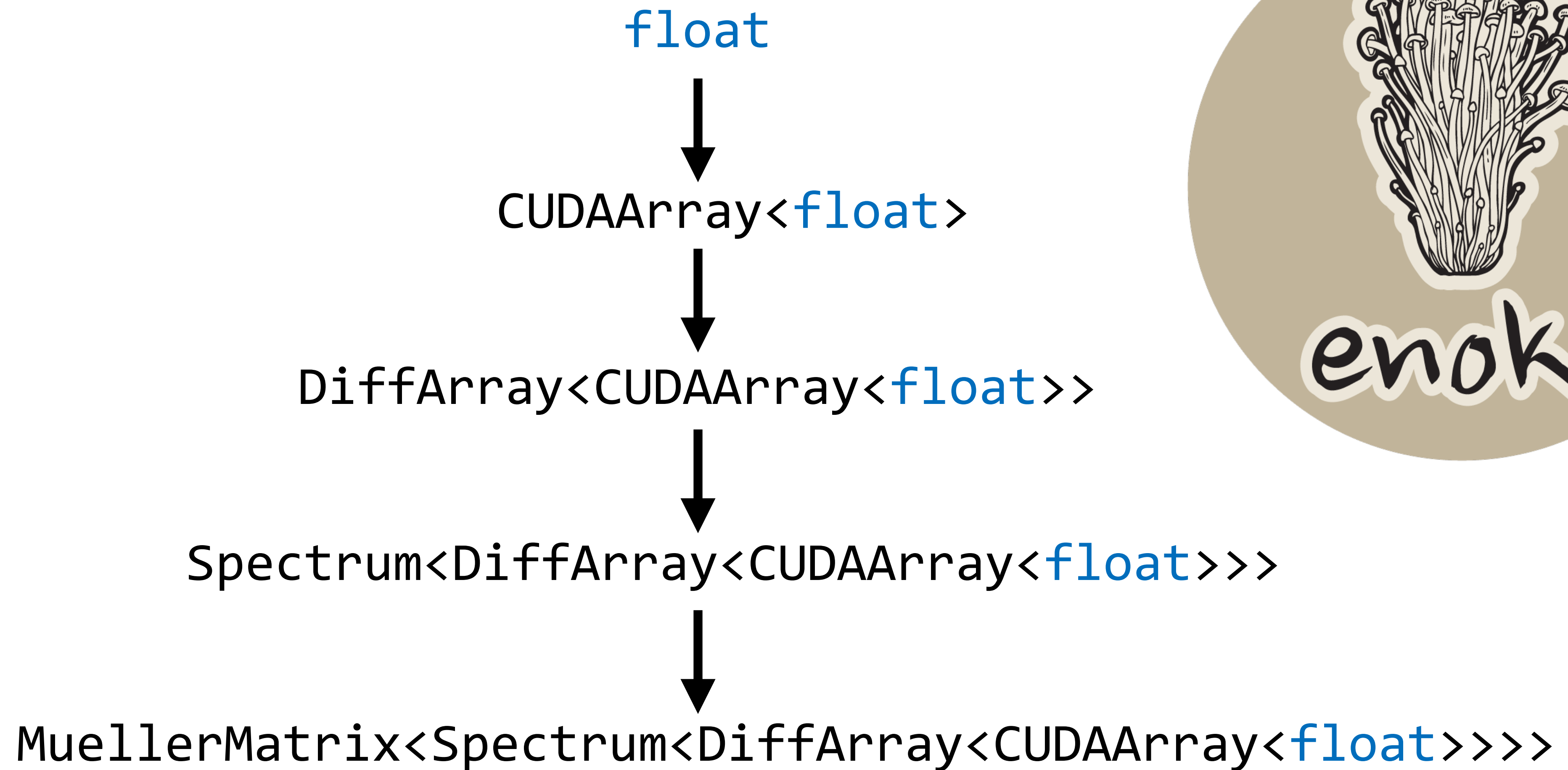
Differentiable rendering

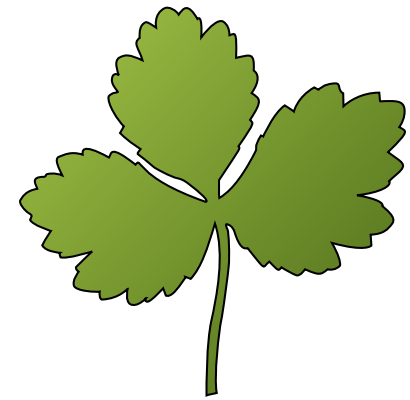


- **Hack Mitsuba to support all of these features?**
 - Not a good idea: each change touches almost every file of the renderer.
 - Want to support various combinations as well
- **Create new programming language for developing rendering systems?**
 - Could deal with variants using automated program transformations.
 - Don't have the manpower for such an effort.

- **Let the type system do all the hard work**
 - Write 1 generic implementation and create variants by substituting types.
- **Key C++ features that enable this**
 - Templates
 - Variadic templates
 - Compile-time computation
 - **if constexpr (...)** { }







Generic rendering algorithms

Float type

Spectrum type



Enoki
Composable array types

Generic plugins

Perspective sensor

Plastic BSDF

Rough conductor BSDF

Path tracing integrator

Area emitter

Environment emitter

Blackbody spectrum

Derived types & data structures

Intersection, sample record, etc

Float type

float, Packet<float>, DiffArray<...>

Spectrum type

Spectrum<Float, 4>, MuellerMatrix<...>

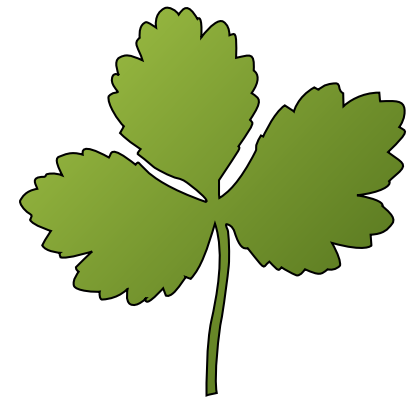
Routing layer

Scalar backend

Vector backends

CUDA backend

Autodiff backend



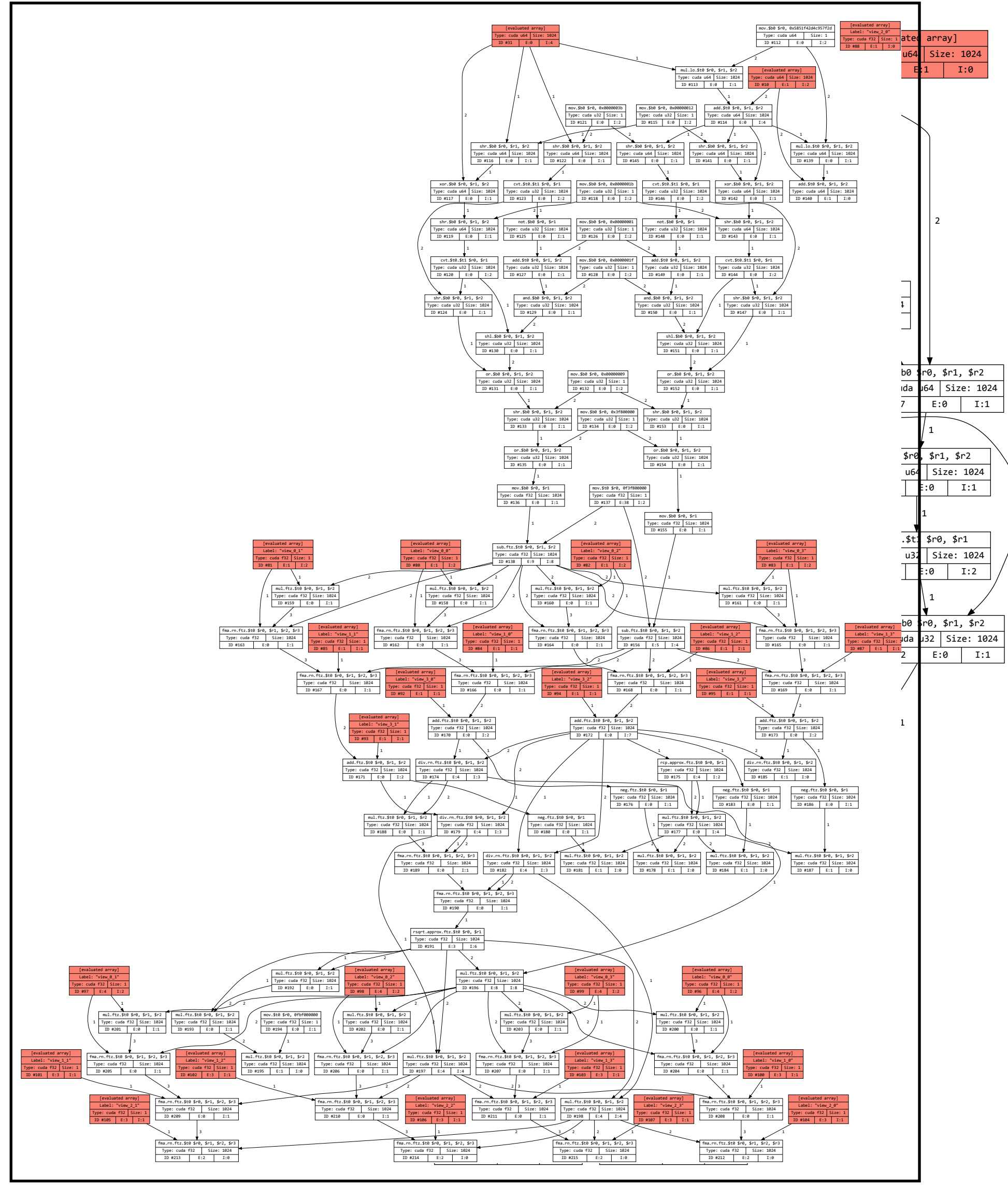
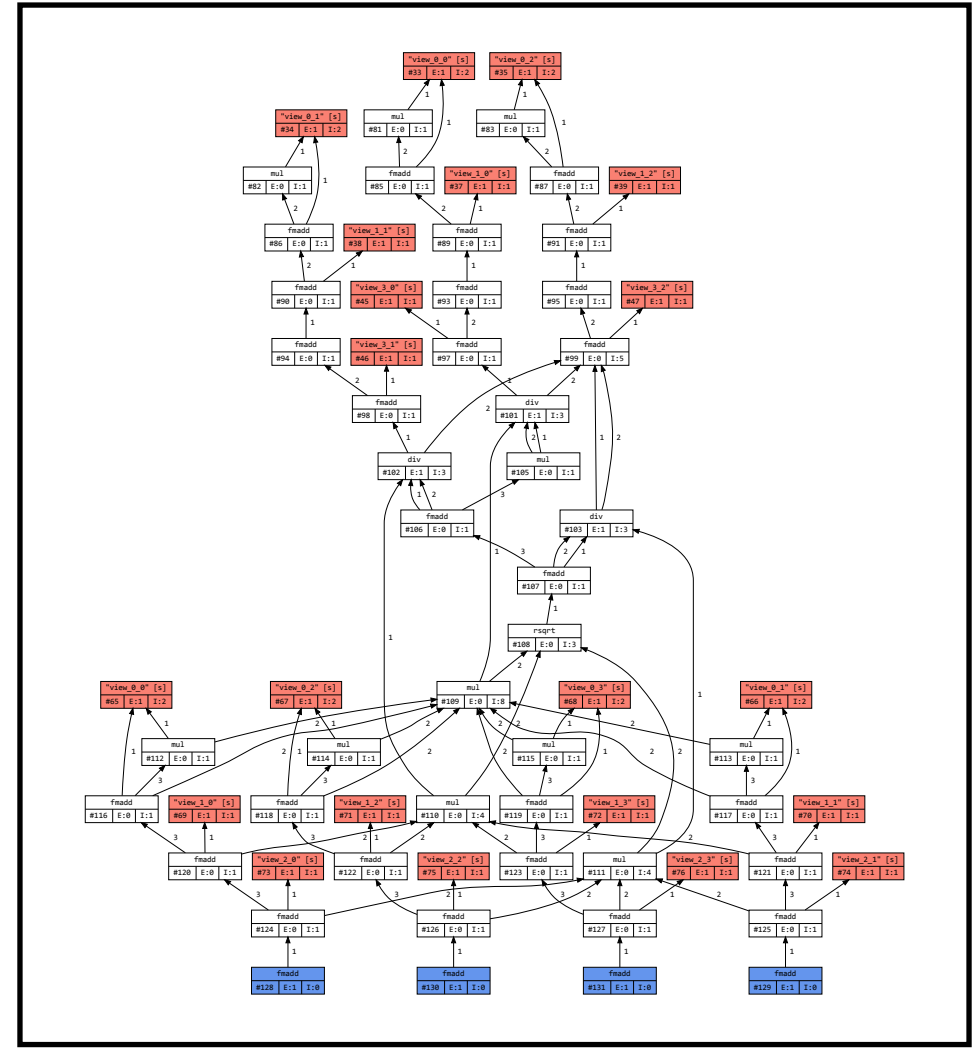
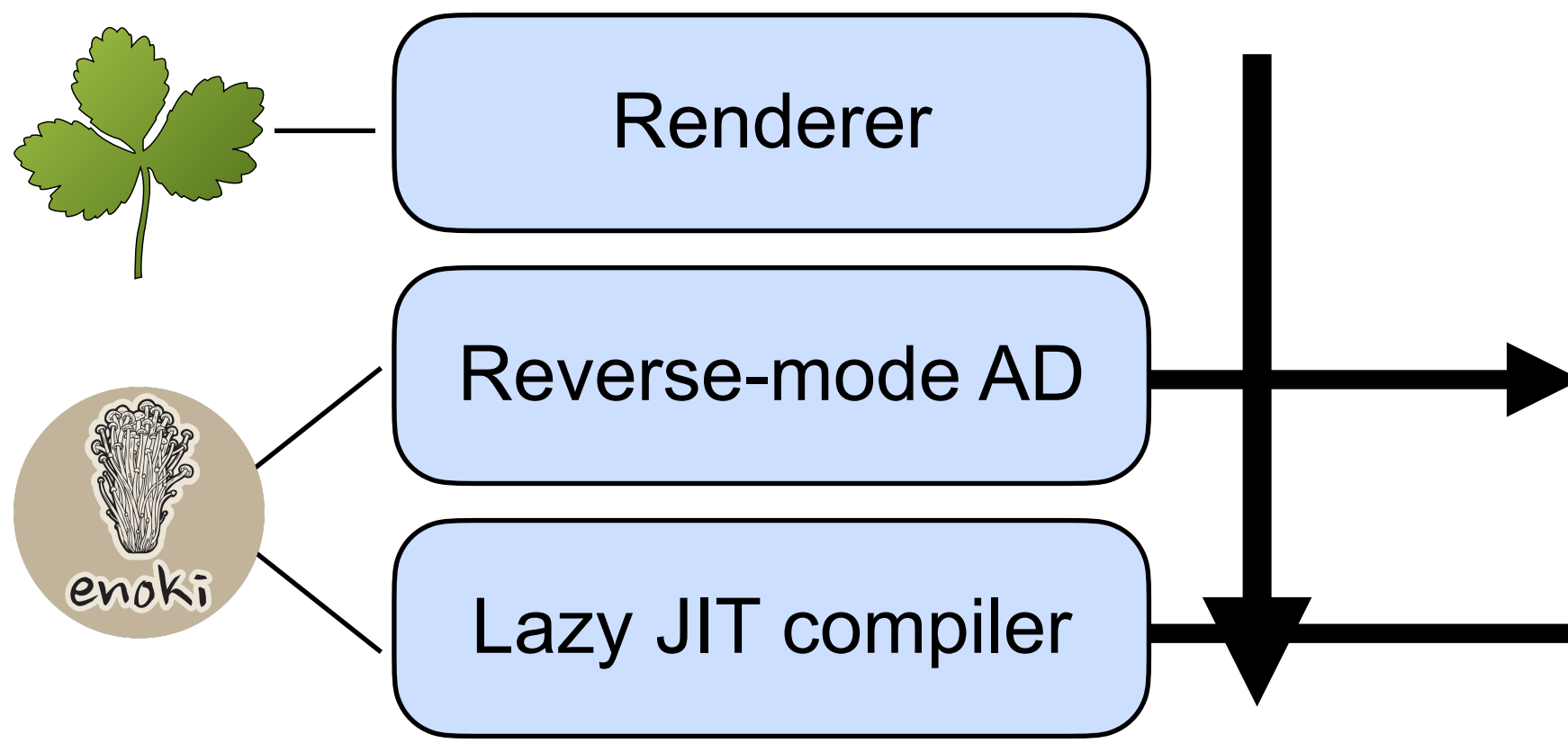
DIFFERENTIABLE RENDERING IN MITSUBA 2

```
Point2f sample = sampler->next_2d();
```

```
Ray3f ray = camera->sample_ray(sample);
```

```
SurfaceInteraction3f si = scene->ray_intersect(ray)
```

```
BSDFSample3f bsdf_sample = si.bsdf->sample(sampler.next_2d())
```



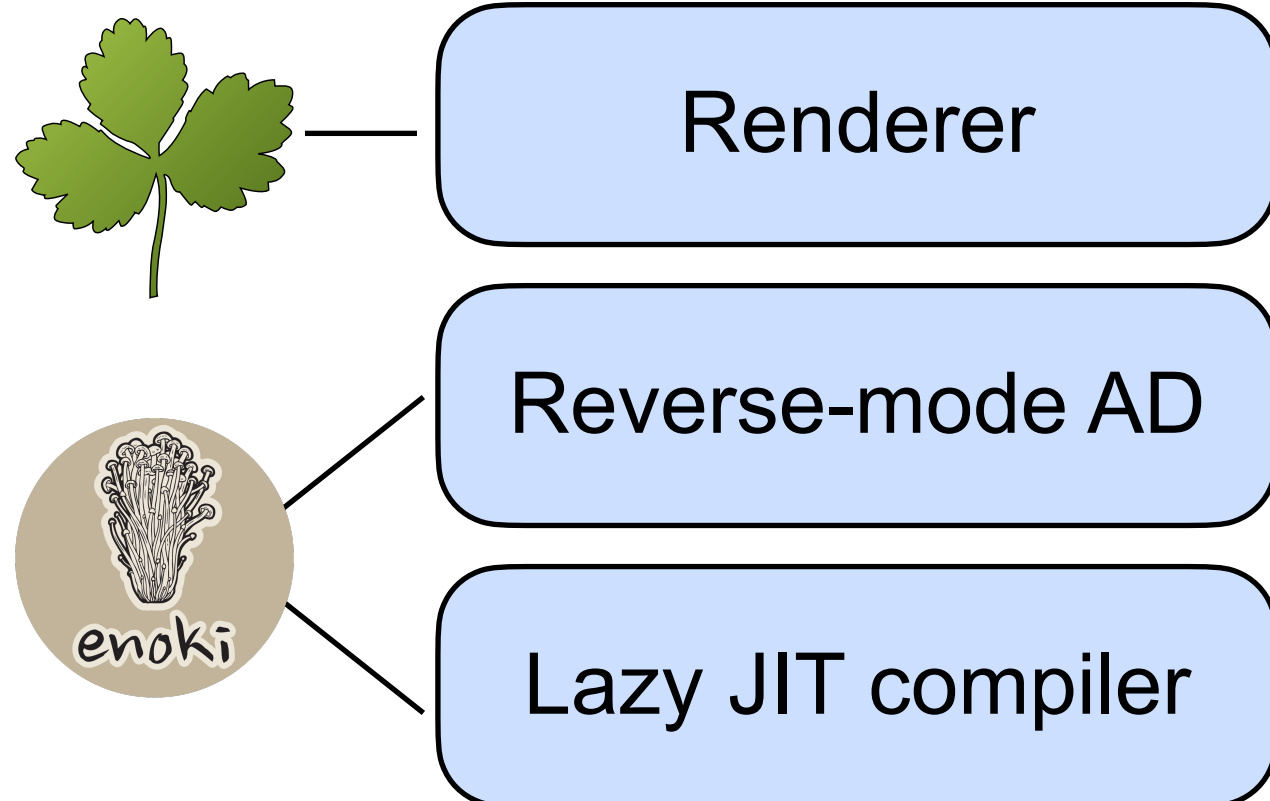

```
Point2f sample = sampler->next_2d();
```

```
Ray3f ray = camera->sample_ray(sample);
```

```
SurfaceInteraction3f si = scene->ray_intersect(ray)
```

```
BSDFSample3f bsdf_sample = si.bsdf->sample(sampler.next_2d())
```

- Compilation is *fast* (~100 us) (just hash table lookups + string concatenation)
- PTX (CUDA), soon: LLVM (CPU)
- Caches compiled kernels
- Can prototype rendering code in Jupyter notebooks with reasonable performance.



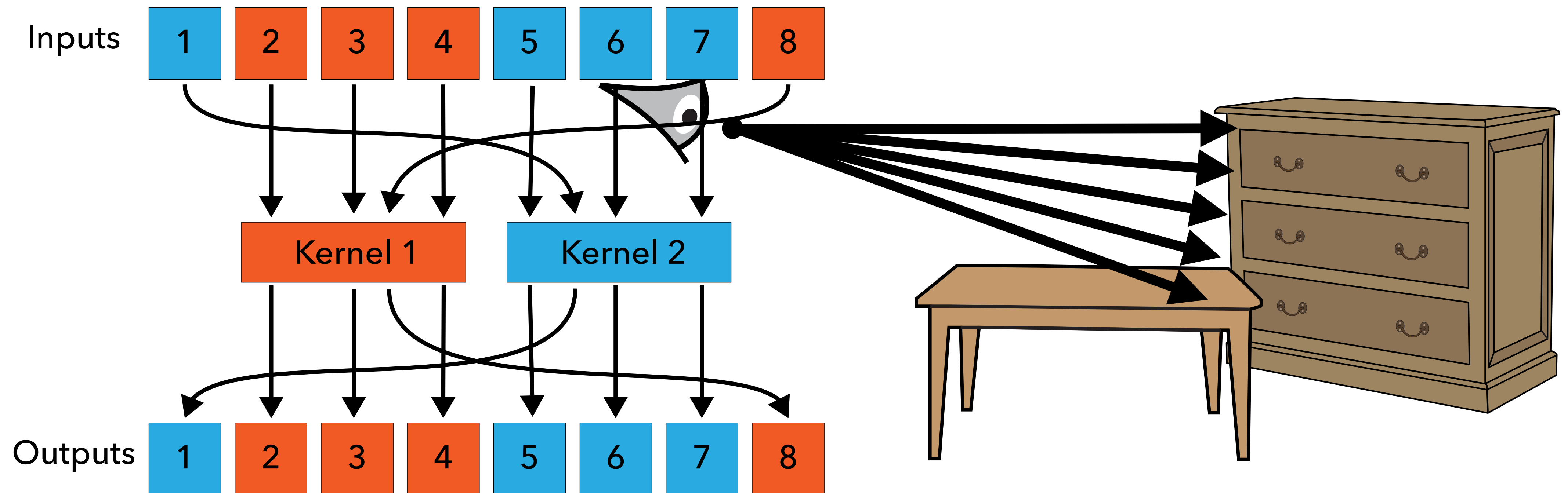
DIFFERENTIABLE RENDERING IN MITSUBA 2

```
Point2f sample = sampler->next_2d();
```

```
Ray3f ray = camera->sample_ray(sample);
```

```
SurfaceInteraction3f si = scene->ray_intersect(ray)
```

```
BSDFSample3f bsdf_sample = si.bsdf->sample(sampler.next_2d())
```




```
import enoki as ek
import Mitsuba
mitsuba.set_variant('gpu_autodiff_rgb')
```

```
from Mitsuba.core import Float, Thread
from Mitsuba.core.xml import load_file
from Mitsuba.python.util import traverse
from Mitsuba.python.autodiff import render, write_bitmap, Adam
```

```
# Load example scene
Thread.thread().file_resolver().append('bunny')
scene = load_file('bunny/bunny.xml')
```

```
# Find differentiable scene parameters
params = traverse(scene)
```

```
opt = Adam(params, lr=.02)
```

```
for it in range(100):
```

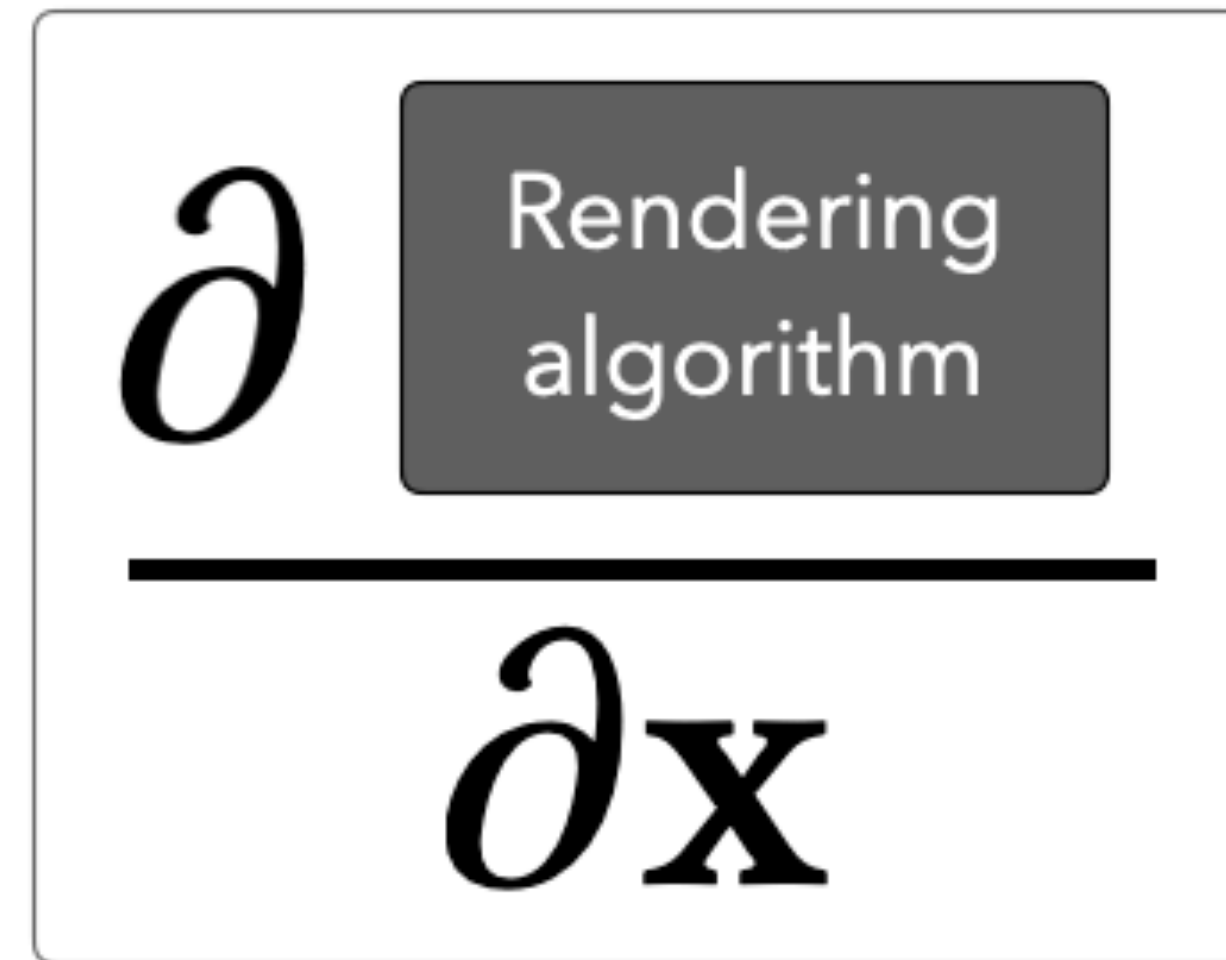
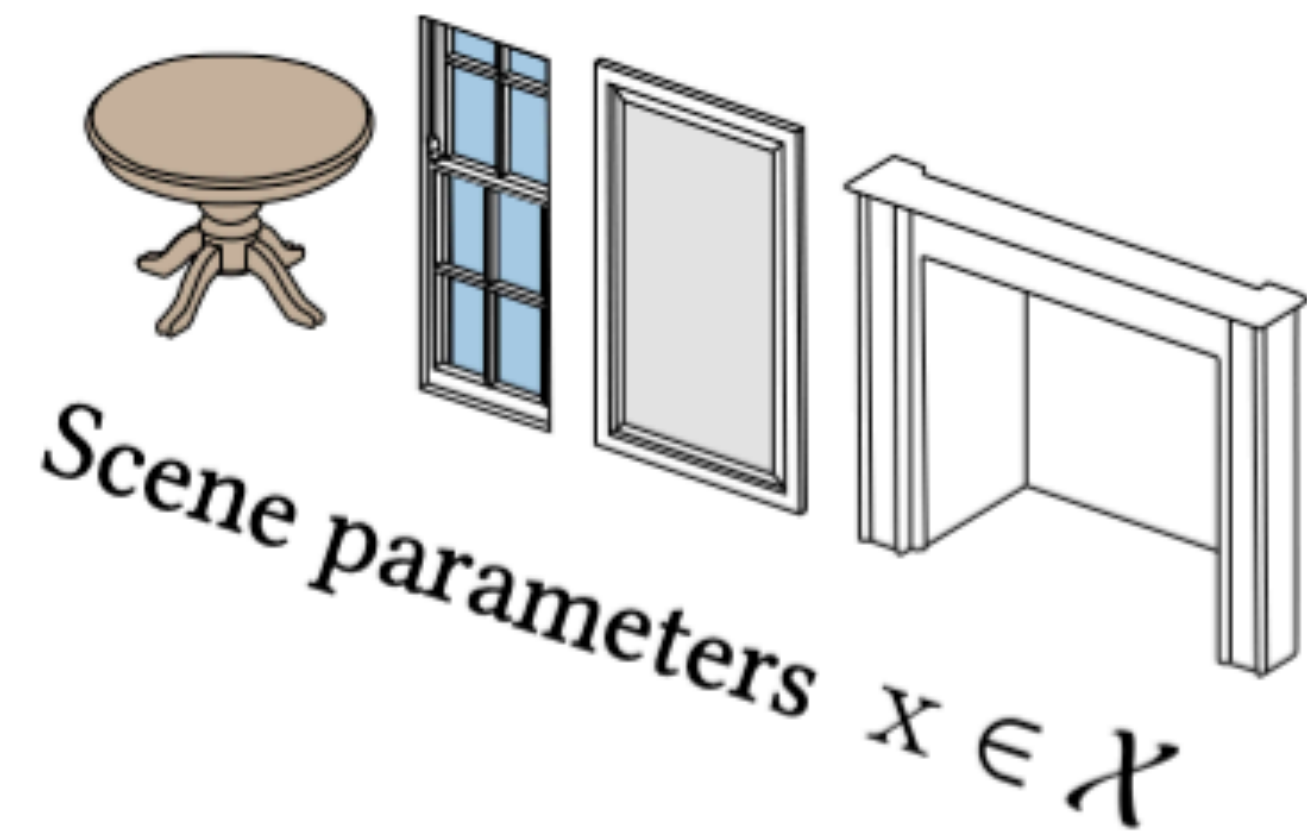
```
    image = render(scene, optimizer=opt, unbiased=True, spp=1)
```

```
    write_bitmap('out_%03i.png' % it, image, crop_size)
```

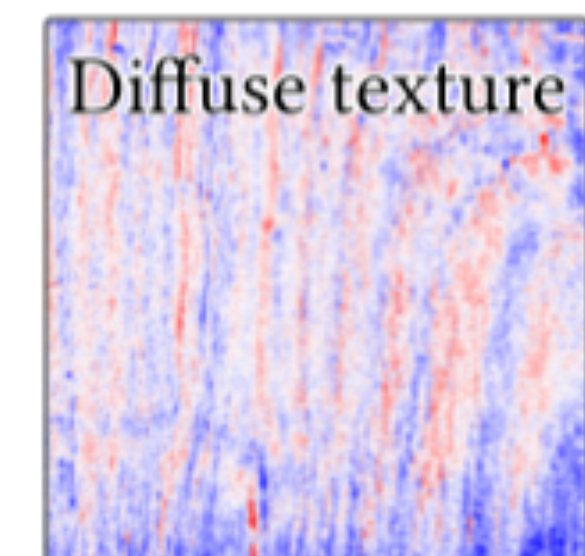
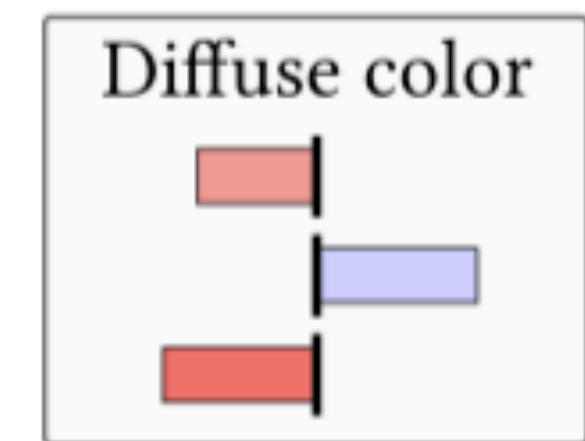
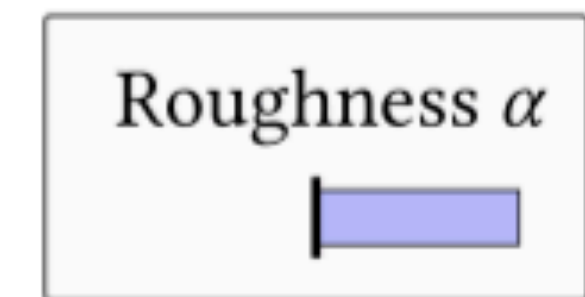
```
    ob_val = ek.hsum(ek.sqr(image - image_ref)) / len(image)
```

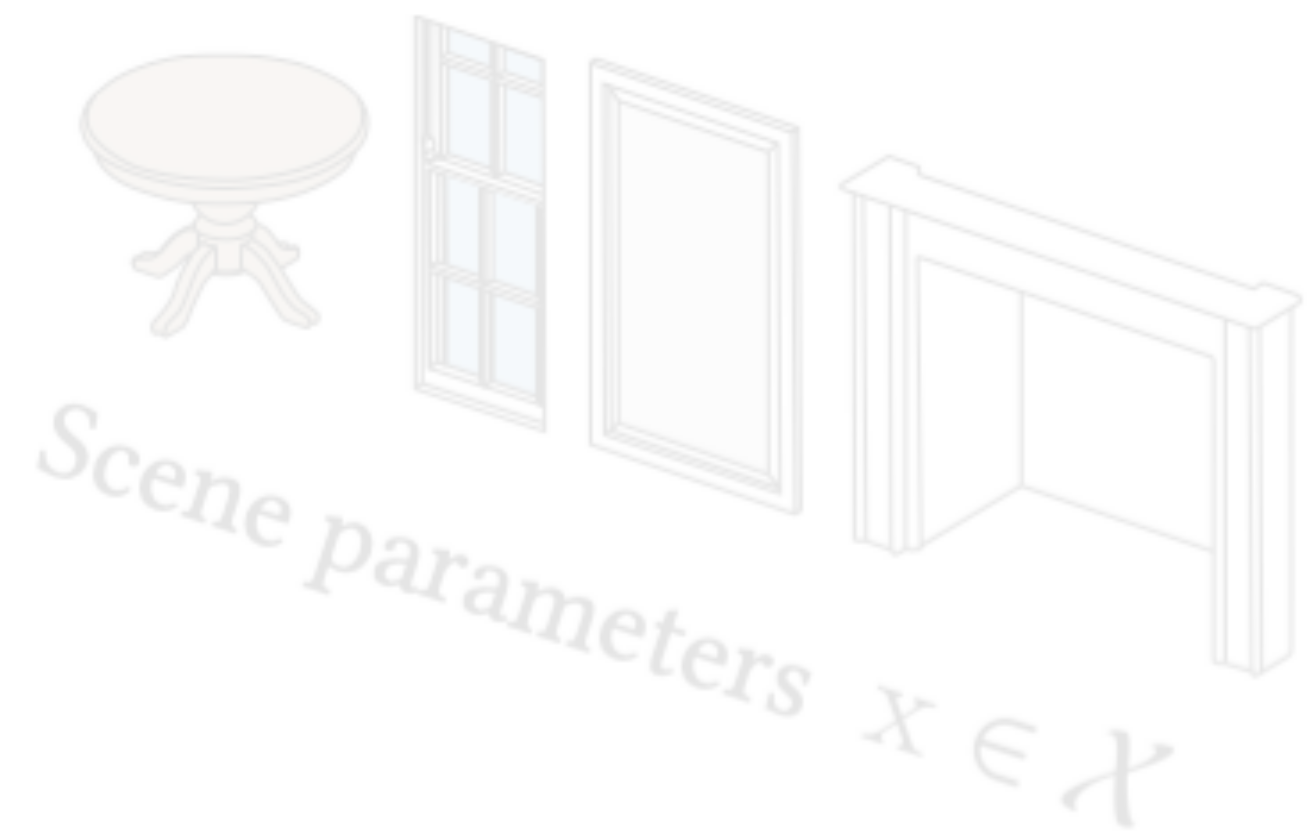
```
    ek.backward(ob_val)
```

```
    opt.step()
```

Gradients





OUT OF MEMORY

Gradients

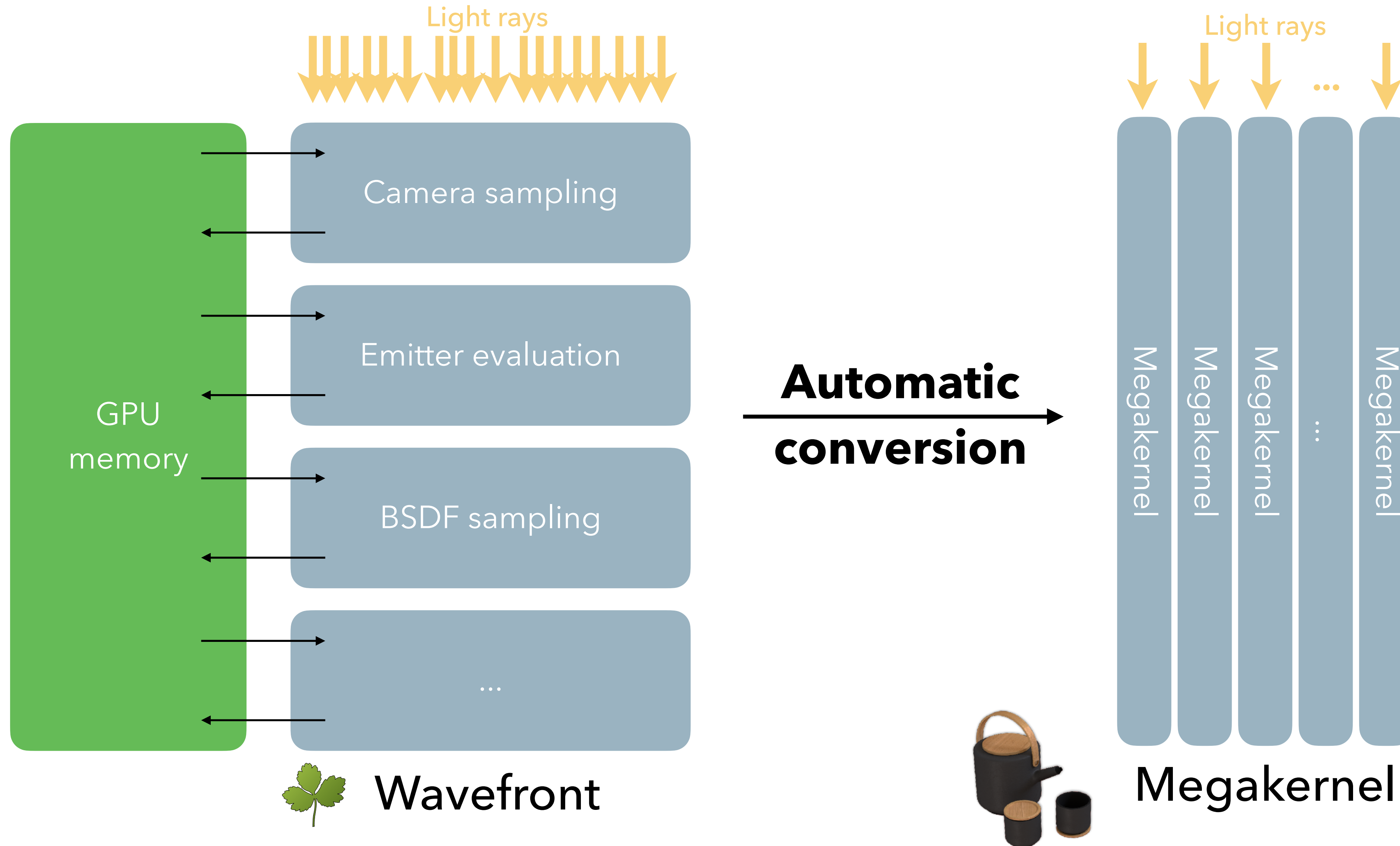
Shininess α

Diffuse color

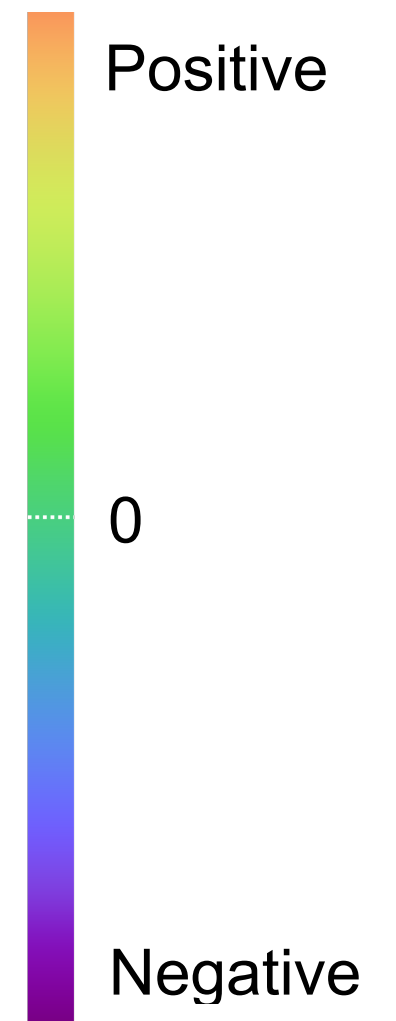
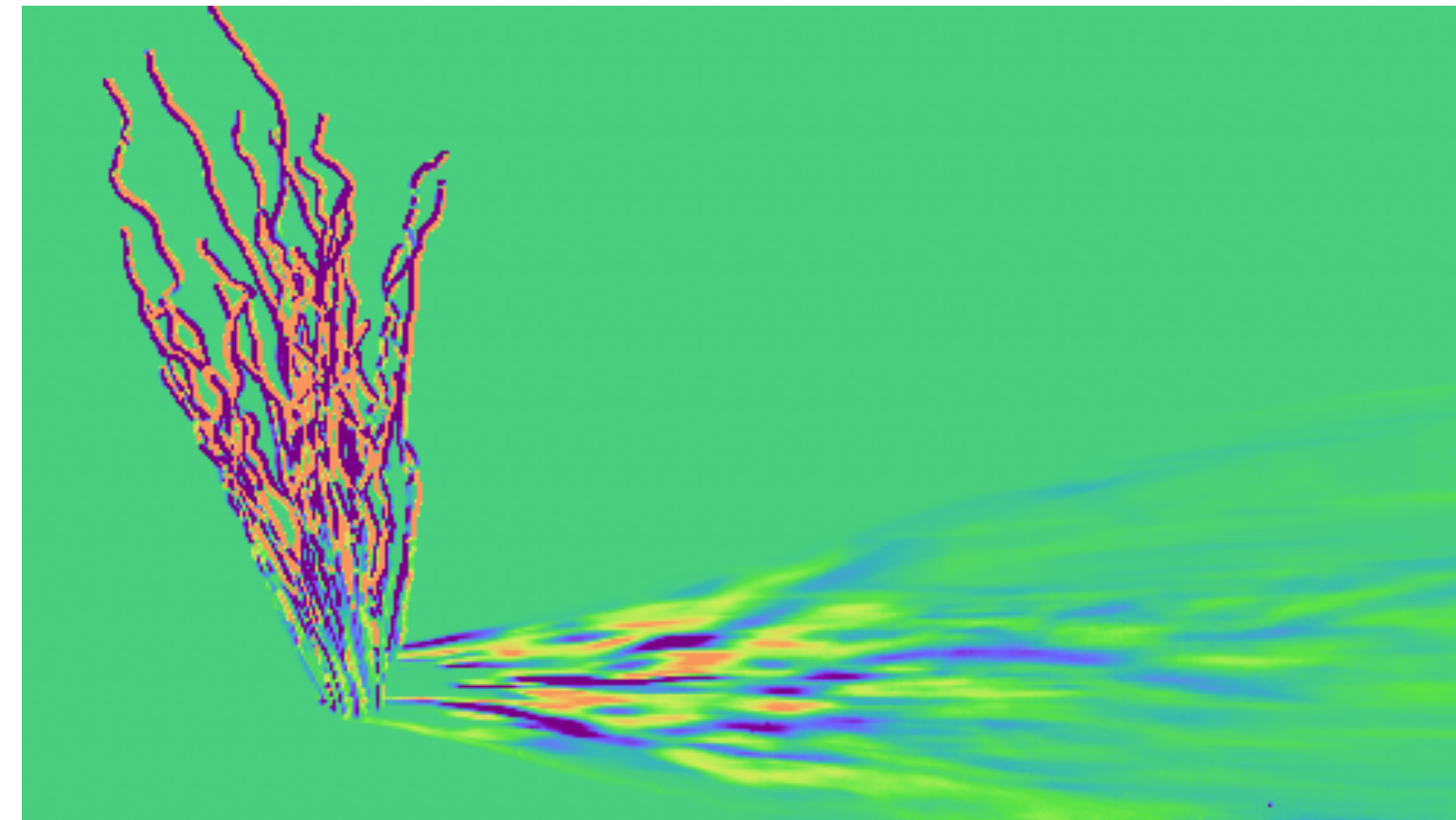
Diffuse texture

Reverse mode AD

WAVEFRONT VS MEGAKERNEL



Parameter: rotation angle of the object



- Implementing differentiable *direct illumination* using the path-space formulation

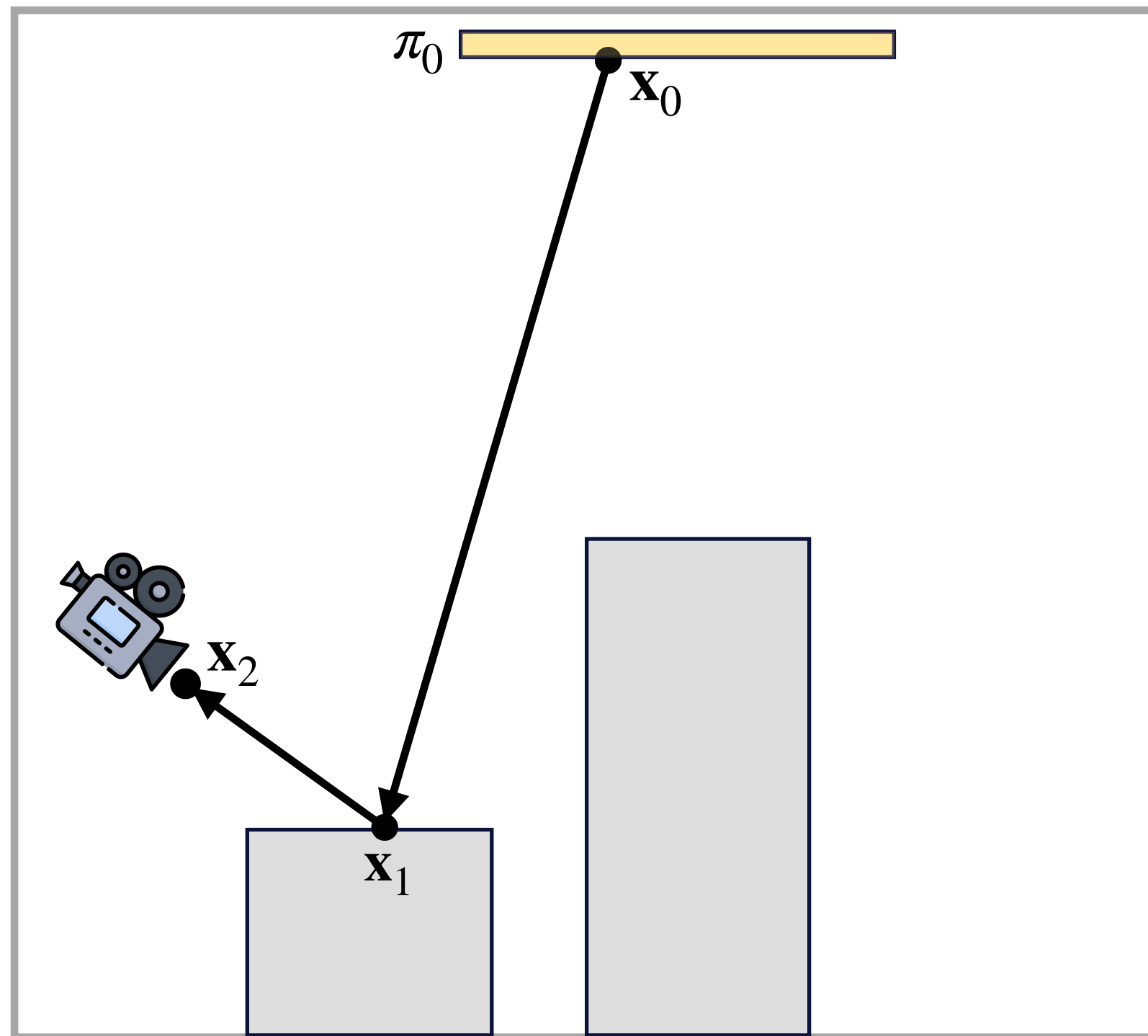
Still nontrivial with complex geometry & motion!

Spatial-form direct-illumination integral

$$I_j = \int_{\mathcal{M}(\pi)^3} \underbrace{f_j(\mathbf{x}_0 \rightarrow \mathbf{x}_1 \rightarrow \mathbf{x}_2)}_{= \bar{\mathbf{x}}} d\mu(\bar{\mathbf{x}})$$

f_j : measurement contribution for pixel j , \mathcal{M} : scene geometry

π controls the position of the area light

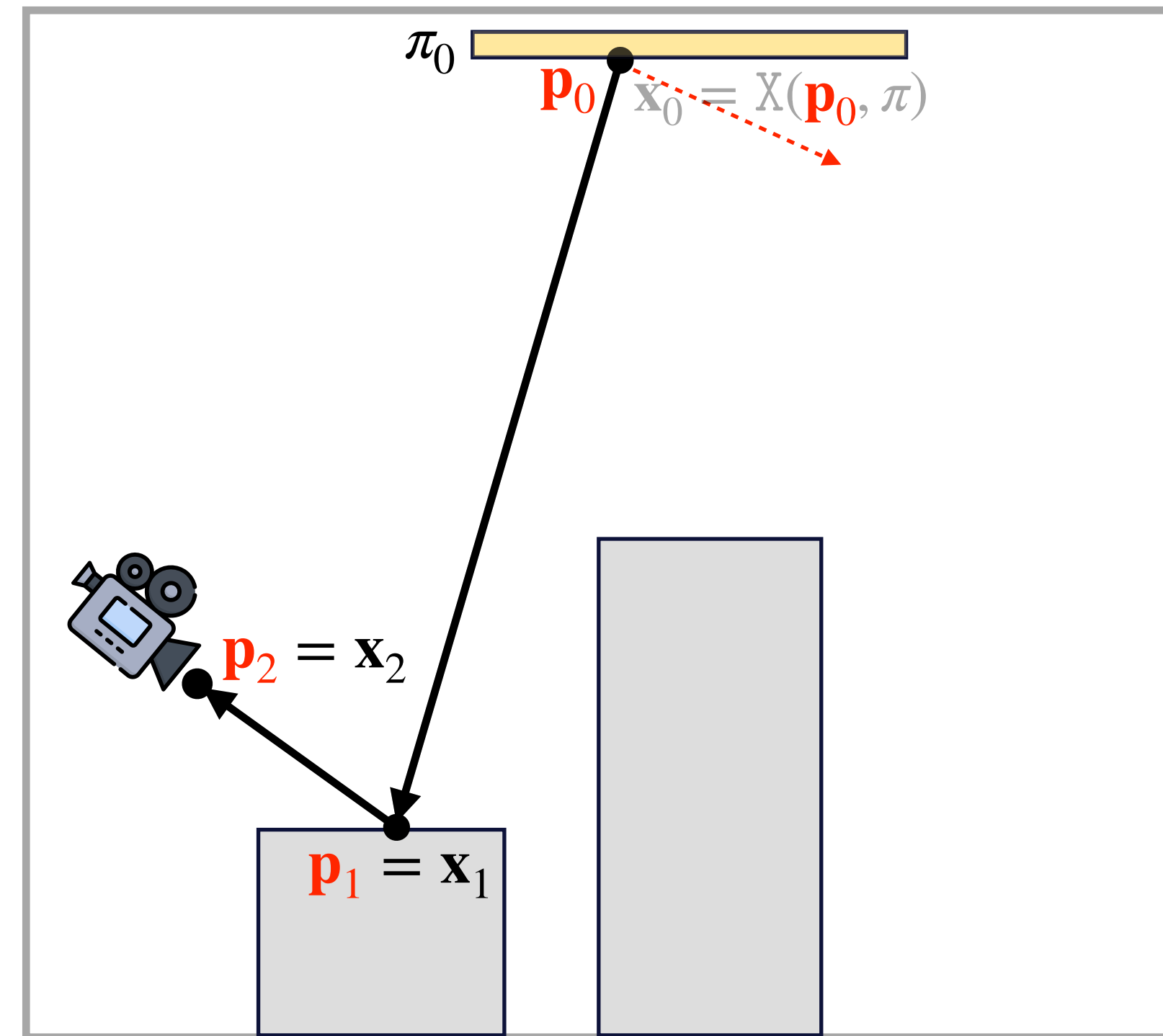


Material-form direct-illumination integral

$$I_j = \int_{\mathcal{M}_0^3} \underbrace{f_j(\mathbf{x}_0 \rightarrow \mathbf{x}_1 \rightarrow \mathbf{x}_2)}_{= f_j(\bar{\mathbf{p}})} \left| \frac{d\mu(\bar{\mathbf{x}})}{d\mu(\bar{\mathbf{p}})} \right| d\mu(\bar{\mathbf{p}})$$

Change of variable: $\mathbf{x}_i = X(\mathbf{p}_i, \pi)$ with $\mathcal{M}_0 = \mathcal{M}(\pi_0)$

π controls the position of the area light

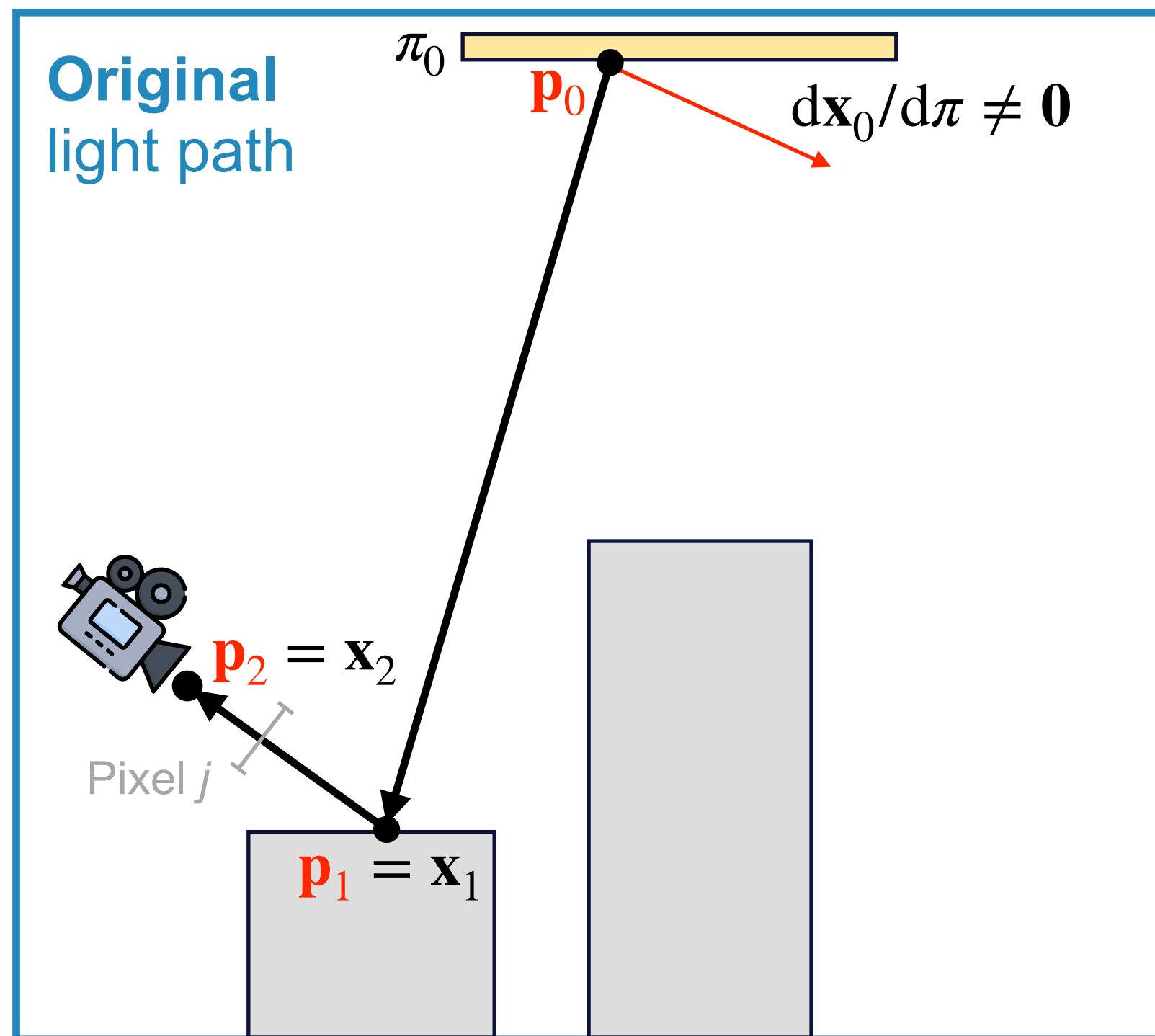


Material-form direct-illumination integral

$$I_j = \int_{\mathcal{M}_0^3} \underbrace{f_j(\mathbf{x}_0 \rightarrow \mathbf{x}_1 \rightarrow \mathbf{x}_2)}_{= f_j(\bar{\mathbf{p}})} \left| \frac{d\mu(\bar{\mathbf{x}})}{d\mu(\bar{\mathbf{p}})} \right| d\mu(\bar{\mathbf{p}})$$

Change of variable: $\mathbf{x}_i = X(\mathbf{p}_i, \pi)$ with $\mathcal{M}_0 = \mathcal{M}(\pi_0)$

π controls the position of the area light



Material-form differential direct-illumination integral

$$\frac{dI_j}{d\pi} = \int_{\mathcal{M}_0^3} \frac{df_j}{d\pi}(\bar{\mathbf{p}}) d\mu(\bar{\mathbf{p}}) + \int_{\partial\mathcal{M}_0^3} g_j(\bar{\mathbf{p}}) d\mu'(\bar{\mathbf{p}})$$

Interior integral Boundary integral

- Consider the problem of estimating $dI_j/d\pi \big|_{\pi=\pi_0}$
 - \mathbf{x}_0 equals \mathbf{p}_0 in value but has nonzero derivative:

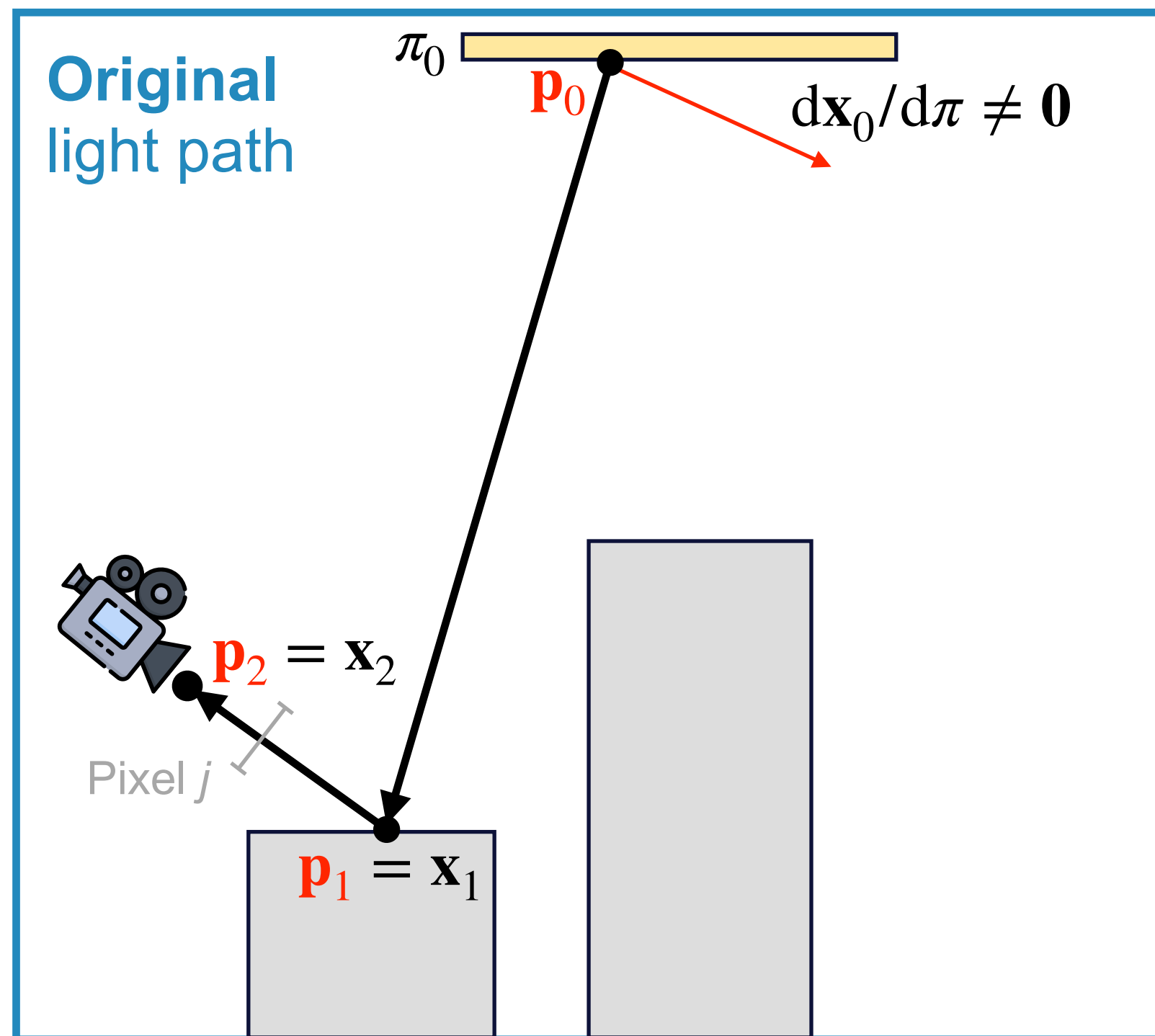
$$d\mathbf{x}_0/d\pi = dX(\mathbf{p}_0, \pi)/d\pi$$
 - This can affect $df_j(\bar{\mathbf{p}})/d\pi$ via:
 - Emission $L_e(\mathbf{x}_0 \rightarrow \mathbf{x}_1)$
 - Geometric term $G(\mathbf{x}_0 \leftrightarrow \mathbf{x}_1)$
 - BSDF $f_s(\mathbf{x}_0 \rightarrow \mathbf{x}_1 \rightarrow \mathbf{x}_2)$
 - Jacobian determinant $|dA(\mathbf{x}_0)/dA(\mathbf{p}_0)|$

Material-form direct-illumination integral

$$I_j = \int_{\mathcal{M}_0^3} \underbrace{f_j(\mathbf{x}_0 \rightarrow \mathbf{x}_1 \rightarrow \mathbf{x}_2)}_{= f_j(\bar{\mathbf{p}})} \left| \frac{d\mu(\bar{\mathbf{x}})}{d\mu(\bar{\mathbf{p}})} \right| d\mu(\bar{\mathbf{p}})$$

Change of variable: $\mathbf{x}_i = X(\mathbf{p}_i, \pi)$ with $\mathcal{M}_0 = \mathcal{M}(\pi_0)$

π controls the position of the area light



Material-form differential direct-illumination integral

$$\frac{dI_j}{d\pi} = \int_{\mathcal{M}_0^3} \frac{df_j}{d\pi}(\bar{\mathbf{p}}) d\mu(\bar{\mathbf{p}}) + \int_{\partial\mathcal{M}_0^3} g_j(\bar{\mathbf{p}}) d\mu'(\bar{\mathbf{p}})$$

Interior integral

- Consider the problem of estimating $dI_j/d\pi \big|_{\pi=\pi_0}$
- Interior integral estimated using *standard methods*:
 - Using scene geometry $\mathcal{M}_0 = \mathcal{M}(\pi_0)$
 - Sample camera ray (through pixel j) that gives $\mathbf{p}_2, \mathbf{p}_1$
 - Sample \mathbf{p}_0 using MIS (area + solid angle sampling)

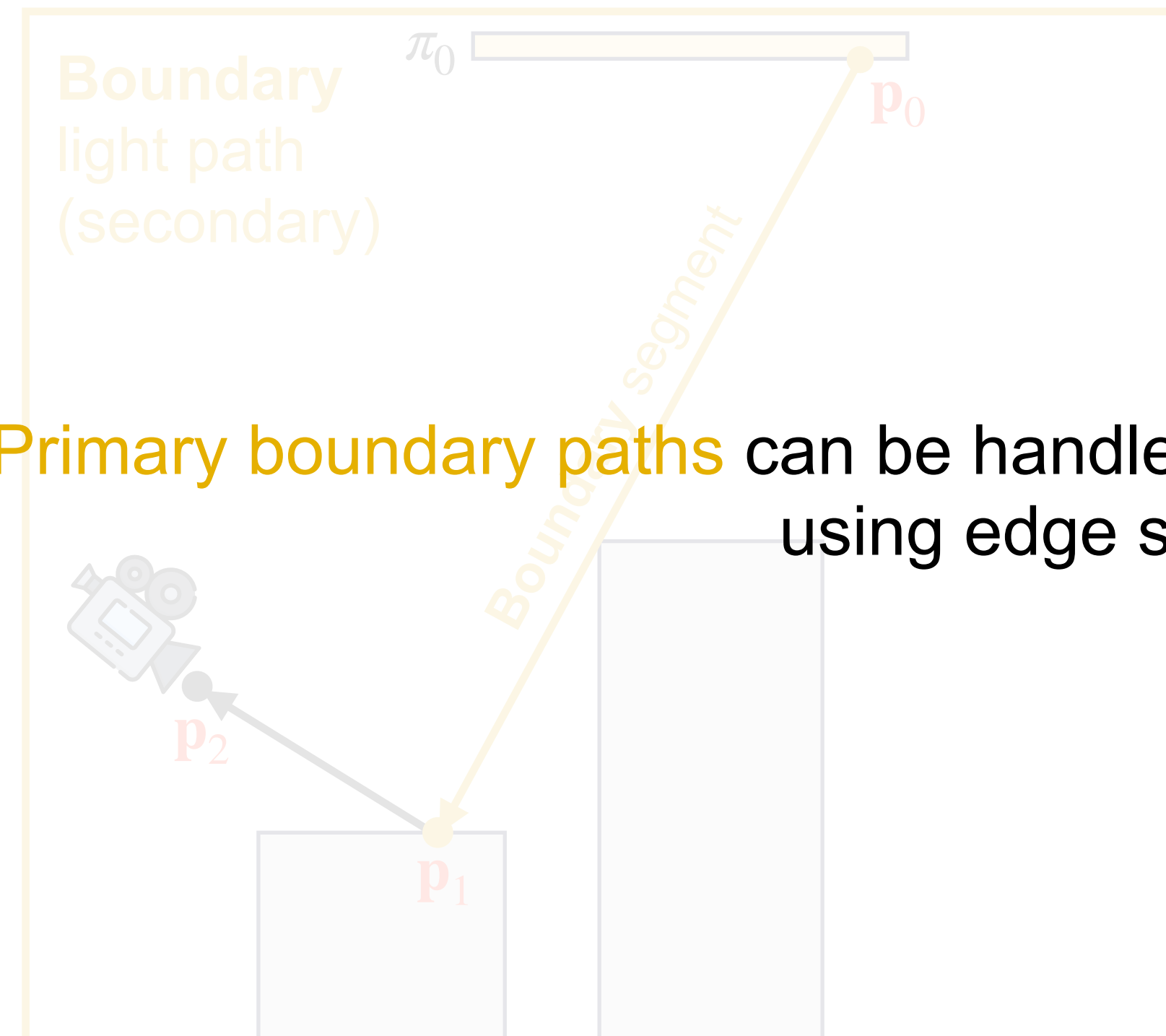
How \mathbf{p}_0 is drawn does NOT affect
 $dx_0/d\pi = dX(\mathbf{p}_0, \pi)/d\pi$

Material-form direct-illumination integral

$$I_j = \int_{\mathcal{M}_0^3} \underbrace{f_j(\mathbf{x}_0 \rightarrow \mathbf{x}_1 \rightarrow \mathbf{x}_2)}_{= f_j(\bar{\mathbf{p}})} \left| \frac{d\mu(\bar{\mathbf{x}})}{d\mu(\bar{\mathbf{p}})} \right| d\mu(\bar{\mathbf{p}})$$

Change of variable: $\mathbf{x}_i = X(\mathbf{p}_i, \pi)$ with $\mathcal{M}_0 = \mathcal{M}(\pi_0)$

π controls the position of the area light



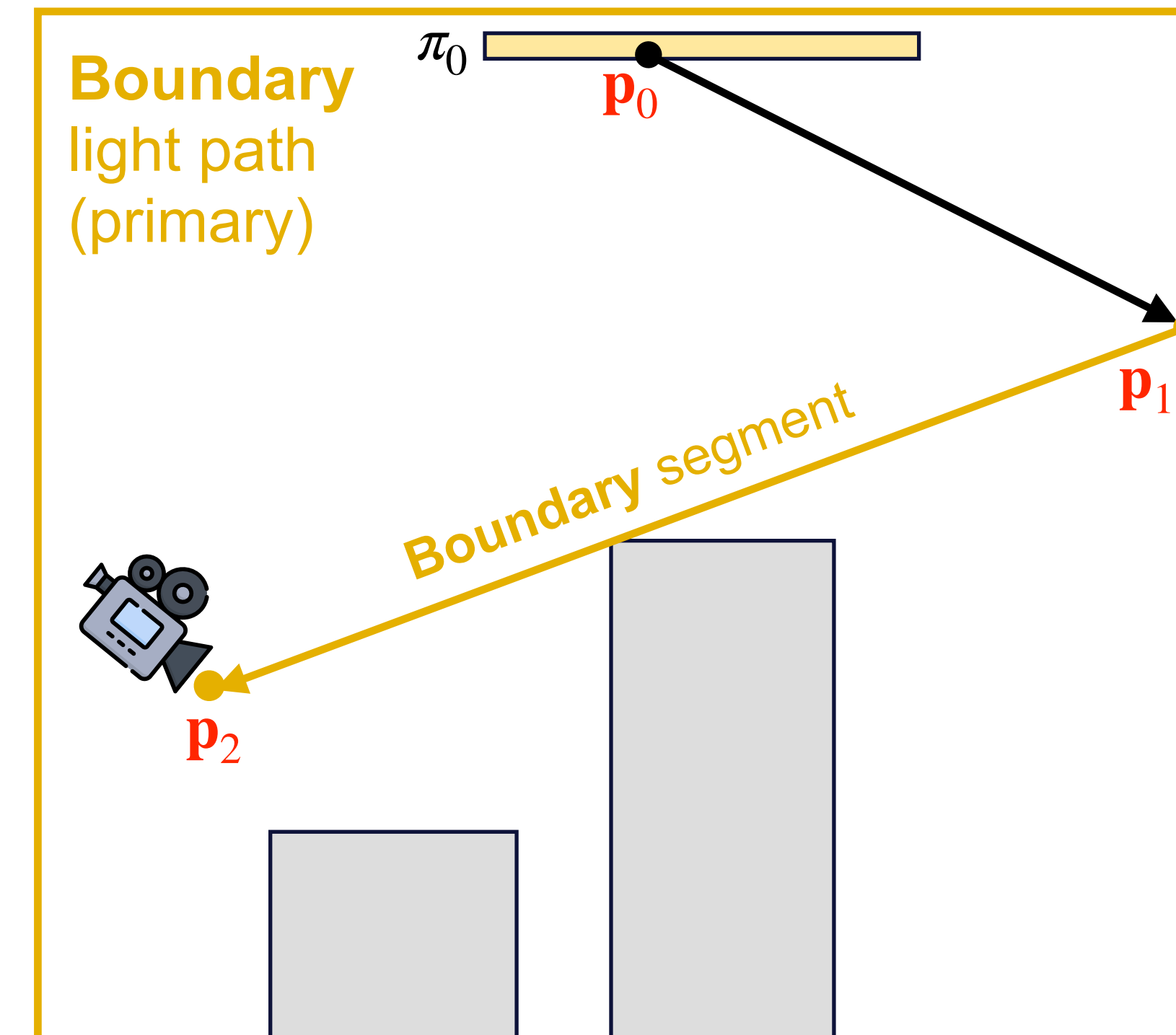
Primary boundary paths can be handled easily using edge sampling

Material-form differential direct-illumination integral

$$\frac{dI_j}{d\pi} = \int_{\mathcal{M}_0^3} \frac{df_j}{d\pi}(\bar{\mathbf{p}}) d\mu(\bar{\mathbf{p}}) + \int_{\partial\mathcal{M}_0^3} g_j(\bar{\mathbf{p}}) d\mu'(\bar{\mathbf{p}})$$

Boundary integral

π controls the position of the area light

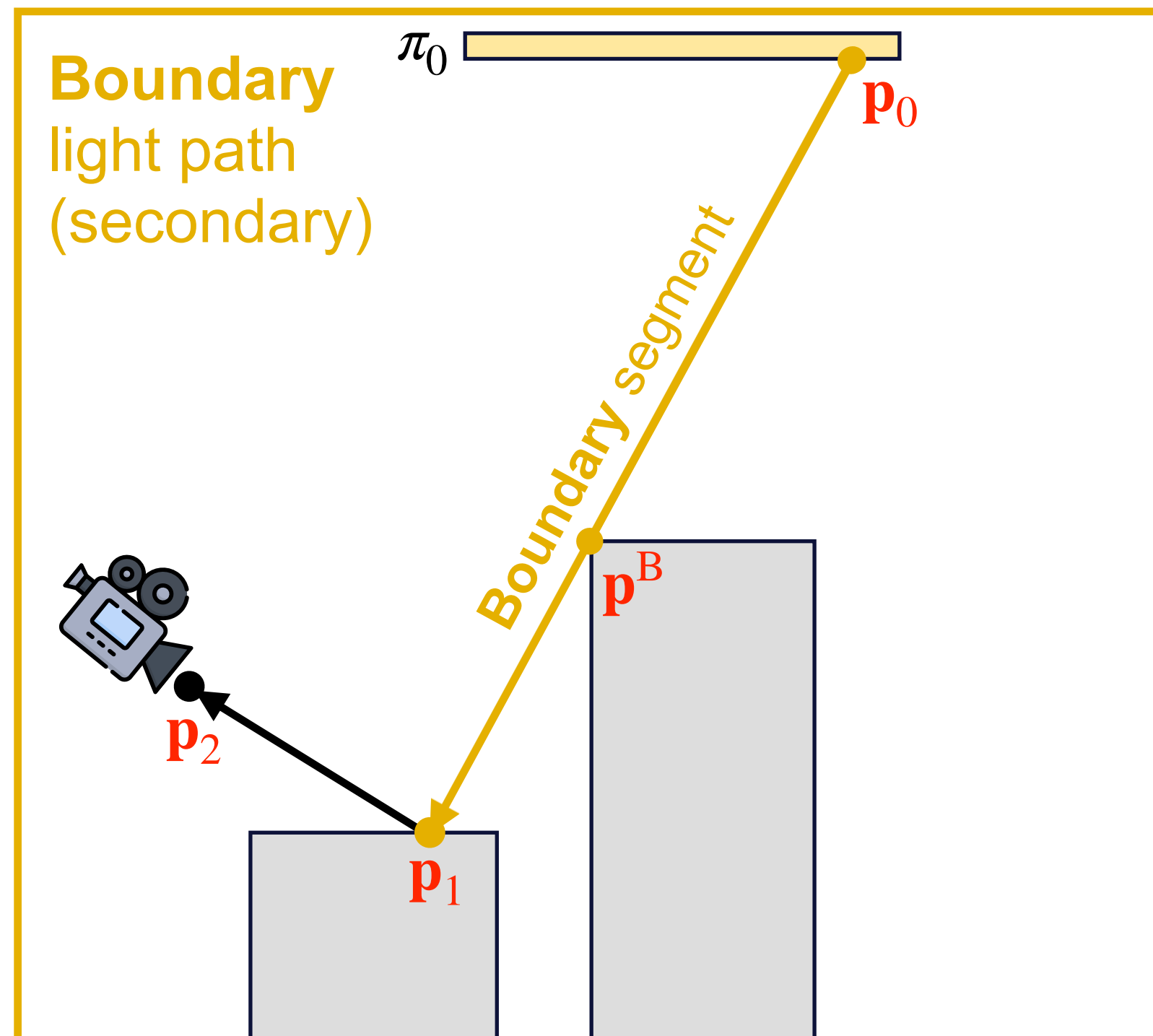


Material-form direct-illumination integral

$$I_j = \int_{\mathcal{M}_0^3} \underbrace{f_j(\mathbf{x}_0 \rightarrow \mathbf{x}_1 \rightarrow \mathbf{x}_2)}_{= f_j(\bar{\mathbf{p}})} \left| \frac{d\mu(\bar{\mathbf{x}})}{d\mu(\bar{\mathbf{p}})} \right| d\mu(\bar{\mathbf{p}})$$

Change of variable: $\mathbf{x}_i = X(\mathbf{p}_i, \pi)$ with $\mathcal{M}_0 = \mathcal{M}(\pi_0)$

π controls the position of the area light



Material-form *differential* direct-illumination integral

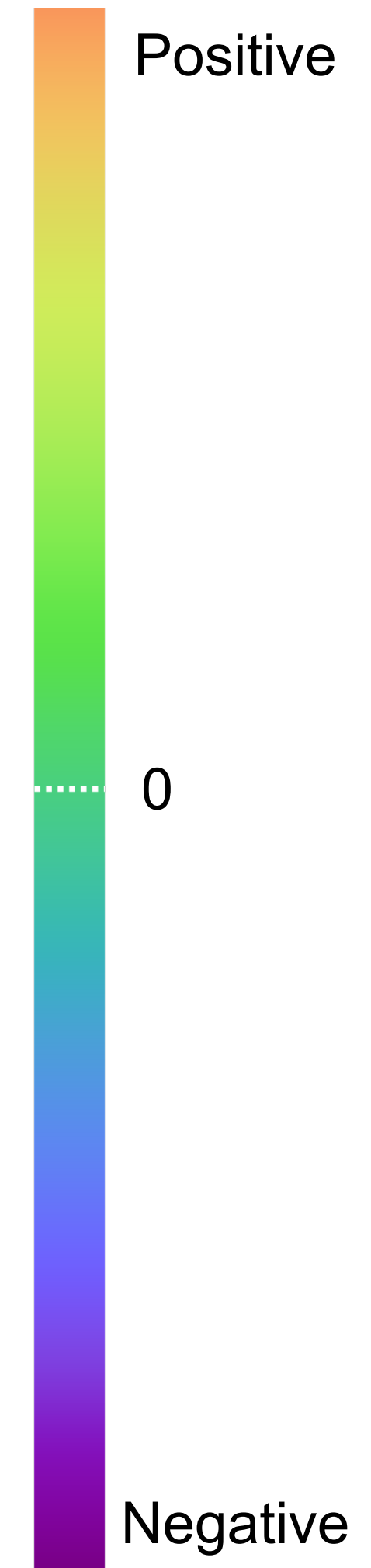
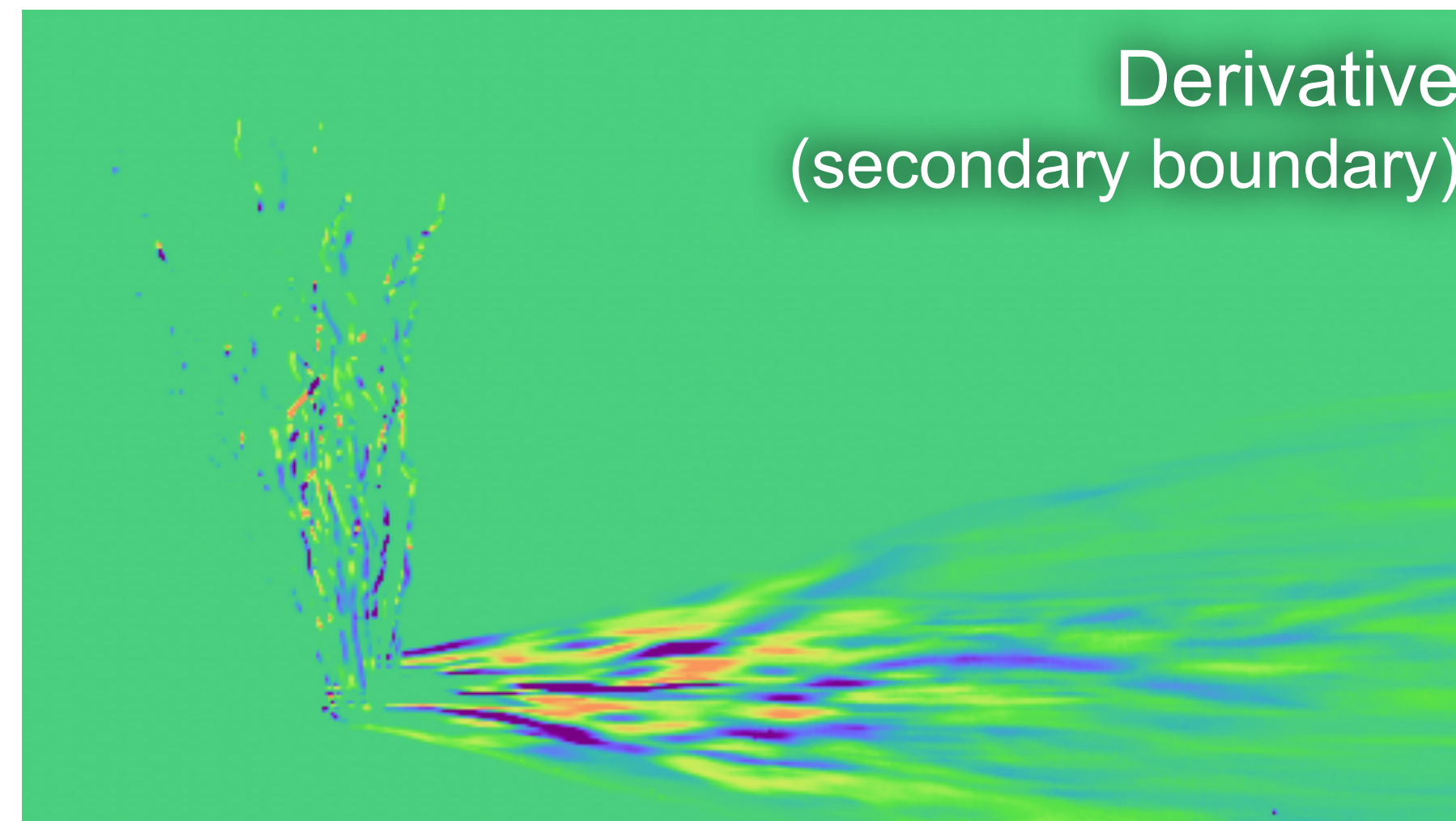
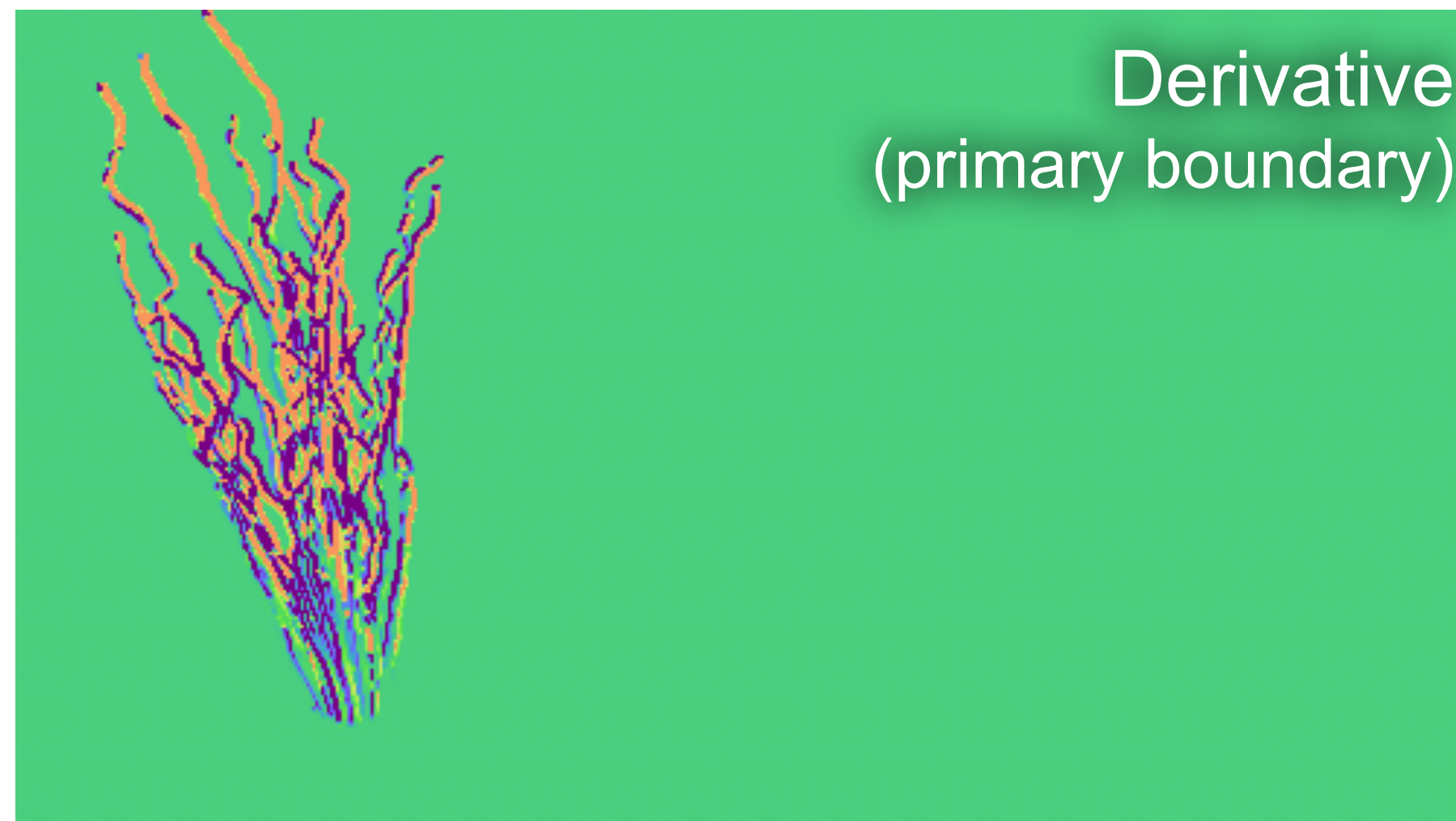
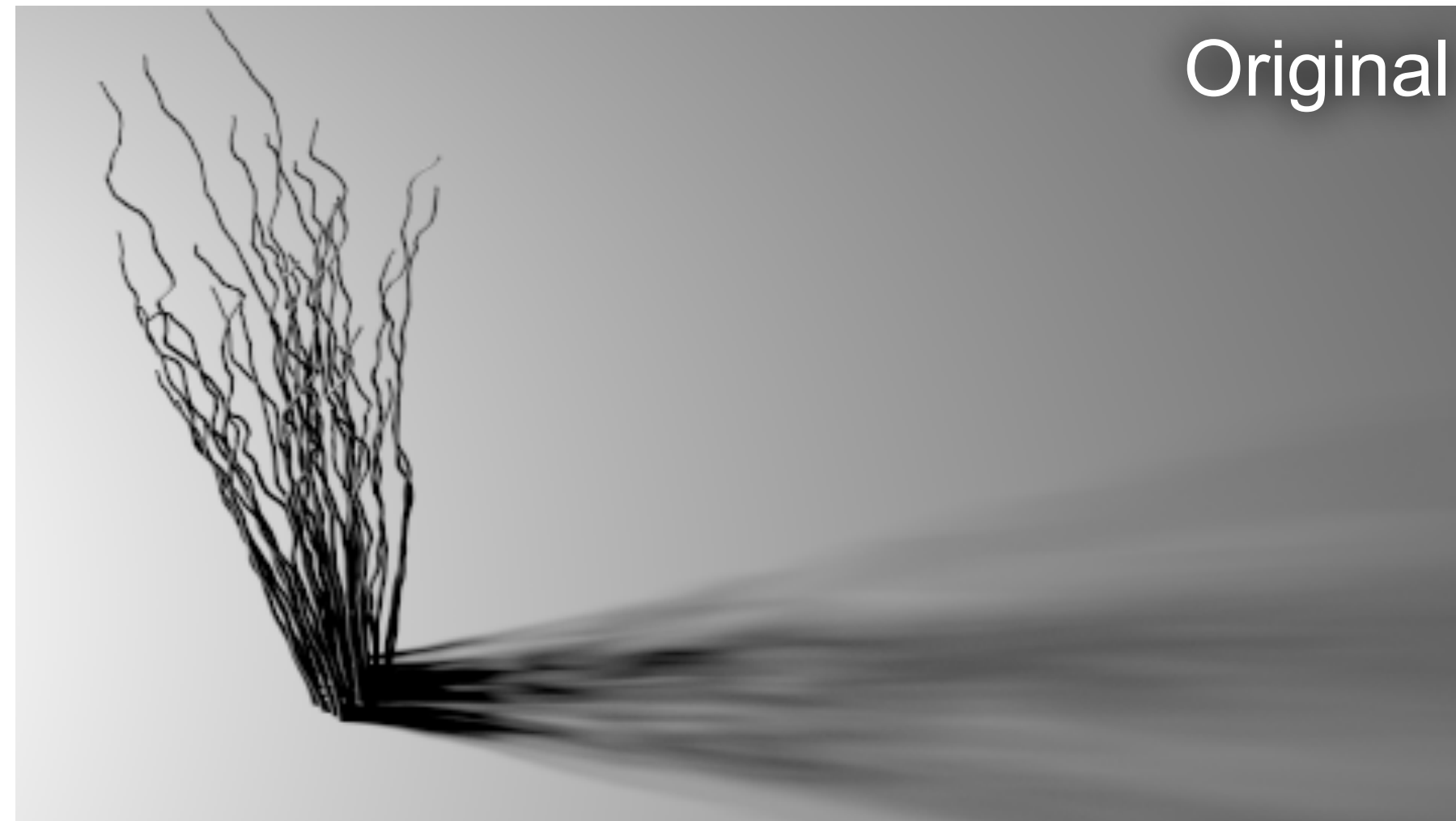
$$\frac{dI_j}{d\pi} = \int_{\mathcal{M}_0^3} \frac{df_j}{d\pi}(\bar{\mathbf{p}}) d\mu(\bar{\mathbf{p}}) + \int_{\partial\mathcal{M}_0^3} g_j(\bar{\mathbf{p}}) d\mu'(\bar{\mathbf{p}})$$

Boundary integral

- Consider the problem of estimating $dI_j/d\pi \big|_{\pi=\pi_0}$
 - Secondary **boundary** light paths:
 - Determined uniquely by the **boundary segment** $\mathbf{p}_0 \mathbf{p}_1$ (with pinhole camera + direct illumination)
 - The **boundary segment** $\mathbf{p}_0 \mathbf{p}_1$:
 - Resides within a 3D manifold
 - For polygonal meshes: can be parameterized with \mathbf{p}^B on a face edge (1D) + \mathbf{p}_0 on the light source (2D)
 - Should be *importance sampled* with a pdf $\propto g_j(\bar{\mathbf{p}})$
 - Sampling can be guided easily!

COMPONENT-WISE VISUALIZATIONS

Parameter: rotation angle of the object



- Physics-based differentiable rendering is a rich topic, and we are just getting started
- Solving inverse-rendering problems is not only about differentiation
 - What loss to use?
 - How to avoid local minima?
 - How to handle non-differentiable things like mesh topology?
 - How to efficiently integrate physics-based rendering into machine learning pipelines?
- We look forward to future collaborations on all these topics!

PHD POSITIONS AT UC IRVINE

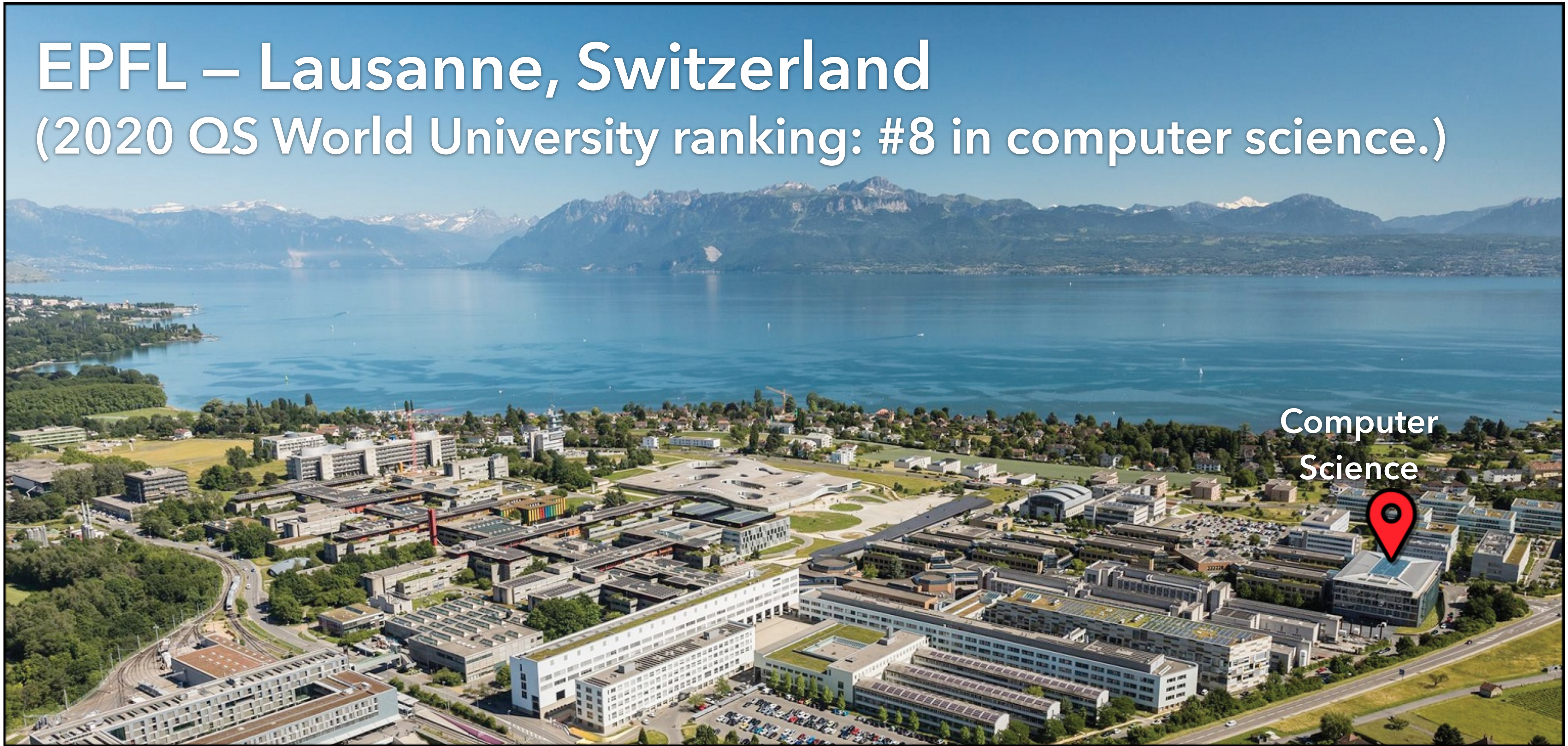


AVAILABLE POSITIONS (4 PHDS & 1 POSTDOC)



EPFL – Lausanne, Switzerland

(2020 QS World University ranking: #8 in computer science.)

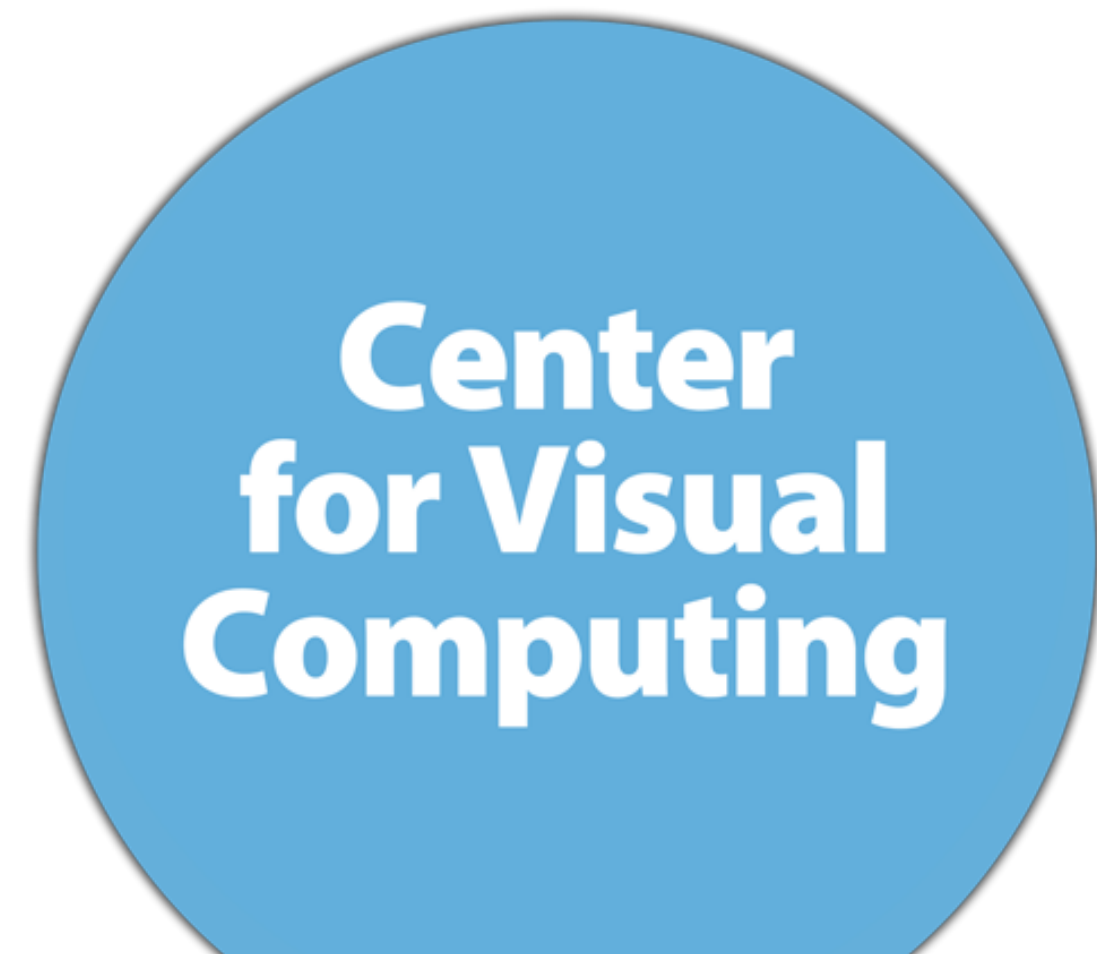


Computer
Science



Apply to UCSD too!

apply to the graduate program/postdoc if you want to work on differentiable graphics!



faculty: Ravi Ramamoorthi, Henrik Jensen, David Kriegman, Manmohan Chandraker, Hao Su, Albert Chern, Nuno Vasconcelos, Xiaolong Wang, Thomas DeFanti, Jurgen Schulze, Zhuowen Tu, and ... **me!**

THANK YOU

- Funding agencies



- Collaborators

- Miika Aittala, Frédo Durand, Ioannis Gkioulekas, Nicolas Holzschuch, Jaakko Lehtinen, Guillaume Loubet, Bailey Miller, Merlin Nimier-David, Ravi Ramamoorthi, Delio Vicini, Lifan Wu, Kai Yan, Tizian Zeltner, Cheng Zhang, Changxi Zheng

- Course website: <https://shuangz.com/courses/pbdr-course-sg20/>